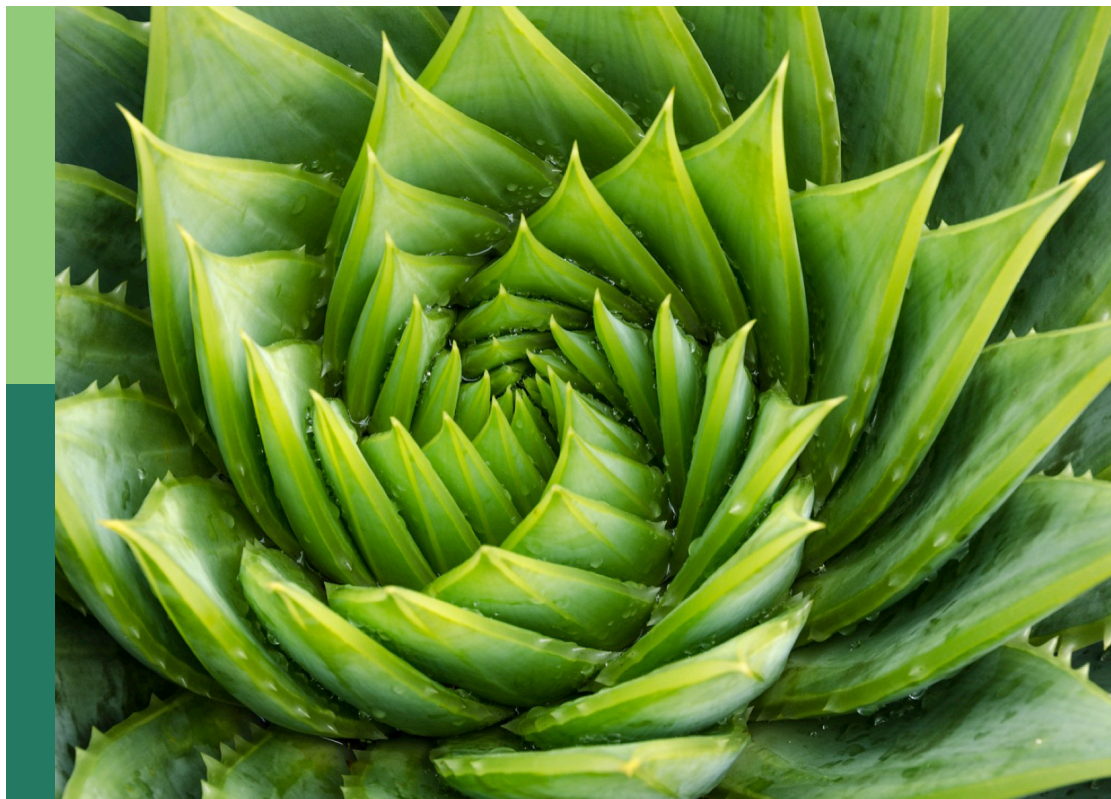# Cereal leaf blights,
volume II

Edited by
Kostya Kanyuka, Stephen Bruce Goodwin, Andres Mäe and
Morten Lillemo

Published in
Frontiers in Plant Science

About Frontiers

Frontiers is more than just an open access publisher of scholarly articles: it is a pioneering approach to the world of academia, radically improving the way scholarly research is managed. The grand vision of Frontiers is a world where all people have an equal opportunity to seek, share and generate knowledge. Frontiers provides immediate and permanent online open access to all its publications, but this alone is not enough to realize our grand goals.

Frontiers journal series

The Frontiers journal series is a multi-tier and interdisciplinary set of open-access, online journals, promising a paradigm shift from the current review, selection and dissemination processes in academic publishing. All Frontiers journals are driven by researchers for researchers; therefore, they constitute a service to the scholarly community. At the same time, the *Frontiers journal series* operates on a revolutionary invention, the tiered publishing system, initially addressing specific communities of scholars, and gradually climbing up to broader public understanding, thus serving the interests of the lay society, too.

Dedication to quality

Each Frontiers article is a landmark of the highest quality, thanks to genuinely collaborative interactions between authors and review editors, who include some of the world's best academicians. Research must be certified by peers before entering a stream of knowledge that may eventually reach the public - and shape society; therefore, Frontiers only applies the most rigorous and unbiased reviews. Frontiers revolutionizes research publishing by freely delivering the most outstanding research, evaluated with no bias from both the academic and social point of view. By applying the most advanced information technologies, Frontiers is catapulting scholarly publishing into a new generation.

What are Frontiers Research Topics?

Frontiers Research Topics are very popular trademarks of the *Frontiers journals series*: they are collections of at least ten articles, all centered on a particular subject. With their unique mix of varied contributions from Original Research to Review Articles, Frontiers Research Topics unify the most influential researchers, the latest key findings and historical advances in a hot research area.

Find out more on how to host your own Frontiers Research Topic or contribute to one as an author by contacting the Frontiers editorial office: frontiersin.org/about/contact

Cereal leaf blights, volume II

Topic editors

Kostya Kanyuka — National Institute of Agricultural Botany (NIAB), United Kingdom

Stephen Bruce Goodwin — Agricultural Research Service, United States Department of Agriculture, United States

Andres Mäe — Estonian Crop Research Institute, Estonia

Morten Lillemo — Norwegian University of Life Sciences, Norway

Citation

Kanyuka, K., Goodwin, S. B., Mäe, A., Lillemo, M., eds. (2023). *Cereal leaf blights, volume II*. Lausanne: Frontiers Media SA. doi: 10.3389/978-2-8325-3083-2

Table of
contents

Check for updates

*CORRESPONDENCE
Juan Zhang
juanzh74@ldu.edu.cn
Hongxia Zhang
hxzhang@sibs.ac.cn

†These authors have contributed
equally to this work

Molecular characterization of a novel strain of *Bacillus halotolerans* protecting wheat from sheath blight disease caused by *Rhizoctonia solani Kühn*

Zhibin Feng[1†], Mingzhi Xu[2,3†], Jin Yang[2,3†], Renhong Zhang[2,3], Zigui Geng[2,3], Tingting Mao[2,3,4], Yuting Sheng[2,3,4], Limin Wang[2,3,4], Juan Zhang[2,3,4*] and Hongxia Zhang[2,4,5*]

[1]College of Life Science, Ludong University, Yantai, China, [2]The Engineering Research Institute of Agriculture and Forestry, Ludong University, Yantai, China, [3]College of Agriculture, Ludong University, Yantai, China, [4]Key Laboratory of Molecular Module-Based Breeding of High Yield and Abiotic Resistant Plants in Universities of Shandong (Ludong University), Ludong University, Yantai, China, [5]Shandong Institute of Sericulture, Shandong Academy of Agricultural Sciences, Yantai, China

Rhizoctonia solani Kühn naturally infects and causes Sheath blight disease in cereal crops such as wheat, rice and maize, leading to severe reduction in grain yield and quality. In this work, a new bacterial strain *Bacillus halotolerans* LDFZ001 showing efficient antagonistic activity against the pathogenic strain *Rhizoctonia solani Kühn* sh-1 was isolated. Antagonistic, phylogenetic and whole genome sequencing analyses demonstrate that *Bacillus halotolerans* LDFZ001 strongly suppressed the growth of *Rhizoctonia solani Kühn* sh-1, showed a close evolutionary relationship with *B. halotolerans* F41-3, and possessed a 3,965,118 bp circular chromosome. Bioinformatic analysis demonstrated that the genome of *Bacillus halotolerans* LDFZ001 contained ten secondary metabolite biosynthetic gene clusters (BGCs) encoding five non-ribosomal peptide synthases, two polyketide synthase, two terpene synthases and one bacteriocin synthase, and a new kijanimicin biosynthetic gene cluster which might be responsible for the biosynthesis of novel compounds. Gene-editing experiments revealed that functional expression of phosphopantetheinyl transferase (SFP) and major facilitator superfamily (MFS) transporter genes in *Bacillus halotolerans* LDFZ001 was essential for its antifungal activity against *R. solani Kühn* sh-1. Moreover, the existence of two identical chitosanases may also make contribution to the antipathogen activity of *Bacillus halotolerans* LDFZ001. Our findings will provide fundamental information for the identification and isolation of new sheath blight resistant genes and bacterial strains which have a great potential to be used for the production of bacterial control agents.

Importance: A new *Bacillus halotolerans* strain *Bacillus halotolerans* LDFZ001 resistant to sheath blight in wheat is isolated. *Bacillus halotolerans* LDFZ001 harbors a new kijanimicin biosynthetic gene cluster, and the functional expression of *SFP* and *MFS* contribute to its antipathogen ability.

Introduction

Wheat sheath blight has become one of worldwide disease causing severe yield loss crop plants (Ghosh et al., 2017). Necrotrophic fungus *Rhizoctonia solani Kühn*, which could produce host specific phytotoxins as pathogenicity or virulence factors, resulting in its widely spread and difficult to control, has been identified as the causal agent of sheath blight in many crops (Srivastava et al., 2016). Although Bacillus species have been widely used to control sheath blight, the antagonistic activity is still not high enough and needs to be improved (Abbas et al., 2019).

To date, various *Bacillus* species have been commercially used as pesticides, surfactants, and biological agents for flavor enhancing and nutrition supplementation, and about half of the commercially available bacterial control agents were originated from *Bacillus* species (Stein, 2005; Ongena and Jacques, 2008; Tareq et al., 2012; Tareq et al., 2014; Kim et al., 2017b; Pereira et al., 2019). The secondary metabolites, hydrolases and peptides, such as ribosomally synthesized and post-translationally modified peptides (RiPPs), nonribosomally synthesized peptides (NRPs), antitumor polyketides (PKs) and terpenes, which constitute a rich assortment of biologically active small molecules in the bio-control process, play a crucial role in plant pathogen inhibition (Tosato et al., 1997; Duitman et al., 1999; Tsuge et al., 2001; Luo et al., 2015b; Torres et al., 2015; Nair et al., 2016; Saggese et al., 2018). Based on the sequences of their genomes, gene clusters corresponding to different biological active molecules have been cloned, and their biological functions have been identified in different bacterial species (Gao et al., 2017; Jin et al., 2017).

To understand the functions of biological active molecules produced by microorganism for plant pathogen protection, complete genome sequencing has been taken as an efficient strategy (Chen et al., 2009b; He et al., 2013; Guo et al., 2015; Shaligram et al., 2016; Jin et al., 2017; Jadeja et al., 2019; Lu et al., 2019; Pereira et al., 2019). Compared with the genome sequence of *B. subtilis* 168, the first sequenced model organism of *Bacillus* species, different sequences responsible for cell wall and antibiotic synthesis have been identified, implying the functional difference of different genome sequences in *Bacillus* species (Guo et al., 2013; Sabaté and Audisio, 2013; Bóka et al., 2019). In the genome of *B. subtilis* 168, almost 4% of the whole genome was predicted to be responsible for the encoding of multifunctional enzymes involved in antibiotic biosynthesis (Kunst et al., 1997). By comparing the genome sequences between different microorganisms, some new gene clusters synthesizing novel antimicrobial products have been predicted (Chen et al., 2009a; Luo et al., 2015a; Mobegi et al., 2017).

Surfactins, the biosurfactant molecules widely identified in *Bacillus* species, have showed multiple bio-activities (Kim et al., 2017a; Li et al., 2021; Han et al., 2022). As a member of lipopeptide family, surfactins synergistically affected the bio-control effectivity of *Bacillus* species (Li et al., 2016; Kim et al., 2017b). Full genome sequence annotation analysis indicated that a surfactin operon, including *srfA*, *srfB*, *srfC*, and *srfD*, was responsible for the biosynthesis of surfactin (Nakano et al., 1991). Meanwhile, a genetic locus *sfp*, encoding a phosphopantetheine transferase, was also required for surfactin production (Wu et al., 2019). Although *B. subtilis* strain 168 possessed a complete *srf* operon, it was unable to produce surfactin due to a frameshift in the *SFP* gene, which resulted in the production of an inactive phosphopantetheine transferase. Integration of a functional *SFP* gene restored the ability of *B. subtilis* 168 to synthesize surfactin (Reuter et al., 1999; Wu et al., 2019).

In addition to *SFP* gene, other genes in *srf* operon, such as major facilitator superfamily (MFS) proteins, were also identified *via* genome sequence analysis. To date, MFS transporter was the largest transporter superfamily, including over 10,000 members divided into 74 families (Marger and Saier 1993; Saier et al., 1999; Wang et al., 2020; Saier et al., 2021). MFS transporters could facilitate the transport of a variety of substrates, including ions, sugar phosphates, drugs, nucleosides, amino acids and peptides, across cytoplasmic and internal membranes (Saier and Paulsen 2001; Lorca et al., 2007; Chen et al., 2008; Yen et al., 2010). Crystallographic structures of MFS members consisted of a typical 12 transmembrane segments and a unique intracellular four-helix domain (Madej and Kaback, 2013). Most MFS transporters in some bacteria

transported specific substrates and were closely related with the immunological issues such as virus invasion and drug resistance (Manel et al., 2005).

Chitosanase could specifically catalyse the hydrolysis of the β-1,4-glycosidic linkage in chitosan, to produce chitosan oligosaccharides, the only natural alkaline amino oligosaccharides widely used in pharmaceutical, food and cosmetic industry (Park et al., 1999; Kurakake et al., 2000; Omumasaba et al., 2000; Yoon et al., 2002; Wang et al., 2008; Johnsen et al., 2010; Kang et al., 2012). Chitosanases also have a function in plant pathogen suppression (Zhao et al., 2011). In prokaryotes, chitosanase, whose target chitosan is not a constituent of the cells, is alleged to work as extracellular enzymes (de Araújo et al., 2016; Park et al., 1999; Liang et al., 2014). A gene cluster encoding chitosanase, which was able to prevent plant from the infection by *Plasmodiophora brassicae*, a common pathogen that causes clubroot disease, has been identified (Guo et al., 2013).

In the past years, a number of *Bacillus* strains have been isolated and the possible functions of some gene clusters in their genomes have been examined. However, *Bacillus* strain showing significantly protection of wheat from sheath blight disease caused by *Rhizoctonia solani Kühn* is still not identified. In the present study, a new *Bacillus* species with high antifungal activity and great potential for sheath blight protection in cereal crops was isolated, and its genome sequence and the possible genes responsible for the antifungal activity were investigated.

Materials and methods

Strains and culture conditions

Bacillus halotolerans LDFZ001 (*B. halotolerans* LDFZ001) was isolated from the sandy soil collected from the coastal zone of Yantai city, Shandong province, China, using serial dilution plating methods. Single colony was cultured on LB medium and stored at -80°C. The control strains *Bacillus subtillis* 168 (*B. subtillis* 168) and *Bacillus halotolerans* F41-3 (*B. halotolerans* F4103) were purchased from BioSciBio (Hangzhou, China). The pathogenic strain *Rhizoctonia solani Kühn* sh-1 is a collection in our lab. All the bacterial and fungus strains used in this study were listed in Table S1.

For the cultivation of *B. halotolerans* LDFZ001, *B. subtillis* 168 and *B. halotolerans* F41-3, nutrient broth (NB) liquid medium consisting of 3 g beef extract, 10 g peptone, 5 g NaCl, 2 g $MgCl_2$ per liter was used. For the growth and preservation of the pathogenic strain *Rhizoctonia solani Kühn* sh-1, potato dextrose agar (PDA) medium consisting of 200 g Patato Destrose Agar (Coolaber, Beijing, China), 20 g sucrose, 20 g agar, was used.

The cloning plasmid pEASY-T1 was purchased from TransGen Biotech (Beijing, China). The expression plasmid pET28a (+) and the host strain *E. coli* BL21 (DE3) were purchased from Novagen (Shanghai, China). The plasmid

pJOE8999 for gene editing with CRISPR-Cas 9 system is a collection in our lab. All the materials for gene cloning and protein purification were purchased from TaKaRa Biotechnology (Dalian, China). HisTrap HP and HiTrap Desalting were purchased from GE Healthcare (München, Germany). Chitosan for enzyme assay was obtained from Sigma-Aldrich (St. Louis, USA). Other chemicals were purchased from Sangon Biotech (Shanghai, China).

Morphology observation and identification of bacterial strain

The morphology of purified strain *B. halotolerans* LDFZ001 was observed with light microscope (Olympus BX41, Japan) at a magnification of × 1000. Genomic DNA, isolated from the purified bacterial strain was used as template to amplify the 16S rRNA gene. The corresponding sequence was applied to phylogenetic analysis using MEGA 7.0 (Kumar et al., 2018).

Antipathogen activity analysis

For antifungal activity analysis, pathogenic microbe strain *R. solani Kühn* sh-1 was inoculated at the center of PDA medium plate and cultured at 28°C alone or with *B. halotolerans* LDFZ001, *Bacillus subtillis* 168 or *B. halotolerans* F41-3 for three days, which was inoculated as a scratch line under the *R. solani Kühn* sh-1 inoculation spot on each plate. Then, the inhibition rate (IR) of *B. halotolerans* LDFZ001, *B. subtillis* 168 and *B. halotolerans* F41-3 against *R. solani Kühn* sh-1 was evaluated as described previously (Chen et al., 2019).

For the inhibition efficiency analysis of *B. halotolerans* LDFZ001, *B. subtillis* 168 and *B. halotolerans* F41-3 on *Rhizoctonia solani Kühn* sh-1 caused wheat sheath blight, *Rhizoctonia solani Kühn* sh-1 cultured on NB solid medium at 28°C for 24 were collected by centrifugation, washed two times with 0.05 M sodium phosphate buffer (pH7.2), and re-suspended with it to a final concentration of 2×10^8 CFU/mL. One-week-old wheat seedlings germinated on filter paper soaked with sterile water were sprayed with 10 mL of the prepared bacterial solution. After 24 h, a 5 mm agar block of *Rhizoctonia solani Kühn* sh-1 grown on NB solid medium were inoculated to the middle of hypocotyls. After incubated at 25°C for 5 days, the phenotypes of seedlings were observed. The disease severity was graded according to the previous reported standard (Chen et al., 2019). The disease incidence rate (DIR) was generated using the following formula:

$$DIR(\%) = \frac{n}{N} \times 100$$

N represents the total number of investigated plants and n is the number of infected plants (Li et al., 2019). In our study, 30

plants were selected to conserve and investigate the DIR for each treatment.

Crude lipopeptide preparation and determination

Cells of *B. halotolerans* LDFZ001, *B. subtillis* 168 and *B. halotolerans* F41-3 were cultivated in NB liquid medium at 28°C for 48 h. The concentrations of the fermentation broths were calibrated to $OD_{600} = 1.0$. Then 100mL of the calibrated fermentation broths from these three bacteria were separately centrifuged at 8000 rpm/min for 10min to remove the bacteria. The supernatants were modified to pH=2 by 6mol/L hydrochloric acid and placed in 4°C refrigerator for more than 12h. After centrifugation at 8000 rpm/min for 10 min, the precipitate was collected. The crude extract was washed twice and dissolved in 100μ of methanol for HPLC analysis and antifungal activity assay. For HPLC analysis, crude extracts were filtered with a 0.22 μm membrane filter. Mobile phase was a mixture of acetonitrile and H_2O (85:15, v/v). The flow rate was 1.00 mL/min. The injection volume was 10μL. The temperature was set at 28°C. Agilent C18 (250×4.6mm, 5μm) column was use and the detection wavelength was 210nm. Lipopeptides were analyzed using an Ultra high liquid chromatography system with a high resolution mass spectrometer (MS) as described previously (Chen et al., 2018).

The Oxford cup method was performed to analyze the antifungal activity of crude lipopeptides. *Rhizoctonia solani Kühn* sh-1 cultured on NB liquid medium at 28°C for 24 h were spread evenly on PDA solid medium. Two days later, four agar blocks (3mm×3mm) with the *Rhizoctonia solani Kühn* sh-1 were cut and place on a PDA solid medium plate, in the center of which a sterilized Oxford cup was placed. Using ddH_2O as a control, 200μL of crude lipopeptide was dripped into the Oxford cup, which was taken away after 12h. The plates containing crude lipopeptide and agar blocks of the *Rhizoctonia solani Kühn* sh-1 were placed in 28°C for 72h. The inhibition zones were observed, photographed and measured.

Genome sequencing and assembly

High-quality genomic DNA isolated from *B. halotolerans* LDFZ001 with Wizard® Genomic DNA Purification Kit (Promega) according to manufacturer's protocol was quantified with TBS-380 fluorometer (Turner BioSystems Inc., Sunnyvale, CA), and applied to a combination of PacBio RS II Single MoleculeReal Time (SMRT) and Illumina sequencing platforms for sequencing. Then, data generated were analyzed using I-Sanger Cloud Platform (www.i-sanger.com) from Shanghai Majorbio (Shanghai, China).

Gene prediction and annotation

CDS, tRNA and rRNA were respectively predicted with Glimmer (version 3.02, http://cbcb.umd.edu/software/glimmer/), tRNA-scan-SE (version 1.23, http://lowelab.ucsc.edu/tRNAs.can-SE) and Barrnap (version 1.2, http://www.cbs.dtu.dk/services/RNAmmer/). The predicted CDSs were annotated from the non-redundant (NR) NCBI database, Swiss-Prot (http://uniprot.org), Pfam, GO, COG (http://www.ncbi.nlm.nih.gov/COG) and KEGG (http://www.genome.jp/kegg/) database using sequence alignment tools BLAST, Diamond and HMMER. Briefly, each set of query proteins was aligned with the databases, and annotations of best-matched subjects (e-value< 10^{-5}) were obtained for gene annotation.

Secondary metabolite gene clusters were predicted with the online tools NP searcher (http://dna.sherman.lsi.umich.edu/) and antiSMASH (http://antismash.secondarymetabolites.org/). The genome of *B. halotolerans* LDFZ001 in a circular format was obtained using Circos.

Plasmid construction and transformation

Deletion of the gene's chromosomal region was performed as described previously (Altenbuchner, 2016). PCR fragments from the upward and downward regions of the gene were inserted into the downstream of T7 promoter in plasmid pJOE8999. To generate plasmids pJOEsfp and pJOEmfs for *B. halotolerans* LDZF001 transformation, the sgDNAs of the relative genes to be deleted based on the database from the internet (http://crispor.tefor.net/crispor.py) were separately inserted into these resultant plasmids *via* homologous recombination (Anagnostopoulos and Spizizen, 1961; Ge et al., 2015; Altenbuchner, 2016). Using conventional two-step procedure, the strain was cultured in a minimal medium (Peptone 10g/L, Yeast extract 5g/L, NaCl 10g/L, Sorbitol 91g/L, pH7.0) to an of OD_{600} value of 0.8 at 30°C. After harvested *via* centrifugation at 4 °C, the cell pellet was re-suspended in ETM buffer (Sorbitol 91g/L, Mannitol 91g/L, 10% Glycerol (v/v), pH 7.0) for electroporation (1800v, 200Ω, 25μF). Competent cells containing pJOEsfp or pJOEmfs plasmid were recovered in RM medium (Peptone 10g/L, Yeast extract 5g/L, NaCl 10g/L, Sorbitol 91g/L, Mannitol 69g/L, pH7.0) and spread on the RM solid plates with supplemented with 40 mg/L kanamycin. The transformant colonies were tested with PCR after the plasmid was cured by being cultured at 37°C for 12-16h.

For heterologous expression of Csn-gene1288 and Csn-gene2656, the two chitosanase genes from *B. halotolerans* LDFZ001 were cloned into pET28a(+) to generate the recombinant plasmids pET28a-Csn1288 and pET28a-Csn2656 *via* homologous recombination (Ge et al., 2015). The resultant constructs were subsequently transformed into *E. coli* BL21 (DE3). After induced with IPTG, the recombinant proteins

were purified *via* immobilized metal affinity chromatography. Chitosanase activity was measured as describe previously (Kurakake et al., 2000; Kang et al., 2012). The reaction was performed at 50°C for 15 min in sodium acetate buffer (pH5.4), followed by the determination of reducing sugar using DNS methods. The optimal condition assays were performed by measuring the activity in sodium acetate buffer (pH 3.6-7.0) at specific temperatures ranging from 30°C to 75°C. All the primer sequences used in this study were shown in Table S2.

Statistical analysis

For the antifungal assay, three replicates were performed. Student's t-test with IBM SPSS Statistics 21 was performed to generate every P value (*P< 0.05).

Results

Isolation and identification of *Bacillus halotolerans* LDFZ001

To identify new antagonistic strain against fungal pathogen, we isolated a total number of 26 bacterial clones from the sandy soil in the coastal zone of Yantai, Shandong Province of China, and assessed their antagonistic activities against the pathogenic strain *Rhizoctonia solani Kühn* sh-1 which caused sheath blight disease in most crop plants. We found that one clone, numbered as LDFZ001, displayed very strong *in vitro* antagonistic activity against *Rhizoctonia solani Kühn* sh-1. Therefore, LDFZ001 was chosen for further studies. It is well known that *Bacillus* species possessed antagonistic activity against various pathogenic fungi. Therefore, two *Bacillus* strains, *B. subtillis* 168 and *B. halotolerans* F41-3, along with LDFZ001, were respectively co-cultivated with *Rhizoctonia solani Kühn* sh-1 on PDA medium. LDFZ001 effectively suppressed the radical growth of *Rhizoctonia solani Kühn* Sh-1, whereas *B. subtillis* 168 and *B. halotolerans* F41-3 did not. LDFZ001 exhibited a 98.8%, whereas *B. subtillis* 168 and *B. halotolerans* F41-3 only showed 2.3% and 1.4%, inhibition rates on the radical growth of *Rhizoctonia solani Kühn* Sh-1, respectively (Figures 1A, C).

Since *Rhizoctonia solani Kühn* Sh-1 can produce basidiospores, which cause the damping off and stem rot in wheat seedlings. We further compared the protective ability of *B. subtillis* 168, *B. halotolerans* F41-3 and LDFZ001 against wheat sheath blight on wheat seedlings caused by *R. solani Kühn* sh-1. We observed that one-week-old wheat seedlings pretreated with LDFZ001 successfully protected the occurrence of wheat sheath blight, but seedlings pretreated with *B. subtillis* 168 or *B. halotolerans* F41-3 did not. The seedlings were susceptible to *R. solani Kühn* Sh-1 and showed almost the same wheat sheath blight phenotype as did the negative control seedlings treated with sodium phosphate buffer, accompanied with a very high disease incidence rate (Figures 1B, D).

To determine the properties of LDFZ001, we performed morphological observation. LDFZ001 colonies cultured on LB medium plate formed approximate circles with creamy smooth surface and regular edge. Morphological analysis with light microscopy demonstrated that LDFZ001 cells were gram-positive and in rod shape (data not shown). To further determine the phylogenetic relationship of LDFZ001 with other bacterial strains, a neighbor-joining tree based on 16S rRNA sequence was constructed with MEGA 7.0. Compared with other *Bacillus* family members, LDFZ001 showed close evolutionary relationship with *B. halotolerans* F41-3 and *B. mojavensis* W1-2 (Figure 1E). Therefore, LDFZ001 was named as *Bacillus halotolerans* LDFZ001, and was deposited in the China General Microbiological Culture Collection Center with an accession number of CGMCC 7187.

The anti-pathogen activity of *Bacillus halotolerans* LDFZ001 is associated with lipopeptide production

Lipopeptides play a crucial role in the protection of plants from fungal pathogen attack. To understand whether lipopeptides also make a contribution to the antagonistic activity of *B. halotolerans* LDFZ001 against *Rhizoctonia solani Kühn* Sh-1, lipopeptide extracts from *B. subtillis* 168, *B. halotolerans* F41-3 and *B. halotolerans* LDFZ001 were separately isolated. Similarly, lipopeptide extract from *B. halotolerans* LDFZ001 significantly prohibited the growth of *Rhizoctonia solani Kühn* Sh-1. A clear inhibition zone of about 6.11 cm^2 against *Rhizoctonia solani Kühn* sh-1 was observed. However, lipopeptide extracts from *B. subtillis* 168 and *B. halotolerans* F41-3 did not. The growth of *Rhizoctonia solani Kühn* Sh-1 was about the same as that on the control plate (Figure 2A). We then carried out HPLC assays with the lipopeptide extracts from *B. subtillis* 168, *B. halotolerans* F41-3 and *B. halotolerans* LDFZ001, a serial of distinct peaks in the profile of *B. halotolerans* LDFZ001, but not in the profiles of *B. subtillis* 168 and *B. halotolerans* F41-3, were observed (Figures 2B, C). Using UPLC-ESI-MS, these distinct peaks were determined as antifungal lipopeptide surfactin A (Figures 2B, C). Ions of m/z values 1022.67, 1036.69 and 1058.67 were also detected in previous reports (Roongsawang et al., 2002; Chen et al., 2019).

High genome sequence identity is observed between *B. halotolerans* LDFZ001 and *B. halotolerans* F41-3

To identify the responsible genes for the antifungal activity of *B. halotolerans* LDFZ001, we performed whole genome sequencing of *B. halotolerans* LDFZ001. The whole genome
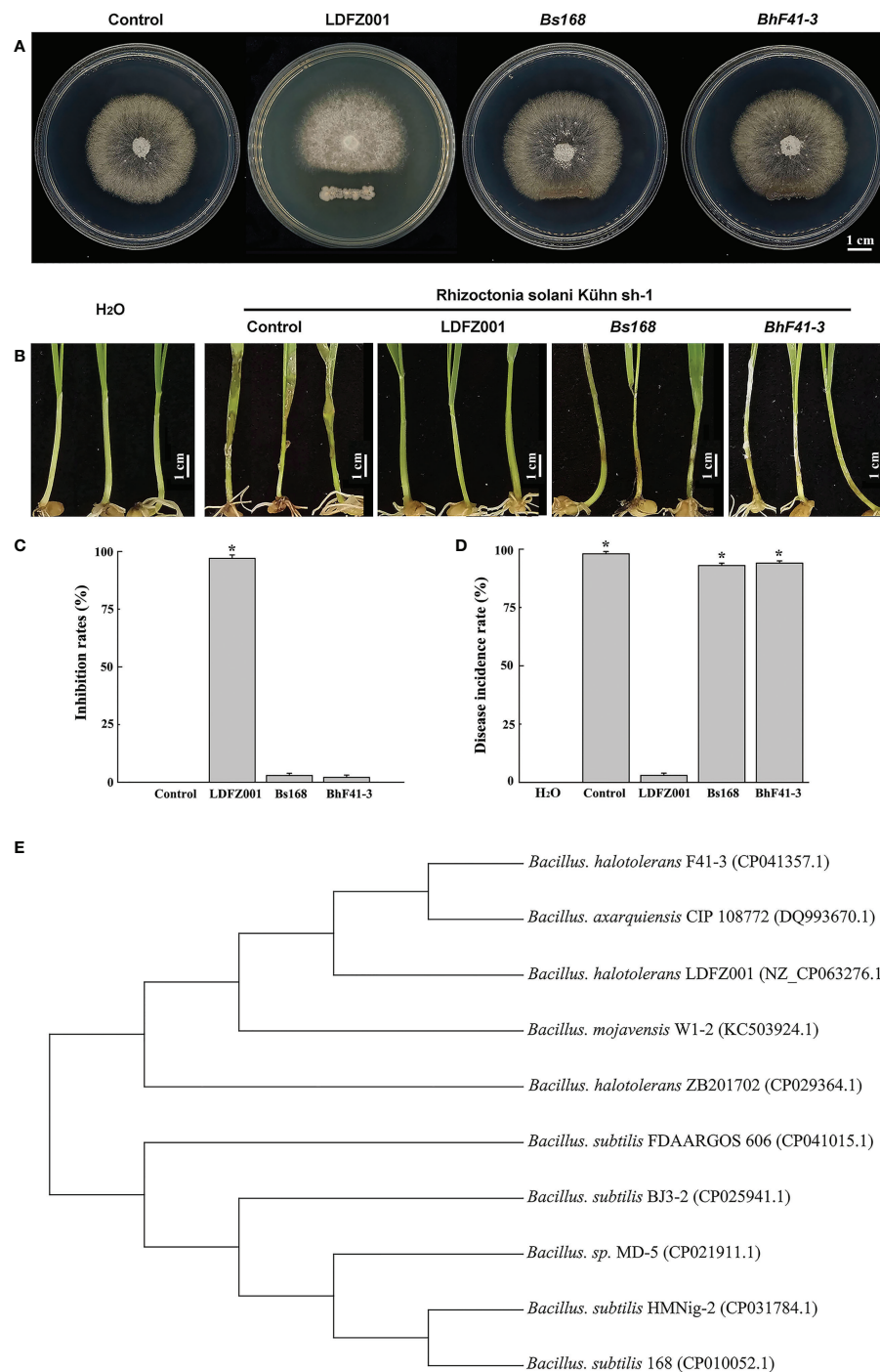
FIGURE 1

Antipathogen activity and phylogenetic relationship analyses. **(A)** Comparison of the antipathogen activity of *B halotolerans* LDFZ001 (LDFZ001) with its relative strains *Bacillus subtillis* 168 (*Bs168*) and *Bacillus halotolerans* F41-3 (*BhF41-3*) against *R. solani Kühn sh-1*, a pathogenic fungus strain cased sheath blight disease in crop plants. *R. solani Kühn sh-1* inoculated at the center of PDA medium plate was cultured three days at 28°C alone or co-cultured with LDFZ001, *Bs168* or *BhF41-3*, which was inoculated as a scratch line under the *R. solani Kühn sh-1* inoculation spot on each plate. **(B)** Susceptibility analysis of wheat seedlings pretreated with LDFZ001, *Bs168* and *BhF41-3* to *R. solani Kühn* Sh-1.The sodium phosphate buffer was used as negative control (control). Wheat seedlings without any treatment were shown in the left as a control, too. **(C)** Inhibition rates (IRs) of *B halotolerans* LDFZ001, *B subtillis* 168 and *B halotolerans* F41-3 against *R. solani Kühn* sh-1 in image **(A)**. **(D)** Disease incidence rates (DIRs) in image **(B)**. Values are the mean $\pm$ SD from three independent experiments (n = 30). *P< 0.05. **(E)** Phylogenetic tree of *B halotolerans* LDFZ001 and other related taxa was generated based on 16S rRNA sequence. MEGA 7 was used to align the sequences.
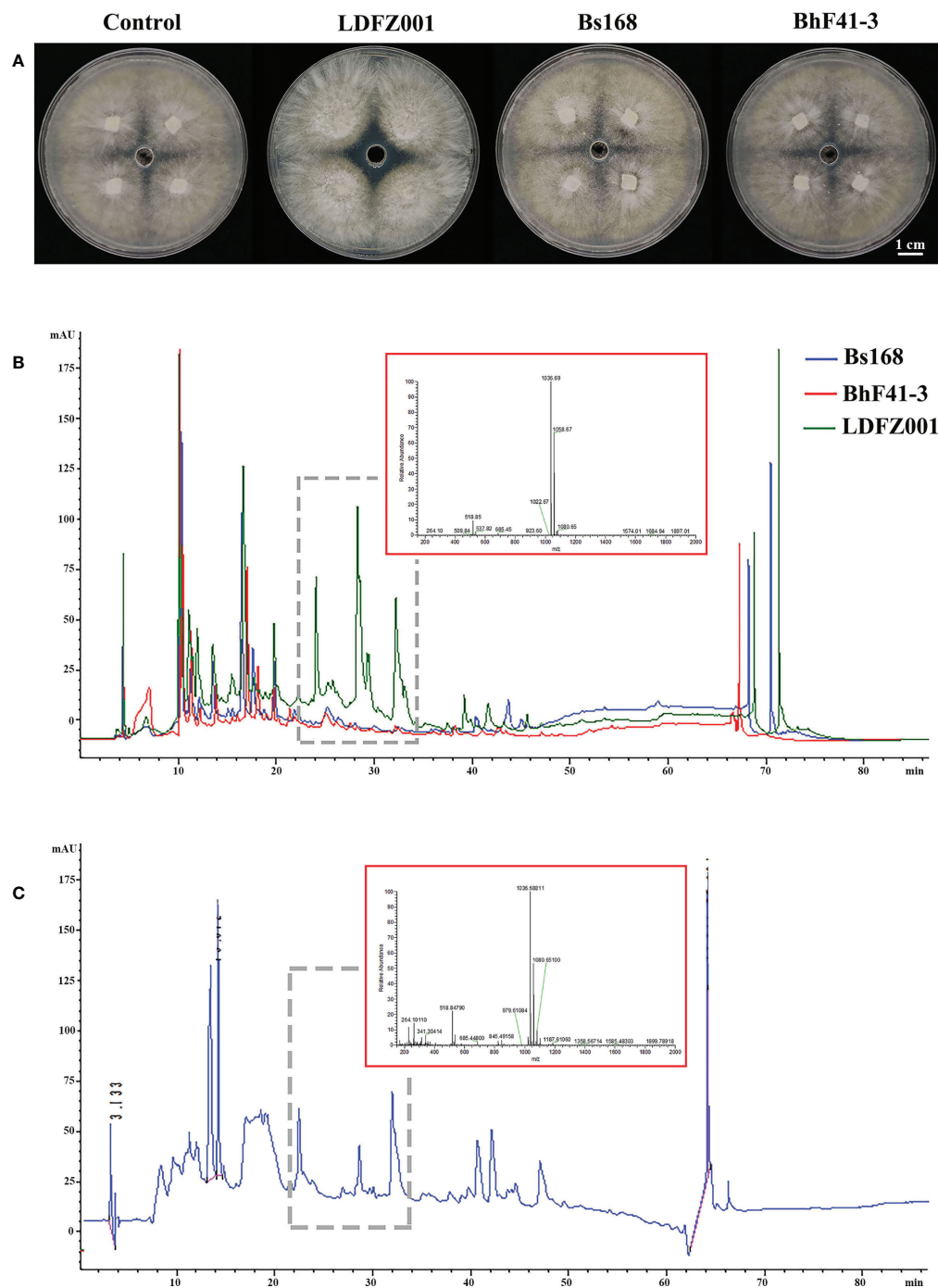
FIGURE 2

Lipopeptide extracts from *B halotolerans* LDFZ001 (LDFZ001), *Bacillus subtillis* 168 (*Bs168*) and *Bacillus halotolerans* F41-3 (*BhF41-3*) were used for antifungal activity and HPLC analyses. **(A)** Antifungal activity assays of putative lipopeptides against *R. solani Kühn* sh-1 **(B, C)** Profiling comparisons of HPLC and the extracted ion flow spectra of m/z 200−2000 from different strains.

was assembled into a 3,965,118 bp circular chromosome with an average genome coverage depth of 475.27-fold and a G+C content of 43.92 (Figure 3). *B. halotolerans* LDFZ001 shares very high sequence identity (97.98%) with *B. halotolerans* F41-3.

A lower sequence identity, from 82.30% to 77.80%, was also observed between *B. halotolerans* LDFZ001 and *B. subtilis* 168, *B. intestinalis* T30, *B. subtilis* ATCC 6633, *B. subtilis* FDAARGOS 606 and *B. subtilis* BJ3-2. Pairwise comparisons

for the average nucleotide identity (ANI) and in silico DNA-DNA hybridization (DDH) between *B. halotolerans* LDFZ001 and these *Bacillus* family members revealed that the ANI values ranged from 87.11 to 97.98% and the DDH values ranged from 32.7 to 81.92% (Table 1). Based on the high ANI and DDH values between *B. halotolerans* LDFZ001 and *B. halotolerans* F41-3, both of them should belong to the same *Bacillus* species.

Genome sequence analyses of *B. halotolerans* LDFZ001

We further performed genome sequence analysis with Glimmer 3.02 and GeneMarks. The whole genome of *B. halotolerans* LDFZ001 was composed of 4,126 coding sequences (CDSs), 73 tRNAs and 24 rRNAs. The 3,500,484 bp CDSs, with an average gene length of 848 bp, accounted for 88.28%, whereas the 22 tandem repeats, with a total DNA length of 6773 bp, accounted for 0.19%, of the whole chromosome DNA (Figure S1). Functional classification of clusters of orthologous gene (COG) showed that the predicted genes in *B. halotolerans* LDFZ001 genome were distributed into 4 COG categories (information storage and processing, metabolism, cellular processes and signaling, and poorly characterized), including 21 COG types and 1237 metabolism, 586 cellular

processes and signaling, 498 information storage and processing, and 836 functionally poorly characterized genes (Figure 4). The complete genome sequence of *B. halotolerans* LDFZ001, with an accession number of NZ_CP063276.1, has been deposited in the NCBI GenBank.

A new kijanimicin biosynthesis cluster is identified in *B. halotolerans* LDFZ001

As one of the well commercialized biological control strains, *Bacillus* family can produce a diverse variety of secondary metabolites. Based on antiSMASH, a total number of 10 secondary metabolite biosynthetic gene clusters (BGCs), encoding 5 non-ribosomal peptide synthases, 2 polyketide synthase, 2 terpene synthases and 1 bacteriocin synthase, were predicted in the *B. halotolerans* LDFZ001 genome (Table 2). These enzymes are involved in the biosynthesis of various secondary metabolites, such as lipopeptides (surfactin and fengycin), lantipeptides (Kijanimicin and subtilosin A), dipeptide antibiotic (bacilysin), polyketides (Bacillaene), siderophores (bacillibactin) and unknown terpenes.

Based on the annotation of secondary metabolite biosynthesis gene clusters, *B. halotolerans* LDFZ001 has a great potential to produce novel antibiotics. Therefore, we compared
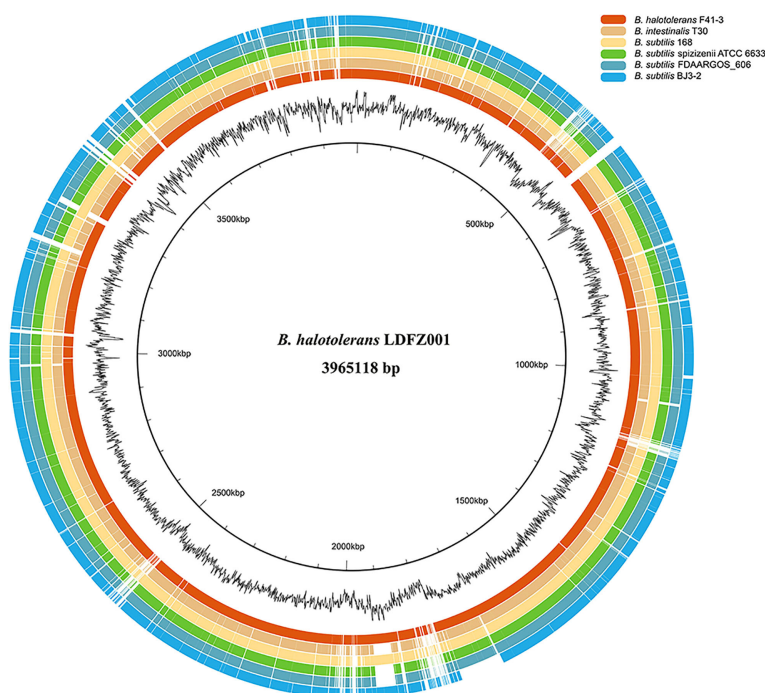
FIGURE 3

Genome comparison of *B halotolerans* LDFZ001 with six of its close *Bacillus* species. The innermost black circle represents the genome of *B halotolerans* LDFZ001 followed by its GC content and the *Bacillus* genomes.

TABLE 1 Comparison of genome information between LDFZ001 and its six closest *Bacillus* species.

Strains	Scaffolds	Genome size (bp)	GC%	LDFZ001	
				ANI	DDH
LDFZ001	1	3965118	43.92%	100%	100%
B. halotolerans F41-3	1	4144458	43.76%	97.98%	81.90%
B. intestinalis T30	1	4031727	43.9%	87.85%	34.30%
B. subtilis 168	1	4215606	43.51%	87.31%	32.80%
B. subtilis ATCC 6633	1	4045538	43.94%	87.94%	34.40%
B. subtilis FDAARGOS 606	1	4045619	43.94%	87.90%	34.40%
B. subtilis BJ3-2	2	4200488	43.64%	87.11%	32.70%

the BGCs of *B. halotolerans* LDFZ001 with other previously reported bacterial strains. Different from the bacilysin, bacillaene, fengycin, bacillibactin and subtilosin A biosynthesis clusters, which shared 100% similarity, and the surfactin biosynthesis cluster, which shared 86% similarity, a new kijanimicin biosynthesis cluster, which shared only 4% similarity, with the reported genome sequences of other bacterial strains, was identified. The schematic representation of the entire gene cluster exhibited that this novel gene cluster contained two lanthionine synthtesase C-like proteins, followed by seven ORFs encoding ATP-binding cassette (ABC) transporter proteins responsible for the translocation of a variety of metabolite compounds across membranes. Although surfactin biosynthesis cluster mainly consists of four genes, *srfAA*, *srfAB*, *srfAC* and *srfAD*, surfactin biosynthesis depends on the phosphopantetheinyl transferase and its adjacent genes. Sequence analysis showed that *B. halotolerans* LDFZ001, and the

reference strains *B. subtilis* 168 and *B. halotolerans* F41-3, all possessed a complete surfactin biosynthesis cluster. However, a frameshift in *sfp* gene, downstream the surfactin biosynthesis cluster in *B. subtilis* 168, and a frameshift in the open reading frame of MFS transporter encoding gene, adjacent to *srfAD* in *B. halotolerans* F41-3, were observed. But no mutation in these two genes was observed in *B. halotolerans* LDFZ001 (Figure 5A).

Using CRISPR-Cas9 system, genes encoding SFP and MFS in *B. halotolerans* LDFZ001 were edited separately by a deletion of part of the gene sequences (Figure 5B). Two *B. halotolerans* LDFZ001 mutants, *Δldfz-sfp* and *Δldfz-mfs* were generated. Confrontation experiments showed that, unlike the wild type *B. halotolerans* LDFZ001, both *Δldfz-sfp* and *Δldfz-mfs* lost their antifungal activity against *Rhizoctonia solani Kühn* sh-1 (Figure 5C). Further HPLC analysis showed that the content of lipopeptide surfactin A was significantly decreased in these two mutants (Figure 5D).
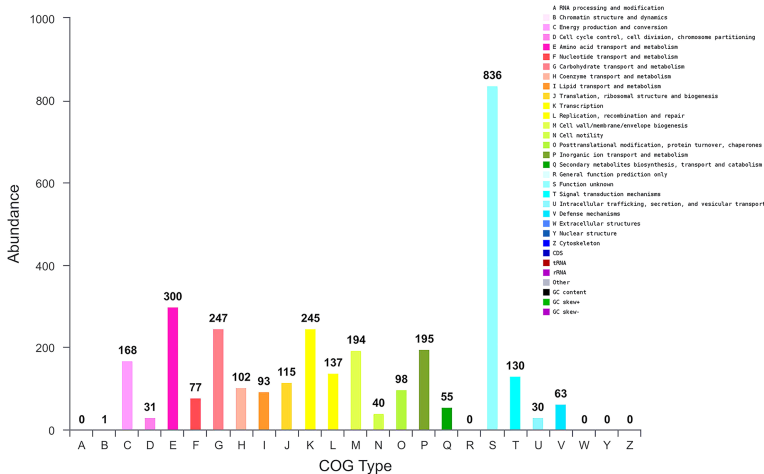
FIGURE 4
Genome sequence analysis of *B halotolerans* LDFZ001. Gene numbers involved in different pathways.

TABLE 2   Biosynthetic gene clusters for secondary metabolites in the genome of *B. halotolerans* LDFZ001.

Cluster ID	Type	Length (bp)	Similar Cluster	Similarity (%)	Gene Numbers
Cluster1	sactipeptide-head_to_tail	21612	Subtilosin_A_biosynthetic_gene_cluster, RiPP	100	21
Cluster2	other	41416	Bacilysin_biosynthetic_gene_cluster, nrps	100	45
Cluster3	nrps-transatpks-otherks	110082	Bacillaene_biosynthetic_gene_cluster, hybrid	100	56
Cluster4	nrps	83464	Fengycin_biosynthetic_gene_cluster, hybrid	100	47
Cluster5	nrps	49736	Bacillibactin_biosynthetic_gene_cluster, nrps	100	42
Cluster6	nrps	65394	Surfactin_biosynthetic_gene_cluster, nrps	86	49
Cluster7	lantipeptide	26864	Kijanimicin_biosynthetic_gene_cluster, polyketide	4	25
Cluster8	terpene	20776	—	–	26
Cluster9	terpene	21898	—	–	22
Cluster10	t3pks	41095	—	–	46

B. halotolerans LDFZ001 harbors two redundant glycoside hydrolase genes

Carbohydrate-active enzymes (CAZymes) can break down cell wall polysaccharides to trigger the death of fungal cells. We found that *B. halotolerans* LDZF001 harbored a large group of potential glycoside hydrolases, including 62 predicted CAZymes such as glycoside hydrolases, glycosyl transferases, carbohydrate esterases and carbohydrate-binding modules (Figure 6A). Interestingly, two members of the glycoside hydrolase GH46 family, Csn-gene1288 and Csn-gene2656, were predicted to be putative chitosanases, with a very high (90.6%) amino acid identity. Sequence alignment analysis of the deduced Csn-gene1288 and Csn-gene2656 with those of other bacterial chitosanases revealed that they were separated into two different branches (Figure 6B). Further enzyme activity analysis with thin-layer chromatography (TLC) showed that

the hydrolysates of chitosan hydrolysed by both purified Csn-gene1288 and Csn-gene2656 were (GlcN)2, (GlcN)3, (GlcN)4, (GlcN)5 and (GlcN)6, with (GlcN) 3, (GlcN)4, and (GlcN)5 as the major products (Figure 6C). The catalytic properties of Csn-gene1288 and Csn-gene2656, with the optimal catalytic condition of pH5.4 at 50°C, were coincidentally similar to those of chitosanases from other *Bacillus* species (Figures 6D, E).

Discussion

Biocontrol microorganisms have been well commercialized as the source of microbial pesticides. They can either be directly used or processed into pesticides. The biocontrol activities of microorganisms were largely determined by the active metabolites and hydrolases they produced (Pal et al., 2000; Nguyen et al., 2017; Chen et al., 2018). During our screening
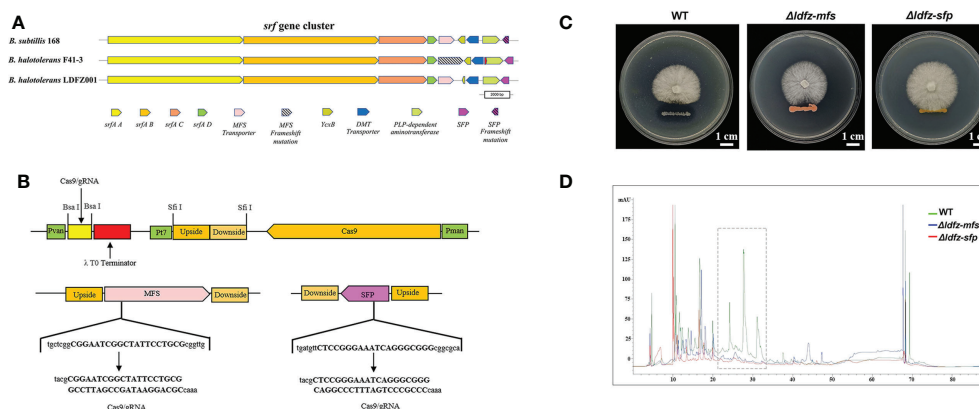
FIGURE 5
Functional analysis of SFP and MFS transporter genes. **(A)** Comparison of core genes in the srf gene clusters from *B halotolerans* LDFZ001, *B subtillis* 168 and *B halotolerans* F41-3. **(B)** A schematic map to show the gRNA sequence positions of *SFPe* and *MFS* genes. **(C)** Δ*ldfz-sfp* and Δ*ldfz-mfs* generated by respectively editing the *SFP* and *MFS* in *B halotolerans* LDFZ001 led to the loss of antifungal activity. **(D)** HPLC profile of lipopeptide extracts from WT and mutant Δ*ldfz-sfp* and Δ*ldfz-mf*.
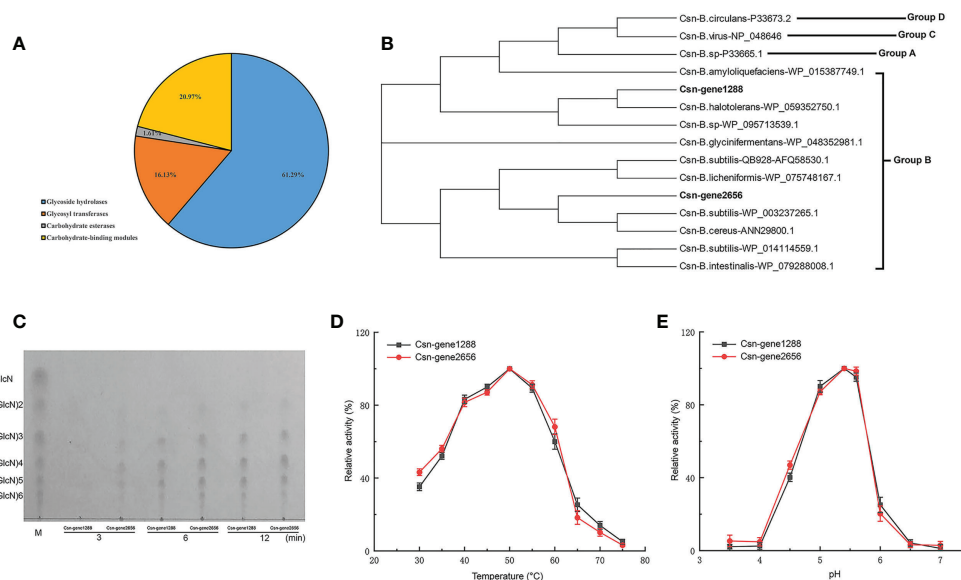
FIGURE 6
Carbohydrate-active enzyme activity analysis of the two chitosanase csn-gene1288 and csn-gene2656. **(A)** Statistical chart of annotated carbohydrate-active enzyme in *B halotolerans* LDFZ001. **(B)** Sequence alignment of csn-gene1288 and csn-gene2656 with that of other GH46 chitosanases. **(C)** Time course profiles of hydrolysis products of csn-gene1288 and csn-gene2656 enzymes on chitosan. **(D)** Effects of temperature on the enzyme activities of csn-gene1288 and csn-gene2656. **(E)** Effects of pH on the enzyme activities of csn-gene1288 and csn-gene2656.

of antifungal pathogen bacterial strains, a new clone, *B. halotolerans* LDFZ001, wich could effectively inhibit the growth of fungal pathogen *Rhizoctonia solani Kühn* sh-1, was isolate (Figures 1A, B). Phylogenetic and whole genome sequencing analyses implied that *B. halotolerans* LDFZ001 and *B. halotolerans* F41-3 fell into the same bacterial strain category (Figure 1C). Although the whole genomic sequence of *B. halotolerans* LDFZ001 was smaller than that of *B. halotolerans* F41-3, they shared as high as 97.98% amino acid sequence identity (Figure 3; Table 1).

To assess the antifungal pathogen activity of *B. halotolerans* LDFZ001, we subsequently performed antagonistic activity analysis. *B. halotolerans* LDFZ001 exhibited very strong suppression, whereas the control strain *B. subtillis* 168 and *B. halotolerans* F41-3 showed nearly no inhibition, against the sheath blight pathogen strain *R. solani Kühn* sh-1 (Figure 2A). Further genome sequence analysis revealed that *B. halotolerans* LDFZ001 genome contained ten gene clusters related to lipopeptide and hydrolase biosynthesis (Table 2). Numerous studies have showed that lipopeptides and hydrolases play crucial roles in antifungal protection. We observed that in contrast to other biocontrol strains, *B. halotolerans* LDFZ001 contained two novel terpene gene clusters, one novel Type III PKS, and a new kijanimicin biosynthesis cluster. The new gene cluster, involved in the biosynthesis of kijanimicin, only shared

4% amino acid similarity with other reported genome sequences in *Bacillus* species (Table 1). With its specific functional mechanism, kijanimicin has provided a vital view for antibiotics research (Castiglione et al., 2008; Crowther et al., 2013). The disclosure of gene cluster for putative kijanimicin biosynthesis in the *B. halotolerans* LDFZ001 genome will provide an important gene source for the future study.

In *Bacillus* species, surfactin is a strong biological surfactant essential for the formation of mycelium (Mukherjee et al., 2006; Shen et al., 2010). Although it does not directly inhibit the growth of plant pathogenic fungi, surfactin can effectively enhance the anti-fungal activity of other lipopeptides (Kobayashi et al., 2002; Kim et al., 2017b). To date, the biosynthetic mechanism of surfactin has been deeply investigated. The *srf* gene cluster has been reported to be *sfp*-dependent. During the domestication of *B. subtilis* 168, the mutation in *sfp* gene caused the loss of its ability to produce NRPs (Wu et al., 2019). Consistently, our genome sequence analysis revealed that *B. halotolerans* LDFZ001 contained complete *sfp* gene reading frame in its *srf* gene cluster, indicating that it had ability to produce surfactin to suppress the growth of pathogenic fungi (Figures 5A–C). MFS transporters also play a vital role in many substances transport in both eukaryotes and prokaryotes (Saier and Paulsen, 2001; Lorca et al., 2007; Chen et al., 2008; Yen et al., 2010). We

observed that, although *B. halotolerans* F41-3 has a complete s*fp* gene, a frame shift mutation was found in the open reading frame of the MFS transporter gene adjacent to *srfAD*. Therefore, the reduced antipathogen activity against *R. solani Kühn* sh-1 in *B. subtillis* 168 and *B. halotolerans* F41-3 could be due to the mutations in the *SFP* and *MFS* genes, as confirmed by the *SFP* and *MFS* gene-editing analysis with CRISPR-Cas9 system in *B. halotolerans* LDFZ001 (Figures 5A–C).

In prokaryotes, gene duplication only occurred among gene products in high demand, such as rRNA and histones, due to the limited sequence size (Zhang, 2003). However, to adapt the environmental changes, specific genes could be generated, giving a great contribution to the divergence of microbes (He and Zhang, 2005; Conant and Wolfe, 2008; Serres et al., 2009; Innan and Kondrashov, 2010). Although chitosanases were found to be widely distributed in both eukaryotes and prokaryotes, chitosanase gene duplication has rarely occurred (Hurst and Smith, 1998; Zhang, 2003). Two chitosanase genes in the genome of *B. halotolerans* LDFZ001 were observed, for the firstly time, in *Bacillus* species (Figures 6B–E). The presence of two redundant chitosanases implied that *B. halotolerans* LDFZ001 has adjusted itself to survival the variable conditions. The high enzyme activity ascribed to the duplication of chitosanase gene will also expand its utilization potential for biocontrol, chitosan production and environmental improvement of *B. halotolerans* LDFZ001.

Taken together, a new bacterial strain *B. halotolerans* LDFZ001 against sheath blight disease caused by *R. solani Kühn* sh-1 was isolated. The growth suppression ability of *B. halotolerans* LDFZ001 on *R. solani Kühn* sh-1 could be ascribed to the functional expression of *SFP* and *MFS* genes. Two redundant chitosanases, which implied the evolutionary adaption to the environment *via* gene duplication, were also verified in *B. halotolerans* LDFZ001. Our findings in this study will provide fundamental information for new candidate gene identification and bacterial strain commercialization in the future.

Data availability statement

The datasets presented in this study can be found in online repositories. The names of the repository/repositories and accession number(s) can be found below: https://www.ncbi.nlm.nih.gov/, NZ_CP063276.1.

Ethics statement

This article does not contain any studies with human participants or animals performed by any of the authors.

Author contributions

Funding

Conflict of interest

The authors declare that the research was conducted in the absence of any commercial or financial relationships that could be construed as a potential conflict of interest.

Publisher's note

All claims expressed in this article are solely those of the authors and do not necessarily represent those of their affiliated organizations, or those of the publisher, the editors and the reviewers. Any product that may be evaluated in this article, or claim that may be made by its manufacturer, is not guaranteed or endorsed by the publisher.

Supplementary material

The Supplementary Material for this article can be found online at: https://www.frontiersin.org/articles/10.3389/fpls.2022.1019512/full#supplementary-material

SUPPLEMENTARY FIGURE 1
A genome map of *B. halotolerans* LDFZ001.

SUPPLEMENTARY TABLE 1
Strains and plasmids used in this study.

SUPPLEMENTARY TABLE 2
Oligonucleotides used in this study.

References

Abbas, A., Khan, S. U., Khan, W. U., Saleh, T. A., Khan, M. H. U., Ullah, S., et al. (2019). Antagonist effects of strains of bacillus spp. against rhizoctonia solani for their protection against several plant diseases: Alternatives to chemical pesticides. *C R Biol.* 342, 124–135. doi: 10.1016/j.crvi.2019.05.002

Altenbuchner, J. (2016). Editing of the *Bacillus subtilis* genome by the CRISPR-Cas9 system. *Appl. Environ. Microbiol.* 82, 5421–5427. doi: 10.1128/AEM.01453-16

Anagnostopoulos, C., and Spizizen, J. (1961). Requirements for transformation in *Bacillus subtilis. J. Bacteriol.* 81, 741–746. doi: 10.1128/jb.81.5.741-746.1961

Bóka, B., Manczinger, L., Kocsubé, S., Shine, K., Alharbi, N. S., Khaled, J. M., et al. (2019). Genome analysis of a *Bacillus subtilis* strain reveals genetic mutations determining biocontrol properties. *World J. Microbiol. Biotechnol.* 35, 52. doi: 10.1007/s11274-019-2625-x

Castiglione, F., Lazzarini, A., Carrano, L., Corti, E., Ciciliato, I., Gastaldo, L., et al. (2008). Determining the structure and mode of action of microbisporicin a potent lantibiotic active against multiresistant pathogens. *Chem. Biol.* 15, 22–31. doi: 10.1016/j.chembiol.2007.11.009

Chen, L., Heng, J., Qin, S., and Bian, K. (2018). A comprehensive understanding of the biocontrol potential of *Bacillus velezensis* LM2303 against fusarium head blight. *PLoS One* 13, e0198560. doi: 10.1371/journal.pone.0198560

Chen, X. H., Koumoutsi, A., Scholz, R., and Borriss, R. (2009a). More than anticipated-production of antibiotics and other secondary metabolites by *Bacillus amyloliquefaciens* FZB42. *J. Mol. Microbiol. Biotechnol.* 16, 14–24. doi: 10.1159/000142891

Chen, X. H., Koumoutsi, A., Scholz, R., Schneider, K., Vater, J., Süssmuth, R., et al. (2009b). Genome analysis of *Bacillus amyloliquefaciens* FZB42 reveals its potential for biocontrol of plant pathogens. *J. Biotechnol.* 140, 27–37. doi: 10.1016/j.jbiotec.2008.10.011

Chen, D. E., Podell, S., Sauer, J. D., Swanson, M. S., and Saier, M. H. (2008). The phagosomal nutrient transporter (Pht) family. *Microbiol. (Reading)* 154, 42–53. doi: 10.1099/mic.0.2007/010611-0

Chen, L., Wu, Y. D., Chong, X. Y., Xin, Q. H., Wang, D. X., and Bian, K. (2019). Seed-borne endophytic *Bacillus velezensis* LHSB1 mediate the biocontrol of peanut stedm rot caused by scleotium rolfsii. *J. Appl. Microbiol.* 128, 803–813. doi: 10.1111/jam.14508

Conant, G. C., and Wolfe, K. H. (2008). Turning a hobby into a job: how duplicated genes find new functions. *Nat. Rev. Genet.* 9, 938–950. doi: 10.1038/nrg2482

Crowther, G. S., Baines, S. D., Todhunter, S. L., Freeman, J., Chilton, C. H., and Wilcox, M. H. (2013). Evaluation of NVB302 versus vancomycin activity in an *in vitro* human gut model of *Clostridium difficile* infection. *J. Antimicrob. Chemother.* 68, 168–176. doi: 10.1093/jac/dks359

de Araújo, N. K., Pimentel, V. C., da Silva, N. M.P., de Araújo Padilha, C. E., de Macedo, G. R., and Dos Santos, E. S. (2016). Recovery and purification of chitosanase produced by Bacillus cereus using expanded bed adsorption and central composite design. *J. Sep.* 39, 709–716. doi: 10.1002/jssc.201500900a

Duitman, E. H., Hamoen, L. W., Rembold, M., Venema, G., Seitz, H., Saenger, W., et al. (1999). The mycosubtilin synthetase of *Bacillus subtilis* ATCC6633: a multifunctional hybrid between a peptide synthetase, an amino transferase, and a fatty acid synthase. *Proc. Natl. Acad. Sci. U S A.* 96, 13294–13299. doi: 10.1073/pnas.96.23.13294

Gao, W., Liu, F., Zhang, W., Quan, Y., Dang, Y., Feng, J., et al. (2017). Mutations in genes encoding antibiotic substances increase the synthesis of poly-γ-glutamic acid in *Bacillus amyloliquefaciens* LL3. *MicrobiologyOpen* 6, e00398. doi: 10.1002/mbo3.398

Ge, J., Li, W., Zhao, Q., Li, N., Chen, M., Zhi, P., et al. (2015). Architecture of the mammalian mechanosensitive Piezo1 channel. *Nature* 527, 64–69. doi: 10.1038/nature15247

Ghosh, S., Kanwar, P., and Jha, G. (2017). Alterations in rice chloroplast integrity, photosynthesis and metabolome associated with pathogenesis of rhizoctonia solani. *Sci. Rep.* 7, 41610. doi: 10.1038/srep41610

Guo, S., Li, X., He, P., Ho, H., Wu, Y., and He, Y. (2015). Whole-genome sequencing of *Bacillus subtilis* XF-1 reveals mechanisms for biological control and multiple beneficial properties in plants. *J. Ind. Microbiol. Biotechnol.* 42, 925–937. doi: 10.1007/s10295-015-1612-y

Guo, S., Mao, Z., Wu, Y., Hao, K., He, P., and He, Y. (2013). Genome sequencing of *Bacillus subtilis* strain XF-1 with high efficiency in the suppression of plasmodiophora brassicae. *Genome Announc.* 1, e0006613. doi: 10.1128/genomeA.00066-13

Han, V. C., Yu, N. H., Yoon, H., Ahn, N. H., Son, Y. K., Lee, B. H., et al. (2022). Identification, characterization, and efficacy evaluation of *Bacillus velezensis* for shot-hole disease biocontrol in flowering cherry. *Plant Pathol. J.* 38, 115–130. doi: 10.5423/PPJ.OA.01.2022.0004

He, P., Hao, K., Blom, J., Rückert, C., Vater, J., Mao, Z., et al. (2013). Genome sequence of the plant growth promoting strain *Bacillus amyloliquefaciens* subsp. plantarum B9601-Y2 and expression of mersacidin and other secondary metabolites. *J. Biotechnol.* 164, 281–291. doi: 10.1016/j.jbiotec.2012.12.014

He, X., and Zhang, J. (2005). Gene complexity and gene duplicability. *Curr. Biol.* 15, 1016–1021. doi: 10.1016/j.cub.2005.04.035

Hurst, L. D., and Smith, N. G. C. (1998). The evolution of concerted evolution. *Proc. R Soc. Lond Ser. B.* 265, 121–127. doi: 10.1098/rspb.1998.0272

Innan, H., and Kondrashov, F. (2010). The evolution of gene duplications: classifying and distinguishing between models. *Nat. Rev. Genet.* 11, 97–108. doi: 10.1038/nrg2689

Jadeja, N. B., Moharir, P., and Kapley, A. (2019). Genome sequencing and analysis of strains bacillus sp. AKBS9 and *Acinetobacter* sp. AKBS16 for biosurfactant production and bioremediation. *Appl. Biochem. Biotechnol.* 187, 518–530. doi: 10.1007/s12010-018-2828-x

Jin, Q., Jiang, Q., Zhao, L., Su, C., Li, S., Si, F., et al. (2017). Complete genome sequence of Bacillus velezensis S3-1, a potential biological pesticide with plant pathogen inhibiting and plant promoting capabilities. *J. Biotechnol.* 259, 199–203. doi: 10.1016/j.jbiotec.2017.07.011

Johnsen, M. D., Hansen, O. C., and Stougaard, P. (2010). Isolation, characterization and heterologous expression of a novel chitosanase from janthinobacterium sp. strain 4239. *Microb. Cell Fact* 9, 5. doi: 10.1186/1475-2859-9-5

Kang, L. X., Chen, X. M., Fu, L., and Ma, L. X. (2012). Recombinant expression of chitosanase from *Bacillus subtilis* HD145 in pichia pastoris. *Carbohydr. Res.* 352, 37–43. doi: 10.1016/j.carres.2012.01.025

Kim, K., Lee, Y., Ha, A., Kim, J. I., Park, A. R., Yu, N. H., et al. (2017a). Chemosensitization of fusarium graminearum to chemical fungicides using cyclic lipopeptides produced by *Bacillus amyloliquefaciens* strain JCK-12. *Front. Plant Sci.* 8, 2010. doi: 10.3389/fpls.2017.02010

Kim, Y. T., Park, B. K., Kim, S. E., Lee, W. J., Moon, J. S., Cho, M. S., et al. (2017b). Organization and characterization of genetic regions in *Bacillus subtilis* subsp. krictiensis ATCC55079 associated with the biosynthesis of iturin and surfactin compounds. *PLoS One* 12, e0188179. doi: 10.1371/journal.pone.0188179

Kobayashi, D., Kondo, K., Uehara, N., Otokozawa, S., Tsuji, N., Yagihashi, A., et al. (2002). Endogenous reactive oxygen species is an important mediator of miconazole antifungal effect. *Antimicrob. Agents Chemother.* 46, 3113–3117. doi: 10.1128/aac.46.10.3113-3117.2002

Kumar, S., Stecher, G., Li, M., Knyaz, C., and Tamura, K. (2018). MEGA X: molecular evolutionary genetics analysis across computing platforms. *Mol. Biol. Evol.* 35, 1547–1549. doi: 10.1093/molbev/msy096

Kunst, F., Ogasawara, N., Moszer, I., Albertini, A. M., Alloni, G., Azevedo, V., et al. (1997). The complete genome sequence of the gram-positive bacterium bacillus subtilis. *Nature* 390, 249–256. doi: 10.1038/36786

Kurakake, M., Yo-u, S., Nakagawa, K., Sugihara, M., and Komaki, T. (2000). Properties of chitosanase from bacillus cereus S1. *Curr. Microbiol.* 40, 6–9. doi: 10.1007/s002849910002

Liang, T. W., Chen, Y. Y., Pan, P. S., and Wang, S. L. (2014). Purification of chitinase/chitosanase from *Bacillus cereus* and discovery of an enzyme inhibitor. *Int. J. Biol. Macromol.* 63, 8–14. doi: 10.1016/j.ijbiomac.2013.10.027

Li, Y., Guo, Q., Wei, X., Xue, Q., and Lai, H. (2019). Biocontrol effects of penicillium griseofulvum against monkshood (Aconitum carmichaelii debx.) root diseases caused by sclerotium rolfsiii and fusarium spp. *J. Appl. Microbiol.* 127, 1532–1545. doi: 10.1111/jam.14382.l

Li, X., Munir, S., Xu, Y., Wang, Y., and He, Y. (2021). Combined mass spectrometry-guided genome mining and virtual screening for acaricidal activity in secondary metabolites of *Bacillus velezensis* W1. *RSC Adv.* 11, 25441–25449. doi: 10.1039/d1ra01326b

Li, X., Zhang, Y., Wei, Z., Guan, Z., Cai, Y., and Liao, X. (2016). Antifungal activity of isolated *Bacillus amyloliquefaciens* SYBC H47 for the biocontrol of peach gummosis. *PLoS One* 11, e0162125. doi: 10.1371/journal.pone.0162125

Lorca, G. L., Barabote, R. D., Zlotopolski, V., Tran, C., Winnen, B., Hvorup, R. N., et al. (2007). Transport capabilities of eleven gram-positive bacteria: comparative genomic analyses. *Biochim. Biophys. Acta* 1768, 1342–1366. doi: 10.1016/j.bbamem.2007.02.007

Luo, C., Liu, X., Zhou, X., Guo, J., Truong, J., Wang, X., et al. (2015b). Unusual biosynthesis and structure of locillomycins from Bacillus subtilis 916. *Appl. Environ. Microbiol.* 81, 6601–6609. doi: 10.1128/AEM.01639-15

Luo, C., Liu, X., Zhou, H., Wang, X., and Chen, Z. (2015a). Nonribosomal peptide synthase gene clusters for lipopeptide biosynthesis in *Bacillus subtilis* 916 and their phenotypic functions. *Appl. Environ. Microbiol.* 81, 422–431. doi: 10.1128/AEM.02921-14

Lu, J. Y., Zhou, K., Huang, W. T., Zhou, P., Yang, S., Zhao, X., et al. (2019). A comprehensive genomic and growth proteomic analysis of antitumor lipopeptide bacillomycin Ib biosynthesis in *Bacillus amyloliquefaciens* X030. *Appl. Microbiol. Biotechnol.* 103, 7647–7662. doi: 10.1007/s00253-019-10019-6

Madej, M. G., and Kaback, H. R. (2013). Evolutionary mix-and-match with MFS transporters II. *Proc. Natl. Acad. Sci. U.S.A.* 110, E4831–E4838. doi: 10.1073/pnas.1319754110

Manel, N., Battini, J. L., Taylor, N., and Sitbon, M. (2005). HTLV-1 tropism and envelope receptor. *Oncogene* 24, 6016–6025. doi: 10.1038/sj.onc.1208972

Marger, M. D., and Saier, M. H.Jr. (1993). A major superfamily of transmembrane facilitators that catalyse uniport, symport and antiport. *Trends Biochem. Sci.* 18, 13–20. doi: 10.1016/0968-0004(93)90081-w

Mobegi, F. M., Zomer, A., de Jonge, M. I., and van Hijum, S. A. F. T. (2017). Advances and perspectives in computational prediction of microbial gene essentiality. *Brief Funct. Genomics* 16, 70–79. doi: 10.1093/bfgp/elv063

Mukherjee, S., Das, P., and Sen, R. (2006). Towards commercial production of microbial surfactants. *Trends Biotechnol.* 24, 509–515. doi: 10.1016/j.tibtech.2006.09.005

Nair, D., Vanuopadath, M., Nair, B. G., Pai, J. G., and Nair, S. S. (2016). Identification and characterization of a library of surfactins and fengycins from a marine endophytic bacillus sp. *J. Basic Microbiol.* 56 (11), 1159–1172. doi: 10.1002/jobm.201600029

Nakano, M. M., Magnuson, R., Myers, A., Curry, J., Grossman, A. D., and Zuber, P. (1991). srfA is an operon required for surfactin production, competence development, and efficient sporulation in *Bacillus subtilis*. *J. Bacteriol.* 173 (5), 1770–1778. doi: 10.1128/jb.173.5.1770-1778.1991

Nguyen, P. A., Strub, C., Fontana, A., and Schorr-Galindo, S. (2017). Crop molds and mycotoxins: alternative management using biocontrol. *Biol. Control* 104, 10–27. doi: 10.1016/j.biocontrol.2016.10.004

Omumasaba, C. A., Yoshida, N., Sekiguchi, Y., Kariya, K., and Ogawa, K. (2000). Purification and some properties of a novel chitosanase from *Bacillus subtilis* KH1. *J. Gen. Appl. Microbiol.* 46 (1), 19–27. doi: 10.2323/jgam.46.19

Ongena, M., and Jacques, P. (2008). *Bacillus* lipopeptides: versatile weapons for plant disease biocontrol. *Trends Microbiol.* 16 (3), 115–125. doi: 10.1016/j.tim.2007.12.009

Pal, K. K., Tilak, K. V., Saxena, A. K., Dey, R., and Singh, C. S. (2000). Antifungal characteristics of a fluorescent *Pseudomonas* strain involved in the biological control of *Rhizoctonia solani*. *Microbiol. Res.* 155 (3), 233–242. doi: 10.1016/S0944-5013(00)80038-5

Park, J. K., Shimono, K., Ochiai, N., Shigeru, K., Kurita, M., Ohta, Y., et al. (1999). Purification, characterization, and gene analysis of a chitosanase (ChoA) from matsuebacter chitosanotabidus 3001. *J. Bacteriol.* 181 (21), 6642–6649. doi: 10.1128/JB.181.21.6642-6649.1999

Pereira, J. Q., Ritter, A. C., Cibulski, S., and Brandelli, A. (2019). Functional genome annotation depicts probiotic properties of *Bacillus velezensis* FTC01. *Gene* 713, 143971. doi: 10.1016/j.gene.2019.143971

Reuter, K., Mofid, M. R., Marahiel, M. A., and Ficner, R. (1999). Crystal structure of the surfactin synthetase-activating enzyme sfp: a prototype of the 4'-phosphopantetheinyl transferase superfamily. *EMBO J.* 18 (23), 6823–6831. doi: 10.1093/emboj/18.23.6823

Roongsawang, N., Thaniyavarn, J., Thaniyavarn, S., Kameyama, T., Haruki, M., Imanaka, T., et al. (2002). Isolation and characterization of a halotolerant bacillus subtilis BBK-1 which produces three kinds of lipopeptides: bacillomycin l, plipastatin, and surfactin. *Extremophiles* 6, 499–506. doi: 10.1007/s00792-002-0287-2

Sabaté, D. C., and Audisio, M. C. (2013). Inhibitory activity of surfactin, produced by different *Bacillus subtilis* subsp. subtilis strains, against listeria monocytogenes sensitive and bacteriocin-resistant strains. *Microbiol. Res.* 168 (3), 125–129. doi: 10.1016/j.micres.2012.11.004

Saggese, A., Culurciello, R., Casillo, A., Corsaro, M. M., Ricca, E., and Baccigalupi, L. (2018). A marine isolate of *Bacillus pumilus* secretes a pumilacidin active against staphylococcus aureus. *Mar. Drugs* 16 (6), 180. doi: 10.3390/md16060180

Saier, M. H., Beatty, J. T., Goffeau, A., Harley, K. T., Heijne, W. H., Huang, S. C., et al. (1999). The major facilitator superfamily. *J. Mol. Microbiol. Biotechnol.* 1 (2), 257–279.

Saier, M. H.Jr., and Paulsen, I. T. (2001). Phylogeny of multidrug transporters. *Semin. Cell Dev. Biol.* 12 (3), 205–213. doi: 10.1006/scdb.2000.0246

Saier, M. H., Reddy, V. S., Moreno-Hagelsieb, G., Hendargo, K. J., Zhang, Y., Iddamsetty, V., et al. (2021). The transporter classification database (TCDB): 2021 update. *Nucleic Acids Res.* 49 (D1), D461–D467. doi: 10.1093/nar/gkaa1004

Serres, M. H., Kerr, A. R., McCormack, T. J., and Riley, M. (2009). Evolution by leaps: gene duplication in bacteria. *Biol. Direct* 4, 46. doi: 10.1186/1745-6150-4-46

Shaligram, S., Kumbhare, S. V., Dhotre, D. P., Muddeshwar, M. G., Kapley, A., Joseph, N., et al. (2016). Genomic and functional features of the biosurfactant producing bacillus sp. AM13. *Funct. Integr. Genomics* 16 (5), 557–566. doi: 10.1007/s10142-016-0506-z

Shen, H. H., Thomas, R. K., Penfold, J., and Fragneto, G. (2010). Destruction and solubilization of supported phospholipid bilayers on silica by the biosurfactant surfactin. *Langmuir* 26, 7334–7342. doi: 10.1021/la904212x

Srivastava, S., Bist, V., Srivastava, S., Singh, P. C., Trivedi, P. K., Asif, M. H., et al. (2016). Unraveling aspects of bacillus amyloliquefaciens mediated enhanced production of rice under biotic stress of rhizoctonia solani. *Front. Plant Sci.* 7. doi: 10.3389/fpls.2016.00587

Stein, T. (2005). *Bacillus subtilis* antibiotics: structures, syntheses and specific functions. *Mol. Microbiol.* 56 (4), 845–857. doi: 10.1111/j.1365-2958.2005.04587.x

Tareq, F. S., Kim, J. H., Lee, M. A., Lee, H. S., Lee, Y. J., Lee, J., et al. (2012). Ieodoglucomides a and b from a marine-derived bacterium. *Bacillus licheniformis*. *Org. Lett.* 14 (6), 1464–1467. doi: 10.1021/ol300202z

Tareq, F. S., Lee, M. A., Lee, H. S., Lee, Y. J., Lee, J. S., Hasan, C. M., et al. (2014). Noncytotoxic antimicrobial linear lipopeptides from a marine bacterium. *Bacillus subtilis*. *Org. Lett.* 16 (3), 928–931. doi: 10.1021/ol403657r

Torres, M. J., Petroselli, G., Daz, M., Erra-Balsells, R., and Audisio, M. C. (2015). Bacillus subtilis subsp. subtilis CBMDC3f with antimicrobial activity against gram-positive foodborne pathogenic bacteria: UV-MALDI-TOF MS analysis of its bioactive compounds. *World J. Microbiol. Biotechnol.* 31 (6), 929–940. doi: 10.1007/s11274-015-1847-9

Tosato, V., Albertini, A. M., Zotti, M., Sonda, S., and Bruschi, C. V. (1997). Sequence completion, identification and definition of the fengycin operon in bacillus subtilis 168. *Microbiol. (Reading)* 143 (Pt11), 3443–3450. doi: 10.1099/00221287-143-11-3443

Tsuge, K., Akiyama, T., and Shoda, M. (2001). Cloning, sequencing, and characterization of the iturin a operon. *J. Bacteriol.* 183 (21), 6265–6273. doi: 10.1128/JB.183.21.6265-6273.2001

Wang, S. L., Chen, S. J., and Wang, C. L. (2008). Purification and characterization of chitinases and chitosanases from a new species strain pseudomonas sp. TKU015 using shrimp shells as a substrate. *Carbohydr. Res.* 343 (7), 1171–1179. doi: 10.1016/j.carres.2008.03.018

Wang, S. C., Davejan, P., Hendargo, K. J., Javadi-Razaz, I., Chou, A., Yee, D. C., et al. (2020). Expansion of the major facilitator superfamily (MFS) to include novel transporters as well as transmembrane-acting enzymes. *Biochim. Biophys. Acta Biomembr.* 1862 (9), 183277. doi: 10.1016/j.bbamem.2020.183277

Wu, Q., Zhi, Y., and Xu, Y. (2019). Systematically engineering the biosynthesis of a green biosurfactant surfactin by bacillus subtilis 168. *Metab. Eng.* 52, 87–97. doi: 10.1016/j.ymben.2018.11.004

Yen, M. R., Chen, J. S., Marquez, J. L., Sun, E. I., and Saier, M. H. (2010). Multidrug resistance: phylogenetic characterization of superfamilies of secondary carriers that include drug exporters. *Methods Mol. Biol.* 637, 47–64. doi: 10.1007/978-1-60761-700-6_3

Yoon, H. G., Lee, K. H., Kim, H. Y., Kim, H. K., Shin, D. H., Hong, B. S., et al. (2002). Gene cloning and biochemical analysis of thermostable chitosanase (TCH-2) from *Bacillus coagulans* CK108. *Biosci. Biotechnol. Biochem.* 66 (5), 986–995. doi: 10.1271/bbb.66.986

Zhang, J. (2003). Evolution by gene duplication: an update. *Trends Ecol. Evol.* 18 (6), 292–298. doi: 10.1016/S0169-5347(03)00033-8

Zhao, J., Xiong, G., Wang, Z., Mao, Z., Wu, Y., and He, Y. (2011). Expression of chitosanase gene of *Bacillus subtilis* XF-1 in *Escherichia coli* and the chitosanase antagonism against the fungal pathogens. *Chinese. J. Biol. Control.* 27, 504–509.

Multi-stage resistance to *Zymoseptoria tritici* revealed by GWAS in an Australian bread wheat diversity panel

Nannan Yang[1], Ben Ovenden[1], Brad Baxter[1],
Megan C. McDonald[2], Peter S. Solomon[3]
and Andrew Milgate[1]*

[1]NSW Department of Primary Industries, Wagga Wagga Agricultural Institute, Wagga Wagga,
NSW, Australia, [2]University of Birmingham, School of Biosciences, Birmingham, West
Midlands, United Kingdom, [3]Division of Plant Sciences, Research School of Biology, The Australian
National University, Canberra, ACT, Australia

Septoria tritici blotch (STB) has been ranked the third most important wheat disease in the world, threatening a large area of wheat production. Although major genes play an important role in the protection against *Zymoseptoria tritici* infection, the lifespan of their resistance unfortunately is very short in modern wheat production systems. Combinations of quantitative resistance with minor effects, therefore, are believed to have prolonged and more durable resistance to *Z. tritici*. In this study, new quantitative trait loci (QTLs) were identified that are responsible for seedling-stage resistance and adult-plant stage resistance (APR). More importantly was the characterisation of a previously unidentified QTL that can provide resistance during different stages of plant growth or multi-stage resistance (MSR). At the seedling stage, we discovered a new isolate-specific QTL, QSt.wai.1A.1. At the adult-plant stage, the new QTL QStb.wai.6A.2 provided stable and consistent APR in multiple sites and years, while the QTL QStb.wai.7A.2 was highlighted to have MSR. The stacking of multiple favourable MSR alleles was found to improve resistance to *Z. tritici* by up to 40%.

KEYWORDS

Zymoseptoria tritici, bread wheat, genome-wide association studies (GWAS), adult plant resistance, multi-stage resistance (MSR), QTL

Introduction

Zymoseptoria tritici (*Mycosphaerella graminicola* (Fuckel) J. Schrot, anamorph *Septoria tritici*, synonym) (Quaedvlieg et al., 2011), severely threatens wheat production in Australia, Europe, and North America. STB disease has been documented as the third most important disease threatening wheat production with an average of 2.44% yield losses

per year (Savary et al., 2019). Thirty to fifty percent yield loss is possible in regions that experience high humidity and mild temperatures during the growing season (Eyal, 1987). The use of fungicides to control the spread of *Z. tritici* is becoming more challenging, due to the increasing levels of resistance to azole fungicides (Milgate, 2014; McDonald et al., 2019) and recently strobilurin resistance (pers. comm F. Lopez-Ruiz) observed in South Australia. Resistance to multiple fungicide chemicals occur in Europe and the US, including azole, strobilurin (Hagerty et al., 2017) and succinate dehydrogenase inhibitors (SDHI) (Dooley et al., 2016; Blake et al., 2018). To reduce the instance of fungicide resistance, fungicides need to be used as a part of an integrated disease management (IDM) system. An important component of effective IDM is the requirement for a robust level of host resistance to *Z. tritici* in cultivated wheat varieties.

Major resistance (*R*) genes are important sources of resistance that wheat breeders can use to protect against *Z. tritici*. To date, twenty-four *Z. tritici* major resistance genes have been reported with tightly linked molecular markers, including 12 isolate-specific genes and 12 non-isolate specific genes from wheat (Aouini, 2018; Tabib Ghaffary et al., 2018; Yang et al., 2018; Langlands-Perry et al., 2022). However, this fungus has a plastic number of chromosomes, sexual and asexual reproduction systems, and the ability of long-distance migration, which increases the threat of the host resistance being overcome (Rudd, 2015; McDonald and Mundt, 2016). For instance, the major seedling resistance genes *Stb4* (Adhikari et al., 2004), *Stb6* (Brading et al., 2002), *Stb2/11/WW* (Raman et al., 2009; Liu et al., 2013; Dreisigacker et al., 2015), and *Stb18* (Tabib Ghaffary et al., 2011) have been overcome in Australia (pers. comm A. Milgate). Thus, new sources of resistance are urgently required by breeders.

Quantitative resistance can be combined with qualitative genes to improve resistance against *Z. tritici* infections. Different types of quantitative resistance have been identified in 89 genomic regions in wheat, of which, 27 were detected at the seedling stage, and 48 at the adult stage (Goudemand et al., 2013; Brown et al., 2015). New quantitative trait loci (QTLs) at the adult-plant stage have also been detected from ten GWAS studies (Arraiano and Brown, 2017; Kidane et al., 2017; Vagndorf et al., 2017; Würschum et al., 2017; Muqaddasi et al., 2019; Yates et al., 2019; Riaz et al., 2020; Alemu et al., 2021; Louriki et al., 2021; Mahboubi et al., 2022). These include notable loci such as QStb.NS-2A associated with APR (Vagndorf et al., 2017), qtl-3 on the control of necrosis lesions (Yates et al., 2019), and QStb.teagasc-4A.1 associated with the STB resistance of flag leaves and flag-1 leaves (Riaz et al., 2020). However, there is a paucity of reports demonstrating the deployment of quantitative genes for *Z. tritici* resistance that can provide stable protection over a long period of time. On the other hand, STB levels can also be reduced by traits such as taller plant height and late heading date or flowering time that contribute to disease escape, which limits the spread of fungal

inoculum within crops (Tavella, 1978; Simón et al., 2004; Arraiano et al., 2009; Brown, 2015), although these traits may be unfavourable in breeding.

Patterns of host resistance differ markedly between *Z. tritici* and other pathogens in wheat. The major seedling resistance genes of wheat against rust pathogens (*Puccinia* spp.) have been described as all-stage resistance or race-specific resistance (Chen, 2005). These major genes provide near immunity at the seedling stage and continue to give high levels of protection at later plant growth stages (Wellings et al., 2012; Ellis et al., 2014). However, for *Z. tritici*, the translation of seedling isolate-specific resistance providing very high protection against infection at the adult plant stage, is seldom observed. In addition, equivalent loci to the rust APR genes have yet to be definitively identified for *Z. tritici*. These genes are typically not effective at the seedling stage, such as *Lr34* (Krattinger et al., 2009) and *Lr67* (Moore et al., 2015), but do provide durable non-specific resistance at the adult-plant stage. Therefore, the search for and combining of different seedling-resistance and APR genes, has long been postulated as a sustainable way of prolonging the durability of disease resistance against *Z. tritici* (Brown, 2015; Niks et al., 2015; Rimbaud et al., 2021). Here we introduce the term "multi-stage resistance" (MSR) to describe those QTLs which are effective at more than one plant growth stage. These are defined as QTLs that reduce disease and or components of disease during both seedling and adult-plant growth stages. QTLs with MSR, which continue providing the resistance from early to later stages of the plant growth will be very desirable breeding targets. In this study, a collection of 273 bread wheat cultivars that represented both the gene pool of recent Australian cultivars and international sources of resistance were applied in a marker and trait genome-wide association analysis.

Materials and methods

Plant materials

Two hundred and seventy-three accessions were selected for inclusion into the AusSTB diversity panel. The panel is comprised of 163 cultivars and breeding lines from breeding programs across Australia, and a selection of *Z. tritici* resistance sources from around the world, that are relevant to Australian *Z. tritici* resistance breeding. These include 13 synthetic hexaploid lines, 59 accessions from CIMMYT, 12 from North America, 10 from Europe, five from the Middle East, three each from New Zealand and Mexico, two each from Brazil and China and one from Russia. (Supplementary Table 1). Accessions were sourced from the Australian Grains Genebank, Horsham Victoria Australia, and accession numbers are also provided in Supplementary Table 1. Accessions were subjected to two generations of single seed descent to decrease genetic heterozygosity prior to phenotyping and DNA extraction.

Experimental design

The package DiGGer (Coombes, 2002) in R (R Core Team, 2020) was used to create randomized complete block (spatial) designs for all experiments in the study. For the glasshouse experiments, the 273 AusSTB lines and six control cultivars 'M1696' (resistant, R) 'Teal' (R), 'Milan' (moderately resistant/moderately susceptible, MR/MS), 'Millewa' (MR/MS), 'Egret' (susceptible, S), and 'Summit'(S) were replicated three times in a 30 row by 30 column array in each experiment. For the field experiments, the 273 AusSTB lines were replicated three times and the balance of entries in each experiment were made up of the susceptible control cultivar 'WW425'. The spatial designs for field experiments were 28 row by 30 column arrays at Wagga Wagga New South Wales (NSW) and 12 rows by 69 columns arrays in Hamilton Victoria (VIC).

Glasshouse screening for *Z. tritici* resistance

Three Australian *Z. tritici* isolates were used in this study. WAI332 was collected from NSW in 1979, WAI251 from VIC in 2012 and WAI161 from Tasmania (TAS) in 2011. Inoculation procedure for the isolates and experimental details for phenotyping *Z. tritici* glasshouse infections are described in Yang et al. (2018). Each isolate was screened on all 273 cultivars in six independent glasshouse screening experiments.

Symptoms of *Z. tritici* were assessed between 21 and 28 days after inoculation. A seedling infection score (STB_S) was scored based on the visually estimated percentage of necrotic lesions containing pycnidia on the infected leaves, according to the methods by Zwart et al. (2010). During the assessment, the percentage of leaf area with necrosis (Nec, 0-100%) on the infected leaf and pycnidia density on the necrotic leaf area (Pyc, 0-100%) were also recorded.

Field experiments

The AusSTB panel was evaluated in four different environments (two locations × two years). Field experiments were conducted at Wagga Wagga Agricultural Institute at Wagga Wagga, NSW, Australia (WGA, -35.04419222, 147.3167896) in 2015 and 2016, and the Department of Economic Development, Jobs, Transport and Resources Hamilton Centre at Hamilton, Victoria, Australia (HLT, -37.828768, 142.082319) in 2015 and 2016. For the field experiments at Wagga Wagga, natural infection of *Z. tritici* was supplemented with an inoculation of stubble debris from wheat with high levels of *Z. tritici* infection. Field experiments at Hamilton relied on natural infections.

Disease severity in the field experiments was visually scored according to Saari and Prescott's severity scale for assessing wheat foliar diseases (Saari and Prescott, 1975). Namely, STB_A

(1-9) was used to record the observations. STB_A (1-9) is used to record *Z. tritici* disease intensity considering the plant growth stage, while STB (1-00%) is used to reflect the disease severity by recording the proportion of plant units with diseased leaves. Two phenotypic scores were collected at Wagga Wagga in 2015, approximately four weeks apart in mid-September (Cycle 1, C1) and mid-October (Cycle 2, C2). One score collected at all other field experiments in mid-October. Additionally, relative maturity was scored using the Zadoks growth scale (Zadoks et al., 1974) at the same time as disease scores were collected. Plant height (HT) measurements of each entry was collected in 2016 and 2017 in December at physiological maturity.

DNA extraction and genotyping

Leaf tissue was harvested from 14-day old seedlings and used for DNA extraction. DNA extraction and genotyping service were conducted by DArT Pty Ltd, Canberra, ACT. Genetic positions of all the markers were assigned according to the custom Chinese Spring Consensus Wheat map v4.0 provided by DArT (pers. comm Dr Andrzej Kilian).

The 273 DNA samples from each line in the population were assayed with two technical replications to derive reproducibility scores. At the first-stage quality control, the reproducibility rate was 0.95 for SNPs and 0.99 for silicoDArTs, and the call rate was 0.85 for SNPs and 0.95 for silicoDArTs. Details of the experimental procedure for generating silicoDArTs are described by Courtois et al. (2013) and Li et al. (2015). At the second stage of quality control, duplicated markers, markers with a Minor Allele Frequency (MAF)< 0.05, and markers not assigned to the chromosome map were excluded. The final marker sets for the association study comprised of 11,200 SNPs and 29,346 silicoDArTs (Table 1).

Linkage disequilibrium and population structure analysis

The R package LDheatmap (Shin et al., 2006), was used to obtain the linkage disequilibrium (LD) squared allelic correlation (r^2) estimates for all pairwise comparisons between markers on each chromosome for each marker set separately. To quantify the pattern of LD decay, syntenic pairwise LD r^2 estimates were plotted against the corresponding pairwise genetic distances for each of the A, B and D genomes and for the overall wheat genome. A second degree locally weighted polynomial regression (LOESS) curve was fitted to each scatter plot (Cleveland and Devlin, 1988) following the approach of Maccaferri et al. (2015). The intersection of the LOESS curve and an r^2 threshold of 0.20 for marker pairs was taken as an estimate of the extent of LD decay within each genome for each marker set and was used to define the confidence intervals of QTL detected in this study (Supplementary Figure 3).

TABLE 1 Summary of the average of Polymorphism Information Content (PIC), the average of Minor Allele Frequency (MAF), and the number of SNP and silicoDArT markers on each chromosome.

Chr	Genetic Length (cM)	SNP			silicoDArT		
		Avg. PIC	Avg. MAF	No. of markers	Avg. PIC	Avg. MAF	No. of markers
1A	255.6	0.28	0.26	617	0.31	0.26	1,113
2A	138.6	0.24	0.25	752	0.3	0.26	1,836
3A	154.2	0.26	0.25	674	0.31	0.26	1,208
4A	135.2	0.25	0.25	540	0.31	0.27	1,612
5A	160	0.26	0.26	568	0.31	0.28	847
6A	105	0.22	0.29	526	0.26	0.26	1,344
7A	160.2	0.23	0.25	658	0.3	0.27	1,739
A	1,108.8	0.25	0.26	4,335	0.3	0.27	9,699
1B	286.6	0.21	0.24	822	0.25	0.21	2,740
2B	110	0.22	0.22	1,468	0.26	0.21	4,377
3B	161.1	0.25	0.27	879	0.31	0.26	2,351
4B	86.3	0.25	0.27	314	0.31	0.28	591
5B	153.7	0.28	0.29	1,041	0.34	0.29	2,134
6B	87.9	0.24	0.26	612	0.29	0.27	1,767
7B	142	0.24	0.25	485	0.3	0.26	1,784
B	1,027.6	0.24	0.26	5,621	0.29	0.25	15,744
1D	139.5	0.21	0.24	244	0.3	0.29	548
2D	166.2	0.21	0.21	400	0.3	0.24	1,351
3D	156.1	0.13	0.21	132	0.28	0.27	665
4D	97.4	0.15	0.22	52	0.27	0.25	152
5D	154.2	0.17	0.28	107	0.29	0.26	311
6D	112.5	0.18	0.27	131	0.28	0.29	379
7D	190.7	0.14	0.25	178	0.24	0.26	497
D	1,016.6	0.17	0.24	1,244	0.28	0.27	3,903
Total	**3,153**	**0.22**	**0.25**	**11,200**	**0.29**	**0.26**	**29,346**

Population structure of the AusSTB panel was analysed using the software package STRUCTURE version 2.3.4 (Pritchard et al., 2000), using 11,200 SNPs and 29,346 silicoDArTs, respectively. An admixture model with 10 predefined subpopulations replicated 10 times was run with 10,000 iterations of burn-in followed by 10,000 recorded Markov-Chain iterations for each marker set. Output from STRUCTURE was analysed in the R package Pophelper (Francis, 2017) to determine the optimal number of subpopulations using the Evanno method (Evanno et al., 2005). STRUCTURE was then re-run with the optimum number of subpopulations (seven) to generate population membership coefficient matrices (**Q**) as well as the corresponding population membership coefficients obtained for each marker set (Figure 1).

Phenotypic data analysis

A multiplicative mixed linear model was used to analyse phenotype data for each trait at each experiment following the approach of Gilmour et al. (1997), using the R software package

ASReml-R version 3 (Butler et al., 2018), in the R statistical software environment (R Core Team 2020). The linear mixed model is given by

$$y = X\tau + Zu + \eta$$

where y is the $(n \times 1)$ data vector of the response variable; τ is a $(t \times 1)$ vector of fixed effects (including genetic line effects and the intercept) with associated design matrix X. The term u is a random component with associated design matrix Z and contains the experimental blocking structures (replicate, range and row) used to capture extraneous variation. Random effects were maintained in the model if they were significant according to log likelihood ratio tests relative to the full model (Stram and Lee, 1994). The residual error is η was assumed to have distribution $\eta \sim N(0, \sigma^2 R)$ where σ^2 is the residual variance for the experiment and R is a matrix that contains a parameterization for a separable autoregressive AR1 ⊗ AR1 process to model potential spatial correlation of the observations.

A total of 31 models were constructed for the traits collected from six experiments in GH and four experiments in the field
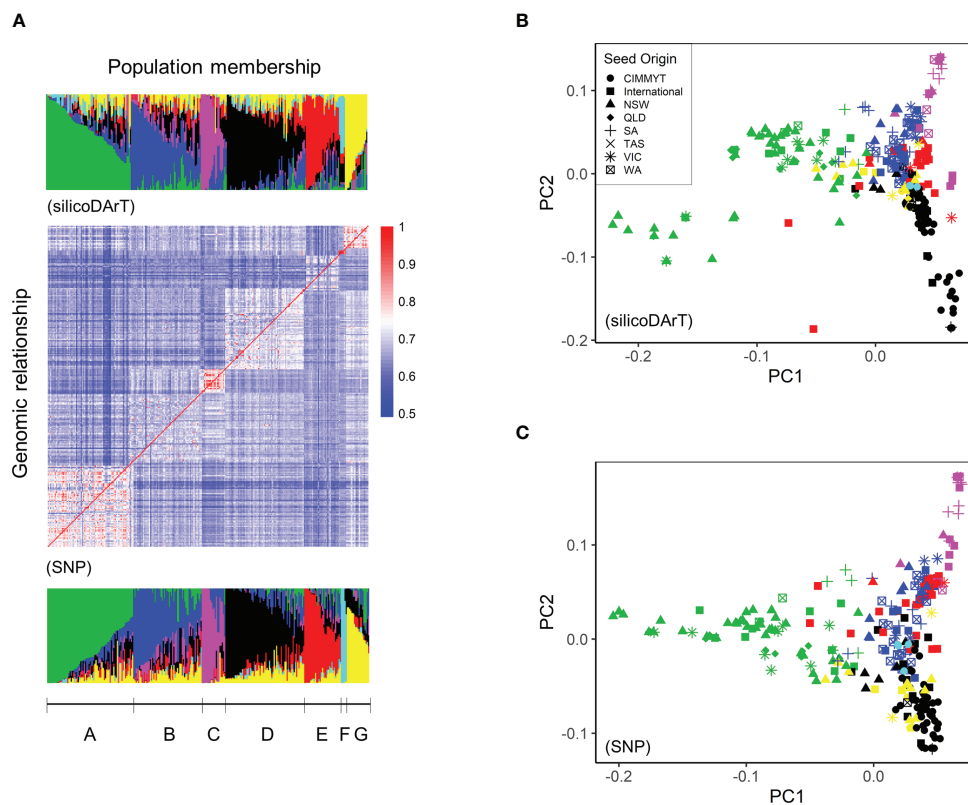
FIGURE 1
Population structure analysis of the AusSTB panel. **(A)** Genomic relationship matrix (*K*) and population membership coefficient matrices (*Q*) showing the seven hypothetical subpopulations derived from the STRUCTURE analysis. **(B)** Principal components analysis of the AusSTB panel using the silicoDArT markers. **(C)** Principal components analysis of the AusSTB panel using the SNPs. The seven sub-populations are displayed in Green (A), Blue (B), Pink (C), Black (D), Red (E), Cyan (F), and Yellow (G). Seed origins of different accessions are CIMMYT (●), International (■), NSW (▲), QLD (♦), SA (+), TAS (×), VIC (✳), and WA (⊠), respectively.

([Supplementary Table 2](#)). Best Unbiased Linear Estimates (BLUEs) were obtained from each model for subsequent use in the association analyses.

Genome-wide association analysis

Association analyses using the phenotype BLUEs described above were performed using the R software package Genome Association and Prediction Integrated Tool (GAPIT) version 2 ([Tang et al., 2016](#)). Missing markers in the two marker sets (consisting of 11,200 SNPs and 29,346 silicoDArTs) were imputed with the major allele at each locus using the imputation function in GAPIT. A separate scaled identity by descent relationship matrix (*K*) after [VanRaden (2008)](#) was calculated for each marker set. Separate association analyses for each trait in each experiment and for the two different marker sets were performed using the compressed mixed linear model approach ([Zhang et al., 2010](#)), implemented in GAPIT as follows:

$$\hat{y} = \mathbf{X}\beta + \mathbf{Z}_g u + \eta$$

where $\hat{y}$ is the vector of BLUEs for one trait measured in one experiment, β is a vector of fixed effects for the corresponding design matrix (*X*) including the molecular marker, population assignments from the STRUCTURE analysis (*Q*) and the intercept. The vector of overall genetic line effects *u* (with associated design matrix $\mathbf{Z}_g$) is modelled as $Var(u) = \mathbf{K}\sigma_a^2$ where *K* is the relationship matrix and σ_a^2 is the estimated additive genetic variance. η is the vector of random residuals.

In order to control for false positive associations, genetic regions, which had marker-trait associations with False Discovery Rate (FDR) adjusted *p*-value less than 0.3 (equivalent to a raw *p*-value of $p < 5e^{-4}$) and were also detected by at least two GWAS, were considered as QTLs ([Maccaferri et al., 2015](#); [Ovenden et al., 2017](#); [Nyine et al., 2019](#)), because repeated detections provide more support for biological association. The confidence interval for QTL is calculated from the genome-wide LD threshold determined above: 1-4 cM for the A and B genomes and 4-6 cM for the D genome. The marker

with the lowest p-value at each QTL was considered the representative marker for the QTL. In addition, to compare the differences among different groups of stacking alleles, Wilcoxon Rank Sum tests was used to generate the p values.

Bioinformatic analysis

The 13 QTLs identified in this study were compared to over 100 QTLs from six GWAS studies, studies using segregating populations and 24 named $Z. tritici$ genes (Aouini, 2018; Tabib Ghaffary et al., 2018; Yang et al., 2018; Langlands-Perry et al., 2022). Firstly, genomic DNA sequences of the 13 QTLs based on the confidence intervals were extracted from the IWGSC RefSeq v1.1 (https://urgi.versailles.inra.fr/). Secondly, the DNA sequences of Simple Sequence Repeats (SSR), silicoDArT and SNP markers tightly linked to reported QTLs were search against the physical QTL regions using blastn. Only those QTLs that overlapped or were detected in our QTL regions were considered as co-localization. All the Coding Sequences (CDS) were then extracted from the 14 QTL regions, and then were BLAST against 314 representative annotated R genes from wheat, maize, rice, and Arabidopsis (Kourelis and van der Hoorn, 2018) to identify candidate R genes in the QTL reported in this study. The annotations of candidate R genes were BLAST and extracted using the software Omics Box™ v2.1.14. The KASP marker wMAS000033, provided by Integrated Breeding Platform (IBP, https://www. integratedbreeding.net/), was used to track the allele frequency of the gene $Vrn-1A$ in the AusSTB panel.

Results

Genotypic data and LD estimation of the AusSTB panel

The consensus map contained all 21 bread wheat chromosomes, covering 3,153 cM, with a total number of 11,200 SNPs and 29,346 silicoDArTs (Table 1). Overall, silicoDArTs were 2-5 times more frequently detected than SNPs on all the 21 chromosomes. Although SNPs and silicoDArTs gave very similar patterns on each of the chromosome, the distribution of silicoDArTs had 9 less gaps than SNPs (Supplementary Figure 1). The average of Minor Allele Frequency (MAF) was similar between SNPs (0.25) and silicoDArTs (0.26) on the A, B, and D genomes. The average of Polymorphism Information Content (PIC) differed slightly between SNPs (0.24) and silicoDArTs (0.25) on A and B genomes, whereas the average of PIC of SNPs (0.17) on D genome was 58% less than that of silicoDArTs (0.27).

Little difference in LD patterns was observed between SNPs and silicoDArTs on the 21 chromosomes, except for a few LD blocks on chromosome 1B, 1D, and 3D (Supplementary Figure 2). An overall average of genetic distance of LD decay was 3 cM for SNPs and 0.68 cM for silicoDArTs at $r^2 = 0.20$ (Supplementary Figure 3c). When estimating LD decays of SNP and silicoDArT individually, SNP LD decay at $r^2 = 0.20$ was 1.2 cM for the A genome, 4.4 cM for the B genome, and 8.5 cM for the D genome (Supplementary Figure 3a). Smaller LD blocks were captured by silicoDArTs than from SNPs in most genomic regions. LD decay values of silicoDArT, were 1.0 cM for the A genome, 0.7 cM for the B genome, and 2.3 cM for the D genome (Supplementary Figure 3b).

AusSTB panel composition and genetic structure

The two sets of markers were used to calculate the genomic relationships matrix (K) and the structure matrices (Q). This analysis indicated there were seven subpopulations amongst the 273 accessions. (Figure 1A). The alignment of members in each subpopulation was not stable between SNPs and silicoDArTs from k = 2 to k = 6 (data not shown), until k = 7 where the discrepancy minimized, and the K matrix matched with the Q matrix (Figure 1A). This population structure was strongly correlated with the seed origins based on the principal component analysis (PCA) (Figures 1B, C). In details, 35 out of 73 members in Sub-population A originated from NSW, 19 out of 58 members in Sub-population B from Western Australia (WA), 8 out of 20 members in Sub-population C from South Australia (SA). Thirty-one members in the Sub-population E, originated from multiple places across the world, was clustered by their growth habits as winter or spring-winter (Supplementary Table 1).

Phenotypic data analysis of the AusSTB panel

The response of the 273 accessions to $Z. tritici$ infection at the seedling stage were tested against three different $Z. tritici$ isolates, which are representative pathotypes for south eastern Australia (WW332, WAI251 and WAI161). Normal frequency distributions were observed in this wheat panel for phenotypic traits Necrosis and STB_S, whereas the frequency distribution of Pycnidia phenotypes was skewed towards zero (Figure 2A). The number of isolate-specific resistant accessions (STB_S scores, 1-2) varied from 23 (WAI161), 17 (WAI251), to 31 (WAI332). Fourteen resistant wheat accessions (STB_S scores, 1-2) were resistant to three $Z. tritici$ isolates in six independent experiments, and five of the most susceptible accessions (STB scores, 3.5-5) were also identified (data not shown).

The response of the 273 accessions to $Z. tritici$ infection at the adult plant stage was evaluated in four environments (two locations × two years) under natural $Z. tritici$ infection. High
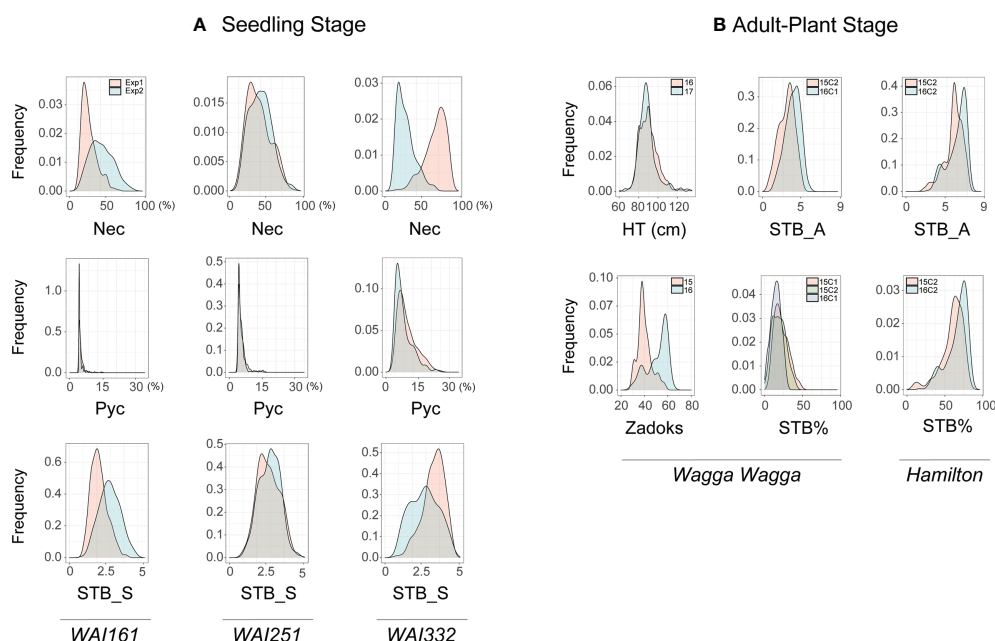
FIGURE 2
Frequency distributions of 31 BLUEs from the AusSTB panel. **(A)** Traits at the seedling stage include the percentage of necrotic leaf area (Nec) on the infected leaves, the pycnidia density (Pyc) in the necrotic leaf area, and the STB_S Scale 1 to 5 using the three STB isolates WAI161, WAI251, and WAI332. **(B)** Traits at the adult-plant stage include Plant Height (HT), Relative maturity (Zadoks scale), STB_A scale 1-9, and the percentage of STB infected leaf area on the whole plant (STB%). Traits HT and Zadoks were only measured at the site of Wagga Wagga.

correlations were observed between four BLUEs of STB_A and five BLUEs of STB%, with Pearson correlation coefficient values ranging from $r = 0.94$ to 0.99 (Supplementary Table 2). This suggests that the two scoring methods captured similar progress of *Z. tritici* infection on plants. A normal frequency distribution was observed on BLUEs of STB_A trait from Wagga Wagga, whereas the distribution shifted towards more susceptibility for the BLUEs of STB_A trait from Hamilton (Figure 2B). Based on the adult-plant assessments in the AusSTB panel, none of the accessions displayed high levels of resistance (R), only five accessions were categorized as moderately resistant (MR). Approximately 20% of the accessions were categorized as being MSS, while the remaining accessions were categorized as susceptible (S) or susceptible/very susceptible (SVS, data not shown).

Association analysis for *Z. tritici* resistance

Thirteen QTLs were detected at the seedling stage and the adult-plant stage (Figure 3 and Supplementary Table 3). These included six QTLs responsible for the *Z. tritici* isolate-specific resistance at seedling stage, which accounted for 3.8-6.9% phenotypic variance. Two QTLs were identified as non-isolate specific resistance as they were detected traits with more than

two *Z. tritici* isolates (3.6-6.9% variance), one QTL at adult plant stage (3.2-4% variance), and four QTLs with multi-stage resistance (MSR, 3.1-6.7% variance).

Three new QTLs were discovered in this study (Figure 2 and Table 2), these are QStb.wai.1A.1 associated with *Z. tritici* resistance against the isolate WAI251, QStb.wai.6A.2 associated with APR and QStb.wai.7A.2 associated with MSR.

Z. tritici resistance associated with HT and Zadoks traits

Plant height (HT) and relative maturity (decimal Zadoks scale) are two important phenological traits known to have various effects on the control of *Z. tritici* resistance. Slight to moderate negative correlations ($r = -0.12$ to -0.41, Supplementary Table 2) were observed between HT and the 18 STB_A and STB% related BLUEs from the field data, suggesting shorter plant tended to have higher susceptibility. In contrast, Zadoks growth scale had strong positive correlations ($r = 0.3-0.83$, Supplementary Table 2) with the 18 STB_A and STB% traits related BLUEs from the field data. The average of STB_A score in the Subpopulation E, which contained the most of the Spring-Winter (intermediate) type and/ or winter-type (slow maturing) plant accessions, was 15% lower than the other subpopulations (data not shown).
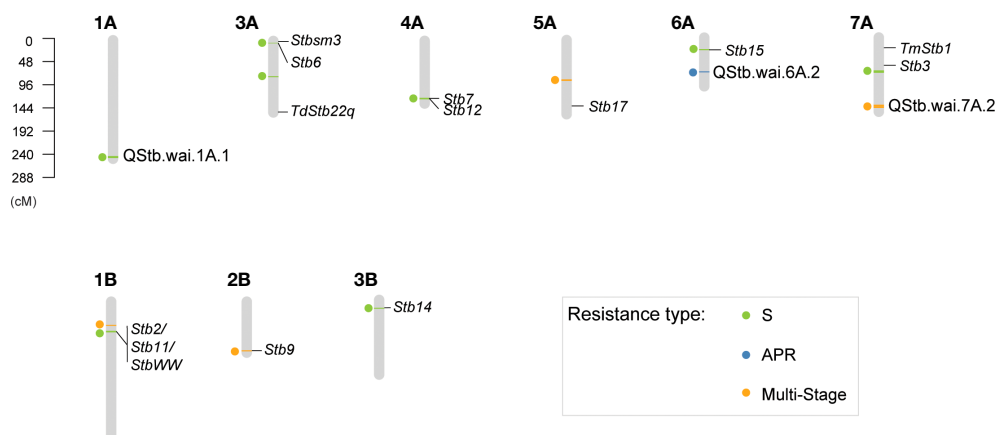
FIGURE 3
Genetic positions of detected QTLs associated with the *Zymoseptoria* resistance at the seedling stage and adult-plant stage. The 13 associations are shown as a solid circle on the left of each chromosome. A bar (linkage disequilibrium confidence interval) is shown in light green for the seedling stage resistance, blue for the adult-plant stage resistance, and orange for the multiple-stage resistance. Names and positions of the previously published *Zymoseptoria* major genes are also shown on the CS consensus genetic linkage map.

QTLs associated with *Z. tritici* resistance at the seedling stage

Six QTLs were associated with the *Z. tritici* isolate-specific resistance, one with WAI161, one with WAI251, and four with WAI332 (Table 2). QStb.wai.6A.1 (resistant allele, C) was associated with the WAI161-specific resistance, with a resistant variant frequency of 0.83. BLAST searches with our markers from the Chinese Spring reference genome indicated that QStb.wai.6A.1 co-located with the major gene *Stb15* (Figure 3). The new putative QTL, QStb.wai.1A.1 (resistant allele, +) was only detected from phenotypes recorded using inoculation with the isolate WAI251 (Figure 3) and accounted for over 5% phenotypic variance. In terms of WAI332-specific associated QTLs, QStb.wai.1B.2 (resistant allele, C) co-located with the major gene locus STB2/STB11/STBWW, QStb.wai.3A.1 (resistant allele, -) co-located with Stb6, and QStb.wai.3B.1 (resistant allele, C) co-located with *Stb14* (Table 2 and Figure 3). The QTL, QStb.wai.4A.1 (resistant allele, -), is co-located with the major gene *Stb7/12* locus. As detailed above, this QTL also co-located with QTL for HT and Zadoks, however there was insufficient data to further improve the resolution in this QTL region.

Two QTLs were detected as non-isolate specific resistance at the seedling stage (Table 2). The resistant QTL, QStb.wai.3A.2 (resistant allele, Y), was associated with pycnidia density, with a variant frequency of 0.12 (Table 2). QStb.wai.3A.2 was detected by phenotypes recorded using the isolates WAI161 and WAI251, with phenotypic variance ranging from 4.1- 7.6%. The QTL, QStb.wai.7A.1 (resistant allele, G), also associated with three traits of WAI251 and WAI332, accounting for 3.6-6.9% phenotypic variance.

QTLs associated with APR and MSR

Five QTLs associated with APR and/or MSR, having variant frequencies from 0.09 to 0.82 were identified (Table 2). These QTLs gave 3.1-6.7% phenotypic contributions to APR (Figure 2).

The QTL, QStb.wai.6A.2, (resistant allele, R or G) is a new QTL, was confined in the region of 73-76 cM, associated with APR in 2015 and 2016 at both Wagga Wagga and Hamilton (Table 2). A blast search found that the tightly linked maker snp_3026774_F_0_34 peaked at the site of 454 Mb according to the Chinese Spring reference genome (Supplementary Table 3).

Four QTLs were categorized as MSR associated with multiple traits at the seedling stage and adult-plant stage (Table 2). The resistant QTL, QStb.wai.2B.1 (resistant allele, +), detected by non-specific isolate resistance at the seedling stage and the adult-plant stage, was found to collocate with the major gene *Stb9* (Figure 3). The second MSR QTL, QStb.wai.1B.1 (resistant allele, +) is close to QStb.wai.1B.2 associated with the resistance at the seedling stage, but our evidence suggests these are two separate QTLs. The genomic region of QStb.1B.1 spanned from 0 to 20 megabases (Mb), while QStb.wai.1B.2 was in the genomic region of 40 to 100 Mb (Supplementary Table 3). Thirdly, QStb.wai.5A.1 (resistant allele, T) highly associated with Zadoks and APR (Table 2 and Supplementary Figure 4). Interestingly, the tagged SNP snp_2262549_F_0_28 of QStb.wai.5A.1 was also detected by two WAI251- seedling related traits, Necrosis and STB_S (Table 2). The fourth QTL, QStb.7A.2 (resistant allele, -) was defined in a genetic span of 4 cM on the distal region of 7AL associated with MSR (Figure 4).

The impact of MSR allele-stacking showed that combinations of QTL alleles with minor effects increased the

TABLE 2   Summary of 13 QTLs detected by five traits associated with *Zymoseptoria tritici* resistance, including the most tightly linked molecular markers (Representative Marker), the location of the QTL (Chromosome and Position), the favorable allele frequency (Variant Freq), the phenotypic contribution of the QTL (Phetypic Variance), and the number of detected BLUEs by the QTL.

QTLs	Representative Marker†	Chr	Pos (cM)	Variant Freq.	Phenotypic Variance (%)	Trait‡ (No. of BLUEs)
(Seedling Stage)						
QStb.wai.1A.1*	pav_1234699 (+/-)	1A	251.5	0.9	5.5-6.5	Necrosis (2), WAI251 specific
QStb.wai.1B.2	snp_1112131_F_0_20 (**C**/A)	1B	63.9	0.63	4.3-5.0	Pycnidia (1), STB_S (1), WAI332 specific
QStb.wai.3A.1	pav_4990595 (+/-)	3A	4.3	0.23	4.8-5.3	Necrosis (1), STB_S (1), WAI332 specific
QStb.wai.3A.2	snp_5325269_F_0_37 (**Y**/T)	3A	77.1	0.12	4.1-6.9	Pycnidia (2), STB1-5 (1), WAI161 and WAI251
QStb.wai.3B.1	snp_4910674_F_0_26 (**C**/G)	3B	17.4	0.64	3.8-6.6	Necrosis (1), Pycnidia (1), STB_S (2), WAI332 specific
QStb.wai.4A.1	pav_3022794 (+/-)	4A	125.4	0.77	4.5-4.9	Pycnidia (1), STB_S (1), WAI332 specific
QStb.wai.6A.1	snp_1233403_F_0_47 (**C**/S)	6A	26.7	0.83	5.1	Necrosis (1), STB_S (1), WAI161 specific
QStb.wai.7A.1	snp_2253221_F_0_65 (**G**/A)	7A	71.9	0.88	3.6-6.9	Necrosis (1), Pycnidia (1), STB_S (1), WAI251 and WAI332
(Adult-plant Stage)						
QStb.wai.6A.2*	snp_3026774_F_0_34 (**R, G**/A)	6A	74.3	0.09	3.2-4	STB_A (2), STB% (1)
(Multi-Stage)						
QStb.wai.1B.1	pav_4991454 (+/-)	1B	51.3	0.11	3.3-4.9	Necrosis (1), Pycnidia (1), STB_S (2), WAI332 specific, STB% (1)
QStb.wai.2B.1	pav_1209089 (+/-)	2B	106.3	0.82	3.2-6.4	Necrosis (1), Pycnidia (1), STB_S (2), STB_A (1), STB% (1)
QStb.wai.5A.1	snp_2262549_F_0_28 (**T**/G)	5A	86.7	0.56	3.2-6.7	Necrosis (1), STB_S (2), WAI251 specific, STB_A (2), STB% (2)
QStb.wai.7A.2*	pav_9364734 (+/-)	7A	145.9	0.14	3.1-6.5	Pycnidia (1), WAI161 specific, STB_A (1), STB% (1)

*New QTLs that are detected in this study.

†The resistant allele is highlighted in bold. The symbol + represents the presence of silicoDArT, and the symbol - represents the absence of silicoDArT. The codominant SNP code Y represents for C/T, S for G/C, and R for A/G.

‡Necrosis represents the percentage of necrotic area on the infected leaves; Pycnidia represents the pycnidia density (%) in the necrotic leaf area. STB_S represents the STB scale 1-5 assessed at the seedling stage, while STB_A represents the STB 1-9 scale assessed at the adult-plant stage.

overall resistance level in phenotypes recorded in this study. Combinations of three MSR alleles (++**T**+ and -+**T**-) showed superior performance, increasing the resistance by 10-30% at Hamilton and by 14-37% at Wagga Wagga (Figure 5). Interestingly, the stacking of MSR alleles ++**T**+ performed better (10% more resistance) than the stacking of -+**T**- at Hamilton, whereas the stacking of MSR alleles ++**T**+ gave ~5% less resistance than -+**T**- at Wagga Wagga. However, no significant differences (*p* values = 0.3) were observed between the combination ++**T**+ of and the combination of -+**T**- at Hamilton and Wagga Wagga. Unfortunately, no accessions in the AusSTB panel had the combination of all four favourable MSR alleles together.

Candidate genes in the QTL regions

Physical genomic regions of thirteen QTLs were BLAST against 341 cloned genes, but only 10 of them were found to

have candidate *R* genes ranging from 1 to 36 (Supplementary Table 4). NBS (Nucleotide-site Binding) like *R* genes were the most abundant in seven of the ten QTLs, with the number varying from 2 to 23. Only one TaWAKL (Wall-Associated Kinase-like) *R* gene was found present in the QTL of QStb.wai.1A.1 associated with the WAI251-specific resistance, while only one RLK (Plant Receptor Kinase) like *R* gene was present in the region of QStb.wai.6A.2 responsible for APR (Table 2).

Discussion

Influence of marker type on the GWAS analysis

The silicoDArT markers performed slightly superior to SNP markers in detecting QTLs. Two to five times more abundance of silicoDArTs than SNPs (Table 1) increased the coverage of makers on the genome (Table 1), possibly explaining why five
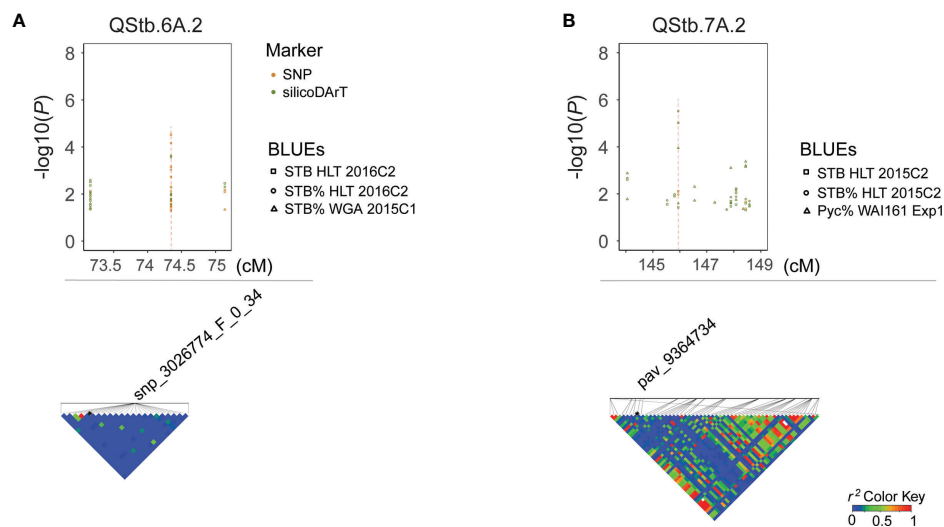
FIGURE 4
Manhattan plots and corresponding linkage disequilibrium r^2 patterns for QStb.wai.6A.2 **(A)** associated with adult-plant resistance, and QStb.wai.7A.2 **(B)** associated with the multiple stage resistance. The upper part of the graph shows -log(P) value plots of marker-trait associations with detected BLUEs (FDR < 0.3). Representative SNP and silicoDArT markers and corresponding local LD r^2 value patterns are presented in the lower part of the graph. Blue color indicates low linkage disequilibrium while red color indicates high linkage disequilibrium.

QTLs were detected by silicoDArTs in comparison to three QTLs by SNPs. In addition, the differences between LD distance decay for the silicoDArT and SNP reported in this study is comparable to previous studies (Chao et al., 2010; Cavanagh et al., 2013; Wang et al., 2014; Ovenden et al., 2017). The more rapid LD decay in the silicoDArTs may have helped to increase the detection of QTLs in smaller regions, therefore increasing the resolution. However, no major difference between silicoDArTs and SNPs was evident in the analysis of population structure. This is possibly due to the existence of large blocks of LD in the AusSTB panel. The recent completion of 1000 exome sequencing of wheat provides another way to enrich LD blocks using low-resolution genotyping services (He et al., 2019), which potentially increase the power to detect QTLs (Jordan et al., 2015; Nyine et al., 2019).

Association between population genetic structure and STB resistance

The genetic characterization of the 273 bread wheat accessions divided the AusSTB panel into seven subpopulations with closely genomic related accessions. The results from the STRUCTURE analysis revealed different levels of admixtures across different subpopulations (Figures 1B, C), reflecting the frequent germplasm exchanges over many years among wheat breeding programs from NSW, VIC, SA, and WA in Australia. However, high levels of resistance were observed to have a high correlation (r > 0.3) with slow-maturing accessions (phenotypes with low Zadoks

scales, Supplementary Table 2) at the adult-plant stage. A high correlation between these characteristics was also observed in several other genetic studies of *Z. tritici* resistance (Arraiano and Brown, 2006; Dreisigacker et al., 2015; Naz et al., 2015; Gerard et al., 2017; Kidane et al., 2017; Muqaddasi et al., 2019). These results imply that winter-type or slow-maturing accessions are inclined to having better *Z. tritici* resistance than the spring type or fast-maturing accessions in the Australian environment. This could be due to the importance of STB resistance in the higher rainfall target environments that these longer season wheat cultivars are developed for, so breeding strategies for these types of cultivars favour the accumulation of STB resistance alleles. This correlation could also indicate that growth stage-dependent resistant QTLs are important in wheat plants at the tillering stage and booting stage, however, few studies have conducted such an exploration.

Known resistance QTLs effectiveness revealed in Australian environments.

Until now breeders targeting *Z. tritici* resistance in Australia have had limited knowledge about which resistance loci are effective in the Australian wheat gene pool, i.e. *Stb2* mapped from 'Veranopolis' (Liu et al., 2013), *Stb3* from 'Israel 493' (Goodwin et al., 2015), *StbWW* from 'WW2449' (Raman et al., 2009), and *Stb19* from 'Lorikeet' (Yang et al., 2018). This GWAS study has revealed seven of the thirteen resistant QTL identified in the AusSTB panel were found to co-locate in regions previously described from international studies as containing
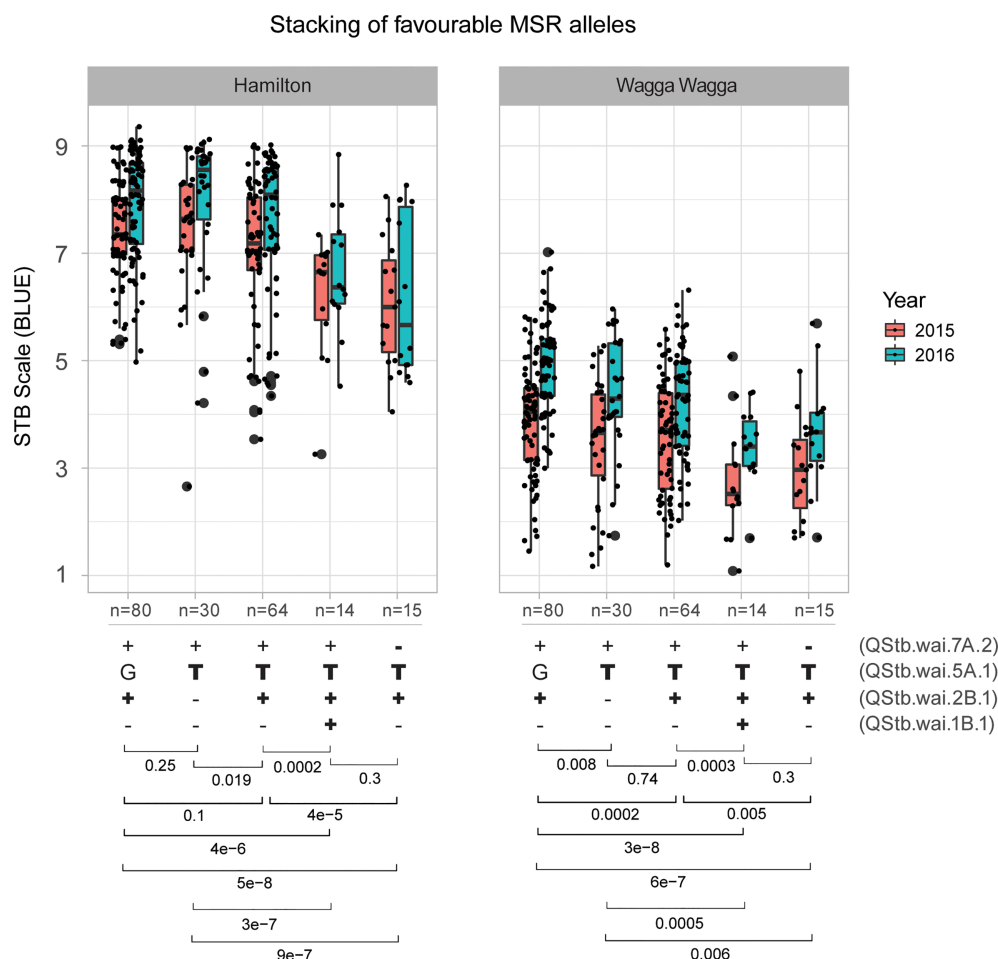
FIGURE 5
Box plot analysis of four QTLs associated with multiple-stage resistance (MSR) using their representative SNP/silicoDArT markers. Four types of stacking of alleles that existed in the AusSTB panel were shown in the lower part of the figure. Favorable alleles of QTLs are highlighted in bold. Significant *p*-values were shown at the bottom, generated by multiple-group Wilcoxon test.

major genes for resistance to *Z. tritici* (Brading et al., 2002; Chartrain et al., 2005a; Chartrain et al., 2005b; Cowling, 2006; Chartrain et al., 2009; Raman et al., 2009; Cuthbert, 2011; Liu et al., 2013). Another four QTLs identified in this study co-located at the same physical chromosome position as previously reported QTLs or within the confidence intervals of the reported QTLs (Arraiano et al., 2007; Goudemand et al., 2013; Dreisigacker et al., 2015). Some of these older reported QTLs have large regions of the chromosome associated with resistance (due to lower mapping resolution in the populations under study) and it is not possible to resolve if the QTLs in this study are the same as the older QTLs or novel resistance loci.

The level of phenotypic variance explained by the identified QTLs ranged from 3.1% to 6.9% (Table 2), even though some of the loci are putative major genes as discussed below. Similar levels of explained variation, 2-11% have been reported in the eight published *Zymoseptoria* resistance GWAS studies using

high-density SNP markers (Kidane et al., 2017; Vagndorf et al., 2017; Würschum et al., 2017; Muqaddasi et al., 2019; Yates et al., 2019; Alemu et al., 2021; Louriki et al., 2021; Mahboubi et al., 2022). It is a reasonable assumption that in a in a diverse germplasm collection such as AusSTB that the *Zymoseptoria* resistance is controlled by multiple QTLs with small effects.

The frequencies of R alleles varied substantially in the whole population (Table 2) and subpopulations (data not shown). Five of the seedling QTLs co-located with known major *R* genes, which is not surprising given the use of cultivars with these *R* genes as parents in Australian breeding over the past 50 years. Several of the favourable allele frequencies are being maintained at high levels, such as QStb.wai.4A.1 (0.77) and QStb.wai.6A.1 (0.83), QStb.wai.7A.1 (0.88) and QStb.wai.1A.1 (0.9), which is notable considering the AusSTB panel is comprised of a wide sample of international, historic, and recent Australian cultivars and that few breeding programs have historically actively

selected for seedling resistance to *Z. tritici*. These QTLs were not detected in the analysis of the adult-plant disease phenotypes. However, they must be contributing to the improved seedling-stage performance in the field to be present in such a high number of accessions in the AusSTB panel. The representative markers described here with the QTLs, enable the selection of multiple favourable alleles and give the ability to remove unfavourable alleles from breeding programs (Table 2).

Two of the five QTLs identified in the adult-plant growth stages may co-locate with known major gene resistance loci. The locus QStb.wai.2B.1 is located physically close to the reported location for *Stb9* (Chartrain et al., 2009) and QStb.wai.5A.1 appears to be close to the physical location reported for *Stb17* (Figure 3). The previous report of INT 6 (Yates et al., 2019) and QStb.sn.2B (Aouini, 2018) also highlighted the importance of loci on chromosome 2BL for resistance. Further, the QTLs, QTL-2BL and Qstb2B_1 were also mapped from the durum wheat 'Agili 39'and are reported to be responsible for *Z. tritici* resistance at both seedling stage and adult-plant stage using multiple isolates. It has also been suggested that this locus could be the major gene *Stb9* (Aouini, 2018; Ferjaoui et al., 2021).

The major gene *Stb17* was sourced from synthetic bread wheat accession 'SH M3', and reportedly accounts for 12-32% of the adult-plant resistance (Tabib Ghaffary et al., 2012). When the available sequences from the report of Tabib Ghaffary et al. (2012) are BLAST searched against the IWGSC reference genome, *Stb17* is possibly located in the region of 520-560 Mb (data not shown), while QStb.wai.5A.1 was in the region of 570-590 Mb (Supplementary Table 3), close to where the *Vrn-A1* is located (IWGSC et al., 2018). In addition, QStb.wai.5A.1 with a resistant frequency of 0.56, was observed to be highly associated with low-Zadoks, APR, and WAI251-specific phenotypes, and appears to be co-located with the previously reported loci QStb.cim-5AL-2 (Dreisigacker et al., 2015) and QStb.B22-5A.a (Naz et al., 2015). It is possible that these reported loci are the gene *Vrn-A1a*, as 162 out of 273 (0.59) accessions in the AusSTB panel were identified as having *Vrn-A1a*. The *Vrn-A1a* gene, which encodes a MADS-box transcription factor 14-like protein (Yan et al., 2003), may have pleiotropic effects on the plant growth and the plant defence on different plant pathogens including *Z. tritici*, Fusarium Head Blight (Xu et al., 2019), tan spot and Septoria nodorum blotch (Hu et al., 2019). However, the association of this locus with a seedling resistance phenotype to the WAI251 isolate suggests otherwise, these loci may be a new gene very close to *Vrn-A1a*. Some probable candidate genes at this locus include a plant receptor kinase or WAKL gene (Supplementary Table 4).

QTLs associated with APR

Generally, APR is considered preferable in breeding programs because of the flexible use in the IDM systems

(Wellings et al., 2012). The putative new locus QStb.wai.6A.2 was detected across multiple sites and years, and the probable physical location for this QTL spanned from 440 Mb to 615 Mb on the Chinese Spring reference genome (Supplementary Table 3). Above the region of QStb.wai.6A.2, QTLs INT 10 and INT 11 were detected based on single year data and was positioned at 411-425 Mb. These QTL are reported to account for the control of *Z. tritici* pycnidia density within lesions at the adult-plant stage, and they were also thought to co-locate with the major gene *Stb15* (Yates et al., 2019). Another QTL, QStb.teagasc-6A.2 (534-580 Mb) was associated with the resistance of flag-1 leaves to *Z. tritici* from a single-year field phenotypes obtained from a Multi-parent Advanced Generation Inter-Cross (MAGIC) population (Riaz et al., 2020). It is possible that the locus QStb.teagasc-6A.2 may be the same as the QStb.wai.6A.2 as the probable physical locations of these loci overlap by approximately 50 Mb on chromosome 6A. However, accessions that carry the resistant alleles from both this study and Riaz et al. (2020) would need to be compared to determine if this is the case.

The genetic control of APR is provided by QTLs that are most effective between tillering and full head emergence, and not necessarily at the seedling stage (Wellings et al., 2012; Ellis et al., 2014). Two potential issues here might impede the utilization of APR-QTLs as breeding targets for resistance. Firstly, if a cultivar is only relying on the combination of several APR-QTLs, it is likely to be vulnerable to disease infection at the seedling stage. In cooler climate and higher rainfall areas of the south-eastern Australian, the *Zymoseptoria* population can start releasing ascospores and infecting seedlings sown in the early planting window from February to May. Secondly, if a cultivar relies only on a single APR gene, the *Z. tritici* population infecting a crop of that cultivar will only need to mutate once to overcome the resistance such as *Lr12* and *Lr37* (McIntosh et al., 1995). One solution to overcome these two issues is to stack a combination of 2-4 major genes resistant at the seedling stage and at the adult-plant stage together in a cultivar. Before this can be attempted, the limited resource of *Z. tritici* resistance will need to be expanded. Only 24 major genes for *Z. tritici* resistance have been reported to date (Aouini, 2018; Tabib Ghaffary et al., 2018; Yang et al., 2018; Langlands-Perry et al., 2022), compared to over 200 rust resistance genes (Zhang et al., 2020). The current stocks of major gene resistance are also being depleted as Australian *Z. tritici* populations evolve to overcome the effectiveness of these loci completely or partially. The loci that are known to have been overcome and are no longer effective in the Australian environment including *Stb2/11/WW* from 'Veranopolis' and 'WW2449', *Stb3* from 'Israel 493', *Stb4* from 'Tadorna', *Stb6* from 'Heraward', *Stb7/12* from 'Currawong', *Stb14* from 'M1696', *Stb18* from 'Balance' (pers. comm A. Milgate). Another possible solution to more sustainable disease resistance would be to stack major genes and APR-QTLs together. Multiple evidence suggests that combinations of different types of partial or quantitative resistance will prolong the life of *Z. tritici* resistance in

cultivars, compared to a single gene of resistance (St Clair, 2010; Brown, 2015; Niks et al., 2015; Rimbaud et al., 2021). In this scenario, stacking of two major genes at seedling stages and two APR-QTLs into a targeted elite cultivar is not trivial, because the success rate to capture one combination of four QTLs into a single genotype is 1/256. In comparison, the combination of two or three MSR-QTLs (1/16 or 1/64) should achieve the same level of resistance but with less breeding effort.

QTLs associated with multi-stage resistance

The results of this study highlight the presence of QTL that provide resistance to the development of disease at multiple growth stages in plants. Multi-stage resistances can be considered different and distinct to APR, as the resistance is continuously expressed through progressive crop development stages from seedlings to grain-filling. From the point of view of resistance breeding, APR loci are attractive breeding targets for incorporation into new cultivars as they provide benefits at the flowering and grain filling stages of crop development, where preservation of green leaf area has a relatively larger contribution to the final grain yield. However, before these growth stages, local transmission of *Z. tritici* inoculum is driven primarily *via* splash-borne pycnidiospores dispersing vertically upwards through the plant canopy from the lower layer of leaves (Eyal, 1987; Robert et al., 2018). The control of *Z. tritici* from the seedling stage to booting stage, to some extent help plants reduce the amount in-crop of inoculum, which in turn alleviates the level of disease infection at later stages of plant development. MSR loci that can provide resistance (i.e., seedling-stage resistance) that reduces early levels of infection, as well as APR-type resistance that protects green leaf area at later growth stages, should be attractive breeding targets for cultivar development, particularly when they can be used in conjunction with other resistance loci for either seedling or APR.

This study introduces the concept of multi-stage resistance as a distinctive classification of loci that confer disease resistance at both seedling and some of the adult growth stages. So far since the first report of the major gene *Stb5* in 2001 (Arraiano et al., 2001), forty-nine genetic studies have reported over 300 genes/QTLs associated with *Z. tritici* resistance, including approx. 200 APR-QTLs and 76 seedling-stage/isolate-(non) specific genes/QTLs (Supplementary Table 6). Among those, approx. twenty previously reported QTLs may fall into the MSR-QTL class of resistance (Supplementary Table 5). For instance, *Stb1*, *Stb4*, *Stb5*, *Stb6*, *Stb16q*, and *Stb18* might be the major genes known to provide MSR (Brown et al., 2015). Additionally 16 reported QTLs with minor effects might also provide MSR (Supplementary Table 5), including those discovered from five segregating populations (Eriksen et al., 2003; Tabib Ghaffary et al., 2011; Tabib Ghaffary et al., 2012; Aouini, 2018; Piaskowska et al., 2021) and two association mapping populations (Goudemand et al., 2013; Louriki et al., 2021). In this study, the four

identified MSR-QTLs are likely to provide resources for the development of *Z. tritici* resistant cultivars both in Australia and globally. In comparison to previously published studies, our detected MSR-QTL QStb.wai.1B.1 was co-located with QStb.cim-1BS (Dreisigacker et al., 2015), and the locus of QStb.wai.2B.1 co-located with QTL-2BL, Qstb2B_1 (Aouini, 2018; Ferjaoui et al., 2021) and the major gene *Stb9* (Chartrain et al., 2009). While the locus of QStb.wai.5A.1 co-located with QStb.cim-5AL-2 (Dreisigacker et al., 2015) and QStb.B22-5A.a (Naz et al., 2015). Finally, QStb.wai.7A.2 is a putative new MSR-QTL located in the distal chromosome of 7A, roughly located in 705-720 Mb based on the CS physical map (Supplementary Table 4). This locus is close to but not overlapping the APR-QTLs, QStb.NS-7A (Vagndorf et al., 2017) and MQTL24 (Goudemand et al., 2013), which are estimated to be located between 680-700 Mb on the CS physical map.

The MSR-QTLs reported in this study were shown to significantly reduced disease levels when at least three were in combination. The MSR-QTL will provide a new resource for *Z. tritici* resistance breeding, although further work will be required to ascertain the genetic architecture of the QTL and validate them across multiple genetic backgrounds. These QTL are likely to be high quality targets for the development of molecular markers and target genome sequencing to identify and clone the underlying resistant genes.

Conclusions

In summary, the study discovered eight QTLs responsible for the seedling resistance, one putative new QTL QStb.6A.2 responsible at the adult-plant stage, four QTLs responsible for MSR including the putative new QStb.wai.7A.2 at multiple stages. The underlying function and how they are acting on the pathogen during infection warrant further detailed studies as they may hold the key to more durable quantitative resistance gene of combinations.

Data availability statement

The original contributions presented in the study are included in the article/Supplementary Material. Further inquiries can be directed to the corresponding author.

Author contributions

Acknowledgments

Conflict of interest

The authors declare that the research was conducted in the absence of any commercial or financial relationships that could be construed as a potential conflict of interest.

Publisher's note

All claims expressed in this article are solely those of the authors and do not necessarily represent those of their affiliated organizations, or those of the publisher, the editors and the reviewers. Any product that may be evaluated in this article, or claim that may be made by its manufacturer, is not guaranteed or endorsed by the publisher.

Supplementary material

The Supplementary Material for this article can be found online at: https://www.frontiersin.org/articles/10.3389/fpls.2022.990915/full#supplementary-material

References

Adhikari, T. B., Cavaletto, J. R., Dubcovsky, J., Gieco, J. O., Schlatter, A. R., and Goodwin, S. B. (2004). Molecular mapping of the *Stb4* gene for resistance to septoria tritici blotch in wheat. *Phytopathology* 94 (11), 1198–1206. doi: 10.1094/PHYTO.2004.94.11.1198

Alemu, A., Brazauskas, G., Gaikpa, D. S., Henriksson, T., Islamov, B., Jorgensen, L. N., et al. (2021). Genome-wide association analysis and genomic prediction for adult-plant resistance to septoria tritici blotch and powdery mildew in winter wheat. *Front. Genet.* 12. doi: 10.3389/fgene.2021.661742

Aouini, L. (2018). Durum wheat and septoria tritici blotch: genes and prospects for breeding. PhD Thesis, (Wageningen University). doi: 10.18174/443719

Arraiano, L., Balaam, N., Fenwick, P., Chapman, C., Feuerhelm, D., Howell, P., et al. (2009). Contributions of disease resistance and escape to the control of septoria tritici blotch of wheat. *Plant Pathol.* 58 (5), 910–922. doi: 10.1111/j.1365-3059.2009.02118.x

Arraiano, L., and Brown, J. (2006). Identification of isolate-specific and partial resistance to septoria tritici blotch in 238 European wheat cultivars and breeding lines. *Plant Pathol.* 55 (6), 726–738. doi: 10.1111/j.1365-3059.2006.01444.x

Arraiano, L. S., and Brown, J. K. (2017). Sources of resistance and susceptibility to septoria tritici blotch of wheat. *Mol. Plant Pathol.* 18 (2), 276–292. doi: 10.1111/mpp.12482

Arraiano, L., Chartrain, L., Bossolini, E., Slatter, H., Keller, B., and Brown, J. (2007). A gene in European wheat cultivars for resistance to an African isolate of *Mycosphaerella graminicola*. *Plant Pathol.* 56 (1), 73–78. doi: 10.1111/j.1365-3059.2006.01499.x

Arraiano, L., Worland, A., Ellerbrook, C., and Brown, J. (2001). Chromosomal location of a gene for resistance to septoria tritici blotch (*Mycosphaerella graminicola*) in the hexaploid wheat 'Synthetic 6x'. *Theor. Appl. Genet.* 103 (5), 758–764. doi: 10.1007/s001220100668

Blake, J. J., Gosling, P., Fraaije, B. A., Burnett, F. J., Knight, S. M., Kildea, S., et al. (2018). Changes in field dose–response curves for demethylation inhibitor (DMI) and quinone outside inhibitor (QoI) fungicides against *Zymoseptoria tritici*, related to laboratory sensitivity phenotyping and genotyping assays. *Pest Manage. Sci.* 74 (2), 302–313. doi: 10.1002/ps.4725

Brading, P. A., Verstappen, E. C., Kema, G. H., and Brown, J. K. (2002). A gene-for-gene relationship between wheat and *Mycosphaerella graminicola*, the septoria tritici blotch pathogen. *Phytopathology* 92 (4), 439–445. doi: 10.1094/PHYTO.2002.92.4.439

Brown, J. K. (2015). Durable resistance of crops to disease: a Darwinian perspective. *Annu. Rev. Phytopathol.* 53, 513–539. doi: 10.1146/annurev-phyto-102313-045914

Brown, J. K., Chartrain, L., Lasserre-Zuber, P., and Saintenac, C. (2015). Genetics of resistance to *Zymoseptoria tritici* and applications to wheat breeding. *Fungal Genet. Biol.* 79, 33–41. doi: 10.1016/j.fgb.2015.04.017

Butler, D., Cullis, B. R., Gilmour, A., Gogel, B., and Thompson, R. (2018). *ASReml-r reference manual version 4* (VSN International Ltd).

Cavanagh, C. R., Chao, S., Wang, S., Huang, B. E., Stephen, S., Kiani, S., et al. (2013). Genome-wide comparative diversity uncovers multiple targets of selection for improvement in hexaploid wheat landraces and cultivars. *PNAS* 110 (20), 8057–8062. doi: 10.1073/pnas.1217133110

Chao, S., Dubcovsky, J., Dvorak, J., Luo, M.-C., Baenziger, S. P., Matnyazov, R., et al. (2010). Population-and genome-specific patterns of linkage disequilibrium and SNP variation in spring and winter wheat (*Triticum aestivum* l.). *BMC Genomics* 11 (1), 727. doi: 10.1186/1471-2164-11-727

Chartrain, L., Berry, S. T., and Brown, J. K. M. (2005a). Resistance of wheat line kavkaz-K4500 L.6.A.4 to septoria tritici blotch controlled by isolate-specific resistance genes. *Phytopathology* 95 (6), 664–671. doi: 10.1094/Phyto-95-0664

Chartrain, L., Joaquim, P., Berry, S., Arraiano, L., Azanza, F., and Brown, J. (2005b). Genetics of resistance to septoria tritici blotch in the Portuguese wheat breeding line TE 9111. *Theor. Appl. Genet.* 110 (6), 1138–1144. doi: 10.1007/s00122-005-1945-4

Chartrain, L., Sourdille, P., Bernard, M., and Brown, J. K. M. (2009). Identification and location of Stb9, a gene for resistance to septoria tritici blotch in wheat cultivars courtot and tonic. *Plant Pathol.* 58 (3), 547–555. doi: 10.1111/j.1365-3059.2008.02013.x

Chen, X. (2005). Epidemiology and control of stripe rust [*Puccinia striiformis* f. sp. *tritici*] on wheat. *Can. J. Plant Pathol.* 27 (3), 314–337. doi: 10.1080/07060660509507230

Cleveland, W. S., and Devlin, S. J. (1988). Locally weighted regression: an approach to regression analysis by local fitting. *J. Am. Stat. Assoc.* 83 (403), 596–610. doi: 10.1080/01621459.1988.10478639

Coombes, N. (2002). "Excavating for designs: SpaDes to DiGGer, spatial design search," in *Australasian Genstat Conference 2002*. Busselton, West Australia

Courtois, B., Audebert, A., Dardou, A., Roques, S., Ghneim-Herrera, T., Droc, G., et al. (2013). Genome-wide association mapping of root traits in a japonica rice panel. *PloS One* 8 (11), e78037. doi: 10.1371/journal.pone.0078037

Cowling, S. G. (2006). Identification and mapping of host resistance genes to septoria tritici blotch of wheat. PhD Thesis, (University of Manitoba).

Cuthbert, R. (2011). Molecular mapping of septoria tritici blotch resistance in hexaploid wheat (*Triticum aestivum* l.) (Canada: University of Manitoba).

Dooley, H., Shaw, M. W., Mehenni-Ciz, J., Spink, J., and Kildea, S. (2016). Detection of *Zymoseptoria tritici* SDHI-insensitive field isolates carrying the SdhC-H152R and SdhD-R47W substitutions. *Pest Manage. Sci.* 72 (12), 2203–2207. doi: 10.1002/ps.4269

Dreisigacker, S., Wang, X., Martinez Cisneros, B. A., Jing, R., and Singh, P. K. (2015). Adult-plant resistance to septoria tritici blotch in hexaploid spring wheat. *Theor. Appl. Genet.* 128 (11), 2317–2329. doi: 10.1007/s00122-015-2587-9

Ellis, J. G., Lagudah, E. S., Spielmeyer, W., and Dodds, P. N. (2014). The past, present and future of breeding rust resistant wheat. *Front. Plant Sci.* 5. doi: 10.3389/fpls.2014.00641

Eriksen, L., Borum, F., and Jahoor, A. (2003). Inheritance and localisation of resistance to *Mycosphaerella graminicola* causing septoria tritici blotch and plant height in the wheat (*Triticum aestivum* l.) genome with DNA markers. *Theor. Appl. Genet.* 107 (3), 515–527. doi: 10.1007/s00122-003-1276-2

Evanno, G., Regnaut, S., and Goudet, J. (2005). Detecting the number of clusters of individuals using the software STRUCTURE: a simulation study. *Mol. Ecol.* 14 (8), 2611–2620. doi: 10.1111/j.1365-294X.2005.02553.x

Eyal, Z. (1987). *The septoria diseases of wheat: concepts and methods of disease management* (CIMMYT).

Ferjaoui, S., Aouini, L., Slimane, R. B., Ammar, K., Dreisigacker, S., Schouten, H. J., et al. (2021). Deciphering resistance to *Zymoseptoria tritici* in the Tunisian durum wheat landrace accession 'Agili39'. *BMC Genomics* 23 (1), 1–20. doi: 10.1186/s12864-022-08560-2

Francis, R. M. (2017). Pophelper: an r package and web app to analyse and visualize population structure. *Mol. Ecol. Resour.* 17 (1), 27–32. doi: 10.1111/1755-0998.12509

Gerard, G. S., Börner, A., Lohwasser, U., and Simón, M. R. (2017). Genome-wide association mapping of genetic factors controlling septoria tritici blotch resistance and their associations with plant height and heading date in wheat. *Euphytica* 213 (1). doi: 10.1007/s10681-016-1820-1

Gilmour, A. R., Cullis, B. R., and Verbyla, A. P. (1997). Accounting for natural and extraneous variation in the analysis of field experiments. *J. Agricul. Biol. Environ. Stat* 2 (3), 269–293. doi: 10.2307/1400446

Goodwin, S. B., Cavaletto, J. R., Hale, I. L., Thompson, I., Xu, S. X., Adhikari, T. B., et al. (2015). A new map location of gene *Stb3* for resistance to septoria tritici blotch in wheat. *Crop Sci.* 55 (1), 35–43. doi: 10.2135/cropsci2013.11.0766

Goudemand, E., Laurent, V., Duchalais, L., Ghaffary, S. M. T., Kema, G. H., Lonnet, P., et al. (2013). Association mapping and meta-analysis: two complementary approaches for the detection of reliable septoria tritici blotch quantitative resistance in bread wheat (Triticum aestivum l.). *Mol. Breed.* 32 (3), 563–584. doi: 10.1007/s11032-013-9890-4

Hagerty, C. H., Graebner, R. C., Sackett, K. E., and Mundt, C. C. (2017). Variable competitive effects of fungicide resistance in field experiments with a plant pathogenic fungus. *Ecol. Appl.* 27 (4), 1305–1316. doi: 10.1002/eap.1524

He, F., Pasam, R., Shi, F., Kant, S., Keeble-Gagnere, G., Kay, P., et al. (2019). Exome sequencing highlights the role of wild-relative introgression in shaping the adaptive landscape of the wheat genome. *Nat. Genet.* 51 (5), 896–904. doi: 10.1038/s41588-019-0382-2

Hu, W., He, X., Dreisigacker, S., Sansaloni, C. P., Juliana, P., and Singh, P. K. (2019). A wheat chromosome 5AL region confers seedling resistance to both tan spot and septoria nodorum blotch in two mapping populations. *Crop J.* 7 (6), 809–818. doi: 10.1016/j.cj.2019.05.004

IWGSC, Appels, R., Eversole, K., Feuillet, C., Keller, B., Rogers, J., et al. (2018). Shifting the limits in wheat research and breeding using a fully annotated reference genome. *Science* 361 (6403), eaar7191. doi: 10.1126/science.aar7191

Jordan, K. W., Wang, S., Lun, Y., Gardiner, L. J., MacLachlan, R., Hucl, P., et al. (2015). A haplotype map of allohexaploid wheat reveals distinct patterns of selection on homoeologous genomes. *Genome Biol.* 16, 48. doi: 10.1186/s13059-015-0606-4

Kidane, Y. G., Hailemariam, B. N., Mengistu, D. K., Fadda, C., Pe, M. E., and Dell'Acqua, M. (2017). Genome-wide association study of *Septoria tritici* blotch resistance in Ethiopian durum wheat landraces. *Front. Plant Sci.* 8. doi: 10.3389/fpls.2017.01586

Kourelis, J., and van der Hoorn, R. A. L. (2018). Defended to the nines: 25 years of resistance gene cloning identifies nine mechanisms for r protein function. *Plant Cell* 30 (2), 285–299. doi: 10.1105/tpc.17.00579

Krattinger, S. G., Lagudah, E. S., Spielmeyer, W., Singh, R. P., Huerta-Espino, J., McFadden, H., et al. (2009). A putative ABC transporter confers durable resistance to multiple fungal pathogens in wheat. *Science* 323 (5919), 1360–1363. doi: 10.1126/science.1166453

Langlands-Perry, C., Cuenin, M., Bergez, C., Krima, S. B., Gélisse, S., Sourdille, P., et al. (2022). Resistance of the wheat cultivar 'Renan' to septoria leaf blotch explained by a combination of strain specific and strain non-specific QTL mapped on an ultra-dense genetic map. *Genes* 13 (1), 100. doi: 10.3390/genes13010100

Liu, Y., Zhang, L., Thompson, I. A., Goodwin, S. B., and Ohm, H. W. (2013). Molecular mapping re-locates the Stb2 gene for resistance to septoria tritici blotch derived from cultivar veranopolis on wheat chromosome 1BS. *Euphytica* 190 (1), 145–156. doi: 10.1007/s10681-012-0796-8

Li, H., Vikram, P., Singh, R. P., Kilian, A., Carling, J., Song, J., et al. (2015). A high density GBS map of bread wheat and its application for dissecting complex disease resistance traits. *BMC Genomics* 16, 216. doi: 10.1186/s12864-015-1424-5

Louriki, S., Rehman, S., El Hanafi, S., Bouhouch, Y., Al-Jaboobi, M., Amri, A., et al. (2021). Identification of resistance sources and genome-wide association

mapping of septoria tritici blotch resistance in spring bread wheat germplasm of ICARDA. *Front. Plant Sci.* 12. doi: 10.3389/fpls.2021.600176

Maccaferri, M., Zhang, J., Bulli, P., Abate, Z., Chao, S., Cantu, D., et al. (2015). A genome-wide association study of resistance to stripe rust (*Puccinia striiformis* f. sp. *tritici*) in a worldwide collection of hexaploid spring wheat (*Triticum aestivum* l.). *G3: Genes|Genomes|Genetics* 5 (3), 449–465. doi: 10.1534/g3.114.014563

Mahboubi, M., Talebi, R., Mehrabi, R., Naji, A. M., Maccaferri, M., and Kema, G. H. (2022). Genetic analysis of novel resistance sources and genome-wide association mapping identified novel QTLs for resistance to *Zymoseptoria tritici*, the causal agent of septoria tritici blotch in wheat. *J. Appl. Genet.* 1-17. doi: 10.1007/s13353-022-00696-x

McDonald, B. A., and Mundt, C. C. (2016). How knowledge of pathogen population biology informs management of septoria tritici blotch. *Phytopathology* 106 (9), 948–955. doi: 10.1094/PHYTO-03-16-0131-RVW

McDonald, M. C., Renkin, M., Spackman, M., Orchard, B., Croll, D., Solomon, P. S., et al. (2019). Rapid parallel evolution of azole fungicide resistance in Australian populations of the wheat pathogen *Zymoseptoria tritici*. *Appl. Environ. Microbiol.* 85 (4), e01908–e01918. doi: 10.1128/AEM.01908-18

McIntosh, R. A., Wellings, C. R., and Park, R. F. (1995). *Wheat rusts: an atlas of resistance genes* (CSIRO publishing).

Milgate, A. (2014) *Septoria tritici blotch has increased in importance in high-rainfall areas of the southern GRDC region and careful attention to fungicide strategies is required to minimise the chances of further resistance developing. ground cover™ issues*. Available at: https://grdc.com.au/resources-and-publications/groundcover/ground-cover-supplements/gcs110/septoria-fungicide-resistance-detected.

Moore, J. W., Herrera-Foessel, S., Lan, C., Schnippenkoetter, W., Ayliffe, M., Huerta-Espino, J., et al. (2015). A recently evolved hexose transporter variant confers resistance to multiple pathogens in wheat. *Nat. Genet.* 47 (12), 1494–1498. doi: 10.1038/ng.3439

Muqaddasi, Q. H., Zhao, Y., Rodemann, B., Plieske, J., Ganal, M. W., and Röder, M. S. (2019). Genome-wide association mapping and prediction of adult stage blotch infection in European winter wheat *via* high-density marker arrays. *Plant Genome* 12 (1), 180029. doi: 10.3835/plantgenome2018.05.0029

Naz, A. A., Klaus, M., Pillen, K., Léon, J., and Miedaner, T. (2015). Genetic analysis and detection of new QTL alleles for septoria tritici blotch resistance using two advanced backcross wheat populations. *Plant Breed.* 134 (5), 514–519. doi: 10.1111/pbr.12301

Niks, R. E., Qi, X., and Marcel, T. C. (2015). Quantitative resistance to biotrophic filamentous plant pathogens: concepts, misconceptions, and mechanisms. *Annu. Rev. Phytopathol.* 53, 445–470. doi: 10.1146/annurev-phyto-080614-115928

Nyine, M., Wang, S., Kiani, K., Jordan, K., Liu, S., Byrne, P., et al. (2019). Genotype imputation in winter wheat using first-generation haplotype map SNPs improves genome-wide association mapping and genomic prediction of traits. *G3: Genes|Genomes|Genetics* 9 (1), 125–133. doi: 10.1534/g3.118.200664

Ovenden, B., Milgate, A., Lisle, C., Wade, L. J., Rebetzke, G. J., and Holland, J. B. (2017). Selection for water-soluble carbohydrate accumulation and investigation of genetic× environment interactions in an elite wheat breeding population. *Theor. Appl. Genet.* 130 (11), 2445–2461. doi: 10.1007/s00122-017-2969-2

Piaskowska, D., Piechota, U., Radecka-Janusik, M., and Czembor, P. (2021). QTL mapping of seedling and adult plant resistance to septoria tritici blotch in winter wheat cv. mandub (*Triticum aestivum* l.). *Agronomy* 11 (6), 1108. doi: 10.3390/agronomy11061108

Pritchard, J. K., Stephens, M., and Donnelly, P. (2000). Inference of population structure using multilocus genotype data. *Genetics* 155 (2), 945–959. doi: 10.1093/genetics/155.2.945

Quaedvlieg, W., Kema, G., Groenewald, J., Verkley, G., Seifbarghi, S., Razavi, M., et al. (2011). *Zymoseptoria* gen. nov.: a new genus to accommodate septoria-like species occurring on graminicolous hosts. *Persoonia - Mol. Phylogeny Evol. Fungi* 26, 57. doi: 10.3767/003158511X571841

Raman, R., Milgate, A., Imtiaz, M., Tan, M.-K., Raman, H., Lisle, C., et al. (2009). Molecular mapping and physical location of major gene conferring seedling resistance to septoria tritici blotch in wheat. *Mol. Breed.* 24 (2), 153–164. doi: 10.1007/s11032-009-9280-0

Riaz, A., KockAppelgren, P., Hehir, J. G., Kang, J., Meade, F., Cockram, J., et al. (2020). Genetic analysis using a multi-parent wheat population identifies novel sources of septoria tritici blotch resistance. *Genes* 11 (8), 887. doi: 10.3390/genes11080887

Rimbaud, L., Fabre, F., Papaix, J., Moury, B., Lannou, C., Barrett, L. G., et al. (2021). Models of plant resistance deployment. *Annu. Rev. Phytopathol.* 59, 125–152. doi: 10.1146/annurev-phyto-020620-122134

Robert, C., Garin, G., Abichou, M., Houles, V., Pradal, C., and Fournier, C. (2018). Plant architecture and foliar senescence impact the race between wheat growth and *Zymoseptoria tritici* epidemics. *Ann. Bot.* 121 (5), 975–989. doi: 10.1093/aob/mcx192

Rudd, J. J. (2015). Previous bottlenecks and future solutions to dissecting the *Zymoseptoria tritici*-wheat host-pathogen interaction. *Fungal Genet. Biol.* 79, 24–28. doi: 10.1016/j.fgb.2015.04.005

Saari, E., and Prescott, J. (1975). Scale for appraising the foliar intensity of wheat diseases. *Plant Dis. Reporter*. 377–380.

Savary, S., Willocquet, L., Pethybridge, S. J., Esker, P., McRoberts, N., and Nelson, A. (2019). The global burden of pathogens and pests on major food crops. *Nat. Ecol. Evol.* 3 (3), 430–439. doi: 10.1038/s41559-018-0793-y

Shin, J.-H., Blay, S., McNeney, B., and Graham, J. (2006). LDheatmap: an r function for graphical display of pairwise linkage disequilibria between single nucleotide polymorphisms. *J. Stat. Software* 16 (3), 1–10. doi: 10.18637/jss.v016.c03

Simón, M., Ayala, F., Cordo, C., Röder, M., and Börner, A. (2004). Molecular mapping of quantitative trait loci determining resistance to septoria tritici blotch caused by *Mycosphaerella graminicola* in wheat. *Euphytica* 138 (1), 41–48. doi: 10.1023/B:EUPH.0000047059.57839.98

St Clair, D. A. (2010). Quantitative disease resistance and quantitative resistance loci in breeding. *Annu. Rev. Phytopathol.* 48, 247–268. doi: 10.1146/annurev-phyto-080508-081904

Stram, D. O., and Lee, J. W. (1994). Variance components testing in the longitudinal mixed effects model. *Biometric* 1, 1171–1177. doi: 10.2307/2533455

Tabib Ghaffary, S. M., Chawade, A., and Singh, P. K. (2018). Practical breeding strategies to improve resistance to septoria tritici blotch of wheat. *Euphytica* 214 (7), 1-18. doi: 10.1007/s10681-018-2205-4

Tabib Ghaffary, S. M., Faris, J. D., Friesen, T. L., Visser, R. G., van der Lee, T. A., Robert, O., et al. (2012). New broad-spectrum resistance to septoria tritici blotch derived from synthetic hexaploid wheat. *Theor. Appl. Genet.* 124 (1), 125–142. doi: 10.1007/s00122-011-1692-7

Tabib Ghaffary, S. M., Robert, O., Laurent, V., Lonnet, P., Margale, E., van der Lee, T. A., et al. (2011). Genetic analysis of resistance to septoria tritici blotch in the French winter wheat cultivars balance and Apache. *Theor. Appl. Genet.* 123 (5), 741–754. doi: 10.1007/s00122-011-1623-7

Tang, Y., Liu, X., Wang, J., Li, M., Wang, Q., Tian, F., et al. (2016). GAPIT version 2: an enhanced integrated tool for genomic association and prediction. *Plant Genome* 9 (2), plantgenome2015-11. doi: 10.3835/plantgenome2015.11.0120

Tavella, C. M. (1978). Date of heading and plant height of wheat varieties, as related to septoria leaf blotch damage. *Euphytica* 27 (2), 577–580. doi: 10.1007/BF00043184

Team, R. C (2020). *R: A language and environment for statistical computing. R Foundation for Statistical Computing. R Foundation for Statistical Computing.* Available at: https://www.R-project.org/.

Vagndorf, N., Nielsen, N. H., Edriss, V., Andersen, J. R., Orabi, J., Jørgensen, L. N., et al. (2017). Genomewide association study reveals novel quantitative trait loci

associated with resistance towards septoria tritici blotch in north European winter wheat. *Plant Breed.* 136 (4), 474–482. doi: 10.1111/pbr.12490

VanRaden, P. M. (2008). Efficient methods to compute genomic predictions. *J. Dairy Sci.* 91 (11), 4414–4423. doi: 10.3168/jds.2007-0980

Wang, S., Wong, D., Forrest, K., Allen, A., Chao, S., Huang, B. E., et al. (2014). Characterization of polyploid wheat genomic diversity using a high-density 90,000 single nucleotide polymorphism array. *Plant Biotechnol. J.* 12 (6), 787–796. doi: 10.1111/pbi.12183

Wellings, C., Park, R. F., Simpfendorfer, S., Wallwork, H., and Shankar, M. (2012). "Adult plant resistance," in *Fact sheet* (GRDC). Available at: https://grdc.com.au/.

Würschum, T., Leiser, W. L., Longin, C. F. H., and Bürstmayr, H. (2017). Molecular genetic characterization and association mapping in spelt wheat. *Plant Breed.* 136 (2), 214–223. doi: 10.1111/pbr.12462

Xu, K., He, X., Dreisigacker, S., He, Z., and Singh, P. K. (2019). Anther extrusion and its association with fusarium head blight in CIMMYT wheat germplasm. *Agronomy* 10 (1), 47. doi: 10.3390/agronomy10010047

Yan, L., Loukoianov, A., Tranquilli, G., Helguera, M., Fahima, T., Dubcovsky, J., et al (2018). Positional cloning of the wheat vernalization gene VRN1. *Proceedings of the National Academy of Sciences* 100 (10), 6263–6268. doi: 10.1073/pnas.093739910

Yang, N., McDonald, M. C., Solomon, P. S., and Milgate, A. W. (2018). Genetic mapping of Stb19, a new resistance gene to *Zymoseptoria tritici* in wheat. *Theor. Appl. Genet.* 131 (12), 2765–2773. doi: 10.1007/s00122-018-3189-0

Yates, S., Mikaberidze, A., Krattinger, S. G., Abrouk, M., Hund, A., Yu, K., et al. (2019). Precision phenotyping reveals novel loci for quantitative resistance to septoria tritici blotch. *Plant Phenomics* 2019, 1–11. doi: 10.34133/2019/3285904

Zadoks, J. C., Chang, T. T., and Konzak, C. F. (1974). A decimal code for the growth stages of cereals. *Weed Res.* 14 (6), 415–421. doi: 10.1111/j.1365-3180.1974.tb01084.x

Zhang, Z., Ersoz, E., Lai, C.-Q., Todhunter, R. J., Tiwari, H. K., Gore, M. A., et al. (2010). Mixed linear model approach adapted for genome-wide association studies. *Nat. Genet.* 42 (4), 355–360. doi: 10.1038/ng.546

Zhang, J., Zhang, P., Dodds, P., and Lagudah, E. (2020). How target-sequence enrichment and sequencing (TEnSeq) pipelines have catalyzed resistance gene cloning in the wheat-rust pathosystem. *Front. Plant Sci.* 11. doi: 10.3389/fpls.2020.00678

Zwart, R. S., Thompson, J. P., Milgate, A. W., Bansal, U. K., Williamson, P. M., Raman, H., et al. (2010). QTL mapping of multiple foliar disease and root-lesion nematode resistances in wheat. *Mol. Breed.* 26 (1), 107–124. doi: 10.1007/s11032-009-9381-9

Stb6 mediates stomatal immunity, photosynthetic functionality, and the antioxidant system during the *Zymoseptoria tritici*-wheat interaction

Fateme Ghiasi Noei[1‡], Mojtaba Imami[1‡], Fardad Didaran[2‡],
Mohammad Amin Ghanbari[3], Elham Zamani[1], Amin Ebrahimi[4],
Sasan Aliniaeifard[2], Mohsen Farzaneh[5],
Mohammad Javan-Nikkhah[1], Angela Feechan[6†]
and Amir Mirzadi Gohari[1*]

[1]Department of Plant Pathology, Faculty of Agricultural Sciences and Engineering, College of Agriculture and Natural Resources, University of Tehran, Karaj, Iran, [2]Photosynthesis Laboratory, Department of Horticulture, Aburaihan Campus, University of Tehran, Tehran, Iran, [3]Department of Horticultural Science, School of Agriculture, Shiraz University, Shiraz, Iran, [4]Agronomy and Plant Breeding Department, Faculty of Agriculture, Shahrood University of Technology, Semnan, Iran, [5]Department of Agriculture, Medicinal Plants and Drugs Research Institute, Shahid Beheshti University, Tehran, Iran, [6]School of Agriculture and Food Science, University College Dublin, Dublin, Ireland

This study offers new perspectives on the biochemical and physiological changes that occur in wheat following a gene-for-gene interaction with the fungal pathogen *Zymoseptoria tritici*. The *Z. tritici* isolate IPO323, carries *AvrStb6*, while *ΔAvrStb6#33*, lacks *AvrStb6*. The wheat cultivar (cv.) Shafir, bears the corresponding resistance gene *Stb6*. Inoculation of cv. Shafir with these isolates results in two contrasted phenotypes, offering a unique opportunity to study the immune response caused by the recognition of AvrStb6 by Stb6. We employed a variety of methodologies to dissect the physiological and biochemical events altered in cv. Shafir, as a result of the AvrStb6-Stb6 interaction. Comparative analysis of stomatal conductance demonstrated that AvrStb6-Stb6 mediates transient stomatal closures to restrict the penetration of *Zymoseptoria tritici*. Tracking photosynthetic functionality through chlorophyll fluorescence imaging analysis demonstrated that AvrStb6-Stb6 retains the functionality of photosynthesis apparatus by promoting Non-Photochemical Quenching (NPQ). Furthermore, the PlantCV image analysis tool was used to compare the H_2O_2 accumulation and incidence of cell death (2, 4, 8, 12, 16, and 21 dpi), over *Z. tritici* infection. Finally, our research shows that the AvrStb6-Stb6 interaction coordinates the expression and activity of antioxidant enzymes, both enzymatic and non-

enzymatic, to counteract oxidative stress. In conclusion, the Stb6-AvrStb6 interaction in the *Z. tritici*-wheat pathosystem triggers transient stomatal closure and maintains photosynthesis while regulating oxidative stress.

Introduction

Zymoseptoria tritici (previously known as *Mycosphaerella graminicola*) which causes septoria tritici blotch (STB) is a notorious fungal pathogen limiting wheat production worldwide and threatening global food security (Quaedvlieg et al., 2011). Under favorable conditions, this destructive pathogen leads to significant yield losses and lowers the grain quality (Eyal, 1999). *Z. tritici* is a typical hemibiotroph whose lifestyle constitutes two distinct stages. The asymptomatic biotrophic growth is initiated by germination of the landed conidia on the leaf surface and penetration directly through the stomata. This fungus then colonizes the mesophyll tissue intercellularly without causing visible damage to the wheat host cells. The biotrophic stage lasts 7–10 days, depending on the fungal isolates and wheat genotypes used. This stage is characterized by the induction of weak plant defence (Rudd et al., 2015). Following this stage, *Z. tritici* undergoes the necrotrophic phase, when it begins to release a plethora of cell wall-degrading enzymes to damage plant tissues, eventually leading to the emergence of STB disease. This rapid colonization plays a pivotal role in the build-up of fungal biomass and developing asexual fruiting bodies (pycnidia) (Kema et al., 1996). At the transition phase, energy is redirected away from other photosynthetic areas in the damaged tissue while genes implicated in the photosynthesis process are noticeably down-regulated during the necrotrophic stage (Rudd et al., 2015).

The effector AvrStb6 and wheat resistance protein Stb6 follow the gene-for-gene paradigm for the *Z. tritici*-wheat interaction. The *Z. tritici* IPO323 isolate has the avirulence protein AvrStb6, which is likely recognized by the matching resistance protein Stb6, culminating in host immunity. The IPO323 isolate fails to infect the wheat cv. Shafir harboring *Stb6*, however the IPO323 mutant lacking *AvrStb6* (*ΔAvrStb6#33*) was pathogenic on this cultivar (Kema et al., 2018).

Photosynthesis is a crucial process in plant physiology in which chlorophyll molecules in the chloroplast receive light energy and utilize it to make oxygen and energy-rich chemicals. The biosynthesis of secondary metabolites and defence-related phytohormones such as jasmonic acid and salicylic acid, as well as the regulation of this process, play a critical role in supplying defensive responses to biotic and abiotic stimuli (Kretschmer et al., 2019). Chlorophyll *a* fluorescence (ChlF) is a sensitive and non-invasive tool to investigate the photochemical efficiency of leaves under biotic and abiotic stress. ChlF offers valuable quantitative data for evaluating the photosynthetic performance (Kalaji et al., 2017). This method has been frequently used to study photosynthetic functionality under abiotic (e.g. heavy metal toxicity, drought and salinity stresses) and biotic (fungal attack) stresses (Paunov et al., 2018; Mihailova et al., 2019).

Under cellular stress, chloroplasts overproduce reactive oxygen species (ROS) to counteract adverse circumstances, such as fungal invasion. It's worth noting that ROS molecules such as H_2O_2 have a dual function: they may either operate as signaling molecules that cause programmed cell death or they can stop fungal development by having a direct antifungal effect (Li and Kim, 2021). Under pathogen attack, the attempted infection sites experience an oxidative burst event, characterized by a quick and extensive accumulation of these harmful free radicals. This biological mechanism plays a key role in defining compatibility/incompatibility (Torres, 2010). A previous study demonstrated that ROS molecules accumulated to higher levels in incompatible interactions than in compatible contexts possibly to halt hyphal growth at the biotrophic phase in the *Z. tritici*-wheat interaction. ROS are produced extensively in the compatible interaction to aid the infection process, which coincides with tissue collapse and the production of pycnidia (necrotrophic stage) (Shetty et al., 2003). However, ROS are continually produced at a low level in chloroplasts during photosynthesis, which is unharmful to live cells because multiple antioxidant enzymes maintain a balance between synthesizing and detoxifying ROS molecules (Apel and Hirt, 2004).

This study compares the physiological and biochemical changes in cv. Shafir inoculated by *Z. tritici* IPO323 and the knockout mutant lacking *AvrStb6* (*ΔAvrStb6#33*). (Kema et al., 2018). The ChlF technique and microscopic analysis were used to evaluate the impact of the AvrStb6-Stb6 interaction on the photosynthetic functionality and stomatal-related features,

respectively. We also employed DAB and trypan blue staining techniques in conjunction with the image analysis program PlantCV to identify and quantify the amount of H_2O_2 accumulated in infected tissues and/or the occurrence of cell death. Oxidative stress was measured by changes in levels of malondialdehyde (MDA) and electrolyte leakage (EC). Five phenolic compounds were investigated as non-enzymatic antioxidant agents using high-performance liquid chromatography (HPLC) in both examined interactions. Proline which has antioxidant activity, was evaluated (Hayat et al., 2012). The activities of five enzymatic antioxidant agents, including the superoxide dismutase (SOD), Catalase (CAT), Guaiacol peroxidase (GPX), Ascorbate peroxidase (APX), and Glutathione reductase (GR) were also investigated during infection with IPO323 and *ΔAvrStb6#33*.

Measurements were undertaken (2, 4, 8, 12, 16 and 21 dpi) corresponding to three phases of *Z. tritici* infection; the biotrophic stage (2-4 dpi)), the transition from biotrophy to necrotrophy (8 dpi), and the necrotrophic stage (12, 16, and 21 dpi). This study revealed that *Stb6* in the cv. Shafir triggers transient stomatal closure and maintains photosynthesis while regulating oxidative stress.

Material and methods

Biological materials

Throughout the experiments, *Z. tritici* IPO323 (WT) and the corresponding mutant strain *ΔAvrStb6#33* were utilized (Kema et al., 2018). Both strains were stored at -80°C before being re-cultured at 18°C on a V8 juice medium (Campbell Foods, Puurs, Belgium). Yeast Malt Dextrose Broth (YMDB) medium (Yeast extract 4 g/L, Malt 4 g/L, and Dextrose 4 g/L) was used to abundantly generate yeast-like spores by growing the strains on this medium and placing the inoculated flasks in an orbital shaker (Innova 4430; New Brunswick Scientific, Nijmegen, The Netherlands) at 18°C for 5-7 days. The wheat cultivar Shafir, which carries the resistance gene *Stb6*, was employed in the infection assay (Mirzadi Gohari et al., 2014; Saintenac et al., 2018). Wheat cv. Shafir infected with IPO323 were designated as incompatible interaction, while those inoculated with *ΔAvrStb6#33* were marked as a compatible interaction.

Stomatal measurement

Stomatal morphological features (including stomatal length, stomatal width, pore aperture, stomatal index, and density), were first calculated using the previously described protocol (Aliniaeifard and Van Meeteren, 2016). Subsequently, stomatal conductance (g_s) of the inoculated and non-inoculated leaves surfaces were measured at 2,4, 8, 12, 16, and 21 dpi by following

the protocol described previously (Fanourakis et al., 2013). Based on the assumption that guard cells inflate to form a circular cross-section, the stomatal pore depth was calculated as being equal to the guard cell width (stomatal width/2). On three randomly chosen areas of the same leaf, stomata were counted and their sizes measured. A total of twelve leaves derived from four biological samples were examined and this was repeated independently twice. One square millimeter of leaf tissue was analyzed on both sides of the main vein. The following equation was utilized to calculate g_s (Fanourakis et al., 2013):

$$\left[gs = \frac{(diffusion\ coefficient) \times (stomatal\ density) \times (\pi \times poreapperture \div 2 \times porelength \div 2)}{(molar\ volume\ of\ air) \times [(pore\ depth) + \sqrt{(pore\ apperture \div 2 \times pore\ length \div 2)]}} \right]$$

Polyphasic chlorophyll fluorescence transients

The OJIP transients of dark-adapted (20 min) plants were measured using a Fluorpen FP 100-MAX (Photon Systems Instruments, Drasov, Czech Republic) at 2, 4, 8, 12, 16, and 21 dpi. The OJIP protocol was used to investigate biophysical and phenomenological parameters related to plant stress and photosystem II (PSII) status (listed in Supplementary Table 1), as described previously (Strasser et al., 2000). The energy fluxes of light absorption (ABS) and trapping (TR) of the excitation energy, as well as electron transport (ET_O) per reaction center (RC), are described in Supplementary Table 1 using parameters derived from the OJIP protocol.

Chlorophyll fluorescence imaging analysis

A FluorCam device (FluorCam FC 1000-H, Photon Systems Instruments, PSI, Czech Republic) was employed to image the chlorophyll fluorescence of dark-adapted (20 min) plants at multiple time points, including 2, 4, 8, 12, 16, and 21 dpi. Maximum quantum yield of photosystem II (F_V/F_M) was determined using a custom protocol depicted previously (Shomali et al., 2021). Measurements of chlorophyll fluorescence began with the samples being exposed to short flashes in darkness, followed by a saturating pulse for longer duration of 3900 mol m^{-2} s^{-1} Photosynthetic photon flux density (PPFD) at the end of the measurement to stop electron transport due to Quinone acceptor reduction (Genty et al., 1989). Two sets of fluorescence data were recorded using the applied protocol: one averaged over the time of short flashes in the dark (Fo) and the other at the time of exposure to saturating flash (F_M). Maximum fluorescence in light-adapted steady-state (F_M') was measured to determine the non-photochemical quenching (NPQ). FluorCam software version 7 (PSI, Czech Republic)

was used to analyze the data. The Fv/F$_M$ was estimated through the following equation: Fv/F$_M$= (F$_M$-F$_O$)/F$_M$. Additionally, the NPQ was calculated based on the following equation: NPQ = (F$_M$/F$_M$')-1.

In planta detection of H$_2$O$_2$ and cell death

Detection of H$_2$O$_2$ in planta was conducted through staining by 3,3 diaminobenzidine (DAB, D-8001, Sigma) (Thordal-Christensen et al., 1997). The inoculated leaves were harvested at 2, 4, 8, 12, 16, and 21 dpi, and placed in a container filled with acidic water (pH 3.8), containing 1 mg/ml DAB under darkness. The container was kept in a desiccator equipped with a vacuum pump to generate a suction force of 0.2 bar for 30 min, and this was maintained overnight. Following the next day, a clearing procedure to eliminate chlorophyll was conducted using absolute ethanol/acetic acid/glycerol (3:1:1) for 30 min at 80 °C (Shetty et al., 2003). Dead cells and fungal structures were stained using trypan blue based on the procedure reported by Koch and Slusarenko (1990) (Koch and Slusarenko, 1990). These assays were repeated independently three times.

Image processing

The integrated optical density (IOD) of leaves areas stained either by DAB or trypan blue was obtained using PlantCV (Gehan et al., 2017). The multiclass naive Bayes approach based on RGB pixel values was utilized for this purpose. The classes included background, unstained, and three staining intensities (low, medium, and high). These classifications are based on how intensely the colour is present in the stained tissues; these intensities were first visually classified, and then the colour spectrum was detected using Photoshop software. For machine learning to define the three intensities level, a table of red, green, and blue color values was created from 50 pixels in each class, with each column of the table allocated to a specific class (Díaz-Tielas et al., 2012). Ultimately, thousands of pixels in all leaves were sorted into these classes using machine learning data. The table was used to generate probability density functions (PDFs) for each of the classes. The RGB values were extracted from the leaf images using Adobe Photoshop (Version 23.1.0).

Infection biology

Inoculated leaves of the wheat cv. Shafir was collected at 2, 4, 8, 12, 16, and 21 dpi to investigate the infection biology of Z. tritici in both compatible and incompatible interactions. At each sampling time, a total of twelve leaves derived from four

biological samples were harvested, followed by clearing using absolute ethanol/acetic acid/glycerol (3:1:1) for 30 min at 80 °C to eliminate the natural pigment of the examined leaves (Shetty et al., 2003). Four biological samples were used in this assay, which was independently performed twice. Afterward, microscopic slides were prepared from the inoculated part of the leaves using lactophenol solution. The prepared slides were examined through an Olympus® light microscope (Olympus, Tokyo, Japan). Studying the quantitative developmental stages of employed strains in planta was conducted based on the previously reported protocol (Shetty et al., 2003).

Antioxidant enzymes activity

Harvested samples were homogenized in an extraction buffer comprising 15% acetic acid and 85% methanol. These homogenates were centrifuged at 12,000 rpm for 15 minutes at 4°C. The resulting supernatant were filtered with a 0.45 µm disposable syringe, and this solution was used to measure antioxidant enzyme activity. The superoxide dismutase (SOD) activity was determined based on its inhibition in the photoreduction reduction by the nitroblue tetrazolium (NBT). The final reaction was read spectrophotometrically through a spectrophotometer device (UV-1800; Shimadzu Corporation, Kyoto, Japan) at a wavelength of 560 nm as documented earlier (Beauchamp and Fridovich, 1971). Catalase (CAT) activity was measured spectrophotometrically, and the absorbance recorded at 240 nm (Ranieri et al., 2003). Guaiacol peroxidase (GPX) activity was estimated at 25°C through a spectrophotometer tool adjusted at 470 nm (Hemeda and Klein, 1990). Ascorbate peroxidase (APX) activity was measured by following the procedure depicted previously (Ranieri et al., 2003). Finally, the Glutathione reductase (GR) activity was spectrophotometrically estimated at 412 nm (Smith et al., 1988).

HPLC-UV analysis of phenolic compounds

As previously reported, the HPLC profile analysis of methanolic extracts was performed using a Waters 2695 Alliance HPLC system with a 996 PDA detector to monitor phenolic compounds (Mansoor et al., 2020). The gradient programme was run for 60 min using (A) methanol+ 0.02 percent TFA; and (B) HPLC grade water+ 0.02 percent TFA, with a flow rate of 0.5 mL min^{-1} on the C18 column (Novapack C18, 4.6 15 mm, 4 m). Peaks were monitored at wavelengths of 200-400 nm, and each phenolic compound was identified by comparing its spectra and retention time to standards. The external standard method was used to make quantitative determinations with commercial standards. Results are

expressed as parts per million (ppm). Here, we traced five phenolic compounds in the investigated interactions as described in Supplementary Table 2.

Proline content

The reported procedure was applied to measure the proline content (Bates et al., 1973). Briefly, 300 mg of leaves were homogenized in 10 ml of 3% sulphosalicylic acid. The solutions were centrifuged at 2,000 g for 5 min. The extract was then mixed with acidic-ninhydrine and glacial acetic acid for 45 min at 100°C. Toluene was used to extract the reaction mixture. Separated toluene's chromophore. Using a UV–Vis spectrophotometer, 515 nm absorbance was read (UV-1800; Shimadzu Corporation, Kyoto, Japan).

Disruption of membrane integrity

To investigate disruption in cell membrane integrity, malondialdehyde (MDA) content and electrolyte leakage were measured. MDA content was calculated as reported previously with minor modification (Stewart and Bewley, 1980). Harvested samples (0.25 g) were homogenized in 5% (w/v) trichloroacetic acid (TCA) and centrifuged at 10000 rpm for 15 min. Sample supernatant (1 mL) was mixed with 5 mL of trichloroacetic acid containing 0.5% thiobarbituric acid (TBA). The mixture was boiled at 95°C for 30 min. The absorbance at 532 and 600 nm was measured. The non-specific absorbance at 600 nm was subtracted from what was measured at the absorbance of 532 nm. The concentration of MDA was measured *via* the extinction coefficient of 155 mM^{-1} cm^{-1}. The electrolyte leakage was estimated by applying the previously documented protocol (Bajji et al., 2002). Briefly, five leaves with 10 ml distilled water were punched. The containers were shaken in an orbital shaker for 24 h at 150 rpm, and the electrolyte conductivity (EC0) was read. The leaves were autoclaved at 120°C for 20 min to determine the maximum leakage, and immediately, electrolyte conductivity (EC1) was estimated after cooling. Eventually, the percentage of leaf electrolytes leakage (EL) was calculated as documented previously (Bajji et al., 2002).

Statistical analysis

The data were analyzed using SAS software (version 9.0). The two-way analysis of variance (ANOVA) was used to find the significant differences (p ≤ 0.05) and then the Duncan multiple comparisons test was used to compare the means. For analyzing chlorophyll fluorescence parameters, obtained data were subjected to two-way ANOVA, and for mean comparison, the Tukey multiple comparison tests were used. For stomatal

characteristics, data was collected from each single leaf on three randomly chosen areas of the same leaf, stomata were counted and their sizes measured. Stomatal features were deemed to be non-independent, and a two-way ANOVA and Tukey multiple comparison tests were used to compare mean values. Odds ratios were calculated for comparison of the variables (percentages) using cv. Shafir inoculated by *ΔAvrStb6#33* as a reference, as previously reported (Shetty et al., 2003). The spider plots were produced using Microsoft Excel 2020, which aided in the accurate evaluation of the parameters gathered from the OJIP data. For all analyses, we assumed a significance level of 0.05.

Results

AvrStb6-Stb6 establishes resistance reaction

The cultivar Shafir which carries *Stb6* (Zhong et al., 2017) was inoculated by IPO323 and *ΔAvrStb6#33* strains to validate the impact of *AvrStb6* deletion on STB development. Typical STB symptoms, including the emergence of small chlorotic specks formed specifically at the tip of the leaves, which become visible at 8 dpi in plants challenged by the *ΔAvrStb6#33* strain while no symptoms appeared in the plants inoculated by IPO323. In the compatible interaction, the chlorotic lesions expanded into larger areas at 12 dpi and, subsequently, coalesced into typical necrotic STB blotches bearing numerous pycnidia at 16 dpi (Supplementary Figure 1A). At 21 dpi, the inoculated leaves became completely necrotic and covered by abundant asexual fruiting bodies; the necrotic leaf area was 100% ± 0 and pycnidia formation was 89% ± 1 following *ΔAvrStb6#33* infection while no pycnidia were formed on plants inoculated by IPO323 (Supplementary Figures 1B, C).

AvrStb6-Stb6 mediates transient stomatal closures

We investigated the stomatal pore width and stomatal conductance (g_s) of treated plants at 2, 4, 8, 12, 16, and 21 dpi to explore stomatal function as a defensive response (Grimmer et al., 2012) towards *Z. tritici* infection. At 2 dpi, the highest pore width was observed in plants infected by *ΔAvrStb6#33*, while the lowest was found for IPO323-inoculated plants. Following the transition stage (8 dpi), the pore width of resistant plants remained constant without further fluctuations by 21 dpi, while that of susceptible plants underwent a dramatic reduction to almost zero at later time points (16 and 21 dpi). The g_s ratio followed the same pattern as described for the stomatal pore width. For instance, the g_s of resistant plants

declined by 32% at 2 dpi, whereas that of mock and susceptible plants remained at the same level, which was around 5000 mmol m^{-2} s^{-1}. Therefore, our microscopic observation at 2 dpi demonstrated that stomatal closure occurred only in plants infected with IPO323, whereas stomata were semi-open in mock treated and open in plants inoculated by isolate *ΔAvrStb6#33* (Figure 1).

AvrStb6-Stb6 interaction maintains photosynthetic functionality primarily by maintaining NPQ

Since *Z. tritici* causes chlorosis and necrotic lesions on wheat leaves, we speculate it may affect the hosts photosynthetic apparatus. The photosynthetic functionality following inoculation with IPO323 and *ΔAvrStb6#33* (incompatible and compatible interactions, respectively) was recorded. F_O, F_i, F_j, F_v and F_m dropped significantly from 78.8-100% in the cv. Shafir inoculated by *ΔAvrStb6#33* compared to those of plants infected by IPO323 at 16 and 21 dpi (Supplementary Table 3). At 8 dpi, the F_V/F_M ratio, as an indicator of PSII's maximum quantum efficiency, was slightly reduced (9.5% from 4 dpi) in plants infected by IPO323, but this ratio increased at 12 dpi (6% from 8 dpi) and remained constant between 12 to 21 dpi. However, in contrast, the F_V/F_M ratio was drastically reduced in compatible interactions following *ΔAvrStb6#33* infection. As a result, following 12 dpi the ratio (0.62) decreased to zero at 16 and 21 dpi (Figure 2A). The PI_{abs} (photosynthetic performance index) was significantly higher at 2dpi in the Mock treated plants and those inoculated with *ΔAvrStb6#33* compared to

IPO323 inoculated plants at 2 dpi. The PI_{abs} significantly decreased in plants inoculated with *ΔAvrStb6#33* from 8 dpi (1.97) to 0 at 16 dpi. During the incompatible interaction (plants inoculated with IPO323), PI_{abs} decreased 50% at 8 dpi (0.52) compared with that of this index measured at 4 dpi (1.34). Following that, this index recovered at 12 dpi and remained stable until 21 dpi (Figure 2B). In the compatible interaction (plants inoculated with *ΔAvrStb6#33*), the highest ABS/RC and DI_0/RC peaked at 12 dpi before falling to 0 at 16 dpi. While ET_0/RC and TR_O/RC parameters suddenly decreased at 16 dpi during the compatible interaction (Figures 3A-D). In contrast during the incompatible interaction, plants inoculated with IPO323 had a relatively constant ABS/RC and DI_0/RC with a small but significant increase between 8 dpi and 12 dpi. The ET_0/RC gradually declined from 2 dpi to 8 dpi before recovering to a similar level to that found for the compatible interaction at 12 dpi and remaining stable until 21 dpi (Figure 3B). TR_O/RC was significantly reduced in the incompatible interaction at the transition stage (8 dpi), but at 12 dpi returned to levels previously found at 2 and 4 dpi (Figure 3C).

The efficiency for electron transfer ($Φ_{E0}$) and energy dissipation ($Φ_{D0}$) were computed to evaluate the energy flow in the photosynthesis process of two studied interactions. The $Φ_{E0}$ was reduced by 36% in the incompatible interaction between 4 and 8 dpi. Afterward, the $Φ_{E0}$ was elevated by 36% between 8 and 12 dpi returning to previous levels and remaining unaltered until 21 dpi. The $Φ_{E0}$ during the compatible interaction dropped by 52% between 8 and 12 dpi, thereafter it had completely stopped by 16 dpi (Supplementary Table 3). The highest $Φ_{D0}$ was found in compatible interactions at 16 and 21 dpi, while no
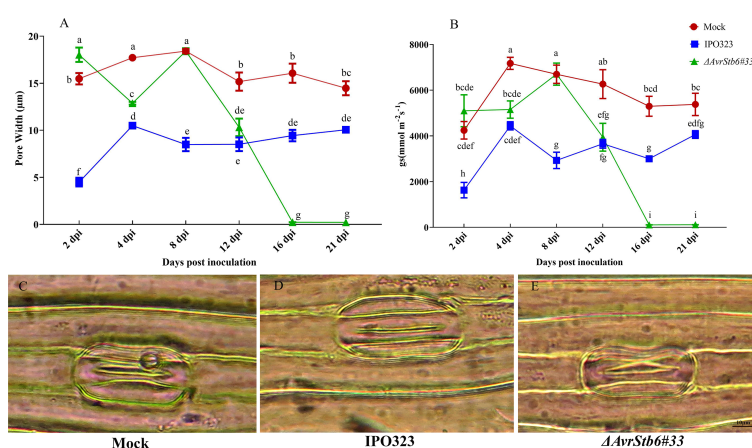
FIGURE 1
The effect of AvrStb6-Stb6 interaction on stomatal pore width and gas exchange. **(A)** Measuring the stomatal pore width of cv. Shafir inoculated by distilled water (Mock), the WT strain carrying the *AvrStb6* (IPO323), and deleted mutant for *AvrStb6* (*ΔAvrStb6#33*); **(B)** estimating the g_s ratio of the treated plants; **(C)** Microscopic picture of a stomata from a plant treated with distilled water (Mock: semi-open); **(D)** inoculated by IPO323 (closed), and **(E)** inoculated by *ΔAvrStb6#33* (open). Data indicate mean $\pm$ SD (Standard Deviation) of twelve individual leaves derived from four biological samples. This assay was repeated independently twice. Different lowercase letters indicate statistically significant differences (P≤0.05).
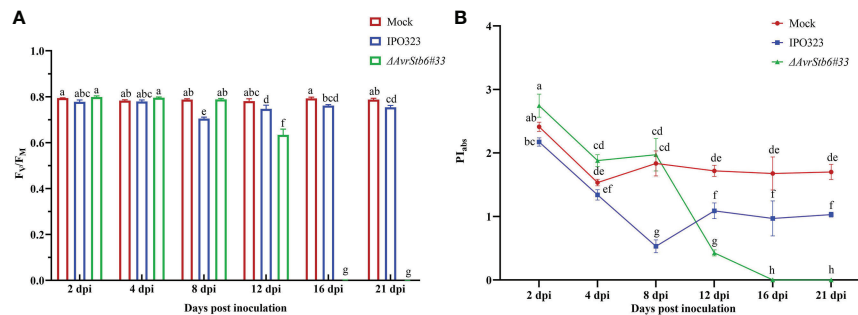
FIGURE 2

The impact of AvrStb6-Stb6 relationship on the maximum quantum yield of PSII (Fv/F$_M$) **(A)** and Performance index (PI$_{abs}$) **(B)** parameters. The leaves of cv. Shafir harboring Stb6 were inoculated with the WT IPO323 and *AvrStb6#33* strains. The essential parameters to calculate the Fv/F$_M$ and PI$_{abs}$ were measured by a Fluorpen FP at several time points, including 2, 4, 8, 12, 16, and 21 days post-inoculation. Data are indicate as mean $\pm$ SD (Standard Deviation) of four biological samples from one independent experiment. Different lowercase letters indicate statistically significant differences (P$\leq$0.05).

fluctuations were found for the mock treated plants throughout (Supplementary Table 3). All of the parameters derived from the chlorophyll fluorescence OJIP curves are presented as a spider plot (Supplementary Figure 2).

The release of energy in the form of heat and fluorescence (NPQ) increased steadily in all interactions, from 2-4 dpi. After 8 dpi, there was a sudden and sharp decrease in NPQ (a 95% decrease) in the compatible interaction between 8-12 dpi,

remaining low without significant changes until 21 dpi. In the incompatible interaction, the NPQ began to rise slowly, by 26.2% between 2-4 dpi and fell 20% between 4-8 dpi. Following the switching stage at 8 dpi, there was an increase of 17% where this ratio reached similar levels to that of control plants at 12 and 16 dpi. The NPQ fell again by 25% between 16 dpi and 21 dpi (Figure 4). Modification occurred in the photosynthetic parameters and chlorophyll fluorescence images of infected
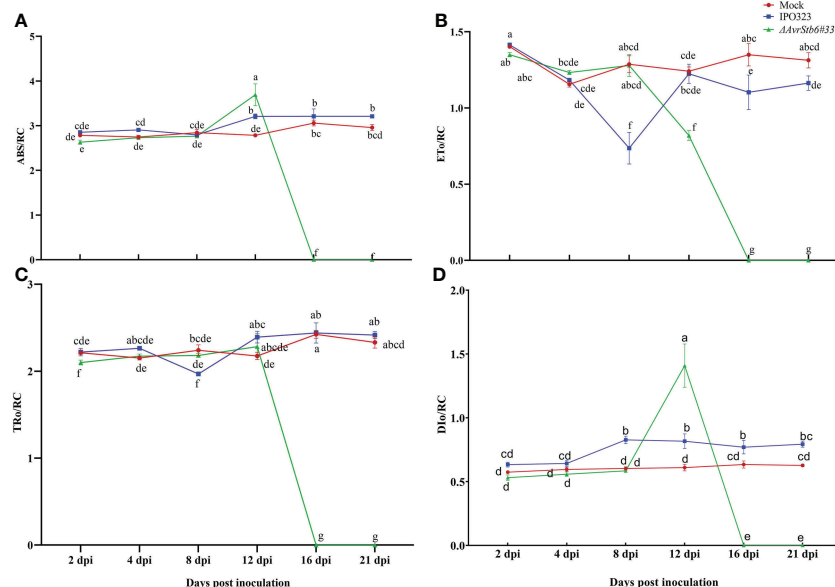
FIGURE 3

AvrStb6-Stb6 interaction impacts ABS/RC **(A)**, ET$_0$/RC (L688) **(B)**, TR$_0$/RC (L688) **(C)**, and DI$_0$/RC (L688) **(D)** H$_2$O$_2$ (L897)parameters. The WT IPO323 and *ΔAvrStb6#33* strains were applied to infect the leaves of cv. Shafir harboring the Stb6. The Fluorpen FP instrument was used to measure the key parameters for calculating the ABS/RC **(A)**, ET$_0$/RC **(B)**, TR$_0$/RC **(C)**, and DI$_0$/RC **(D)** parameters at multiple days post-inoculation, including 2, 4, 8, 12, 16, and 21 days. Data are indicate as mean $\pm$ SD (Standard Deviation) of four biological samples from one independent experiment. Different lowercase letters indicate statistically significant differences (P$\leq$0.05).
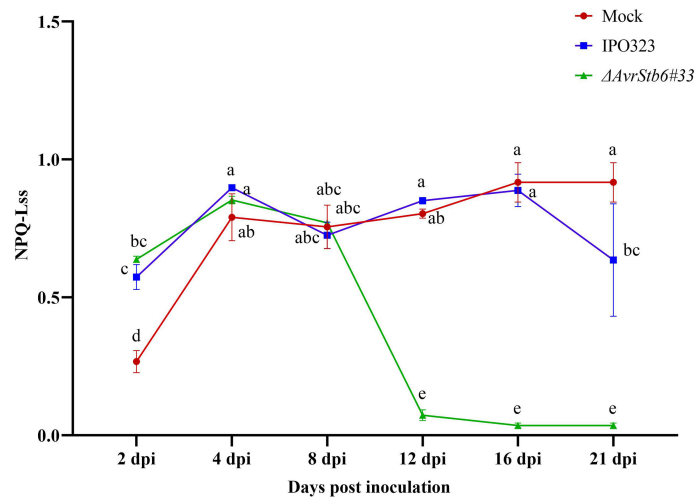
FIGURE 4

AvrStb6-Stb6 interaction leads to high non-photochemical quenching (NPQ). The leaves of cv. Shafir with Stb6 was infected with either the WT IPO323 and *ΔAvrStb6#33* strains and NPQ was recorded at 2, 4, 8, 12, 16, and 21 days post-inoculation. Data are indicate as mean ± SD (Standard Deviation) of four biological samples from one independent experiment. Different lowercase letters indicate statistically significant differences (P≤0.05).

wheat leaves taken at 2, 4, 8, 12, 16, and 21 dpi were presented in the Supplementary Figure 3.

AvrStb6-Stb6 regulates H_2O_2 accumulation and cell death occurrence

We histochemically compared the accumulation of H_2O_2 and the onset of cell death at several time points, including 2, 4, 8, 12, 16, and 21 dpi, to assess the role of H_2O_2 and cell death in two studied interactions. In the incompatible interaction, the timing and accumulation of H_2O_2 and cell death was found at low levels 2-4 dpi peaking at 8 dpi (Figure 5). Following the switch (8 dpi), no extensive generation and localization of H_2O_2 or widespread cell death were observed at the necrotrophic stage (12, 16, and 21 dpi). Plants infected with the *ΔAvrStb6#33* (compatible interaction), on the other hand, showed steady H_2O_2 accumulation and cell death from 2 dpi onwards displaying high levels of H_2O_2 accumulation and the occurrence of cell death at the necrotrophic growth stage (12, 16, and 21 dpi). Therefore, in the compatible interaction, dramatic and uncontrolled H_2O_2 accumulations occurs, leading to the complete death of the inoculated leaves at 21 dpi. The PlantCV program was also used to quantify the stained area of infected leaves by DAB. Our findings demonstrated that the incompatible interaction produces substantially more H_2O_2 than the susceptible plants during the transition stage (8 dpi) (Figure 5A). Similar results were achieved for trypan blue staining and the PlantCV tool. At 8 dpi, substantial cell death

occurred in the incompatible interaction compared with the compatible interaction. Additionally, high levels of cell death occurred following infection of wheat with *ΔAvrStb6#33* at the necrotrophic stage (Figure 5B).

AvrStb6-Stb6 blocks fungal growth and pycnidial formation

The spores of the employed strains germinated by forming thin germ tubes penetrated directly through stomata by 2 dpi (Figures 6A–E). The percentage of spores that germinated was low (15–29%) (Supplementary Table 4), but it did not differ significantly between the compatible and incompatible interaction at each of the time-points. The directions of germ tubes derived from germinating spores were divided into three categories, but there were no significant differences in the number of germ tubes in each category between the two interactions, as shown in Supplementary Table 4. In the incompatible interaction, H_2O_2 accumulated in stained cells 2-8 dpi to a higher level than found in plants inoculated by the *ΔAvrStb6#33* strain (Figures 5A, 6B–F). This occurred particularly around the substomatal cavity where penetration happened (Figure 6B). H_2O_2 accumulated around the fungal hyphae starting to move into mesophyll cells, and no hyphal growth beyond the H_2O_2 accumulation was observed. In the compatible interaction, hyphal growth was found at the switching phase (8 dpi) possibly as the accumulated H_2O_2 was inadequate to suppress the hyphal progression (Figure 6G). Cell collapse associated with cytoplasmic-like shrinkage was also found in the
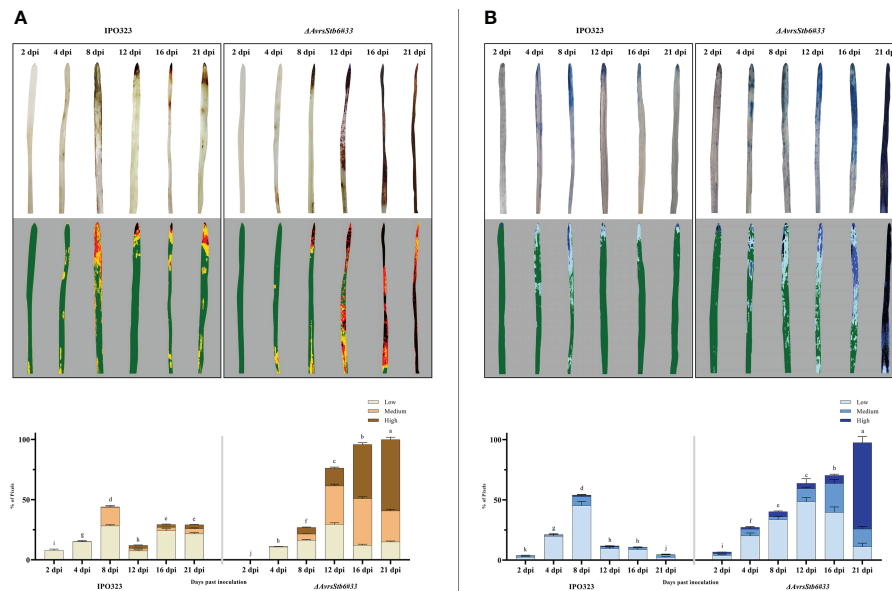
FIGURE 5

AvrStb6-Stb6 interaction affects both the accumulation of hydrogen peroxide (H_2O_2) following staining by DAB signified by the red-brown areas **(A)** and the occurrence of cell death indicated as dark-blue areas stained by the trypan blue **(B)**. Pictures were taken at 2, 4, 8, 12, 16, and 21 dpi. The images were analyzed by the PlantCV software to obtain the integrated optical density (IOD), displaying the percentage of the stained cells by DAB and trypan blue. Data are indicate as mean $\pm$ SD (Standard Deviation) of four biological samples from three independent experiments. Different lowercase letters indicate statistically significant differences (P$\leq$0.05).

incompatible context at 8 dpi (Figure 6D). Massive H_2O_2 accumulation was observed at 12 dpi, coinciding with the pycnidial formation and tissue collapse. Mature asexual fruiting bodies (Figure 6H) along with cell death of plant tissues were found at 16 and 21 dpi, respectively.

AvrStb6-Stb6 manipulates the activities of enzymatic antioxidant agents

Since H_2O_2 accumulation was observed in the interaction, the activities of five enzymatic antioxidant agents (e.g. SOD,
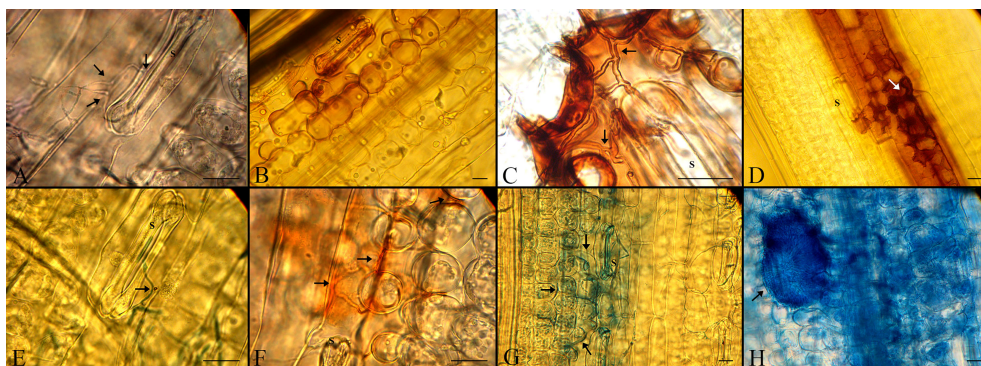
FIGURE 6

Histopathological events in the cv. Shafir infected by either the WT IPO323 (incompatible interaction) or the ΔAvrStb6#33 (compatible interaction) strains. **(A, E)** Both fungal strains germinated by 2 dpi and penetrated directly through stomata (S stands for the stomata and arrows represent the germinated spores). **(B, F)** Accumulation of H_2O_2 as seen by the formation of red-brown staining in the incompatible (upper panel) and compatible interactions (lower panel), respectively at 4 dpi. **(C, G)** Extensive accumulation of H_2O_2 in the cv. Shafir infected by IPO323, blocks further hyphal growth while hyphal growth of ΔAvrStb6#33 was found in the cv. Shafir at 8 dpi. **(D)** Cytoplasmic-like shrinkage occurred in the incompatible context at 8 dpi. **(H)** A-sexual flask-shaped fruiting buddings were formed in the compatible interaction at 12 dpi. The scale bars are 20 μm.

CAT, GPX, APX, and GR) were measured following infection by the employed strains to examine their potential role in the pathosystem, complying with the *AvrStb6-Stb6* relationship. SOD activity was significantly higher in the incompatible interaction than in the compatible interaction at all-time points, except for 4 and 16 dpi, while SOD was highest in the compatible interaction at 16 dpi (Figure 7A). CAT was considerably activated in the compatible interaction as compared to the incompatible interaction except at 4 and 12 dpi (Figure 7B). GPX was notably activated at 16 dpi in the compatible interaction compared to the incompatible context where GPX was activated significantly at 21 dpi (Figure 7C). The highest APX activity peaks occurred at 2 and 12 dpi in the IPO323-infected plants, whereas lowest peak occurred at 21 dpi in plants infected with *ΔAvrStb6#33* (Figure 7D). The GR activity showed high initial and final values (at 2 and 21 dpi) in the incompatible interaction compared with the compatible interaction (Figure 7E). At 21 dpi, the activity of all antioxidant enzymes in the compatible interaction was consistently retarded and clearly diminished, which is indicative of an abated antioxidant defence system of the plant.

AvrStb6-Stb6 orchestrates the activities of non-enzymatic antioxidant agents

Our findings show that five phenolic chemicals known as nonenzymatic antioxidant agents alter dramatically in the incompatible and compatible systems that follows the gene for gene interaction. Ferulic acid was significantly increased in plants infected with IPO323 when compared to levels measured in plants inoculated with *ΔAvrStb6#33*. At 2-4 dpi, 42-41 ppm were found before falling to 25 ppm at 8 dpi (Figure 8A) and increasing back to 42 ppm between 12-21 dpi. Between 2 and 8 dpi, Apigenin fell during the incompatible interaction. The level of Apigenin remained stable during the remaining sample time-points (8-21 dpi) and was comparable between each of the investigated interactions (Figure 8B). The highest amount of Rutin (3.5 ppm)
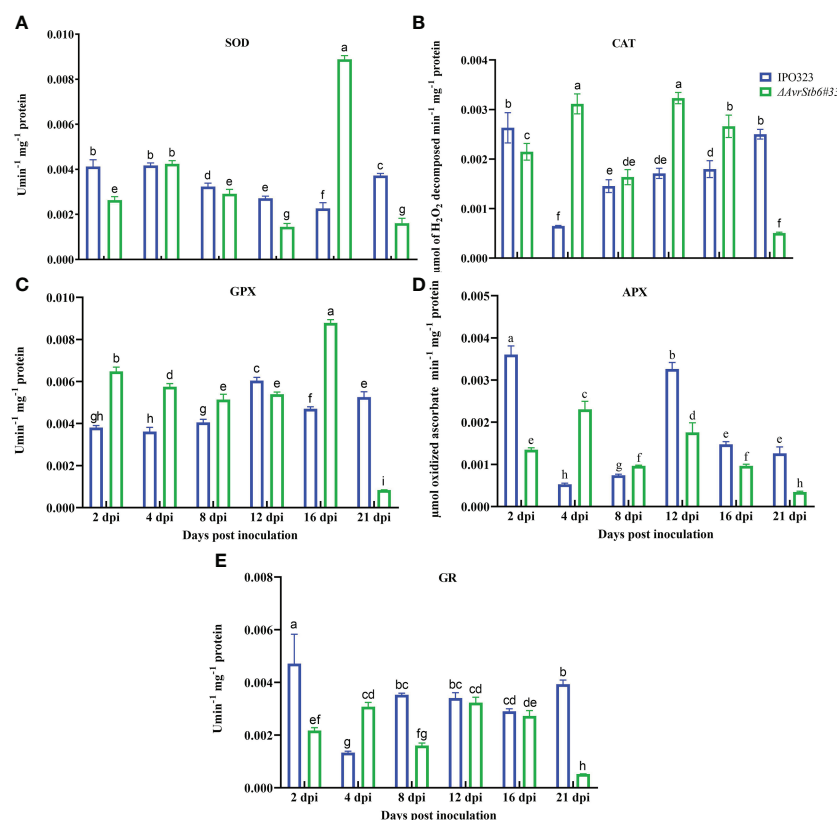
FIGURE 7
AvrStb6-Stb6 interaction manipulates the activities of five enzymatic antioxidant agent. Activities of five antioxidant enzymes: **(A)** superoxide dismutase (SOD), **(B)** Catalase (CAT), **(C)** Guaiacol peroxidase (GPX), **(D)** Ascorbate peroxidase (APX), and **(E)** Glutathione reductase measured spectrophotometrically following infection of cv. Shafir by WT IPO323 or *ΔAvrStb6#33* strains. Data are indicate as mean $\pm$ SD (Standard Deviation) of four biological samples from one independent experiment. Different lowercase letters indicate statistically significant differences (P$\leq$0.05).
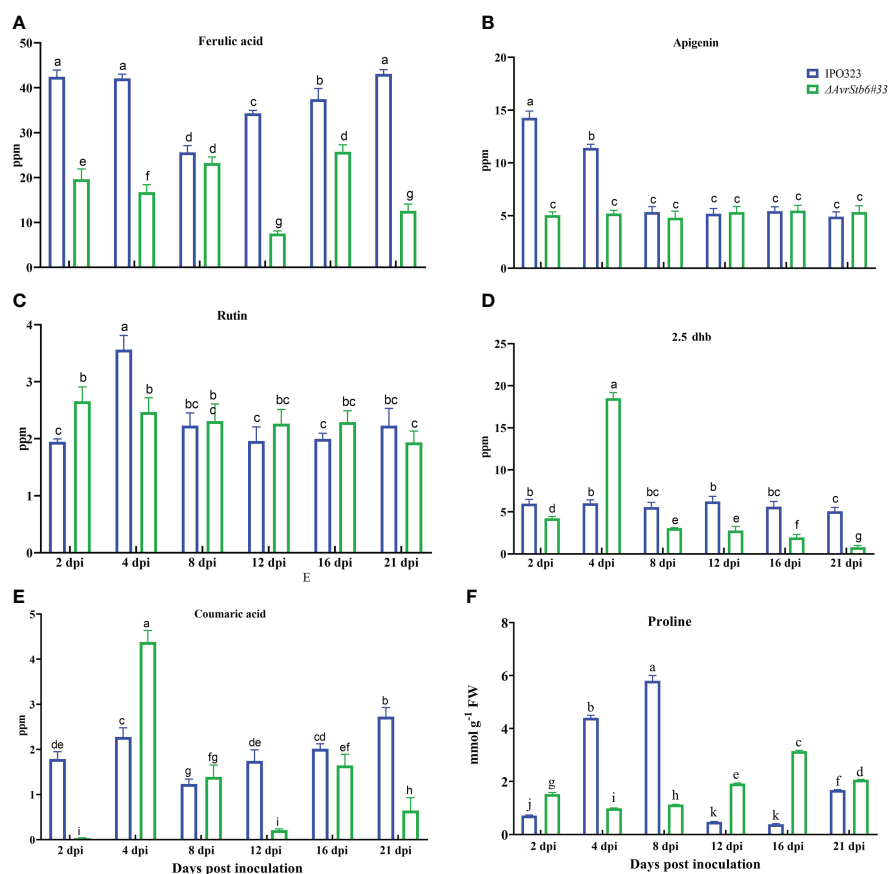
FIGURE 8
AvrStb6-Stb6 interaction orchestrates the activities of six non-enzymatic antioxidant agent: **(A)** Ferulic acid, **(B)** Apigenin, **(C)** Rutin, **(D)** 2,5-Dihydroxybenzoic aci (2.5 dhb), and **(E)** coumaric acid, and **(F)** Proline. Data are indicate as mean $\pm$ SD (Standard Deviation) of four biological samples from one independent experiment. Different lowercase letters indicate statistically significant differences (P$\leq$0.05).

was found in the incompatible interaction at 4 dpi (Figure 8C). Rutin remained at stable levels over the other timepoints for both interactions. When compared to the incompatible interaction, both 2.5 dhb and coumaric acid followed the same pattern in that they are high in the compatible interactionat 4 dpi. 2.5 dhb and coumaric acid levels were 18.5 ppm and 4.3 ppm, respectively (Figures 8D, E). Finally, the activity of proline as non-enzymatic antioxidant agent was assessed in the studied interactions. Proline was elevated in the incompatible interaction between 2-8 dpi compared with its level in the compatible interaction (Figure 8F).

AvrStb6-Stb6 maintains the integrity of plasma membrane

The MDA content and EC parameter were used to explore the effects of the AvStb6/Stb6 on lipid peroxidation and membrane integrity. The MDA content in the compatible interaction increased steadily from 4 dpi, peaking at 21 dpi,

but that of the incompatible interaction remained relatively unchanged over 2-21 dpi (except for a dip at 4 dpi) (Figure 9A). The EC index follows a similar trend as recorded for the MDA content of investigated interactions (Figure 9B).

Discussion

Here, we compared some physiological and biochemical events that occurred in the cv. Shafir while responding differently to inoculation by IPO323 (carrying *AvrStb6*) or *ΔAvrStb6#33* (knock-out for *AvrStb6*) (Supplementary Figure 1). This system follows the gene-for-gene (GFG) model in which the indirect recognition of AvrStb6 *via* Stb6 results in an immune response (Kema et al., 2018; Saintenac et al., 2018).

The intriguing finding was that Stb6 temporarily mediates stomatal closure at an early point (2 dpi) presumably to prevent fungal penetration at the stomatal gate. This finding was confirmed by measuring the pore width and g_s of the treated
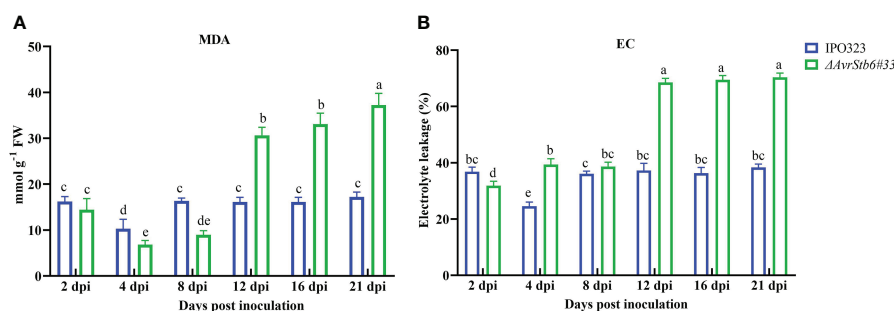
FIGURE 9
AvrStb6-Stb6 interaction impacts the **(A)** malondialdehyde (MDA) content, and **(B)** electrolyte leakage (EC) parameter measured in cv. Shafir infected by WT IPO323 or ΔavrStb6#33 strains. Data are indicate as mean ± SD (Standard Deviation) of four biological samples from one independent experiment. Different lowercase letters indicate statistically significant differences (P≤0.05).

leaves over time (Figure 1). This outcome was consistent with a recent study that found Stb16q mediates an early and temporary stomatal closure in response to an avirulent *Z. tritici* isolate (Battache et al., 2022). Typically, each stomatal pore is surrounded by two guard cells, that are extremely specialized in structure and function, and variations in the turgor pressure of these cells regulate the pore aperture size. Stomata are the potential gates for the entrance of pathogenic agents such as fungi and bacteria, and they are closed to prevent the pathogen's entry into the plant tissues. It is worth mentioning that recent evidence has demonstrated that both salicylic acid (SA) and abscisic acid (ABA) pathways play central roles in stomatal closure (Zhang et al., 2008), which could be an intriguing subsequent project to investigate the impacts of these pathways in the examined interaction.

This study shows that when the AvrStb6-Stb6 interaction is lost, the ChlF transient curve of the *ΔAvrStb6#33*-infected leaves observed at 16 and 21 dpi rapidly and sharply declines (Supplementary Figure 4). These times correspond to the necrotrophic stage, during which the STB necrotic lesions enlarge, and the entire leaf turns brown and dies. F_O, indicating changes in PSII antenna proteins (protein D1) (Schäfer et al., 1993) and its fluctuations reflecting modification of PSII photochemical reactions (Kalaji et al., 2017), declined sharply in the compatible interaction at 16 and 21 dpi (Supplementary Table 1). These events coincided with extending necrotic lesions covered by numerous pycnidia, which can be associated to extreme damage to the antenna proteins. Maximum quantum yield of photosystem II (F_V/F_M) is a reliable, indirect marker for studying stressed plants, with values of around 0.83 for healthy unstressed plants. A decrease in this parameter (lower than 0.8) indicates photoinhibition, oxidative burst, or PSII down-regulation (Murchie and Lawson, 2013). Our results showed that the value of F_V/F_M decreased significantly from 0.79 to 0.70 in the incompatible interaction at 8 dpi. Afterward, this returned to the original level (0.79)

without remarkable changes by 21 dpi. This finding suggested that during the incompatible interaction plants undergo a significant shock at the transition phase (8 dpi). Following on, plants could resist and maintain their PSII performance (Figure 2A). Additionally, the F_V/F_M of plants during the compatible interaction completely stopped at 16 and 21 dpi due to irreversible damage occurring in the reaction centers, thereby leading to the complete annihilation of the photosynthetic apparatus. Our results were in agreement with the previous reports demonstrating a decrease in F_V/F_M by 40% in the susceptible wheat cv. Enola challenged with *Z. tritici* (Mihailova et al., 2019). Other studies revealed that infection by *Colletotrichum gloeosporioides* and *C. lindemuthianum* led to the drop of F_V/F_M below the equipment threshold, when massive tissue colonization and cell death occurred (Bassanezi et al., 2002; Otero-Blanca et al., 2021). Additionally, infection of susceptible wheat plants by *Bipolaris sorokiniana* led to a progressive reduction of F_V/F_M matched up with the expansion of the lesions (Rios et al., 2017). Performance index (PI_{abs}) could sensitively represent the functionality of both PSII and PSI providing quantitative data, exhibiting the current physiological state of plant performance under environmental stress (Strasser et al., 2004). We observed a similar trend of PI_{abs} fluctuations among the investigated treatment to that observed for F_V/F_M (Figure 2B). This finding suggested that during the incompatible interaction resistant plants could inhibit *Z. tritici* infection at 8 dpi, hindering further STB symptom development. Contrastingly, this component declined dramatically in the compatible interaction at 21 dpi since all reaction centers of PSII were destroyed due to infection by *Z. tritici*. Previously, it was demonstrated that *(blank)*infection of wheat by *B. sorokiniana* led to the reduction of PI_{abs} by 28% at 14 dpi compared to reaction centre (RC) of non-inoculated plants (Matorin et al., 2018). The ABS/RC represents the average antenna size and expresses the total number of photons absorbed by PSII antenna chlorophylls divided by the total

number of active RCs. The depression of some active RCs due to environmental stresses can lead to ABS/RC elevation while destroying the RCs can result in a decrease this parameter (Straaer, 1995). Our finding (Figure 3A) aligned with a report revealing that the ABS/RC index in wheat leaves infected by *B. sorokiniana* was elevated by 25% compared to the control at 14 dpi, once disease symptoms started to initiate (Matorin et al., 2018). ET_0/RC defines as electron transport flux in an active RC of PSII and reflects the functionality of an active RC (Force et al., 2003). The pattern of ET_0/RC recorded in the incompatible interaction indicated that plants withstood the imposed infection by *Z. tritici* IPO323 at 8 dpi and recovered the functionality of their active RCs (Figure 3B). Dramatic reduction of ET_0/RC at the necrotrophic stage of a compatible interaction in susceptible plants corroborated that there is no active RC in the PSII since the fungus kills all living cells to gain nourishment from the dead material (Kema et al., 1996). Our data were supported by the report that the ET_0/RC declined significantly in the highly susceptible wheat cv. Tika Taka infected by *Fusarium graminearum* at 10 dpi (Katanić et al., 2021). DI_0/RC indicates the dissipated energy flux mainly as heat per PSII reaction center, and this value is affected through the ratios of active/inactive RCs. An increase in this parameter demonstrated that the number of inactive RCs of PSII increased (Strasser et al., 2004). Our finding on changing the DI_0/RC ratio (Figure 3D) verified that numerous active RCs become silenced as the *Z. tritici* fungus causes extensive necrotic lesions on the inoculated leaves. Furthermore, this parameter reached below the device threshold (0) during the compatible interaction, at 16 and 21 dpi, which coincides with the time the entire leaves became necrotic, and no active RCs exist in the PSII. These data were supported by the study showing that the Fusarium head blight (FHB) caused an increase in the DI_0/RC in the winter wheat variety Tika Taka at 10 dpi (Katanić et al., 2021). NPQ is a central photoprotective tactic aiming to aid the plants' ability to cope with the molecular damage caused by excess absorbed light energy. This event leads to the inactivation of the biochemical process that happens in the active RCs of PSII and down-regulates the photosynthetic activity (Ruban, 2016). Our analysis showed that the NPQ value was down-regulated remarkably in plants infected by *ΔAvrStb6#33* at 16-21 dpi (Figure 4). This timing coincides with STB symptom expression as the emergence of the chlorotic and necrotic lesions on the inoculated leaves. This finding stated that NPQ plays a pivotal role as a photoprotective mechanism to prevent the induction of ROS accumulation as this parameter remained unchangeable in the resistant plants against *Z. tritici*. This finding agreed with the previous reports validating that *Z. tritici* infection led to a significant enhancement of NPQ value in the highly resistant wheat cv. Ariana at the necrotrophic phase (23 dpi). In contrast, the NPQ was remarkably dampened in the highly STB susceptible wheat cv. Enola by 73% at 23 dpi (Mihailova et al., 2019). Our discovery followed a report that

NPQ was significantly downregulated in soybean leaflets challenged with *C. truncatum* from 36 to 120 hai, which corresponds to an increase in anthracnose severity on the main vein (Dias et al., 2018).

Our finding demonstrated that the correlation between photosynthetic metrics of the leaves in the *ΔAvrStb6#33* (compatible interaction) was strongly positive, with the exception of ϕDo, which was negatively correlated with all photosynthesis parameters. However, in the IPO323-infected plants, the correlation of photosynthesis parameter and electron transfer chain (ETC) dropped drastically (Supplementary Figure 5).

Our histopathological study suggested that H_2O_2 is a pivotal substance to restrict and halt the fungal growth in the incompatible interaction involving AvrStb6-Stb6. As *Z. tritici* is a hemibiotroph, this fungus exploits two distinct pathogenicity stages, including biotrophic and necrotrophic phases, to complete its infection cycle (Kema et al., 1996). We observed that H_2O_2 accumulated in the plants infected by IPO323 at the biotrophic stage (Figure 5A). This observation corroborated its potential role in stopping the fungal growth similar to that documented previously for the biotrophic fungal pathogens such as *Blumeria graminis* f.sp. *hordei* (Thordal-Christensen et al., 1997) and also *Z. tritici* (Shetty et al., 2003). Following the transition phase, massive H_2O_2 accumulation took place in the mesophyll cells during the compatible interaction coinciding with STB symptom expression and initiation of the tissue collapse. This event was observable in the plant inoculated by *ΔAvrStb6#33* by eye (Figure 5A). Therefore, *Z. tritici* may hijack the defence system at the necrotrophic growth stage similar to *Botrytis cinerea* to facilitate the infection process (Govrin and Levine, 2000).

Enzymatic antioxidants such as SOD, CAT, GPX, APX, and GR, are key players in maintaining the balance between the generation and degradation of ROS molecules. These chloroplast-produced enzymes are essential for plant antioxidant defence. Except for GPX, all of the investigated antioxidant enzymes were significantly stimulated in the incompatible interaction at 2 dpi, indicating that they may play a role in detoxifying free radicals in an attempt to protect living cells from the damaging effects of the oxidative burst (Figure 7). We additionally quantified the amount of five phenolic compounds as nonenzymatic antioxidants. For instance, Ferulic acid was highly induced in the incompatible interaction at all time points, suggesting an essential role in rendering the resistance reaction by neutralizing free radicals such as H_2O_2 at the biotrophic growth stage and preventing the oxidative burst as suggested formerly (Boz, 2015). A significant increase of Ferulic acid in the stem of chickpea beyond the infection area caused by *sclerotium rolfsii* led to such a conclusion that this substance may play a role in preventing the infection of chickpea by *S. rolfsii* (Sarma and Singh, 2003). Rutin was also activated significantly in the incompatible interaction at 4 dpi, suggesting a potential role for this

compound in providing resistance in the Shafir-IPO323 context. Rutin has antifungal activity toward phytopathogenic agents and possesses a powerful antioxidant capacity (Báidez et al., 2007; Ismail et al., 2015). Apigenin levels were specifically enhanced in the incompatible interaction at the early biotrophic stage (2 and 4 dpi). This chemical probably increases notably at the biotrophic stage, when WT IPO323 faces more H_2O_2, to induce antioxidant enzymes. A previous report showed that Apigenin-treated rice seedlings had lower levels of lipid peroxidation and H_2O_2 concentration due to increased antioxidant enzyme activity (Mekawy et al., 2018). Coumaric acid was significantly increased in the compatible interaction at 4 dpi, followed by a sharp decline by 21 dpi. We concluded that this induction is a general response to infection, or this phenolic compound may be triggered by oxidative stress in the incompatible interaction to halt the fungal growth (Ansari et al., 2013). We noticed that during the compatible interaction the plant traded energy between defence and growth because this phenolic acid was low during the necrotrophic phase (Figure 8). However, there is accumulating evidence demonstrating that Coumaric acid plays a role in providing a resistance response in host-microbe interactions (Morales et al., 2017). We additionally discovered that the proline content, a known non-enzymatic antioxidant agent, was overproduced in the incompatible context, implying proline content may play a role in establishing the resistance response in the AvrStb6-Stb6 interaction (Figure 8F).

Our findings showed that the MDA content, a valuable biomarker for lipid peroxidation, and the EC parameter, a hallmark for cellular damages, gradually increased in the compatible interaction and peaked at 21 dpi, corresponding to massive tissue collapse and widespread cell death. These findings were consistent with those of a previous study comparing susceptible and resistant wheat genotypes inoculated with *Z. tritici* (Mihailova et al., 2019). This indicated that the AvrStb6-Stb6 interaction plays a pivotal role in maintaining the membrane integrity and preventing cellular electrolyte leakage

To sum up, a variety of methodologies were used to investigate the GFG model system where Stb6 recognizes AvrStb6 and causes an immune response in the *Z. tritici*-wheat pathosystem, concluding that several mechanisms are involved in mounting defence reactions. The resistant interaction between AvrStb6 and Stb6 is crucial for stomatal opening/closure and maintaining the efficiency of the photosynthetic apparatus. Preserving membrane integrity and regulating the level of oxidative stress are crucial for the resistance response. We recommend that future studies take advantage of this system providing two distinct phenotypes to discover defense-related genes or compounds using RNA-seq and metabolomics approaches.

Data availability statement

The original contributions presented in the study are included in the article/Supplementary Material. Further inquiries can be directed to the corresponding author.

Author contributions

AMG designed, supervised, and coordinated the study. FGN, MI, and EZ performed the infection assay. FGN conducted the infection biology, DAB and tryptophan assays and was involved in the photosynthetic related-assay. MI conducted the experiment related to HPLC and spectrophotometry. FD performed and analyzed the assay associated with photosynthetic part. AE conducted and analyzed the spectrophotometric assays. MAG employed PlantCV tool to analysis images associated with DAB and tryptophan blue staining. AG wrote the manuscript with substantial input from SA, MF, MJ-N, and AF. All authors contributed to the article and approved the submitted version.

Conflict of interest

The authors declare that the research was conducted in the absence of any commercial or financial relationships that could be construed as a potential conflict of interest.

Publisher's note

All claims expressed in this article are solely those of the authors and do not necessarily represent those of their affiliated organizations, or those of the publisher, the editors and the reviewers. Any product that may be evaluated in this article, or claim that may be made by its manufacturer, is not guaranteed or endorsed by the publisher.

Supplementary material

The Supplementary Material for this article can be found online at: https://www.frontiersin.org/articles/10.3389/fpls.2022.1004691/full#supplementary-material

SUPPLEMENTARY FIGURE 1

AvrStb6-Stb6 interaction establishes immunity response. **(A)** Fully expanded first leaves were inoculated with the WT IPO323 or *ΔAvrStb6#33* strains by a hand sprayer **(B)** The percentage of necrotic area formed on the inoculated leaves. (C) The percentage of pycnidia produced on the necrotic lesions. Pictures were taken at 2, 4, 8, 12, 16, and 21 days post-inoculation. Error bars are SD.

SUPPLEMENTARY FIGURE 2

Spider plot of the chlorophyll fluorescence parameters in wheat cv. Shafir inoculated by distilled water (Mock), WT IPO323, and *ΔAvrStb6#33* after 2, 4, 8, 12, 16, and 21 days post-inoculation.

SUPPLEMENTARY FIGURE 3

A schematic model illustrating changes that occurred in the photosynthetic parameter in cv. Shafir inoculated by IPO323 WT or *ΔAvrStb6#33* along with the Chlorophyll fluorescence images of infected wheat leaves taken at 2, 4, 8, 12, 16, and 21 dpi. Increases or declines in parameter's amount are represented by size changes of boxes embedded each parameter.

SUPPLEMENTARY FIGURE 4

The impact of AvrStb6-Stb6 interaction on OJIP curve of cv. Shafir inoculated by distilled water (Mock), WT IPO323, and *ΔAvrStb6#33*. Data are shown as fluorescence intensity.

SUPPLEMENTARY FIGURE 5

Graphical representation of a correlation matrix of initial plant enzymatic and non-enzymatic antioxidant as well as photosynthesis parameters in cv. Shafir inoculated either with *ΔAvrStb6#33* **(A)** or IPO323 **(B)**. Red color represents positive correlation whereas blue represents negative correlation. Color intensity is proportional to the correlation, which depicted in the legend at the bottom.

References

Aliniaeifard, S., and Van Meeteren, U. (2016). Stomatal characteristics and desiccation response of leaves of cut chrysanthemum (*Chrysanthemum morifolium*) flowers grown at high air humidity. *Sci. Hortic.* 205, 84–89. doi: 10.1016/j.scienta.2016.04.025

Ansari, M. A., Anurag, A., Fatima, Z., and Hameed, S. (2013). "Natural phenolic compounds: a potential antifungal agent", in: *Microbial Pathogens and Strategies for Combating Them: Science, Technology and Education* ed. A., Méndez-Vilas ((Badajoz: Formatex Research Center), 189–195.

Apel, K., and Hirt, H. (2004). Reactive oxygen species: metabolism, oxidative stress, and signaling transduction. *Annu. Rev. Plant Biol.* 55, 373. doi: 10.1146/annurev.arplant.55.031903.141701

Báidez, A. G., Gómez, P., Del Río, J. A., and Ortuño, A. (2007). Dysfunctionality of the xylem in *Olea europaea* l. plants associated with the infection process by *Verticillium dahliae* kleb. role of phenolic compounds in plant defense mechanism. *J. Agric. Food Chem.* 55, 3373–3377. doi: 10.1021/jf063166d

Bajji, M., Kinet, J.-M., and Lutts, S. (2002). The use of the electrolyte leakage method for assessing cell membrane stability as a water stress tolerance test in durum wheat. *Plant Growth Regul.* 36, 61–70. doi: 10.1023/A:1014732714549

Bassanezi, R., Amorim, L., Filho, A. B., and Berger, R. (2002). Gas exchange and emission of chlorophyll fluorescence during the monocycle of rust, angular leaf spot and anthracnose on bean leaves as a function of their trophic characteristics. *J. Phytopathol.* 150, 37–47. doi: 10.1046/j.1439-0434.2002.00714.x

Bates, L. S., Waldren, R. P., and Teare, I. (1973). Rapid determination of free proline for water-stress studies. *Plant Soil* 39, 205–207. doi: 10.1007/BF00018060

Battache, M., Lebrun, M.-H., Sakai, K., Soudière, O., Cambon, F., Langin, T., et al. (2022). Blocked at the stomatal gate, a key step of wheat Stb16q-mediated resistance to *Zymoseptoria tritici*. *Front. Plant Sci.* 13. doi: 10.3389/fpls.2022.921074

Beauchamp, C., and Fridovich, I. (1971). Superoxide dismutase: improved assays and an assay applicable to acrylamide gels. *Analyt. Biochem.* 44, 276–287. doi: 10.1016/0003-2697(71)90370-8

Boz, H. (2015). Ferulic acid in cereals-a review. *Czech J. Food Sci.* 33, 1–7. doi: 10.17221/401/2014-CJFS

Dias, C. S., Araujo, L., Chaves, J., Damatta, F. M., and Rodrigues, F. A. (2018). Water relation, leaf gas exchange and chlorophyll a fluorescence imaging of soybean leaves infected with *Colletotrichum truncatum*. *Plant Physiol. Biochem.* 127, 119–128. doi: 10.1016/j.plaphy.2018.03.016

Díaz-Tielas, C., Grana, E., Sotelo, T., Reigosa, M. J., and Sánchez-Moreiras, A. M. (2012). The natural compound transchalcone induces programmed cell death in *Arabidopsis thaliana* roots. *Plant Cell Environ.* 35, 1500–1517.

Eyal, Z. (1999). The *Septoria tritici* and *Stagonospora nodorum* blotch diseases of wheat. *Eur. J. Plant Pathol.* 105, 629–641. doi: 10.1023/A:1008716812259

Fanourakis, D., Heuvelink, E., and Carvalho, S. M. (2013). A comprehensive analysis of the physiological and anatomical components involved in higher water loss rates after leaf development at high humidity. *J. Plant Physiol.* 170, 890–898. doi: 10.1016/j.jplph.2013.01.013

Force, L., Critchley, C., and Van Rensen, J. J. (2003). New fluorescence parameters for monitoring photosynthesis in plants. *Photosynth. Res.* 78, 17–33. doi: 10.1023/A:1026012116709

Gehan, M. A., Fahlgren, N., Abbasi, A., Berry, J. C., Callen, S. T., Chavez, L., et al. (2017). PlantCV v2: Image analysis software for high-throughput plant phenotyping. *PeerJ* 5, e4088. doi: 10.7717/peerj.4088

Genty, B., Briantais, J.-M., and Baker, N. R. (1989). The relationship between the quantum yield of photosynthetic electron transport and quenching of chlorophyll fluorescence. *Biochim. Biophys. Acta (BBA)-Gen. Subj.* 990, 87–92. doi: 10.1016/S0304-4165(89)80016-9

Govrin, E. M., and Levine, A. (2000). The hypersensitive response facilitates plant infection by the necrotrophic pathogen *Botrytis cinerea*. *Curr. Biol.* 10, 751–757. doi: 10.1016/S0960-9822(00)00560-1

Grimmer, M. K., John Foulkes, M., and Paveley, N. D. (2012). Foliar pathogenesis and plant water relations: a review. *J. Exp. Bot.* 63, 4321–4331. doi: 10.1093/jxb/ers143

Hayat, S., Hayat, Q., Alyemeni, M. N., Wani, A. S., Pichtel, J., and Ahmad, A. (2012). Role of proline under changing environments: a review. *Plant Signaling Behav.* 7, 1456–1466. doi: 10.4161/psb.21949

Hemeda, H., and Klein, B. (1990). Effects of naturally occurring antioxidants on peroxidase activity of vegetable extracts. *J. Food Sci.* 55, 184–185. doi: 10.1111/j.1365-2621.1990.tb06048.x

Ismail, H., Maksimović, J. D., Maksimović, V., Shabala, L., Živanović, B. D., Tian, Y., et al. (2015). Rutin, a flavonoid with antioxidant activity, improves plant salinity tolerance by regulating k+ retention and na+ exclusion from leaf mesophyll in quinoa and broad beans. *Funct. Plant Biol.* 43, 75–86. doi: 10.1071/FP15312

Kalaji, H. M., Schansker, G., Brestic, M., Bussotti, F., Calatayud, A., Ferroni, L., et al. (2017). Frequently asked questions about chlorophyll fluorescence, the sequel. *Photosynth. Res.* 132, 13–66. doi: 10.1007/s11120-016-0318-y

Katanić, Z., Mlinarić, S., Katanić, N., Ćosić, J., and Španić, V. (2021). Photosynthetic efficiency in flag leaves and ears of winter wheat during fusarium head blight infection. *Agronomy* 11:1–22. doi: 10.3390/agronomy11122415

Kema, G. H., Mirzadi Gohari, A., Aouini, L., Gibriel, H. A., Ware, S. B., Van Den Bosch, F., et al. (2018). Stress and sexual reproduction affect the dynamics of the wheat pathogen effector AvrStb6 and strobilurin resistance. *Nat. Genet.* 50, 375–380. doi: 10.1038/s41588-018-0052-9

Kema, G. H., Yu, D., Rijkenberg, F. H., Shaw, M. W., and Baayen, R. P. (1996). Histology of the pathogenesis of *Mycosphaerella graminicola* in wheat. *Phytopathology* 86, 777–786. doi: 10.1094/Phyto-86-777

Koch, E., and Slusarenko, A. (1990). Arabidopsis is susceptible to infection by a downy mildew fungus. *Plant Cell* 2, 437–445. doi: 10.1105/tpc.2.5.437

Kretschmer, M., Damoo, D., Djamei, A., and Kronstad, J. (2019). Chloroplasts and plant immunity: where are the fungal effectors? *Pathogens* 9, 19. doi: 10.3390/pathogens9010019

Li, M., and Kim, C. (2021). Chloroplast ROS and stress signaling. *Plant Commun.* 9, 100264. doi: 10.1016/j.xplc.2021.100264

Mansoor, S., Sharma, V., Mir, M. A., Mir, J. I., Un Nabi, S., Ahmed, N., et al. (2020). Quantification of polyphenolic compounds and relative gene expression studies of phenylpropanoid pathway in apple (*Malus domestica* borkh) in response to *Venturia inaequalis* infection. *Saudi J. Biol. Sci.* 27, 3397–3404. doi: 10.1016/j.sjbs.2020.09.007

Matorin, D., Timofeev, N., Glinushkin, A., Bratkovskaja, L., and Zayadan, B. (2018). Effect of fungal infection with *Bipolaris sorokiniana* on photosynthetic light reactions in wheat analyzed by fluorescence spectroscopy. *Moscow Univ. Biol. Sci. Bull.* 73, 203–208. doi: 10.3103/S0096392518040065

Mekawy, A. M. M., Abdelaziz, M. N., and Ueda, A. (2018). Apigenin pretreatment enhances growth and salinity tolerance of rice seedlings. *Plant Physiol. Biochem.* 130, 94–104. doi: 10.1016/j.plaphy.2018.06.036

Mihailova, G., Stoyanova, Z., Rodeva, R., Bankina, B., Bimšteine, G., and Georgieva, K. (2019). Physiological changes in winter wheat genotypes in response to the *Zymoseptoria tritici* infection. *Photosynthetica* 57, 428–437. doi: 10.32615/ps.2019.054

Mirzadi Gohari, A., Mehrabi, R., Robert, O., Ince, I. A., Boeren, S., Schuster, M., et al. (2014). Molecular characterization and functional analyses of ZtWor1, a transcriptional regulator of the fungal wheat pathogen *Zymoseptoria tritici*. *Mol. Plant Pathol.* 15, 394–405. doi: 10.1111/mpp.12102

Morales, J., Mendoza, L., and Cotoras, M. (2017). Alteration of oxidative phosphorylation as a possible mechanism of the antifungal action of p-coumaric acid against *Botrytis cinerea*. *J. Appl. Microbiol.* 123, 969–976. doi: 10.1111/jam.13540

Murchie, E. H., and Lawson, T. (2013). Chlorophyll fluorescence analysis: a guide to good practice and understanding some new applications. *J. Exp. Bot.* 64, 3983–3998.

Otero-Blanca, A., Pérez-Llano, Y., Reboledo-Blanco, G., Lira-Ruan, V., Padilla-Chacon, D., Folch-Mallol, J. L., et al. (2021). Physcomitrium patens infection by *Colletotrichum gloeosporioides*: Understanding the fungal–bryophyte interaction by microscopy, phenomics and RNA sequencing. *J. Fungi* 7, 677. doi: 10.3390/jof7080677

Paunov, M., Koleva, L., Vassilev, A., Vangronsveld, J., and Goltsev, V. (2018). Effects of different metals on photosynthesis: cadmium and zinc affect chlorophyll fluorescence in durum wheat. *Int. J. Mol. Sci.* 19, 787. doi: 10.3390/ijms19030787

Quaedvlieg, W., Kema, G., Groenewald, J., Verkley, G., Seifbarghi, S., Razavi, M., et al. (2011). Zymoseptoria gen. nov.: a new genus to accommodate septoria-like species occurring on graminicolous hosts. *Persoonia-Mol. Phylogeny Evol. Fungi* 26, 57–69. doi: 10.3767/003158511X571841

Ranieri, A., Castagna, A., Pacini, J., Baldan, B., Mensuali Sodi, A., and Soldatini, G. (2003). Early production and scavenging of hydrogen peroxide in the apoplast of sunflower plants exposed to ozone. *J. Exp. Bot.* 54, 2529–2540. doi: 10.1093/jxb/erg270

Rios, J., Aucique-Pérez, C., Debona, D., Cruz Neto, L., Rios, V., and Rodrigues, F. (2017). Changes in leaf gas exchange, chlorophyll a fluorescence and antioxidant metabolism within wheat leaves infected by *Bipolaris sorokiniana*. *Ann. Appl. Biol.* 170, 189–203. doi: 10.1111/aab.12328

Ruban, A. V. (2016). Nonphotochemical chlorophyll fluorescence quenching: mechanism and effectiveness in protecting plants from photodamage. *Plant Physiol.* 170, 1903–1916. doi: 10.1104/pp.15.01935

Rudd, J. J., Kanyuka, K., Hassani-Pak, K., Derbyshire, M., Andongabo, A., Devonshire, J., et al. (2015). Transcriptome and metabolite profiling of the infection cycle of *Zymoseptoria tritici* on wheat reveals a biphasic interaction with plant immunity involving differential pathogen chromosomal contributions and a variation on the hemibiotrophic lifestyle definition. *Plant Physiol.* 167, 1158–1185. doi: 10.1104/pp.114.255927

Saintenac, C., Lee, W.-S., Cambon, F., Rudd, J. J., King, R. C., Marande, W., et al. (2018). Wheat receptor-kinase-like protein Stb6 controls gene-for-gene resistance to fungal pathogen *Zymoseptoria tritici*. *Nat. Genet.* 50, 368–374. doi: 10.1038/s41588-018-0051-x

Sarma, B., and Singh, U. (2003). Ferulic acid may prevent infection of *Cicer arietinum* by *Sclerotium rolfsii*. *World J. Microbiol. Biotechnol.* 19, 123–127. doi: 10.1023/A:1023205522032

Schäfer, C., Vogg, G., and Schmid, V. (1993). Evidence for loss of D1 protein during photoinhibition of *Chenopodium rubrum* l. culture cells. *Planta* 189, 433–439. doi: 10.1007/BF00194442

Shetty, N., Kristensen, B., Newman, M.-A., Møller, K., Gregersen, P. L., and Jørgensen, H. L. (2003). Association of hydrogen peroxide with restriction of *Septoria tritici* in resistant wheat. *Physiol. Mol. Plant Pathol.* 62, 333–346. doi: 10.1016/S0885-5765(03)00079-1

Shomali, A., Aliniaeifard, S., Didaran, F., Lotfi, M., Mohammadian, M., Seif, M., et al. (2021). Synergistic effects of melatonin and gamma-aminobutyric acid on protection of photosynthesis system in response to multiple abiotic stressors. *Cells* 10:1–24. doi: 10.3390/cells10071631

Smith, I. K., Vierheller, T. L., and Thorne, C. A. (1988). Assay of glutathione reductase in crude tissue homogenates using 5, 5′-dithiobis (2-nitrobenzoic acid). *Analyt. Biochem.* 175, 408–413. doi: 10.1016/0003-2697(88)90564-7

Stewart, R. R., and Bewley, J. D. (1980). Lipid peroxidation associated with accelerated aging of soybean axes. *Plant Physiol.* 65, 245–248. doi: 10.1104/pp.65.2.245

Straaer, B. (1995). Measuring fast fluorescence transients to address environmental questionsL; the JIP-test. *Photosynth.: light to biosphere*, 5, 977–980. doi: 10.1007/978-94-009-0173-5_1142

Strasser, R. J., Srivastava, A., and Tsimilli-Michael, M. (2000). The fluorescence transient as a tool to characterise and screen photosynthetic samples", in *Mechanisms, Regulation and Adaptation*. Eds. Yunus, M.Pathre, U. Moanty, P (London, UK: Taylor and Francis) pp.25445–483.

Strasser, R. J., Tsimilli-Michael, M., and Srivastava, A. (2004). "Analysis of the chlorophyll a fluorescence transient," in *Chlorophyll a fluorescence* (Dordrecht: Springer), 321–362.

Thordal-Christensen, H., Zhang, Z., Wei, Y., and Collinge, D. B. (1997). Subcellular localization of H2O2 in plants. H2O2 accumulation in papillae and hypersensitive response during the barley–powdery mildew interaction. *Plant J.* 11, 1187–1194. doi: 10.1046/j.1365-313X.1997.11061187.x

Torres, M. A. (2010). ROS in biotic interactions. *Physiol. Plant.* 138, 414–429. doi: 10.1111/j.1399-3054.2009.01326.x

Zhang, W., He, S. Y., and Assmann, S. M. (2008). The plant innate immunity response in stomatal guard cells invokes G-protein-dependent ion channel regulation. *Plant J.* 56, 984–996. doi: 10.1111/j.1365-313X.2008.03657.x

Zhong, Z., Marcel, T. C., Hartman, F. E., Ma, X., Plissonneau, C., Zala, M., et al (2017). A small secreted protein in Zymoseptoria tritici is responsible for avirulence on wheat cultivars carrying the Stb6 resistance gene. *New Phytologist* 214, 619–631.

Shifting sensitivity of septoria tritici blotch compromises field performance and yield of main fungicides in Europe

Lise Nistrup Jørgensen[1]*, Niels Matzen[1], Thies Marten Heick[1], Aoife O'Driscoll[2], Bill Clark[2], Katherine Waite[2], Jonathan Blake[3], Mariola Glazek[4], Claude Maumene[5], Gilles Couleaud[5], Bernd Rodemann[6], Stephan Weigand[7], Charlotte Bataille[8], Bán R[9], Pierre Hellin[8], Steven Kildea[10] and Gerd Stammler[11]

[1]Department of Agroecology, Aarhus University, Slagelse, Denmark, [2]NIAB, Cambridge, United Kingdom, [3]ADAS Rosemaund, Hereford, United Kingdom, [4]Institute of Plant Protection, Sosnicowice, Poland, [5]Arvalis Institut du végétal, Station Expérimentale, Boigneville, France, [6]JKI, Braunschweig, Germany, [7]Institut für Pflanzenschutz, Bayerische Landesanstalt für Landwirtschaft, Freising-Weihenstephan, Germany, [8]CRA-W, Plant and Forest Health Unit, Gembloux, Belgium, [9]Institute of Plant Protection, Department of Integrated Plant Protection, Hungarian University of Agriculture and Life Sciences (MATE), Gödöllő, Hungary, [10]Teagasc, Carlow, Ireland, [11]BASF Limburgerhof, Limburgerhof, Germany

Septoria tritici blotch (STB; *Zymoseptoria tritici*) is a severe leaf disease on wheat in Northern Europe. Fungicide resistance in the populations of *Z. tritici* is increasingly challenging future control options. Twenty-five field trials were carried out in nine countries across Europe from 2019 to 2021 to investigate the efficacy of specific DMI and SDHI fungicides against STB. During the test period, two single DMIs (prothioconazole and mefentrifluconazole) and four different SDHIs (fluxapyroxad, bixafen, benzovindiflupyr and fluopyram) along with different co-formulations of DMIs and SDHIs applied at flag leaf emergence were tested. Across all countries, significant differences in azole performances against STB were seen; prothioconazole was outperformed in all countries by mefentrifluconazole. The effects also varied substantially between the SDHIs, with fluxapyroxad providing the best efficacy overall, while the performance of fluopyram was inferior to other SDHIs. In Ireland and the UK, the efficacy of SDHIs was significantly lower compared with results from continental Europe. This reduction in performances from both DMIs and SDHIs was reflected in yield responses and also linked to decreased sensitivity of *Z. tritici* isolates measured as EC_{50} values. A clear and significant gradient in EC_{50} values was seen across Europe. The lower sensitivity to SDHIs in Ireland and the UK was coincident with the prevalence of SDH-C-alterations T79N, N86S, and sporadically of H152R. The isolates' sensitivity to SDHIs showed a clear cross-resistance between fluxapyroxad, bixafen, benzovindiflupyr and fluopyram, although the links with the latter were less apparent. Co-formulations of DMIs + SDHIs performed well in all trials conducted in 2021. Only minor differences were seen between

fluxapyroxad + mefentrifluconazole and bixafen + fluopyram + prothioconazole; the combination of benzovindiflupyr + prothioconazole gave an inferior performance at some sites. Fenpicoxamid performed in line with the most effective co-formulations. This investigation shows a clear link between reduced field efficacy by solo SDHIs as a result of increasing problems with sensitivity shifting and the selection of several SDH-C mutations. The presented data stress the need to practice anti-resistance strategies to delay further erosion of fungicide efficacy.

1 Introduction

Severe fungal leaf disease attacks cause economically significant losses in winter wheat each year (Oerke, 2006; Savary et al., 2019). Despite efforts to mitigate these losses by employing resistant cultivars and adjusting cultural practices, frequent fungicide applications are indispensable. In Northern Europe, septoria tritici blotch (STB), caused by the ascomycete *Zymoseptoria tritici*, is one of the most devastating leaf diseases in wheat (Fones and Gurr, 2015). Besides, yellow rust (*Puccinia striiformis*) and brown rust (*Puccinia triticina*) may cause major problems depending on the region and the season (Jørgensen et al., 2014; Singh et al., 2016). Current fungicide strategies for the control of STB in most European countries are mainly built around 14α-demethylase inhibitors (DMI; FRAC group 3 and from here on referred to as azoles; e.g. prothioconazole and mefentrifluconazole), succinate dehydrogenase inhibitors (SDHI, FRAC group 11, e.g. bixafen, fluxapyroxad, and fluopyram), quinone inside inhibitors (QiI; FRAC group 21; currently only represented by the picolinamide fenpicoxamid), and multi-site fungicides (e.g. folpet and sulfur).

Over the past four decades, the intensive use of azoles in Europe has led to significant reductions in the sensitivity of contemporary European *Z. tritici* populations toward the azole fungicides (Heick et al., 2017; Blake et al., 2018; Garnault et al., 2019; Jørgensen et al., 2021a; Klink et al., 2021). The emergence of reduced sensitivity to the azoles coincided with the commercialization of novel SDHIs with activity against *Z. tritici*, starting with boscalid in 2006 and a suite of additional SDHIs from the early 2010s onwards. Since then, these SDHIs

have become an integral component of disease control in cereals throughout Europe (Rehfus et al., 2018a, Turner et al., 2021). As previously seen with azoles, the increased dependency on SDHIs for control of STB has gradually led to the selection of SDHI-resistant strains of *Z. tritici*. Several key point mutations have been reported in the different *SDH* sub-units, leading to amino acid alterations in the succinate dehydrogenase (SDH) enzyme (FRAC, 2021). The most widespread of these include C-T79N and C-N86S, rendering strains moderately resistant to most SDHIs (Rehfus et al., 2020; Hellin et al., 2021). The alteration C-H152R has been identified as causing complete resistance to all the major SDHIs, and has been detected in European field *Z. tritici* populations at a low frequency; first in Ireland in 2015 and later in the United Kingdom (UK) and sporadically in Northern France, Germany, the Netherlands, and Belgium (Scalliet et al., 2012; Dooley et al., 2016; Gutiérrez-Alonso et al., 2017; Rehfus et al., 2018a; Hellin et al., 2020; FRAC, 2021; Hellin et al., 2021). Whereas the development of fungicide resistance has been problematic for the fungicide groups mentioned above, a recent study showed that target-site resistance to the newly introduced QiI fenpicoxamid was non-existing in the European *Z. tritici* population (Kildea et al., 2022). However, this active ingredient might also be at risk for resistance development, with expected increased use in the future.

The rapid development of fungicide resistance in *Z. tritici* is partially favored by its lifecycle. *Zymoseptoria tritici* causes epidemic outbreaks due to the high density and mobility of spores and widespread sexual reproduction, which allows the perpetual recombination of alleles (McDonald and Linde, 2002), followed by asexual cycles typically driven by splash events and high humidity. Therefore, anti-resistance strategies should be mandatory and followed from the introduction to keep the frequencies of resistant strains low.

The present study's primary aim was to generate updated efficacy profiles for key azoles and SDHI fungicides commonly used for STB control in wheat across Europe. More specifically,

these were: (1) to investigate the field performances of two azoles and four SDHIs against the current *Z. tritici* populations across Europe, including dose responses and efficacy of co-formulations of azoles and SDHIs, (2) to elucidate the interrelation of field performances, *in-vitro* sensitivity of *Z. tritici* populations and CYP51 and SDH-C alterations frequencies across Europe, (3) to discuss the interrelationship between EC_{50} values, specific mutations, and field performances, (4) to investigate the tested products impact on yield. This project is a continuation of a previous collaboration in the EuroWheat group – initiated by activities in the European Network of excellence - ENDURE (Jørgensen et al., 2014) and the network for comparison of azoles efficacy against STB across Europe (Jørgensen et al., 2018; Jørgensen et al., 2021a).

2 Methods and materials

2.1 Field trial setup and fungicide applications

The study was carried out over the growing seasons of 2019, 2020, and 2021 at a range of locations across Europe, covering various climate zones and agricultural practices. In total, 33 trials were carried out across Denmark, England, Poland, France, Germany, Ireland, Belgium, the Netherlands, and Hungary by local scientific organizations (Figure 1 and Table S1). The number of trials used in each analysis is presented in Table S2. All experiments were carried out to standard procedures using a randomized plot design with a minimum plot size of 10 m² and three to four replicates at each location. Wheat varieties with

moderate to high susceptibility to STB were chosen for all trials to ensure significant levels of STB. All trials have been conducted in fields with natural infections and in regions with a history of at least moderate STB attack. Except for fungicides, each trial was managed according to local agricultural practices. Fungicides were applied using various equipment, including knapsack sprayers and self-propelled sprayers, depending on local options, with both water volumes (196 – 300 L/ha) used and pressures (1.8 – 4 bar) applied reflective of local equipment and practices. All applications were made to coincide with flag leaf emergence at the growth stage (GS) 37-39 (BBCH) (Lancashire et al., 1991). In a few cases, the trials were treated with cover sprays to mitigate early attacks of powdery mildew, yellow rust, and STB as required.

2.2 Fungicide application scheme

Over the three seasons, a total of four different trial protocols were used, but as commonalities existed between them, it is possible to examine three different factors a) comparisons between key solo azoles and SDHIs (Table 1); b) comparisons between full and half rates for selected azoles and SDHIs (Table 1); c) comparisons of azole/SDHI mixtures and the novel QiI fenpicoxamid (Table 2). The objective and specific details of each are further outlined below. The fungicides used in all trials were supplied by BASF SE (Limburgerhof, Germany).

a) Azole & SDHI comparisons

In each of the three seasons, the efficacy of the azoles mefentrifluconazole (MFA) and prothioconazole (PTH), and the SDHIs fluxapyroxad (FXP), bixafen (BIX) and
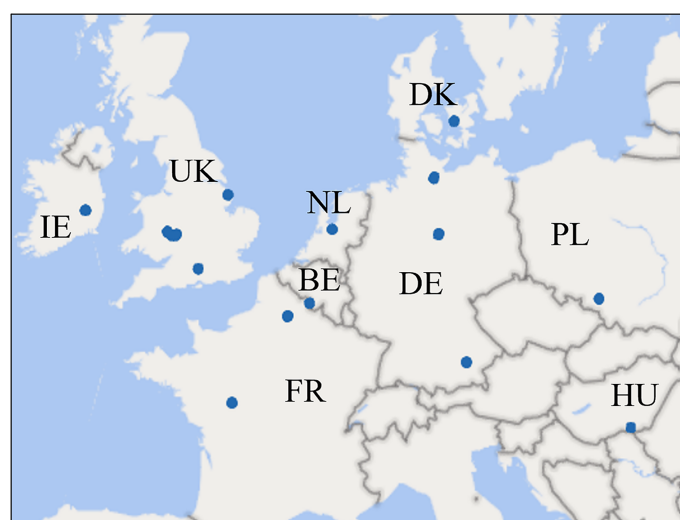
FIGURE 1
Locations of trials carried out from 2019-2021.

TABLE 1   Treatments used in all trials with full dose applications were carried out at growth stage GS 37-39.

Treatments	Active ingredient	Abbreviation	Active group	Years	Dose (l/ha)	g a.i./ha
Untreated control	-				-	-
Revysol, BASF	Mefentrifluconazole	MFA	DMI	2019, 2020, 2021	1.5	150
Proline 250, Bayer	Prothioconazole	PTH	DMI	2019, 2020, 2021	0.8	200
Imtrex, BASF	Fluxapyroxad	FXP	SDHI	2019, 2020, 2021	2	125
Thore, Bayer	Bixafen	BIX	SDHI	2019, 2020, 2021	1	125
Elatus, Syngenta	Benzovindiflupyr	BVF	SDHI	2019, 2020, 2021	0.75	75
Luna, Bayer	Fluopyram	FLP	SDHI	2019, 2020	0.2	100

In 2019, also half rates were tested for the included actives.
In 2019, also half rates were tested.

benzovindiflupyr (BVF) were investigated as solo products, with fluopyram (FLP) included in only 2019 and 2020 (Table 1).

b) Comparisons between full and half doses

In 2019, treatments with the solo azoles MFA and PTH and the solo SDHIs FXP, BVF, BIX, and FLP were tested at half rates (Table 1) in addition to the full rates.

c) Azole/SDHI mixtures & QiI fenpicoxamid

In 2021, comparisons between full label rate treatments were made using the co-formulations of the azoles and SDHIs FXP +MFA, BVF+PTH, and BIX+FLP+PTH, the SDHIs BIX+FLP and the QiI fenpicoxamid (FPX) (Table 2).

2.3 Field assessments

The severity of STB was assessed following EPPO guidelines (1/26 (4)) (Oepp/Eppo, 2014). Assessments were carried out individually on the flag leaf (F) and flag leaf minus one (F-1), by visually scoring the average percent leaf area with symptoms either at four different spots in each plot or on ten main stems selected from throughout the plot. The assessment carried out at GS 73-75 was emphasized, corresponding to 27-55 days after application (DAA). The analyzed assessments on F-1 were generally carried out at an earlier timepoint than those on flag leaves. All trials were carried through to harvest, and grain yields were measured for every plot and adjusted to 85% dry matter.

2.4 *Zymoseptoria tritici* fungicide sensitivity testing and molecular analyses

Twenty leaves with STB symptoms were collected per replicate from the fungicide untreated plots at GS 75 from every trial. Ten leaves were sent to BASF SE (Limburgerhof, Germany) for analysis of alterations associated with azole and SDHI resistance (pyrosequencing and qPCR) and ten were sent to EpiLogic (Freising, Germany) for fungicide sensitivity testing (microtitre assessment and EC_{50} calculations). To determine the frequency of key alteration associated with azole and SDHI resistance, leaves from each of the four replicates of individual trials were pooled into one bulk sample of 40 leaves. All diseased material from the pooled- leaves was collected in one sample (15 to 30 mg), which was ground for 1 min at 20 hz (Retsch) in the presence of a metal bead. Genomic DNA was extracted using NucleoSpin Plant II kit (Macherey-Nagel) following the manufacturer's protocol. Mutation analysis was carried out using a combination of pyrosequencing or qPCR (Rehfus, 2018b; Huf, 2020). The specific mutations investigated were SDH-B alterations N225I, N225T, H267X, T268I, and I269V, SDH-C alterations T79I, T79N, W80S, N86S and H152R in all three seasons, G90R in 2019 and 2020 and S83G in 2021, and CYP51 alterations D134G, V136A, V136C, A379G, I381V and S524T in all three seasons. In the case of samples analyzed for CYP51 mutations in 2019 and sensitivity to PTH-D, five trials were located away from the trial site where efficacy were

TABLE 2   Treatment mixtures and fenpicoxamid at full label doses from trials carried out in 2021.

Treatments	Active ingredient	Abbreviation	Active group	Dose (l/ha)	g a.i./ha
Untreated control	-			-	-
Questar, Corteva	Fenpicoxamid	FPX	QiI	2.0/1.5*	100/75
Revystar XL, BASF	Fluxapyroxad+ mefentrifluconazole	FXP+MFA	SDHI+DMI	1.5	75 +150
Revytrex, BASF	Fluxapyroxad+ mefentrifluconazole	FXP+MFA	SDHI+DMI	1.5	100 + 100
Elatus Era, Syngenta	Benzovindiflupyr+ prothioconazole	BVF+PTH	SDHI+DMI	1.0	75 + 150
Ascra Xpro, Bayer	Bixafen+fluopyram +prothioconazole	BIX+FLP +PTH	SDHI+SDHI +DMI	1.5	98 + 98 + 195
Silvron Xpro, Bayer	Bixafen+fluopyram	BIX+FLP	SDHI+SDHI	1	100 + 100

*The lower dose was used in FR and BE in accordance with the authorized rate in these countries.

measured, but both are expected to reflect their national level of sensitivity in 2019 (Table S1).

To determine the sensitivity of the local *Z. tritici* population in each trial to the SDHI and azole fungicides, ten single pycnidium isolates were retrieved from the other 40 leaves collected across the fungicide untreated plots in most cases (Table S3). Sensitivity was determined using a microtitre plate assay as previously described by Rehfus et al. (2018), with the SDHI fungicides FXP, BIX, FLP, and BVF and azole prothioconazole-desthio (PTH-D) tested each year and the azole MFA tested in only 2020 and 2021. The range of fungicide concentrations included differed depending on the fungicide (Table 1). No sensitivity data was generated for three trials in the United Kingdom, the Netherlands, and Germany in 2019 and one trial in Hungary in 2021, as no disease was present.

2.5 Statistical analyses

Statistical analyses were carried out using RStudio version 09.2 + 382 (RStudio, 2021) with α = 0.05 for all tests. The data were checked for normal distribution using QQ-plots and the Shapiro-Wilk normality test. Furthermore, residual plots and Bartlett's test were used to check for homogeneity of variance. However, it was not possible to correct the residuals by a transformation of variables and removal of outliers. Thus, all analyses were carried out using the non-parametric Kruskal-Wallis test and differences between groups were distinguished using Dunn's test, using the appropriate functions from the FSA R package (Ogle et al., 2022). For the correlation analysis, Pearson's r correlation coefficients and probability values were

calculated using *corr.test* of the "psych" package. Holm's correction was used to adjust for multiple comparisons.

3 Results

3.1 Overall disease pressures

Of the 25 trials included in the STB dataset, which were conducted over three seasons, a total of 18 and 19 trials developed adequate levels of STB on flag leaves (F) and F-1, respectively. Disease severity above 4% was considered a minimum for inclusion in the dataset. Disease pressures varied across seasons, with the highest pressures observed in 2019, followed by 2021, with the lowest levels recorded in 2020, which was regarded as a low-pressure season across much of Europe (Figure 2 and Table S4). Similarly, disease levels varied between countries, with the highest levels observed in Belgium (albeit it was only included in 2021) and Denmark, moderate levels in Germany, Ireland and Poland, and low levels in the UK (Figure 2). Across the three seasons, levels of STB in France varied considerably.

3.2 Fungicide efficacies

a) Azole & SDHI comparisons

Although levels of control provided by the individual solo treatments when applied at the full recommended field rate varied considerably between locations, a pattern of control could be observed. On the flag leaf, the azole MFA provided the most
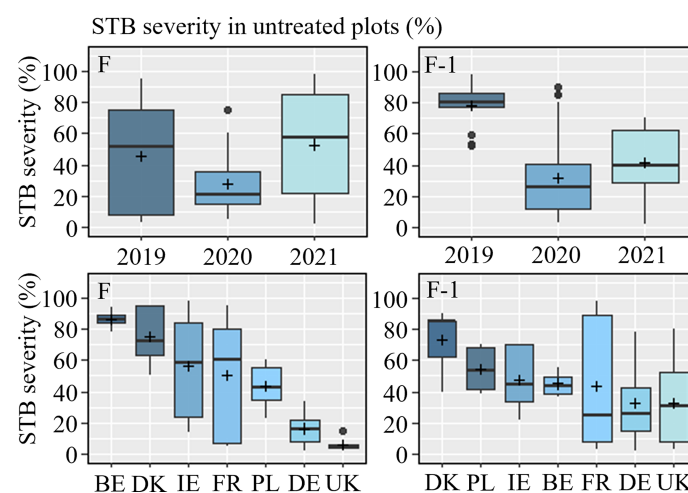

FIGURE 2
Septoria tritici blotch (STB) severity in untreated plots (%) on flag leaves (F) (left) and flag leaf minus one (F-1) (right) from 2019–2021, sorted by year (top) and country (bottom). The line inside the boxes indicates the median and '+' indicates the average.

control, followed by the SDHI FXP, which was superior to the SDHIs BIX and BVF, both of which provided only moderate levels of control comparable to the azole PTH, but significantly more when compared to the SDHI FLP (Table 3 and Figure 3). The variations in levels of control from the different treatments were similar across all trials (Figure 3), with standard deviations ranging from 24.5-30.7% for PTH, FXP, FLP, BIX and BVF on flag leaves, while the level of control from MFA was least variable (sd=18.1%). The efficacy patterns were similar on F-1, but at moderately lower levels, than those seen on flag leaves (Table 4 and Figure 3).

As significant differences have previously been observed in the frequencies of key alterations affecting both the azoles and SDHIs between Ireland and the UK with the rest of Europe (Hellin et al., 2021), levels of efficacy were separately analyzed for Ireland and the UK, and Continental Europe (Belgium, Denmark, France, Germany, Poland). In Ireland and the UK, on the flag leaf, the azole MFA provided the best control (76%), which was significantly greater than any of the other fungicides. FXP only provided moderate levels of disease control (46%) and

was not significantly better than either the SDHI BIX or the azole PTH, both of which did not provide significantly better control than the remaining SDHIs BVF or FLP. On F-1, the only differences observed were between MFA and all other fungicides, with MFA providing superior control (70%). This contrasts with Continental Europe, where on the flag leaf the SDHI FXP provided equal high levels of disease control (83%) to MFA (84%), which were significantly better than the good levels of control provided by BIX (63%) and BVF (61%), which were also significantly better than levels provided by either PTH (48%) or FLP (47%). Similar levels of control and differences were observed on F-1, with the exception that the difference between PTH and FLP was significant, with PTH providing better disease control.

b) Comparisons between full and half doses

Full and half doses were tested in 2019, and usable data on the effects against STB were collected from five trials (DK, UK, IE, FR, DE) (Table S1). The full dose of every compound tended to provide better STB control than the half doses; this was most pronounced in the case of FXP and MFA (Figure 4 and Table S5). The exception to

TABLE 3 Overview of septoria tritici blotch (STB) control and disease severity (%) in untreated (untr.) plots on flag leaves.

STB control (%), flag leaf					Untr.	FXP	BIX	BVF	FLP	PTH	MFA
Year	Trial	Ctry.	GS	DAA		125 g/ha	125 g/ha	75 g/ha	100 g/ha	200 g/ha	150 g/ha
2019	19309-1	DK	75	43	95.0	88	68	17	9	11	84
	19309-3	UK	75	40	4.1	36	13	17	13	13	41
	19309-4	IE	75	28	58.3	39	47	38	15	25	76
	19309-6	FR	75	55	65.9	97	70	86	34	34	94
	19309-7	DE	73	30	7.7	100	69	61	26	70	79
2020	20334-1	DK	75	42	61.3	96	93	92	72	58	97
	20334-3	DE	75-77	43	17.5	93	69	84	66	69	93
	20334-4	FR	85	58	6.2	90	74	69	56	76	92
	20334-5	PL	75	48	31.3	80	72	62	61	61	90
	20334-8	IE	75	49	18.6	42	11	25	21	39	73
2021	21328-1	DK	77	43	70.0	81	73	73	–	36	65
	21328-3	UK	75	38	8.0	72	50	22	–	50	100
	21328-4	IE	75	51	91.3	42	20	9	–	51	90
	21328-5	BE	75	38	86.1	65	25	30	–	29	82
	21328-6	FR	75	48	92.5	75	58	70	–	66	87
	21328-7	PL	75	45	55.0	81	61	73	–	39	75
	21328-9	DE	75	30	29.2	90	58	62	–	60	91
	21328-10	DE	83	40	10.7	44	33	28	–	28	65
Avg., 2019					45.2	70.7	52.4	41.6	18.9	30.2	73.9
Avg., 2020					28.1	79.5	63.1	66.3	55.2	59.8	89.0
Avg., 2021					52.9	68.5	46.9	45.1	–	43.4	81.7
Avg., 2019-2021					43.8	72.1	52.9	50.0	37.5	44.3	81.5
Avg., continental Europe, 2019-2021					47.0	82.7	63.0	61.3	46.5	47.9	83.8
Avg., Ireland, and UK, 2019-2021					36.1	46.2	28.0	22.1	16.4	35.8	76.0

STB severity was assessed at growth stage (GS) 73-85, 30-58 days after application (DAA) in 18 trials from 2019-2021. Trials from Continental Europe were carried out in Denmark (DK), France (FR), Germany (DE), Poland (PL) and Belgium (BE). Tested fungicides included mefentrifluconazole (MFA), prothioconazole (PTH), fluxapyroxad (FXP), bixafen (BIX), benzovindiflupyr (BVF), fluopyram (FLP). Colors signify ranking of treatment effects within individual trials. Efficacy data was ranked using a color gradient for each individual trial; the ranking should therefore be read horizontally and not vertically. Green: highest rating. Yellow: medium rating. Orange: lowest rating.
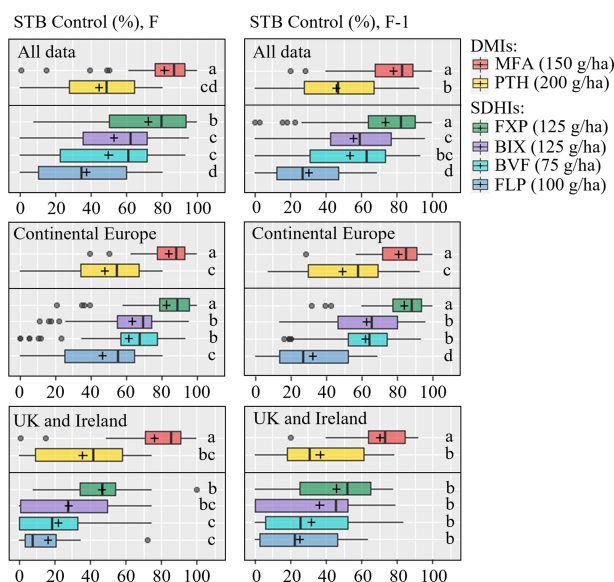
FIGURE 3
Septoria tritici blotch (STB) control (%) on flag leaves (left) and F-1 (right) were assessed at growth stage 65-85, 22-58 days after application in 18 trials on flag leaf and 19 on F-1 from 2019-2021. Trials from Continental Europe were carried out in Denmark, France, Germany, Poland and Belgium. Tested fungicides included mefentrifluconazole (MFA), prothioconazole (PTH), fluxapyroxad (FXP), bixafen (BIX), benzovindiflupyr (BVF), fluopyram (FLP). FLP was not included in 2021. The line inside the boxes indicates the median and '+' indicates the average. Different letters represent significant differences between treatments within boxplot as determined by Dunn's test.

this dose-response was in Ireland where FXP, FLP and PTH had lower efficacies at full dose than at half dose. On F-1, a similar overall pattern in efficacy was observed, although the difference between full and half rate MFA was not significantly different.

c) Azole/SDHI mixtures & QiI fenpicoxamid

During the 2021 trial season five commercial co-formulations were tested in 10 trials, of which 9 provided useable data (Table 5). Four of the co-formulations were based on the combination of azole + SDHI(s). For comparison, one co-formulation containing two SDHIs (Silvron Xpro) was tested and compared with the most potent solo SDHI (FXP in the form of Imtrex), solo azole (MFA, in the form of Revysol), and the new QiI fenpicoxamid (in the form of Questar). This testing clearly showed a stable and improved control of the co-formulations compared with either the azole or the SDHI used alone (Table 5). While MFA solo provided on average 72% and 76% control on F-1 and flag leaf, respectively; FXP similarly gave 69% and 82% control. Elatus ERA and Silvron Xpro gave comparable control to solo FXP, while both Revystar XL, Revytrex, Ascra Xpro and the new QiI fungicide Questar gave the highest average control. On F-1, the effects of the different solutions were overall very similar (Figure 5). If looking specifically at the UK and Irish trial sites, the efficacies from the solo SDHIs were clearly lower compared with the efficacy from the co-formulations.

d) Effect of azoles, SDHIs, mixtures of azoles/SDHIs and fenpicoxamid on yield responses

Yields from 21 trials were included in the analysis of solo actives (Figure 6). Generally the yield responses were best from MFA and FXP, which overall performed better than the rest of the tested active ingredients. The data also showed that FLP was significantly inferior to BIX and BVF and PTH. The SDHIs BIX, BVF and FLP gave significantly lower yield increases than MFA in UK and Ireland, which was also the case in Continental Europe. Nevertheless, the average yield increase suggested that FXP performed more in line with MFA in Continental Europe, and FLP gave significantly lower yield increases than all other treatments. Yield responses from fungicide mixtures were tested in 9 trials in 2021 (Figure 7). This analysis shows that all products increased yields significantly. Still, the three solo solutions and the five mixtures gave similar increases, and no statistically significant differences were found between the tested fungicides.

3.3 *Zymoseptoria tritici* azole and SDHI sensitivity

3.3.1 *In vitro* sensitivity

In vitro testing was carried out based on isolates from 29 trials. With a few exceptions ten *Z. tritici* isolates were successfully collected from each trial, and their sensitivity was analyzed (Table S3). These exceptions included: only four isolates were obtained from Poland in 2020 and again 2021;

TABLE 4 Overview of septoria tritici blotch (STB) control and disease severity (%) in untreated (untr.) plots on flag leaves minus one (F-1).

STB control (%), flag leaf -1					Untr.	FXP	BIX	BVF	FLP	PTH	MFA
Year	Trial	Ctry.	GS	DAA		125 g/ha	125 g/ha	75 g/ha	100 g/ha	200 g/ha	150 g/ha
2019	19309-1	DK	73	33	86.3	86	62	42	20	20	83
	19309-3	UK	75	40	61.1	23	12	8	11	11	50
	19309-6	FR	75	55	92.5	83	43	56	8	13	72
	19309-7	DE	73	30	77.1	90	28	19	12	30	59
2020	20334-1	DK	75	42	85.0	76	77	69	22	18	89
	20334-2	DE	75	37	27.3	52	40	43	25	33	66
	20334-3	DE	75-77	43	17.5	84	56	74	56	63	77
	20334-4	FR	75	44	6.3	93	48	65	44	68	79
	20334-5	PL	75	48	40.5	80	80	68	67	72	92
	20334-6	UK	78	43	5.7	32	35	17	16	23	72
	20334-8	IE	75	49	32.3	49	34	43	49	54	82
2021	21328-1	DK	75	35	47.5	94	92	93	–	50	89
	21328-2	UK	69	41	30.4	69	53	61	–	54	79
	21328-4	IE	65	35	63.3	55	48	30	–	41	69
	21328-5	BE	75	27	45.0	93	64	70	–	64	91
	21328-6	FR	71	33	24.6	97	94	90	–	84	93
	21328-7	PL	71	30	68.3	98	76	70	–	63	89
	21328-9	DE	69	22	36.4	89	72	68	–	55	90
	21328-10	DE	70	27	5.6	62	43	46	–	60	61
Avg., 2019					78.4	69.6	35.9	29.5	13.3	18.9	65.6
Avg., 2020					31.5	65.7	52.9	53.7	39.7	46.5	79.6
Avg., 2021					41.2	81.7	67.0	65.4	–	57.9	82.2
Avg., 2019-2021					45.3	73.3	55.4	53.7	30.3	45.7	77.8
Avg., Continental Europe, 2019-2021					47.9	83.7	62.6	62.0	32.2	49.1	80.6
Avg., Ireland + UK, 2019-2021					38.6	45.7	36.4	31.8	25.4	36.5	70.4

STB severity was assessed at growth stage (GS) 69-78, 22-55 days after application (DAA) in 19 trials from 2019-2021. Trials from Continental (Cont.) Europe were carried out in Denmark (DK), France (FR), Germany (DE), Poland (PL) and Belgium (BE). Tested fungicides included mefentrifluconazole (MFA), prothioconazole (PTH), fluxapyroxad (FXP), bixafen (BIX), benzovindiflupyr (BVF), fluopyram (FLP). Colors signify ranking of treatment effects within individual trials. Efficacy data were ranked using a color gradient for each individual trial; the ranking should therefore be read horizontally and not vertically. Green: highest rating. Yellow: medium rating. Orange: lowest rating.

only five isolates were obtained from the trial in Northern Germany in 2021, only three isolates were obtained from Belgium in 2021, which was the only trial conducted in Belgium across the trial series, and given this limited number these were excluded from further analysis. The sensitivity of _Z. tritici_ to MFA was only analyzed on isolates recovered in 2020 and 2021.

Amongst the isolates wide ranges in sensitivity (EC_{50}) were observed for each fungicide (BIX: 0.01 – 5.79 mg/l; BVF: 0.003 – 2.55 mg/l; FLP: 0.07 – 9.85 mg/l; PTH-D: 0.01 – 2.13 mg/l; MFA: 0.001 – 0.64 mg/l). Sensitivity also varied widely across the countries, and with the exception of MFA this variation was broadly similar for each fungicide (Figure 8 and Table S6). For all compounds except MFA, the least sensitive isolates were collected from Ireland and the UK, and the most sensitive came from Denmark and Poland. This was reflected in the differences observed between the countries in terms of their sensitivity to the SDHIs. No significant differences were seen between the sensitivity of isolates from Ireland and the UK, but both

countries had significantly less sensitive isolates than other countries. Statistically significant differences were identified between Denmark, France, Germany and Poland, but these were dependent on the specific SDHI (Figure 8), with both Denmark and Poland being the most sensitive, although not always significantly more sensitive than the collection from France. The Irish collection was significantly less sensitive to PTH-D compared to all other collections, including that from the UK. The differences between the PTH-D sensitivity of isolates from other countries were similar to those observed for the SDHIs (Figure 8).

No clear shift in the sensitivity was seen from 2019-2021, and no statistically significant differences were found between EC_{50} values in the different years overall. When grouped by country, significant differences were only observed among years in Germany for BVF, from which decreasing EC_{50} values were measured each year (data not shown).

Very high levels of correlation were found between the sensitivity of isolates towards FXP and BIX, BIX and BVF
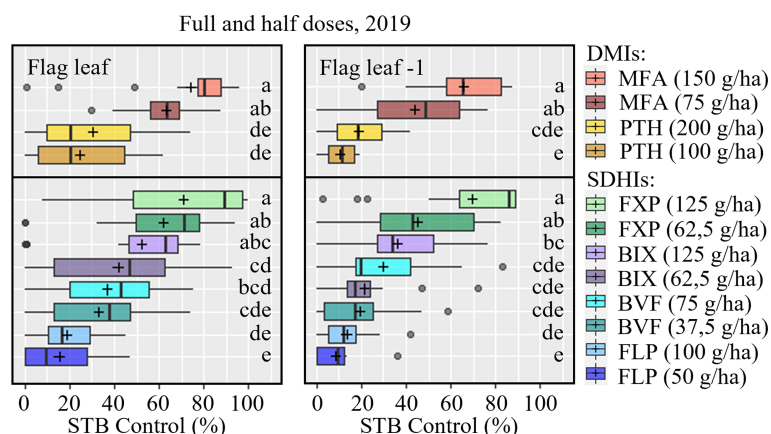
FIGURE 4
STB control (%) of full and half doses on flag leaves (left) and F-1 leaves (right) were assessed at growth stage 73-75, 33-55 days after application in five trials in 2019. The trials were carried out in Denmark, the United Kingdom, Ireland, France, and Germany. The tested fungicides included mefentrifluconazole (MFA), prothioconazole (PTH), fluxapyroxad (FXP), bixafen (BIX), benzovindiflupyr (BVF), fluopyram (FLP). The line inside the boxes indicates the median and '+' indicates the average. Different letters represent significant differences between treatments within boxplot as determined by Dunn's test.

(r=0.94 for both comparisons) and FXP and BVF (r=0.93). The correlations between FXP and FLP, BIX and FLP and FLP and BVF were slightly lower (r ranging from 0.72-0.76) (Figure 9). It was possible to analyze the correlation between MFA and PTH-D in 2020 and 2021, but no correlation was found.

Moderate levels of negative correlations were found between the average sensitivity of isolates *in vitro* (EC_{50} values) towards the specific SDHIs and the field efficacy (R^2 = 0.2-0.46) (data not presented).

3.3.2 Target site alteration frequencies

Amongst the leaf collections analyzed no SDH-B mutations were detected, nor were the SDH-C mutations T79I and G90R. Only the SDH-C mutations T79N, W80S, N86S and H152R were found, and the frequencies varied greatly across locations (Table 6). It should, however, be noted that due to the limits of detection associated with the methods used only frequencies above a threshold of 5% are reported. T79N and N86S were found most frequently, while W80S and H152R were only detected in the UK, in 4 and 2 locations, respectively, with frequencies ranging from 5-15%. T79N was found only in the UK and Ireland, where this mutation was found in every trial. The frequencies of this mutation were highest in Ireland ranging from 60% to 64%, while frequencies of 13-25% were found in the UK trials. Among the SDH-C mutations, only N86S was detected in countries other than the UK and Ireland. While this mutation was found at frequencies of 11-37% in Belgium, Germany, Hungary, the Netherlands, and Poland, it was most frequently detected in the UK and Ireland. Only in one trial in 2021 in the UK was this mutation not found, and in the remaining trials of this region the frequencies ranged from 18-41%. No clear development was seen from 2019-2021.

The CYP51 mutations were more evenly detected across Europe, but clear patterns were still discernible. The most widespread mutation was I381V, which was found at high frequencies in all samples. D134G and V136A were also present at high frequencies at most locations, with average frequencies of 38% and 55%, respectively, and only one Polish and one German trial had frequencies below 21%, while neither mutation was found in Hungary. A379G was found at intermediate frequencies with an average of 26% across all trials. This mutation was found at all locations, but a clear distinction was seen between the regions, and while 17% of isolates from Continental Europe carried this mutation on average, the frequency was 43% on average in The UK and Ireland. V136C was detected least frequently in an average of 15% across all trials, and the difference between the regions was less pronounced. However, in five trials located in Denmark, France, Hungary and Poland V136C was not detected, while the same was the case in one Irish trial. The greatest difference between the regions was seen for S524T, which was found with an average frequency of 23% in Continental Europe, while the average frequency was 79% in The UK and Ireland.

4 Discussion

Resistance emergence and gradual sensitivity shifting in *Z. tritici* populations towards SDHIs and azoles have become a widespread problem in many areas of European wheat production.This challenges current fungicide control practices, where SDHIs and azoles still are the most widely used fungicides for the control of STB (Jørgensen and Heick 2021, Turner et al.,

TABLE 5 Overview STB control from mixtures and FPX and disease severity (%) in untreated (untr.) plots.

STB Control (%), mixtures and FPX, flag leaf, 2021				Untr.	Revysol	Imtrex	Questar	Revystar XL	Revytrex	Elatus ERA	Ascra Xpro EC 260	Silvron Xpro
					MFA	FXP	FPX*	FXP+MFA	FXP+MFA	BVF+PTH	BIX+FLP+PTH	BIX+FLP
Trial	Ctry.	GS	DAA	-	150 g/ha	125g/ha	100/75 g/ha	75 + 150 g/ha	100 + 100 g/ha	75 + 150 g/ha	98 + 98 + 195 g/ha	100 + 100 g/ha
21328-1	DK	77	43	70.0	65	81	80	87	80	79	79	81
21328-3	UK	75	38	8.0	100	72	100	96	100	81	96	90
21328-4	IE	75	51	91.3	90	42	95	94	92	63	88	68
21328-5	BE	75	38	86.1	82	65	71	87	92	58	75	54
21328-6	FR	75	48	92.5	87	75	85	98	98	81	90	86
21328-7	PL	75	45	55.0	75	81	72	84	91	95	92	91
21328-9	DE	75	30	29.2	91	90	84	96	97	76	87	81
21328-10	DE	83	40	10.7	65	44	73	81	71	68	78	61
STB Control (%), F -1, 2021				Untr.	MFA	FXP	FPX	FXP+MFA	FXP+MFA	BVF+PTH	BIX+FLP+PTH	BIX+FLP
21328-1	DK	75	35	47.5	89	94	94	95	94	94	94	93
21328-2	UK	69	41	30.4	79	69	86	84	89	70	82	77
21328-4	IE	65	35	63.3	69	55	66	69	58	56	60	50
21328-5	BE	75	27	45.0	91	93	96	98	96	83	91	77
21328-6	FR	71	33	24.4	93	97	96	98	99	97	99	99
21328-7	PL	71	30	68.3	89	98	81	96	97	93	93	90
21328-9	DE	69	22	36.4	90	89	91	94	93	78	89	93
21328-10	DE	70	27	5.6	61	62	59	71	59	59	66	54
Avg., flag leaf				55.4	81.7	68.5	82.4	90.4	90.0	75.2	85.6	76.5
Avg., flag leaf -1				40.1	82.2	67.0	83.7	88.2	85.7	78.7	84.1	79.0

Assessments were carried out at growth stage (GS) 65-83, 27-45 days after application (DAA) in 9 trials in 2021. Tested fungicides included mefentrifluconazole (MFA), fluxapyroxad (FXP), fenpicoxamid (FPX), fluxapyroxad + mefentrifluconazole (FXP+MFA) (Revystar XL and Revytrex), benzovindiflupyr + prothioconazole (BVF+PTH), bixafen + fluopyram + prothioconazole (BIX+FLP+PTH) and bixafen + fluopyram (BIX+FLP). Colors signify the ranking of treatment effects within individual trials. Efficacy data were ranked using a color gradient for each individual trial; the ranking should therefore be read horizontally and not vertically. Green: highest rating. Yellow: medium rating. Orange: lowest rating.
*The lower dose was used in FR and BE in accordance with the authorized rate in these countries.

2021). Previous studies within the Eurowheat framework have investigated both *Z. tritici* sensitivity to azoles, CYP51 mutation, and azole field efficacies, which verified that sensitivity to the azoles is variable across Europe and, in general, decreases from Eastern to Western Europe (Jørgensen et al., 2021a). A similar trend has been described by Hellin et al. (2021). The more rapid local adaptation of the *Z. tritici* populations to fungicides in countries such as Ireland and Great Britain was also confirmed in those studies, which the authors attributed to (i) a higher disease pressure and (ii) more intensive fungicide usage to combat these pressures (Hellin et al., 2021; Jørgensen and Heick, 2021b).

The present study confirms that the presence of alterations conferring resistance to azole and SDHI fungicides are widespread throughout the European *Z. tritici* populations (Table 6). As also observed in other studies (Rehfus et al., 2018a; Rehfus et al., 2020; FRAC, 2021; Hellin et al., 2021), the most common SDH mutations found in this study are C-T79N and C-N86S, conferring moderate resistance to *Z. tritici* (Hellin et al., 2021). The target site mutation C-H152R is causing particular interest as it drastically decreases the sensitivity to all SDHIs. In this study, C-H152R was only detected in two of

the trials, both from the United Kingdom. Although previously detected in other continental European populations, some studies suggest that C-H152R comes with a fitness cost to the pathogen (Dooley et al., 2016; Rehfus et al., 2020), which makes it less likely to increase dramatically and may explain why it was not detected elsewhere in the presented trials series

The *in vitro* resistance testing in this study confirmed a reduced sensitivity towards all tested SDHIs in the Irish and British trials and that a gradual but still significant shifting also has taken place in Germany and Belgium compared with the sensitivity measured in Poland, Denmark, and France. These differences correspond to the differences in SDH-C mutations detected between the different countries. In this way, the previously seen gradient of increasing azole-resistant *Z. tritici* populations from east to west (Jørgensen et al., 2021a) can also be confirmed to apply to SDHI resistance. Previous studies have shown a good correlation between field efficacies and EC_{50} values from *in vitro* testing (Blake et al., 2018). The current study with SDHI fungicides shows a similar relationship. The current study with SDHI fungicides shows a similar relationship, however, the specific correlations between field efficacy on STB and EC_{50} values are only moderate (R^2=0.2-0.46), indicating that
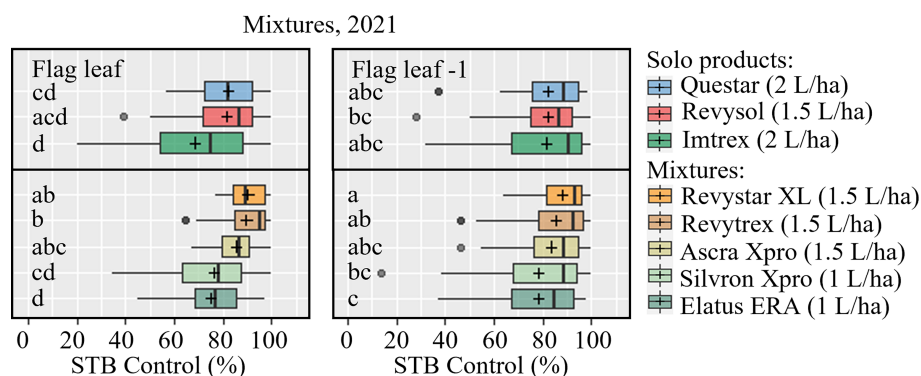
FIGURE 5

STB control (%) of mixtures on flag leaves (left) and F-1 leaves (right) were assessed at growth stage 65-83, 27-51 days after application in 9 trials in 2021. The trials were carried out in Denmark, the United Kingdom, Ireland, Belgium, France, Poland, and Germany. The tested fungicides included Questar (fenpicoxamid), Revysol (mefentrifluconazole), Imtrex (fluxapyroxad), Revystar and Revytrex (fluxapyroxad + mefentrifluconazole), Ascra Xpro (bixafen + fluopyram + prothioconazole), Silvron Xpro (bixafen + fluopyram), Elatus ERA (benzovindiflupyr + prothioconazole). The line inside the boxes indicates the median and '+' indicates the average. Different letters represent significant differences between treatments within boxplot as determined by Dunn's test.

also other factors like level of disease attack and timing impact the specific performances in individual trials.

Although the azole group of fungicides has been authorized for the control of foliar diseases in wheat since the late 1970s, this group is still regarded as among the most important fungicide groups available to growers. This goes for the control of diseases in wheat but also for most other major crops (Jørgensen and Heick, 2021b). Despite the erosion of efficacy measured for most azoles, it is also clear that the levels of efficacy they bring differ depending on the CYP51 mutations dominating the different European populations. Data collected since 2015 have confirmed that when applied at full rates, the older generation of azoles (epoxiconazole, metconazole, tebuconazole, difenoconazole, and prothioconazole) still provide moderate control (typically 40-70%) of STB (Jørgensen et al., 2018; Jørgensen et al., 2020). However, it is also clear that their field efficacy has been reduced (Kildea, 2016; Heick et al., 2017; Blake et al., 2018).

Prothioconazole is the second newest azole on the European fungicide market and has been used intensively as part of cereal disease control strategies for approximately 20 years (Jørgensen and Heick, 2021). In the current study, PTH still provided moderate control with an average of ca. 45% control from a single application at GS 37-39, although with a wide range of control observed (11-84%), depending on disease pressure, site, and season. The newest azole on the market, MFA, was authorized for control of STB in 2021. In the presented trials it provided good control of STB with an average of 82% control, covering a range of 41-100%. These results align with previous trials, where MFA similarly outperformed the older azoles giving an average control of ca. 80% (Jørgensen et al., 2020). As shown in this study, the reduced efficacy from PTH not only impacted field control of STB, but also gave reduced yields compared to
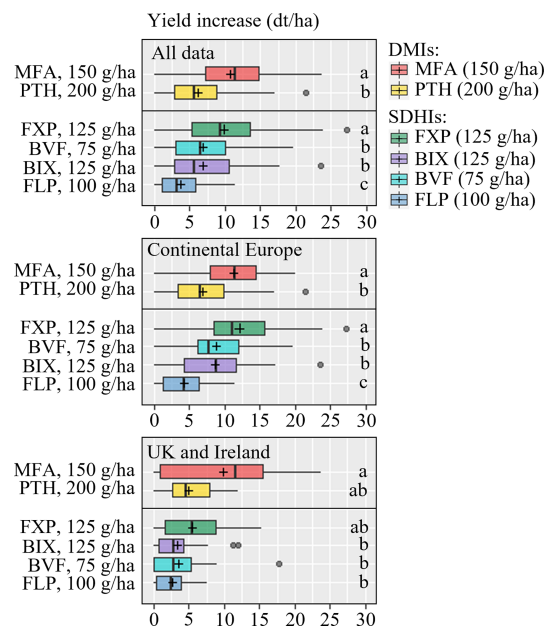
FIGURE 6

Yield increases from 21 field trials with the azoles mefentrifluconazole (MFA), prothioconazole (PTH) and the SDHIs fluxapyroxad (FXP), bixafen (BIX), fluopyram (FLP) and benzovindiflupyr (BVF). Trials from Continental Europe were carried out in Denmark (DK), France (FR), Germany (DE), Poland (PL) and Belgium (BE). FLP was not included in 2021. The line inside the boxes indicates the median and '+' indicates the average. Different letters represent significant differences between treatments within boxplot as determined by Dunn's test.
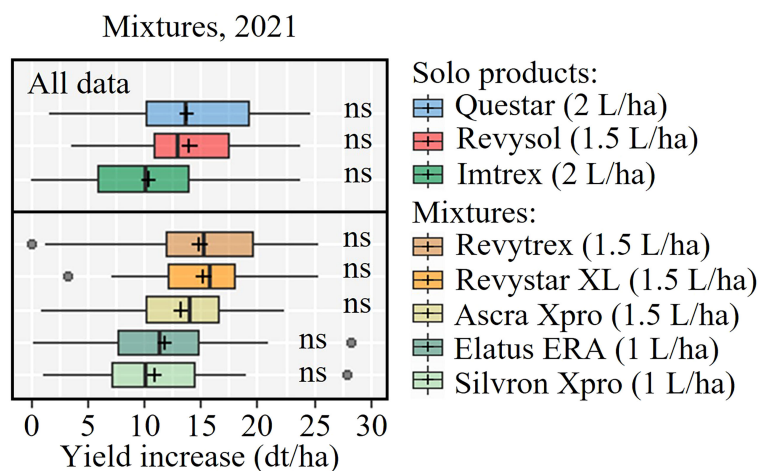
FIGURE 7
Yield increases from nine field trials with Questar (fenpicoxamid), Revysol (mefentrifluconazole), Imtrex (fluxapyroxad), Revytrex and Revystar (fluxapyroxad + mefentrifluconazole), Ascra Xpro (bixafen + fluopyram + prothioconazole), Elatus ERA (benzovindiflupyr + prothioconazole) and Silvron Xpro (bixafen + fluopyram). The line inside the boxes indicates the median and '+' indicates the average. NS = no significant differences were found between treatments determined by Dunn's test.

FIGURE 8
Sensitivity (log EC$_{50}$) of *Z. tritici* isolates, collected in Europe from 2019 to 2021, to SDHI fungicides fluxapyroxad (FXP), bixafen (BIX), fluopyram (FLP), and benzovindiflupyr (BVF), and the azoles prothioconazole-desthio (PTH-D) and mefentrifluconazole (MFA). Data is divided by countries Poland (PL), Denmark (DK), France (FR), Germany (DE), Belgium (BE), Ireland (IE), and the United Kingdom (UK). Different letters below the boxes represent significant differences between treatments within the plot as determined by Dunn's test.
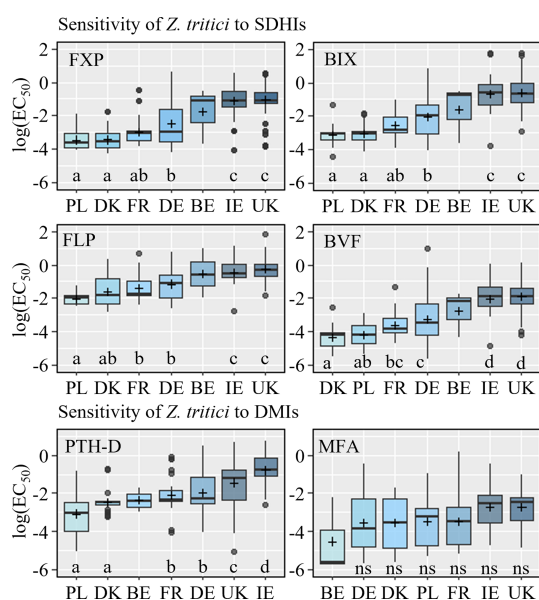
the more effective azole, MFA. On average, PTH yielded 107.2% (5.9 dt/ha) and MFA 112.3% (10.3 dt/ha). These differences are more pronounced than the differences seen by Jørgensen et al. (2020), where MFA only yielded 3 dt/ha more than PTH based on 17 trials across Europe in 2017-18. Despite a difference in cost between products with PTH and MFA, it is still clear that MFA will be a more profitable treatment than PTH.

Mefentrifluconazole has been seen to have a stronger binding efficiency ensuring good control even of highly shifted isolates with complex *CYP51*-haplotypes (Strobel et al., 2020). It is currently unclear whether MFA selects for specific alterations. Still, cross-resistance studies have shown a high correlation between MFA and difenoconazole/tebuconazole (Heick et al., 2020), and the effects of these actives are strongly impeded by alterations such as D134G and V136C.

As a result of historical experiences and the previously provided anti-resistance strategies, it is still strongly recommended to include anti-resistance strategies for MFA. These should include elements of not using the product repeatedly during the season- preferably once per season, avoiding applying solo products, using mixtures where all mixing partners are equally effective against STB, and not using it at excessive rates (van den Bosch et al., 2014).

4.1 Dose effect

An overall dose effect was observed for all tested fungicides in the five trials from 2019, where full and half rates were compared (Figure 4 and Table S5), although differences were not significant
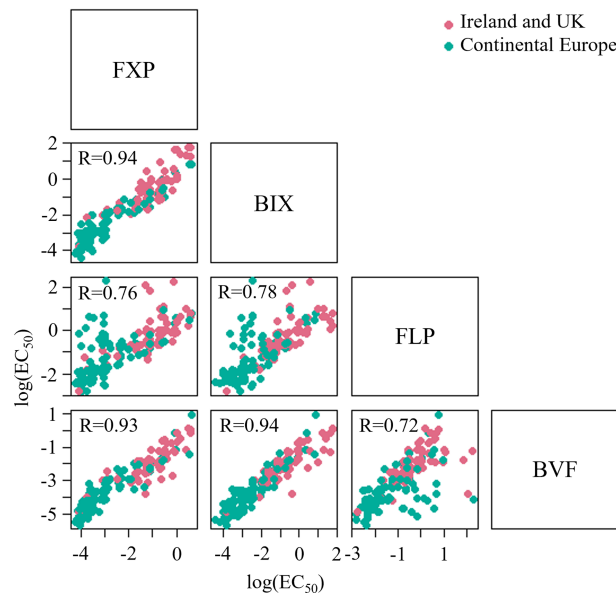
FIGURE 9
Cross-resistance between SDHI fungicides based on sensitivity data (EC$_{50}$) from 3 seasons and 202 *Z. tritici* isolates. Samples were collected from trials located in Ireland and UK, and continental Europe, including Denmark, Germany, Belgium, France and Poland.

as shown in Figure 4. The data showed a clearer dose-response for some active ingredients than for others, which also indicates that specific actives have a more considerable reduction potential than others. Specifically, for PTH, FLP, and BVF the impact from dose rates was relatively minor, around 10% or less, while it was more pronounced for the more potent products like MFA, FXP, and BIX. It is, however, worth mentioning that despite always giving inferior control on average, reducing the dose by 50% did not significantly impact the efficacy of any of the tested actives. Overall, a slightly poorer control was seen on the F-1 compared to the flag leaves, which given the treatment timing at GS 37-39, represented a more curative control on F-1, and a more preventive control on the flag leaves, which is in accordance with other investigations from the UK and Ireland (Blake et al., 2018).

Overall, keeping down the dose might be desirable to reduce environmental impact and selection for target site selection in accordance with van den Bosch et al. (2014). The economically optimal rate for any given fungicide type is highly variable and depends on grain price, site, seasons, and cultivars. Results from Ireland suggest that varieties exhibiting strong STB resistance may allow confident reductions in fungicide programs (Lynch et al., 2017).The use of fungicides at less than the recommended dose has been widely adopted in many countries (Jørgensen et al., 2017). The basis on which those dose decisions are being made is less clear, suggesting a gap between research and its translation into practice. The presented data in this paper show

that the potential for reductions is variable and more likely for effective mixtures than for solo solutions giving low to moderate control as presented in this paper. Practical farming in Western Europe uses typically 2-3 treatments per season. These treatments will consist of various products, most likely co-formulations, which include all available modes of action to ensure sufficient disease control.

4.2 Co-formulations

The tested co-formulations of an SDHI with an azole and showed more stable and improved control compared with either solo azoles or SDHIs (Figure 5 and Table 5). This is in line with previous findings from Ireland, which have shown that averaged across the margin above fungicide cost was greater for crops treated with the azole + SDHI treatment than an azole-only treatment for all varieties evaluated (Lynch et al., 2017).

If looking specifically at the UK and Irish sites and one of the German trials, which had EC$_{50}$ values for both chemistries, the efficacy from solo SDHIs was reduced (Figure 3). This likely confirms a link between reduced efficacy and higher EC$_{50}$ values. It is therefore recommended to apply co-formulations, as these will provide a more stable level of disease control and are expected to slow down resistance development, as described by van den Bosch et al. (2014). In regions now already challenged

TABLE 6 Frequencies of sdh-c and cyp51mutations.

			CYP51									SDH-C			
Year	Trial	Ctry.	D134G	V136A	V136C	A379G	I381V	S524T	Year	Trial	Ctry.	T79N	W80S	N86S	H152R
2021	21328-5	BE	53	67	21	15	95	30	2021	21328-5	BE	0	0	14	0
2019	19341-5	DE	31	38	0	21	99	32	2019	19309-7	DE	0	0	11	0
2019	19341-6	DE	53	59	10	19	98	22	2020	20334-2	DE	0	0	0	0
2020	20334-2	DE	64	74	11	17	100	24	2020	20334-3	DE	0	0	30	0
2020	20334-3	DE	11	24	28	29	100	62	2021	21328-9	DE	0	0	0	0
2021	21328-9	DE	62	71	15	22	97	24	2021	21328-10	DE	0	0	0	0
2021	21328-10	DE	25	40	17	18	100	71	2019	19309-1	DK	0	0	0	0
2019	19341-1	DK	59	68	0	12	99	5	2020	20334-1	DK	0	0	0	0
2020	20334-1	DK	40	50	13	13	99	7	2021	21328-1	DK	0	0	0	0
2021	21328-1	DK	45	54	0	10	100	5	2019	19309-6	FR	0	0	0	0
2019	19341-7	FR	42	63	0	19	79	23	2020	20334-4	FR	0	0	0	0
2020	20334-4	FR	46	61	18	11	96	24	2021	21328-6	FR	0	0	0	0
2021	21328-6	FR	42	60	18	12	95	19	2021	21328-8	HU	0	0	21	0
2021	21328-8	HU	0	0	0	38	98	0	2019	19309-5	NL	0	0	16	0
2019	19341-8	PL	14	20	0	20	96	6	2020	20334-5	PL	0	0	0	0
2020	20334-5	PL	24	35	15	11	99	23	2021	21328-7	PL	0	0	37	0
2021	21328-7	PL	26	34	13	11	100	13							
2019	19341-4	IE	45	80	0	24	97	88	2019	19309-4	IE	60	0	18	0
2020	20334-8	IE	51	93	16	46	100	97	2020	20334-8	IE	61	0	26	0
2021	21328-4	IE	62	86	15	35	100	96	2021	21328-4	IE	64	0	21	0
2019	19341-2	UK	23	42	23	36	98	63	2019	19309-2	UK	13	5	41	0
2019	19341-3	UK	33	61	19	45	98	71	2019	19309-3	UK	14	11	31	7
2020	20334-6	UK	34	60	28	42	100	52	2020	20334-6	UK	20	15	39	0
2020	20334-7	UK	36	69	35	50	98	90	2020	20334-7	UK	23	0	41	0
2021	21328-2	UK	32	58	31	52	98	66	2021	21328-2	UK	17	12	20	0
2021	21328-3	UK	38	58	34	57	100	92	2021	21328-3	UK	25	0	0	10
2019			37	54	6	24	95	39				12	3	20	1
2020			38	58	21	27	99	47				13	1.9	17	0
2021			39	53	16	27	98	42				11	1.2	11	1
Continental Europe			37	48	11	17	97	23				0	0	8	0
UK and Ireland			39	67	22	43	99	79				31	5	28	2

Screening was also carried out for the sdh-b mutations N225I, N225T, H267X, T268I, I269V, sdh-c mutations T79I and G90R which were not found at any of the locations. Colors signify the following ranges of mutation frequencies: green: 0%, light yellow: 1-20%, dark yellow: 21-40%, orange: 41-60%, red: 61-100%.

with shifs in sensitivity to both SDHIs and azoles, co-formulations can help maintain disease control, whilst in regions not yet challenged they will delay such shifting from occurring.

The benefits from co-formulations can, apart from the actives giving a broader control, also be the result of increased dose input. The SDHI co-formulation Silvron Xpro, including the two SDHIs BIX and FLP was also included in the trials to compare the efficacy of the SDHI component of the three-way mixture product, Ascra Xpro which also contains the azole PTH and is widely applied throughout Europe. The co-formulation of

BIX and FLP performed well and better than any of the solo SDHIs. Adding PTH to the two SDHIs increased control only slightly by 5-8%. Yield data from the co-formulation trials showed a similar pattern of treatment responses as seen for the field effects on STB. The yield increases were on average between 1 and 1.5 T/ha. The variation of yield increases from the three solo products and the five mixtures was limited, and no statistically significant differences were found between them (Figure 7). Treatment cost varies across Europe depending on specific national conditions, grain prices, etc. However, with a roughly estimated treatment cost equivalent to 2-4 dt/ha, the

solo treatments applied at GS 39 in this project have generally been very profitable and cost-effective.

The QiI fungicide FPX was included and compared with the efficacy of the different co-formulations. Although FPX performed in line with the better co-formulations, it is also important to emphasize that this active ingredient should not be used as a solo treatment. Resistance risk evaluations of FPX have shown that the product also is at risk of developing resistance and therefore only should be used in mixtures with other actives and only once per season (Owen et al., 2017; Fouché et al., 2022).

4.3 Cross-resistance

The degree of cross-resistance among SDHIs for several fungal pathogens has been discussed intensively (Yamashita and Fraaije, 2018). The current study confirms a clear cross-resistance between all tested SDHIs. Although significant positive cross-resistance was identified between FLP and BIX/FXP the scatterplots of these relationships indicated the presence of outliers that did not follow the overall positive pattern. Other studies have found FLP not always showing a clear cross-resistance pattern with other SDHIs (Yamashita and Fraaije, 2018; Steinhauer et al., 2019). It is generally accepted that cross-resistance patterns among SDHIs are complex and will continue to be so as many mutations confer full cross-resistance while others do not. The nature of the mutations found in populations varies with species and the selection compound used, but cross-resistance between all SDHIs has to be assumed at the population level (Sierotzki and Scalliet, 2013). Specifically in relation to FLP, a pre-existing non-target site resistance mechanism has been identified in *Z. tritici*, which has been found to be present at variable levels in different field populations (Yamashita and Fraaije, 2018), this might have impacted the lower levels of cross-resistance also seen in this study.

5 Conclusion

European testing of four SDHI fungicides for control of STB during three seasons confirms that shifting in fungicide efficacy against STB is challenged in some countries, while the efficacy is still good in other countries. The efficacy assessments based on field data, supported by *in vitro* testing, also clearly confirmed a significant shifting in *Z. tritici's* sensitivity from Eastern to Western Europe for all SDHIs tested. These changes were supported by differences in the composition of specific SDH-C

mutations between local *Z. tritici* populations. A high degree of cross-resistance between the SDHIs tested was seen based on EC_{50} values; however, the values of FLP were slightly less correlated with those of the other actives. Across all European countries, the azole MFA performed better for control of STB than PTH. The sensitivity to PTH also showed an East-West gradient across Europe based both on EC_{50} values and CYP51 mutations. The sensitivity to MFA did not differ significantly between the included countries. The reduced efficacy from both PTH and the tested SDHIs also impacted the yield responses, which were substantially reduced in Ireland and the UK compared with continental Europe. Co-formulations based on azoles and SDHIs, and the new QiI fungicide FPX proved to be the most effective solutions for the control of STB. This benefit was clearest where the populations had shifted to lower sensitivity to both azoles and SDHIs.

Data availability statement

The raw data supporting the conclusions of this article will be made available by the authors, without undue reservation.

Conflict of interest

GS was employed by company BASF. JB was employed by company ADAS.

The remaining authors declare that the research was conducted in the absence of any commercial or financial relationships that could be construed as a potential conflict of interest.

Although BASF funded this project, their primary role has been to assist in analysing specific target site alterations and provide the tested chemicals. The products included in the testing represent key fungicide actives and co-formulations belonging to both BASF and their competitors. BASF did not influence the experimental design, selection of locations, or computation and presentation of data.

Publisher's note

All claims expressed in this article are solely those of the authors and do not necessarily represent those of their affiliated organizations, or those of the publisher, the editors and the reviewers. Any product that may be evaluated in this article, or claim that may be made by its manufacturer, is not guaranteed or endorsed by the publisher.

Supplementary material

The Supplementary Material for this article can be found online at: https://www.frontiersin.org/articles/10.3389/fpls.2022.1060428/full#supplementary-material

References

Blake, J. J., Gosling, P., Fraaije, B. A., Burnett, F. J., Knight, S. M., Kildea, S., et al. (2018). Changes in field dose-response curves for demethylation inhibitor (DMI) and quinone outside inhibitor (QoI) fungicides against *Zymoseptoria tritici*, related to laboratory sensitivity phenotyping and genotyping assays. *Pest Manage. Sci.* 74 (2), 302–313. doi: 10.1002/ps.4725

Dooley, H., Shaw, M. W., Mehenni-Ciz, J., Spink, J., and Kildea, S. (2016). Detection of *Zymoseptoria tritici* SDHI-insensitive field isolates carrying the SdhC-H152R and SdhD-R47W substitutions. *Pest Manage. Sci.* 72, 2203–2207. doi: 10.1002/ps.4269

Fones, H., and Gurr, S. (2015). The impact of septoria tritici blotch disease on wheat: An EU perspective. *Fungal Genet. Biol.* 79, 3–7. doi: 10.1016/j.fgb.2015.04.004

Fouché, G., Michel, T., Lalève, A., Wang, N. X., Young, D. H., Meunier, B., et al. (2022). Directed evolution predicts cytochrome b G37V target site modification as probable adaptive mechanism towards the QiI fungicide fenpicoxamid in *Zymoseptoria tritici*. *Environ. Microbiol.* 24, 1117–1132. doi: 10.1111/1462-2920.15760

FRAC (2021) *Minutes of the succinate dehydrogenase inhibitor (SDHI) working grou.* Available at: https://www.frac.info/docs/default-source/working-groups/sdhi-fungicides/sdhi-meeting-minutes/minutes-of-the-2021-sdhi-meeting-20-21th-of-january-2021-with-recommendations-for-2021.pdf?sfvrsn=66eb499a_2.

Garnault, M., Duplaix, C., Leroux, P., Couleaud, G., Carpentier, F., David, O., et al. (2019). Spatiotemporal dynamics of fungicide resistance in the wheat pathogen *Zymoseptoria tritici* in France. *Pest. Manage. Sci.* 75, 1794–1807. doi: 10.1002/ps.5360

Gutiérrez-Alonso, O., Hawkins, N. J., Cools, H. J., Shaw, M. W., and Fraaije, B. A. (2017). Dose-dependent selection drives lineage replacement during the experimental evolution of SDHI fungicide resistance in *Zymoseptoria tritici*. *Evol. Appl.* 10, 1055–1066. doi: 10.1111/eva.12511

Heick, T. M., Justesen, A. F., and Jørgensen, L. N. (2017). Resistance of wheat pathogen *Zymoseptoria tritici* to DMI and QoI fungicides in the Nordic-Baltic region – a status. *Eur. J. Plant Pathol.* 149, 669–682. doi: 10.1007/s10658-017-1216-7

Heick, T. M., Matzen, N., and Jørgensen, L. N. (2020). Reduced field efficacy and sensitivity of demethylation inhibitors in the Danish and Swedish *Zymoseptoria tritici* populations. *Eur. J. Plant Pathol.* 157 (3), 625–636. doi: 10.1007/s10658-020-02029-2

Hellin, P., Duvivier, M., Clinckemaillie, A., Bataille, C., Legrève, A., Heick, T. M., et al. (2020). Multiplex qPCR assay for simultaneous quantification of CYP51-S524T and SdhC-H152R substitutions in European populations of *Zymoseptoria tritici*. *Plant Pathol.* 69, 1666–1677. doi: 10.1111/ppa.13252

Hellin, P., Duvivier, M., Heick, T. M., Fraaije, B. A., Bataille, C., Clinckemaillie, A., et al. (2021). Spatio-temporal distribution of DMI and SDHI fungicide resistance of *Zymoseptoria tritici* throughout Europe based on frequencies of key target-site alterations. *Pest Manage. Sci.* 77, 5576–5588. doi: 10.1002/ps.6601

Huf, A. (2020). *Characterisation of the sensitivity of zymoseptoria tritici to demethylation inhibitors in Europe* (Stuttgart (DE: Fakultät Agrarwissenschaften, Universität Hohenheim, Institut für Phytomedizin).

Jørgensen, L. N., and Heick, T. M. (2021b). Azole use in agriculture, horticulture, and wood preservation – is it indispensable? *Front. Cell. Infect. Microbiol.* 11:730297. doi: 10.3389/fcimb.2021.730297

Jørgensen, L. N., Hovmøller, M. S., Hansen, J. G., Lassen, P., Clark, B., Bayles, R., et al. (2014). IPM strategies and their dilemmas including an introduction to www.Eurowheat.org. *J.Integr. Agric.* 13, 265–281. doi: 10.1016/S2095-3119(13)60646-2

Jørgensen, L. N., Matzen, N., Hansen, J. G., Semaskiene, R., Korbas, M., Danielewicz, J., et al. (2018). Four azoles' profile in the control of septoria, yellow rust and brown rust in wheat across Europe. *Crop Prot.* 105, 16–27. doi: 10.1016/j.cropro.2017.10.018

Jørgensen, L. N., Matzen, N., Havis, N., Holdgate, S., Clark, B., Blake, J., et al. (2020). "Efficacy of common azoles and mefentrifluconazole against septoria, brown rust and yellow rust in wheat across Europe," in *Modem fungicides and antifungal compounds IX*. Eds. H. B. Deising, B. Fraaije, A. Mehl, E. C. Oerke, H. Sierotzki and G. Stammler (Braunschweig: Deutsche Phytomedizinische Gesellschaft), 27–34.

Jørgensen, L. N., Matzen, N., Heick, T. M., Havis, N., Holdgate, S., Clark, B., et al. (2021a). Decreasing azole sensitivity of z. tritici in Europe contributes to reduced and varying field efficacy. *J. Plant Dis. Prot.* 128 (1), 287–301. doi: 10.1007/s41348-020-00372-4

Jørgensen, L. N., van den Bosch, F., Oliver, R. P., Heick, T. M., and Paveley, N. D. (2017). Targeting fungicide inputs according to need. *Annu. Rev. Phytopathol.* 55, 181–203. doi: 10.1146/annurev-phyto-080516-035357

Kildea, S. (2016). "Wheat disease control and resistance issues," in *National Tillage Conference 2016*, Vol. 39 (Teagasc: Oak Park, Crop Research, Carlow).

Kildea, S., Hellin, P., Heick, T. M., and Hutton, F. (2022). Baseline sensitivity of European *Zymoseptoria tritici* populations to the complex III respiration inhibitor fenpicoxamid. *Pest Manage. Sci.* 78(11):4488–4496. doi: 10.1002/ps.7067

Klink, H., Verreet, J.-A., Hasler, M., and Birr, T. (2021). Will triazoles still be of importance in disease control of *Zymoseptoria tritici* in the future? *Agron.* 11, 933. doi: 10.3390/agronomy11050933

Lancashire, P. D., Bleiholder, H., Langelüddecke, P., Stauss, R., Weber, E., and Witzenberger, A. (1991). A uniform decimal code for growth stages of crops and weeds. *Ann. Appl. Biol.* 119, 561–601. doi: 10.1111/j.1744-7348.1991.tb04895.x

Lynch, J. P., Glynn, E., Kildea, S., and Spink, J. (2017). Yield and optimum fungicide dose rates for winter wheat (*Triticum aestivum* l.) varieties with contrasting ratings for resistance to septoria tritici blotch. *Field Crops Res.* 204, 89–100. doi: 10.1016/j.fcr.2017.01.012

McDonald, B. A., and Linde, C. (2002). Pathogen population genetics, evolutionary potential, and durable resistance. *Annu. Rev. Phytopathol.* 40, 349–379. doi: 10.1146/annurev.phyto.40.120501.101443

Oepp/Eppo (2014). *Foliar and ear diseases on cereals* Vol. 44 (EPPO Bulletin).

Oerke, E. (2006). Crop losses to pests. *J. Agric. Sci.* 144, 31–43. doi: 10.1017/S0021859605005708

Ogle, D. H., Doll, J. C., Wheeler, P., and Dinno, A. (2022). *FSA: Fisheries stock analysis* (R package version 0.9.3). Available at: https://github.com/fishR-Core-Team/FSA.

Owen, W. J., Yao, C., Myung, K., Kemmitt, G., Leader, A., Meyer, K. G., et al. (2017). Biological characterisation of fenpicoxamid, a new fungicide with utility in cereals and other crops. *Pest Manage. Sci.* 73, 2005–2016. doi: 10.1002/ps.4588

Rehfus, A. (2018b). *Analysis of the emerging situation of resistance to succinate dehydrogenase inhibitors in pyrenophora teres and zymoseptoria tritici in Europe.*

Rehfus, A., Katamadze, A., Strobel, D., Bryson, R., and Stammler., G. (2020). "Evoloution of sdh adaptation in cereal pathogens in Europe," in *Modern fungicides and antifungal compounds*. Eds. H. B. Deising, B. Fraaije, A. Mehl, E. C. Oerke, H. Sierotzki and G. Stammler (Deutsche: Phytomedizinische Gesellschaft, Braunschweig), 99–104.

Rehfus, A., Strobel, D., Bryson, R., and Stammler, G. (2018a). Mutations in sdh genes in field isolates of *Zymoseptoria tritici* and impact on the sensitivity to various succinate dehydrogenase inhibitors. *Plant Pathol.* 67, 175–180. doi: 10.1111/ppa.12715

RStudio (2021). 09.2+382 "Ghost Orchid" Release (fc9e217980ee9320 126e33cdf334d4f4e105dc4f, 2022-01-04) for Windows. Mozilla/5.0 (Windows NT 10.0; Win64; x64) AppleWebKit/537.36 (KHTML, like Gecko). QtWebEngine/5.12.8 Chrome/69.0.3497.128 Safari/537.36.

Savary, S., Willocquet, L., Pethybridge, S. J., Esker, P., McRoberts, N., and Nelson, A. (2019). The global burden of pathogens and pests on major food crops. *Nat. Ecol. Evol.* 3, 430–439. doi: 10.1038/s41559-018-0793-y

Scalliet, G., Bowler, J., Luksch, T., Kirchhofer-Allan, L., Steinhauer, D., Ward, K., et al. (2012). Mutagenesis and functional studies with succinate dehydrogenase inhibitors in the wheat pathogen *Mycosphaerella graminicola*. *PloS One* 7 (4), e35429. doi: 10.1371/journal.pone.0035429

Sierotzki, H., and Scalliet, G. (2013). A review of current knowledge of resistance aspects for the next-generation succinate dehydrogenase inhibitor fungicides. *Phytopathology* 103, 880–887. doi: 10.1094/PHYTO-01-13-0009-RVW

Singh, R. P., Singh, P. K., Rutkoski, J., Hodson, D. P., He, X., Jørgensen, L. N., et al. (2016). Disease impact on wheat yield potential and prospects of genetic control. *Annu. Rev. Phytopathol.* 54, 303–322. doi: 10.1146/annurev-phyto-080615-095835

Steinhauer, D., Salat, M., Frey, R., Mosbach, A., Luksch, T., Balmer, D., et al. (2019). A dispensable paralog of succinate dehydrogenase subunit c mediates standing resistance towards a subclass of SDHI fungicides in *Zymoseptoria tritici*. *PloS Pathog.* 15 (12), 1–35. doi: 10.1371/journal.ppat.1007780

Strobel, D., Bryson, R., Semar, M., Stammler, G., Kienle, M., and Smith, J. (2020). "Mefentrifluconazole (Revysol) the first isopropanol-azole," in *Modern fungicides and antifungal compounds*. Eds. B. H, B. Fraaije, A. Mehl, E. C. Oerke, H. Sierotzki and G. Stammler (Deutsche: Phytomedizinische Gesellschaft, Braunschweig), 259–264.

Turner, J. A., Chantry, T., Taylor, M. C., and Kennedy, M. C. (2021). Changes in agronomic practices and incidence and severity of diseases in winter wheat in England and Wales between 1999 and 2019. *Plant Pathol.* 70, 1759–1778. doi: 10.1111/ppa.13433

van den Bosch, F., Oliver, R., van den Berg, F., and Paveley, N. (2014). Governing principles can guide fungicide-resistance management tactics. *Annu. Rev. Phytopathol.* 52, 175–195. doi: 10.1146/annurev-phyto-102313-050158

Yamashita, M., and Fraaije, B. (2018). Non-target site SDHI resistance is present as standing genetic variation in field populations of *Zymoseptoria tritici*. *Pest Manage. Sci.* 74, 672–681. doi: 10.1002/ps.4761

Check for updates

A new NLR disease resistance gene *Xa47* confers durable and broad-spectrum resistance to bacterial blight in rice

Yuanda Lu[1,2], Qiaofang Zhong[1], Suqin Xiao[1], Bo Wang[1],
Xue Ke[1], Yun Zhang[1], Fuyou Yin[1], Dunyu Zhang[1], Cong Jiang[1],
Li Liu[1], Jinlu Li[1], Tengqiong Yu[1], Lingxian Wang[1],
Zaiquan Cheng[1]* and Ling Chen[1]*

[1]Biotechnology and Germplasm Resources Institute, Yunnan Academy of Agricultural Sciences,
Yunnan Provincial Key Lab of Agricultural Biotechnology, Kunming, China, [2]College of Plant
Protection, Yunnan Agricultural University, Kunming, China

Bacterial blight (BB) induced by *Xanthomonas oryzae* pv. *oryzae* (Xoo) is a devastating bacterial disease in rice. The use of disease resistance (*R*) genes is the most efficient method to control BB. Members of the nucleotide-binding domain and leucine-rich repeat containing protein (NLR) family have significant roles in plant defense. In this study, *Xa47*, a new bacterial blight *R* gene encoding a typical NLR, was isolated from G252 rice material, and XA47 was localized in the nucleus and cytoplasm. Among 180 rice materials tested, *Xa47* was discovered in certain BB-resistant materials. Compared with the wild-type G252, the knockout mutants of *Xa47* was more susceptible to Xoo. By contrast, overexpression of *Xa47* in the susceptible rice material JG30 increased BB resistance. The findings indicate that *Xa47* positively regulates the Xoo stress response. Consequently, *Xa47* may have application potential in the genetic improvement of plant disease resistance. The molecular mechanism of *Xa47* regulation merits additional examination.

KEYWORDS

Xa47, NLR, *Xanthomonas oryzae* pv. *oryzae*, broad-spectrum resistance, bacterial blight

Introduction

Crop production occurs in complex and changing ecological environments, and plants inevitably experience many biotic stresses, including attacks by fungi, bacteria, viruses, and insects (Savary et al., 2019; Zhang et al., 2020). To prevent onset of disease, plants evolved innate immune mechanisms to stop the invasion of pathogens primarily by recognizing

pathogenic signals by various genes and associated gene products (Ahuja et al., 2012; Bednarek, 2012). When a pathogen invades, the first level of a plant defense system is activated, and pattern recognition receptors on plant cell membranes recognize pathogen/microbe-associated molecular patterns (PAMPs/MAMP), triggering PAMPs/MAMPs-induced immunity (PTI/MTI), which inhibits further pathogen spread (Tena et al., 2011). To interfere with or break plant PTI/MTI, pathogens secrete effectors or virulence factors that enter plant cells directly or indirectly to cause infection (Chen and Ronald, 2011). However, because of co-evolution with pathogens, the effectors can be recognized directly or indirectly by plant resistance proteins to trigger effector-triggered immunity (ETI), a second level of a plant immune system, which is also known as "gene-to-gene" disease resistance (Jones and Dangl, 2006; Dodds and Rathjen, 2010). Activation of ETI is usually accompanied by a burst of reactive oxygen species and a hypersensitive response (HR), among other actions, to prevent pathogen colonization (Spoel and Dong, 2012; Withers and Dong, 2017).

Rice is one of the most important agricultural crops and is consumed by more than half of the global population (Ainsworth, 2008). Rice production is often threatened by pathogens, and rice leaf blight (BB) caused by *Xanthomonas oryzae* pv. *oryzae* (Xoo) can cause 10% to 30% reductions in yield or even crop failure (Liu et al., 2014). Compared with chemical applications, cultivating resistant varieties is a more effective and environmentally friendly method to control BB in rice (Ke et al., 2017; Li et al., 2020; Zhang et al., 2020). The interaction between rice and Xoo has become an important model in analyzing plant disease resistance and bacterial pathogens (Niño-Liu et al., 2006). Clarifying the various molecular mechanisms of this interaction is of great importance to basic research and crop breeding (Jiang et al., 2020). To date, 12 genes against Xoo have been isolated: *Xa1*, *Xa3/Xa26*, *Xa4*, *xa5*, *Xa7*, *Xa10*, *xa13*, *Xa21*, *Xa23*, *xa25*, *Xa27*, and *xa41* (Song et al., 1995; Yoshimura et al., 1998; Iyer and McCouch, 2004; Sun et al., 2004; Gu et al., 2005; Jiang et al., 2006; Xiang et al., 2006; Yang et al., 2006; Liu et al., 2011; Tian et al., 2014; Wang et al., 2015; Hutin et al., 2016; Hu et al., 2017; Chen et al., 2021). The genes encode multiple protein types and are an important in the rice–Xoo interaction. Notably, nine of the genes (*Xa1*, *Xa7*, *Xa10*, *Xa23*, *Xa27*, *xa5*, *xa13*, *xa25*, and *xa41*) are related to the transcription activator-like effectors (TALEs) secreted by the type III secretion system (T3SS) of pathogens in the resistance mechanism of host cells (Boch and Bonas, 2010; Jiang et al., 2020).

The TALEs are important pathogenic factors secreted by Xoo that enter the host nucleus with the assistance of T3SS and then bind to a specifically identified target gene promoters to regulate the transcription of downstream genes (Bogdanove et al., 2010). The promoter regions that bind to TALEs are effector binding elements (EBEs). The target genes to which TALEs bind can be either susceptibility genes that regulate host plant physiology to help a pathogen survive and increase colonization or disease resistance genes that mediate the production of plant ETI (Boch et al., 2014; Peng et al., 2019). For example, instance, the expression of the rice executor resistance (*R*) genes *Xa7*, *Xa10*, *Xa23*, and *Xa27* leads to transcriptional activation by the TALEs AvrXa7/PthXo3, AvrXa10, AvrXa23, and AvrXa27, respectively, triggering a host-induced HR response to prevent Xoo colonization in rice and achieve strong disease resistance (Luo et al., 2021). Alternatively, Xoo TALEs (PthXo1, PthXo2, AvrXa7/Tal5/PthXo3/TalC) can directly target EBEs of the corresponding *OsSWEET* genes (*Xa13/OsSWEET11/Os8N3*, *Xa25/OsSWEET13*, and *Xa41/OsSWEET14/Os11N3*), thereby up-regulating the expression in rice, which supplies sufficient sugar for the growth of Xoo in host cells and increases susceptibility to BB (Yuan et al., 2009; Streubel et al., 2013; Zhou et al., 2015). Moreover, mutations in the EBEs of *xa13*, *xa25*, and *xa41* interfere with Xoo TALE interactions, resulting in cryptic resistance to BB (Chu et al., 2006; Yang et al., 2006; Liu et al., 2011; Yuan et al., 2011; Hutin et al., 2015; Zhou et al., 2015). In addition, *Xa1* and its alleles (*Xa2*, *Xa14*, *Xa31*, and *Xa45*) encode atypical nucleotide binding site-leucine-rich repeat (NBS-LRR) containing proteins that recognize multiple Xoo TALEs (PthXo1, Tal4, and Tal9d) and can confer resistance to BB in rice (Zhang et al., 2020). However, interfering TALEs (iTALEs), which are truncated to lack a transcriptional activation domain, can interfere with XA1, XA2, XA14, and XA45 to confer resistance to Xoo in rice (Zhang et al., 2020).

Previously, the gene *Xa47* was localized in a 26.24-kb interval between molecular markers R13I14 and 13rbq-71 and was found to co-segregate with the InDel marker Hxjy-1 (Xing et al., 2021). Based on analyses of the Gramene database and the rice genome RGAP annotation database, *LOC_Os11g46200* (in this study, *xa47*) was ultimately selected as the target gene of *Xa47* (Xing et al., 2021). The gene *Xa47* was originally discovered in the Yuanjiang common wild rice infiltration line material G252, but the gene has not been cloned. However, whether G252, a broad-spectrum, highly resistant rice germplasm material, is endowed with the resistance function of *Xa47* is unknown. Therefore, in this study, the *Xa47* gene was cloned, its function in improving resistance to BB was investigated, and its potential mechanism of resistance was examined.

Materials and methods

Plant materials and bacterial inoculation

The rice G252, a BC_2F_{16} generation material of the Yuanjiang common wild rice infiltration line (IL), was the donor material for *Xa47* cloning and gene editing. Indica varieties susceptible to Xoo strains PXO99 and PB included IR24,IRBB1, and IRBB14. Dr. Zaiquan Cheng (Biotechnology & Genetic Germplasm Institute, Yunnan Academy of Agricultural Sciences, Yunnan, China) kindly provided 80 rice landraces and 100 ILs. Transgenic

plants were grown in an artificial climate chamber at 28°C for 12 h (light) and 20°C for 12 h (dark) with relative humidity of 65% to 80%. The other rice materials were grown in the field.

The Xoo strains included the Chinese strains YN18 (C1), YN1 (C2), GD414 (C3), HEN11 (C4), ScYc-b (C5), YN7 (C6), JS49-6 (C7), FuJ (C8), and YN24 (C9), the Filipino strain PXO99, and PB, a strain with Tal3a and Tal3b genes knocked out from PXO99 (Ji et al., 2016). All Xoo strains were grown at 28°C on nutrient agar medium (1 g/L yeast extract, 12 g/L sucrose, 18 g/L agar, 5 g/L peptone, 3 g/L beef extract). Cultured Xoo strains were eluted with sterile water, and concentrations of bacterial suspensions were configured to 3×10^8 colony forming units/mL (OD600 = 0.5). Rice plants at the gestation stage were inoculated with a Xoo strain using the sword leaf tip-clipping method. Disease lesion length (resistant: ≤6 cm; susceptible: >6 cm) was measured approximately 14 d after inoculation when disease development of the susceptible control material JG30 stabilized, as described previously (Chen et al., 2008). Each Xoo strain was tested in three replicates, each with three rice plants. A detailed description of the Xoo strains involved in this study can be found in Supplementary Table 1.

Cloning and sequence analysis of *Xa47*

The CTAB method was used to extract rice genomic DNA (Porebski et al., 1997). Based on the sequence of *LOC_Os11g46200* (*xa47*), the primer pair Xa47-12F/R, with forward primer 5'-TGGTGCCTATACCTTCATTG-3' and reverse primer 5'-AATTCGTCATGTTCTACTAGC-3', was designed and used to clone the gene. PCR amplification of *Xa47* was performed using primers Xa47-12F/R and G252 genomic DNA, and the PCR products were used for sequencing. Based on the sequencing results, the CDS sequence of *Xa47* was obtained using SnapGene 6.0 software (GSL Biotech, USA). BLASTP[1] (https://blast.ncbi.nlm.nih.gov/Blast.cgi) was used for the *Xa47* homologous gene search, and CD-search (https://www.ncbi.nlm.nih.gov/Structure/cdd/wrpsb.cgi) was used to predict protein structural domains. Multiple sequence alignment and phylogenetic analysis was performed using DNAMAN8.0 (Lynnon Biosoft, USA) and (Kumar et al., 2016), and bootstrap testing was performed with 500 replicates using the neighbor-joining method.

Detection of *Xa47* in different germplasm resources

The gene *Xa47* was detected in 180 germplasm resources (Supplementary Tables 2, 3) using a molecular marker screening method combined with homologous cloning, in which the primers used were Hxjy-1F/R and Xa47-12F/R, in that order. In parallel, the rice materials were evaluated for resistance to strains C5 and C9 (described above).

Subcellular localization of XA47

An Eastep® Super Total RNA Isolation kit (Proegal, Shanghai, China) was used to extract total RNA from rice leaves. A HiScript® III RT SuperMix for qPCR kit (Vazyme Biotech Co., Ltd., Nanjing, China) was used to synthesize cDNA. Based on the *Xa47* gene sequence and the pBE221-GFP expression vector, primers with double restriction enzyme sites XbaI and SalI were designed to amplify the *Xa47* CDS sequence without a terminator. Polyethylene glycol mediated the transient expression of the XA47::GFP and pBE221-GFP constructs in rice protoplasts under the control of the 35S promoter. Sixteen hours after inoculation, resulting protoplasts were observed using a laser scanning confocal microscope (Nikon A1, Tokyo, Japan).

CRISPR-Cas9-based gene editing in rice

The target vector pH-ubi-cas9 and the entry vector pOs-sgRNA were generously provided by Dr. Liang Chen (College of Life Sciences, Xiamen University, China). The selection and design of sgRNA target sequences were based on the web tool CRISPR-P2.0 (http://crispr.hzau.edu.cn/CRISPR2/news.php) (He et al., 2021). The pOs-*Xa47*-sgRNA was obtained by ligation reaction of sgRNA with BsaI-digested pOs-sgRNA vector by T4 DNA Ligase (New England Biolabs Ltd., Beijing, China). Similarly, the *Xa47*-ubi-Cas9 recombinant vector was obtained by ligation reaction of pOs-*Xa47*-sgRNA vector and pH-ubi-cas9 vector by T4 Polynucleotide Kinase (New England Biolabs Ltd., Beijing, China). The *Xa47*-ubi-Cas9 vector was introduced into G252 by an *Agrobacterium*-mediated method (Zhang et al., 2016). All CRISPR plants were genotyped, target locus regions were amplified, and PCR products were Sanger sequenced.

35S::*Xa47* expression vector construction and transformation

The *Xa47*-CDS containing the homologous sequence of pCAMBIA1305 was amplified using the appropriate double digestion sites NcoII and BstEI based on the CDS sequence of *Xa47* and the pCAMBIA1305 expression vector. This approach used the primers *Xa47*-CDS-F/R and Xa47-35S-F/R (attached). The *Xa47* was ligated to the pCAMBIA1305 vector in the presence of T4 DNA Ligase (TaKaRa, Dalian, China), resulting in the CaMV35S promoter-driven 35S::Xa47. An *Agrobacterium*-mediated approach was used to deliver the 35S::*Xa47* expression vector into the indica rice variety JG30, which is sensitive to Xoo strains. All transgenic plants were screened for thaumatin resistance. The resistant transgenic plants were planted in greenhouse until maturity. The continuous PCR test for *Xa47* was carried out. T_2 homozygous transgenic plants were selected for further analysis.

Gene expression assays

From the inverted second leaves of wild-type and mutant lines (described above), RNA was isolated, and cDNA was synthesized. Reverse transcription quantitative PCR (RT-qPCR) using ChamQTM Universal SYBR® qPCR Master Mix (Vazyme Biotech Co., Ltd., Nanjing, China) was performed on a LightCycler® 96 platform (Roche, Shanghai, China). The rice *Actin1* gene was used as the endogenous control. All reactions were conducted three times. The $2^{-\triangle\triangle Cq}$ approach (Livak and Schmittgen, 2001) was used to examine relative expression. The primers used in this work are listed in Supplementary Table 4.

Statistical analyses

For statistical analysis with Student's *t*-tests, SPSS 26.0 (IBM, USA) was used. To prepare figures, TBtools (Chen et al., 2020) and GraphPad Prism 8.0 software (GraphPad Software, China) were used.

Results

Cloning of *Xa47*

Previously, to isolate *Xa47*, an F2 population obtained by crossing the IL G252 with the susceptible cultivar 02428, which therefore included plants with or without *Xa47*, was inoculated with different strains of Xoo to trigger *Xa47*-mediated BB resistance in rice (Xing et al., 2021). After gene linkage and lesion length analyses, the *Xa47* gene was localized to a 2.6-kb

area on chromosome 11 between markers Hxjy-14 and 13rbq-71 (Figure 1A). In addition, *Xa47* in G252 was identified as a dominant disease-resistance gene (Xing et al., 2021). According to the reference sequence of the rice cultivar Nipponbare (NPB), the NLR-encoding gene *LOC_Os11g46200* was chosen as the target gene for *Xa47* (Xing et al., 2021).

Homologous cloning was used to clone *Xa47* in sequential rice materials G252 and 02428 (Supplementary Figures 1A–C). Notably, the *xa47* sequences in rice materials 02428 and NPB were consistent, whereas the *Xa47* sequences in G252 differed from those sequences (Supplementary Figure 2). The gene *Xa47* was 4,240 bp in length, had three exons and two introns (Figure 1B), and encoded 802 amino acids (aa) (Figure 1C). The protein XA47 (G252) contained a typical NB-ARC domain and a leucine-rich repeat (LRR) protein, consisting of 237 and 178 aa, respectively (Figure 1C). In addition, XA47 (G252) also contained an Rx N-terminal domain (Figure 1C). Further multisequence alignment and phylogenetic analysis showed that all homologous genes of *Xa47* were distributed in graminaceous crops. Notably, XA47 (G252) was slightly more homologous to EAY84977.1 than to XA47 (NPB) (Supplementary Figure 3).

Xa47 is in some bacterial blight-resistant rice

The functional marker Hxjy-1 of *Xa47* and homologous cloning were used to detect *Xa47* in 180 rice materials. Twenty of 100 ILs contained *Xa47* (Figures 2A, B and Supplementary Table 2), and eight of 80 rice landraces contained *Xa47* (Figure 2C and Supplementary Table 3). To confirm whether
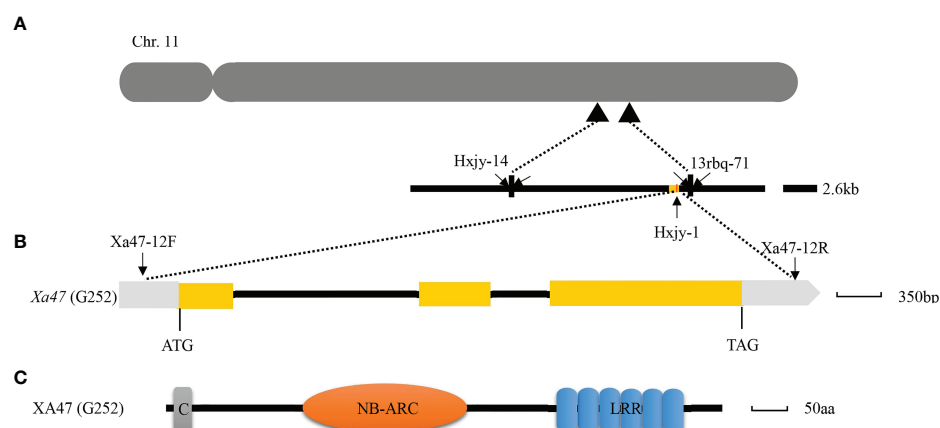

FIGURE 1
Map-based cloning of *Xa47*. **(A)** Physical mapping of *Xa47* on chromosome 11 of rice based on the Nipponbare reference genome. **(B)** Structure of the *Xa47* gene. Yellow rectangles indicate exons, and the black line indicates introns. **(C)** Prediction of the functional domain of XA47. C, Rx N-terminus; NB-ARC, NB-ARC domain; LRR, leucine-rich repeat protein.

the materials were resistant to BB, a disease assessment was performed. Almost all *Xa47*-containing materials showed resistance to C5 and C9 strains (Figure 2B).

Xa47 is localized in the nucleus and cytoplasm

To determine the subcellular localization of XA47 in cells, a 35S::Xa47-GFP vector was constructed for transient expression in rice protoplasts. Laser scanning confocal microscopy showed that the fluorescence signal of cells transfected with 35S::GFP was uniformly distributed throughout cells, whereas the strong fluorescence signal of cells transfected with 35S::Xa47-GFP was distributed in the nucleus and cytoplasm. Thus, XA47 was localized in the nucleus and cytoplasm (Figure 3).

Loss-of-function mutations of *Xa47* result in loss of resistance against *Xanthomonas oryzae* pv. *oryzae*

Previously, when locating the *Xa47* gene, it was predicted to be a new *R* gene that conferred resistance to Xoo in rice (Xing et al., 2021). Therefore, a sgRNA was designed to specifically target the second exon of *Xa47* (sequence 'CAAGGTGCCGG AAAAAAGAA'), and it was cloned into a Ubi-Cas9 vector. When G252 was transformed with the constructed knockout vector, 30 T_0 transgenic plants were obtained. The mutation sites were sequenced, and six mutations were identified in T_0 transgenic plants. Two homozygous mutant lines were selected, one with two base pairs inserted at the target site ($X^{\text{Cas9+2}}$) and one with eight base pairs missing ($X^{\text{Cas9-8}}$), which were used in further molecular and phenotypic analyses (Figures 4A, B).

The X^{Cas9} and G252 (WT) plants were grown to the late tillering stage, and leaf specimens were collected at 0, 24, 48, and 72 h after inoculation with Xoo and subjected to RT-qPCR. At each time point, the expression level of *Xa47* in X^{Cas9} lines was much lower than that in G252 (WT) lines, which further confirmed the successful knockdown of *Xa47* in G252 (Figures 5A-D). Transcript levels of the defense-related marker genes *OsNPR1*, *OsPR1a*, and *OsPR10* were also measured. At nearly all time points, expression levels of the three genes were considerably lower in X^{Cas9} plants than in G252 plants, which suggested that the defense response was affected in mutant plants. Therefore, the two T_1 X^{cas9} mutants were inoculated with nine Xoo strains at the rice booting stage using the leaf tip-clipping method. At 14 d following inoculation, all X^{Cas9} plants exhibited much longer lesions than those in G252 plants (Figure 6). Collectively, the findings revealed that X^{Cas9} mutations caused *Xa47* to lose its resistance to BB.

Overexpression of *Xa47* increases resistance of JG30 to bacterial blight

The indica rice cultivar JG30 is extremely vulnerable to Xoo because it lacks *R* genes for BB resistance. Notably, the *Xa47* genotype in JG30 was consistent with that of NPB and 02428. To determine whether *Xa47* could increase resistance in JG30 to BB, an expression vector 35S::Xa47 was constructed, and then, *Xa47* was overexpressed in JG30. Overexpression (35S::Xa47-JG30-1 and 35S::Xa47-JG30-2) and JG30 (WT) plants were grown to the late tillering stage, and leaf specimens were collected at 0, 24, 48, and 72 h after inoculation with Xoo and subjected to RT-qPCR. At each time point, the expression level of *Xa47* in 35S::Xa47-JG30 lines was much higher than that in JG30 lines, which confirmed the successful transformation of 35S::Xa47 in JG30 (Figures 7A-D). Transcript levels of the defense-related marker genes *OsNPR1*, *OsPR1a*, and *OsPR10* were also measured. At nearly all time points, expression levels of the three genes were significantly up-regulated in 35S::Xa47-JG30 plants compared with JG30 plants. The data indicated that overexpression of *Xa47* in rice could activate its defenses. Therefore, 35S::Xa47-JG30 plants were inoculated with nine Xoo strains at the rice booting stage using the leaf tip-clipping method. At 14 d following inoculation, all overexpression plants exhibited much shorter lesions than those of JG30 plants (Figure 8). Notably, the growth of 35S-Xa47-JG30 plants was similar to that of JG30-WT (Supplementary Figures 4A-H). Collectively, the findings revealed that overexpression of *Xa47* increased the resistance of JG30 to BB.

Interfering transcription activator-like effectors reduce resistance mediated by *Xa47*

As NLR genes specific to rice resistance to BB, *Xa1* and its alleles (*Xa2*, *Xa14*, *Xa31*, and *Xa45*) have identified various TALEs (PthXo1 and Tal4 and Tal9d) to induce resistance to Xoo. Nonetheless, certain iTALEs, such Tal3a and Tal3b in PXO99, reduce this resistance (Zhang et al., 2020). Notably, *Xa47*, a newly identified NLR gene in rice BB resistance after *Xa1* and its alleles, also possessed a functional structural domain similar to that of *Xa1*. Nevertheless, XA47 had little sequence similarity to XA1 and XA2/XA31 and XA14 and XA45 proteins. To investigate whether *Xa47* was influenced by iTALEs, PXO99 and PB (which does not secrete iTALEs) strains were used for identification. After inoculation with PXO99, JG30, 35S::Xa47-1 and 35S::Xa47-2, and $X^{\text{Cas9+2}}$ and $X^{\text{Cas9-8}}$ plants were as susceptible as IRBB1, IRBB2, and IR24 plants, but the opposite was observed for G252 (Figures 9A, B). By contrast, the resistance of 35S::Xa47-1 and 35S::Xa47-2 and G252 plants after PB inoculation was similar to that observed in IRBB1 and IRBB2 plants (Figures 9A, B). However, $X^{\text{Cas9+2}}$ and $X^{\text{Cas9-8}}$
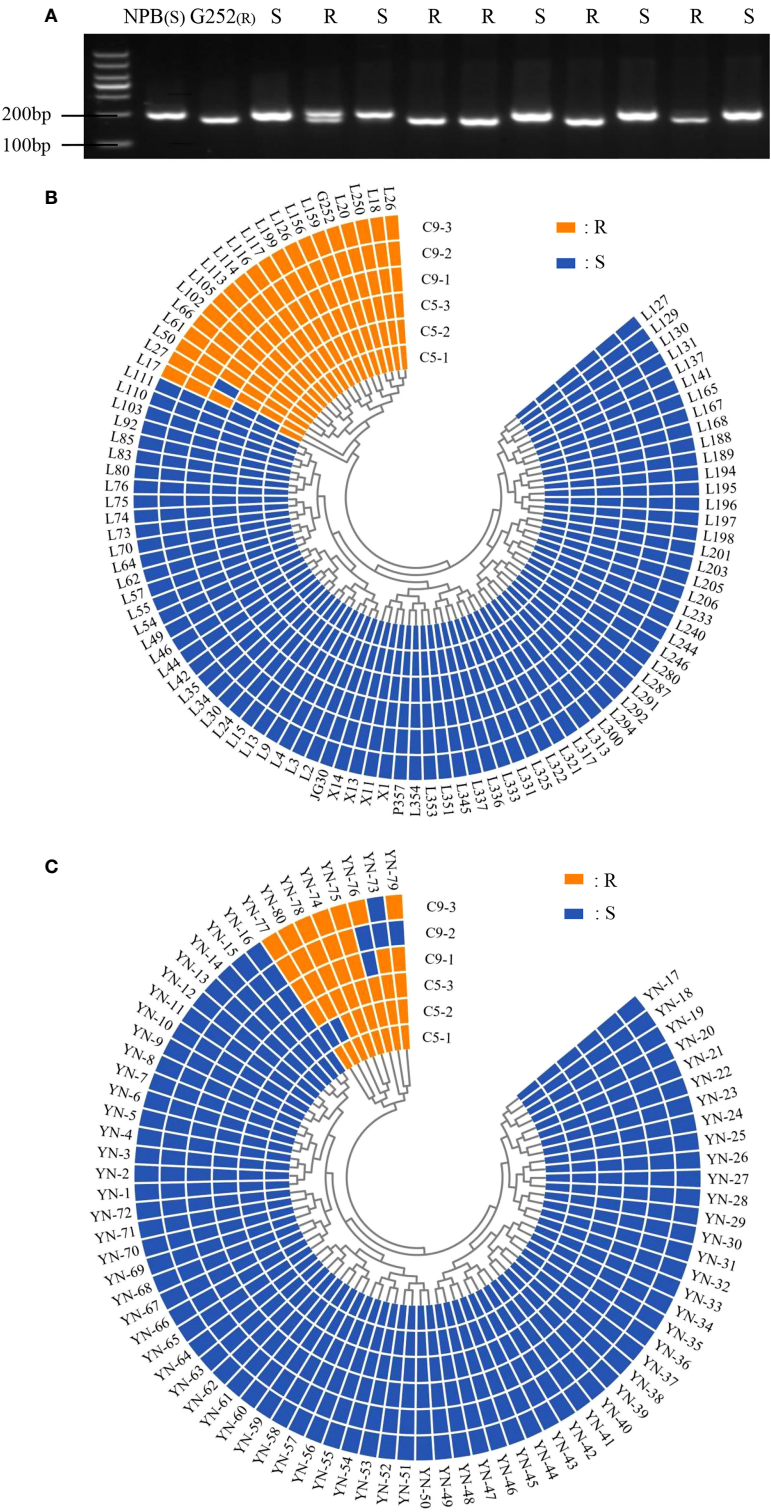
FIGURE 2

Identification of *Xa47* in 180 rice varieties. **(A)** Detection of rice resistance gene *Xa47* using the molecular marker Hxjy-1. R indicates *Xa47* disease resistance allele fragment of 170 bp; S indicates *Xa47* disease susceptibility allele fragment of 210 bp.NBP was the susceptible control material and G252 was the susceptible control material. **(B)** Reactions of 100 infiltration lines inoculated with C5 and C9 strains of *Xanthomonas oryzae* pv. *oryza* (Xoo). R: resistant (lesion length ≤ 6 cm); S: susceptible (lesion length > 6 cm). **(C)** Reactions of 80 Yunnan (YN) landraces inoculated with C5 and C9 strains of Xoo. R, resistant (lesion length ≤ 6 cm); S, susceptible (lesion length > 6 cm).

FIGURE 3
Subcellular localization of XA47 in rice protoplasts. Fluorescence detection of XA47-GFP fusion protein in rice protoplast cells with pBE221::GFP transformed rice protoplast cells as controls.

and JG30 plants after PB inoculation were as susceptible as IR24 plants (Figures 9A, B). The findings suggested that iTALEs can also reduce *Xa47*-mediated resistance.

Discussion

The *R* genes have essential roles in the competition between rice and Xoo, and the discovery of new *R* genes will be crucial to ric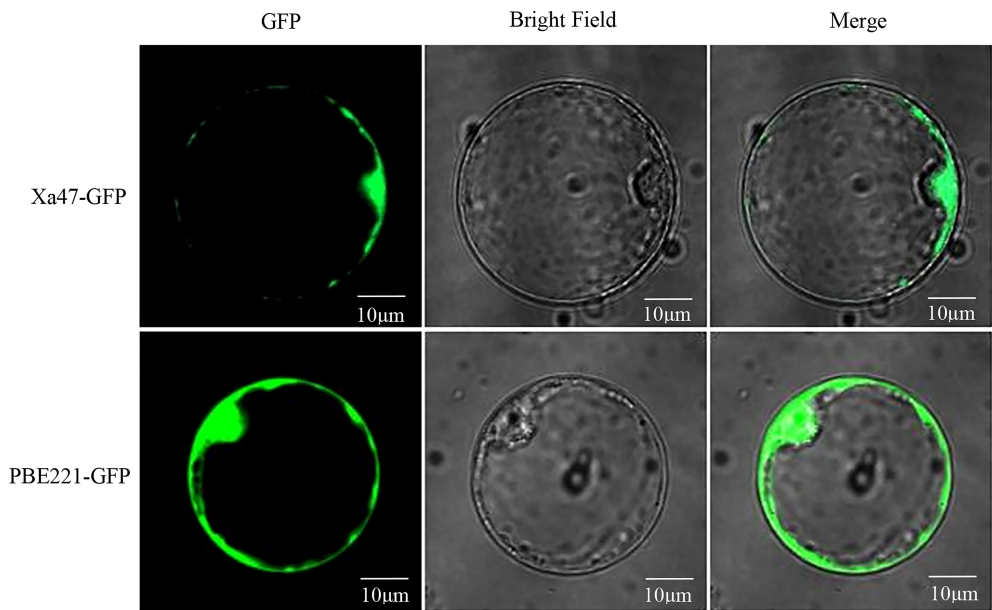e success. Nearly one-third of the *Xa* genes are localized on chr. 11, including *Xa3/Xa26*, *Xa4*, *Xa10*, *Xa21*, *Xa22*, *Xa23*, *Xa30*, *Xa32*, *Xa35*, *Xa36*, *Xa39*, *Xa40*, *xa41*, *Xa43*, *xa44-1*, *xa44-*

2, *Xa46*, and *Xa47* (Sun et al., 2004; Xiang et al., 2006; Tian et al., 2014; Wang et al., 2014; Kim et al., 2015; Zhang et al., 2015; Kim, 2018; Chen et al., 2020; Neelam et al., 2020; Xing et al., 2021). Even though many *R* genes have been identified, relatively few have been cloned or used in breeding. For example, *Xa4*, *Xa21*, and *Xa23* have been used most frequently in breeding for disease resistance in hybrid rice (Balachiranjeevi et al., 2018). The primary cause of this problem is that most *R* genes have disadvantages, such as a limited resistance spectrum or insufficient resistance. To overcome such problems, the exploration for new *Xa* genes with broad-spectrum resistance must be continuous. In addition to identifying new *Xa* genes
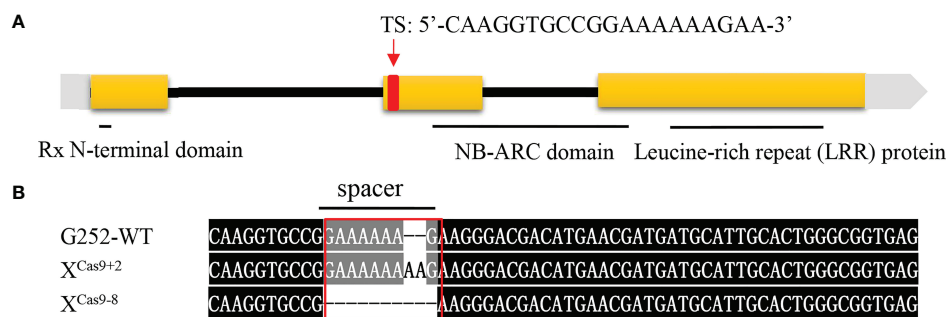

FIGURE 4
Xa47 knockout mutant lines. **(A)** Design of target site (TS) sequences. **(B)** Sequence mutations at the *Xa47* target site in two T[0]-generation X[Cas9] rice plants. The TS sequence is from G252.
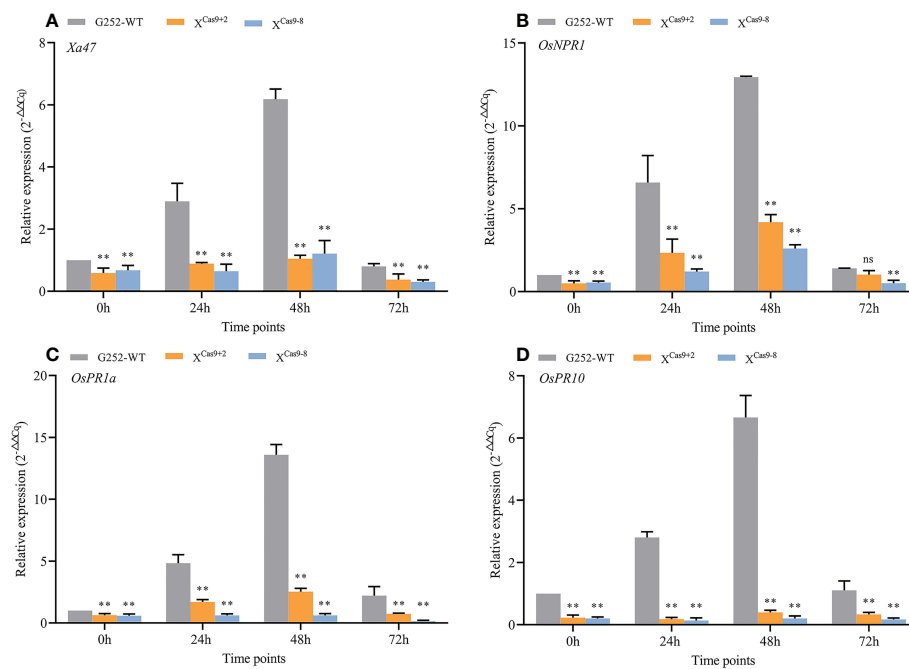
FIGURE 5
Expression of defense-related genes in X^{Cas9} plants after inoculation with *Xanthomonas oryzae* pv. *oryzae* (Xoo). **(A–D)** Relative expression level of *Xa47*, *OsNPR1*, *OsPR1a*, and *OsPR10* in the G252 and two X^{Cas9} lines at 0, 24, 48, and 72 h post-inoculation with Xoo. Values are the mean $\pm$ SD (n = 3). Asterisks indicate significant differences compared with the wild type (WT), based on Student's *t*-tests (**P < 0.01). Each experiment was performed with three biological replicates.

with broad-spectrum resistance, multiple *Xa* genes can be aggregated into the same variety to produce disease-resistant varieties (Dash et al., 2016; Wu et al., 2019). Additionally, rice variants with broad-spectrum resistance can be developed using gene editing technologies (Tao et al., 2021).

In this study, a new NLR gene, *Xa47*, was cloned from G252 (Figure 1C). The cloning of *Xa47* increased the number of NLR

genes for BB resistance to two (*Xa1* and *Xa47*, not including alleles). Allelic variety in functional genes is prevalent in plants, and that variation is essential for plant evolution (Zhang et al., 2020). In rice, *Xa1* and *Xa2/Xa31*, *Xa14*, and *Xa45* are alleles of one another, and there are sequence differences among them. Notably, *Xa47* and *xa47* are alleles of one another, and there were sequence differences between them (Supplementary Figure 2).

FIGURE 6
Lesion length of rice after infection with nine *Xanthomonas oryzae* pv. *oryzae* isolates (C1–C9). Values are the mean $\pm$ SD (n = 9). Asterisks indicate significant differences compared with the wild type (WT), based on Student's *t*-tests (**P < 0.01). Each experiment was performed with three biological replicates.

FIGURE 7
Expression of defense-related genes in 35S::Xa47-JG30 plants after inoculation with *Xanthomonas oryzae* pv. *oryzae* (Xoo). **(A–D)** Relative expression levels of *Xa47*, *OsNPR1*, *OsPR1a*, and *OsPR10* in the G252 and two 35S::Xa47-JG30 lines at 0, 24, 48, and 72 h post-inoculation with Xoo. Values are the mean $\pm$ SD (n = 3). Asterisks indicate significant differences compared with the wild type (WT), based on Student's t-tests (**P < 0.01). Each experiment was performed with three biological replicates.

This result also indicated that *Xa47* is variable at natural loci, which warrants additional study. Most plant *R* genes code for NLRs, which are composed of an N-terminal signaling domain, a central nucleotide-binding region (NBS), and a C-terminal leucine zipper repeat region (LRR) (Mermigka et al., 2020). The NLRs are split into two types based on the N-terminal structure. The TIR-NBS-LRR has a toll/interleukin receptor (TIR) structural domain,

whereas the CC-NBS-LRR contains a coiled-coil (CC) motif (van Wersch et al., 2020). In addition, some NLRs contain other structural domains, such as kinase, WRKY, and BED finger domains (Le Roux et al., 2015; Kroj et al., 2016; Bailey et al., 2018). In this study, XA47 was a typical CC-NBS-LRR resistance protein (Figure 1C), whereas XA1 was not a typical CC-NBS-LRR resistance protein and contained other structural domains (Zhang
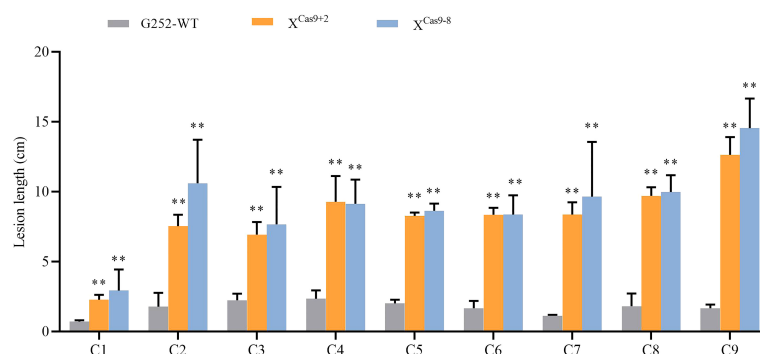

FIGURE 8
Lesion length of rice after infection with nine *Xanthomonas oryzae* pv. *oryzae* isolates (C1–C9). Values are the mean $\pm$ SD (n = 9). Asterisks indicate significant differences compared with the wild type (WT), based on Student's t-tests (**P < 0.01). Each experiment was performed with three biological replicates.
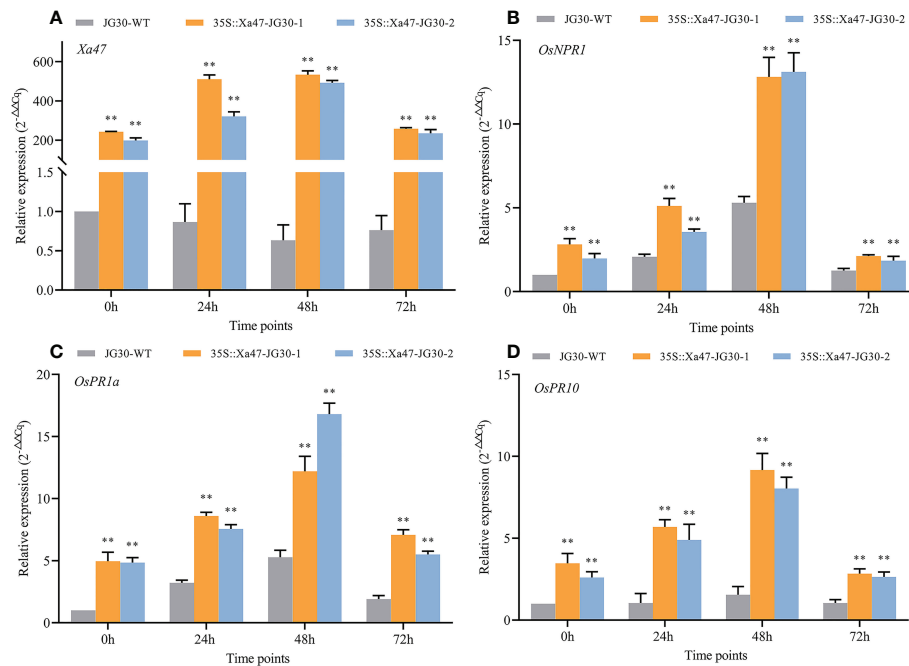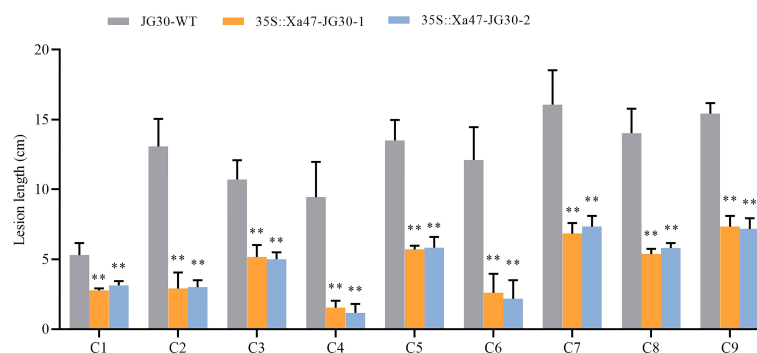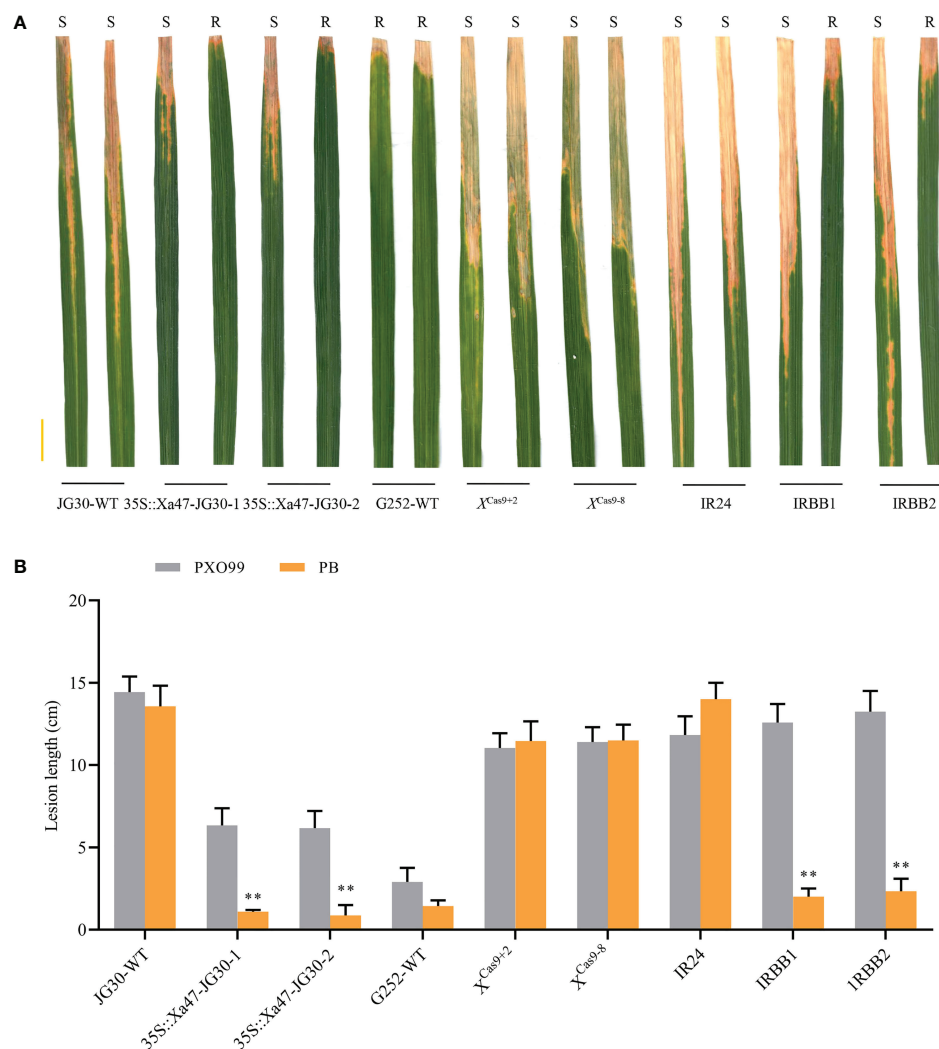
FIGURE 9
Xa47-mediated resistance is attenuated by interfering transcription activator-like effectors. **(A)** Photographs of infected leaves of different rice materials 2 weeks after inoculation with *Xanthomonas oryzae* pv. *oryzae* strains PXO99 and PB. Scale bar: 2 cm. Two leaves of each rice variety show disease spots after inoculation with PXO99 and PB. **(B)** Lesion lengths on infected leaves in **(A)**. Values are the mean $\pm$ SD (n = 9). Asterisks indicate significant differences compared with the wild type (WT), based on Student's t-tests (**P < 0.01). Each experiment was performed with three biological replicates.

et al., 2020). The results indicated that XA47 and XA1 have distinct functions in disease resistance.

The NLR genes are critical in plant immune systems, because they recognize specific pathogens and activate resistance responses (Lei and Li, 2020). The NLR gene-mediated disease resistance response has a dose effect (Howles et al., 2005). Simultaneously, NLR proteins can lead to activation of plant disease resistance responses (Tao et al., 2000). However, during normal plant development, NLR genes are strictly regulated to prevent induced self-activating reactions (Du et al., 2021), hence preventing abnormal plant growth and development. In this study, in the mutant lines overexpressing *Xa47*, cell death was not observed (Supplementary Figures 4A-

H), and thus, the overexpression of *Xa47* did not spontaneously activate the rice ETI response to the HR-like phenotype.

The gene *OsNPR1* is essential for plant disease resistance, especially for resistance to rice bacterial blight (Chern et al., 2005). The *OsNPR1* gene was expressed in response to Xoo at different times after inoculation in 35S::Xa47-JG30 plants, and *OsNPR1* expression was significantly higher in 35S::Xa47-JG30 plants than in those of the wild type. Expression of the *OsNPR1* gene in X^{Cas9} plants was also induced by Xoo at different times after inoculation, but expression was significantly lower in X^{Cas9} plants than in those of the wild type. Therefore, *Xa47* can strongly activate the expression of *OsNPR1* and thus stimulate OsNPR1-mediated disease resistance response in rice. Expression of pathogenesis

related(*PR*) genes tends to promote plant cell death, hence inhibiting the spread of harmful microorganisms (Kim et al., 2011; Hu et al., 2017). Notably, both disease process-related genes *OsPR1a* and *OsPR10* were significantly activated with significantly higher expression in the 35S::Xa47-JG30 strain than in the wild type when resisting infestation by Xoo (Figures 7A-D). Both *OsPR1a* and *OsPR10* were also significantly activated with significantly higher expression in G252 than in X^{Cas9} plants in response to Xoo infestation (Figures 5A-D). The results suggested that *Xa47* regulates the resistance response in rice.

Identifying the level of resistance of an *R* gene to pathogens is also an assessment of the value and potential of the application of that gene (Feng et al., 2022). In this study, *Xa47* was determined to be an *R* gene with broad-spectrum resistance by multiple methods. There were three essential observations: (1) *Xa47* occurred in some BB-resistant rice; (2) loss-of-function mutations of *Xa47* led to loss of resistance against Xoo; and (3) overexpression of *Xa47* increased the resistance of JG30 to BB (Figures 2-7). China is a rice-producing nation, and most rice-growing regions are affected by Xoo (Lu et al., 2021). Representative Xoo strains, including C1, C2, C3, C4, C5, C6, C7, C8, and C9, have been discovered in the disease-endemic regions. Therefore, the use of isolates from diverse rice-growing regions in China to evaluate the resistance of rice lines to BB, particularly during gestation, was an important aspect of this work.

Previously, it was reported that iTALEs reduce *Xa1*-mediated resistance (Zhang et al., 2020). In this study, the resistance mediated by *Xa47* was also inhibited by iTALEs. Notably, G252 showed resistance to PXO99 and PB strains. In 35S::Xa47-JG30 plants inoculated with PXO99 strains, lesion length was approximately 6.0 cm, whereas the lesion length in JG30 and IRBB1 plants was more than 10 cm (Figures 9A, B). The difference in resistance between G252 and 35S::Xa47-JG30 plants might be attributed to differences in genetic background. Moreover, the results indicated that *Xa47*-mediated resistance exceeds *Xa1* resistance. The isolation and identification of *Xa47* will not only reduce yield loss of rice due to Xoo infection but will also enable crop breeders to include *Xa47* in breeding programs. Notably, 100 BC_2F_{16} generations of Yuanjiang common wild rice IL materials, which possess a diverse antimicrobial spectrum, were available for selection of rice varieties. The varieties containing *Xa47* (YN-80, YN-79, YN-78, YN-77, YN-76, YN-75, YN-74, and YN-73) that were isolated from 80 local rice varieties can be used as novel donors in rice breeding efforts. Therefore, the results of this study can help expedite the development of leaf blight-resistant cultivars in Yunnan Province and adjacent areas.

Data availability statement

The original contributions presented in the study are included in the article/Supplementary Material. Further inquiries can be directed to the corresponding authors.

Author contributions

ZC and LC designed the research. YL, XK, YZ, FY, DZ, CJ, LL, JL, TY and LW performed the experiments and analyzed the data. YL and LC wrote the manuscript. QZ, SX and BW revised the manuscript. All authors contributed to the article and approved the submitted version.

Funding

Acknowledgments

Conflict of interest

The authors declare that the research was conducted in the absence of any commercial or financial relationships that could be construed as a potential conflict of interest.

Publisher's note

All claims expressed in this article are solely those of the authors and do not necessarily represent those of their affiliated organizations, or those of the publisher, the editors and the reviewers. Any product that may be evaluated in this article, or claim that may be made by its manufacturer, is not guaranteed or endorsed by the publisher.

Supplementary material

The Supplementary Material for this article can be found online at: https://www.frontiersin.org/articles/10.3389/fpls.2022.1037901/full#supplementary-material

References

Ahuja, I., Kissen, R., and Bones, A. M. (2012). Phytoalexins in defense against pathogens. *Trends Plant Sci.* 17, 73–90. doi: 10.1016/j.tplants.2011.11.002

Ainsworth, E. A. (2008). Rice production in a changing climate: A meta-analysis of responses to elevated carbon dioxide and elevated ozone concentration. *Glob. Change Biol.* 14, 1642–1650. doi: 10.1111/j.1365-2486.2008.01594.x

Bailey, P. C., Schudoma, C., Jackson, W., Baggs, E., Dagdas, G., Haerty, W., et al. (2018). Dominant integration locus drives continuous diversification of plant immune receptors with exogenous domain fusions. *Genome Biol.* 19, 23. doi: 10.1186/s13059-018-1392-6

Balachiranjeevi, C. H., Naik, S. B., Kumar, V. A., Harika, G., Mahadev, S. H. K., Hajira, S., et al. (2018). Marker-assisted pyramiding of two major, broad-spectrum bacterial blight resistance genes, *Xa21* and *Xa33* into an elite maintainer line of rice, DRR17B. *PLoS One* 13, e0201271. doi: 10.1371/journal.pone.0201271

Bednarek, P. (2012). Chemical warfare or modulators of defence responses-the function of secondary metabolites in plant immunity. *Curr. Opin. Plant Biol.* 15, 407–414. doi: 10.1016/j.pbi.2012.03.002

Boch, J., and Bonas, U. (2010). *Xanthomonas* AvrBs3 family-type III effectors: Discovery and function. *Annu. Rev. Phytopathol.* 48, 419–436. doi: 10.1146/annurev-phyto-080508-081936

Boch, J., Bonas, U., and Lahaye, T. (2014). TAL effectors-pathogen strategies and plant resistance engineering. *New Phytol.* 204, 823–832. doi: 10.1111/nph.13015

Bogdanove, A. J., Schornack, S., and Lahaye, T. (2010). TAL effectors: finding plant genes for disease and defense. *Curr. Opin. Plant Biol.* 13, 394–401. doi: 10.1016/j.pbi.2010.04.010

Chen, S., Huang, Z., Zeng, L., Yang, J., Liu, Q., and Zhu, X., et al. (2020). TBtools: An integrative toolkit developed for interactive analyses of big biological data. *Mol. Plant* 13, 1194–1202. doi: 10.1016/j.molp.2020.06.009

Chen, S., Huang, Z., Zeng, L., Yang, J., Liu, Q., and Zhu, X. (2008). High-resolutionmapping and gene prediction of *Xanthomonas oryzae* pv. *oryzae* resistance gene *Xa7*. *Mol. Breeding* 22, 433–441. doi: 10.1007/s11032-008-9187-1

Chen, X., Liu, P., Mei, L., , X., Chen, L., Liu, H., et al. (2021). *Xa7*, a new executor *R* gene that confers durable and broad-spectrum resistance to bacterial blight disease in rice. *Plant Commun.* 2, 100143. doi: 10.1016/j.xplc.2021.100143

Chen, X., and Ronald, P. C. (2011). Innate immunity in rice. *Trends Plant Sci.* 16, 451–459. doi: 10.1016/j.tplants.2011.04.003

Chen, S., Wang, C., Yang, J., Chen, B., and Zhu, X. (2020). Identification of the novel bacterial blight resistance gene *xa46(t)* by mapping and expression analysis of the rice mutant h120. *Sci. Rep.* 10, 12642. doi: 10.1038/s41598-020-69639-y

Chern, M., Fitzgerald, H. A., Canlas, P. E., Navarre, D. A., and Ronald, P. C. (2005). Overexpression of a rice *NPR1* homolog leads to constitutive activation of defense response and hypersensitivity to light. *Mol. Plant Microbe Interact.* 18, 511–520. doi: 10.1094/MPMI-18-0511

Chu, Z., Yuan, M., Yao, J., Ge, X., Yuan, B., Xu, C., et al. (2006). Promoter mutations of an essential gene for pollen development result in disease resistance in rice. *Genes Dev.* 20, 1250–1255. doi: 10.1101/gad.1416306

Dash, A. K., Rao, R. N., Rao, G. J., Verma, R. L., Katara, J. L., Mukherjee, A. K., et al. (2016). Phenotypic and marker-assisted genetic enhancement of parental lines of rajalaxmi, an elite rice hybrid. *Front. Plant Sci.* 13. doi: 10.3389/fpls.2016.01005

Dodds, P. N., and Rathjen, J. P. (2010). Plant immunity: towards an integrated view of plant-pathogen interactions. *Nat. Rev. Genet.* 11, 539–548. doi: 10.1038/nrg2812

Du, D., Zhang, C. W., Xing, Y. D., Lu, X., Cai, L. J., Yun, H., et al. (2021). The CC-NB-LRR *OsRLR1* mediates rice disease resistance through interaction with *OsWRKY19*. *Plant Biotechnol. J.* 19, 1052–1064. doi: 10.1111/pbi.13530

Feng, Z., Li, M., Xu, Z., Gao, P., Wu, Y., Wu, K., et al. (2022). Development of rice variety with durable and broad-spectrum resistance to blast disease through marker-assisted introduction of pigm gene. *Front. Plant Sci.* 13. doi: 10.3389/fpls.2022.937767

Gu, K., Yang, B., Tian, D., Wu, L., Wang, D., Sreekala, C., et al. (2005). *R* gene expression induced by a type-III effector triggers disease resistance in rice. *Nature.* 435, 1122–1125. doi: 10.1038/nature03630

He, C., Liu, H., Chen, D., Xie, W. Z., Wang, M., Li, Y., et al. (2021). CRISPR-Cereal: a guide RNA design tool integrating regulome and genomic variation for wheat, maize and rice. *Plant Biotechnol. J.* 19, 2141–2143. doi: 10.1111/pbi.13675

Howles, P., Lawrence, G., Finnegan, J., McFadden, H., Ayliffe, M., Dodds, P., et al. (2005). Autoactive alleles of the flflax L6 rust resistance gene induce non-race-specific rust resistance associated with the hypersensitive response. *Mol. Plant Microbe Interact.* 18, 570–582. doi: 10.1094/MPMI-18-0570

Hu, K., Cao, J., Zhang, J., Xia, F., Ke, Y., Zhang, H., et al. (2017). Improvement of multiple agronomic traits by a disease resistance gene *via* cell wall reinforcement. *Nat. Plants* 3, 17009. doi: 10.1038/nplants.2017.9

Hutin, M., Sabot, F., Ghesquiére, A., Koebnik, R., and Szurek, B. (2015). A knowledge-based molecular screen uncovers a broad-spectrum OsSWEET14 resistance allele to bacterial blight from wild rice. *Plant J.* 84, 694–703. doi: 10.1111/tpj.13042

Hutin, M., Sabot, F. O., Ghesquie`re, A., Koebnik, R., and Szurek, B. (2016). A knowledge-based molecular screen uncovers a broadspectrum *OsSWEET14* resistance allele to bacterial blight from wild rice. *Plant J.* 84, 694–703. doi: 10.1111/tpj.13042

Hu, L., Wu, Y., Wu, D., Rao, W. W., Guo, J. P., Ma, Y. H., et al. (2017). The coiled-coil and nucleotide binding domains of BROWN PLANTHOPPER RESISTANCE14 function in signaling and resistance against planthopper in rice. *Plant Cell.* 29, 3157–3185. doi: 10.1105/tpc.17.00263

Iyer, A. S., and McCouch, S. R. (2004). The rice bacterial blight resistance gene *xa5* encodes a novel form of disease resistance. *Mol. Plant Microbe Interact.* 17, 1348–1354. doi: 10.1094/MPMI.2004.17.12.1348

Jiang, G., Xia, Z., Zhou, Y., Wan, J., Li, D., Chen, R., et al. (2006). Testifying the rice bacterial blight resistance gene *xa5* by genetic complementation and further analyzing *xa5* (*Xa5*) in comparison with its homolog TFIIAg1. *Mol. Genet. Genomics* 275, 354–366. doi: 10.1007/s00438-005-0091-7

Jiang, N., Yan, J., Liang, Y., Shi, Y., He, Z., Wu, Y., et al. (2020). Resistance genes and their interactions with bacterial blight/leaf streak pathogens (*Xanthomonas oryzae*) in rice (*Oryza sativa* l.)- an updated review. *Rice* 13, 3. doi: 10.1186/s12284-019-0358-y

Ji, Z., Ji, C., Liu, B., Zou, L., Chen, G., and Yang, B. (2016). Interfering TAL effectors of *Xanthomonas oryzae* neutralize r-gene-mediated plant disease resistance. *Nat. Commun.* 7, 13435. doi: 10.1038/ncomms13435

Jones, J. D., and Dangl, J. L. (2006). The plant immune system. *Nature* 444, 323–329. doi: 10.1038/nature05286

Ke, Y., Deng, H., and Wang, S. (2017). Advances in understanding broad-spectrum resistance to pathogens in rice. *Plant J.* 90, 738–748. doi: 10.1111/tpj.13438

Kim, S. M. (2018). Identification of novel recessive gene *xa44(t)* conferring resistance to bacterial blight races by QTL linkage analysis using an SNP chip. *Theoret Appl. Genet.* 131, 2733–2743. doi: 10.1007/s00122-018-3187-2

Kim, S. G., Kim, S. T., Wang, Y., Yu, S., Choi, I. S., Kim, Y. C., et al. (2011). The RNase activity of rice probenazole-induced protein1 (PBZ1) plays a key role in cell death in plants. *Mol. Cells* 31, 25–31. doi: 10.1007/s10059-011-0004-z

Kim, S. M., Suh, J. P., Qin, Y., Noh, T. H., Reinke, R. F., and Jena, K. K. (2015). Identification and fine-mapping of a new resistance gene, *Xa40*, conferring resistance to bacterial blight races in rice (*Oryza sativa* l.). *Theoret Appl. Genet.* 128, 1933–1943. doi: 10.1007/s00122-015-2557-2

Kroj, T., Chanclud, E., Michel-Romiti, C., Grand, X., and Morel, ,. J. B. (2016). Integration of decoy domains derived from protein targets of pathogen effectors into plant immune receptors is widespread. *New Phytol.* 210, 618–626. doi: 10.1111/nph.13869

Kumar, S., Stecher, G., and Tamura, K. (2016). MEGA7: Molecular evolutionary genetics analysis version 7.0 for bigger datasets. *Mol. Biol. Evol.* 33, 1870–1874. doi: 10.1093/molbev/msw054

Le, R. C., Huet, G., Jauneau, A., Camborde, L., Tremousaygue, D., Kraut, A., et al. (2015). A receptor pair with an integrated decoy converts pathogen disabling of transcription factors to immunity. *Cell .* 161, 1074–1088. doi: 10.1016/j.cell.2015.04.025

Lei, T., and Li, X. (2020). Enzyme formation by immune receptors. *Science* 370, 1163–1164. doi: 10.1126/science.abf2833

Li, W., Deng, Y., Ning, Y., He, Z., and Wang, G. L. (2020). Exploiting broad-spectrum disease resistance in crops: from molecular dissection to breeding. *Annu. Rev. Plant Biol.* 71, 575–603. doi: 10.1146/annurev-arplant-010720-022215

Liu, W., Liu, J., Triplett, L., Leach, J. E., and Wang, G. L. (2014). Novel insights into rice innate immunity against bacterial and fungal pathogens. *Annu. Rev. Phytopathol.* 52, 213–241. doi: 10.1146/annurev-phyto-102313-045926

Liu, Q., Yuan, M., Zhou, Y., Li, X., Xiao, J., and Wang, S. (2011). A paralog of the MtN3/saliva family recessively confers race-specific resistance to xanthomonas oryzae in rice. *Plant Cell Environ.* 34, 1958–1969. doi: 10.1111/j.1365-3040.2011.02391.x

Livak, K. J., and Schmittgen, T. D. (2001). Analysis of relative gene expression data using real-time quantitative PCR and the $2^{-\triangle\triangle Cq}$ method. *Methods* 25, 402–408. doi: 10.1006/meth.2001.1262

Lu, J. L., Li, Q. L., Wang, C. C., Wang, M. M., Zeng, D., Zhang, F., et al. (2021). Identification of quantitative trait loci associated with resistance to x*anthomonas oryzae* pv. oryzae pathotypes prevalent in south China. *Crop J.* 10, 498–507. doi: 10.1016/j.cj.2021.05.009

Luo, D., Huguet-Tapia, J. C., Raborn, R. T., White, F. F., Brendel, V. P., and Yang, B. (2021). The *Xa7* resistance gene guards the susceptibility gene *SWEET14* of rice against exploitation by bacterial blight pathogen. *Plant Commun.* 2, 100164. doi: 10.1016/j.xplc.2021.100164

Mermigka, G., Amprazi, M., Mentzelopoulou, A., Amartolou, A., and Sarris, . P. F. (2020). Plant and animal innate immunity complexes: Fighting different enemies with similar weapons. *Trends Plant Sci.* 25, 80–91. doi: 10.1016/j.tplants.2019.09.008

Neelam, K., Mahajan, R., Gupta, V., Bhatia, D., Gill, B. K., Komal, R., et al. (2020). High-resolution genetic mapping of a novel bacterial glight resistance gene *xa-45(t)* identified from *Oryza* glaber-rima and transferred to oryza sativa. *Theor. Appl. Genet.* 133, 689–705. doi: 10.1007/s00122-019-03501-2

Niño-Liu, D., Ronald, P., and Bogdanove, A. (2006). *Xanthomonas oryzae* pathovars: model pathogens of a model crop. *Mol. Plant Pathol.* 7, 303–324. doi: 10.1111/j.1364-3703.2006.00344.x

Peng, Z., Hu, Y., Zhang, J., Huguet-Tapia, J. C., Block, A. K., Park, S., et al. (2019). *Xanthomonas translucens* commandeers the host rate-limiting step in ABA biosynthesis for disease susceptibility. *Proc. Natl. Acad. Sci.* 116, 20938–20946. doi: 10.1073/pnas.1911660116

Porebski, S., Bailey, L. G., and Baum, B. R. (1997). Modification of a CTAB DNA extraction protocol for plants containing high polysaccharide and polyphenol components. *Plant mol. Biol. Rep.* 15, 8–15. doi: 10.1007/bf02772108

Savary, S., Willocquet, L., Pethybridge, S. J., Esker, P., McRoberts, N., and Nelson, A. (2019). The global burden of pathogens and pests onmajor food crops. *Nat. Ecol. Evol.* 3, 430–439. doi: 10.1038/s41559-018-0793-y

Song, W., Wang, G., Chen, L., Kim, H. S., Pi, L., Holsten, T., et al. (1995). A receptor kinase-like protein encoded by the rice disease resistance gene, *Xa21*. *Science* 270, 1804–1806. doi: 10.1126/science.270.5243.1804

Spoel, S. H., and Dong, X. (2012). How do plants achieve immunity? defence without specialized immune cells. *Nat. Rev. Immunol.* 12, 89–100. doi: 10.1038/nri3141

Streubel, J., Pesce, C., Hutin, M., Koebnik, R., Boch, J., and Szurek, B. (2013). Five phylogenetically close rice *SWEET* genes confer TAL effector-mediated susceptibility to *Xanthomonas oryzae* pv. *Oryzae New Phytol.* 200 (3), 808–819. doi: 10.1111/nph.12411

Sun, X., Cao, Y., Yang, Z., Xu, C., Li, X., Wang, S., et al. (2004). *Xa26*, a gene conferring resistance to *Xanthomonas oryzae* pv. *oryzae* in rice, encodes an LRR receptor kinase-like protein. *Plant J.* 37, 517–527. doi: 10.1046/j.1365-313x.2003.01976.x

Tao, H., Shi, X., He, F., Wang, D., Xiao, N., Fang, H., et al. (2021). Engineering broad-spectrum disease-resistant rice by editing multiple susceptibility genes. *J. Integr. Plant Biol.* 63, 1639–1648. doi: 10.1111/jipb.13145

Tao, Y., Yuan, F. H., Leister, R. T., Ausubel, F. M., and Katagiri, F. (2000). Mutational analysis of the arabidopsis nucleotide binding site-leucine-rich repeat resistance gene RPS2. *Plant Cell.* 12. doi: 10.1105/tpc.12.12.2541

Tena, G., Boudsocq, M., and Sheen, J. (2011). Protein kinase signaling networks in plant innate immunity. *Curr. Opin. Plant Biol.* 14, 519–529. doi: 10.1016/j.pbi.2011.05.006

Tian, D., Wang, J., Zeng, X., Gu, K., Qiu, C., Yang, X., et al. (2014). The rice TAL effectordependent resistance protein XA10 triggers cell death and calcium

depletion in the endoplasmic reticulum. *Plant Cell.* 26, 497–515. doi: 10.1105/tpc.113.119255

van Wersch, S., Tian, L., Hoy, R., and Li, X. (2020). Plant NLRs: the whistleblowers of plant immunity. *Plant Commun.* 1, 100016. doi: 10.1016/j.xplc.2019.100016

Wang, C., Fan, Y., Zheng, C., Qin, T., Zhang, X., and Zhao, K. (2014). High-resolution genetic mapping of rice bacterial blight resistance gene *Xa23*. *Mol. Genet. Genom.* 289, 745–753. doi: 10.1007/s00438-014-0848-y

Wang, C., Zhang, X., Fan, Y., Gao, Y., Zhu, Q., Zheng, C., et al. (2015). XA23 is an executor r protein and confers broad-spectrum disease resistance in rice. *Mol. Plant* 8, 290–302. doi: 10.1016/j.molp.2014.10.010

Withers, J., and Dong, X. (2017). Post-translational regulation of plant immunity. *Curr. Opin. Plant Biol.* 38, 124–132. doi: 10.1016/j.pbi.2017.05.004

Wu, Y., Xiao, N., Chen, Y., Yu, L., Pan, C., Li, Y., et al. (2019). Comprehensive evaluation of resistance effects of pyramiding lines with different broad-spectrum resistance genes against magnaporthe oryzae in rice (*Oryza sativa* l.). *Rice (N Y)* 1, 12–11. doi: 10.1186/s12284-019-0264-3

Xiang, Y., Cao, Y., Xu, C., Li, X., and Wang, S. (2006). *Xa3*, conferring resistance for rice bacterial blight and encoding a receptor kinaselike protein, is the same as *Xa26*. *Theor. Appl. Genet.* 113, 1347–1355. doi: 10.1007/s00122-006-0388-x

Xing, J. X., Zhang, D. Y., Yin, F. Y., Zhong, Q. F., Wang, B., Xiao, S. Q., et al. (2021). Identification and fine-mapping of a new bacterial blight resistance gene, *Xa47(t)*, in G252, an introgression line of yuanjiang common wild rice (*Oryza rufipogon*). *Plant Dis.* 105, 4106–4112. doi: 10.1094/PDIS-05-21-0939-RE

Yang, B., Sugio, A., and White, . F. F. (2006). *Os8N3* is a host diseasesusceptibility gene for bacterial blight of rice. *Proc. Natl. Acad. Sci.USA.* 103, 10503–10508. doi: 10.1073/pnas.0604088103

Yoshimura, S., Yamanouchi, U., Katayose, Y., Toki, S., Wang, Z., Kono, I., et al. (1998). Expression of *Xa1*, a bacterial blight-resistancegene in rice, is induced by bacterial inoculation. *Proc. Nat. Acad. Sci. U. S. A.* 95, 1663–1668. doi: 10.1073/pnas.95.4.1663

Yuan, M., Chu, Z., Li, X., Xu, C., and Wang, S. (2009). Pathogen-induced expressional loss of function is the key factor in race-specific bacterial resistance conferred by a recessive. *R Gene Xa13 Rice Plant Cell Physiol.* 50 (5), 947–955. doi: 10.1093/pcp/pcp046

Yuan, M., Chu, Z., Li, X., Xu, C., and Wang, S. (2010). The bacterial pathogen Xanthomonas oryzae overcomes rice defenses by regulating host copper redistribution. *Plant Cell.* 22, 3164–3176. doi: 10.1105/tpc.110.078022

Zhang, Y., Li, J., and Gao, C. X. (2016). Generation of stable transgenic rice (*Oryza sativa* l.) by *Agrobacterium*-mediated transformation. *Curr. Protoc. Plant Biol.* 1, 235–246. doi: 10.1002/cppb.20004

Zhang, B., Zhang, H., Li, F., Ouyang, Y., Yuan, M., Li, X., et al. (2020). Multiple alleles encoding atypical NLRs with unique central tandem repeats in rice confer resistance to *Xanthomonas oryzae* pv. *oryzae*. *Plant Commun.* b1, 100088. doi: 10.1016/j.xplc.2020.100088

Zhang, F., Zhuo, D. L., Huang, L. Y., Wang, W. S., and Zhou, . Y. L. (2015). *Xa39*, a novel dominant gene conferring broad-spectrum resistance to *Xanthomonas oryzae* pv. *oryzae* in rice. *Plant Pathol.* 64, 568–575. doi: 10.1111/ppa.12283

Zhou, J., Peng, Z., Long, J., Sosso, D., Liu, B., Eom, J. S., et al. (2015). Gene targeting by the TAL effector PthXo2 reveals cryptic resistance gene for bacterial blight of rice. *Plant J.* 82, 632–643. doi: 10.1111/tpj.12838

frontiers | Frontiers in Plant Science

A large bioassay identifies *Stb* resistance genes that provide broad resistance against Septoria tritici blotch disease in the UK

Henry Tidd[1]*, Jason J. Rudd[1], Rumiana V. Ray[2], Ruth Bryant[3] and Kostya Kanyuka[4]*

[1]Protecting Crops and the Environment, Rothamsted Research, Harpenden, United Kingdom, [2]Division of Plant and Crop Sciences, School of Biosciences, University of Nottingham, Sutton Bonington, Loughborough, United Kingdom, [3]RAGT Seeds, Ickleton, United Kingdom, [4]NIAB, Cambridge, United Kingdom

Introduction: Septoria tritici blotch (STB) is one of the most damaging fungal diseases of wheat in Europe, largely due to the paucity of effective resistance genes against it in breeding materials. Currently dominant protection methods against this disease, e.g. fungicides and the disease resistance genes already deployed, are losing their effectiveness. Therefore, it is vital that other available disease resistance sources are identified, understood and deployed in a manner that maximises their effectiveness and durability.

Methods: In this study, we assessed wheat genotypes containing nineteen known major STB resistance genes (Stb1 through to *Stb19*) or combinations thereof against a broad panel of 93 UK *Zymoseptoria tritici* isolates. Seedlings were inoculated using a cotton swab and monitored for four weeks. Four infection-related phenotypic traits were visually assessed. These were the days post infection to the development of first symptoms and pycnidia, percentage coverage of the infected leaf area with chlorosis/necrosis and percentage coverage of the infected leaf area with pycnidia.

Results: The different *Stb* genes were found to vary greatly in the levels of protection they provided, with pycnidia coverage at four weeks differing significantly from susceptible controls for every tested genotype. *Stb10, Stb11, Stb12, Stb16q, Stb17,* and *Stb19* were identified as contributing broad spectrum disease resistance, and synthetic hexaploid wheat lines were identified as particularly promising sources of broadly effective STB resistances.

Discussion: No single *Z. tritici* isolate was found to be virulent against all tested resistance genes. Wheat genotypes carrying multiple *Stb* genes were found to provide higher levels of resistance than expected given their historical levels of use. Furthermore, it was noted that disease resistance controlled by different

Stb genes was associated with different levels of chlorosis, with high levels of early chlorosis in some genotypes correlated with high resistance to fungal pycnidia development, potentially suggesting the presence of multiple resistance mechanisms. The knowledge obtained here will aid UK breeders in prioritising Stb genes for future breeding programmes, in which optimal combinations of resistance genes could be pyramided. In addition, this study identified the most interesting Stb genes for cloning and detailed functional analysis.

Introduction

Septoria tritici blotch (STB), caused by the fungal pathogen *Zymoseptoria tritici*, is one of the most damaging wheat diseases across Europe, with the capacity to cause up to 50% crop losses under disease-favourable conditions (Fones and Gurr, 2015). Approximately 70% of the fungicides used in Europe can be for the purpose of preventing *Z. tritici* epidemics (Duveiller et al., 2007; Torriani et al., 2015). Developing methods for protecting wheat from STB is therefore a high priority for UK wheat breeders and researchers.

Traditionally, STB protection has been achieved through the widespread application of fungicides reinforced with the deployment of a small number of *Stb* resistance genes. However, the sexual reproductive cycle that *Z. tritici* undergoes around the end of the cropping season can contribute to high levels of genetic diversity in the pathogen, leading to the rapid loss of effectiveness from fungicides. Resistant strains now exist for every major fungicide group used against them (Fraaije et al., 2005; Cools and Fraaije, 2008; Stammler and Semar, 2011; Hillocks, 2012; van den Berg et al., 2013; Estep et al., 2015), or their development has been demonstrated to be possible through directed evolution, e.g. the case of quinone inside inhibitors (Fouché et al., 2021). A similar lack of durability has proven an issue with *Stb* resistance genes. For example, *Stb6* and *Stb15* have both been widely used in Northern Europe and were initially highly effective however, both have since been widely broken by *Z. tritici* due to the selection pressures caused by their widespread use (Chartrain, 2004b; Arraiano et al., 2009; Stephens et al., 2021). *Stb16q* has also been brought into wide use more recently in some European countries, and initially offered very broad STB resistance. However, isolates of *Z. tritici* virulent on wheat cultivars carrying *Stb16q* have already been reported in Iran, Ireland

and France (Dalvand et al., 2018; Kildea et al., 2020; Orellana-Torrejon et al., 2022a) and are likely to spread rapidly within field populations, making this resistance gene less useful in future breeding programmes. The lack of broad spectrum STB resistance in wheat leaves agricultural systems vulnerable when major resistance genes are broken (e.g. the cultivar Gene in the USA, which was fully resistant in 1992 but become widely susceptible by 1995, causing substantial crop losses (Cowger et al., 2000), or Cougar, which has become unpopular due to the development of Cougar-virulent strains of *Z. tritici* in the UK (Kildea et al., 2021). Such problems will only become more frequent as effective fungicide protection options become more limited (Birr et al., 2021).

It is also noteworthy that some individual major resistance genes that have been widely used in breeding so far have proved to be more durable than others. For example, *Stb1* was introduced to the grower market in the cultivar Oasis in 1975 and has been used in many other cultivars (e.g. Sullivan) since 1979 and remained effective in the field up until mid-2000's (Cowger et al., 2000; Adhikari et al., 2004b; Singh et al., 2016). *Stb4* also proved to be reasonably durable, lasting for approximately 15 years. After its introduction to breeding programs in 1975 (in a cross between Tadorna, Cleo and Inia 66), the first cultivar containing *Stb4* underwent a commercial release in 1984 (Somasco et al., 1996), and this gene remained effective until 2000 (Jackson et al., 2000). However, no individual *Stb* gene so far identified appears to be completely durable. Gene pyramiding may be able to mitigate this rapid breakdown of disease resistance by producing additional obstacles to fungal populations in the evolution of new virulences. For example, Kavkaz-K4500 is one of the most durable sources of field resistance used for breeding and has been shown to possess at least five qualitative resistance genes, including *Stb6*, *Stb10* and *Stb12* (Chartrain et al., 2005a). This combination of *Stb* genes

seems to be sufficient to make Kavkaz-K4500 resistant to STB under field conditions despite the fact that many international *Z. tritici* isolates are virulent on it in laboratory tests (Chartrain et al., 2004a; Chartrain et al., 2005a) – this may suggest high genetic diversity differences between UK and international *Z. tritici* populations, or could be related to the different levels of inoculum used in laboratory vs field trials.

The currently limited availability of data on the interaction between modern *Z. tritici* isolates and wheat [due to limited numbers of isolates being tested in most studies and the fact that many older isolates are reused in many studies for example, 22 isolates from one set of plots at a single location were used in Cowger et al. (2000), ten isolates from a range of Iranian farms in Dalvand et al. (2018) and only one 1996 isolate in Ali et al. (2008)], along with the difficulty in comparing data from different sources, is problematic as it has limited our ability to identify useful sources of quantitative resistances to this disease (Chartrain et al., 2004a). This combined with the limited historical breeding for STB resistance, has led to a dearth of cultivars with significant quantitative resistance to the disease.

Further issues arise from the lack of standardised, modern wild-type *Z. tritici* isolates among the standard model strains for this disease, which represents a significant obstacle to the development of durable STB resistance in wheat due to the difficulties it causes in designing experiments that produce useful information on the likely field efficacy of resistance genes and quantitative trait loci (QTLs) for breeders and can be easily compared to other work in the same field. It is therefore important that new field isolates of *Z. tritici* are collected from all regions of interest for breeders to be used in the testing of new resistance genes. A database of *Z. tritici* isolates with known virulence profiles could help identify combinations of *Stb* resistance genes that could provide several independent resistances for each tested *Z. tritici* isolate. This could allow us to identify combinations of resistance genes that would require several independent mutations in any *Z. tritici* isolate in order for that isolate to gain virulence.

This rapid breakdown of existing resistances makes it particularly important that breeders have access to novel STB resistance genes effective against local *Z. tritici* populations. Several known major resistance genes, such as *Stb5*, *Stb17* and *Stb19*, have not previously been widely used in Europe, and could perhaps be used to replace those that have already been overcome (e.g. *Stb6* and *Stb16q*). Unfortunately, little data is currently available to breeders regarding which of these genes are sufficiently broadly effective to be worth using in breeding programs.

It is therefore clear that a future priority in wheat breeding is likely to be the development of elite lines containing a greater variety of disease resistance genes. Major resistance genes are likely to be a large part of this as they can be identified easily and

applied quickly in breeding programs, and major genes not yet broken will provide excellent field resistance. More than twenty *Stb* resistance genes that could be used in wheat breeding programs have thus far been identified, providing natural protection against a variety of *Z. tritici* isolates at the different stages of the wheat life cycle (referred to as seedling and adult resistance genes) (Dreisigacker et al., 2015). For many of these *Stb* genes we have some information relating to their chromosomal locations, but in the majority of cases this data is imprecise.

Overall, large pathology screens are necessary to assess the effectiveness of *Stb* genes more accurately. Conducting these screens on more genetically diverse germplasm (particularly non-elite landraces and ancestor species) may help to identify novel *Stb* genes highly effective against current *Z. tritici* populations. Here we carried out a broad screen of 2015-2017 UK *Z. tritici* isolates against a panel of wheat lines of diverse origin containing known *Stb* resistance genes to produce estimates of the effectiveness of each of these genes against contemporary field populations of *Z. tritici* in the UK. Several *Stb* genes were identified as contributing broad spectrum disease resistance, and synthetic hexaploid wheat lines were identified as promising sources of broadly effective STB resistance.

Materials and methods

Library of fungal isolates

One hundred *Z. tritici* isolates were donated by Bart Fraaije (NIAB, UK). These isolates were collected from locations around the UK in the years 2015-2017. These isolates were originally drawn from many sources with different naming conventions, and were renamed for ease of use in this project – a list of the original names of these isolates on receipt is included in the Supplementary Data.

In preparation for use in these experiments, the isolates were grown on 7% (w/v) YPD agar (Formedium Ltd., Hunstanton, UK) plates containing 1 unit of penicillin and 1 µg/mL streptomycin (Merck Life Science UK Limited, Gillingham, UK) to remove bacterial contamination. Approximately 25 µl of original *Z. tritici* glycerol stocks were used per plate. Inoculated plates were incubated at 16°C for four to seven days before the fungus was harvested using a sterile loop into 50% (w/v) glycerol and stored at -80°C. This was then repeated using antibiotic free YPD agar plates to ensure the fungi used were not stressed. Fungi from antibiotics-free plates were harvested and stored identically.

Where bacterial contaminants proved resistant to the antibiotics used, contaminated glycerol stock was diluted (approximately by a factor of 100, depending on

concentration), allowing individual colonies to form from single spores or cells. Suitable uncontaminated *Z. tritici* colonies were harvested into 50% glycerol and re-plated to produce pure stocks.

Wheat lines used

Wheat lines were chosen for use in this study that collectively contained *Stb* resistance genes *Stb1-Stb19*. These lines and the *Stb* genes they contain are listed in Table 1. Taichung 29 and KWS Cashel were both included as known susceptible controls (of these, KWS Cashel was the primary control and Taichung 29 was included as a second control in case KWS Cashel was found to be resistant to any *Z. tritici* isolates used).

Inoculation of wheat plants

Z. tritici isolates used in inoculations were cultured on antibiotic-free YPD agar plates and grown for four to seven days at 16°C. Fungal blastospores were then harvested using sterile loops into 5mL of 0.1% Silwet L-77 surfactant (Momentive Performance Materials, Waterford, NY, USA) in H_2O and diluted to a concentration of 10^7 spores per mL using the average of two replicated measurements from a haemocytometer.

High concentrations and the presence of a surfactant are not reflective of field conditions but were included to encourage rapid infection to reduce the time needed per bioassay.

Plants were grown for approximately three weeks (adapted for variable growth rates where necessary) at 16-hour day, 8-hour night cycles under halogen or white LED lamps at a temperature of 21°C and ambient humidity. After inoculation, these plants were transferred to 17°C and the same 16-hour day, 8-hour night cycle. The second leaf was inoculated where possible, although for some cultivars (e.g. Israel 493) the third leaves were used due to their larger size. One leaf each from a minimum of three plants was used for testing each wheat genotype - *Z. tritici* isolate interaction.

Leaves were affixed to aluminium inoculation tables using double sided sticky tape and rubber bands, which also defined the area inoculated and scored. Cotton buds were used to inoculate each spore suspension onto leaves of three plants of each wheat line (four strokes per leaf, ensuring an even layer of moisture on leaf surface). Non-inoculated leaves were trimmed to ensure light access to inoculated leaves.

After inoculation, plants were placed in high humidity boxes (Supplementary Figure 1) for three days before the inner tray (perforated to allow for water uptake) was removed and placed in a larger plastic watering tray to minimise the risk of causing leaf damage or cross-contamination from direct watering.

Plants were maintained for 28 days after inoculation to allow symptom development. They were watered three times per week

TABLE 1   Wheat lines used in this study with known *Stb* genes.

Wheat Genotype	Known *Stb* genes	Reference
Taichung 29	No *Stb* genes known	-
KWS Cashel	No *Stb* genes known	-
Bulgaria 88	*Stb1, Stb6*	Adhikari et al., 2004b
Veranopolis	*Stb2, Stb6*	Liu et al., 2013
Israel 493	*Stb3, Stb6*	Goodwin et al., 2015
Tadinia	*Stb4, Stb6*	Adhikari et al., 2004a
Synthetic 6X	*Stb5*	Arraiano et al., 2001
Estanzuela Federal	*Stb7*	McCartney et al., 2003
Synthetic M6 (Previously W7984)	*Stb8*	Adhikari et al., 2003
Tonic	*Stb9*	Chartrain et al., 2009
Kavkaz-K4500	*Stb6, Stb7, Stb10, Stb12*	Chartrain et al., 2005a
TE9111	*Stb6, Stb7, Stb11*	Chartrain et al., 2005b
Salamouni	*Stb6, Stb13, Stb14*	Cowling, 2006
Riband	*Stb15*	Arraiano et al., 2007
Synthetic M3	*Stb16q, Stb17*	Tabib Ghaffary et al., 2012
Balance	*(Stb6), Stb18*	Tabib Ghaffary et al., 2011
Lorikeet	*Stb6, Stb19*	Yang et al., 2018

and kept trimmed to ensure light access to inoculated leaves. From ten days post inoculation (dpi), plants were checked regularly (every two days where possible) for chlorosis, necrosis and pycnidia development, and symptoms were recorded. Photographs were taken at each check for later verification.

The final screen included 973 tested interactions. Due to the large number of wheat genotype – *Z. tritici* isolate interactions tested, one replicate was normally performed for each of these interactions in the bioassay.

Visual symptom assessments

Necrosis, chlorosis and pycnidia development symptoms were assessed visually. Assessment of the rate of symptom and pycnidia development began ten days after seedling inoculation by *Z. tritici* for each plant. Assessments were then carried out three times a week at regular intervals until 28 days after the initial inoculation date. Leaf status was recorded as no infection (i.e. clean), chlorosis present (showing yellow chlorotic tissue but which had not yet progressed to necrosis), necrosis present (where necrotic lesions were visible), chlorosis with pycnidia (chlorotic symptoms present with small black pycnidia visible on the inoculated leaf surface) or necrosis with pycnidia. The first date on which chlorosis or necrosis was seen was used to determine the "days until symptom development" trait value, while the date on which pycnidia were first noted was used to determine the "days until pycnidia development" trait value. Photographs were taken at each check in case needed for later verification of results.

At 28 days post infection, before leaves were harvested, the "percentage leaf area covered by symptoms" and "percentage leaf area covered by pycnidia" traits were visually assessed. The values for each leaf were rounded to 0, 20, 40, 60, 80 or 100% for each leaf. Photographs were taken in case needed for later verification of results.

Statistical analysis

Statistical tests were carried out using the statistics package R (R Core Team, 2017) to run paired Student's *t*-tests on data from different wheat lines (results obtained using the same *Z. tritici* isolate in the same experimental set were treated as paired) using standard R commands for this function. The large numbers of *Z. tritici* isolates tested against the wheat genotypes of interest allowed for statistical assessments of the average broad resistance of each line. ANOVA tests were used when data from multiple wheat lines was to be compared, and to verify results produced from the *t*-tests – this was done using standard R and Excel Data Analysis commands.

Results

The assessment of multiple phenotypic traits for a large panel of *Z. tritici* isolate – wheat genotype interactions

Seventeen wheat genotypes carrying no known *Stb* genes, a single *Stb* gene, or a combination of *Stb* genes were screened against up to 100 current UK *Z. tritici* isolates. The symptoms of each genotype were compared to those of KWS Cashel, used as the susceptible control. The *P*-values derived using a standard student's *t*-test to compare the average % pycnidia coverage of inoculated leaf area for each *Z. tritici* isolate-resistant wheat line to the equivalent averages from interactions with the KWS Cashel susceptible control are shown in Table 2 – these data show which lines have significantly different symptom development levels overall compared to KWS Cashel (*P*<0.05). Mean average values the full set of genotype-isolate comparisons tested on each wheat line are given in Table 3 for each of the four measured traits. The proportion of isolate-wheat line interactions for which disease symptoms were entirely absent

TABLE 2 A comparison of the % pycnidia coverage of inoculated leaf area for each *Z. tritici* isolate-resistant wheat genotype interaction and the equivalent values derived from the *Z. tritici* isolate's interactions with the KWS Cashel susceptible control.

Wheat Genotype	*P*-value
Taichung 29	1.5×10^{-5}
Riband	3×10^{-4}
Synthetic 6X	4.6×10^{-12}
Synthetic M3	1.6×10^{-10}
Kavkaz-K4500	4×10^{-13}
Tadinia	7.3×10^{-8}
Estanzuela Federal	1×10^{-10}
Israel 493	7.2×10^{-16}
TE9111	5.8×10^{-18}
Bulgaria 88	2.1×10^{-6}
Veranopolis	1.9×10^{-6}
Synthetic M6	4.4×10^{-5}
Tonic	1.3×10^{-2}
Salamouni	3×10^{-4}
Balance	2.3×10^{-6}
Lorikeet	5.9×10^{-7}

A mean average from each interaction (calculated using the standard function in excel) were compared to that with KWS Cashel using a two-tailed Student's *t*-test from the excel data analysis tool. The *P*-values resulting from this analysis are shown. All interactions show significant differences to the KWS Cashel susceptible control.

TABLE 3 The average symptoms on inoculated leaves of each wheat genotype.

Wheat Genotype	Level of resistance	*Stb* genes	No. *Z. tritici* isolates tested	Average No. days to appearance of symptoms	Average No. of days to appearance of pycnidia	Average final % of inoculated leaf area covered by chlorosis/ necrosis	Average final % of inoculated leaf area covered by pycnidia
Taichung 29	Low	*None known*	68	13.0	16.4	97	21
Riband	Low	*Stb15*	90	14.2	17.7	79	23
KWS Cashel	Low	*None known*	85	14.7	17.6	84	36
Synthetic 6X	High	*Stb5*	70	15.4	25.3	50	1
Synthetic M3	High	*Stb16q, Stb17*	44	15.7	No pycnidia developed*	34	0
Kavkaz-K4500	High	*Stb6, Stb7, Stb10, Stb12*	65	17.7	No pycnidia developed*	22	0
Tadinia	Intermediate	*Stb4, Stb6*	71	17.1	19.6	55	9
Estanzuella Federal	Low/ Intermediate	*Stb7*	62	14.1	19.1	85	10
Israel 493	High	*Stb3, Stb6*	74	13.6	22.7	59	1
TE9111	High	*Stb6, Stb7, Stb11*	84	17.8	20.7	31	1
Bulgaria 88	Intermediate/ High	*Stb1, Stb6*	38	16.8	25.0	50	3
Veranopolis	Intermediate	*Stb2, Stb6*	37	15.9	23.2	47	6
Synthetic M6	Intermediate	*Stb8*	41	16.5	22.7	57	10
Tonic	Low/ Intermediate	*Stb9*	29	15.1	21.1	78	15
Salamouni	Intermediate	*Stb6, Stb13, Stb14*	31	17.3	22.8	50	3
Balance	Intermediate	*Stb6, Stb18*	46	16.6	23.7	61	3
Lorikeet	High	*Stb6, Stb19*	31	18.9	No pycnidia developed*	22	0

* No visible pycnidia at time of assessment.

for chlorosis/necrosis and for pycnidia development is shown in Table 4.

Inoculated wheat plants were assessed for four STB disease associated traits: the times (dpi) taken to the development of chlorosis/necrosis symptoms and fungal pycnidia, the final percentage of the inoculated leaf sections covered by chlorosis/necrosis and the final percentage of the inoculated leaf sections covered by pycnidia. Attempts were also made to quantify fungal

sporulation in the inoculated leaves at 28 days post inoculation using spectrophotometry, but the obtained data was considered unreliable due to systemic over-estimation of spores by this method and was thus omitted for clarity.

Trait 1: Time to appearance of first symptoms

The time to the appearance of symptoms development for each seedling was measured as the number of days taken from

TABLE 4 The proportion of *Z. tritici* isolates that did not generate symptoms of each type on each wheat genotype in any interaction.

Wheat genotype	Overall level of resistance	*Stb* genes	No. *Z. tritici* isolates tested	% *Z. tritici* isolates that did not induce chlorosis/necrosis	% *Z. tritici* isolates that did not sporulate
Taichung 29	Low	none known	68	0	29
Riband	Low	*Stb15*	90	0	14
KWS Cashel	Low	none known	85	0	15
Synthetic 6X	High	*Stb5*	70	11	93
Synthetic M3	High	*Stb16q, Stb17*	44	32	100
Kavkaz-K4500	High	*Stb6, Stb7, Stb10, Stb12*	65	26	97
Tadinia	Intermediate	*Stb4, Stb6*	71	3	48
Estanzuella Federal	Low to intermediate	*Stb7*	62	0	34
Israel 493	High	*Stb3, Stb6*	74	5	92
TE9111	High	*Stb6, Stb7, Stb11*	84	10	92
Bulgaria 88	Intermediate to high	*Stb1, Stb6*	38	0	74
Veranopolis	Intermediate	*Stb2, Stb6*	37	3	68
Synthetic M6	Intermediate	*Stb8*	41	5	41
Tonic	Low to intermediate	*Stb9*	29	0	45
Salamouni	Intermediate	*Stb6, Stb13, Stb14*	31	3	68
Balance	Intermediate	*Stb6, Stb18*	46	0	80
Lorikeet	High	*Stb6, Stb19*	31	35	100

inoculation to the first visible chlorosis or necrosis on the inoculated leaf area. There was significant biological variation in the rates of development of chlorosis and necrosis symptoms and percentage of leaf coverage by chlorosis/necrosis in some wheat line – *Z. tritici* isolate interactions (potentially caused by variation in factors such as sunlight levels, natural senescence or mechanical damage done during inoculation). This trait is therefore considered the least reliable indicator of fungal virulence of presented here. The wheat genotype that showed chlorosis/necrosis symptoms soonest on average was Taichung 29 at just 13 days post inoculation (dpi), although Israel 493 and Estanzuella Federal were close to this (13.6 and 14.1 dpi, respectively). The slowest average development of infection symptoms was in Lorikeet, with an average of 18.9 dpi.

Trait 2: Time to appearance of first pycnidia

The time to the appearance of pycnidia for each seedling was measured as the number of days taken from inoculation to the first visible pycnidia on the inoculated leaf area. The lowest average time to the appearance of pycnidia was 16.4 dpi in the

wheat genotype Taichung 29. This value could not be obtained for Synthetic M3, Kavkaz-K4500 or Lorikeet due to the complete lack of pycnidia development in these genotypes. It should be noted that as this trait was not usually measurable in incompatible (resistance) interactions, the values provided for this apply only to interactions that enabled some level of pycnidia formation.

Trait 3: Inoculated leaf coverage by symptoms

The final percentage of the inoculated area of the leaf covered by chlorosis and necrosis at 28 days post inoculation was expected to provide an estimate of the relative levels of photosynthetic loss that could be expected from each wheat genotype when challenged with an isolate of *Z. tritici*. This trait showed high levels of variation both within and between wheat genotypes (Figure 1). Only highly resistant or highly susceptible genotypes showed more restricted ranges, with Estanzuella Federal leaves having consistently high symptoms coverage and leaves of Kavkaz-K4500 displaying consistently lower symptoms coverage. Due to these high ranges in the results
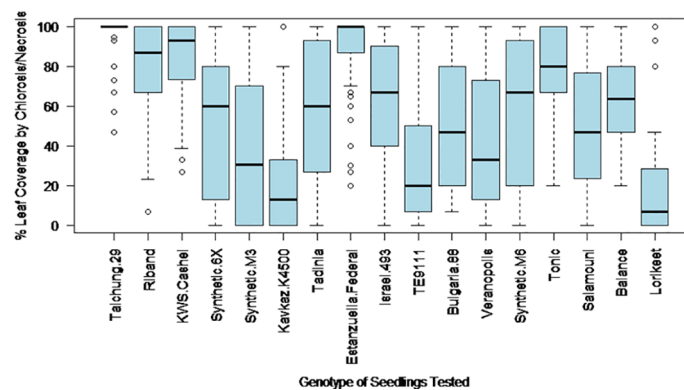
FIGURE 1
The variation in leaf coverage by chlorosis and necrosis induced by different *Z. tritici* isolates as observed at 28 days post inoculation on each of the 17 studied wheat genotypes.

obtained from most genotypes and the potential for occasional leaf damage due to the inoculation procedure (leading to the overestimation of symptoms), this phenotypic trait was considered less reliable than Trait 4.

Trait 4: Inoculated leaf coverage by pycnidia

The final percentage of the inoculated area of the leaf covered by pycnidia at 28 days post inoculation was expected to provide an estimate of the extent to which each isolate of the pathogen could effectively complete its asexual reproductive cycle on each wheat genotype, which is likely to be the strongest measured indicator of the capacity of each isolate to generate an epidemic in the field. The percentage of leaf area covered by pycnidia was more consistent for wheat genotype – *Z. tritici* isolate interactions than Trait 3, and thus became the primary factor used to differentiate between disease resistance

and susceptibility. The variation in pycnidia coverage levels for each wheat genotype over the range of *Z. tritici* isolates tested is shown in Figure 2. The highest average level of pycnidia coverage was 36% in KWS Cashel, while the lowest were 0% for Synthetic M3, Kavkaz-K4500 and Lorikeet.

The percentage leaf coverage by pycnidia in all other tested genotypes was significantly lower compared to the susceptible control KWS Cashel in two-tailed paired Student's t-tests (Table 2). This includes Taichung 29, which contains no known *Stb* genes. This may be due to possible differences in the plant leaf architecture resulting in fewer fungal penetration events, or potentially due to previously unidentified minor-effect resistance QTL(s). This indicates that all other wheat genotypes tested were significantly more resistant than KWS Cashel using this phenotypic trait, which is most directly connected to these isolates' ability to cause an epidemic in the field.
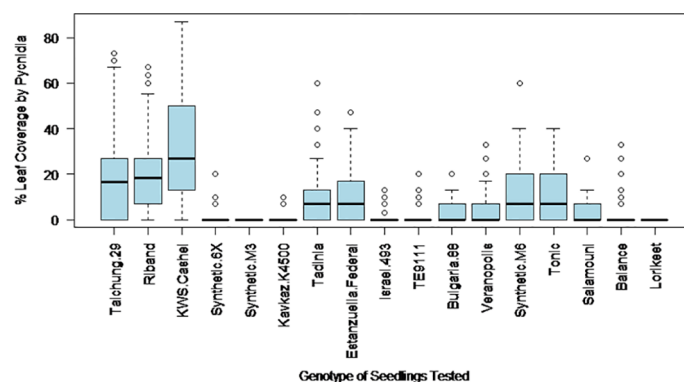

FIGURE 2
The variation in leaf coverage by pycnidia at 28 days post inoculation with different *Z. tritici* isolates on each of the 17 studied wheat genotypes.

Comparative assessment of average levels of *Z. tritici* resistance in wheat genotypes based on four phenotypic traits

It should be emphasised that these results are calculated by averaging disease assessment scores from many individual *Z. tritici* isolates tested for each wheat genotype. Resistant genotypes, such as TE9111, Kavkaz-K4500 and Synthetic 6X were generally resistant to almost all isolates tested. However, genotypes, such as Tadinia had far more variable resistance, with some isolates inducing high infection scores across all assessment criteria while others produced no symptoms, generating intermediate average scores (Table 3). This suggests that these resistances are specific to fungal isolates carrying particular avirulence factors (a "gene-for-gene" relationship) which are each present in only some UK *Z. tritici* isolates. This also indicates that the underlying resistance mechanisms are highly effective when recognition occurs early in *Z. tritici* development, even against isolates with the potential to be highly virulent on other lines.

In most cases, wheat genotypes displayed similar symptom severity across all measurements. However, for some genotypes (e.g. Israel 493) the development rate and final percentage leaf coverage of chlorosis were high compared to the final percentage of pycnidia leaf coverage. Similarly, early chlorosis followed by high resistance to pycnidia development were seen in Synthetic 6X and Synthetic M3, although not all *Z. tritici* isolates stimulated visible chlorosis development in these lines (e.g. RResHT-8 and RResHT-10 induced 33-86% chlorosis in both Synthetic 6X and Synthetic M3, whereas RResHT-21 and RResHT-24 generated 0-7% chlorosis in both lines).

The results obtained in this study demonstrate great variability between the resistances of different wheat lines to UK *Z. tritici* isolates. As expected, wheat lines containing no known *Stb* genes are by far the least resistant group, with almost all tested isolates being highly virulent against KWS Cashel and Taichung 29. This indicates the very low levels of non-specific resistance for *Z. tritici* present in most wheat lines.

Overall, in addition to the wheat genotypes Taichung 29 and KWS Cashel (no known *Stb* genes), Riband [*Stb15*-common and widely broken in Europe (Arraiano et al., 2009)] was more susceptible than other lines. Estanzuela Federal (*Stb7*) also showed low resistance to most isolates tested (though higher than in fully susceptible lines for pycnidia coverage), indicating that UK *Z. tritici* populations are virulent towards *Stb7* and *Stb15*. Tonic also showed relatively low resistance although it was less susceptible than Taichung 29, KWS Cashel or Riband.

Israel 493 (*Stb3* and *Stb6*) and TE9111 (*Stb6, Stb7* and *Stb11*) showed relatively high levels of resistance, indicating that *Stb3* and *Stb11* could be of high potential interest to UK breeders. The synthetic and synthetic-derived lines Synthetic 6X,

Synthetic M3 and Lorikeet also demonstrated high levels of resistance, likely due to their novel *Stb* resistance genes (*Stb5, Stb16q* and *Stb17*, and *Stb19* respectively). Kavkaz-K4500 (*Stb6, Stb7, Stb10* and *Stb12*) provides good levels of resistance, likely due to the presence of *Stb10* and *Stb12* (as *Stb6* is known to be widely broken and *Stb7* has been shown to be ineffective due to the susceptibility of Estanzuela Federal).

The lines Tadinia, Balance, Synthetic M6, Bulgaria 88, Veranopolis, and Salamouni had more intermediate average levels of resistance, indicating that the genes *Stb1, Stb2, Stb4, Stb8, Stb9, Stb13, Stb14* and *Stb18* all provided partial resistance, or provided resistance to some but not all *Z. tritici* isolates tested. These *Stb* genes could also be interesting to breeders as most would take relatively little effort to move into new wheat cultivars, and are likely to produce reasonable levels of resistance under field conditions (where inoculum levels will be lower than in these screens). However, the genetic variability of *Z. tritici* in the field suggests that individually these genes are unlikely to offer stable resistance, as at least one *Z. tritici* isolate will be virulent against each. It is likely that these genes would have to be stacked to provide durable resistance, slowing and complicating the breeding process.

It was notable that Riband, Estanzuela Federal and Tonic possessed the least resistance among *Stb* gene containing genotypes. Riband showed the highest levels of pycnidia amongst the lines possessing at least one *Stb* gene. This is likely to be because *Stb15* is known to have been widely present in European wheat lines historically (Arraiano et al., 2009), meaning that the local *Z. tritici* populations have adapted to its presence. Tonic had the second highest levels of pycnidiospore production and Estanzuela Federal having the second highest levels of pycnidia coverage. This suggests that the *Stb* genes found in these lines (*Stb7, Stb9* and *Stb15*) do not provide good resistance to most *Z. tritici* isolates present in the UK population and should be considered low priority breeding targets for UK wheat lines (although these genes may be more effective against *Z. tritici* populations in other parts of the world).

Identification of preferential breeding targets for maximising the durability of STB resistance genes

The broadest complete resistances were found in Synthetic M3, Kavkaz-K4500, TE9111 and Lorikeet. These genotypes collectively contain *Stb6, Stb7, Stb10, Stb11, Stb12, Stb16q, Stb17*, and *Stb19*. However, the *Z. tritici* isolates used in this test were selected from a dataset of isolates known to be virulent against lines containing *Stb6*. Additionally, *Stb6* and *Stb7* were present in less resistant lines (e.g. Veranopolis and Estanzuela Federal), likely indicating that these *Stb* genes contributed minimally to the resistances of these cultivars.

In Kavkaz-K4500 and Synthetic M3, *Stb10* is paired with *Stb12* and *Stb16q* is paired with *Stb17*, respectively. As none of the genotypes tested contained these genes individually, it is difficult to determine from these results what proportion of the resistances each gene in these pairs was responsible for. It should be noted that previous experiments and field observations demonstrate that *Stb16q* provides extremely broad resistance to the UK *Z. tritici* population present in 2015-2017 (Tabib Ghaffary et al., 2012; Saintenac et al., 2021) whilst *Stb17* was demonstrated to act primarily in adult plants, older than the seedlings used in this study (Tabib Ghaffary et al., 2012), indicating that *Stb16q* is likely to be responsible for most of the resistance seen in Synthetic M3.

Further experimentation using nearly isogenic lines containing each of these genes individually will aid determining for certain which provide the broadest resistance – until such time as this work is completed, *Stb5*, *Stb11* and *Stb19* appear to be the highest priority breeding targets found in these bioassays.

Identification of a class of STB resistance responses associated with strong early leaf chlorosis and reduced pycnidia production

An examination of the level of resistance to different symptoms of *Z. tritici* infection in each wheat genotype also reveals a broader category of potentially interesting *Stb* genes that show high levels of resistance to pycnidia development but do not protect from the early development and high final coverages of chlorotic and necrotic symptoms on the leaves. For example, Israel 493 (containing *Stb3* and *Stb6*) shows the sixth highest average symptom coverage score of all tested genotypes (the fourth highest amongst genotypes possessing at least one *Stb* gene), yet has negligibly low average levels of pycnidia coverage, as shown in Figure 3. This could indicate the presence of resistance genes that act specifically to disrupt the pycnidia formation stage of fungal pathogen development or the presence of resistance pathways which cause chlorosis as a side effect less damaging then allowing the fungus to grow unimpeded, although it seems unlikely that chlorosis is directly tied to the resistance mechanism as chlorosis is usually linked with cell death and *Z. tritici* is primarily necrotrophic.

This unusual combination of symptoms could indicate the activation of resistance mechanisms involving a hypersensitive response, likely involving early reactive oxygen species-producing reactions in the chloroplasts (as indicated by the early and strong chlorosis response). This resistance mechanism seems likely to be effective at preventing the spread of a *Z. tritici* epidemic in the field by preventing pycnidia development, although there may also be some loss of photosynthetic potential from individual plants. This could suggest that *Stb3* and other resistance genes whose action is associated with high levels of chlorosis could provide more durable resistance if deployed in combination with other resistance genes, whose action is not associated with chlorosis, as the two different resistance mechanisms would be difficult for any *Z. tritici* isolate to adapt to. However, the utility of these resistances is likely to depend on the level of loss of photosynthetic potential in the field, which cannot easily be estimated from this work, as the high levels of inoculum used to ensure infection here are unrealistic to occur under normal field conditions. Additionally, it is not known which resistance response would be activated against isolates avirulent on wheat genotypes containing both resistance genes associated with chlorosis and those that do not associate with chlorosis. Further experimentation and fieldwork are needed to determine the utility of combining these two mechanistically different types of resistance responses.
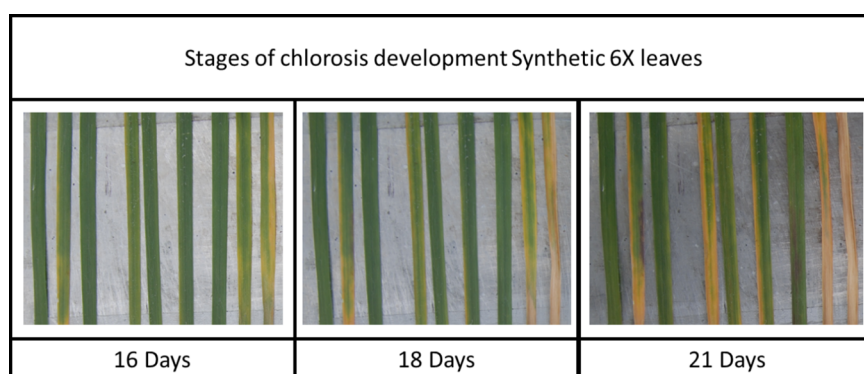

FIGURE 3
The early chlorosis symptoms and lack of fungal pycnidia observed on Synthetic 6X leaves at 28 days post inoculation with three different *Z. tritici* strains.

Discussion

Zymoseptoria tritici is one of the most important pathogens in the wheat-based agricultural systems of Europe, and chemical defences against it do not seem likely to be durable in the long term. It is therefore vital that breeders be able to effectively utilise *Stb* resistance genes to prevent major epidemics. This study provides data that will help to target UK breeding efforts to the most effective *Stb* resistance genes.

Data provided by field trials can be difficult to standardise due to genetic differences in *Z. tritici* populations locally (Berraies et al., 2013; Mekonnen et al., 2020) and globally, and due to the dramatic effect of weather conditions (particularly rainfall) on STB disease development, which can cause large fluctuations in readings between years at the same sites (Ouaja et al., 2020). Additional complexities are added to data analysis by wheat lines with resistance levels that change over the wheat life cycle (e.g. high seedling and low adult resistance) and by imperfect correlations between the levels of different infection symptoms (e.g. necrosis levels and pycnidia counts) (Ouaja et al., 2020). This information is particularly lacking for novel STB disease resistance sources, such as synthetic hexaploid wheats. Overall, the results presented here suggest that the lines Lorikeet (containing *Stb19*) and Synthetic M3 (containing *Stb16q* and *Stb17*) should be of the greatest interest to breeders, as these genotypes were resistant to pycnidia formation from every *Z. tritici* isolate they were challenged with in our bioassays, along with Kavkaz-K4500 (containing *Stb6, Stb7, Stb10* and *Stb12*), Synthetic 6X (containing *Stb5*) and TE9111 (containing *Stb6, Stb7* and *Stb11*), which had very high overall resistance. However, Synthetic M3 carries two *Stb* genes, *Stb16q* and *Stb17*. Of these, previous research suggests that *Stb17* is effective only in adult plants (Tabib Ghaffary et al., 2012), suggesting that the Synthetic M3 resistance is primarily due to the effect of *Stb16q*, which is known to provide broad resistance against *Z. tritici*. However, it should be noted that the resistance provided by *Stb16q* in the field is likely to be less complete than these results suggest, as the bioassays described here used UK *Z. tritici* isolates collected between 2015 and 2017. Since these dates, use of *Stb16q* in elite wheat lines has led to selection for *Z. tritici* isolates capable of virulence against lines containing this resistance gene, e.g. those found in Ireland and Iran (Dalvand et al., 2018; Kildea et al., 2020), which will likely lead to reductions in the field effectiveness of *Stb16q* over the coming years (as has previously been seen for *Stb6* and *Stb15*). This effect has not yet been noted for the resistance gene *Stb19*, which has not been used in the UK thus far. However, it seems likely that wider use of *Stb19* in elite lines would favour the development of *Z. tritici* isolates capable of breaking this resistance, leading to the loss of efficacy of this resistance gene. It is therefore important that when *Stb19* is used, it is supported by additional genes that provide broad resistance to the local *Z. tritici* population.

The results of this bioassay suggest Kavkaz-K4500 (*Stb6, Stb7, Stb10* and *Stb12*), Synthetic 6X (*Stb5*) and TE9111 (*Stb6, Stb7* and *Stb11*) as good potential sources for these protective *Stb* resistance genes. These genotypes show no pycnidia development from 98%, 96% and 95% of tested *Z. tritici* isolates respectively, with low pycnidia coverages (a maximum of 20% average) from the remaining isolates. All isolates tested against all three genotypes proved avirulent against at least one. As results from Estanzuella Federal and previous research suggest that *Stb6* and *Stb7* provide little or no resistance from UK *Z. tritici* populations (Czembor et al., 2011; Makhdoomi et al., 2015; Stephens et al., 2021), it seems likely that *Stb5, Stb11* and either *Stb10* or *Stb12* are responsible for these resistances. As *Stb10* and *Stb12* were not available for testing in isolation, it was not possible in this study to assess proportion of the total Kavkaz-K4500 resistance associated with each of these genes. Therefore currently *Stb5* and *Stb11* appear to be the optimal resistances to protect the durability of *Stb19* in future wide use. The long-term effectiveness of the Kavkaz-K4500 resistance despite the widespread use of this genotype in breeding suggests that such pyramids of mutually protective *Stb* genes are likely to be effective in slowing the development of virulence against them in *Z. tritici* populations.

The most useful *Stb* genes identified here are novel genes originating from synthetic hexaploid wheat lines and those that have historically been protected by the presence of multiple resistances in a single breeding line. This may cause issues during the breeding process, as synthetic-derived lines could carry undesirable genes (causing linkage drag when resistances are transferred to elite lines, possibly reducing yields) and effective resistances may be difficult to identify from wheat lines in which they coexist with several ineffective resistances. The high average resistance of novel lines aligns well with the results of (Arraiano and Brown, 2006), which found that of 238 wheat genotypes tested, the line with the highest non-specific resistance in their study was the Italian landrace Rieti. Although the resistances identified as broadly effective in this study were highly specific rather than non-specific, both results still indicate that the time given for *Z. tritici* to adapt to widely used resistances is a vital determining factor in their effectiveness. However, the (Arraiano and Brown, 2006) paper utilised isolates, which are now severely outdated and several generations removed from current wild *Z. tritici* populations, along with detached leaf assays, which may cause issues with measuring symptoms such as necrosis coverage (which (Arraiano and Brown, 2006) did not attempt to monitor). This study used more recent field isolates of *Z. tritici* collected from a more localised region around the UK and tested against a smaller set of wheat genotypes, producing a dataset more optimally targeted

for identifying resistance genes of interest to breeders in this area. This study also selected wheat genotypes for testing based on the presence of known major resistance genes whereas (Arraiano and Brown, 2006) aimed to test a broader set of wheat genotypes for any resistance regardless of genetic origin, which together with the more modern *Z. tritici* isolates used in the present study makes it difficult to draw direct conclusions from differences in the average resistances observed.

Resistance to *Z. tritici* is a relatively new target in wheat breeding, meaning that much of the research relating to this pathogen and its interactions with crop plants is still in the early stages and major details of the infection and resistance processes (e.g. potential *Z. tritici* effector impacts on host chloroplast function or the mechanisms of most *Stb* gene-for-gene resistances) are largely unknown at a molecular level. Up so far, only *Stb6* and *Stb16q* have been cloned (along with the corresponding fungal effector AvrStb6 recognised by *Stb6*) (Zhong et al., 2017; Saintenac et al., 2018; Saintenac et al., 2021). Much of the research conducted thus far has utilised the model isolate held by most laboratories, IPO 323 – however, this isolate is not reflective of modern field isolates in important ways. For example, IPO 323 is naïve to all modern fungicides and avirulent on cultivars with disease resistance genes that have now been broken down by a large majority of isolates found in the field (e.g. *Stb6*). It is therefore important that novel *Stb* resistance genes be tested more broadly against collections rather than single *Z. tritici* isolates, to assess whether they act sufficiently broadly to be useful in a commercial growing context. The *Z. tritici* isolates utilised in this study were selected from UK fields between the years 2015 and 2017, and are virulent against *Stb6*. Although these isolates have not been sequenced, the range of different resistance responses they triggered in some wheat genotypes suggests a high level of genetic diversity. This is supported by the well-established genetic diversity of *Z. tritici* even in limited geographic regions (Berraies et al., 2013; Mekonnen et al., 2020; Orellana-Torrejon et al., 2022b) and indicates that the results identified here should be broadly applicable to UK *Z. tritici* populations.

Although broadly resistant wheat genotypes shared resistance to some specific *Z. tritici* isolates with each other, no statistically significant associations were found between the specific isolates that were included in this resistance and those which remain virulent against each host genotype (data not shown). This suggests that most of the *Stb* resistance genes tested here operate through the recognition of different avirulence factors. No *Z. tritici* isolate tested here was shown to be virulent against all host genotypes assessed in this study. Therefore, it should be possible to develop highly resistant breeding lines by stacking many *Stb* genes. Such gene pyramids would likely improve the durability of all *Stb* genes included (provided that these *Stb* genes were only used in such gene pyramids), as it is much less likely that any given isolate would gain all of the required mutations for virulence at once

and thus overcome the resistance. This could be extremely useful in the long term – for example, Kavkaz-K4500 has been considered an STB resistant breeding line for many years and still appeared effective in our experiments, suggesting that combinations of resistance genes that utilise different mechanisms may not only help to increase the durability of each individual gene, but could also be broadly effective due to the collective action of these genes. The use of modern genetic markers and breeding techniques will be necessary to overcome potential obstacles to breeding such as linkage drag and epistasis effects – for example, markers could help track specific resistance genes present in breeding materials derived from genotypes containing multiple *Stb* genes, and the production of nearly isogenic lines assisted through genotyping using such markers could limit the effect of linkage drag on new breeding lines. However, it is likely that significant breeding work would still be required to introgress the majority of the *Stb* genes examined here into the regionally adapted elite breeding lines, as the corresponding disease resistance sources used in this study were originally bred for different environments and growth habits (e.g. Bulgaria 88 is a Bulgarian winter type wheat, whereas Israel 493 is an Israeli spring type wheat) and most are not recent but were developed years or decades ago.

In summary, this study revealed that sufficiently diverse *Stb* genes exist to give broad and durable protection from UK *Z. tritici* isolates to new wheat lines. However, generating this protection in a sustainable form will require extensive breeding efforts. We identified suitable *Stb* genes to prioritise for pyramiding. However, further work will be necessary to identify modern high-throughput markers such as Kompetitive Allele Specific PCR (KASP) markers (Semagn et al., 2014) for each *Stb* gene of interest to ensure that multiple broadly effective genes can be stacked in a single line (as otherwise epistatic effects may make their presence difficult to confirm), and to produce lines containing each *Stb* gene from highly resistant lines individually for further detailed characterization. There therefore remains much work to be done collaboratively between UK wheat breeders and the scientific community to ensure the desired level of resistance in future wheat.

Data availability statement

The original contributions presented in the study are included in the article/Supplementary Material. Further inquiries can be directed to the corresponding authors.

Author contributions

All authors contributed to the writing of this paper, with HT acting as lead writer. KK and RB conceived this project and contributed materials to this project. HT acted as primary

experimenter and performed measurement, compilation and statistical analysis of results. All authors contributed to the article and approved the submitted version.

Funding

Conflict of interest

Publisher's note

Supplementary material

The Supplementary Material for this article can be found online at: https://www.frontiersin.org/articles/10.3389/fpls.2022.1070986/full#supplementary-material

References

Adhikari, T. B., Anderson, J. M., and Goodwin, S. B. (2003). Identification and molecular mapping of a gene in wheat conferring resistance to mycosphaerella graminicola. *Phytopathology* 93, 1158–1164. doi: 10.1094/PHYTO.2003.93.9.1158

Adhikari, T. B., Cavaletto, J. R., Dubcovsky, J., Gieco, J. O., Schlatter, A. R., and Goodwin, S. B. (2004a). Molecular mapping of the Stb4 gene for resistance to septoria tritici blotch in wheat. *Phytopathology* 94, 1198–1206. doi: 10.1094/PHYTO.2004.94.11.1198

Adhikari, T. B., Yang, X., Cavaletto, J. R., Hu, X., Buechley, G., Ohm, H. W., et al. (2004b). Molecular mapping of Stb1, a potentially durable gene for resistance to septoria tritici blotch in wheat. *Theor. Appl. Genet.* 109, 944–953. doi: 10.1007/s00122-004-1709-6

Ali, S., Singh, P. K., McMullen, M. P., Mergoum, M., and Adhikari, T. B. (2008). Resistance to multiple leaf spot diseases in wheat. *Euphytica* 159, 167–179. doi: 10.1007/s10681-007-9469-4

Arraiano, L. S., Balaam, N., Fenwick, P. M., Chapman, C., Feuerhelm, D., Howell, P., et al. (2009). Contributions of disease resistance and escape to the control of septoria tritici blotch of wheat. *Plant Pathol.* 58, 910–922. doi: 10.1111/j.1365-3059.2009.02118.x

Arraiano, L. S., and Brown, J. K. M. (2006). Identification of isolate-specific and partial resistance to septoria tritici blotch in 238 European wheat cultivars and breeding lines. *Plant Pathol.* 55, 726–738. doi: 10.1111/j.1365-3059.2006.01444.x

Arraiano, L. S., Chartrain, L., Bossolini, E., Slatter, H. N., Keller, B., and Brown, J. K. M. (2007). A gene in European wheat cultivars for resistance to an African isolate of mycosphaerella graminicola. *Plant Pathol.* 56, 73–78. doi: 10.1111/j.1365-3059.2006.01499.x

Arraiano, L. S., Worland, A. J., Ellerbrook, C., and Brown, J. K. M. (2001). Chromosomal location of a gene for resistance to septoria tritici blotch (Mycosphaerella graminicola)in the hexaploid wheat 'Synthetic 6x'. *Theor. Appl. Genet.* 103, 758–764. doi: 10.1007/s001220100668

Berraies, S., Gharbi, M. S., Belzile, F., Yahyaoui, A., Hajlaoui, M. R., Trifi, M., et al. (2013). High genetic diversity of mycospaherella graminicola (Zymoseptoria tritici) from a single wheat field in Tunisia as revealed by SSR markers. *Afr. J. Biotechnol.* 12, 1344–1349. doi: 10.5897/AJB12.2299

Birr, T., Hasler, M., Verreet, J.-A., and Klink, H. (2021). Temporal changes in sensitivity of zymoseptoria tritici field populations to different fungicidal modes of action. *Agriculture* 11, 269. doi: 10.3390/agriculture11030269

Chartrain, L., Berry, S. T., and Brown, J. K. M. (2005a). Resistance of wheat line kavkaz-K4500 L.6.A.4 to septoria tritici blotch controlled by isolate-specific resistance genes. *Phytopathology* 95, 664–671. doi: 10.1094/PHYTO-95-0664

Chartrain, L., Brading, P. A., Makepeace, J. C., and Brown, J. K. M. (2004a). Sources of resistance to septoria tritici blotch and implications for wheat breeding. *Plant Pathol.* 53, 454–460. doi: 10.1111/j.1365-3059.2004.01052.x

Chartrain, L., Brading, P. A., Widdowson, J. P., and Brown, J. K. M. (2004b). Partial resistance to septoria tritici blotch (Mycosphaerella graminicola) in wheat cultivars arina and riband. *Phytopathology* 94, 497–504. doi: 10.1094/PHYTO.2004.94.5.497

Chartrain, L., Joaquim, P., Berry, S. T., Arraiano, L. S., Azanza, F., and Brown, J. K. M. (2005b). Genetics of resistance to septoria tritici blotch in the Portuguese wheat breeding line TE 9111. *Theor. Appl. Genet.* 110, 1138–1144. doi: 10.1007/s00122-005-1945-4

Chartrain, L., Sourdille, P., Bernard, M., and Brown, J. K. M. (2009). Identification and location of Stb9, a gene for resistance to septoria tritici blotch in wheat cultivars courtot and tonic. *Plant Pathol.* 58, 547–555. doi: 10.1111/j.1365-3059.2008.02013.x

Cools, H. J., and Fraaije, B. A. (2008). Are azole fungicides losing ground against septoria wheat disease? resistance mechanisms in mycosphaerella graminicola. *Pest Manage. Sci.* 64, 681–684. doi: 10.1002/ps.1568

Cowger, C., Hoffer, M. E., and Mundt, C. C. (2000). Specific adaptation by mycosphaerella graminicola to a resistant wheat cultivar. *Plant Pathol.* 49, 445–451. doi: 10.1046/j.1365-3059.2000.00472.x

Cowling, S. G. (2006). Identification and mapping of host resistance genes to septoria tritici blotch of wheat. Available online at: https://mspace.lib.umanitoba.ca/xmlui/handle/1993/20699 (Accessed December 22, 2022).

Czembor, P. C., Radecka-Janusik, M., and Mańkowski, D. (2011). Virulence spectrum of mycosphaerella graminicola isolates on wheat genotypes carrying known resistance genes to septoria tritici blotch. *J. Phytopathol.* 159, 146–154. doi: 10.1111/j.1439-0434.2010.01734.x

Dalvand, M., Soleimani Pari, M. J., and Zafari, D. (2018). Evaluating the efficacy of STB resistance genes to Iranian zymoseptoria tritici isolates. *J. Plant Dis. Prot.* 125, 27–32. doi: 10.1007/s41348-017-0143-3

Dreisigacker, S., Wang, X., Martinez Cisneros, B. A., Jing, R., and Singh, P. K. (2015). Adult-plant resistance to septoria tritici blotch in hexaploid spring wheat. *Theor. Appl. Genet.* 128, 2317–2329. doi: 10.1007/s00122-015-2587-9

Duveiller, E., Singh, R. P., and Nicol, J. M. (2007). The challenges of maintaining wheat productivity: Pests, diseases, and potential epidemics. *Euphytica* 157, 417–430. doi: 10.1007/s10681-007-9380-z

Estep, L. K., Torriani, S. F. F., Zala, M., Anderson, N. P., Flowers, M. D., McDonald, B. A., et al. (2015). Emergence and early evolution of fungicide

resistance in north American populations of zymoseptoria tritici. *Plant Pathol.* 64, 961–971. doi: 10.1111/ppa.12314

Fones, H., and Gurr, S. (2015). The impact of septoria tritici blotch disease on wheat: An EU perspective. *Fungal Genet. Biol.* 79, 3–7. doi: 10.1016/j.fgb.2015.04.004

Fouché, G., Michel, T., Lalève, A., Wang, N. X., Young, D. H., Meunier, B., et al. (2021). Directed evolution predicts cytochrome b G37V target site modification as probable adaptive mechanism towards the QiI fungicide fenpicoxamid in zymoseptoria tritici. *Environ. Microbiol.* 24 (3), 985–1688. doi: 10.1111/1462-2920.15760

Fraaije, B. A., Cools, H. J., Fountaine, J., Lovell, D. J., Motteram, J., West, J. S., et al. (2005). Role of ascospores in further spread of QoI-resistant cytochrome b alleles (G143A) in field populations of mycosphaerella graminicola. *Phytopathology* 95, 933–941. doi: 10.1094/PHYTO-95-0933

Goodwin, S. B., Cavaletto, J. R., Hale, I. L., Thompson, I., Xu, S. S., Adhikari, T. B., et al. (2015). A new map location of gene Stb3 for resistance to septoria tritici blotch in wheat. *Crop Sci.* 55, 35–43. doi: 10.2135/cropsci2013.11.0766

Hillocks, R. J. (2012). Farming with fewer pesticides: EU pesticide review and resulting challenges for UK agriculture. *Crop Prot.* 31, 85–93. doi: 10.1016/j.cropro.2011.08.008

Jackson, L. F., Dubcovsky, J., Gallagher, L. W., et al. (2000) *2000 regional barley and common and durum wheat performance tests in California.* Available at: http://mwqdesign.com/agronomy/reports/272-2000RegionalBarleyandCommonandDurumWheatPerformanceTestsinCalifornia.pdf.

Kildea, S., Byrne, J. J., Cucak, M., and Hutton, F. (2020). First report of virulence to the septoria tritici blotch resistance gene Stb16q in the Irish zymoseptoria tritici population. *New Dis. Rep.* 41, 13. doi: 10.5197/j.2044-0588.2020.041.013

Kildea, S., Sheppard, L., Cucak, M., and Hutton, F. (2021). Detection of virulence to septoria tritici blotch (STB) resistance conferred by the winter wheat cultivar cougar in the Irish zymoseptoria tritici population and potential implications for STB control. *Plant Pathol.* 70 (9), 2137–2147. doi: 10.1111/ppa.13432

Liu, Y., Zhang, L., Thompson, I. A., Goodwin, S. B., and Ohm, H. W. (2013). Molecular mapping re-locates the Stb2 gene for resistance to septoria tritici blotch derived from cultivar veranopolis on wheat chromosome 1BS. *Euphytica* 190, 145–156. doi: 10.1007/s10681-012-0796-8

Makhdoomi, A., Mehrabi, R., Khodarahmi, M., and Abrinbana, M. (2015). Efficacy of wheat genotypes and stb resistance genes against Iranian isolates of zymoseptoria tritici. *J. Gen. Plant Pathol.* 81, 5–14. doi: 10.1007/s10327-014-0565-8

McCartney, C. A., Brûlé-Babel, A. L., Lamari, L., and Somers, D. J. (2003). Chromosomal location of a race-specific resistance gene to mycosphaerella graminicola in the spring wheat ST6. *Theor. Appl. Genet.* 107, 1181–1186. doi: 10.1007/s00122-003-1359-0

Mekonnen, T., Haileselassie, T., Goodwin, S. B., and Tesfayea, K. (2020). Genetic diversity and population structure of zymoseptoria tritici in Ethiopia as revealed by microsatellite markers. *Fungal Genet. Biol.* 141, 103413. doi: 10.1016/j.fgb.2020.103413

Orellana-Torrejon, C., Vidal, T., Boixel, A.-L., Gélisse, S., Saint-Jean, S., and Suffert, F. (2022a). Annual dynamics of zymoseptoria tritici populations in wheat cultivar mixtures: A compromise between the efficacy and durability of a recently broken-down resistance gene? *Plant Pathol.* 71, 289–303. doi: 10.1111/ppa.13458

Orellana-Torrejon, C., Vidal, T., Gazeau, G., Boixel, A.-L., Gélisse, S., Lageyre, J., et al. (2022b). Multiple scenarios for sexual crosses in the fungal pathogen zymoseptoria tritici on wheat residues: Potential consequences for virulence gene transmission. *Fungal Genet. Biol.* 163, 103744. doi: 10.1016/j.fgb.2022.103744

Ouaja, M., Aouini, L., Bahri, B., Ferjaoui, S., Medini, M., Marcel, T. C., et al. (2020). Identification of valuable sources of resistance to zymoseptoria tritici in the Tunisian durum wheat landraces. *Eur. J. Plant Pathol.* 156, 647–661. doi: 10.1007/s10658-019-01914-9

R Core Team. (2017). R: A language and environment for statistical computing. Available at: https://www.r-project.org

Saintenac, C., Cambon, F., Aouini, L., Verstappen, E., Ghaffary, S. M.T., Poucet, T., et al. (2021). A wheat cysteine-rich receptor-like kinase confers broad-spectrum resistance against septoria tritici blotch. *Nat. Commun.* 12, 433. doi: 10.1038/s41467-020-20685-0

Saintenac, C., Lee, W.-S., Cambon, F., Rudd, J. J., King, R. C., Marande, W., et al. (2018). Wheat receptor-kinase-like protein Stb6 controls gene-for-gene resistance to fungal pathogen zymoseptoria tritici. *Nat. Genet.* 50, 368–374. doi: 10.1038/s41588-018-0051-x

Semagn, K., Babu, R., Hearne, S., and Olsen, M. (2014). Single nucleotide polymorphism genotyping using kompetitive allele specific PCR (KASP): Overview of the technology and its application in crop improvement. *Mol. Breed.* 33, 1–14. doi: 10.1007/s11032-013-9917-x

Singh, R. P., Singh, P. K., Rutkoski, J., Hodson, D. P., He, X., Jørgensen, L. N., et al. (2016). Disease impact on wheat yield potential and prospects of genetic control. *Annu. Rev. Phytopathol.* 54, 303–322. doi: 10.1146/annurev-phyto-080615-095835

Somasco, O. A., Qualset, C. O., and Gilchrist, D. G. (1996). Single-gene resistance to septoria tritici blotch in the spring wheat cultivar 'Tadinia.'. *Plant Breed.* 115, 261–267. doi: 10.1111/j.1439-0523.1996.tb00914.x

Stammler, G., and Semar, M. (2011). Sensitivity of mycosphaerella graminicola (anamorph: Septoria tritici) to DMI fungicides across Europe and impact on field performance. *EPPO Bull.* 41, 149–155. doi: 10.1111/j.1365-2338.2011.02454.x

Stephens, C., Ölmez, F., Blyth, H., McDonald, M., Bansal, A., Turgay, E. B., et al. (2021). Remarkable recent changes in the genetic diversity of the avirulence gene AvrStb6 in global populations of the wheat pathogen zymoseptoria tritici. *Mol. Plant Pathol.* 22, 1121–1133. doi: 10.1111/mpp.13101

Tabib Ghaffary, S. M., Faris, J. D., Friesen, T. L., Visser, R. G. F., van der Lee, T. A. J., Robert, O., et al. (2012). New broad-spectrum resistance to septoria tritici blotch derived from synthetic hexaploid wheat. *Theor. Appl. Genet.* 124, 125–142. doi: 10.1007/s00122-011-1692-7

Tabib Ghaffary, S. M., Robert, O., Laurent, V., Lonnet, P., Margalé, E., van der Lee, T. A. J., et al. (2011). Genetic analysis of resistance to septoria tritici blotch in the French winter wheat cultivars balance and Apache. *Theor. Appl. Genet.* 123, 741–754. doi: 10.1007/s00122-011-1623-7

Torriani, S. F. F., Melichar, J. P. E., Mills, C., Pain, N., Sierotzki, H., and Courbot, M. (2015). Zymoseptoria tritici: A major threat to wheat production, integrated approaches to control. *Fungal Genet. Biol.* 79, 8–12. doi: 10.1016/j.fgb.2015.04.010

van den Berg, F., van den Bosch, F., and Paveley, N. D. (2013). Optimal fungicide application timings for disease control are also an effective anti-resistance strategy: A case study for zymoseptoria tritici (Mycosphaerella graminicola) on wheat. *Phytopathology* 103, 1209–1219. doi: 10.1094/PHYTO-03-13-0061-R

Yang, N., McDonald, M. C., Solomon, P. S., and Milgate, A. W. (2018). Genetic mapping of Stb19, a new resistance gene to zymoseptoria tritici in wheat. *Theor. Appl. Genet.* 131, 2765–2773. doi: 10.1007/s00122-018-3189-0

Zhong, Z., Marcel, T. C., Hartmann, F. E., Ma, X., Plissonneau, C., Zala, M., et al. (2017). A small secreted protein in zymoseptoria tritici is responsible for avirulence on wheat cultivars carrying the Stb6 resistance gene. *New Phytol.* 214, 619–631. doi: 10.1111/nph.14434

frontiers | Frontiers in Plant Science

Check for updates

Deciphering immune responses primed by a bacterial lipopeptide in wheat towards *Zymoseptoria tritici*

Rémi Platel[1]*, Anca Lucau-Danila[1], Raymonde Baltenweck[2], Alessandra Maia-Grondard[2], Pauline Trapet[1], Maryline Magnin-Robert[3], Béatrice Randoux[3], Morgane Duret[1], Patrice Halama[1], Jean-Louis Hilbert[1], François Coutte[1], Philippe Jacques[4], Philippe Hugueney[2], Philippe Reignault[3] and Ali Siah[1]*

[1]Joint Research Unit 1158 BioEcoAgro, Junia, Université de Lille, Université de Liège, UPJV, Université d'Artois, ULCO, INRAE, Lille, France, [2]Université de Strasbourg, INRAE SVQV UMR A1131, Colmar, France, [3]Unité de Chimie Environnementale et Interactions sur le Vivant, Université du Littoral Côte d'Opale, Calais Cedex, France, [4]Joint Research Unit 1158 BioEcoAgro, TERRA Teaching and Research Centre, MiPI, Gembloux Agro-Bio Tech, Université de Liège, Gembloux, Belgium

Plant immunity induction with natural biocontrol compounds is a valuable and promising ecofriendly tool that fits with sustainable agriculture and healthy food. Despite the agroeconomic significance of wheat, the mechanisms underlying its induced defense responses remain obscure. We reveal here, using combined transcriptomic, metabolomic and cytologic approach, that the lipopeptide mycosubtilin from the beneficial bacterium *Bacillus subtilis*, protects wheat against *Zymoseptoria tritici* through a dual mode of action (direct and indirect) and that the indirect one relies mainly on the priming rather than on the elicitation of plant defense-related mechanisms. Indeed, the molecule primes the expression of 80 genes associated with sixteen functional groups during the early stages of infection, as well as the accumulation of several flavonoids during the period preceding the fungal switch to the necrotrophic phase. Moreover, genes involved in abscisic acid (ABA) biosynthesis and ABA-associated signaling pathways are regulated, suggesting a role of this phytohormone in the indirect activity of mycosubtilin. The priming-based bioactivity of mycosubtilin against a biotic stress could result from an interaction of the molecule with leaf cell plasma membranes that may mimic an abiotic stress stimulus in wheat leaves. This study provides new insights into induced immunity in wheat and opens new perspectives for the use of mycosubtilin as a biocontrol compound against *Z. tritici*.

1 Introduction

Wheat is one of the most consumed cereal crops worldwide, serving as primary ingredient in human nutrition, food industry, and livestock feed. Wheat cultivation has to cope with a wide range of phytopathogenic microorganisms impacting its growth, productivity, and the quality of its production (Savary et al., 2019). The most frequently occurring and damaging pathogen on wheat crop is the hemibiotrophic fungus *Zymoseptoria tritici*, responsible for Septoria tritici blotch (STB) disease, causing severe yield losses of up to 50% during high-level pressure years (Fones and Gurr, 2015). The infection process of this hemibiotrophic pathogen consists of an initial asymptomatic biotrophic phase followed by a necrotrophic phase, the latter being characterized by the apparition of visual symptoms (Steinberg, 2015). Even if progresses have been accomplished in wheat resistance breeding during the last decades, with 22 major resistance genes described against *Z. tritici*, disease control of STB relies mainly on synthetic fungicides (Brown et al., 2015; Torriani et al., 2015; Yang et al., 2018). In Europe, 70% of the total currently applied fungicides are used to protect wheat against *Z. tritici* (Fones and Gurr, 2015). Nevertheless, fungicide resistance developed by *Z. tritici* populations is an increasing concern for wheat producers (Cools and Fraaije, 2013; McDonald et al., 2019). Therefore, a strong need for substitutes and alternatives have emerged in the recent years, reinforced by all the concerns about the potential impacts of chemical inputs on the environment and human health.

Biosurfactants are surface-active biomolecules produced by a broad range of microorganisms, including bacteria and fungi. These molecules are often classified according to their chemical structure, such as mannosylerythritol lipids, trehalose dimycolate, trehalolipids, sophorolipids, rhamnolipids, and lipopeptides (Crouzet et al., 2020). Even though they may be very diverse both in their structure and origin, they all are amphiphilic molecules, composed by hydrophilic and hydrophobic moieties. They also exhibit a high potential for application in many fields, including human health, cosmetic, food industry, petroleum industry, soil and water remediation, nanotechnology and agriculture (Sachdev and Cameotra, 2013; Shekhar et al., 2015; Kourmentza et al., 2021). Regarding their use in crop protection, many studies have reported them as promising ecofriendly candidates for biocontrol of crop diseases (Ongena and Jacques, 2008; D'aes et al., 2010; Sachdev and Cameotra, 2013; Crouzet et al., 2020). Moreover, green surfactants have often been described as displaying high biodegradability, as well as low toxicity and ecotoxicity, two major advantages required for the development of sustainable agriculture (Shekhar et al., 2015).

The possible modes of action of biosurfactants in plant protection against pathogens are diverse. For instance, they can display direct antimicrobial activity towards pathogens, modify the bio-availability of nutrients used by the pathogens, and/or induce plant immune defenses (D'aes et al., 2010). The compounds inducing the plant immune defenses may be distinguished into two categories, including elicitors, that directly activate host defense responses after their application, and priming agents, that require additional signals, such as pathogen recognition, to trigger full defense responses (Paré et al., 2005). Primed plants may develop a stronger and/or faster response pattern than so-called naïve (unprimed) plants. They can also detect the pathogen invasion at a lower threshold and hence react in a more sensitized way. Finally, primed plants can exhibit other response networks, involving specific defense pathways (Conrath et al., 2002; Paré et al., 2005; Lämke and Bäurle, 2017).

Bacillus spp. are considered as microbial factories for the production of metabolites of interest, especially biosurfactant molecules such as lipopeptides. Lipopeptides consist of a hydrophobic fatty acid tail linked to a short linear or cyclic oligopeptide (CLPs), and were, initially, mainly studied for their direct antimicrobial activities against phytopathogenic agents. However, many investigations have also been carried out on their stimulating effect of host defense mechanisms (Ongena and Jacques, 2008; Raaijmakers et al., 2010; Chowdhury et al., 2015; Crouzet et al., 2020). Three main groups of CLPs have been reported to exhibit significant biological activities, including surfactins, iturins and fengycins. The two latter possess a significant antimicrobial activity against a wide range of fungi and oomycetes, likely due to their ability to interact directly with pathogen plasma membranes, hence resulting in their destabilization, pore formation and cytoplasmic leakage, leading *in fine* to cell death or to an inhibition of spore germination (Chitarra et al., 2003; Pérez-García et al., 2011; Desmyttere et al., 2019; Crouzet et al., 2020). However, some authors suggest that CLPs could also display antifungal activity by interacting with fungal intracellular targets (Qi et al., 2010). Concerning their ability to induce plant immunity, many studies have highlighted the potential of mainly two families of CLPs, fengycin and surfactin, to trigger defense reactions in various plants, such as bean, citrus, grapevine, lettuce, tomato, melon, rye grass, sugar beet, and wheat, as reviewed by Crouzet et al. (2020). Mycosubtilin, another CLP was also shown to induce defense responses in grapevine cells (Farace et al., 2015). Supposedly, CLPs are able to fit into the lipid bilayer of host plant plasma membranes, slightly altering the lipid dynamics, hence leading to the activation of defense reactions, as eliciting or priming agents (Nasir et al., 2010; Schellenberger et al., 2019).

Although the innate immunity of wheat towards *Z. tritici* is extensively studied (*e.g.* Rudd et al., 2015; Seybold et al., 2020), the literature regarding the induced resistance in wheat against this major fungal pathogen, with exogenous treatments, is relatively poor. Regarding CLPs, only one single study showing the potential of surfactin to activate defense

mechanisms in wheat against *Z. tritici* has been recently reported
(Le Mire et al., 2018). Nevertheless, the ability of mycosubtilin, a
CLP from the iturin family, to induce defense reactions in wheat
against this disease has never been investigated, while its direct
antimicrobial activity against *Z. tritici* has already been
examined (Mejri et al., 2018). Omics tools, including
transcriptomics and metabolomics, have significantly
improved these later years the understanding of plant-
pathogen cross-talks. Although such approaches have already
been used to investigate the interactions between wheat and *Z.
tritici*, they have not been deployed so far to examine the induced
resistance in this pathosystem. The aim of the present study was
thus to determine whether mycosubtilin is able to trigger
immunity reactions in wheat towards *Z. tritici* as an eliciting
(in absence of fungal infection) or a priming (in presence of
fungal infection) molecule, by using transcriptomic and
metabolomic tools. The analyses allowed to decipher the
mechanisms as well as the plant-defense related pathways
induced by the biomolecule. Cytological bioassays were also
performed to better understand the mode of action of
mycosubtilin on both the fungus and the host plant.

2 Materials and methods

2.1 Plant growth, treatment and inoculation

Seeds of the cultivar (cv.) Alixan (Limagrain, France),
susceptible to STB, were pregerminated in square Petri dishes (12
× 12 cm) on moist filter paper as described by Siah et al. (2010a),
and germinated grains were delicately transferred into three-liter
pots filled with universal loam (Gamm Vert, France). The prepared
pots were then placed in the greenhouse at 21 ± 2°C with a 16/8 h
day-night cycle. For each condition and each sampling modality,
three pots harboring 12 wheat plants each (n=36), were used. At day
0 (D0), corresponding to three weeks after sowing, plants of each
pot were hand-sprayed with 30 mL of either a solution of 100 mg.L⁻¹
mycosubtilin from *Bacillus subtilis* (Lipofabrik, Lesquin, France)
or mock (control) treatment. Mycosubtilin was first dissolved in
dimethyl sulfoxide (DMSO, Sigma-Aldrich, Saint-Louis, USA),
leading to a final DMSO concentration of 0.1% in the treatment
solution, also supplemented with 0.05% of polyoxyethylene-
sorbitan monolaurate (Tween 20, Sigma-Aldrich, Saint-Louis,
USA) serving as wetting agent. Mock treatment consisted of a
solution of 0.1% DMSO supplemented with 0.05% of Tween 20. At
two days after treatment (D2), half of the plants treated with
mycosubtilin, as well as control plants, were inoculated by hand-
spraying 30 mL of *Z. tritici* spore suspension (10⁶ spores.mL⁻¹),
mixed with 0.05% of Tween 20, on the plants of each pot. Fungal
spores were obtained by growing the *Z. tritici* single-spore strain
T02596 (isolated in 2014 in Northern France) on potato dextrose
agar (PDA) medium during one week in dark conditions, according

to Siah et al. (2010a). The other half of the plants were mock
inoculated by hand spraying 30 mL of a 0.05% Tween 20 solution
on the plants of each pot. All pots, even the mock inoculated ones,
were then immediately covered with a clear polyethylene bag for
three days in order to ensure a high humidity level on the surface of
the leaves, a required condition for the success of the infection. At
23 days after treatment (D23), the disease severity level was assessed
by scoring, on the plant third leaves, the area of lesions (chlorosis
and necrosis) bearing or not pycnidia. Leaf samples were harvested
at two (D2), five (D5) and fifteen (D15) days after treatment for
further cytological, biochemical, or molecular analyses. In addition
to the protection efficacy assay, a phytotoxicity biotest was
performed in order to evaluate the impact of mycosubtilin at
different concentrations (0, 0.8, 4, 20, 100, and 500 mg L⁻¹) on
leaf appearance and plant fresh biomass. The assay was carried out
in the greenhouse using the same conditions of plant growth and
treatment described above. Leaf appearance was assessed on the
third leaves at two (D2), seven (D7), and 15 (D15) days after
treatment, while the plant fresh biomass was determined at 15 days
after treatment. Three pots of nine plants each (27 plants in total)
were used as replicates for each molecule concentration condition.

2.2 *In vitro* antifungal activity assay in solid medium

The *in vitro* antifungal effect of mycosubtilin was determined
by measuring the growth of *Z. tritici* strain T02596 on
PDA medium, as described by Platel et al. (2021).
Briefly, mycosubtilin was dissolved in DMSO (0.1% final
DMSO concentration) and different concentrations of this
biomolecule (0.19, 0.39, 0.78, 1.56, 3.125, 6.25, 12.5, 25, 50,
and 100 mg.L⁻¹) were mixed with an autoclaved PDA medium at
approximatively 40°C. Each well of sterile 12-well plates
(Cellstar standard®, Greiner Bio-One GmbH, Kremsmünster,
Austria) was filled with 3 mL of the mixture. After PDA
solidification, a drop of 5 µL of *Z. tritici* spore suspension at
5.10⁵ spores.mL⁻¹ was spotted on the center of each plate well.
After drop drying in sterile conditions, the plates were incubated
in a growth chamber at 20 ± 1°C in dark conditions. Ten days
later, the growth of fungal colonies was assessed by measuring
their two perpendicular diameters. Control wells supplemented
or not with 0.1% DMSO and inoculated or not with fungal
spores were also used. This experiment was repeated twice and
three wells were used as replicates for each condition.

2.3 *In vitro* direct activity bioassays in liquid medium

The *in vitro* direct antifungal activity of mycosubtilin in
liquid medium was assessed by measuring the cell viability of *Z.
tritici* strain T02596 using resazurin staining, as proposed by

Siah et al. (2010b). Sterile 12-well plates were also used for the bioassay. Plate wells were filled with 2 mL of autoclaved glucose peptone medium supplemented with mycosubtilin at different concentrations (0.8, 4, 20, 100, and 500 mg.L^{-1}), before inoculation with fungal spore suspension already prepared in sterile glucose peptone medium, for a final concentration of 5.10^4 spores.mL^{-1}. Mycosubtilin was first dissolved in DMSO at a final concentration of 0.5% in the wells. Controls with and without 0.5% DMSO and with or without the fungus, were also used. After incubation for ten days at 20 ± 1°C under agitation at 150 rpm in dark conditions, 140 µL of the content of each well were sampled and deposited in flat-bottomed polystyrene 96-well microplates (Corning Costar®, Corning, USA). Then, 10 µL Alamar blue (AbD Serotec, UK) were added to each well before incubating the microplates for 4h in the same conditions described above. Cell viability was evaluated by measuring the absorbance at 540 nm using a microplate reader (Multiskan GO, Thermo Fischer Scientific, France). Six biological replicates were used for each condition.

The inhibitory effect of mycosubtilin towards unique wheat cells (cv. Alixan) was assessed in sterile 12-well plates. Wheat unique cells were obtained using the protocol of Biesaga-Kościelniak et al. (2008), with few modifications. Briefly, wheat caryopses were plunged for 5 min in 70% ethanol, rinsed twice with sterile osmotic water, and disinfected for 20 min in a 15% calcium hypochlorite solution, before being cleansed again at least twice. Mature embryos were delicately separated from the rest of the grain and were gently ground in a mortar. Fifty embryos were required to initiate wheat-cell suspension in 200 mL Erlenmeyer flask. These flasks contained 20 mL of autoclaved Gamborg B5 medium including vitamins (Duchefa Biochemie B.V, Netherlands), supplemented with 20 g.L^{-1} sucrose and 3.5 mg.L^{-1} 2,4-dichlorophenoxyacetic acid (Thermo Fischer Scientific, France). Wheat cell suspensions were incubated at 20 ± 1°C in dark conditions under agitation at 80 rpm. At three and six days after inoculation, 20 mL of sterile medium were added to each flask. At 10 days, the mixture was filtered through a 1 mm sieve, to get rid of ungrounded agglomerate tissue. Fresh medium was added to the filtrates to obtain 80 mL suspension in each flask. Seven days later, 20 mL of Gamborg B5 fresh medium were supplemented. Finally, every week, 25% of the suspension was discarded and replaced by fresh medium. After two months of subculture, 12-well plate wells were filled with 2 mL of wheat cell suspension as well as 2 mL of fresh Gamborg B5 medium supplemented with mycosubtilin at different concentrations (0.8, 4, 20, 100, and 500 mg.L^{-1}). The plates were then placed into a growth chamber at 20 ± 1°C in the dark with an agitation of 80 rpm. Three weeks after incubation, the number of wheat cells were counted for each condition using a Malassez hemocytometer under a light microscope (Nikon, Champigny-sur-Marne, France). Representative pictures were obtained using a digital camera (DXM1200C, Nikon, Champigny-sur-Marne, France) coupled with the image

capture software NIS-Elements BR (Nikon, Champigny-sur-Marne, France).

2.4 *In planta* cytological assays

The direct antifungal activity of mycosubtilin at 100 mg.L^{-1} on *Z. tritici* spore germination as well as on the epiphytic hyphal growth of the fungus on the leaf surface was assessed in planta at D5 using Fluorescent Brightener 28 (Calcofluor, Sigma-Aldrich, Saint-Louis, USA), a chitin staining dye. Third-leaf segments (2 cm) harvested from wheat plants grown in the greenhouse, inoculated with *Z. tritici* and treated or not with mycosubtilin in the same conditions described above, were sampled and immersed for 5 min in a solution of 0.1% (w/v) Calcofluor buffered with 0.1 M Tris-HCl, pH 8.5. Leaf segments were then rinsed twice in sterile osmosed water for 2 min before being dried in dark conditions at room temperature. Finally, they were deposited on a glass slide, covered with cover slip, and observed with an optic microscope (Eclipse 80i, Nikon, Champigny-sur-Marne, France) under UV-light. The proportion of different spore classes was determined from 100 distinct spores on each third-leaf segment. Spore classes were defined as follows; class 1, non-germinated spore; class 2, germinated spore with a small germ tube; class 3, germinated spore with developed germ tube; and class 4, geminated spore with a strongly developed germ tube. Nine leaf segments, randomly selected from three different pots (three segments per pot), were used as replicates for each condition. Pictures were obtained using digital camera (DXM1200C, Nikon, Champigny-sur-Marne, France) coupled with the image capture software NIS-Elements BR (Nikon, Champigny-sur-Marne, France).

2.5 Sampling design for transcriptomic and metabolomic analyses

Samples were collected at two days (D2) and five days (D5) after treatment for transcriptomic analyses. For each condition, *i.e.* plants treated with mycosubtilin (M) or not (control, C), and inoculated with *Z. tritici* (i) or not (Ni), nine third leaves sampled from three different pots (three leaves per pot) were randomly harvested, bulked per pot, immediately frozen in liquid nitrogen and stored at -80°C for further analyses. Thereafter, 100 mg of frozen pooled leaves were ground in a mortar with liquid nitrogen for RNA extraction. Regarding metabolomic analyses, samples were collected at D2, D5, as well as fifteen days after treatment (D15). For each modality, nine third leaves were randomly harvested from three different pots (three leaves per pot), immediately frozen in liquid nitrogen, and stored at -80°C for further analyses. Leaves were later freeze-dried using Alpha 2-4 LSCplus lyophilizer (Martin Christ Gefriertrocknungsanlagen GmbH, Osterode am Harz,

Germany) and ground with iron beads using a MM2 Retsch mixer-mill (Retsch GmbH, Haan, Germany) in order to obtain a fine powder, suitable for analyses. Sampling design for both transcriptomic and metabolomic analyses is illustrated in Supplementary Figure S1.

2.6 RNA extraction and microarray analyses

Total RNA was extracted from wheat leaves using RNeasy Plant Mini Kit (Qiagen, Courtaboeuf, France). RNA quality was determined with Nanodrop One/One[C] (Thermo Fisher Scientific, USA) by analyzing their absorbance ratios A260/280 and A260/230, which were found to range between 2.0 and 2.2. Moreover, RNA quality was also examined with Bioanalyzer 2100 (Agilent, France) and a minimal RNA integrity number (RIN) of 8 was required for all samples. For microarray analyses, hybridization for all conditions were performed in triplicate with three sets of total RNA extracted from bulked wheat leaves (see above Sampling design section). Wheat Gene Expression Microarrays GE 4x44 (Agilent, Santa Clara, CA, USA) were used to study the gene expression profile between the different conditions. RNA amplification, staining, hybridization, and washing steps were conducted according to the manufacturer's specifications. Slides were scanned at 5 μm/pixel resolution using the GenePix 4000B scanner (Molecular Devices Corporation, Sunnyvale, CA, USA). Images were used for grid alignment and expression data digitization with GenePix Pro 6.0 software (Molecular Devices Corporation, Sunnyvale, CA, USA). Gene expression data were normalized by Quantile algorithm. The three control samples were filtered for $P < 0.05$ and the average was calculated for each gene. A fold change (FC) value was calculated for each gene between individual treated samples and the mean of corresponding controls. Differentially expressed genes (DEGs) were selected for a significant threshold > 2.0 or < 0.5 ($P < 0.05$). Functional annotation of DEGs was based on NCBI GenBank and related-genes physiological processes were assigned with NCBI, AmiGO 2 Gene Ontology and UniProt. KEGG pathway analysis was also used to identify relevant biological pathways for the selected genes. All microarray data have been submitted to the NCBI GEO: archive for functional genomics data with the accession number GSE169298.

2.7 Metabolite extraction and UHPLC-MS analyses

Metabolites were extracted from powdered freeze-dried wheat leaves (30-50 mg per sample) using 25 μL of methanol per mg dry weight. The extract was then incubated in an ultrasound bath for 10 minutes, before centrifugation at 13000 g at 10°C for 10 minutes. The supernatant was analyzed using a Dionex Ultimate 3000 UHPLC system (Thermo Fisher Scientific, USA). The chromatographic separations were performed on a Nucleodur C18 HTec column (150 × 2 mm, 1.8 μm particle size; Macherey-Nagel, Germany) maintained at 30°C. The mobile phase consisted of acetonitrile/formic acid (0.1%, v/v, eluant A) and water/formic acid (0.1%, v/v, eluant B) at a flow rate of 0.3 mL.min^{-1}. The gradient elution was programed as follows: 0 to 1 min, 95% B; 1 to 2 min, 95% to 85% B; 2 to 7 min, 85% to 0% B; 7 to 9 min, 100% A. The sample volume injected was 1 μL. The UHPLC system was coupled to an Exactive Orbitrap mass spectrometer (Thermo Fischer Scientific, USA), equipped with an electrospray ionization (ESI) source operating in positive mode. Parameters were set at 300°C for ion transfer capillary temperature and 2500 V for needle voltages. Nebulization with nitrogen sheath gas and auxiliary gas were maintained at 60 and 15 arbitrary units, respectively. The spectra were acquired within the m/z (mass-to-charge ratio) mass ranging from 100 to 1000 atomic mass units (a.m.u.), using a resolution of 50,000 at m/z 200 a.m.u. The system was calibrated internally using dibutyl-phthalate as lock mass at m/z 279.1591, giving a mass accuracy lower than 1 ppm. The instruments were controlled using the Xcalibur software (Thermo Fischer Scientific, USA). LC-MS grade methanol and acetonitrile were purchased from Roth Sochiel (France); water was provided by a Millipore water purification system. Apigenin and chloramphenicol (Sigma-Aldrich, France) were used as internal standards.

Metabolites belonging to different chemical families were identified based on published works about benzoxazinoids (de Bruijn et al., 2016), flavonoids (Wojakowska et al., 2013) and hydroxycinnamic acid amides (Li et al., 2018) from wheat. Putative metabolite identifications were proposed based on expertized analysis of the corresponding mass spectra and comparison with published literature. Further information was retrieved from the KEGG (Kyoto Encyclopedia of Genes and Genomes, http://www.genome.ad.jp/kegg/) and PubChem (http://pubchem.ncbi.nlm.nih.gov) databases. Relative quantification of the selected metabolites was performed using the Xcalibur software. For some metabolites, identity was confirmed with the corresponding standard provided by Sigma-Aldrich (France).

2.8 Statistical analyses

Protection efficacy data set was analyzed using One-Way analysis of variance (ANOVA) at $p \leq 0.05$, while data obtained for *in planta* spore germination and hyphal growth were analyzed using ANOVA followed by the Tukey's test at $p \leq 0.05$, using GraphPad Prism software version 9 (GraphPad Software Inc., San Diego, USA). Regarding the *in vitro* antifungal activity assay, the half-maximal inhibitory concentration (IC_{50}) was also determined with the GraphPad

Prism software version 9. Differential metabolomic analyses were performed with the W4M platform (Guitton et al., 2017), using the Tukey's Honest Significant Difference method followed by a false discovery rate (FDR) correction using the Benjamini-Hochberg procedure (Benjamini and Hochberg, 1995). Metabolites of interest were considered differentially accumulated when the false discovery rate was below 5% (FDR ≤ 0.05).

3 Results

3.1 Foliar application of mycosubtilin protects wheat against *Z. tritici* and reduces fungal spore germination and hyphal epiphytic growth

The ability of mycosubtilin to protect wheat against *Z. tritici* was assessed in the greenhouse using the wheat cv. Alixan and the pathogenic *Z. tritici* strain T02596. At 21 days after inoculation, the disease severity level was 55.7% in the non-treated inoculated plants. Preventive foliar application of mycosubtilin at 100 mg.L^{-1} two days before inoculation resulted in significant disease reduction (23.3% of diseased leaf

area, corresponding to a 58.1% decrease) in treated plants when compared to non-treated inoculated plants (Figure 1A). *In planta* fungal staining assays using Calcofluor revealed that the treatment with mycosubtilin significantly reduced the rates of both spore germination and epiphytic growth of *Z. tritici* at three days after inoculation, *i.e* five days after treatment (D5) (Figure 1B). In treated wheat plants, non-germinated spores (class 1) were significantly more abundant (approximatively five-fold) than in the control plants. Moreover, the number of germinated spores with either developed germ tube (class 3) or strongly developed germ tube (class 4) was significantly reduced (by three- and seven-fold, respectively) on treated plants when compared to the control ones.

3.2 Mycosubtilin impacts *in vitro* growth of both *Z. tritici* and wheat single cells, but at different concentration thresholds

The effect of mycosubtilin on the *Z. tritici in vitro* growth was evaluated on solid PDA medium in 12-well plates. The biomolecule exhibited a strong antifungal activity against the pathogen, with IC$_{50}$ and MIC values of 0.57 and 0.78 mg.L^{-1}, respectively (Supplementary Figure S2). In order to gain more
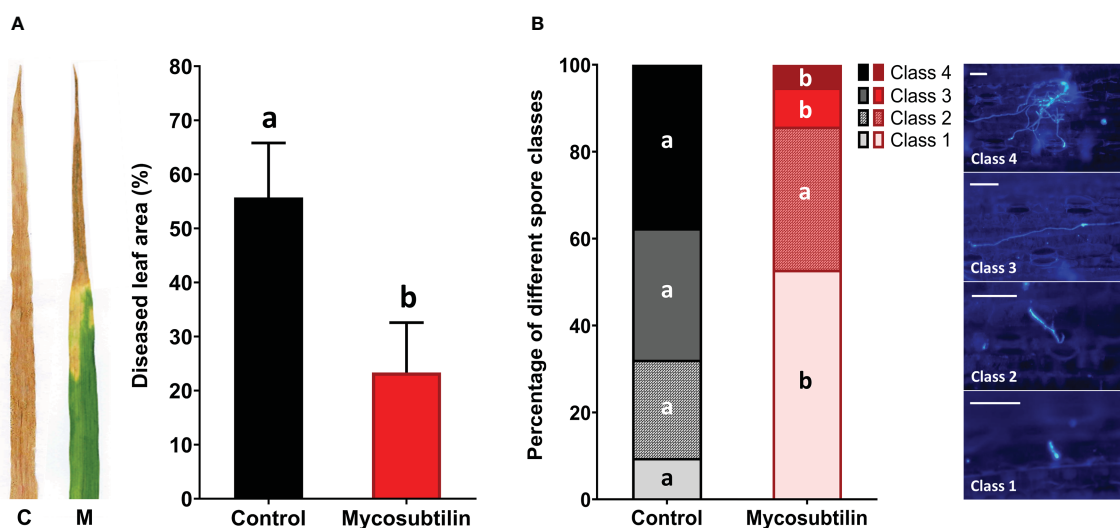
FIGURE 1
Disease severity level **(A)** and rates of *in planta* spore germination and epiphytic growth **(B)** of *Zymoseptoria tritici* (T02596 strain) on wheat leaves (cv. Alixan) pre-treated with mycosubtilin (M) at 100 mg.L^{-1} or not (C, control). **(A)** Disease severity level was scored 21 days after inoculation (*i.e* 23 days after mycosubtilin treatment) by assessing the area of lesions (chlorosis and necrosis) on the third leaf of each wheat plant (n=36). Means tagged with the same letter are not significantly different according to One-way ANOVA test ($P \leq 0.05$). **(B)** Proportions of four different development stages of fungal spores were assessed by using Calcofluor staining recorded three days after inoculation (*i.e.* five days after mycosubtilin treatment). The different spore development classes are defined as followed: Class 1, non-germinated spore; Class 2, germinated spore with a small germ tube; Class 3, germinated spore with a developed germ tube; Class 4, germinated spore with a strongly developed germ tube. For each condition, the different classes were determined from 100 distinct spores chosen randomly on each third-leaf segment. Within each spore class, the presence of different letters indicates a significant difference according to the Tukey test at $p \leq 0.05$. Scale bar = 25 µm.

insights into the mode of action of mycosubtilin on the host plant as well as on the pathogen, further bioassays were performed in liquid medium to examine the effect of the lipopeptide on the development (cell multiplication) of either wheat single cells or *Z. tritici* spores. Microscopic observation of the fungal spores grown in glucose peptone liquid medium showed that mycosubtilin totally inhibits the fungal growth from the concentration of 4 mg.L^{-1}. Besides, the lipopeptide exhibits also an effect on the growth of wheat single cells cultivated in suspension in MS liquid medium, but with a total inhibiting concentration of 500 mg.L^{-1} (Figure 2). Hence, the activity threshold of mycosubtilin seems to be 125-fold higher towards wheat single cells than against *Z. tritici* spores in liquid medium. However, no phytotoxic effect of mycosubtilin was observed at this concentration when the biomolecule is applied on wheat leaves. Indeed, no visible leaf necrosis and no

significant effect on the total fresh biomass were observed on the treated plants at all tested concentrations (Figure 2).

3.3 Mycosubtilin regulates several defense-associated genes in wheat against *Z. tritici*

Transcriptomic analyses using RNA microarray assay were performed in order to examine both eliciting and priming effects of mycosubtilin in wheat towards *Z. tritici* during the early stages of the fungal infection. The bioassay was performed in non-inoculated conditions at two days after treatment (D2), and in both non-inoculated and inoculated conditions at five days after treatment (D5), *i.e* three days after inoculation. The eliciting effect was examined at D2 and D5 by comparing the treated non-
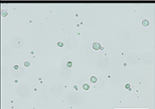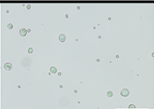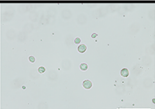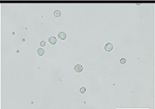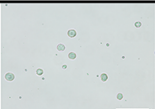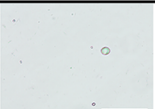
Mycosubtilin (mg.L^{-1})	Control	DMSO	0.8	4	20	100	500
Fungal cell suspension							
ΔDO (540 nm)	1.39 (± 0.10)	1.47 (± 0.20)	1.36 (± 0.23)	~0	~0	~0	~0
Wheat cell suspension							
Wheat cell (cells.mL^{-1})	12x10^4 (± 11.4x10^4)	10x10^4 (± 8.2x10^4)	11x10^4 (± 11.0x10^4)	12x10^4 (± 10.3x10^4)	7x10^4 (± 10.6x10^4)	1x10^4 (± 3.2x10^4)	< 1x10^4
Wheat leaf surface							
Visible tissue damage	No necrosis	No necrosis	No necrosis	No necrosis	No necrosis	No necrosis	No necrosis
Wheat aerial biomass							
Fresh weight (g per pot)	102.3 (± 11.5)	102.0 (± 15.6)	103.7 (± 6.7)	102.0 (± 7.2)	98.9 (± 8.5)	101.4 (± 8.8)	102.5 (± 10.2)

FIGURE 2
Effect of mycosubtilin at different concentrations on the growth of either *Zymoseptoria tritici* or wheat cells in liquid medium *in vitro* in twelve well microplates, on leaf appearance and on plant fresh biomass of whole plants grown in the greenhouse. Fungal growth was assessed using resazurin staining and optical density measurement 10 days after inoculation (dai) of glucose peptone medium with *Z. tritici* spores (n=6), while wheat cell growth was evaluated using Malassez hemocytometer at 21 days after inoculation of Gamborg B5 medium with wheat cell suspension (n=10). Leaf appearance was assessed visually at two, seven and fifteen days after plant treatment (n=27), while the fresh biomass was determined by weighting nine whole plants from each pot (n=3). Representative pictures of either *Z. tritici* or wheat cell cultures observed under a light microscope at magnification 10x and 20x respectively, as well as the microplate wells used for *Z. tritici* culture medium staining with resazurin, are shown. Likewise, representative pictures of leaf appearance and plant fresh aerial biomass, at fifteen days after treatment, are also presented. Scale bar = 100 μm.

inoculated plants to non-treated and non-inoculated plants. The priming effect was investigated at D5 by comparing treated and inoculated plants to non-treated inoculated plants, and by taking into account the elicitation modality at both D2 and D5. Moreover, in order to have a reliable conclusion and comprehensive view on the data linked to the priming effect, additional comparisons (treated and inoculated plants *versus* treated non-inoculated plants, and treated and inoculated plants *versus* non-treated non-inoculated plants), were also performed (Supplementary Table S1 and Figures S3, S4). The fungal effect was investigated at D5 by comparing non-treated and inoculated plants to non-treated and non-inoculated ones. The different comparisons will thereafter be referred to as eliciting, fungal, and priming effects, corresponding to eliciting, infection alone, and priming modalities, respectively.

A total of 130 genes were regulated (*i.e.* when taking into account both up and down regulations) when examining eliciting, fungal, and priming effects and considering all time points (Supplementary Table S2). Overall, treatment with mycosubtilin led to a broader gene regulation response in priming modality at D5 when compared to both elicitation modalities at D2 or D5 (Figures 3-5). When considering the eliciting effect at both D2 and D5, only 40 differentially expressed genes (DEGs) were highlighted, with 18, 6, and 16 DEGs specifically scored at D2, both D2 and D5, and D5, respectively. Among them, 28 were upregulated and 12 were downregulated (Figure 3A). At D5, priming modality displayed considerably more DEGs (80) when

compared to the eliciting effect at D5 (22), with 13 DEGs found in common among the two modalities. Globally, when considering all investigated modalities at D5 (eliciting, fungal, and priming effects), a total of 116 DEGs were recorded (Figure 3B). Out of the detected 116 DEGs, 8, 27 and 59, were specifically noticed during either elicitation, fungal or priming effect modalities, respectively. (Figure 3B).

Functional groups of DEGs recorded during wheat eliciting or priming by mycosubtilin at D5 were compared (Figure 4). Consistently with the findings highlighted above in Venn diagrams, priming conditions clearly exhibited more DEGs annotated in the highlighted functional groups when compared to the eliciting conditions at D5. Among the sixteen identified functional groups of DEGs, those linked to stress responses were the most regulated upon treatment with mycosubtilin, especially in priming conditions, followed by those involved in chloroplast and light harvesting, as well as growth and development. Few functional groups of DEGs were found only in priming modality, including those related to pigment biosynthesis, photosynthesis, flowering and seed maturation, cell wall structure and function, and primary metabolic pathways (carbohydrate, amino acid, protein, and lipid metabolisms). Moreover, a relative strong increase in the number of DEGs involved in transcription regulation, RNA-processing and translation, as well as secondary metabolism, was observed in priming when compared to elicitation modalities (Figure 4).
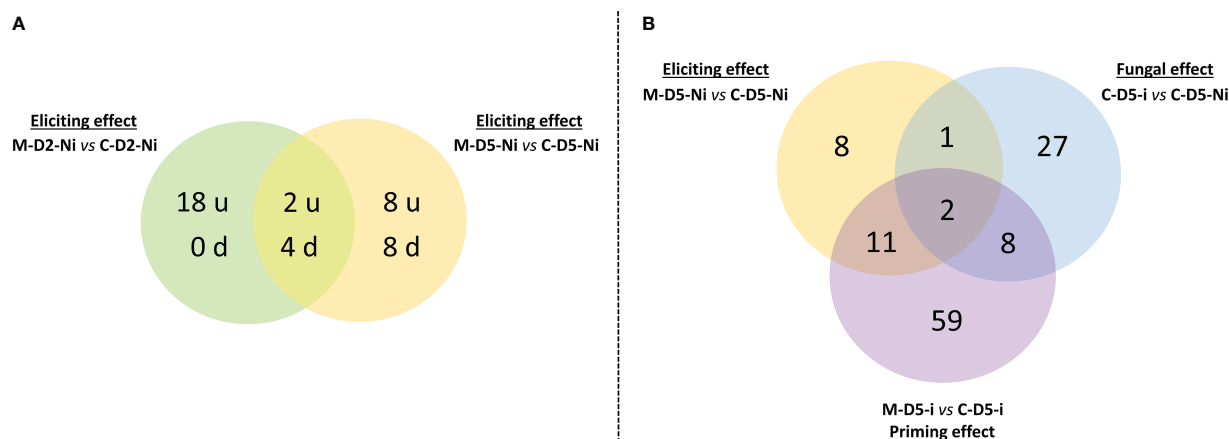
FIGURE 3
Venn diagrams underlying **(A)** the number of up-regulated (u) or down-regulated (d) genes observed after mycosubtilin treatment in non-inoculated conditions with *Zymoseptoria tritici* as well as **(B)** the number of differentially expressed genes in the different tested conditions at five days after treatment with mycosubtilin (*i.e.* three days after wheat inoculation with *Z. tritici*). In **(A)**, the potential early elicitation effect of mycosubtilin at two days after treatment (M-D2-Ni vs C-D2-Ni) on the levels of wheat leaf gene expression is compared to the later one at five days after treatment (M-D5-Ni vs C-D5-Ni). In **(B)**, The eliciting effect of mycosubtilin (M-D5-Ni vs C-D5-Ni) is compared to the fungus effect (C-D5-i vs C-D5-Ni) and to the priming effect of mycosubtilin (M-D5-i vs C-D5-i). M refers to plants treated with mycosubtilin whereas C stands for mock treated ones. Ni stands for mock inoculated whereas i indicates that plants were inoculated with *Z. tritici*. D2 and D5 signify that leaves were sampled respectively at two and five days after mycosubtilin treatment.

FIGURE 4

Functional groups of differentially expressed genes (DEGs) highlighting eliciting (M-D5-Ni vs C-D5-Ni) or priming (M-D-5i vs C-D5-i) effects of wheat defenses after treatment with mycosubtilin. Functional annotation of DEGs was performed based on NCBI GenBank and related-gene physiological processes were assigned with NCBI, AmiGO 2 Gene Ontology and UniProt. M refers to plants treated with mycosubtilin whereas C stands for mock treated ones. Ni stands for mock inoculated whereas i indicates that plants were inoculated with *Zymoseptoria tritici*. D5 signifies that leaves were sampled at five days after mycosubtilin treatment.

When examining the gene regulation in detail, mycosubtilin-induced eliciting effect observed at D2 mainly involved DEGs associated to responses to pathogens, oxidative stress, and abiotic stress; most of them were significantly upregulated, except *peroxidase* and *peroxidase 2*, which were significantly downregulated (Figure 5 and Supplementary Table S2). Noticeably, three DEGs involved in signaling, transcription, and translation (Ca^{2+}/H^+ *exchanging protein*, *zinc finger protein WZF1*, and *histone H1 WH1A.3*) were found overexpressed at D2 (Figure 5). Additionally, at D5, a downregulation of eight other DEGs, three associated with responses to pathogens (*thaumatin-like protein TL4*, *chitinase*, and *chitinase*2), as well as an upregulation of eight DEGs, with two linked with responses to pathogens, were recorded. In the priming modality at D5, mycosubtilin induced the regulation of a substantial number of genes related to several physiological pathways. Among them, a subset of 26 genes is linked to responses to stresses, including thirteen to oxidative stress, nine to pathogens, and four to abiotic stress. Interestingly, several genes involved in abscisic acid (ABA) biosynthesis (*beta-carotene hydroxylase* and *lycopene β-cyclase*) and ABA-associated signaling pathways (*ARK protein*, *aquaporins*, *aldose reductase*, *ABC1 family protein-like*, *glutathione peroxidase-like protein GPX15Hv*, *nicotianamine synthase 3*, *chlorophyll a/b binding protein of LHCII type III chloroplast precursor*, *light-harvesting complex 1* and *S-adenosylmethionine synthetase*) were also regulated in priming modality at D5 (Figure 5). Regarding

the effect of the fungal infection alone on the wheat leaf transcriptome at D5, only an upregulation of six DEGs involved in response to abiotic stress and pathogens was obtained, whereas a set of 32 DEGs was downregulated by the fungus alone at this time point, among them some are also related to responses to abiotic stress and pathogens. However, the most remarkable effect of *Z. tritici* is the downregulation of an important number of genes involved in cell-wall structure, amino acid metabolism, and protein metabolism (Figure 5).

3.4 Mycosubtilin primes flavonoid accumulation in wheat against *Z. tritici*

Metabolomic analyses using UHPLC-MS were undertaken to assess the effect of mycosubtilin on the wheat leaf metabolome in both non-inoculated and inoculated conditions, and at the same time points than those targeted in the above described transcriptomic assay (D2 and D5), with an additional time point corresponding to 15 days after treatment (D15), *i.e* 13 days after inoculation, corresponding to the late stage of *Z. tritici* biotrophic phase. The eliciting effect was investigated at D2, D5, and D15 by comparing the treated non-inoculated plants to non-treated and non-inoculated plants. The priming effect was examined at D5 as well as D15, on the one hand, by comparing treated and inoculated plants to non-treated inoculated plants, and on the other hand, by considering the elicitation modalities at D2, D5, and D15. Besides, further comparisons (treated and inoculated plants *versus* treated non-inoculated plants, and treated and inoculated plants *versus* non-treated non-inoculated plants), were also carried out in order to have a comprehensive picture on the data linked to the priming effect on leaf metabolome (Supplementary Figure S5). As described in the transcriptomic assay, the different comparisons in the metabolomic assay will also be referred to as eliciting, fungal, and priming effects, corresponding to eliciting, infection alone, and priming modalities, respectively.

The analyses were targeted on 54 metabolites belonging to major chemical families that were detected and quantified using UHPLC-MS (Figure 6 and Supplementary Table S3). Plant treatment with mycosubtilin and/or inoculation with *Z. tritici* resulted in marked differentiations among wheat leaf metabolite patterns, as highlighted by the PCA analysis (Supplementary Figure S6). The largest changes in the accumulation of the selected metabolites were observed during fungal infection alone or during priming modalities, whereas only minor modifications were scored in eliciting modalities (Figure 6). In all eliciting modalities, only eight differentially accumulated metabolites (DAMs) were recorded. Among them, four DAMs were under-accumulated, two at D2 (asparagine and chry-C-hexo-O-hexo), one at D5 (MeJA), and one at D15

FIGURE 5
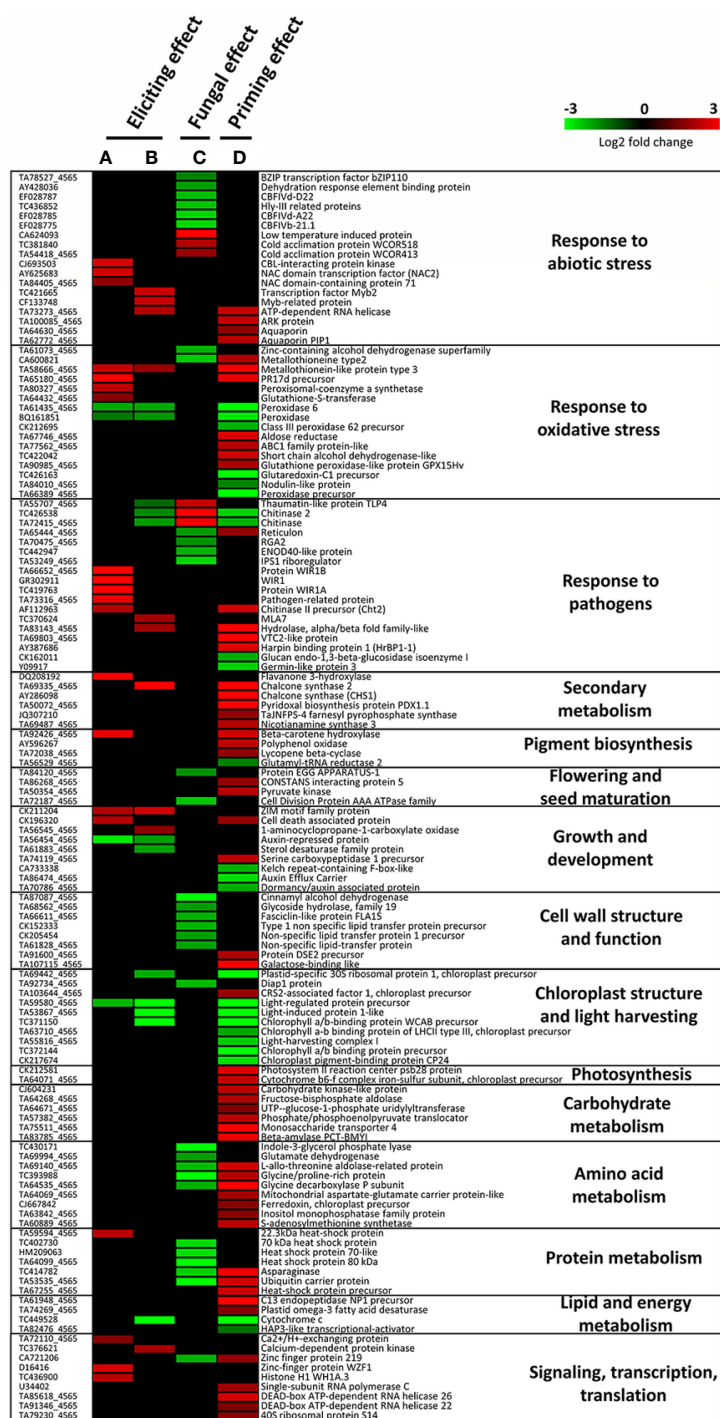
Heatmap showing significantly up- or down-regulated genes in wheat third-leaves (cv. Alixan) treated or not with 100 mg.L^{-1} mycosubtilin and inoculated or not with *Zymoseptoria tritici* (strain T02596), recorded at two days after treatment in non-inoculated conditions **(A, B)** and at five days after treatment (*i.e.* three days after inoculation) in inoculated conditions **(C, D)**. A and B highlight the eliciting effect, C shows the fungal effect, while D reveals the priming effect induced by mycosubtilin. Gene-related physiological processes are represented on the right part of the graph and were determined using NCBI, AmiGO 2 Gene Ontology, KEGG and UniProt. **(A)**, M-D2-Ni *vs* C-D2-Ni; **(B)**, M-D5-Ni *vs* C-D5-Ni; **(C)**, C-D5-i *vs* C-D5-Ni; **(D)**, M-D5-i *vs* C-D5-i. Significant relative change in gene expression is presented in Log2 ratio, according to the color scale, using the WebMev software. M refers to plants treated with mycosubtilin whereas C stands for mock treated ones. Ni stands for mock inoculated whereas i indicates that plants were inoculated with *Z. tritici*. D2 and D5 signify that leaves were sampled respectively at two and five days after mycosubtilin treatment.

(tricin), and four were over-accumulated at D15, including three amino acids (glutamic acid, threonine and proline) and one hormone (ABA-Glc). However, in the priming modalities, a higher number of DAMs was scored, including 16 DAMs at D5 and 16 DAMs at D15 (Figure 6). At D5, only metabolite down-accumulation was detected (corresponding mainly to those over-accumulated in the fungal modalities), whereas at D15, both increases and decreases in metabolite concentration were observed. At D15, a decrease in the concentration of three hydroxycinnamic acid amides (coumaroylputrescine, coumaroylcadaverine, and caffeoylputrescine) and five amino acids and derivatives (leucine-isoleucine, arginine, threonine, glutamine, and methyl-pipecolate) was found. Interestingly, seven metabolites belonging to flavonoids and one benzoxazinoid were over-accumulated specifically in the priming modality at D15 (Figure 6).

Fungal infection alone induced substantial modifications in metabolite accumulation patterns at D5 and D15, with marked changes at D5, corresponding to the early stages of infection (Figure 6). Indeed, at D15, only significant changes in the concentration of glutamine, methyl-pipecolate, salicylic acid, and four hydroxycinnamic acid amides were noticed. However, at D5, a total of 26 DAMs, about half of the quantified molecules, were significantly regulated, with 18 molecules over-accumulated and eight under-accumulated. Seven amino acids, six benzoxazinoids, and five hydroxycinnamic acid amides were more concentrated, while three phytohormone precursors or derivatives (OPDA, MeJA and MeSA), five flavonoids, four luteolin derivatives, and one chrysoeriol derivative were down-accumulated (Figure 6). The proposed model on the effects of mycosubtilin-induced priming and *Z. tritici* infection at D5 and D15 on both hydroxycinnamic acid amide and flavonoid biosynthesis pathways within wheat leaves is illustrated (Figure 7).

4 Discussion

We have combined here transcriptomic and metabolomic approaches to unravel the resistance mechanisms induced in wheat, using the *B. subtilis* lipopeptide mycosubtilin as a treatment and *Z. tritici* as a phytopathogenic model. Only few previous works have used Omics to characterize the induced resistance in plants, whereas such tools could be helpful and informative about the molecular and physiological changes occurring during plant resistance activation using exogenous treatments (*e.g.* Gauthier et al., 2014; Fiorilli et al., 2018). Our results revealed that mycosubtilin likely acts on the wheat-*Z. tritici* pathosystem through a double activity (direct and indirect) and that the indirect activity relies mainly on the priming of wheat defense mechanisms.

4.1 Mycosubtilin displays direct antifungal activity towards *Z. tritici* and likely interacts with wheat leaf cells without causing *in planta* phytotoxicity

Foliar application of mycosubtilin at 100 mg.L^{-1} decreased *Z. tritici* symptoms on wheat plants by more than half (58.1%), thus agreeing with previous results obtained on this pathosystem (Mejri et al., 2018). Mycosubtilin has also been reported to biocontrol other pathogens, such as *Bremia lactucae* on lettuce, *Botrytis cinerea* on grapevine, and *Fusarium oxysporum* f. sp. *iridacearum* on *Iris* sp. (Deravel et al., 2014; Farace et al., 2015; Mihalache et al., 2018). Our *in vitro* and *in planta* bioassays have shown that mycosubtilin exhibits a direct antifungal effect on both spore germination and epiphytic growth of *Z. tritici* on wheat leaves, hence corroborating previous findings on this fungus (Mejri et al., 2018). Interestingly, our results revealed that mycosubtilin exhibits growth inhibiting activity on fungal as well as wheat single cells grown in suspension, suggesting that the lipopeptide interacts with the cells of both organisms with a common process. Indeed, it has been reported that the mode of action of mycosubtilin could rely on the destabilization of cytoplasmic membranes (Nasir et al., 2010; Nasir and Besson, 2012), that could lead to loss of cell integrity, cytoplasm leakage, and ultimately cell death. We can, thus, hypothesize that the biological activities of mycosubtilin on both *Z. tritici* and wheat cells may be associated with its ability to interact with the plasma membranes of both organisms. Nevertheless, the *in vitro* threshold concentration of the molecule activity on both species varies strongly, with a difference of 125-fold between *Z. tritici* and wheat cells, even though fungal cells growing in contact with the biomolecule during the bioassay were protected by cell-walls, while wheat cells grown in suspension didn't likely develop complete cell-walls. However, no visible phytotoxicity caused by mycosubtilin on the whole plants was observed even at the highest tested concentration (500 mg.L^{-1}), presumably because leaves are overall more robust (presence of cuticle, etc.) than single wheat cells growing *in vitro*. An effect of mycosubtilin at 50 mg.L^{-1} on the growth of grapevine single cells has previously been observed, with a significant increase in the amounts of cell death (23% of the total cells compared with 11% in the control) observed at 24h post-treatment, thus agreeing with our results (Farace et al., 2015). Taken together, these results suggest that, when applied on wheat plants at 100 mg.L^{-1}, mycosubtilin is able, on the one hand, to display direct antimicrobial activity towards the pathogen and, on the other hand, to interact with the plasma membranes of plant leaf cells without causing damages that could lead to their death. More likely, this interaction of the molecule with the plasma membranes of plant cells could be the initial stimulus triggering the downstream defense reactions highlighted in wheat plants in the transcriptomic and metabolomic assays. This defense-
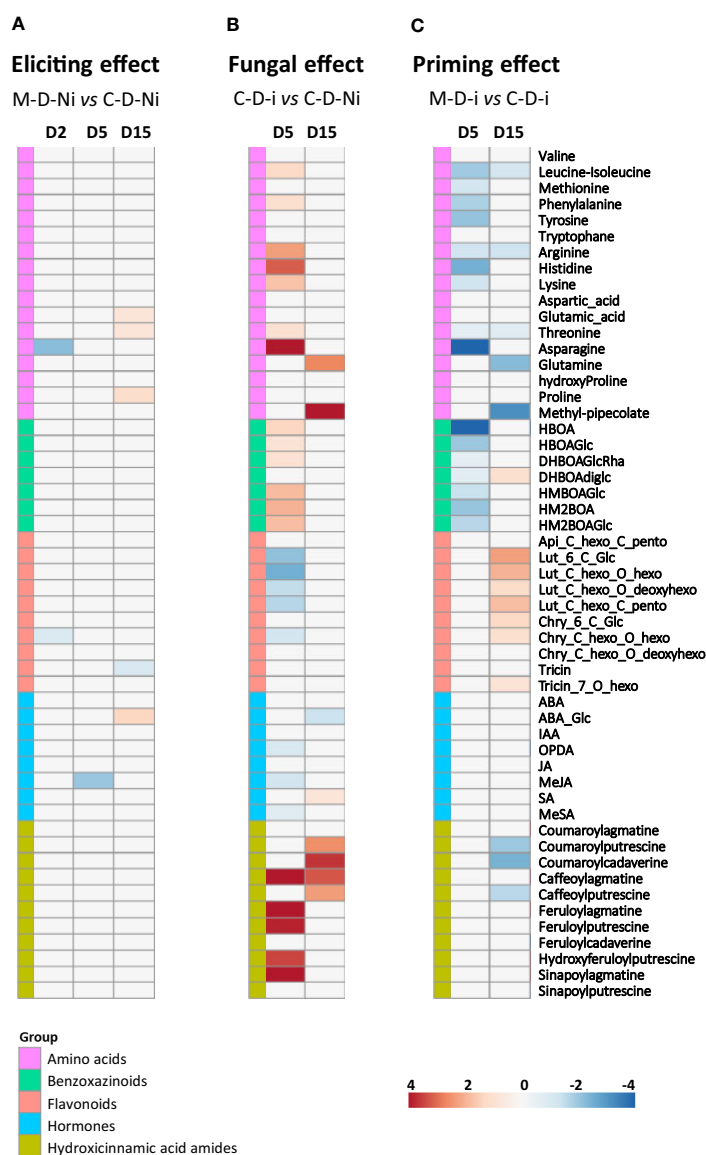
FIGURE 6

Heatmap of significant relative changes in metabolite patterns within wheat third-leaves (cv. Alixan) treated or not with 100 mg.L^{-1} mycosubtilin and inoculated or not with *Zymoseptoria tritici* (strain T02596) at different time points (n = 9 plants). **(A)**, potential elicitation effect of mycosubtilin in non-inoculated conditions at 2 (M-D2-Ni vs C-D2-Ni), 5 (M-D5-Ni vs C-D5-Ni) and 15 (M-D15-Ni vs C-D15-Ni) days after treatment (dat). **(B)**, Fungal effect on wheat leaf metabolome at 5 (C-D5-i vs C-D5-Ni) and 15 (C-D15-i vs C-D15-Ni) dat, *i.e.* at 3 and 13 days after wheat inoculation (dai) with *Z. tritici*, respectively. **(C)**, Priming effect of mycosubtilin in inoculated conditions at 5 (M-D5-i vs C-D5-i) and 15 (M-D15-i vs C-D15-i) dat (*i.e.* at 3 and 13 dai, respectively). M refers to plants treated with mycosubtilin whereas C stands for mock treated ones. Ni stands for mock inoculated whereas i indicates that plants were inoculated with *Z. tritici*. D2, D5 and D15 signify that leaves were sampled respectively at two, five and fifteen days after mycosubtilin treatment. Log2 of significant metabolite fold changes for indicated pairwise comparisons are given by shades of red or blue colors according to the scale bar. Metabolites were grouped according to their functional or chemical family as amino acids, benzoxazinoids, flavonoids, hormones and hydroxycinnamic acid amides. Data represent mean values of nine biological replicates for each condition and time point. Statistical analyses were performed using the Tukey's Honest Significant Difference method followed by a false discovery rate (FDR) correction, with FDR < 0.05. For FDR $\geq$ 0.05, Log2 fold changes were set to 0.

initiating stimulus could be attributed, as suggested in other plant models, to the potential biophysical and biochemical interactions of mycosubtilin with the lipid bilayer of the leaf cell plasma membranes (Crouzet et al., 2020). The insertion of the lipopeptide within them could, hence, modify their fluidity as an "abiotic stress-like" agent, like a thermal or drought stress (Niu and Xiang, 2018; Couchoud et al., 2019). This "abiotic stress-like" mechanism could therefore explain the accumulation of gene transcripts involved in plant defenses against abiotic and oxidative stresses found in eliciting conditions.
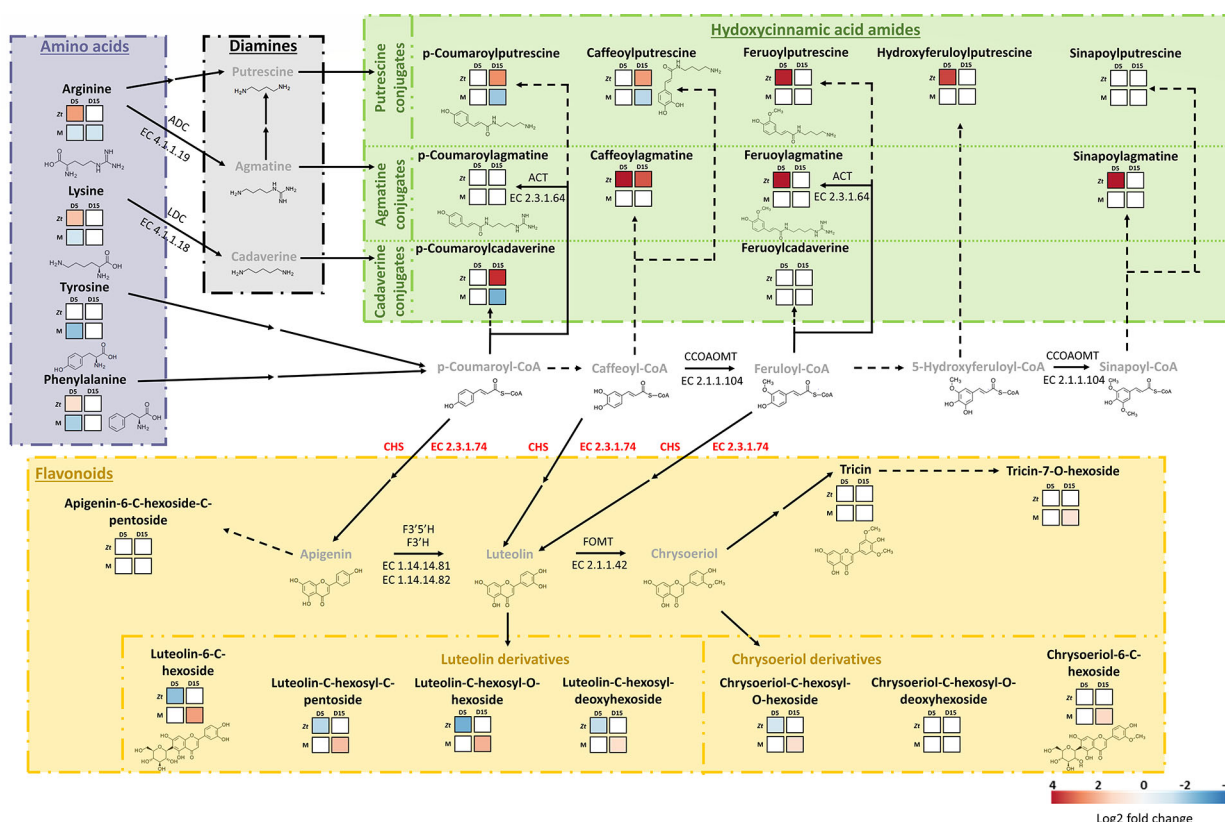
FIGURE 7

Metabolic map of the biosynthesis pathways and patterns of accumulation of major hydroxycinnamic acid amides and flavonoids within wheat third leaves (cv. Alixan) inoculated with *Zymoseptoria tritici* (strain T02596) pre-treated or not with mycosubtilin. Metabolic pathways are based on KEGG pathways (map00310, map00330, map00940, map00941, map00944). Amino acids, diamines, hydroxycinnamic acid amides and flavonoids metabolite families are separated and indicated in block of different colors, respectively purple, black, green and orange. Heatmaps show significant Log2 fold changes in metabolite accumulation, according to the corresponding scale bar. For each analyzed metabolite, the two upper squares represent the fungus effect on the relative accumulation of the compound, from the left to the right, at five (C-D5-i vs C-D5-Ni) and fifteen (C-D15-i vs C-D15-Ni) days after treatment (dat), *i.e* 13 days after inoculation. The two lower squares represent the effect of application of mycosubtilin (priming) prior to inoculation with *Z. tritici* on the wheat metabolome at five (M-D5-i vs C-D5-i) and fifteen (M-D15-i vs C-D15-i) dat. Metabolites in grey were not analyzed in this study. Solid arrows stand for enzymatic reactions completely described in the abovementioned KEGG pathways whereas dashed arrows are for suggested ones. Double arrows represent two or more metabolic steps. With ACT, agmatine N4-coumaroyltransferase; ADC, arginine decarboxylase; CCOAOMT, caffeoyl-CoA O-methyltransferase; CHS, chalcone synthase; F3'5'H, flavonoid 3';5'-hydroxylase, F3'H, flavonoid 3'-monooxygenase; FOMT, flavone 3'-O-methyltransferase; LDC, lysine decarboxylase. Genes coding for chalcone synthase were significantly upregulated when plants were primed with mycosubtilin at five days after treatment (M-D5-i vs C-D5-i), hence CHS is presented in red. M refers to plants treated with mycosubtilin whereas C stands for mock treated ones. Ni stands for mock inoculated whereas i indicates that plants were inoculated with *Z. tritici*. D5 and D15 signify that leaves were sampled respectively at five and fifteen days after mycosubtilin treatment.

4.2 Perception of mycosubtilin by wheat leaves leads to the elicitation of few genes associated with plant defense

Transcriptomic analyses revealed that in wheat plants treated with mycosubtilin (100 mg.L^{-1}), the expression of genes involved in plant responses to stresses and other biological functions was significantly regulated. At D2, in the elicitation modality, 24 DEGs were recorded, among which, three involved in signaling, transcription and translation were upregulated, including a gene encoding for Ca^{2+}/H$^+$ exchanging protein, a crucial regulatory protein of cytoplasm calcium homeostasis. Moreover, we found in the same modality and time point an overexpression of a *CBL-interacting protein kinase* (*CIPK*) gene, encoding for a protein functioning as a calcium sensor displaying a large range of activity in plant responses to stresses (Cui et al., 2018). Calcium influx into the cytoplasm is considered as one of the first cellular reactions after stress signal perception, that can trigger subsequent downstream defense reactions upon detection of the elevation of calcium concentration, by calcium-dependent protein kinases (CDPKs) (Harmon et al., 2000). The accumulation of *Ca2+/H+ exchanging protein* and *CIPK* transcripts detected in our conditions could likely be linked to the mycosubtilin-induced initial stimulus suggested above on the wheat cell plasma

membranes, leading to a modification in Ca^{2+} concentration inside wheat cells and hence to the subsequent triggered defense reactions observed in wheat leaves. In addition, among the DEGs still highlighted at D2 in the elicitation modality, 14 are associated to responses to either oxidative, pathogen, or abiotic stresses, suggesting that mycosubtilin confers to wheat an increased resistance level to these stresses. Notably, the upregulation of three genes encoding for a Pathogenesis-related (PR) protein or precursors (*pathogen-related protein*, *chitinase II precursor*, and *PR17d precursor*), known to play a major role in plant resistance to pathogens, was observed. Chitinases are enzymes known to be involved in wheat defenses against *Z. tritici* by degrading the chitin of fungal cell-wall (Kettles and Kanyuka, 2016). PR-17 is a class of PR proteins with an unknown mode of action, discovered by Christensen et al. (2002) and which could be involved in wheat defense against powdery mildew (Görlach et al., 1996). WIR1 is a membrane protein that was reported to contribute to wheat defense responses against fungal infections, including powdery mildew and stripe rust, supposedly by increasing the adhesion of the cellular membrane to the cell wall during the pathogen attack (Bull et al., 1992; Coram et al., 2008). The accumulation of these transcripts at D2, *i.e* just before the moment of plant inoculation, may contribute to wheat protection against *Z. tritici*. Nevertheless, further investigations are needed to determine the role of these proteins during the studied compatible interaction.

At D5, still in the elicitation context, 22 DEGs were found, six of them were also reported at D2, including three involved in responses to oxidative stress (*peroxidase*, *peroxidase 6* and *metallothionein-like protein type 3*) and two in growth and development (*ZIM motif family protein* and *auxin-repressed protein*). Genes encoding for ZIM motif family protein have been described as key repressors of the jasmonic acid (JA) signaling pathway (Chini et al., 2009), being, hence, involved in the regulation of many physiological processes, especially in the mediation of plant responses to biotic and abiotic stresses (Sun et al., 2017; Ruan et al., 2019). A large number of genes belonging to this family have been found to be regulated by other hormones such as gibberellins and ABA (Zheng et al., 2020). Considering DEGs involved in the growth and development functional group, the upregulation of *1-aminocyclopropane-1-carboxylate (ACC) oxidase* is to be noticed. This enzyme has been shown to be of prior importance for ethylene (ETH) production in plants (Houben and Van de Poel, 2019). As ETH is a gaseous plant hormone playing a crucial role in several biological processes, including tolerance to stresses, wheat responses to mycosubtilin could hence include ETH-responses (Adie et al., 2007a). Remarkably, Chandler et al. (2015) showed that mycosubtilin induces changes in gene expression in rice cells *in vitro*, with, especially, an increase in the amount of *ACC synthase* (*ACS1*) transcripts, another key enzyme in ETH synthesis. Regarding DEGs involved in response to pathogens, genes encoding for PR proteins (*thaumatin-like protein TLP4* and *chitinases*) were found to be downregulated, whereas *MLA7*, an homolog of a resistance

gene against powdery mildew in barley (Caldo et al., 2004), and *hydrolase alpha/beta fold family-like*, encoding for a protein family displaying large varieties of functions in plants (Mindrebo et al., 2016), were upregulated. In addition to this ability of mycosubtilin to regulate wheat defenses against biotic stress, we also observed significant modifications in the expression of genes involved in responses to abiotic stress, suggesting that mycosubtilin triggers multifaceted cross-talks in wheat defense pathways. In fact, three DEGs involved in response to abiotic stress were upregulated in the elicitation modality at D5, including genes encoding for transcription factor (TF) MYB2 (myeloblastosis), MYB-related protein, and ATP-dependent RNA helicase. MYB TFs were particularly studied for their critical importance in plant growth and stress tolerance, as reviewed by Ambawat et al. (2013). More precisely, a MYB2 was reported to participate in rice tolerance to salt, cold, and dehydration stress (Yang et al., 2012). The authors also showed that this TF was regulated by ABA. ATP-dependent helicases are major actors involved in various biological processes involving RNA, such as RNA splicing and decay as well as translation initiation (Nakamura et al., 2004). Zhang et al. (2014) reported that wheat RNA helicase 1 (*TaRH1*) may play a regulatory role during plant responses to both biotic and abiotic stresses.

4.3 Mycosubtilin primes genes associated with several metabolic pathways in wheat

In the priming modality at D5, we observed DEG patterns different from those detected in the elicitation ones at D2 and D5, with a number of DEGs drastically higher than in the other tested modalities, suggesting that mycosubtilin acts on wheat as a priming compound. This hypothesis is supported by the upregulation of the gene encoding for histone H1 WH1A.3 recorded at D2 in elicitation modality. Indeed, histone modifications are supposed to play a central role in priming memorization and transcription reprogramming after the stressing cue, corresponding here to mycosubtilin application (Lämke and Bäurle, 2017). Out of the 80 DEGs noticed in the priming modality, 26 are involved in stress responses (oxidative, pathogen and abiotic stresses). Among them, we observed significant downregulation of the expression of genes encoding for chitinases, glucan endo-1,3- beta glucosidase isoenzyme 1 and a germin-like protein. In addition, as observed in elicitation modalities, transcripts of *peroxidase* were also downregulated, suggesting that mycosubtilin may negatively regulate peroxidase-related defense mechanisms. On the other hand, mycosubtilin priming led to the overexpression of DEGs involved in responses to pathogens such as *harpin binding protein (HrBP1-1)*, a gene encoding a protein located in plant cell walls known to promote anti-pathogen responses and SAR in plants (Chen et al., 2012). We also found DEGs potentially

involved in carotenoids and ABA biosynthesis, such as *beta-carotene hydroxylase* and *lycopene β-cyclase* (Finkelstein, 2013). Remarkably, a significant number of DEGs described to play a part in ABA signaling and response pathways were regulated, such as genes encoding for ARK protein, aquaporins, aldose reductase, glutathione peroxidase-like protein GPX15Hv, nicotianamine synthase 3, chlorophyll a/b binding protein of LHCII type III chloroplast precursor, light-harvesting complex 1 and S-adenosylmethionine synthetase (Karuna Sree et al., 2000; Inoue et al., 2003; Finkelstein, 2013; Liu et al., 2013; Zhai et al., 2013; Kim et al., 2015; Saruhashi et al., 2015). The expression of some of these genes could potentially lead to significant protective activity in wheat. For instance, aquaporins (AQPs) are membrane proteins found in a large variety of organisms, mainly known for their role in water transport. As described by Tian et al. (2016), a member of AQP subfamily PIP1, AtPIP1;4, found in *Arabidopsis thaliana*, has been shown to play a central role in pathogen associated-molecular patterns (PAMPs)-triggered immunity (PTI) and SAR in the plant, by regulating H_2O_2 transport across the plasma membrane, from the apoplast to the cytoplasm, hence playing an active role in triggering H_2O_2-dependent host defenses. Another AQP, AtPIP1;2, has been reported to be involved in PTI and ABA-dependent stomatal closure in *A. thaliana* (Rodrigues et al., 2017). Additionally, genes involved in carbohydrate metabolism were over-transcribed in the priming modality. ABA has been described as primordial in the regulation of carbohydrate metabolism during plant stresses (Kempa et al., 2008). Another identified relevant DEG in the priming modality is *ABC1-family like*. Indeed, Wang et al. (2013) have recently reported that *TaAbc1* upregulation is associated with hypersensitive response against stripe rust in wheat. We also found an overexpression of DEGs involved in amino acid, protein, lipid and energy metabolism, that could be regulated by mycosubtilin to compensate the potential deleterious effect of *Z. tritici* infection on wheat metabolism. Finally, four DEGs associated with signaling, transcription and translation were upregulated in the priming modality, highlighting the significant broader amplitude of responses displayed in mycosubtilin-primed and infected wheat plants than in naïve infected plants.

4.4 Mycosubtilin did not elicit marked metabolite regulation but primes flavonoid accumulation in wheat leaves

Metabolomic analyses showed a substantially higher number of DAMs in the priming modality than in the elicitation ones, thus agreeing with transcriptomic findings. Indeed, only a few metabolites were regulated upon treatment with mycosubtilin in the elicitation modality, such as methyl jasmonate (MeJA) at D5. At D15, a flavonoid (tricin) was found under-accumulated, whereas four metabolites were detected in higher concentrations,

i.e glutamic acid, threonine as well as, remarkably, ABA glucose ester (ABA-Glc), and proline. Proline is an osmolyte amino acid involved in adaptation to abiotic stress, especially salt, osmotic, and drought stresses (Szabados and Savouré, 2010). Proline accumulation is supposed to be regulated by ABA (Finkelstein, 2013). Although the concentration of ABA and derivatives was not significantly regulated in treated wheat leaves, except at D15 for ABA-Glc, many DEGs and DAMs associated to ABA-dependent pathways were scored, suggesting that wheat responses to mycosubtilin may involve this hormone (both in elicitation and priming modalities). Whereas the role of ABA in plant tolerance to abiotic stress, such as drought, salinity, cold, and heavy metals has been extensively investigated, its effect on plant pathogen resistance remains unclear (Asselbergh et al., 2008; Vishwakarma et al., 2017). As reviewed by Lievens et al. (2017), a negative effect of this phytohormone on plant resistance has been reported for many pathosystems, such as tomato-*B. cinerea* and rice-*Magnaporthe oryzae*. In the rice-*M. grisea* pathosystem, ABA has been shown to compromise rice resistance against the pathogen by acting antagonistically towards SA-dependent pathway (Jiang et al., 2010). Some phytopathogens were even able to biosynthesize their own ABA, such as *B. cinerea* and *M. oryzae*, most likely to modulate host defenses and enhance their pathogenicity (Ding et al., 2015; Spence et al., 2015). However, in the later years, this phytohormone has also been described to display positive effects on plant resistance in other pathosystems, such as *A. thaliana-Pythium irregulare* and *Brassica napus-Leptosphaeria maculans* (Adie et al., 2007b; Kaliff et al., 2007). Two ABA-dependent modes of action on plant resistance against pathogens have been highlighted, including the regulation of stomatal closure to prevent pathogens from invading the plant, and callose deposition (Ton et al., 2009). In addition, ABA has also recently been proposed as a potential key actor in molecular cross-talks for plant-microbe symbiosis at the rhizosphere level (Stec et al., 2016). In the wheat-*Z. tritici* pathosystem, the role of ABA, as well as ethylene, in the host resistance mechanisms has, so far, been clearly overlooked. Hence, further investigations focusing on this phytohormone may provide new insights on its role in wheat resistance against *Z. tritici*.

In the priming modality at D5, only an under-accumulation of metabolites was observed, with patterns of amino acids and benzoxazinoids in opposition to those scored in the fungal effect modality at the same time point. This result suggests that mycosubtilin treatment (weakening the fungus pathogenicity) may reduce the expected fungal effect on benzoxazinoid and amino acid pathways in wheat, likely due (i) to its direct antifungal activity and/or (ii) to a countering by the plant of *Z. tritici* effect on these two pathways thanks to a compensatory mechanism. However, at D15, we observed significant changes in metabolite accumulation. The most remarkable result was clearly the increased accumulation of almost all targeted flavonoids, especially luteolin-derivatives (Figures 6, 7). Noticeably, at D5 in the priming modality, the genes encoding chalcone synthase 1 and 2, enzymes involved in

flavonoid biosynthesis, were significantly upregulated (Figure 7). Flavonoids are known to exhibit a range of biological activities in plant protection, not only antimicrobial activity but also strong antioxidant activity and cell-wall reinforcing (Lam et al., 2015; Lan et al., 2015; Al Aboody and Mickymaray, 2020). Accumulation of compounds displaying these three activities could be greatly beneficial for the host, especially just at the moment preceding the *Z. tritici* switch to necrotrophic phase. Indeed, at this time, *Z. tritici* growth increases, and the fungus produces toxins to induce wheat cell apoptosis, in order to feed on the released nutrients (Steinberg, 2015). Hence, cell-wall strengthening and the increase in antioxidant capacity may very likely help wheat mesophyll cells to resist to the pathogen attack. On the other hand, hydroxycinnamic acid amides (coumaroylputrescine, coumaroylcadaverine, and caffeoylputrescine) were significantly under-accumulated. The decrease in the concentration of these metabolites in wheat leaves may be linked with the hypotheses regarding mycosubtilin effect on plant metabolome during the priming modality emitted above (due to direct mycosubtilin antifungal effect and/or plant compensatory mechanism). Nevertheless, another reason would be the reorganization of metabolic pathways due to the mycosubtilin priming effect, as illustrated in Figure 7. Hence, during infection, flavonoid biosynthesis pathway would be enhanced to the detriment of the hydroxycinnamic acid amide pathway, leading to this differential accumulation in wheat leaves in the priming modalities. Interestingly, flavonoid biosynthesis can be induced by ABA, highlighting once again that ABA-dependent responses may be crucial to understand wheat responses to mycosubtilin (Gai et al., 2020).

In conclusion, this study provides new insights into the mechanisms underlying the bioactivity of the *B. subtilis* lipopeptide mycosubtilin on the wheat-*Z. tritici* pathosystem. This promising biomolecule likely confers protection to wheat through a dual activity, *i.e.* directly by displaying an antimicrobial activity against the fungus, and indirectly by priming the host defense responses. Taken together, these findings reveal that mycosubtilin acts on wheat as a priming agent, likely by involving ABA, and ETH biosynthesis and signaling pathways. Stimulation of the plant immune system by mycosubtilin probably results from the interaction of the biomolecule with the plasma membranes of leaf cells leading to the activation of abiotic stress-like responses in the plant. However, further investigations are required to unravel the precise mechanisms by which wheat leaf cells perceive mycosubtilin within the membranes.

Data availability statement

The datasets presented in this study can be found in online repositories. The names of the repository/repositories and accession number(s) can be found in the article/Supplementary Material.

Author contributions

All authors listed have made a substantial, direct, and intellectual contribution to the work and approved it for publication.

Funding

Conflict of interest

FC and PJ from the University of Lille and University of Liège, respectively, are the two co-founders of Lipofabrik company, which markets lipopeptides from *B. subtilis*.

The remaining authors declare that the research was conducted in the absence of any commercial or financial relationships that could be construed as a potential conflict of interest.

Publisher's note

All claims expressed in this article are solely those of the authors and do not necessarily represent those of their affiliated organizations, or those of the publisher, the editors and the reviewers. Any product that may be evaluated in this article, or claim that may be made by its manufacturer, is not guaranteed or endorsed by the publisher.

Supplementary material

The Supplementary Material for this article can be found online at: https://www.frontiersin.org/articles/10.3389/fpls.2022.1074447/full#supplementary-material

References

Adie, B., Chico, J. M., Rubio-Somoza, I., and Solano, R. (2007a). Modulation of plant defenses by ethylene. *J. Plant Growth Regul.* 26, 160–177. doi: 10.1007/s00344-007-0012-6

Adie, B. A. T., Pérez-Pérez, J., Pérez-Pérez, M. M., Godoy, M., Sánchez-Serrano, J.-J., Schmelz, E. A., et al. (2007b). ABA is an essential signal for plant resistance to pathogens affecting JA biosynthesis and the activation of defenses in arabidopsis. *Plant Cell* 19, 1665–1681. doi: 10.1105/tpc.106.048041

Al Aboody, M. S., and Mickymaray, S. (2020). Anti-fungal efficacy and mechanisms of flavonoids. *Antibiotics (Basel)* 9, 45. doi: 10.3390/antibiotics9020045

Ambawat, S., Sharma, P., Yadav, N. R., and Yadav, R. C. (2013). MYB transcription factor genes as regulators for plant responses: an overview. *Physiol. Mol. Biol. Plants* 19, 307–321. doi: 10.1007/s12298-013-0179-1

Asselbergh, B., De Vleesschauwer, D., and Höfte, M. (2008). Global switches and Fine-Tuning–ABA modulates plant pathogen defense. *MPMI* 21, 709–719. doi: 10.1094/MPMI-21-6-0709

Benjamini, Y., and Hochberg, Y. (1995). Controlling the false discovery rate: A practical and powerful approach to multiple testing. *J. R. Stat. Society Ser. B (Methodological)* 57, 289–300. doi: 10.1111/j.2517-6161.1995.tb02031.x

Biesaga-Kościelniak, J., Kościelniak, J., Filek, M., and Janeczko, A. (2008). Rapid production of wheat cell suspension cultures directly from immature embryos. *Plant Cell Tiss Organ Cult* 94, 139. doi: 10.1007/s11240-008-9397-6

Brown, J. K. M., Chartrain, L., Lasserre-Zuber, P., and Saintenac, C. (2015). Genetics of resistance to *Zymoseptoria tritici* and applications to wheat breeding. *Fungal Genet. Biol.* 79, 33–41. doi: 10.1016/j.fgb.2015.04.017

Bull, J., Mauch, F., Hertig, C., Rebmann, G., and Dudler, R. (1992). Sequence and expression of a wheat gene that encodes a novel protein associated with pathogen defense. *Mol. Plant Microbe Interact.* 5, 516–519. doi: 10.1094/mpmi-5-516

Caldo, R. A., Nettleton, D., and Wise, R. P. (2004). Interaction-dependent gene expression in mla-specified response to barley powdery mildew. *Plant Cell* 16, 2514–2528. doi: 10.1105/tpc.104.023382

Chandler, S., Van Hese, N., Coutte, F., Jacques, P., Höfte, M., and De Vleesschauwer, D. (2015). Role of cyclic lipopeptides produced by *Bacillus subtilis* in mounting induced immunity in rice (*Oryza sativa* l.). *Physiol. Mol. Plant Pathol.* 91, 20–30. doi: 10.1016/j.pmpp.2015.05.010

Chen, Z., Zeng, M., Song, B., Hou, C., Hu, D., Li, X., et al. (2012). Dufulin activates HrBP1 to produce antiviral responses in tobacco. *PLoS One* 7:e37944. doi: 10.1371/journal.pone.0037944

Chini, A., Fonseca, S., Chico, J. M., Fernández-Calvo, P., and Solano, R. (2009). The ZIM domain mediates homo- and heteromeric interactions between arabidopsis JAZ proteins. *Plant J.* 59, 77–87. doi: 10.1111/j.1365-313X.2009.03852.x

Chitarra, G. S., Breeuwer, P., Nout, M. J. R., van Aelst, A. C., Rombouts, F. M., and Abee, T. (2003). An antifungal compound produced by bacillus subtilis YM 10-20 inhibits germination of *Penicillium roqueforti* conidiospores. *J. Appl. Microbiol.* 94, 159–166. doi: 10.1046/j.1365-2672.2003.01819.x

Chowdhury, S. P., Uhl, J., Grosch, R., Alquéres, S., Pittroff, S., Dietel, K., et al. (2015). Cyclic lipopeptides of *Bacillus amyloliquefaciens* subsp. *plantarum* colonizing the lettuce rhizosphere enhance plant defense responses toward the bottom rot pathogen *Rhizoctonia solani*. *MPMI* 28, 984–995. doi: 10.1094/MPMI-03-15-0066-R

Christensen, A. B., Cho, B. H., Næsby, M., Gregersen, P. L., Brandt, J., Madriz-Ordeñana, K., et al. (2002). The molecular characterization of two barley proteins establishes the novel PR-17 family of pathogenesis-related proteins. *Mol. Plant Pathol.* 3, 135–144. doi: 10.1046/j.1364-3703.2002.00105.x

Conrath, U., Pieterse, C. M. J., and Mauch-Mani, B. (2002). Priming in plant–pathogen interactions. *Trends Plant Sci.* 7, 210–216. doi: 10.1002/ps.3348

Cools, H. J., and Fraaije, B.A. (2013). Update on mechanisms of azole resistance in Mycosphaerella graminicola and implications for future control. *Pest Manag. Sci.* 69, 150–155. doi: 10.1002/ps.3348

Coram, T. E., Settles, M. L., and Chen, X. (2008). Transcriptome analysis of high-temperature adult-plant resistance conditioned by Yr39 during the wheat–*Puccinia striiformis* f. sp. *tritici* interaction. *Mol. Plant Pathol.* 9, 479–493. doi: 10.1111/j.1364-3703.2008.00476.x

Couchoud, M., Der, C., Girodet, S., Vernoud, V., Prudent, M., and Leborgne-Castel, N. (2019). Drought stress stimulates endocytosis and modifies membrane lipid order of rhizodermal cells of *Medicago truncatula* in a genotype-dependent manner. *BMC Plant Biol.* 19, 221. doi: 10.1186/s12870-019-1814-y

Crouzet, J., Arguelles-Arias, A., Dhondt-Cordelier, S., Cordelier, S., Pršić, J., Hoff, G., et al. (2020). Biosurfactants in plant protection against diseases:

Rhamnolipids and lipopeptides case study. *Front. Bioeng Biotechnol.* 8. doi: 10.3389/fbioe.2020.01014

Cui, X.-Y., Du, Y.-T., Fu, J., Yu, T.-F., Wang, C.-T., Chen, M., et al. (2018). Wheat CBL-interacting protein kinase 23 positively regulates drought stress and ABA responses. *BMC Plant Biol.* 18, 93. doi: 10.1186/s12870-018-1306-5

D'aes, J., De Maeyer, K., Pauwelyn, E., and Höfte, M. (2010). Biosurfactants in plant-*Pseudomonas* interactions and their importance to biocontrol. *Environ. Microbiol. Rep.* 2, 359–372. doi: 10.1111/j.1758-2229.2009.00104.x

de Bruijn, W. J. C., Vincken, J.-P., Duran, K., and Gruppen, H. (2016). Mass spectrometric characterization of benzoxazinoid glycosides from rhizopus-elicited wheat (*Triticum aestivum*) seedlings. *J. Agric. Food Chem.* 64, 6267–6276. doi: 10.1021/acs.jafc.6b02889

Deravel, J., Lemière, S., Coutte, F., Krier, F., Van Hese, N., Béchet, M., et al. (2014). Mycosubtilin and surfactin are efficient, low ecotoxicity molecules for the biocontrol of lettuce downy mildew. *Appl. Microbiol. Biotechnol.* 98, 6255–6264. doi: 10.1007/s00253-014-5663-1

Desmyttere, H., Deweer, C., Muchembled, J., Sahmer, K., Jacquin, J., Coutte, F., et al. (2019). Antifungal activities of *Bacillus subtilis* lipopeptides to two *Venturia inaequalis* strains possessing different tebuconazole sensitivity. *Front. Microbiol.* 10. doi: 10.3389/fmicb.2019.02327

Ding, Z.-T., Zhang, Z., Luo, D., Zhou, J.-Y., Zhong, J., Yang, J., et al. (2015). Gene overexpression and RNA silencing tools for the genetic manipulation of the s-(+)-Abscisic acid producing ascomycete *Botrytis cinerea*. *Int. J. Mol. Sci.* 16, 10301–10323. doi: 10.3390/ijms160510301

Farace, G., Fernandez, O., Jacquens, L., Coutte, F., Krier, F., Jacques, P., et al. (2015). Cyclic lipopeptides from *Bacillus subtilis* activate distinct patterns of defence responses in grapevine. *Mol. Plant Pathol.* 16, 177–187. doi: 10.1111/mpp.12170

Finkelstein, R. (2013). Abscisic acid synthesis and response. *Arabidopsis book*, 1, 11:e0166. doi: 10.1199/tab.0166

Fiorilli, V., Vannini, C., Ortolani, F., Garcia-Seco, D., Chiapello, M., Novero, M., et al. (2018). Omics approaches revealed how arbuscular mycorrhizal symbiosis enhances yield and resistance to leaf pathogen in wheat. *Sci. Rep.* 8, 9625. doi: 10.1038/s41598-018-27622-8

Fones, H., and Gurr, S. (2015). The impact of septoria tritici blotch disease on wheat: An EU perspective. *Fungal Genet. Biol.* 79, 3–7. doi: 10.1016/j.fgb.2015.04.004

Gai, Z., Wang, Y., Ding, Y., Qian, W., Qiu, C., Xie, H., et al. (2020). Exogenous abscisic acid induces the lipid and flavonoid metabolism of tea plants under drought stress. *Sci. Rep.* 10, 12275. doi: 10.1038/s41598-020-69080-1

Gauthier, A., Trouvelot, S., Kelloniemi, J., Frettinger, P., Wendehenne, D., Daire, X., et al. (2014). The sulfated laminarin triggers a stress transcriptome before priming the SA- and ROS-dependent defenses during grapevine's induced resistance against *Plasmopara viticola*. *PloS One* 9, e88145. doi: 10.1371/journal.pone.0088145

Görlach, J., Volrath, S., Knauf-Beiter, G., Hengy, G., Beckhove, U., Kogel, K. H., et al. (1996). Benzothiadiazole, a novel class of inducers of systemic acquired resistance, activates gene expression and disease resistance in wheat. *Plant Cell* 8, 629–643. doi: 10.1105/tpc.8.4.629

Guitton, Y., Tremblay-Franco, M., Le Corguillé, G., Martin, J.-F., Pétéra, M., Roger-Mele, P., et al. (2017). Create, run, share, publish, and reference your LC-MS, FIA-MS, GC-MS, and NMR data analysis workflows with the Workflow4Metabolomics 3.0 galaxy online infrastructure for metabolomics. *Int. J. Biochem. Cell Biol.* 93, 89–101. doi: 10.1016/j.biocel.2017.07.002

Harmon, A. C., Gribskov, M., and Harper, J. F. (2000). CDPKs – a kinase for every Ca2+ signal? *Trends Plant Sci.* 5, 154–159. doi: 10.1016/S1360-1385(00)01577-6

Houben, M., and Van de Poel, B. (2019). 1-Aminocyclopropane-1-Carboxylic acid oxidase (ACO): The enzyme that makes the plant hormone ethylene. *Front. Plant Sci.* 10. doi: 10.3389/fpls.2019.00695

Inoue, H., Higuchi, K., Takahashi, M., Nakanishi, H., Mori, S., and Nishizawa, N. K. (2003). Three rice nicotianamine synthase genes, *OsNAS1*, *OsNAS2*, and *OsNAS3* are expressed in cells involved in long-distance transport of iron and differentially regulated by iron. *Plant J.* 36, 366–381. doi: 10.1046/j.1365-313X.2003.01878.x

Jiang, C.-J., Shimono, M., Sugano, S., Kojima, M., Yazawa, K., Yoshida, R., et al. (2010). Abscisic acid interacts antagonistically with salicylic acid signaling pathway in rice-*Magnaporthe grisea* interaction. *Mol. Plant Microbe Interact.* 23, 791–798. doi: 10.1094/MPMI-23-6-0791

Kaliff, M., Staal, J., Myrenås, M., and Dixelius, C. (2007). ABA is required for *Leptosphaeria maculans* resistance *via* ABI1- and ABI4-dependent signaling. *Mol. Plant Microbe Interact.* 20, 335–345. doi: 10.1094/MPMI-20-4-0335

Karuna Sree, B., Rajendrakumar, C. S. V., and Reddy, A. R. (2000). Aldose reductase in rice (*Oryza sativa* l.): stress response and developmental specificity. *Plant Sci.* 160, 149–157. doi: 10.1016/s0168-9452(00)00376-9

Kempa, S., Krasensky, J., Santo, S. D., Kopka, J., and Jonak, C. (2008). A central role of abscisic acid in stress-regulated carbohydrate metabolism. *PLoS One* 3, e3935. doi: 10.1371/journal.pone.0003935

Kettles, G. J., and Kanyuka, K. (2016). Dissecting the molecular interactions between wheat and the fungal pathogen *Zymoseptoria tritici*. *Front. Plant Sci.* 7. doi: 10.3389/fpls.2016.00508

Kim, S. H., Kim, S. H., Palaniyandi, S. A., Yang, S. H., and Suh, J.-W. (2015). Expression of potato s-adenosyl-L-methionine synthase (*SbSAMS*) gene altered developmental characteristics and stress responses in transgenic *Arabidopsis* plants. *Plant Physiol. Biochem.* 87, 84–91. doi: 10.1016/j.plaphy.2014.12.020

Kourmentza, K., Gromada, X., Michael, N., Degraeve, C., Vanier, G., Ravallec, R., et al. (2021). Antimicrobial activity of lipopeptide biosurfactants against foodborne pathogen and food spoilage microorganisms and their cytotoxicity. *Front. Microbiol.* 11. doi: 10.3389/fmicb.2020.561060

Lämke, J., and Bäurle, I. (2017). Epigenetic and chromatin-based mechanisms in environmental stress adaptation and stress memory in plants. *Genome Biol.* 18, 124. doi: 10.1186/s13059-017-1263-6

Lam, P. Y., Liu, H., and Lo, C. (2015). Completion of tricin biosynthesis pathway in rice: Cytochrome P450 75B4 is a unique chrysoeriol 5'-hydroxylase. *Plant Physiol.* 168, 1527–1536. doi: 10.1104/pp.15.00566

Lan, W., Lu, F., Regner, M., Zhu, Y., Rencoret, J., Ralph, S. A., et al. (2015). Tricin, a flavonoid monomer in monocot lignification. *Plant Physiol.* 167, 1284–1295. doi: 10.1104/pp.114.253757

Le Mire, G., Siah, A., Brisset, M.-N., Gaucher, M., Deleu, M., and Jijakli, M. H. (2018). Surfactin protects wheat against *Zymoseptoria tritici* and activates both salicylic acid- and jasmonic acid-dependent defense responses. *Agriculture* 8, 11. doi: 10.3390/agriculture8010011

Lievens, L., Pollier, J., Goossens, A., Beyaert, R., and Staal, J. (2017). Abscisic acid as pathogen effector and immune regulator. *Front. Plant Sci.* 8. doi: 10.3389/fpls.2017.00587

Liu, R., Xu, Y.-H., Jiang, S.-C., Lu, K., Lu, Y.-F., Feng, X.-J., et al. (2013). Light-harvesting chlorophyll a/b-binding proteins, positively involved in abscisic acid signalling, require a transcription repressor, WRKY40, to balance their function. *J. Exp. Bot.* 64, 5443–5456. doi: 10.1093/jxb/ert307

Li, Z., Zhao, C., Zhao, X., Xia, Y., Sun, X., Xie, W., et al. (2018). Deep annotation of hydroxycinnamic acid amides in plants based on ultra-High-Performance liquid chromatography–High-Resolution mass spectrometry and its in silico database. *Anal. Chem.* 90, 14321–14330. doi: 10.1021/acs.analchem.8b03654

McDonald, M. C., Renkin, M., Spackman, M., Orchard, B., Croll, D., Solomon, P. S., et al. (2019). Rapid parallel evolution of azole fungicide resistance in Australian populations of the wheat pathogen *Zymoseptoria tritici*. *Appl. Environ. Microbiol.* 85, e01908–18. doi: 10.1128/AEM.01908-18

Mejri, S., Siah, A., Coutte, F., Magnin-Robert, M., Randoux, B., Tisserant, B., et al. (2018). Biocontrol of the wheat pathogen *Zymoseptoria tritici* using cyclic lipopeptides from *Bacillus subtilis*. *Environ. Sci. pollut. Res. Int.* 25, 29822–29833. doi: 10.1007/s11356-017-9241-9

Mihalache, G., Balaes, T., Gostin, I., Stefan, M., Coutte, F., and Krier, F. (2018). Lipopeptides produced by *Bacillus subtilis* as new biocontrol products against fusariosis in ornamental plants. *Environ. Sci. pollut. Res.* 25, 29784–29793. doi: 10.1007/s11356-017-9162-7

Mindrebo, J. T., Nartey, C. M., Seto, Y., Burkart, M. D., and Noel, J. P. (2016). Unveiling the functional diversity of the alpha-beta hydrolase fold in plants. *Curr. Opin. Struct. Biol.* 41, 233–246. doi: 10.1016/j.sbi.2016.08.005

Nakamura, T., Muramoto, Y., Yokota, S., Ueda, A., and Takabe, T. (2004). Structural and transcriptional characterization of a salt-responsive gene encoding putative ATP-dependent RNA helicase in barley. *Plant Sci.* 167, 63–70. doi: 10.1016/j.plantsci.2004.03.001

Nasir, M. N., and Besson, F. (2012). Interactions of the antifungal mycosubtilin with ergosterol-containing interfacial monolayers. *Biochim. Biophys. Acta (BBA) - Biomembranes* 1818, 1302–1308. doi: 10.1016/j.bbamem.2012.01.020

Nasir, M. N., Thawani, A., Kouzayha, A., and Besson, F. (2010). Interactions of the natural antimicrobial mycosubtilin with phospholipid membrane models. *Colloids Surf B Biointerfaces* 78, 17–23. doi: 10.1016/j.colsurfb.2010.01.034

Niu, Y., and Xiang, Y. (2018). An overview of biomembrane functions in plant responses to high-temperature stress. *Front. Plant Sci.* 9. doi: 10.3389/fpls.2018.00915

Ongena, M., and Jacques, P. (2008). *Bacillus* lipopeptides: versatile weapons for plant disease biocontrol. *Trends Microbiol.* 16, 115–125. doi: 10.1016/j.tim.2007.12.009

Paré, P. W., Farag, M. A., Krishnamachari, V., Zhang, H., Ryu, C.-M., and Kloepper, J. W. (2005). Elicitors and priming agents initiate plant defense responses. *Photosynth Res.* 85, 149–159. doi: 10.1007/s11120-005-1001-x

Pérez-García, A., Romero, D., and de Vicente, A. (2011). Plant protection and growth stimulation by microorganisms: biotechnological applications of bacilli in agriculture. *Curr. Opin. Biotechnol.* 22, 187–193. doi: 10.1016/j.copbio.2010.12.003

Platel, R., Chaveriat, L., Le Guenic, S., Pipeleers, R., Magnin-Robert, M., Randoux, B., et al. (2021). Importance of the C12 carbon chain in the biological activity of rhamnolipids conferring protection in wheat against *Zymoseptoria tritici*. *Molecules* 26, 40. doi: 10.3390/molecules26010040

Qi, G., Zhu, F., Du, P., Yang, X., Qiu, D., Yu, Z., et al. (2010). Lipopeptide induces apoptosis in fungal cells by a mitochondria-dependent pathway. *Peptides* 31, 1978–1986. doi: 10.1016/j.peptides.2010.08.003

Raaijmakers, J. M., De Bruijn, I., Nybroe, O., and Ongena, M. (2010). Natural functions of lipopeptides from *Bacillus* and *Pseudomonas*: more than surfactants and antibiotics. *FEMS Microbiol. Rev.* 34, 1037–1062. doi: 10.1111/j.1574-6976.2010.00221.x

Rodrigues, O., Reshetnyak, G., Grondin, A., Saijo, Y., Leonhardt, N., Maurel, C., et al. (2017). Aquaporins facilitate hydrogen peroxide entry into guard cells to mediate ABA- and pathogen-triggered stomatal closure. *PNAS* 114, 9200–9205. doi: 10.1073/pnas.1704754114

Ruan, J., Zhou, Y., Zhou, M., Yan, J., Khurshid, M., Weng, W., et al. (2019). Jasmonic acid signaling pathway in plants. *Int. J. Mol. Sci.* 20, 2479. doi: 10.3390/ijms20102479

Rudd, J. J., Kanyuka, K., Hassani-Pak, K., Derbyshire, M., Andongabo, A., Devonshire, J., et al. (2015). Transcriptome and metabolite profiling of the infection cycle of *Zymoseptoria tritici* on wheat reveals a biphasic interaction with plant immunity involving differential pathogen chromosomal contributions and a variation on the hemibiotrophic lifestyle Definition1[OPEN]. *Plant Physiol.* 167, 1158–1185. doi: 10.1104/pp.114.255927

Sachdev, D. P., and Cameotra, S. S. (2013). Biosurfactants in agriculture. *Appl. Microbiol. Biotechnol.* 97, 1005–1016. doi: 10.1007/s00253-012-4641-8

Saruhashi, M., Kumar Ghosh, T., Arai, K., Ishizaki, Y., Hagiwara, K., Komatsu, K., et al. (2015). Plant raf-like kinase integrates abscisic acid and hyperosmotic stress signaling upstream of SNF1-related protein kinase2. *Proc. Natl. Acad. Sci. U.S.A.* 112, E6388–E6396. doi: 10.1073/pnas.1511238112

Savary, S., Willocquet, L., Pethybridge, S. J., Esker, P., McRoberts, N., and Nelson, A. (2019). The global burden of pathogens and pests on major food crops. *Nat. Ecol. Evol.* 3, 430–439. doi: 10.1038/s41559-018-0793-y

Schellenberger, R., Touchard, M., Clément, C., Baillieul, F., Cordelier, S., Crouzet, J., et al. (2019). Apoplastic invasion patterns triggering plant immunity: plasma membrane sensing at the frontline. *Mol. Plant Pathol.* 20, 1602–1616. doi: 10.1111/mpp.12857

Seybold, H., Demetrowitsch, T. J., Hassani, M. A., Szymczak, S., Reim, E., Haueisen, J., et al. (2020). A fungal pathogen induces systemic susceptibility and systemic shifts in wheat metabolome and microbiome composition. *Nat. Commun.* 11, 1910. doi: 10.1038/s41467-020-15633-x

Shekhar, S., Sundaramanickam, A., and Balasubramanian, T. (2015). Biosurfactant producing microbes and their potential applications: A review. *Crit. Rev. Environ. Sci. Technol.* 45, 1522–1554. doi: 10.1080/10643389.2014.955631

Siah, A., Deweer, C., Duyme, F., Sanssené, J., Durand, R., Halama, P., et al. (2010a). Correlation of *in planta* endo-beta-1,4-xylanase activity with the necrotrophic phase of the hemibiotrophic fungus *Mycosphaerella graminicola*. *Plant Pathol.* 59, 661–670. doi: 10.1111/j.1365-3059.2010.02303.x

Siah, A., Deweer, C., Morand, E., Reignault, Ph., and Halama, P. (2010b). Azoxystrobin resistance of French mycosphaerella graminicola strains assessed by four *in vitro* bioassays and by screening of G143A substitution. *Crop Prot.* 29, 737–743. doi: 10.1016/j.cropro.2010.02.012

Spence, C. A., Lakshmanan, V., Donofrio, N., and Bais, H. P. (2015). Crucial roles of abscisic acid biogenesis in virulence of rice blast fungus *Magnaporthe oryzae*. *Front. Plant Sci.* 6. doi: 10.3389/fpls.2015.01082

Stec, N., Banasiak, J., and Jasiński, M. (2016). Abscisic acid - an overlooked player in plant-microbe symbioses formation? *Acta Biochim. Pol.* 63, 53–58. doi: 10.18388/abp.2015_1210

Steinberg, G. (2015). Cell biology of *Zymoseptoria tritici*: Pathogen cell organization and wheat infection. *Fungal Genet. Biol.* 79, 17–23. doi: 10.1016/j.fgb.2015.04.002

Sun, H., Chen, L., Li, J., Hu, M., Ullah, A., He, X., et al. (2017). The JASMONATE ZIM-domain gene family mediates JA signaling and stress response in cotton. *Plant Cell Physiol.* 58, 2139–2154. doi: 10.1093/pcp/pcx148

Szabados, L., and Savouré, A. (2010). Proline: a multifunctional amino acid. *Trends Plant Sci.* 15, 89–97. doi: 10.1016/j.tplants.2009.11.009

Tian, S., Wang, X., Li, P., Wang, H., Ji, H., Xie, J., et al. (2016). Plant aquaporin AtPIP1;4 links apoplastic H2O2 induction to disease immunity pathways. *Plant Physiol.* 171, 1635–1650. doi: 10.1104/pp.15.01237

Ton, J., Flors, V., and Mauch-Mani, B. (2009). The multifaceted role of ABA in disease resistance. *Trends Plant Sci.* 14, 310–317. doi: 10.1016/j.tplants.2009.03.006

Torriani, S. F. F., Melichar, J. P. E., Mills, C., Pain, N., Sierotzki, H., and Courbot, M. (2015). *Zymoseptoria tritici*: A major threat to wheat production, integrated approaches to control. *Fungal Genet. Biol.* 79, 8–12. doi: 10.1016/j.fgb.2015.04.010

Vishwakarma, K., Upadhyay, N., Kumar, N., Yadav, G., Singh, J., Mishra, R. K., et al. (2017). Abscisic acid signaling and abiotic stress tolerance in plants: A review on current knowledge and future prospects. *Front. Plant Sci.* 8. doi: 10.3389/fpls.2017.00161

Wang, X., Wang, X., Duan, Y., Yin, S., Zhang, H., Huang, L., et al. (2013). *TaAbc1*, a member of Abc1-like family involved in hypersensitive response against the stripe rust fungal pathogen in wheat. *PLoS One* 8, e58969. doi: 10.1371/journal.pone.0058969

Wojakowska, A., Perkowski, J., Góral, T., and Stobiecki, M. (2013). Structural characterization of flavonoid glycosides from leaves of wheat (*Triticum aestivum* l.) using LC/MS/MS profiling of the target compounds. *J. Mass Spectrometry* 48, 329–339. doi: 10.1002/jms.3160

Yang, A., Dai, X., and Zhang, W.-H. (2012). A R2R3-type MYB gene, *OsMYB2*, is involved in salt, cold, and dehydration tolerance in rice. *J. Exp. Bot.* 63, 2541–2556. doi: 10.1093/jxb/err431

Yang, N., McDonald, M. C., Solomon, P. S., and Milgate, A. W. (2018). Genetic mapping of Stb19, a new resistance gene to *Zymoseptoria tritici* in wheat. *Theor. Appl. Genet.* 131, 2765–2773. doi: 10.1007/s00122-018-3189-0

Zhai, C.-Z., Zhao, L., Yin, L.-J., Chen, M., Wang, Q.-Y., Li, L.-C., et al. (2013). Two wheat glutathione peroxidase genes whose products are located in chloroplasts improve salt and H2O2 tolerances in arabidopsis. *PloS One* 8, e73989. doi: 10.1371/journal.pone.0073989

Zhang, X., Zhao, X., Feng, C., Liu, N., Feng, H., Wang, X., et al. (2014). The cloning and characterization of a DEAD-box RNA helicase from stress-responsive wheat. *Physiol. Mol. Plant Pathol.* 88, 36–42. doi: 10.1016/j.pmpp.2014.07.004

Zheng, Y., Chen, X., Wang, P., Sun, Y., Yue, C., and Ye, N. (2020). Genome-wide and expression pattern analysis of JAZ family involved in stress responses and postharvest processing treatments in *Camellia sinensis*. *Sci. Rep.* 10, 2792. doi: 10.1038/s41598-020-59675-z

Managing spot blotch disease in wheat: Conventional to molecular aspects

Chandan Roy[1], Xinyao He[2], Navin C. Gahtyari[3],
Sunita Mahapatra[4] and Pawan K. Singh[2]*

[1]Department of Genetics and Plant Breeding, Agriculture University, Jodhpur, Rajasthan, India, [2]Global Wheat Program, International Maize and Wheat Improvement Center (CIMMYT), Mexico DF, Mexico, [3]Crop Improvement Division, ICAR−Vivekanand Parvatiya Krishi Anushandhan Sansthan, Almora, Uttarakhand, India, [4]Department of Plant Pathology, Bidhan Chandra Krishi Viswavidyalaya, Mohanpur, West Bengal, India

Spot blotch (SB) caused by *Bipolaris sorokiniana* (teleomorph *Cochliobolus sativus*) is one of the devastating diseases of wheat in the warm and humid growing areas around the world. *B. sorokiniana* can infect leaves, stem, roots, rachis and seeds, and is able to produce toxins like helminthosporol and sorokinianin. No wheat variety is immune to SB; hence, an integrated disease management strategy is indispensable in disease prone areas. A range of fungicides, especially the triazole group, have shown good effects in reducing the disease, and crop-rotation, tillage and early sowing are among the favorable cultural management methods. Resistance is mostly quantitative, being governed by QTLs with minor effects, mapped on all the wheat chromosomes. Only four QTLs with major effects have been designated as *Sb1* through *Sb4*. Despite, marker assisted breeding for SB resistance in wheat is scarce. Better understanding of wheat genome assemblies, functional genomics and cloning of resistance genes will further accelerate breeding for SB resistance in wheat.

KEYWORDS

Bipolaris sorokiniana, disease management, resistance breeding, spot blotch, wheat

Introduction

Spot blotch (SB) caused by the hemibiotrophic fungus *Bipolaris sorokiniana* (teleomorph *Cochliobolus sativus*) syn. *Drechslera sorokiniana*, syn. *Helminthosporium sativum* is the most devastating disease of wheat grown in warm and humid areas. In Eastern Gangetic Plains (EGP) of India, Bangladesh and Nepal, *B. sorokiniana* appears in a complex with *Pyrenophora tritici-repentis* (Died.) Drechs. (anamorph *Drechslera tritici-repentis* (Died.) Shoemaker) responsible for tan spot (TS) and is commonly known as Helminthosporium leaf blight (HLB) (Duveiller et al., 2005). Occurrence of SB is more frequent in the humid and warmer wheat growing areas of South Asia (SA), Latin America and Africa (He et al., 2022) (Figure 1). Globally, the disease appears in approximately 25-million-hectare (mha) areas, out of which 10 mha areas are present in EGP. Besides, wheat grown under subtropical lowland of Bolivia, Brazil and Argentina in Latin America, Tanzania, rainfed areas of Zambia

FIGURE 1
Worldwide distribution of spot blotch of wheat caused by *Bipolaris sorokiniana*.
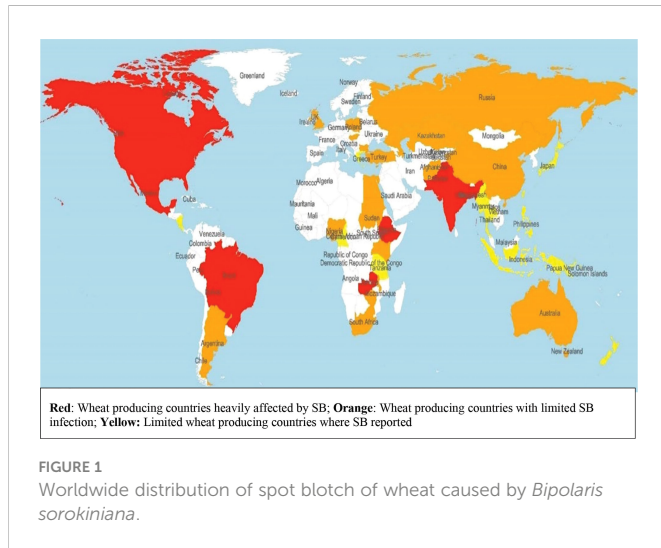
and Madagascar in Africa provides congenial environments for SB (van Ginkel and Rajaram, 1998). Under favorable conditions, the disease may cause yield loss of above 50% (Sharma and Duveiller, 2004), with an average yield loss of 15-20% in SA, and yield loss in the farmer's field reported up to 16% in Nepal and 15% in Bangladesh (Villareal et al., 1995; Saari, 1998; Duveiller, 2002).

B. sorokiniana causes a typical symptom of light brown colored lesions of oval or oblong to elliptical shape on leaves, sheath, nodes or glume of its host plants. Size of the lesion gradually increases, then partial to whole leaf may become chlorotic, turning brown and drying up (Figure 2). The pathogen transmits through infected seeds, stubbles and soil, and secondary infection may take place through air. Other than SB, *B. sorokiniana* is also responsible for seedling blight, common root rot, head blight and black point in wheat (Al-Sadi, 2021). No positive association was found among spot blotch, root rot and black point in wheat, indicating that different mechanisms of host resistance exist in different plant parts (Conner, 1990). Cross infection between different species is rarely reported; one such example is isolates collected from wheat root were able to infect barley (Valjavec-Gratian and Steffenson, 1997). A number of articles have been published pertaining to pathogen biology, disease management, breeding and molecular aspects, including genome sequence of *B. sorokiniana*, gene/QTL mapping, marker-assisted selection (MAS) and genomic selection. The present

FIGURE 2
Lesions of spot blotch on infected leaves and plants.

work aims to summarize the most important findings, especially those reported in recent years, in the area of SB management in wheat.

Pathogen biology

The pathogen produces olive brown mycelia and light grayish colonies on potato dextrose agar (PDA) medium at early stage, which turns into black at later stage. Conidia are brown colored, elliptical, straight or curved multiple celled with 3-9 septa tapering at the ends, measuring $10\text{-}28 \times 40\text{-}120$ μm (Acharya et al., 2011). Variability under natural conditions among the *B. sorokiniana* isolates is sufficiently high (Sultana et al., 2018). *Bipolaris sorokiniana* is the asexual stage of the pathogen, which multiplies mostly through conidia. Its sexual stage has not been reported in natural conditions except in Zambia, due to a lack of sexual compatibility between the opposite mating (A, a) types. Under controlled conditions, sexual spores of *B. sorokiniana* were isolated from barley (Zhong and Steffenson, 2001) and recently from wheat in Bangladesh (Sultana et al., 2018).

The fungus can produce toxins like helminthosporol and hydrolytic enzymes that trigger pathogenesis. Prehelminthosporium is the most abundant and active compound produced by *B. sorokiniana*, which damages membrane permeability and affects mitochondrial oxidative phosphorylation and chloroplast photophosphorylation (Kumar et al., 2002). A necrotrophic effector gene *ToxA* interacts with the susceptibility gene *Tsn1* in wheat to initiate disease development (McDonald et al., 2017). *ToxA* was initially identified in *P. tritici-repentis* and then in *Parastagonospora nodorum*, but molecular evidence indicated that the gene in the former was acquired from the latter through horizontal gene transfer (Friesen et al., 2006). *ToxA* was found in *B. sorokiniana* populations from Australia (McDonald et al., 2017), USA (Friesen et al., 2018), India (Navathe et al., 2019b) and Mexico (Wu et al., 2020), with various occurrence frequencies, from 10.2% in Mexico to 86.7% in USA.

Molecular markers may be useful to detect the pathogen on wheat plants before the appearance of visible symptoms, as well as on alternative hosts and volunteer plants. A sequence characterized amplified region (SCAR) marker SCARBS$_{600}$ was developed to diagnose *B. sorokiniana* (Aggarwal et al., 2011). Alternatively, DNA sequence of ribosomal internal transcribe spacer (ITS), β-tubulin gene and translational elongation factor 1-α (EF-1α) can also be used to diagnose this pathogen, as did in a study to detect *B. sorokiniana* in volunteer plants in China (Sun et al., 2015). Using universal rice primers (URP), Aggarwal et al. (2010) successfully grouped 40 *B. sorokiniana* isolates from different geographical origins of India. High level of genetic diversity among the isolates from Brazil and Mexico was reported using UPR markers (Mann et al., 2014).

Draft genome sequences of eight virulent accessions of *B. sorokiniana* from India, Australia, USA and China are currently available (https://www.ncbi.nlm.nih.gov/data-hub/genome/?taxon=45130). A highly virulent isolate BS_112 (GenBank accession number KU201275) from India has a genome size of 35.64 Mb and 10,460 genes were predicted with an average gene length of 435-545 bp and gene density of 250-300 genes/Mb (Aggarwal et al., 2019). A phylogenetic analysis was carried out among 254 isolates of *B. sorokiniana* with global origin using gene sequences of ITS, TEF-1

and GAPDH, and the results indicated the presence of a broad and geographically undifferentiated global population (Sharma et al., 2022).

Biochemical and molecular events associated with SB infection

Bipolaris sorokiniana initially has a biotrophic phase represented by the epidermal invasion and fungal hyphal growth, followed by the necrotrophic phase in the mesophyll cells (Kumar et al., 2002). The germinating conidia penetrates the cuticle and epidermis of wheat plant with the help of an appressorium at its germinating tube, getting entered mostly through the anticlinal cell walls. The levels of sesquiterpene molecule 'prehelminthosporol' increases in the extracellular matrix of the cell at the site of apposition, helping pathogen to intrude further into the cell (Jansson and Akesson, 2003).

The first toxin compound known to confer virulence to *B. sorokiniana* was named 'Victoxinin' and the second one was 'sorokinianin'. Another toxin isolated and characterized was 'bipolaroxin', which was again structurally a sesquiterpene and had a role in pathogenicity and host selectivity (Jahani, 2005). Helminthosporol was found to enhance the susceptibility of genotypes like Sonalika and CIANO T79. However, it is important to note that helminthosporol and its derivatives are not solely responsible for deciding the susceptibility of a genotype. A multitude of other factors like cell wall apposition, cuticle thickness, leaf anatomy, pathogen specificity, host defense responses etc., are also involved in the pathosystem, making both resistance/susceptibility of the host and virulence/avirulence of the pathogen (Ibeagha et al., 2005; Jahani et al., 2014).

For initial invasion, *B. sorokiniana* produces various cell wall degrading enzymes like glucosidase, cellulases, pectinases, xylanase. Endopolygalacturonase (EPG) loosens the cell wall by cleaving α-(1→4) linkages of the homogalacturonan, an important constituent of the middle lamella of the cell wall (Ridley et al., 2001; Janni et al., 2008). To protect the host cell from EPG, plant cell produces polygalacturonase inhibiting protein (PGIP), which elicits the defense response of a plant by accumulating oligogalacturonides (Ridley et al., 2001). PGIPs have a proven role against the fungal colonization in many dicot species as well as wheat plant against *Bipolaris* (Kemp et al., 2003).

Epidemiology and host range

Generally, temperature between 16-32°C enables SB development (Acharya et al., 2011), and in Indian subcontinent, the disease predominantly spread when temperature exceeds 26°C as it favors heavy sporulation (Chaurasia et al., 2000). Teleomorph develops in a range of 16-24°C with the optimum temperature of 20°C and can survive up to seven months under natural conditions in Zambia; while the anamorph can survive sufficiently large range of temperature from 4-36°C (Duveiller and Sharma, 2009). High temperature and high relative humidity enhance disease severity, SB outbreak in Brazil occurred when the leaves remain wet for >18 hrs in a day with a mean temperature of >18°C (Reis, 1991). In EGP, leaf

wetness period >12hrs due to rainfall or dew coinciding with high temperature and humidity are believed to favor the onset of infection (Duveiller et al., 2005). In addition, delayed sowing of wheat due to the rice-wheat cropping system causes yield loss due to terminal heat stress (Hasan et al., 2021; Narendra et al., 2021); besides, high residual soil moisture and increased duration of leaf wetness due to foggy weather can also increase the disease severity (Duveiller, 2004; Duveiller et al., 2005). The waterlogged condition due to flooding in the Ganges belt sharply declines the conidia viability, and *B. sorokiniana* conidia isolated from soil after August, the monsoon month with high rainfall, becomes non-pathogenic (Pandey et al., 2005). This in turn implies that seeds might be the main source of inoculum in EGP.

SB is a polycyclic disease with the initial sources of inoculum being contaminated seeds, infected soil, straw, volunteer plants and secondary hosts. *B. sorokiniana* has a large host range, and more than 65 graminaceous hosts have been identified in China (Chang and Wu, 1998). Among the cereals, hexaploid wheat and barley are most common hosts, along with durum and emmer wheat, triticale, oats, rice, rye, maize, pearl millet, foxtail millet and several grass species like *Phalaris minor*, *Agropyron pectinatum*, *A. repens*, *Festuca* spp. (Gupta et al., 2017). A list of plant species that harbors *B. sorokiniana* is given in Table 1. The three most common species, *Setaria glauca*, *Echinochloa colonum* and *Pennisetum typhoids* act as a natural harbor of *B. sorokiniana* in EGP (Pandey et al., 2005). In rice-wheat cropping system, rice plants may serve as a host for the pathogen (Acharya et al., 2011); but in eastern India the source of primary inoculum is still debatable, with infected seeds and weeds being the most probable inoculum sources (Neupane et al., 2010).

Disease management strategies

Management of SB through resistant varieties is the most economical and environment-friendly approach, which, however, is compromised by a lack of highly resistant varieties. Under this circumstance, cultivation of resistant varieties may be supplemented with other strategies like adjusting sowing time and fungicides application to reduce the SB severity in disease prone areas. Details of these strategies are described below.

Chemical control

Seed treatment is always useful to avoid the introduction of additional inoculum. Seed treatment with carboxin or thiram can effectively reduce the load of primary inoculum, especially for seeds with more than 20% infection rate (Mehta et al., 1992). However, seed treatment alone cannot guarantee low spot blotch infection in field (Singh et al., 2014) and foliar fungicidal application is often indispensable. Triazole fungicides like propiconazole, tebuconazole, flutriafol, iprodione, prochloraz, and triadimenol are effective in SB management, e.g., application of Opus (epoxiconazole) significantly reduced the disease severity and maintained it below 10% (Sharma and Duveiller, 2006). In addition, application of Carbendazim and Azoxystrobin has also shown efficacy in controlling the disease (Navathe et al., 2019a). Applying both seed treatment and foliar

TABLE 1   Host species of *B. sorokiniana* (Modified from Manamgoda et al., 2014).

Family	Species group	Species
Poaceae	Cultivated species	*Triticum aestivum, T. durum, Hordeum vulgare, Secale cereale, Tribulus terrestris, Zea mays, Oryza sativa, Eleusine coracana*
	Wild species and grasses	*Aegilops cylindrica, Agropyron buonapartis, A. ciliare, A. cristatum, A. distichum, A. repens, A. trachycaulum var. trachycaulum, A. trachycaulum var. unilaterale, Agrostis capillaries, A. gigantea, A. palustris, Agrostis sp., A. stolonifera var. palustris, Alopecurus pratensis, Aneurolepidium chinense, Arrhenatherum elatius, Avena byzantina, A. sativa, Brachiaria plantaginea, Bromus inermis, B. japonicus, B. marginatus, B. uniloides, B. willdenowii, Buchloe dactyloides, Chloris virgata, Cynodon dactylon, C. transvaalensis, Dactylis glomerata, Dendrobium sp., Digitaria sanguinalis, Echinochloa crusgalli, Ehrharta calycina, E. indica, Elymus breviaristatus, E. canadensis, E. riparius, E. sibiricus, E. trachycaulus, E. virginicus, Elytrigia intermedia, E. repens, Eragrostis cilianensis, Festuca arundinacea, F. ovina, F. pratensis, F. rubra, Holcus lanatus, Hordeum brevisubulatum, H. jubatum, H. leporinum, H. murinum, H. sativum, Hystrix patula, Leymus angustus, L. cinereus, Lolium multiflorum, L. perenne, Microlaena stipoides, Microstegium vimineum, Miscanthus sinensis var. zebrinus, Panicum dichotomiflorum, P. lacromanianum, P. virgatum, Paspalum notatum, Pennisetum clandestinum, Phalaris arundinacea, P. canariensis, Phleum pratense, Phleum sp., Poa annua, P. pratensis, P. sylvestris, P. trivialis, Psathyrostachys juncea, Roegneria hirsuta, Saccharum sp., Secale montanum, Setaria viridis, Sporobolus vaginiflorus, Stenotaphrum secundatum, Tribulus terrestris, T. secale, Triticum sp., T. sphaerococcum, T. vulgare, Zizania aquatica, Z. palustris*
Non-poaceae	-	*Allium sp., Helianthus annuus, Calluna vulgaris* (Alliaceae), *Taraxacumkok-saghyz* (Compositae), (Ericaceae), *Cicer arietinum, Lablab purpureus, Medicago sativa, Phaseolus vulgaris* (Fabaceae), *Linum usitatissimum* (Linaceae), *Lythrum salicaria* (Lythraceae) *Broussonetia papyrifera* (Moraceae), *Fagopyrum esculentum* (Polygonaceae), *Amaranthus viridis, Glycine max.*

spray can further reduce the disease, especially when the latter is conducted twice, e.g., upon the appearance of initial infection symptom and 10-20 days later (Singh et al., 2014; Navathe et al., 2019a). Systemic fungicides are more effective than contact fungicides, but the recommended dose should be strictly followed to avoid the emergence of resistant pathotypes against fungicides.

Despite its effectiveness in SB management, fungicidal application increases the cost of cultivation and brings environmental hazardousness. An estimated cost of 153.5 million AUD including application cost is required for fungicides to control wheat diseases in Australia (Murray and Brennan, 2009). Besides, excessive use of systemic fungicides may lead to changes in pathogenic virulence and development of resistance against fungicides. Fungicide resistance has been reported for leaf blight related pathogens *P. tritici-repentis* causing tan spot (Sautua and Carmona, 2021). This is due to the directional selection on pathogen population for resistant pathotypes.

Poor nutrient management is reported to be associated with higher SB infection (Sharma and Duveiller, 2004). Appropriate nitrogen application reduces SB infection, and balanced application of nitrogen along with phosphorus and potassium can further reduce SB severity (Sharma et al., 2006a). Exogenous use of silicon significantly reduces SB severity by increasing the incubation period of the pathogen in wheat (Domiciano et al., 2010). Similarly, application of silver nanoparticles significantly reduced SB infection in wheat, with the induced lignin deposition in vascular bundles (Mishra et al., 2014).

Cultural practices

Crop rotation is an effective practice for minimizing the primary inoculum load of *B. sorokiniana* in wheat, and the rotation systems of wheat-rice, wheat-oat, wheat-sunflower, and wheat-soybean may be adopted instead of wheat monoculture. Crop rotation provides time to decompose the infected stubble in the field, which helps in improving soil health. Crop residue burning reduces inoculum load up to 90%; but is associated with environmental hazardousness. Alternatively, tillage can be adopted to minimize the load of

primary inoculum from the infected stubble. But this may delay the sowing of wheat crop particularly in rice-wheat cropping system, exposing wheat to SB conducive conditions. Zero tillage, minimum tillage or use of happy seeder are alternatives to traditional tillage practices in rice-wheat cropping system (Acharya et al., 2011). Zero tillage facilitates the sowing 10-15 days earlier which helps in escaping the terminal heat stress and results in yield gain by 10-25% in EGP (Joshi et al., 2007c; McDonald et al., 2022). Early sowing is effective in reducing SB, subjected to selection of suitable variety for early sowing as 1) the genotypes must have capacity to tolerate high temperature at early crop growth stage; 2) proper management of foliar blight diseases; as sometimes higher leaf bight incidence was observed upon early sowing due to high residual moisture and humidity (Duveiller, 2004). Therefore, judicial selection of resistant variety is required to minimize the trade off in yield gain by early sowing and higher incidence of leaf blight. In a study, PBW 343, HUW 234 and HUW 468 were found suitable for growing under zero tillage practices (Joshi et al., 2007a).

Disease resistance

Growing resistant variety is the most effective method of managing crop disease. It is noteworthy that commercial varieties are moderately resistant to susceptible, and such varieties could be heavily infected under SB conducive environment. An early study by Sharma and Dubin (1996) showed increased resistance using multiline mixture resulted in reduction of area under disease progress curve (AUDPC) up to 57% and increased yield up to 8.6% than the component lines. Evaluation of wheat germplasm under different agro-climatic conditions has led to the identification of resistant genotypes. Genotypes SW 89-5193, SW 89-3060 and SW 89-5422 were resistant with 3.9, 2.6 and 3.5% reduction in grain weight, respectively, due to HLB, compared to 33% and 27.6% loss in susceptible cultivars BL 1135 and Sonalika, respectively (Sharma et al., 2004a). Sharma et al. (2004b) reported that SW 89-5422, Yangmai-6, Ning 8201, Chirya 7, Chirya 1 and CIGM90.455 were HLB resistant. These genotypes have been used in developing resistant lines. Furthermore, increasing the level of resistance in new varieties will be

TABLE 2 QTLs/MTAs (PVE of ≥10%) mapped on different chromosomes for spot blotch resistance using linkage mapping and GWAS.

Chromosome	Flanking markers/MTAs	QTL interval (cM)/Marker position (bp)	PVE (%)	References
Linkage mapping				
4B	985312 - 1241652	39.5 – 41.5	13.7	(Gahtyari et al., 2021)
5D	1058378–1048778	38.5–51.5	15.0	
4D	BS00036421_51-1119387	70.49–90.31	12.2	(Roy et al., 2021a)
5A	1067537-2257572	331.49–332.06	10.3	
5A	2341646-Vrn-A1	44.2-48.6	19.4	(He et al., 2020)
5A	987242-IWA4449	174.6-188.2	25.6	
5B	996745-10592866	73.9-77.7	17.2	
5A	Vrn-A1-3064415	175.9–179.4	12.5	(Singh et al., 2018)
5A	1135154-2260918	147.5–148.4	25.1	
7B	wmc758-wmc335	8.6	11.4	(Singh et al., 2016)
Sb2/QSb.bhu-5B/5BL	Xgwm639-Xgwm1043	0.62	42.4	(Kumar et al., 2015)
QSb.cim-3B	990937|F|0–1123330|F|0	2.7	17.6	(Zhu et al., 2014)
QSb.cim-5A	1086218|F|0–982608|F|0	12.1	12.3	
QSb.bhu-2A/2AS	Xgwm425-Xbarc159	8.5	15.2	(Kumar et al., 2010)
QSb.bhu-2B/2BS	Xgwm148-Xbarc91	21.2	23.7	
QSb.bhu-2D/2DS	Xgwm455-Xgwm815	9.0	10.7	
QSb.bhu-5B/5BL	Xgwm067-Xgwm213	9.0	10.7	
QSb.bhu-7B/7BS	Xgwm263-Xgwm255	5.0	10.2	
QSb.bhu-7D/7DS	Xgwm111-Xgwm1168	3.0	39.2	
QSb.bhu-2A/2AL	Xbarc353-Xgwm445	37.4	14.8	(Kumar et al., 2009)
QSb.bhu-2B/2BS	Xgwm148-Xgwm374	15.0	20.5	
QSb.bhu-5B/5BL	Xgwm067-Xgwm371	13.2	38.6	
QSb.bhu-6D/6DL	Xbarc175-Xgwm732	30.1	22.5	
Genome wide Association studies (GWAS)				
2A	AX-94710084	764783606	31.3	Kumar et al., 2022
2A	AX-94865722	765138703	32.0	
2A	AX-95135556	764819041	31.7	
2B	AX-95217784	800119910	30.1	
2D	AX-94901587	640297481	31.3	
3B	AX-94529408	719773163	31.8	
4D	AX-94560557	442164847	31.4	
Q.Sb.bisa-1A	S1A_497201550 & S1A_497201682	497200000	18.8	Tomar et al. (2021)
Q.Sb.bisa-1B	S1B_636840957	636840000	16.3	
Q.Sb.bisa-1D	S1D_89835681	89840000	24.0	
Q.Sb.bisa-2A	S2A_703111105- S2A_704446408	703110000-704450000	22.8	
Q.Sb.bisa-2B	S2B_419320960-S2B_423836280	419320000-423840000	30.7	
Q.Sb.bisa-4A	S4A_725538462 & S4A_725660945	725540000-725660000	23.0	
Q.Sb.bisa-5B	S5B_682958475 & S5B_683240735	682960000-683240000	31.4	
Q.Sb.bisa-6D	S6D_6395796-S6D_7194112	640000-7190000	20.2	

(Continued)

TABLE 2 Continued

Chromosome	Flanking markers/MTAs	QTL interval (cM)/Marker position (bp)	PVE (%)	References
3A	1085203	595935042	17.7	(Bainsla et al., 2020)
3A	1220348	598916422	13.2	
4A	991620	658343324	12.3	
5A	100177527	3319047	17.6	
5A	5411867	586600348	17.7	
5A	998276	569660176	10.6	
1A	S1A_582293281	582293281	10.0	(Jamil et al., 2018)
1D	S1D_479711997	479711997	11.0	
2A	S2A_16824871	16824871	10.0	
2D	S2D_389463371	389463371	10.0	
3A	S3A_180419285	180419285	13.0	
3A	S3A_741852990	741852990	10.0	
4B	S4B_554842477	554842477	13.0	
5A	S5A_50162259	50162259	11.0	
5B	S5B_501480761	501480761	10.0	
5B	S5B_502451973	502451973	10.0	
5B	S5B_503326206	503326206	10.0	
5B	S5B_504309131	504309131	12.0	
5B	S5B_508031185	508031185	10.0	
5B	S5B_513590441	513590441	11.0	
5B	S5B_528990456	528990456	12.0	
6B	S6B_9296088	9296088	12.0	
7A	S7A_483878120	483878120	10.0	
7B	S7B_749474154	749474154	14.0	

effective in managing SB in disease prone areas. Near immune line has been developed from the crosses between resistant genotypes (Kumar et al., 2019); yet further field evaluations are needed to confirm the stability of their resistance as well as their performance in other traits for possible release as varieties.

Genetics of disease resistance

Quantitative nature of SB resistance is predominantly reported in wheat (Singh et al., 2018; Bainsla et al., 2020; He et al., 2020), but reports are also available for major gene(s) governing SB resistance. Single dominant gene was postulated in the resistant genotypes Chirya 3 and MS#7 when they were crossed with common susceptible parent BL1473 (Neupane et al., 2007). Likewise, single dominant gene was reported in the resistant genotype DT 188, whereas digenic dominant resistance was reported in the lines E5895, HD 1927 and Motia (Adlakha et al., 1984). More genes were estimated in other resistant varieties, e.g., 2-3 genes in Gisuz, Cugap, Chirya 1 and Sabuf (Velazquez-Cruz, 1994), and three genes

in Acc.8226, Mon/Ald and Suzhoe#8 (Joshi et al., 2004b). Populations in these two studies have already began to show a pattern similar to polygenic segregation, implying that most resistant sources are governed by multiple genes with minor effects, which increases the chances of deriving transgressive segregants in the progenies (Singh et al., 2018; He et al., 2020). The magnitude of heritability (h^2) for SB resistance varied greatly in different studies, e.g., from 0.21 to 0.64 in Sharma et al. (2006b) and 0.85 to 0.89 in He et al. (2020), whereas most studies exhibited moderate to high heritability, providing a good opportunity to select resistant genotypes in breeding programs.

Detection of quantitative trait loci (QTL)

Quantitative disease resistance slows down the disease development by increasing the latency period, though, does not always show a clear-cut difference from qualitative resistance conferred by gene-for-gene interaction (Krattinger and Keller, 2016). Most of the QTLs for SB resistance were detected using bi-

parental mapping population (Table 2), and four major QTLs have been designated as *Sb1* through *Sb4*. *Sb1* was mapped on chromosome arm 7DS, being co-located with *Lr34* (Lillemo et al., 2013) that has been cloned and encodes an ABC (ATP binding cassette) transporter (Krattinger et al., 2009). *Sb2* was detected on chromosome arm 5BL (Kumar et al., 2015), and proposed to be the same locus earlier mapped as *QSb.bhu-5B* in Yangmai 6 (Kumar et al., 2009). Later, *Sb3* was identified in a winter wheat resistant line 621-7-1, being located on chromosome arm 3BS flanked by the markers *Xbarc133* and *Xbarc147* (Lu et al., 2016). Recently, *Sb4* was detected and fine mapped on chromosome arm 4BL flanked by the markers *YK12831* and *YK12928* (Zhang et al., 2020). Besides, a necrosis insensitivity gene *tsn1* was mapped on 5BL associated with *ToxA* insensitivity, and selection for genotypes with *tsn1* may confer resistance against *B. sorokiniana* isolates with *ToxA* (Navathe et al., 2019b).

Genome wide association studies (GWAS) have been widely performed to detect SB resistance QTLs in wheat. In a study using 566 spring wheat landraces, Adhikari et al. (2012) reported four genomic regions on 1A, 3B, 7B and 7D that were associated with SB resistance. One of the markers, wPt-1159 on 3B, was also associated with resistance to powdery mildew, yellow rust and grain yield (Crossa et al., 2007), and thus could be more useful in breeding. A GWAS on 528 spring wheat landraces with global origin reported 11 significant markers on chromosomes 1B, 5A, 5B, 6B and 7B with phenotypic variation explained (PVE) ranging from 0.14 to 5.80% (Gurung et al., 2014). Recently, 25 significant marker-trait associations (MTA) were identified in a panel of 301 Afghan wheat lines, being located on chromosomes 1A, 1B, 1D, 2B, 2D, 3A, 3B, 4A, 5A, 5B, 6A, 7A, and 7D with PVE ranging from 2.0-17.7% (Bainsla et al., 2020). Major challenges are faced by wheat breeders due to most identified QTLs/MTAs are of minor effects and have no diagnostic markers. Till date, diagnostic markers are available only for *Sb1* (*Lr34*) (Krattinger et al., 2009) and *tsn1* (Faris et al., 2010). A list of QTLs/MTAs for SB resistance is shown in Table 2, and an integrated map indicating major genes, QTLs and MTAs on different wheat chromosomes is shown in Figure 3.

Traits associated with SB resistance

Association of SB resistance with plant height and heading date has been well established, with high stature and late maturity often associated with low SB severity (Singh et al., 2015; He et al., 2020). This is mostly due to disease escape mechanisms; though, the possibility of tight linkage of *Rht* and *Vrn* genes with SB resistance genes cannot be ruled out (Zhu et al., 2014; He et al., 2020). Nevertheless, such linkages can be broken, as early and short lines with good SB resistance have been identified in some studies (Joshi et al., 2002; Sharma and Duveiller, 2004; Joshi et al., 2007d). Such early lines are especially important for SA, where terminal heat stress and SB are major yield constraints.

Leaf orientation influences the plant micro-climate, particularly temperature and humidity, through regulating evapotranspiration, and germplasm with erect to semi-erect leaves often showed good SB resistance (Joshi and Chand, 2002). Leaf tip necrosis associated with SB resistance serves as a good morphological marker (Joshi et al., 2004a). Stay-green (SG) genotypes are photosynthetically more active under biotic and abiotic stress conditions, and a positive correlation of SG with SB resistance was reported (Joshi et al., 2007b).

FIGURE 3
An integrated map showing genes and QTLs for SB resistance and their flanking markers (green color).
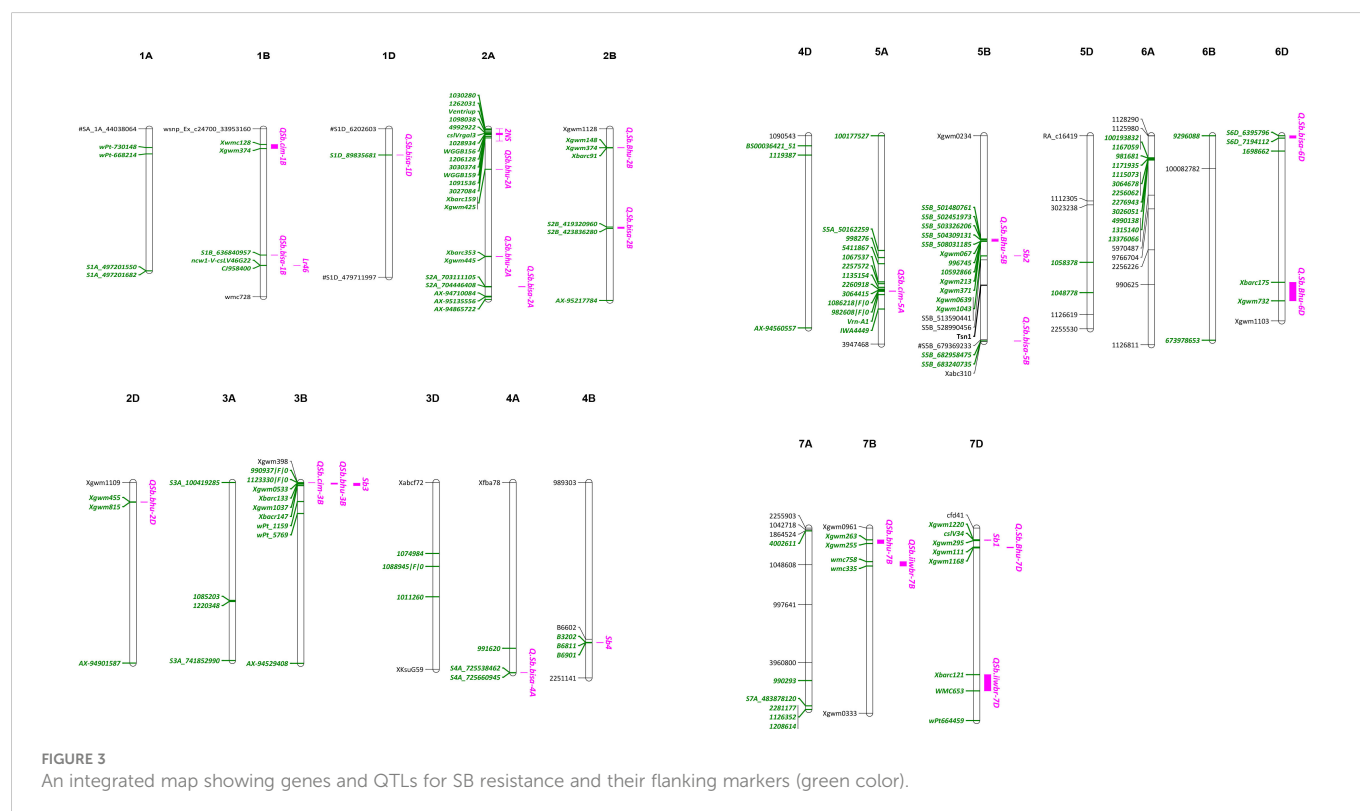
Breeding for disease resistance

Sources of SB resistance

Green revolution has resulted in the development of cultivars of semi-dwarf, fertilizer responsive and wider adaptability, enabling the cultivation of wheat in non-traditional areas, including the humid and hot regions with severe SB epidemics. Significant genetic variation for SB resistance was observed among the genotypes evaluated in India, Nepal and Bangladesh (Sharma et al., 2004a; Joshi et al., 2007d). Large-scale SB screening programs were initiated in the late 1980s when the disease became a major threat to wheat production in SA (Duveiller and Sharma, 2012). Initially, resistant sources were identified from Latin American particularly Brazilian germplasm like BH 1146, CNT 1, Ocepar 7, as well as from China like Shanghai 1 to 8, Suzhoe 1 to 10, Wuhan 1 to 3, Ning 8201, Longmai 10 and Yangmai #6 (van Ginkel and Rajaram, 1998). Using such lines as resistant donors, promising genotypes were developed at CIMMYT-Mexico, which exhibited good resistance against SB when tested in Bolivia, Nepal, India and Bangladesh (Sharma et al., 2004b; Sharma and Duveiller, 2007). Recent large-scale germplasm screening activities involve a work on screening 19,460 accessions from Indian national gene bank under field conditions, and 868 accessions were found to be resistant to moderately resistant (Kumar et al., 2016). Further screening of unexplored germplasm from gene bank has identified near immune response in the genotypes EC664204, IC534306 and IC535188 (Kumar et al., 2022).

Wild relatives are a rich source of SB resistance. The 2NS chromosome segment transferred from *Ae. ventricose* has been associated with resistance against wheat blast (Singh et al., 2021; Roy et al., 2021b), rusts (Helguera et al., 2003), cereal cyst nematode (Jahier et al., 2001) and lodging (Singh et al., 2019), and recently it was also associated with SB resistance (Juliana et al., 2022b). *Thinopyrum curvifolium* (Mujeeb-Kazi et al., 1996; van Ginkel and Rajaram, 1998) and synthetic hexaploid wheat derived from crosses between *T. turgidum* and *Aegilops tauschii* (Mujeeb-Kazi et al., 2007) serve as additional resistant sources. Good examples are Chirya genotypes derived from wide hybridization and exhibited good SB resistance, like Chirya 1, Chirya 3 and Chirya 7 (Sharma et al., 2007; Joshi et al., 2007b). High proportion of SB resistance was reported among the synthetic hexaploids evaluated under controlled conditions (Lozano-Ramirez et al., 2022). However, genotypes with high level of field SB resistance are scarce, a major limitation in the progress of breeding program.

Development of resistant genotypes

Breeding for resistant genotypes through crossing programs were started in 1980s in CIMMYT, Mexico and still this center is playing an important role in global SB resistance breeding. Ever since 2009, a special nursery was formed as CSISA-SB (presently known as Helminthosporium Leaf Blight Screening Nursery, HLBSN), comprising high yielding SB resistant genotypes for testing over the different countries in SA, Africa and Latin America (Singh et al., 2015). Testing of the 4th CSISA-SB nursery at seven locations in

Mexico, India and Bangladesh identified two stably resistant lines (CHUKUI#1 and VAYI#1) consistent over the locations (Singh et al., 2015).

The progress in achieving genetic gain for SB resistance is slow, due to reasons like quantitative inheritance, moderate heritability, strong genotype × environmental interaction, and high variability of the pathogen over time. Phenotypic selection is often associated with confounding traits, and molecular markers can be used to assist the pyramiding of resistance QTLs and selection for SB resistant genotypes (He et al., 2020). Superior genotypes have been developed from a marker assisted backcross program *via* transferring *Qsb.bhu-2A* and *Qsb.bhu-5B* from Chirya 3 and *Qsb.bhu-2A* from Ning 8201 into the genetic background of HUW 234 (Vasistha et al., 2015). Increased resistance up to near immunity could be obtained by stacking effective QTLs from multiple donors (Kumar et al., 2019). However, such QTL stacking could be compromised by QTL × QTL interaction, as demonstrated by Kumar et al. (2019) in a cross between "Yangmai#6" and "Chirya#3", where QTLs on 6D and 7D have a masking effect on each other. This highlights the importance of understanding the mode of action (additive, dominant, or epistatic) of the QTLs to be utilized in breeding.

Genomic selection can improve the efficiency of breeding program by reducing phenotyping cost, time and increasing selection intensity and genetic gain. Studies on genomic selection for SB in wheat are limited, and a successful example was reported by Juliana et al. (2022a), where genomic selection showed significantly higher accuracy than the fixed effect model using few selected markers. However, there is a long way to go for genomic selection to completely replace phenotypic selection in wheat breeding.

Biotechnological approaches

Gene silencing through RNAi is a powerful tool for controlling insects, nematodes, viruses, fungal diseases like powdery mildew, and rusts (Qi et al., 2019). Utilization of RNAi in functional genomic analysis in *B. sorokiniana* was reported by Leng et al. (2011), and it can be further explored in SB pathogenesis and resistance breeding in wheat.

Liu et al. (2012) developed a new mapping strategy combining bulk segregant analysis and RNA-Seq called 'BSR-Seq', where transcripts are sequenced from extreme bulks, being a potential technique for marker discovery in large polyploid genome like wheat. Using BSR-Seq, five SB-resistance associated transcripts were identified on 5B and 3B chromosomes and their potential role in SB resistance were inferred (Saxesena et al., 2022).

Transgenic lines expressing foreign genes proved to be a potential approach to control insect and diseases in several crop plants. Examples include the heteroexpression of *PvPGIP2* (Janni et al., 2008) and overexpression of *TaPIMP1* and *TaPIMP2* (Zhang et al., 2012; Wei et al., 2017) in transgenic wheat lines that enhanced the resistance against *B. sorokiniana*. However, government regulations on transgenic development are major concerns for researchers.

Additional techniques like genome editing (Zhang et al., 2017) and Eco-Tilling (Ajaz et al., 2021) have been increasingly utilized in

wheat, having great potential to contribute to SB resistance breeding in near future.

Conclusion

Spot blotch is a disease of concern in warmer wheat growing areas of South Asia, Latin America and Africa. Most of the commercially grown cultivars are moderately resistant to susceptible and are subjected to significant yield losses under conducive climatic conditions. An integrated disease management strategy involving cultural practices, chemical control, resistant cultivars, etc., is needed to combat the disease. In addition, modern biotechnology brings new tools for the rapid and efficient development of resistant cultivars in wheat.

Author contributions

CR, XH, and PS conceptualized the manuscript. CR drafted the first version. NG and SM collected information and improved the first draft. XH and PS edited and approved the submitted version. All authors contributed to the article and approved the submitted version.

Conflict of interest

The authors declare that the research was conducted in the absence of any commercial or financial relationships that could be construed as a potential conflict of interest.

The reviewer SN declared a past collaboration with author PS to the handling editor at the time of review.

Publisher's note

All claims expressed in this article are solely those of the authors and do not necessarily represent those of their affiliated organizations, or those of the publisher, the editors and the reviewers. Any product that may be evaluated in this article, or claim that may be made by its manufacturer, is not guaranteed or endorsed by the publisher.

References

Acharya, K., Dutta, A. K., and Pradhan, P. (2011). *Bipolaris sorokiniana* (Sacc.) shoem.: The most destructive wheat fungal pathogen in the warmer areas. *Aust. J. Crop Sci.* 5, 1064–1071.

Adhikari, T. B., Gurung, S., Hansen, J. M., Jackson, E. W., and Bonman, J. M. (2012). Association mapping of quantitative trait loci in spring wheat landraces conferring resistance to bacterial leaf streak and spot blotch. *Plant Genome* 5, 1–16. doi: 10.3835/plantgenome2011.12.0032

Adlakha, K., Wilcoxson, R., and Raychaudhuri, S. (1984). Resistance of wheat to leaf spot caused by. *Bipolaris sorokiniana. Plant Dis.* 68, 320–321. doi: 10.1094/PD-69-320

Aggarwal, R., Gupta, S., Banerjee, S. A., and Singh, V. B. (2011). Development of a SCAR marker for detection of *Bipolaris sorokiniana* causing spot blotch of wheat. *Can. J. Microbiol.* 57, 934–942. doi: 10.1139/w11-089

Aggarwal, R., Sharma, S., Singh, K., Gurjar, M. S., Saharan, M. S., Gupta, S., et al. (2019). First draft genome sequence of wheat spot blotch pathogen *Bipolaris sorokiniana* BS_112 from India, obtained using hybrid assembly. *Microbiol.* 8, e00308-19. doi: 10.1128/MRA.00308-19

Aggarwal, R., Singh, V. B., Shukla, R., Gurjar, M. S., Gupta, S., and Sharma, T. R. (2010). URP-based DNA fingerprinting of *Bipolaris sorokiniana* isolates causing spot blotch of wheat. *J. Phytopathol.* 158, 210–216. doi: 10.1111/j.1439-0434.2009.01603.x

Ajaz, S., Benbow, H. R., Christodoulou, T., Uauy, C., and Doohan, F. M. (2021). Evaluation of the susceptibility of modern, wild, ancestral, and mutational wheat lines to septoria tritici blotch disease. *Plant Pathol.* 70, 1123–1137. doi: 10.1111/ppa.13369

Al-Sadi, A. M. (2021). *Bipolaris sorokiniana*-induced black point, common root rot, and spot blotch diseases of wheat: A review. *Front. Cell Infect. Microbiol.* 11, 584899. doi: 10.3389/fcimb.2021.584899

Bainsla, N. K., Phuke, R. M., He, X., Gupta, V., Bishnoi, S. K., Sharma, R. K., et al. (2020). Genome-wide association study for spot blotch resistance in afghan wheat germplasm. *Plant Pathol.* 69, 1161–1171. doi: 10.1111/ppa.13191

Chang, N., and Wu, Y. (1998). "Incidence and current management of Spot blotch of wheat in China," in *Helminthosporium blights of wheat: Spot blotch and tan spot*. Eds. E. Duveiller, H. J. Dubin, J. Reeves and A. McNab (El Batan, Mexico: CIMMYT), 119–125.

Chaurasia, S., Chand, R., and Joshi, A. K. (2000). Relative dominance of *Alternaria triticina* pras. et prab. and *Bipolaris sorokiniana* (Sacc.) shoemaker in different growth stages of wheat (*T. aestivum*). *J. Plant Dis. Protect.* 107, 176–181.

Conner, R. (1990). Interrelationship of cultivar reactions to common root rot, black point, and spot blotch in spring wheat. *Plant Dis.* 74, 224–227. doi: 10.1094/PD-74-0224

Crossa, J., Burgueno, J., Dreisigacker, S., Vargas, M., Herrera-Foessel, S. A., Lillemo, M., et al. (2007). Association analysis of historical bread wheat germplasm using additive

genetic covariance of relatives and population structure. *Genetics* 177, 1889–1913. doi: 10.1534/genetics.107.078659

Domiciano, G. P., Rodrigues, F. A., Vale, F. X. R., Filha, M. S. X., Moreira, W. R., Andrade, C. C. L., et al. (2010). Wheat resistance to spot blotch potentiated by silicon. *J. Phytopathol.* 158, 334–343. doi: 10.1111/j.1439-0434.2009.01623.x

Duveiller, E. (2002). "Helminthosporium blights of wheat: challenges and strategies for a better disease control," in *Advance of wheat breeding in China: Proceedings of the first national wheat breeding conference* (Jinan, Shandong, People Republic of China: China Science and Technology Press), 57–66.

Duveiller, E. (2004). Controlling foliar blights of wheat in the rice-wheat systems of Asia. *Plant Dis.* 88, 552–556. doi: 10.1094/PDIS.2004.88.5.552

Duveiller, E., Kandel, Y. R., Sharma, R. C., and Shrestha, S. M. (2005). Epidemiology of foliar blights (spot blotch and tan spot) of wheat in the plains bordering the Himalayas. *Phytopathology* 95, 248–256. doi: 10.1094/PHYTO-95-0248

Duveiller, E. M., and Sharma, R. C. (2009). Genetic improvement and crop management strategies to minimize yield losses in warm non-traditional wheat growing areas due to spot blotch pathogen *Cochliobolus sativus*. *J. Phytopathol.* 157, 521–534. doi: 10.1111/j.1439-0434.2008.01534.x

Duveiller, E., and Sharma, R. C. (2012). "Wheat resistance to spot blotch or foliar blight," in *Disease resistance in wheat*. Ed. I. Sharma (Cambridge, MA: CABI, Wallingford, Oxfordshire, UK), 120–135.

Faris, J. D., Zhang, Z., Lu, H., Lu, S., Reddy, L., Cloutier, S., et al. (2010). A unique wheat disease resistance-like gene governs effector-triggered susceptibility to necrotrophic pathogens. *Proc. Natl. Acad. Sci. U. S. A.* 107, 13544–13549. doi: 10.1073/pnas.1004090107

Friesen, T. L., Holmes, D. J., Bowden, R. L., and Faris, J. D. (2018). ToxA is present in the U.S. *Bipolaris sorokiniana* population and is a significant virulence factor on wheat harboring *Tsn1. Plant Dis.* 102, 2446–2452. doi: 10.1094/PDIS-03-18-0521-RE

Friesen, T. L., Stukenbrock, E. H., Liu, Z., Meinhardt, S., Ling, H., Faris, J. D., et al. (2006). Emergence of a new disease as a result of interspecific virulence gene transfer. *Nat. Genet.* 38, 953–956. doi: 10.1038/ng1839

Gahtyari, N. C., Roy, C., He, X., Roy, K. K., Reza, M. M. A., Hakim, M. A., et al. (2021). Identification of QTLs for spot blotch resistance in two bi-parental mapping populations of wheat. *Plants* 10, 973. doi: 10.3390/plants10050973

Gupta, P. K., Chand, R., Vasistha, N. K., Pandey, S. P., Kumar, U., Mishra, V. K., et al. (2017). Spot blotch disease of wheat: the current status of research on genetics and breeding. *Plant Pathol.* 67, 508–531. doi: 10.1111/ppa.12781

Gurung, S., Mamidi, S., Bonman, J. M., Xiong, M., Brown-Guedira, G., and Adhikari, T. B. (2014). Genome-wide association study reveals novel quantitative trait loci associated

with resistance to multiple leaf spot diseases of spring wheat. *PloS One* 9, e108179. doi: 10.1371/journal.pone.0108179

Hasan, U. W., Roy, C., Chattopadhyay, T., Ranjan, R. D., and De, N. (2021). Effects of heat and drought stress on yield and physiological traits in wheat (*Triticum aestivum* l.). *J. Crop Weed.* 17 (1), 203–210. doi: 10.22271/09746315.2021.v17.i1.1424

He, X., Dreisigacker, S., Sansaloni, C., Duveiller, E., Singh, R. P., and Singh, P. K. (2020). QTL mapping for spot blotch resistance in two bi-parental mapping populations of bread wheat. *Phytopathology* 110, 1980–1987. doi: 10.1094/PHYTO-05-20-0197-R

He, X., Gahtyari, N. C., Roy, C., Dababat, A. A., Brar, G. S., and Singh, P. K. (2022). "Globally important non-rust diseases of wheat," in *Wheat improvement*. Eds. M. P. Reynolds and H. J. Braun (Cham: Springer), 143–158. doi: 10.1007/978-3-030-90673-3_9

Helguera, M., Khan, I. A., Kolmer, J., Lijavetzky, D., Zhong-qi, L., and Dubcovsky, J. (2003). PCR assays for the *Lr37-Yr17-Sr38* cluster of rust resistance genes and their use to develop isogenic hard red spring wheat lines. *Crop Sci.* 43, 1839–1847. doi: 10.2135/cropsci2003.1839

Ibeagha, A. E., Hückelhoven, R., Schäfer, P., Singh, D. P., and Kogel, K. H. (2005). Model wheat genotypes as tools to uncover effective defense mechanisms against the hemibiotrophic fungus *Bipolaris sorokiniana*. *Phytopathology* 95, 528–532. doi: 10.1094/PHYTO-95-0528

Jahani, M. (2005). *Characterization of toxin from bipolaris sorokiniana and development of molecular marker for identification of the pathogen* (New Delhi: Indian Agricultural Research Institute). dissertation/Ph D thesis.

Jahani, M., Aggarwal, R., Gupta, S., Sharma, S., and Dureja, P. (2014). Purification and characterization of a novel toxin from *Bipolaris sorokiniana*, causing spot blotch of wheat and analysis of variability in the pathogen. *Cereal Res. Commun.* 42, 252–261. doi: 10.1556/CRC.2013.0053

Jahier, A., Tanguy, D., Rivoal, K., and Bariana, H. S. (2001). The *Aegilops ventricosa* segment on chromosome 2AS of the wheat cultivar 'VPM1' carries the cereal cyst nematode resistance gene *Cre5*. *Plant Breed.* 120, 125–128. doi: 10.1046/j.1439-0523.2001.00585.x

Jamil, M., Ali, A., Gul, A., Ghafoor, A., Ibrahim, A. M. H., and Mujeeb-Kazi, A. (2018). Genome-wide association studies for spot blotch (Cochliobolus sativus) resistance in bread wheat using genotyping-by-sequencing. *Phytopathology* 108, 1307–1314.

Janni, M., Sella, L., Favaron, F., Blechl, A. E., De Lorenzo, G., and D'Ovidio, R. (2008). The expression of a bean PGIP in transgenic wheat confers increased resistance to the fungal pathogen *Bipolaris sorokiniana*. *Mol. Plant Microbe In.* 21, 171–177. doi: 10.1094/MPMI-21-2-0171

Jansson, H. B., and Akesson, H. (2003). Extracellular matrix, esterase and the phytotoxin prehelminthosporol in infection of barley leaves by *Bipolaris sorokiniana*. *Eur. J. Plant Pathol.* 109, 599–605. doi: 10.1023/A:1024773531256

Joshi, A. K., and Chand, R. (2002). Variation and inheritance of leaf angle, and its association with spot blotch (*Bipolaris sorokiniana*) severity in wheat (*Triticum aestivum*). *Euphytica* 124, 283–291. doi: 10.1023/A:1015773404694

Joshi, A. K., Chand, R., and Arun, B. (2002). Relationship of plant height and days to maturity with resistance to spot blotch in wheat. *Euphytica* 123, 221–228. doi: 10.1023/A:1014922416058

Joshi, A. K., Chand, R., Arun, B., Singh, R. P., and Ortiz, R. (2007a). Breeding crops for reduced-tillage managementin the intensive, rice–wheat systems of south Asia. *Euphytica* 153, 135–151. doi: 10.1007/s10681-006-9249-6

Joshi, A. K., Chand, R., Kumar, S., and Singh, R. P. (2004a). Leaf tip necrosis: A phenotypic marker associated with resistance to spot blotch disease in wheat. *Crop Sci.* 44, 792–796. doi: 10.2135/cropsci2004.7920

Joshi, A. K., Kumar, S., Chand, R., and Ortiz-Ferrara, G. (2004b). Inheritance of resistance to spot blotch caused by *Bipolaris sorokiniana* in spring wheat. *Plant Breed.* 123, 213–219. doi: 10.1111/j.1439-0523.2004.00954.x

Joshi, A. K., Kumari, M., Singh, V. P., Reddy, C. M., Kumar, S., Rane, J., et al. (2007b). Stay green trait: Variation, inheritance and its association with spot blotch resistance in spring wheat (*Triticum aestivum* l.). *Euphytica* 153, 59–71. doi: 10.1007/s10681-006-9235-z

Joshi, A. K., Mishra, B., Chatrath, R., Ferrara, G. O., and Singh, R. P. (2007c). Wheat improvement in India: present status, emerging challenges and future prospects. *Euphytica* 157, 431–446. doi: 10.1007/s10681-007-9385-7

Joshi, A. K., Ortiz-Ferrara, G., Crossa, J., Singh, G., Sharma, R. C., Chand, R., et al. (2007d). Combining superior agronomic performance and terminal heat tolerance with resistance to spot blotch (*Bipolaris sorokiniana*) of wheat in the warm humid gangetic plains of south Asia. *Field Crop Res.* 103, 53–61. doi: 10.1016/j.fcr.2007.04.010

Juliana, P., He, X., Poland, J., Roy, K. K., Malaker, P. K., Mishra, V. K., et al. (2022a). Genomic selection for spot blotch in bread wheat breeding panels, full–sibs and half–sibs and index–based selection for spot blotch, heading and plant height. *Theor. Appl. Genet.* 135, 1965–1983. doi: 10.1007/s00122-022-04087-y

Juliana, P., He, X., Poland, J., Shrestha, S., Joshi, A. K., Huerta-Espino, J., et al. (2022b). Genome-wide association mapping indicates quantitative genetic control of spot blotch resistance in bread wheat and the favorable effects of some spot blotch loci on grain yield. *Front. Plant Sci.* 13. doi: 10.3389/fpls.2022.835095

Kemp, G., Bergmann, C. W., Clay, R., van der Westhuizen, A., and Pretorius, Z. A. (2003). Isolation of a polygalacturonase-inhibiting protein (PGIP) from wheat. *Mol. Plant Microbe Interact.* 16, 955–961. doi: 10.1094/MPMI.2003.16.11.955

Krattinger, S. G., and Keller, B. (2016). Molecular genetics and evolution of disease resistance in cereals. *New Phytol.* 212, 320e332. doi: 10.1111/nph.14097

Krattinger, S. G., Lagudah, E. S., Spielmeyer, W., Singh, R. P., Huerta-Espino, J., McFadden, H., et al. (2009). A putative ABC transporter confers durable resistance to multiple fungal pathogens in wheat. *Science* 323, 1360–1363. doi: 10.1126/science.1166453

Kumar, S., Archak, S., Tyagi, R. K., Kumar, J., Vk, V., Jacob, S., et al. (2016). Evaluation of 19,460 wheat accessions conserved in the Indian national genebank to identify new sources of resistance to rust and spot blotch diseases. *PloS One* 11, e0167702. doi: 10.1371/journal.pone.0167702

Kumar, U., Joshi, A. K., Kumar, S., Chand, R., and Röder, M. S. (2009). Mapping of resistance to spot blotch disease caused by *Bipolaris sorokiniana* in spring wheat. *Theor. Appl. Genet.* 118, 783–792. doi: 10.1007/s00122-008-0938-5

Kumar, U., Joshi, A. K., Kumar, S., Chand, R., and Röder, M. S. (2010). Quantitative trait loci for resistance to spot blotch caused by *Bipolaris sorokiniana* in wheat (*T. aestivum* l.) lines 'Ning 8201' and 'Chirya 3'. *Mol. Breed.* 26, 477–491. doi: 10.1007/s11032-009-9388-2

Kumar, U., Kumar, S., Prasad, R., Röder, M. S., Kumar, S., Chand, R., et al. (2019). Genetic gain on resistance to spot blotch of wheat by developing lines with near immunity. *Crop Breed. Genet. Genom.* 1, e190017. doi: 10.20900/cbgg20190017

Kumar, S., Pradhan, A. K., Kumar, U., Dhillon, G. S., Kaur, S., Budhlakoti, N., et al. (2022). Validation of novel spot blotch disease resistance alleles identified in unexplored wheat (*Triticum aestivum* l.) germplasm lines through KASP markers. *BMC Plant Biol.* 22, 618. doi: 10.1186/s12870-022-04013-w

Kumar, S., Röder, M. S., Tripathi, S. B., Kumar, S., Chand, R., Joshi, A. K., et al. (2015). Mendelization and fine mapping of a bread wheat spot blotch disease resistance QTL. *Mol. Breed.* 35, 218. doi: 10.1007/s11032-015-0411-5

Kumar, J., Schäfer, P., Hückelhoven, R., Langen, G., Baltruschat, H., Stein, E., et al. (2002). *Bipolaris sorokiniana*, a cereal pathogen of global concern: cytological and molecular approaches towards better control. *Mol. Plant Pathol.* 3, 185–195. doi: 10.1046/j.1364-3703.2002.00120.x

Leng, Y., Wu, C., Liu, Z., Friesen, T. L., Rasmussen, J. B., and Zhong, S. (2011). RNA-Mediated gene silencing in the cereal fungal pathogen *Cochliobolus sativus*. *Mol. Plant Pathol.* 12, 289–298. doi: 10.1111/j.1364-3703.2010.00666.x

Lillemo, M., Joshi, A. K., Prasad, R., Chand, R., and Singh, R. P. (2013). QTL for spot blotch resistance in bread wheat line Saar co-locate to the biotrophic disease resistance loci *Lr34* and *Lr46*. *Theor. Appl. Genet.* 126, 711–719. doi: 10.1007/s00122-012-2012-6

Liu, S., Yeh, C. T., Tang, H. M., Nettleton, D., and Schnable, P. S. (2012). Gene mapping *via* bulked segregant RNA-seq (BSR-seq). *PloS One* 7, e36406. doi: 10.1371/JOURNAL.PONE.0036406

Lozano-Ramirez, N., Dreisigacker, S., Sansaloni, C. P., He, X., Sandoval-Islas, J. S., Pérez-Rodríguez, P., et al. (2022). Genome-wide association study for spot blotch resistance in synthetic hexaploid wheat. *Genes* 13, 1387. doi: 10.3390/genes13081387

Lu, P., Liang, Y., Li, D., Wang, Z., Li, W., Wang, G., et al. (2016). Fine genetic mapping of spot blotch resistance gene *Sb3* in wheat (*Triticum aestivum*). *Theor. Appl. Genet.* 129, 577–589. doi: 10.1007/s00122-015-2649-z

Manamgoda, D. S., Rossman, A. Y., Castlebury, L. A., Crous, P. W., Madrid, H., Chukeatirote, E., et al. (2014). The genus bipolaris. *Stud. Mycol.* 79, 221–288. doi: 10.1016/j.simyco.2014.10.002

Mann, M. B., Minotto, E., Feltrin, T., Milagre, L. P., Spadari, C., and van der Sand, S. T. (2014). Genetic diversity among monoconidial and polyconidial isolates of *Bipolaris sorokiniana*. *Curr. Microbiol.* 69, 874–879. doi: 10.1007/s00284-014-0667-8

McDonald, M. C., Ahren, D., Simpfendorfer, S., Milgate, A., and Solomon, P. S. (2017). The discovery of the virulence gene ToxA in the wheat and barley pathogen *Bipolaris sorokiniana*. *Mol. Plant Pathol.* 19, 432–439. doi: 10.1111/mpp.12535

McDonald, A. J., Singh, B., Keil, A., Srivastava, A., Craufurd, P., Kishore, A., et al. (2022). Time management governs climate resilience and productivity in the coupled rice–wheat cropping systems of eastern India. *Nat. Food.* 3, 542–551. doi: 10.1038/s43016-022-00549-0

Mehta, Y., Riede, C., Campos, L., and Kohli, M. (1992). Integrated management of major wheat diseases in Brazil: an example for the southern cone region of Latin America. *Crop Prot.* 11, 517–524. doi: 10.1016/0261-2194(92)90168-5

Mishra, S., Singh, B. R., Singh, A., Keswani, C., Naqvi, A. H., and Singh, H. B. (2014). Biofabricated silver nanoparticles act as a strong fungicide against *Bipolaris sorokiniana* causing spot blotch disease in wheat. *PloS One* 9, e97881. doi: 10.1371/journal.pone.0097881

Mujeeb-Kazi, A., Gul, A., Ahmad, I., Farooq, M., Rizwan, S., Bux, H., et al. (2007). *Aegilops tauschii*, as a spot blotch (Cochliobolus sativus) resistance source for bread wheat improvement. *Pak. J. Bot.* 39, 1207–1216.

Mujeeb-Kazi, A., Villareal, R., Gilchrist, L., and Rajaram, S. (1996). Registration of five wheat germplasm lines resistant to helminthosporium leaf blight. *Crop Sci.* 36, 216–217. doi: 10.2135/cropsci1996.0011183X003600010054x

Murray, G. M., and Brennan, J. P. (2009). *The current and potential costs from diseases of wheat in Australia* Vol. 69 (Barton: Grain Research and Development Corporation, Australia).

Narendra, M. C., Roy, C., Kumar, S., Virk, P., and De, N. (2021). Effect of terminal heat stress on physiological traits, grain zinc and iron content in wheat (*Triticum aestivum* l.). *Czech J. Genet. Plant Breed.* 57, 43–50. doi: 10.17221/63/2020-CJGPB

Navathe, S., Chand, R., Mishra, V. K., Pandey, S. P., Kumar, U., and Joshi, A. K. (2019a). Management of spot blotch and heat stress in spring wheat through azoxystrobin-mediated redox balance. *Agr. Res.* 9 (2), 169–178. doi: 10.1007/s40003-019-00417-7

Navathe, S., Yadav, P. S., Chand, R., Mishra, V. K., Vasistha, N. K., Meher, P. K., et al. (2019b). ToxA-Tsn1 interaction for spot blotch susceptibility in Indian wheat: An example of inverse gene-for-gene relationship. *Plant Dis.* 104, 71–81. doi: 10.1094/PDIS-05-19-1066-RE

Neupane, R. B., Sharma, R. C., Duveiller, E., Ortiz-Ferrara, G., Ojha, B. R., Rosyara, U. R., et al. (2007). Major gene controls of field resistance to spot blotch in wheat genotypes 'Milan/Shanghai 7' and 'Chirya.3'. *Plant Dis.* 91, 692–697. doi: 10.1094/PDIS-91-6-0692

Neupane, A. C., Sharma, R. C., Duveiller, E., and Shrestha, S. M. (2010). Sources of *Cochliobolus sativus* inoculum causing spot blotch under warm wheat growing conditions in south Asia. *Cereal Res. Commun.* 38 (4), 541–549. doi: 10.1556/CRC.38.2010.4.11

Pandey, S. P., Kumar, S., Kumar, U., Chand, R., and Joshi, A. K. (2005). Sources of inoculum and reappearance of spot blotch of wheat in rice-wheat cropping systems in eastern India. *Eur. J. Plant Pathol.* 111, 47–55. doi: 10.1007/s10658-004-2404-9

Qi, T., Guo, J., Peng, H., Liu, P., Kang, Z., and Guo, J. (2019). Host-induced gene silencing: A powerful strategy to control diseases of wheat and barley. *Int. J. Mol. Sci.* 20, 206. doi: 10.3390/ijms20010206

Reis, E. M. (1991). Integrated disease management: the changing concept of controlling head blight and spot blotch. In: DA Saunders and GP Hettel eds. *Wheat in Heat Stressed Environments: Irrigated, Dry Areas and Rice Wheat Systems* Mexico, DF: CIMMYT, 165–170.

Ridley, B. L., O'Neill, M. A., and Mohnen, D. (2001). Pectins: Structure, biosynthesis, and oligogalacturonide-related signaling. *Phytochemistry* 57, 929–967. doi: 10.1016/S0031-9422(01)00113-3

Roy, C., Gahtyari, N. C., He, X., Mishra, V. K., Chand, R., Joshi, A. K., et al. (2021a). Dissecting quantitative trait loci for spot blotch resistance in south Asia using two wheat recombinant inbred line populations. *Front. Plant Sci.* 12, 641324. doi: 10.3389/fpls.2021.641324

Roy, C., Juliana, P., Kabir, M. R., Roy, K. K., Gahtyari, N. C., Marza, F., et al. (2021b). New genotypes and genomic regions for resistance to wheat blast in south Asian germplasm. *Plants* 10, 2693. doi: 10.3390/plants10122693

Saari, E. (1998). Leaf blight disease and associated soil-borne fungal pathogens of wheat in South and South East Asia. In: E. Duveiller, H. J. Dubin, J. Reeves and A. McNab eds. *Helminthosporium Blights of wheat: spot blotch and tan spot* Mexico, DF: CIMMYT, 37–51.

Sautua, F. J., and Carmona, M. A. (2021). Detection and characterization of QoI resistance in *Pyrenophora tritici-repentis* populations causing tan spot of wheat in Argentina. *Plant Pathol.* 70 (9), 2125–2136. doi: 10.1111/ppa.13436

Saxesena, R. R., Mishra, V. K., Chand, R., Kumar, U., Chowdhury, A. K., Bhati., J., et al. (2022). SNP discovery using BSR-seq approach for spot blotch resistance in wheat (*Triticum aestivum* l.), an essential crop for food security. *Front. Genet.* 13. doi: 10.3389/fgene.2022.859676

Sharma, R. C., and Dubin, H. J. (1996). Effect of wheat cultivar mixtures on spot blotch (*Bipolaris sorokiniana)* and grain yield. *Field Crop Res.* 48, 95–101. doi: 10.1016/S0378-4290(96)01031-3

Sharma, R. C., and Duveiller, E. (2004). Effect of helminthosporium leaf blight on performance of timely and late-seeded wheat under optimal and stressed levels of soil fertility and moisture. *Field Crop Res.* 89, 205–218. doi: 10.1016/j.fcr.2004.02.002

Sharma, R. C., and Duveiller, E. (2006). Spot blotch continues to cause substantial grain yield reductions under resource-limited farming conditions. *J. Phytopathol.* 154, 482–488. doi: 10.1111/j.1439-0434.2006.01134.x

Sharma, R. C., and Duveiller, E. (2007). Advancement toward new spot blotch resistant wheats in south Asia. *Crop Sci.* 47, 961–968. doi: 10.2135/cropsci2006.03.0201

Sharma, R. C., Duveiller, E., Ahmed, F., Arun, B., Bhandari, D., Bhatta, M. R., et al. (2004b). Helminthosporium leaf blight resistance and agronomic performance of wheat genotypes across warm regions of south Asia. *Plant Breed.* 123, 520–524. doi: 10.1111/j.1439-0523.2004.01006.x

Sharma, R., Duveiller, E., Gyawali, S., Shrestha, S., Chaudhary, N., and Bhatta, M. (2004a). Resistance to helminthosporium leaf blight and agronomic performance of spring wheat genotypes of diverse origins. *Euphytica* 139, 33–44. doi: 10.1007/s10681-004-2292-2

Sharma, R. C., Duveiller, E., and Ortiz-Ferrara, G. (2007). Progress and challenge towards reducing wheat spot blotch threat in the Eastern gangetic plains of south Asia: Is climate change already taking its toll? *Field Crop Res.* 103, 109–118. doi: 10.1016/j.fcr.2007.05.004

Sharma, P., Duveiller, E., and Sharma, R. C. (2006a). Effect of mineral nutrients on spot blotch severity in wheat, and associated increases in grain yield. *Field Crop Res.* 95, 426–430. doi: 10.1016/j.fcr.2005.04.015

Sharma, P., Mishra, S., Singroha, G., Kumar, R. S., Singh, S. K., and Singh, G. P. (2022). Phylogeographic diversity analysis of *Bipolaris sorokiniana* (Sacc.) shoemaker causing spot blotch disease in wheat and barley. *Genes* 13, 2206. doi: 10.3390/genes13122206

Sharma, R. C., Pandey-Chhetri, B., and Duveiller, E. (2006b). Heritability estimates of spot blotch resistance and its association with other traits in spring wheat crosses. *Euphytica* 147, 317–327. doi: 10.1007/s10681-005-9018-y

Singh, P. K., Gahtyari, N. C., Roy, C., Roy, K. K., He, X., Tembo, B., et al. (2021). Wheat blast: A disease spreading by intercontinental jumps and its management strategies. *Front. Plant Sci.* 12. doi: 10.3389/fpls.2021.710707

Singh, P. K., He, X., Sansaloni, C. P., Juliana, P., Dreisigacker, S., Duveiller, E., et al. (2018). Resistance to spot blotch in two mapping populations of common wheat is controlled by multiple QTL of minor effects. *Int. J. Mol. Sci.* 19, 4054. doi: 10.3390/ijms19124054

Singh, D. P., Kumar, A., Solanki, I. S., Singh, S. P., Verma, J., Mahapatra, S., et al. (2014). Management of spot blotch of wheat caused by *Bipolaris sorokiniana* in wheat using fungicides. *Indian Phytopath.* 67 (3), 308–310.

Singh, V., Singh, G., Chaudhury, A., Ojha, A., Tyagi, B. S., Chowdhary, A. K., et al. (2016). Phenotyping at hot spots and tagging of QTLs conferring spot blotch resistance in bread wheat. *Mol. Bio Rep.* 43, 1293–1303. doi: 10.1007/s11033-016-4066-z

Singh, D., Wang, X., Kumar, U., Gao, L., Noor, M., Imtiaz, M., et al. (2019). High-throughput phenotyping enabled genetic dissection of crop lodging in wheat. *Front. Plant Sci.* 10, 394. doi: 10.3389/fpls.2019.00394

Singh, P. K., Zhang, Y., He, X., Singh, R. P., Chand, R., Mishra, V. K., et al. (2015). Development and characterization of the 4th CSISA-spot blotch nursery of bread wheat. *Eur. J. Plant Pathol.* 143, 595–605. doi: 10.1007/s10658-015-0712-x

Sultana, S, Adhikary, SK, Islam, MM, and Rahman, SMM. (2018). Evaluation of pathogenic variability based on leaf blotch disease development components of *Bipolaris sorokiniana* in *Triticum aestivum* and agroclimatic origin. *Plant Pathol J.* 34, 93–103.

Sun, X. F., Zhang, D. X., Gong, G. S., Qi, X. B., Ye, K. H., Zhou, Y., et al. (2015). Spot blotch on volunteer wheat plants in sichuan, China. *J. Plant Path.* 97, 173–176.

Tomar, V., Singh, D., Dhillon, G. S., Singh, R. P., Poland, J., Joshi, A. K., et al. (2021). New QTLs for spot blotch disease resistance in wheat (*Triticum aestivum* l.) using genome-wide association mapping. *Front. Genet.* 11. doi: 10.3389/fgene.2020.613217

Valjavec-Gratian, M., and Steffenson, B. J. (1997). Pathotypes of *Cochliobolus sativus* in barley in north Dakota. *Plant Dis.* 81, 1275–1278. doi: 10.1094/PDIS.1997.81.11.1275

van Ginkel,, and Rajaram, S. (1998). "Breeding for resistance to spot blotch in wheat: Global perspective," in *Helminthosporium blight of wheat: Spot blotch and tan spot.* Eds. E. Duveiller, H. J. Dubin, J. Reeves and A. McNab (Mexico: DF: CIMMYT), 376.

Vasistha, N. K., Balasubramaniam, A., Mishra, V. K., Chand, R., Srinivasa, J., Yadav, P. S., et al. (2015). Enhancing spot blotch resistance in wheat by marker-aided backcross breeding. *Euphytica* 207, 119–133. doi: 10.1007/s10681-015-1548-3

Velazquez-Cruz, C. (1994). *Genetica de la resistencia a bipolaris sorokiniana en trigos harineros* (Mexico: Colegio de Post-Graduados, Montecillo). dissertation/MSc Thesis.

Villareal, R. L., Mujeeb-Kazi, A., Gilchrist, L. I., and Del Toro, E. (1995). Yield loss to spot blotch in spring bread wheat in warm nontraditional wheat production areas. *Plant Dis.* 79, 893–897. doi: 10.1094/PD-79-0893

Wei, X., Shan, T., Hong, Y., Xu, H., Liu, X., and Zhang, Z. (2017). TaPIMP2, a pathogen-induced MYB protein in wheat, contributes to host resistance to common root rot caused by *Bipolaris sorokiniana*. *Sci. Rep.* 7, 1754. doi: 10.1038/s41598-017-01918-7

Wu, L., He, X., Lozano, N., Zhang, X., and Singh, P. K. (2020). ToxA, a significant virulence factor involved in wheat spot blotch disease, exists in the Mexican population of *Bipolaris sorokiniana*. *Trop. Plant Path.* 46, 201–206. doi: 10.1007/s40858-020-00391-4

Zhang, Y., Bai, Y., Wu, G., Zou, S., Chen, Y., Gao, C., et al. (2017). Simultaneous modification of three homoeologs of TaEDR1 by genome editing enhances powdery mildew resistance in wheat. *Plant J.* 91, 714–724. doi: 10.1111/tpj.13599

Zhang, P., Guo, G., Wu, Q., Chen, Y., Xie, J., Lu, P., et al. (2020). Identification and fine mapping of spot blotch (*Bipolaris sorokiniana*) resistance gene Sb4 in wheat. *Theor. Appl. Genet.* 133, 2451–2459. doi: 10.1007/s00122-020-03610-3

Zhang, Z., Liu, X., Wang, X., Zhou, M., Zhou, X., Ye, X., et al. (2012). An R2R3 MYB transcription factor in wheat, TaPIMP1, mediates host resistance to *Bipolaris sorokiniana* and drought stresses through regulation of defense and stress-related genes. *New Phytol.* 196, 1155–1170. doi: 10.1111/j.1469-8137.2012.04353.x

Zhong, S., and Steffenson, B. J. (2001). Virulence and molecular diversity in *Cochliobolus sativus*. *Phytopathol.* 91, 469–476. doi: 10.1094/PHYTO.2001.91.5.469

Zhu, Z., Bonnett, D., Ellis, M., Singh, P., Heslot, N., Dreisigacker, S., et al. (2014). Mapping resistance to spot blotch in a CIMMYT synthetic-derived bread wheat. *Mol. Breed.* 34, 1215–1228. doi: 10.1007/s11032-014-0111-6

Fungal plant pathogen "mutagenomics" reveals tagged and untagged mutations in *Zymoseptoria tritici* and identifies SSK2 as key morphogenesis and stress-responsive virulence factor

Hannah R. Blyth[1], Dan Smith[1], Robert King[1†], Carlos Bayon[1], Tom Ashfield[2], Hannah Walpole[3], Eudri Venter[3†], Rumiana V. Ray[4], Kostya Kanyuka[1†] and Jason J. Rudd[1*]

[1]Protecting Crops and the Environment, Rothamsted Research, Harpenden, United Kingdom, [2]Crop Health and Protection (CHAP), Rothamsted Research, Harpenden, United Kingdom, [3]Bioimaging Unit, Rothamsted Research, Harpenden, United Kingdom, [4]Division of Plant and Crop Sciences, School of Biosciences, University of Nottingham, Loughborough, United Kingdom

"Mutagenomics" is the combination of random mutagenesis, phenotypic screening, and whole-genome re-sequencing to uncover all tagged and untagged mutations linked with phenotypic changes in an organism. In this study, we performed a mutagenomics screen on the wheat pathogenic fungus *Zymoseptoria tritici* for altered morphogenetic switching and stress sensitivity phenotypes using *Agrobacterium*-mediated "random" T-DNA mutagenesis (ATMT). Biological screening identified four mutants which were strongly reduced in virulence on wheat. Whole genome re-sequencing defined the positions of the T-DNA insertion events and revealed several unlinked mutations potentially affecting gene functions. Remarkably, two independent reduced virulence mutant strains, with similarly altered stress sensitivities and aberrant hyphal growth phenotypes, were found to have a distinct loss of function mutations in the Zt*SSK2* MAPKKK gene. One mutant strain had a direct T-DNA insertion affecting the predicted protein's N-terminus, while the other possessed an unlinked frameshift mutation towards the C-terminus. We used genetic complementation to restore both strains' wild-type (WT) function (virulence, morphogenesis, and stress response). We demonstrated that ZtSSK2 has a non-redundant function with ZtSTE11 in virulence through the biochemical activation of the stress-activated HOG1 MAPK pathway. Moreover, we present data suggesting that SSK2 has a unique role in activating this pathway in response to specific stresses. Finally, dual RNAseq-based transcriptome profiling of WT and SSK2 mutant strains revealed many HOG1-dependent transcriptional changes in the fungus during early infection and suggested that the host

response does not discriminate between WT and mutant strains during this early phase. Together these data define new genes implicated in the virulence of the pathogen and emphasise the importance of a whole genome sequencing step in mutagenomic discovery pipelines.

Introduction

Plant and animal health are consistently threatened by microbial pathogens causing infections and diseases (Fisher et al., 2012). Many (but not all) of these disease-causing agents have relatively small compact genomes and are also haploid in the case of some bacteria and fungi. The next-generation sequencing (NGS) advances now provide highly cost-effective and comprehensive comparative genome analysis for many pathogenic microbes. Combined, these are proving particularly useful in identifying natural genetic variation within populations and allowing genome-wide associated linkage studies to highlight candidate genes related to virulence-associated traits (Zhong et al., 2017; Meile et al., 2018).

Forwards genetics screens performed on pathogenic microbes, including fungal plant pathogens, have used several different methods/approaches. These experiments facilitate an unbiased gene discovery process to dissect the molecular basis of virulence. Nevertheless, before the more recent NGS-based technologies, the genomic analysis of induced experimental mutants was challenging, often reliant upon plasmid rescue or PCR-based approaches to try to identify coding sequences affected by, for example, plasmid insertional screens (Singer & Burke, 2003; Nan & Walbot, 2009). For certain fungal species, the development of *Agrobacterium*-mediated T-DNA-based mutagenesis revolutionised functional gene studies as the procedure generated mostly single insertion events in what are often haploid genomes. Previously the positional analysis of these mutation events required methods such as TAIL-PCR or plasmid rescue to identify candidate genes tagged by T-DNA insertion. Untagged mutations were much more challenging to locate without sequencing technologies. Therefore, the advances in whole genome sequencing have significantly increased the precision of mutation detection in forward genetics experiments resulting in a new field of "mutagenomics" becoming established. This differs from previous approaches in that whole genomes are interrogated in mutant strains/genotypes of plants and microbes to ascertain the full range of all mutations. This approach was first mentioned in the literature by Penna & Jain (2017) and was recently utilised in the model plant *Arabidopsis thaliana* (Hodgens et al., 2020). Mutagenomics enables experimentally generated mutants of pathogens to be genome re-sequenced to ascertain the full spectrum of potentially causative mutations beyond tagged mutations caused by select mutagenesis methods (e.g. T-DNA or plasmid sequence).

The ascomycete fungus *Zymoseptoria tritici* causes the disease Septoria Tritici Blotch (STB) in wheat (*Triticum aestivum*) and is responsible for significant economic losses worldwide. *Z. tritici* has a biphasic infection cycle with an extended symptomless growth phase followed by a switch to a necrotrophic phase when the symptoms of infection begin to show (Goodwin et al., 2011; Steinberg, 2015). The fungus is strictly apoplastic and is not known to invade host cells physically. While interactions between the fungus and wheat leaf cells are not fully understood, hyphal filament extension from "yeast-like" spores is considered essential for successful leaf infection, which occurs predominantly through leaf stomates (Mehrabi et al., 2006b; Motteram et al., 2011; King et al., 2017; Yemelin et al., 2017). This switch between yeast-like and hyphal growth forms is typical of "dimorphic" fungi, and for *Z. tritici in vitro* this depends on nutritional sources and temperature (Rossman et al., 2015). Among the filamentous ascomycetes, this is a unique aspect of *Z. tritici* biology, enabling studies targeting the critical yeast to hyphal growth state switch (Steinberg, 2015; Kilaru et al., 2022). Mutations that affect hyphal growth are lethal to most filamentous fungal pathogens, but in *Z. tritici*, these mutants are culturable in their "yeast-like" form. However, the failure of yeast-like cells to transition into hyphae, or reduction of overall filamentation, results in reduced virulence. A fungus with a lower capacity for stomatal penetration limits the ability for subsequent intercellular colonisation and could severely delay or outright abolish virulence (King et al., 2017; Mohammadi et al., 2020). For this reason, assays that easily identify "switching" mutants are a quick valuable screen for putatively identifying reduced virulence mutants. For *Z. tritici*, the switch to hyphal growth from yeast-like blastospores can be induced and monitored easily following inoculation onto nutrient-poor agar such as tap water agar (TWA) (King et al., 2017).

A reference isolate of *Z. tritici*, IPO323, was one of the first filamentous fungi to have a fully sequenced genome (Testa et al., 2015). The 39.7 Mb genome is arranged in 21 chromosomes, of which the smallest eight (chromosomes 14–21) are mainly considered dispensable for asexual plant infection (Goodwin et al., 2011). With faster, more accurate and cheaper sequencing technologies, further isolates of *Z. tritici* have since been fully sequenced. These include strains 1A5, 1E4, 3D1 and 3D7, all isolated in 1999 from infected wheat fields in Switzerland, as well as single isolates of the related *Zymoseptoria* fungi *Z. brevis*, *Z. pseudotritici* and *Z. ardabiliae* (Lendenmann et al., 2014;

Grandaubert et al., 2015; Plissonneau et al., 2018). Work on all these reference strains has illuminated much about the genomics of this important wheat pathogen. *Z. tritici* has been shown to have a high rate of genome plasticity, with regions contributing to low-level "background" mutations occasionally observable within a single strain (Möller et al., 2018; Plissonneau et al., 2018; Oggenfuss et al., 2021). The haploid genome of *Z. tritici* is also amenable to multiple mutagenesis methods, with commonly used and well-established protocols working at different throughputs. *Agrobacterium tumefaciens*-mediated transformation (ATMT) is now widely used for gene deletion, reporter strain generation and studying protein localisation in a targeted manner (Michielse et al., 2005). However, the method can also generate "random" genomic T-DNA insertions to facilitate forward genetics or mutagenomics screens when combined with whole genome re-sequencing.

The global impact of transformation techniques on the genomes of target organisms remains undefined. As previously mentioned, before the advent of and advancements in NGS technologies, researchers used molecular methods to identify the "tagged" sites of genomic integrations (Urban et al., 2015). However, these methods cannot provide information regarding potential "untagged", spontaneous, or otherwise non-specifically induced mutations that might occur during experimental manipulations and mutagenesis. These untagged mutations can generate a loss of function or missense mutations in proteins and result in observable phenotypic changes. In such cases, a tagged insertion event may unwittingly be ascribed to an impact that an untagged change is causal of. For example, in a transposon tagging experiment in *Arabidopsis thaliana*, the phenotype was attributed to a Ds element jumping more than once in the host genome, impacting multiple sites, and leaving behind a molecular scar (Østergaard & Yanofsky, 2004). Fully re-sequencing genomes from generated mutants enables the detection of any specific "tagged" integration events whilst simultaneously allowing the identification of untagged or "off-target" mutations.

This current study used a whole genome re-sequencing mutagenomics pipeline to investigate T-DNA integrations and untagged mutations in the genomes of five IPO323 mutants, most of which (four) exhibited reduced virulence on wheat. This work identified untagged mutations; some were common amongst the mutant isolates, whereas others were unique to individual isolates. Furthermore, we present and characterise an example of a single gene affected in two of the five mutants, once by direct T-DNA insertion and once by an unlinked Single Nucleotide Polymorphism (SNP) mutation introducing a frameshift. Loss of function of this gene, encoding a putative MAP kinase kinase kinase (MAPKKK) SSK2, imparted many phenotypic changes, including markedly reduced virulence on wheat leaves and differences in responses to stress. Finally, through dual RNAseq, we also present the early *in planta* expressed transcriptome of SSK2 mutants and the comparable host (wheat) transcriptome. These data indicate that whilst SSK2 loss of function reduces the expression of many fungal genes, the host transcriptome does not respond differently to mutants and WT strains, indicating that early responses to the fungus are unchanged. Our study emphasises the key role of whole genome re-sequencing in mutagenomics discovery pipelines and sets a framework for similar studies in other systems.

Materials and methods

In vitro culture conditions and fungal strains

The reference isolate of *Z. tritici* IPO323, collected in the Netherlands, is the parental strain for the ATMT collection. This strain is virulent towards the experimental wheat cultivar used, cv. Riband.

For all experiments, fungal spores were harvested from 5–6-days-old cultures on Yeast extract peptone dextrose (YPD) agar plates at 16°C. Hygromycin B resistance was conferred by introducing a hygromycin resistance gene cassette as a selectable marker in the original library. To ensure that all mutant isolates were stably transformed, YPD was amended with hygromycin to a final concentration of 100 µg ml^{-1}. For later experiments involving complementation mutants, wherein an additional selectable marker was required to enable the selection of positive transformants, a geneticin (G418) resistance gene cassette was introduced. Therefore, hygromycin (100 µg ml^{-1}) and geneticin (Sigma Aldrich) to a final working concentration of 200 µg ml^{-1} were added to the YPD media to ensure these isolates were stably transformed.

In planta infection assays and quantitative analysis *via* image analysis

Second leaves of wheat cv. Riband seedlings grown for 21 days in complete compost were inoculated with spores of mutant isolates collected from YPD cultures, which had been washed and re-suspended in dH$_2$O+0.01% Tween 20 to a density of 1×10^7 spores ml^{-1}. Infection assays were performed as previously described (Keon et al., 2007). In addition, a wild-type (WT) parental strain of IPO323 was used on each seedling tray to compare the rate of disease symptom development by transformed strains. A minimum of 3 leaves from 3 independent seedlings were tested against each fungal isolate. Additionally, each isolate was tested in this infection assay in at least four replica experiments.

Leaves were photographed periodically, with final photos taken at 21 dpi. For quantitative analysis of disease levels, the LemnaGrid (LemnaTech) software was used as recently described (Chen et al., 2023). In brief, photographs of diseased leaves (TIFs) were imported into the LemnaGrid software. Next, leaves were segmented based on a combination of intensity thresholding and a colour-based classification. Finally, the proportion of diseased tissue for each leaf was quantified using an additional colour-based classification (for chlorotic, necrotic or healthy tissue) which converted data into a percentage of each category for each leaf. Scores were then exported for subsequent quantitative and statistical analysis.

In vitro assays for hyphal growth and stress sensitivity tests

A range of media was used to compare *in vitro* growth phenotypes of *Z. tritici* mutants. For the following assays *in vitro*,

blastospores were grown from glycerol stocks and then collected from 5–6-day YPD amended with hygromycin incubated at 16°C. Approximately 1×10^7 spores ml^{-1} (or a dilution series thereof) were suspended in dH$_2$0+0.01% Tween20 and then spotted as drops of 5 μl, allowed to air dry on the agar surface before plates were then sealed with parafilm.

Spore suspensions were also spot-inoculated (as above) onto the surfaces of 1% tap-water agar (TWA) plates for filamentous growth assays. TWA plates were sealed and kept at room temperature. Growth was monitored 2-, 5- and 8-days post-inoculation (dpi). Final macroscopic photographs of hyphal development (radial growth of hyphae from the central spot) were taken at 10 dpi.

YPD media was also amended with various stressors at concentrations used in previous literature (Mehrabi et al., 2006b; Motteram et al., 2011; Yemelin et al., 2017; Francisco et al., 2019). A 200 μg ml^{-1} of calcofluor white was used to induce cell wall integrity stress. To cause oxidative stress, YPD media containing hydrogen peroxide at a concentration of 5 mM. A concentration of 1 M sorbitol was used for osmotic stress conditions. Finally, to test for the resistance of ZtSsk2 disrupted mutants to the phenylpyrrole fungicide fludioxonil (Fluka), a working concentration of 30 μg ml^{-1} was used. Both YPD and YPD amended plates were sealed and kept at 16°C for 5 days. Growth was monitored from 2 dpi, and final photographs of yeast-like growth levels were taken 5 days post-inoculation (dpi).

In planta inoculation for scanning electron microscopy (SEM)

A different approach was used from the standard attached wheat leaf bioassay to prevent damage to the wheat leaf surface. Instead, a 0.1% Tween20-water solution with a spore concentration of 1×10^7 spores ml^{-1} was paint brush inoculated onto leaf surfaces.

For the scanning electron microscopy (SEM), approximately 5 mm square regions were cut from the leaf samples and attached to aluminium stubs with a 50:50 mixture of graphite:TissueTek. The samples were frozen in liquid nitrogen and transferred to the GATAN ALTO 2100 cryo prep system. Samples were etched and coated in a thin layer of gold. Micrographs were collected using a JEOL 6360 scanning electron microscope at 5kV.

Genome re-sequencing and identification of T-DNA insertion sites

Genomic DNA from YPD-grown liquid cultures collected by vacuum filtration was prepared using the Illustra Phytopure DNA extraction kit (GE Healthcare) following the manufacturer's instructions for all samples and sent for genome re-sequencing by Illumina HiSeq2500 with a 250 bp paired-end read metric and a target of 100× coverage (BGI genomics).

Read quality was assessed using Fastqc (v0.11.9, https://www.bioinformatics.babraham.ac.uk/projects/fastqc/) and Trimmomatic (v0.38-Java-1.8, http://www.usadellab.org/cms/?page=trimmomatic) was used to remove any remaining Illumina

adaptors. The position of the T-DNA insertion was determined by mapping paired-end reads to the T-DNA plasmid reference. Where one mate was mapped and the other mate was unmapped, this unmapped read was likely to inform the boundary position of the T-DNA insertion site. A stack of forward reads represents the 5' T-DNA insertion boundary loci boundary, and the stack of reverse reads represents the 3' T-DNA insertion boundary loci. The gap between these stacks, therefore, represented any deleted sequence. Copies of T-DNA insertion are determined by the average coverage of mapped reads to the T-DNA versus mapping the raw data to the fungal genome. Detailed instructions on running the FindInsertSeq workflow are available in the previous publication (Urban et al., 2015; https://github.com/Rothamsted/script-collection/tree/master/FindInsertSeq).

Determination of non-T-DNA mutation sites in *Z. tritici* genomes

Variants (SNPs/indels) were called against the reference IPO323 genome assembly using FreeBayes (v. 1.2.0.4-intel.2019.01). Raw variant counts were filtered using SNPsift (v.1.7.0_161) by the depth equal to, or greater than ten, and a quality score equal to, or greater than, 30. To categorise and assess the likely impacts on annotated genes SNPeff 4.3t (build 2017-11-24 10:18) was used. For high/medium impact variants of interest or concern, PROVEAN (Protein Variation Effect Analyser; http://provean.jcvi.org/index.php) with default settings was also used to predict whether an amino acid substitution or indel impacted the biological function of a protein.

Agrobacterium-mediated transformation of *Z. tritici*

The original library generation was detailed in Motteram et al. (2011). The vector pCHYG (providing resistance to Hygromycin B) was transformed into an IPO323 isolate by random *Agrobacterium*-mediated transformation using *Agrobacterium* strain AGL-1. For the generation of the complementation construct used in this study the Gibson assembly method and a pCGEN vector, conferring geneticin resistance was used. Primers used in construct building for Gibson assembly were designed using the NEBuilder tool (https://nebuilder.neb.com/). The plasmid was assembled following the Gibson Assembly® Protocol (E5510) and reagents produced by NEB. The generated transformation plasmid was verified by restriction digest using colony PCR of transformed *E. coli* ahead of miniprep. The manufacturer's protocol for transforming chemically competent cells NEB® 5-alpha Competent *E. coli* (High Efficiency, DH5α) was followed. After overnight incubation, the vector was isolated using a QIAprep spin miniprep kit (Qiagen) following the manufacturer's instructions.

Electrocompetent AGL-1 *Agrobacterium* cells were transformed following the protocol described in Motteram et al. (2009), using 1 μg of generated pCGGEN+ZtSSK2 plasmid DNA and the default Agro setting on a BioRad Micropulser. LB Miller agar amended

with Kanamycin was used to select for successfully transformed *A. tumefaciens*. Stocks were then made in 50% glycerol and stored at −80°C. *Agrobacterium*-mediated transformation of *Z. tritici* was carried out following a protocol first outlined by Zwiers & De Waard (2001) and further developed by Mehrabi et al. (2006b). Briefly, *Z. tritici* spores and *A. tumefaciens* cells were co-cultivated on cellophane disks on the surface of induction media agar containing acetosyringone. The discs were subsequently transferred to *Aspergillus nidulans* minimal medium agar, which was amended with hygromycin, geneticin and timentin to select stable fungal transformants. Putative transformants were typically observed after 14 days and were subcultured onto YPD agar plates amended with hygromycin or geneticin and timentin. Finally, 50% glycerol stocks were made and stored at −80°C.

Anti-active MAPK western blotting for oxidative stress responses

Z. tritici isolates were grown for 6 days in YPD broth, starting with a single 10 µL loop of blastospores taken from YPD agar. After 6 days of growth shaking in fresh YPD broth, the fungal cultures were "spiked" with 25 mM H_2O_2. Fungal cells were collected by vacuum filtration 30 and 60 minutes after exposure and snap-frozen, then stored at −80°C before protein extraction.

Frozen cells were transferred to 2 mL tubes with two small ball bearings and freeze-dried using LyoDry Compact Benchtop Freeze Dryer (MechaTech Systems) overnight for total protein extraction. First, to lyse the samples, Y-PER™ Yeast Protein Extraction Reagent (ThermoScientific) was added. Then, typically for 150 mg fungal material, 1.5 ml was added with a Protease Inhibitor Cocktail (100X) (ThermoScientific). Next, a TissueLyserII was used to agitate and homogenise the mixture for 5 min at 20 Hz. Next, the samples were spun in a centrifuge (14,000 g, 10 min), and the supernatant was transferred to a fresh tube. For storage, 200 µL protein extracts were added to 50 µL 5X SDS loading buffer and kept at −20°C.

Sodium dodecyl sulphate-polyacrylamide gel electrophoresis (SDS-PAGE) protocol was performed as described in Rudd et al. (2008) using 10% resolving gels. Benchmark ladder and MagicMark XP ladder (ThermoFisher) were used for protein size estimations. Following electrophoresis, proteins were blotted onto nitrocellulose membranes (GE Healthcare, 0.1 µm pore size). Correct transfer to the membrane was assessed by staining with ponceau S. The membrane was first washed three times (5 min, RT) in TBS-T buffer before blocking in 5% non-fat milk (Marvel Skimmed Milk Powder) in TBS-Tween buffer. The membrane was rewashed three times (5 min, RT) in TBS-Tween, before subsequent probing and blotting according to the supplier's guidelines for the Anti-p44/42 and p38 antibodies (Cell Signalling Technologies) using 5% BSA TBS-Tween buffer with the primary antibodies. The secondary antibody, horseradish peroxidase-conjugated goat anti-rabbit antibody (Invitrogen), was used at a 1:10,000 dilution in TBS-T + 5% non-fat milk powder. Finally, chemiluminescence was performed with ECL reagents (GE Healthcare) and blot imaging using an Odyssey Fc imager (Li-Cor), with a 10 min exposure time. Images were optimised and saved using Image Studio 5.2. Protein

loading controls were generated by counter-straining membranes with Naphthol blue black (Amido Black).

RNA sequencing and GO term analyses

The WT IPO323 and T-DNA insertion mutant strain 4-124 were inoculated onto susceptible wheat leaves (cv Riband as previously described). Infected leaf tissues were excised at 6 and 24 h and snap-frozen. Each technical and biological replicate incorporated five leaves. Total RNA was isolated using the TRIZOL procedure (Invitrogen), and RNA quality was assessed using Nanodrop and gel electrophoresis. Directional mRNA polyA enriched library preparation and sequencing were performed by Novogene (Cambridge, UK) using Illumina NovaSeq paired-end 150 bp sequencing.

Quality control of reads was performed using MultiQC. Sequence trimming of recognised adaptors was performed using Trimmomatic (Bolger et al., 2014). Reads were mapped to the *Z. tritici* IPO323 genome using HiSat2 (Kim et al., 2019). Principal Component Analysis (PCA) was performed on sample differences of variance stabilising transformed (vsd) gene count data to confirm that biological replicates clustered together. Count determination was performed using featureCounts (Liao et al., 2014). Library normalisation and differential expression (DE) calling were done using the Bioconductor package DESeq2 (Love et al., 2014; https://bioconductor.org/packages/release/bioc/html/DESeq2.html) in R studio. Gene expression levels were individually compared between WT IPO323 and the 4-124 ATMT mutant samples for each time point. DEGs were identified by applying a log2 fold change filter of ≥ 1 or ≤ −1, and the DESeq2 implementation of Benjamini-Hochberg (Benjamini & Hochberg, 1995) was used to control for multiple testing (FDR<0.05).

Gene Ontology (GO) enrichment analysis was performed for all significantly up-and down-regulated *Z. tritici* genes using OmicsBox to identify the overrepresented GO term BLAST2GO Enrichment. This list of fungal differentially expressed genes was then subjected to PAM (partition around medoids) clustering, with the number of clusters determined using the pamk function in R (*fpc* package version 2.2-9).

The same process was applied to the reads mapping to the Chinese Spring (v1.1) wheat genome, with the exception of a BLAST2GO GO enrichment analysis. To rapidly functionally profile the identified differentially expressed genes g:Prolfiler (https://biit.cs.ut.ee/gprofiler/gost) "g:OSt functional profiling" was performed using default values and ENSEMBL Plants *Triticum aestivum* (taestivum version: IWGSC) (Raudvere et al., 2019).

KnetMiner knowledge graphs and keyword searches

Zymoseptoria KnetMiner (https://knetminer.com/Zymoseptoria_tritici/) can generate knowledge graphs using *Z. tritici* JGI genome identifiers (e.g. Mycgr3G67344). These graphs identify related proteins, genes, domains, associated phenotypic

information and more from databases and broader literature (Hassani-Pak et al., 2021). A prototype Zymoseptoria KnetMiner currently draws on data and literature from a few fungi, including Saccharomyces yeast, *Fusarium graminearum*, *Neurospora crassa* and *Aspergillus nidulans*.

The KnetMiner keyword search function was used to identify a list of candidate genes associated in the literature with "HOG1", "oxidative stress", "osmotic stress", "cell wall integrity", "hyphal growth", "filamentous growth", and "dimorphism" from data from select model fungi and the yeast *S. cerevisiae*. These keyword searches generated a list of 1964 genes "linked" to those search terms, with duplicate entries removed. We compared this to our list of differentially expressed genes from our *in planta* RNA sequencing experiment.

Results

In planta characterisation of *Agrobacterium tumefaciens* mediated (ATMT) *Z. tritici* transformants

We had previously carried an initial high throughput virulence screen on the library of 631 random ATMT mutants of *Z. tritici* IPO323 as the parental strain for reduced *in planta* infection on the susceptible wheat cv. Riband (Rudd, unpublished). In this initial screen, performed only on single leaves, fourteen transformants were identified as either non-pathogenic or with reduced virulence. The mutants in this library all have Hygromycin B resistance conferred by use of the vector pCHYG for ATMT. Two from this collection had previously been further analysed, describing the impact of mutations detected in the *ZtALG2* (previously published as *MgAlg2*) and *ZtGT2* genes on *Z. tritici* virulence (Motteram et al., 2011; King et al., 2017). From the remaining non-pathogenic or reduced virulence mutants, which had not been further characterised, five isolates are explored herein.

Each isolate was retested for virulence against the susceptible wheat cv. Riband, on three leaves, and symptom development on wheat was monitored for 21 days post-inoculation. Photos were taken 21 days post-inoculation (Figure 1A). Altogether, each isolate was tested in an attached wheat leaf screen at least four times with an IPO323 WT control to compare symptom progression. Four of the five mutant isolates tested had reproducibly reduced virulence on wheat leaves, manifesting as delayed symptom development restricted to only limited chlorosis by 21 dpi (Figure 1A). In contrast, isolate 9-70 (the ninth transformation round, picked colony 70) showed disease symptom development that was not significantly distinguishable from WT strains, going against the observations from an initial one-leaf phenotypic screen (Rudd, unpublished). The typical levels of disease symptoms for each strain are shown in Figure 1A. These assays confirmed previous work, suggesting mutant isolates 4-124, 4-158, 5-51, and 15-120 were reduced virulence mutants of *Z. tritici*.

Further characterisation of the T-DNA mutants for *in vitro* growth and stress defects

Further phenotyping of the T-DNA mutant isolates *in vitro* was carried out using different fungal stressors, imparting osmotic, oxidative and cell wall stress, and for hyphal growth induction on tap water agar (TWA). For stress sensitivity testing, each isolate was tested a minimum of three times against each stress, and final images of fungal growth spotting plates were taken after five days. The typical results of these assays are shown in Figure 1B. Isolates 4-124 and 4-158 displayed hypersensitivity to both osmotic and oxidative stress, whilst 15-120, 5-51 and 9-70 appeared to tolerate all the fungal growth stress conditions tested.

To assess the ability of the five isolates to switch to hyphal growth each was also spotted onto TWA, with an IPO323 spot used as the WT control comparison (Figure 1C). Two of the five mutant isolates (5-51 and 9-70) in the hyphal growth assays showed a typical WT hyphal growth phenotype. In contrast, mutant isolate 15-120 displayed the most drastic reduced hyphal growth, compared to the other mutant isolates, with only a few short branches very close to the spot edge. A reduction was also seen for isolates 4-124 and 4-158, exhibiting a similar short, hyperbranched hyphal growth phenotype. This reduction paralleled a similar reduction in virulence and was also associated with hypersensitivity to oxidative and osmotic stress in both strains, suggesting potential functional links between these phenotypes.

Detection of T-DNA insertion sites in the four T-DNA mutant isolates

Whole-genome re-sequencing was then performed on the four ATMT IPO323 mutants described. The initial objective was to determine the number and location of T-DNA insertions in the four strains with reduced virulence on wheat.

Previous analysis of *Agrobacterium tumefaciens*-mediated transformation (ATMT) in fungi has demonstrated that a single T-DNA insertion event is the most frequent (Michielse et al., 2005). In agreement, only one T-DNA insert was detected in each strain for the four ATMT mutant isolates with reduced virulence analysed. Table 1 shows the seven genes potentially affected by these integrations across all four strains. Of these seven, six genes were identified as potentially being affected by intergenic insertion, insertion occurring in close proximity to 5′-upstream regions or 3′-downstream regions of a gene(s). One gene was directly impacted by intragenic insertion of the T-DNA, that is insertion within a gene. Figure 2A shows the chromosomal locations of the genes affected by the T-DNA inserts and untagged variants. The figure emphasises that there was no obvious locational bias for the T-DNA integration events for the small number of events investigated.
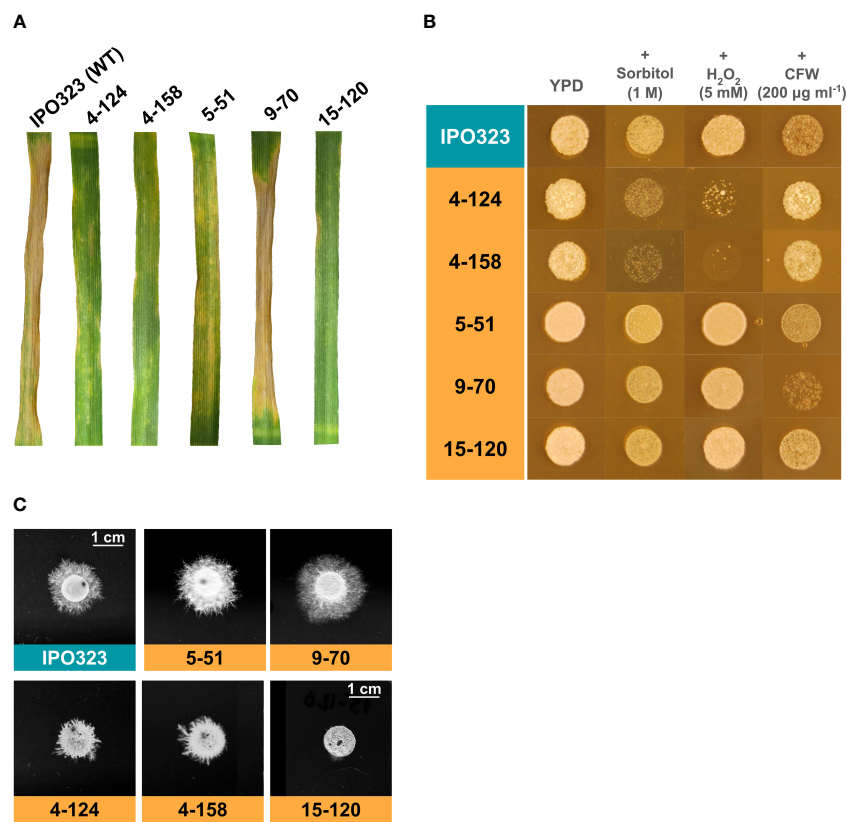
FIGURE 1

Characterisation of *Z. tritici* T-DNA mutants for virulence on wheat and stress responses. **(A)** The five mutants were tested alongside the WT control isolate for their virulence on the leaves of a susceptible wheat cultivar. The mutants 4-124, 4-158, 5-51, and 15-120 exhibited reduced virulence when scored 21 days post-infection. In contrast, 9-70 exhibited WT levels of virulence. **(B)** The five strains were tested alongside the WT for sensitivity to stress on rich agar plates. Stress conditions were osmotic (sorbitol), oxidative (H$_2$O$_2$), and cell wall stress (Calcofluor White – CFW). The T-DNA mutants 4-124 and 4-158 exhibited hypersensitivity to oxidative and osmotic stress. **(C)** *In vitro* hyphal growth assays on tap water agar (TWA). Each strain was spotted onto TWA and incubated for 10 days to enable radial hyphal growth. Diminished hyphal growth rates were observed for strains 4-124, 4-158 and 15-120.

TABLE 1 Genes affected by T-DNA insertion.

IPO323 Mutant Isolate	IPO323 Chromosome	T-DNA Insert Location	Putatively Impacted Genes	Interpro Name	Insert Location
4-124	1	5313974-5315085	ZtritIPO323_04g02061	Mitogen-activated protein (MAP) kinase kinase kinase Ssk2/Ssk22	Intragenic
			ZtritIPO323_04g02062	WD40-repeat-containing domain superfamily	Upstream
4-158	3	99207-99214	ZtritIPO323_04g07162	Gamma-glutamyl cyclotransferase-like	Downstream, 3'UTR
			ZtritIPO323_04g07163	Zn(2)-C6 fungal-type DNA-binding domain	Downstream, 3'UTR
5-51	2	1057013-1057051	ZtritIPO323_04g05837	Major facilitator superfamily	Downstream, 3'UTR
15-120	4	2261923-2261926	ZtritIPO323_04g09207	Molybdenum cofactor sulfurase, C-terminal;MOSC, N-terminal beta barrel	Downstream, 3'UTR
			ZtritIPO323_04g09208	Arf GTPase activating protein	Upstream
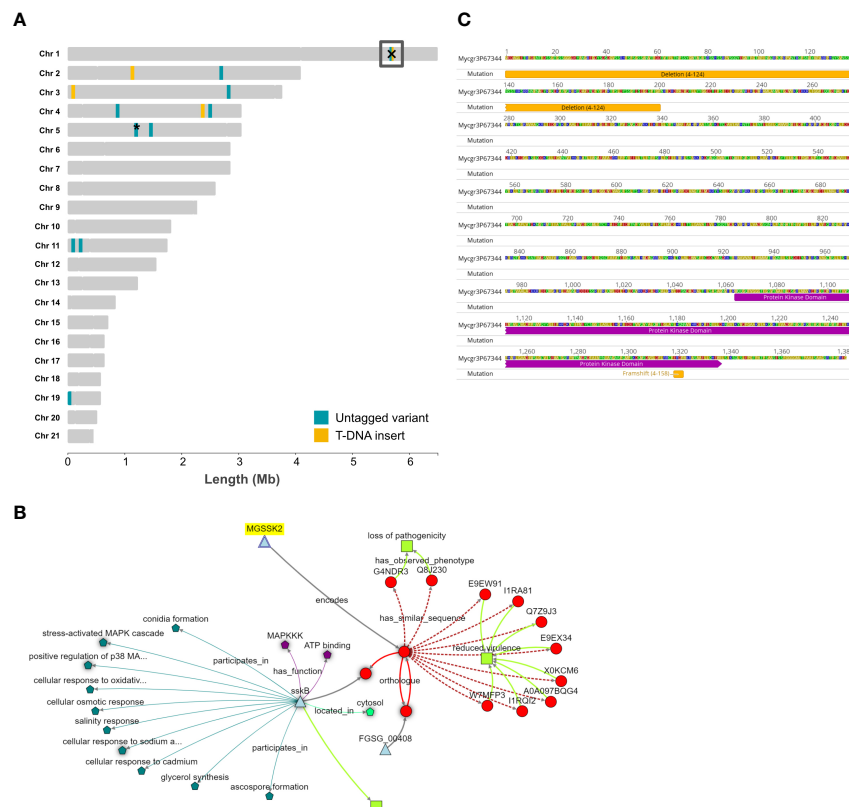
FIGURE 2
The "landscape" of genomic mutation events and the identification of a gene, SSK2, affected by mutations in two independent T-DNA strains.
(A) The 21 chromosomes of the reference isolate IPO323 with the positions of tagged (T-DNA) and untagged (SNPs/indels) identified in the re-sequenced mutant strains. Generated using R package chromoMap (v. 0.3.1) (Anand & Rodriguez Lopez, 2022). Yellow shading indicates T-DNA insertion sites, blue shading represents untagged mutations. The box on chromosome 1 highlights a particular gene affected by both types of mutations in two independent mutant strains, 4-124 and 4-158. The asterisk on chromosome 5 represents that there are untagged variants in genes that are close neighbours, namely ZtritIPO323_04g09806 and ZtritIPO323_04g09809. **(B)** The gene commonly affected by the mutations, *SSK2*, in mutants 4-124 and 4-158, with the positions of the mutation events indicated. **(C)** Zymoseptoria KnetMiner knowledge network analysis indicating that *SSK2* is an orthologue of the corresponding yeast and fungal gene encoding a mitogen-activated kinase kinase kinase (MAPKKK).

A number of intragenic untagged SNP variants were also detected in the T-DNA insertion mutants

As previously discussed, "untagged" variations, including SNPs, insertions and deletions (indels), can occur in genomes and potentially be responsible for phenotypic changes. Our focus was on detecting intragenic variation that could most readily explain the mutant phenotypes. As a result, the full scope of intergenic variation has not been assessed. We next sought to determine the presence and number of additional intragenic untagged mutations in the mutant strains. These were labelled either isolate-specific, present in a single isolate only, or common, in two or more isolates. This analysis identified seventeen intragenic untagged variants, seven of which were single isolate specific. SNPeff identified four isolate-specific high-impact changes to proteins with predicted functions, two of which were in the 15-120 mutant. The genes were affected by three frameshifts, while one gained a stop codon mutation, as listed in Table 2. Three further moderate impact untagged mutations specific to isolate 15-120 were also identified (Table 2).

No predicted high-impact untagged mutations were common to all four isolates (Table 2). However, the same "common" frameshift

mutation was seen in two isolates, 4-124 and 5-51, in a predicted gene of unknown function (Table 2, ZtritIPO323_04g09806). Irrespective of this, the frameshift in this gene was considered unlikely to explain the phenotypes, supported by the fact that isolate 5-51 had a different hyphal growth phenotype compared to 4-124 (Figure 1C). There were two predicted moderate-impact SNP mutations in three mutant isolates and one common low-impact mutation (Table 2). These three variants were in the same position and were of the same type in mutants 4-124 and 5-51. Two of these same variants were also in the 4-158 mutant, but a moderate missense variant was absent (Table 2, ZtritIPO323_04g09929). Labelled with an asterisk in Figure 2A on chromosome 5 is a region where two common variants occurred in the same neighbourhood of genes. On Table 2 these are ZtritIPO323_04g09806 and ZtritIPO323_04g09809.

Altogether this makes four common variants, one predicted high impact, two moderate and one low. The 4-124, 4-158, and 5-51 mutant isolates were generated using potentially the same parental IPO323 glycerol stock (strain names indicate transformation experiments four and five, followed by their respective colony numbers). The presence of these "common" untagged mutations could result from the random mutagenesis method causing similar mutations or, we consider more likely, to be present in the IPO323 stock used in the experiment prior to

TABLE 2 Genes affected by unlinked mutations.

IPO323 Mutant Isolate	IPO323 Chromosome	Putatively Impacted Genes	Interpro Name	SNPeff Predicted Impact	Mutation
4-124	5	ZtritIPO323_04g09806	N/A	High	Frameshift[1]
	4	ZtritIPO323_04g08686	N/A	Moderate	Conservative in-frame deletion[2]
	5	ZtritIPO323_04g09929	P-type ATPase	Moderate	Missense variant[3]
	5	ZtritIPO323_04g09809	Alpha/beta hydrolase fold-3	Low	Synonymous variant[4]
4-158	1	ZtritIPO323_04g02061	Mitogen-activated protein (MAP) kinase kinase kinase Ssk2/Ssk22	High	Frameshift
	4	ZtritIPO323_04g08686	N/A	Moderate	Conservative in-frame deletion[2]
	5	ZtritIPO323_04g09809	Alpha/beta hydrolase fold-3	Low	Synonymous variant[3]
5-51	5	ZtritIPO323_04g09806	N/A	High	Frameshift[1]
	11	ZtritIPO323_04g03036	Zinc finger,GATA-type;PAS domain;PAC motif	High	Frameshift
	4	ZtritIPO323_04g08686	N/A	Moderate	Conservative in-frame deletion[2]
	5	ZtritIPO323_04g09929	P-type ATPase	Moderate	Missense variant[3]
	5	ZtritIPO323_04g09809	Alpha/beta hydrolase fold-3	Low	Synonymous variant[4]
15-120	2	ZtritIPO323_04g06395	Transglutaminase-like	High	Stop gained
	11	ZtritIPO323_04g02979	Pyridoxal phosphate-dependent transferase	High	Frameshift
	3	ZtritIPO323_04g08085	Piwi domain;PAZ domain; Argonaute, linker 1 domain	Moderate	Disruptive in-frame deletion
	4	ZtritIPO323_04g09248	ATPase, V0 complex, subunit e1/e2	Moderate	Missense variant
	19	ZtritIPO323_04g05318	N/A	Moderate	Missense variant

[1]Matching frameshift mutation; [2]Matching in-frame deletion; [3]Matching missense variants; [4]Matching synonymous variants. N/A, not applicable (no InterPro name found).

the mutagenesis. Regardless, we were confident that the "common" variants described in 4-124, 4-158, and 5-51 were unlikely to explain the differing hyphal growth properties.

There was one remarkable finding amongst the isolate-specific untagged high-impact variants which generate loss-of-function mutations in proteins. The previous analysis of T-DNA insertion sites in mutant 4-124 identified an intragenic insertion in the promoter and N-terminal region of a putative MAPKKK protein, orthologous to those encoded by the *SSK2/SSK22* genes in yeast (Maeda et al., 1995: protein ID YNR031C). While analysing the untagged mutations in strain 4-158, we identified a high-impact frameshift mutation in the same gene (Mycgr3G67344/ZtritIPO323_04g02061). Therefore, this gene is listed in Tables 1 and 2 and highlighted with a box on chromosome 1 in Figure 2A. Incidentally, both 4-124 and 4-158 mutant isolates were shown to have reduced virulence and similar stress sensitivities and hyphal growth defects. These similar sensitivities indicated that there may have been a common genetic basis for the shared phenotypes of these two mutant strains, which was later uncovered by genome sequencing. Figure 2B highlights that the respective individual mutations occurred at opposite ends of the predicted protein, with the SNP frameshift

occurring towards the C-terminal protein end but still within a conserved protein kinase sub-domain.

KnetMiner analysis supports ZtSSK2 as an orthologue of yeast and fungal SSK2 MAPKKKs which function in one arm of the HOG1 MAPK pathway

Ahead of any functional complementation attempts and to seek out further information on the Zt*SSK2* candidate gene, we performed a KnetMiner analysis (Hassani-Pak et al., 2021) for predicted orthologues and any associated phenotypic information. The Zymoseptoria KnetMiner draws knowledge graphs from large biological databases and literature from a select few fungi, including *Saccharomyces* yeast, *Fusarium graminearum*, *Neurospora crassa* and *Aspergillus nidulans* (https://knetminer.com/Zymoseptoria_tritici/). Figure 2C shows the knowledge graph generated for Zt*SSK2* using its JGI identifier Mycgr3G67344. The *Z. tritici* gene (MGSSK2) is highlighted and linked to the protein it encodes. It is then further linked to orthologues and proteins with "similar sequences". This

analysis identified orthologues in *Fusarium graminearum* (NCBI: txid5518) and *Aspergillus nidulans* FGSC A4 (NCBI:txid227321). The database for the latter has more associated information on cellular activities and functions. For the similar sequences identified, the majority also share a similar predicted or validated phenotype, "reduced virulence", which agrees well with the observed phenotype of the 4-124 and 4-158 mutants.

Complementation with WT Zt*SSK2* restored full *in planta* disease symptoms, hyphal growth and WT stress responses to both 4-124 and 4-158

We generated gene complementation constructs to determine whether the loss of function of ZtSSK2 was responsible for the reduced virulence and stress sensitivity of the 4-124 and 4-158 mutants. PCR products were obtained that included the native promoter, the complete coding sequence, and the terminator regions of the gene. These were cloned into vector pCGEN and used in

Agrobacterium-mediated fungal transformation on the 4-124 and 4-158 mutants. The resulting transformants were then tested for increased ability to cause STB disease relative to the original mutants and compared to the WT strain. Figure 3A shows that multiple independent complemented strains from each parental background were restored for virulence on wheat, supporting the notion that the loss of SSK2 function in both the 4-124 and 4-158 strains was responsible for the reduction in virulence. Figure 3B provides quantitative data for the observed disease levels incorporating multiple replications.

The "High Osmolarity Glucose" HOG1 pathway is activated in fungi in response to multiple stresses. Figure 1C showed mutant isolates 4-124 and 4-158 have increased sensitivity to oxidative (hydrogen peroxide) and osmotic stress (sorbitol) during blastosporulation on rich nutrient agar. Using the original mutants, the WT strains, and the complemented strains, we next tested whether the re-introduction of functional SSK2 would restore normal sensitivity (reduced hypersensitivity) to these stressors. Figure 3C shows the results of these assays for a complemented strain (representative of three tested with identical results). The figure shows that the re-
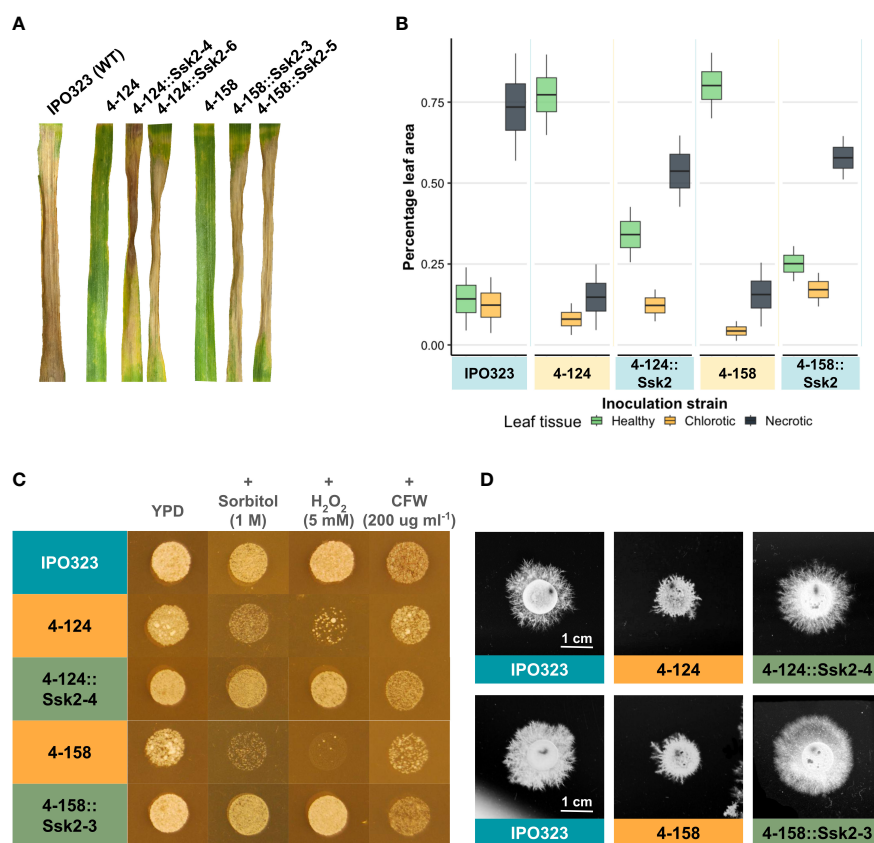
FIGURE 3
Re-introduction of the WT allele of SSK2 restores full virulence and stress responses to both the 4-124 and the 4-158 mutants. **(A)** Wheat leaf infection assays performed with the WT fungus, the two mutant isolates and both mutant isolates complemented with the WT *SSK2* gene (2 independent strains for each shown). The re-introduction of the functional *SSK2* gene restored virulence to both mutants. Photos were taken at 21 dpi. **(B)** Image-based (LemnaGrid) quantification of disease levels on the mutants and *SSK2* complemented strains on infected leaves. The percentage of infected tissue expressing no symptoms (healthy), chlorosis or necrosis is shown. **(C)** The *SSK2* complemented strains restored WT osmotic and oxidative stress sensitivity levels to the original 4-124 and 4-158 mutants. **(D)** The *SSK2* complemented strains generated WT levels of hyphal growth on TWA. Images were taken 10 days after inoculation.

introduction of *SSK2* into both the 4-124 and 4-158 mutants resulted in a loss of the hypersensitivity to osmotic and oxidative stress seen in both original mutants. In contrast, there was no change in sensitivity to calcofluor white (CFW) which is commonly used to impose cell wall stress and is primarily thought to evoke activation of the cell wall integrity MAPK pathway mediated through SLT2 (Mehrabi et al., 2006a).

The other commonly shared phenotype in the Zt*SSK2* mutant strains was the aberrant hyphal growth exhibited on TWA. The two mutant strains consistently produced less extended filaments, which appeared to be hyper-branched compared to its parental strain, IPO323. Figure 3D shows this alongside the complementation results with a functional Zt*SSK2* after 10 dpi on TWA. The representative complementation (one of three tested with identical results) mutant shown displays the restored typical WT hyphal growth phenotype *in vitro*. Figure 3D shows that the re-introduction of *SSK2* fully restores hyphal growth to both the 4-124 and 4-158 mutants, again supporting that loss of this gene was responsible for the original phenotypes observed for both strains. The data also confirm a previously suggested link between reduced virulence phenotypes and aberrant growth morphologies for both strains.

Fungicide sensitivity and kinase activity assays place ZtSSK2p upstream of ZtHOG1p and with non-redundant functionality to the MAPKKK, ZtSTE11

Based on knowledge of Saccharomyces yeasts and other fungi, *SSK2* is likely to function as one of two MAPKKKs that can activate the HOG1 MAPK in response to specific cues (Cheetham et al., 2007; Brewster & Gustin, 2014). Figure 4A shows a representation of the HOG1 signalling pathways. Many orthologous genes in these pathways have been identified in the *Z. tritici* genome, and the MAPKKK STE11 and HOG1 are required for full virulence (Mehrabi et al., 2006b; Kramer et al., 2009). Two previous studies on Zt*SSK1* (upstream of *SSK2*) and Zt*HOG1* mutants have also demonstrated increased resistance to a class of fungicides in mutants, as has also been seen for orthologues in other fungal pathogens (Mehrabi et al., 2006b; Yemelin et al., 2017). To place the predicted *SSK2* in the HOG1 pathway, we tested whether the original mutants exhibited this increased sensitivity and whether sensitivity was restored by complementation with *SSK2*. To this end, we performed a fungicide sensitivity *in vitro* growth assay. This assay revealed that Zt*SSK2* disrupted mutants 4-124 and 4-158
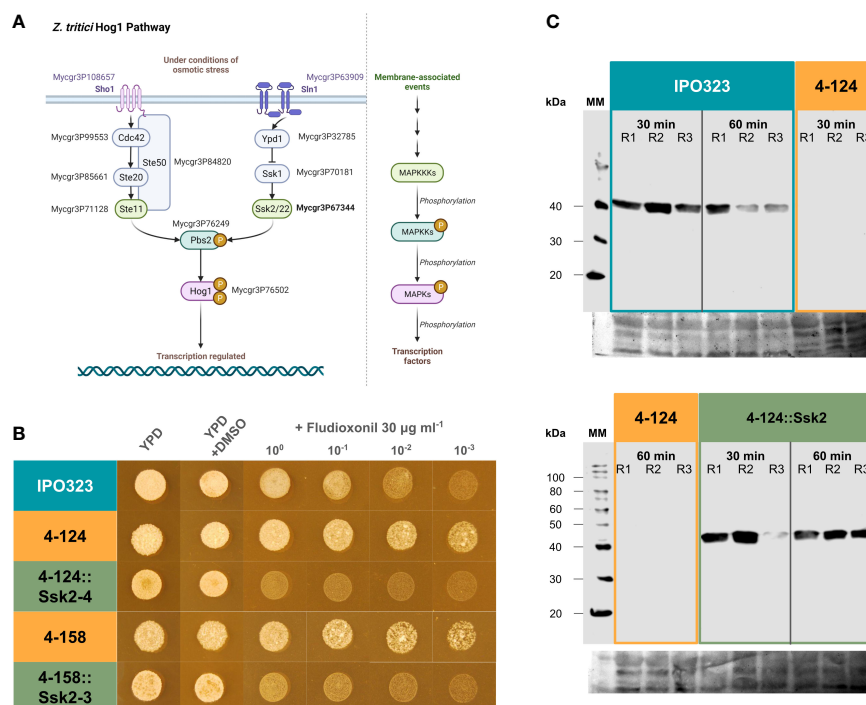
FIGURE 4
The SSK2 MAPKKK is an upstream activator of the HOG1 MAPK pathway and functions non-redundantly to activate the HOG1 protein under stress. **(A)** Representation of the HOG1 signalling pathways characterised in the yeast *Saccharomyces cerevisiae*. Note that HOG1 can be activated by two discrete arms involving either the STE20 or SSK2 MAPKKKs. The orthologous *Z. tritici* genes are labelled with the JGI protein identifiers; Mycgr3P108657 (Sho1), Mycgr3P63909 (Sln1), Mycgr3P99553 (Cdc42), Mycgr3P85661 (Ste20), Mycgr3P71128 (Ste11), Mycgr3P84820 (Ste50) Mycgr3P32785 (Ypd1), Mycgr3P70181 (Ssk1), Mycgr3P67344 (Ssk2), Mycgr3P76249 (Pbs2) and Mycgr3P76502 (HOG1). Created with BioRender.com. **(B)** Fludioxonil sensitivity assays indicate that *SSK2* is an upstream activator of HOG1. HOG1 mutants are less sensitive to this fungicide. The 4-124 and 4-158 strains had a similar reduced sensitivity. However, sensitivity was restored in the complemented strains. The spots indicate serial dilutions of spores. **(C)** HOG1 protein activity assays demonstrate that SSK2 is solely responsible for activating HOG1 in response to oxidative stress. Western blotting using anti-p38 MAPK antibodies to report on the activation of fungal HOG1 proteins. This protein displayed no activity without SSK2p, which was restored in the complemented strains. R1-R3 = replicated experiments. The fungicide sensitivity data and the HOG1 kinase activity data suggest that SSK2p has non-redundant functionality with the STE20 MAPKKK in activating HOG1 under specific conditions.

displayed increased resistance to the phenylpyrrole fungicide fludioxonil, exhibiting similar enhanced growth phenotypes at higher concentrations (Figure 4B). This observation supports previous reports by Mehrabi et al. (2006b) and Yemelin et al. (2017) on HOG1 and SSK1, respectively. Unlike the disrupted mutant isolates, the IPO323 reference strain and ΔZtSSK2::ZtSSK2 complementation strain on YPD supplemented with 30 µg ml^{-1} fludioxonil were more sensitive to fludioxonil. Therefore, these data are consistent with the idea that ZtSSK2p also acts upstream of ZtHOG1p and contributes to fungicide sensitivity independent of the other MAPKKK, STE11.

Much of the previous data has implied that the SSK2 MAP3K functions upstream of the HOG1 MAPK in one of the two potential arms leading to HOG1 kinase activation. To test this link more directly, we studied the activation of the HOG1 protein using anti-active MAPK antibodies and western blotting. Activated MAPK proteins can be detected using anti-active antibodies, which only cross-react with MAPKs when dual phosphorylated in the activation loop region. This dual phosphorylation is performed by the upstream MAPKK, activated by phosphorylation through MAPKKKs. We performed western blots using MAPK p38 anti-active antibodies, which recognise the mammalian ortholog of the fungal HOG1. As such, (anti-rabbit) p38 MAPK antibodies can also be used to test for the activation of HOG1 in fungi (Han et al., 1994). Western blotting was done on protein extracts from 4-124, 4-124::SSK2 complemented strains and IPO323 under oxidative stress induced by H_2O_2. Figure 4C shows that the activation (phosphorylation) of HOG1 was abolished entirely in the ZtSSK2 mutant (4-124), whereas the WT IPO323 and representative ΔZtSSK2::ZtSSK2 complementation strain isolate displayed strong activation. These data provide direct supporting evidence that HOG1 activation, through its dual phosphorylation, is an event downstream and requires the function of the SSK2 MAPKKK in response to oxidative stress. The data suggests, like the fungicide data, that the ZtSTE11 MAPKKK cannot compensate for the loss of function of ZtSSK2 in this response.

Analysis of early ZtSSK2-mediated fungal gene expression on wheat leaves by global RNA-sequencing

To probe the consequence of loss of SSK2 function on infection-related gene expression, we analysed the in planta transcriptome of the 4-124 mutant isolate through RNA-sequencing. Samples were taken at two early in planta infection time points, 6 h and 24 h. These span the normal early switch to hyphal growth seen in the WT strain (including first stomatal penetration events), used as a control to compare overall gene expression across this period. Unfortunately, due to a technical error in RNA sequencing, one replicate from the 6 h IPO323 samples was unusable in the analyses. Another important initial observation was that the "WT" IPO323 strain appeared to have lost a small accessory chromosome, chromosome eighteen. This loss was flagged by the high number

of differentially expressed (DE) genes mapping to the chromosome, followed by discovering the lack of reads mapping to any gene on this chromosome in the WT strain. This dispensable chromosome is highly prone to loss during strain cultivation (Kellner et al., 2014; Möller et al., 2018) but has no known impact on virulence or any other associated phenotype. Therefore, all reads mapped to chromosome eighteen in the SSK2 mutant were removed from subsequent analyses to identify DE genes elsewhere in the genome.

Figure 5A, depicting a principal component analysis (PCA), shows that the biological replicates cluster together (circled) and that principal components split the samples by strain and timepoint. This plot indicates that the mutant isolate 4-124 and WT IPO323 expression patterns differed more by strain than by sampling time. Gene expression levels were then individually compared between the Z. tritici mutant 4-124 and IPO323 strain at each time point. Genes were considered "differentially expressed" at a cut-off where the average expression was affected by a factor of 1-log2 fold (equates to 2-fold change in expression), and false discovery rate adjusted p-values were less than or equal to 0.05. However, due to the failed run of a biological replicate in IPO323 at 6 h, the WT expression is based on only two replicates, increasing the chance of false positives and negatives. As a result, for this analysis, more emphasis was placed on investigating differentially expressed genes (DEGs) identified in the strain contrast (4-124 vs WT) at 24 h, where 3 biological replicates were available for both mutant and WT strain.

In total, 252 significantly differentially expressed genes (DEGs) were identified, listed in Supplementary Table S1. This list included 100 genes from the 4-124 vs IPO323 strain comparison at 24 h, and 74 DEGs at 6 h. Figure 5B shows that an additional 78 genes overlap between the different comparisons. This overlap indicates that similar biological responses occur at both timepoints, most probably due to the relatively close sampling time points (6 h and 24 h). Figure 5B also shows the percentage of up/down-regulated genes in 4-124 versus IPO323. From this, we can see that more genes were downregulated in the ZtSSK2 mutant than IPO323, with 135 unique DEGs across the three comparisons versus 117 up-regulated. Two clusters of genes were identified through PAM K-medoids testing, as shown in Figure 5C. Genes in cluster one are up-regulated in IPO323 compared to 4-124, whilst genes in cluster two show the opposite pattern.

Classification of DEGs into their predicted functions identified 44 functional groups, annotated through GO and Joint Genome Institute data, combined with results retrieved from BLASTp, InterProScan and Blast2GO analyses. This was done similarly to Yemelin et al. (2021), who reported a recent in vitro growth transcriptome analysis on mutant isolates, which included a ΔZtHOG1 mutant isolate (the downstream MAPK activated by the MAPKKK ZtSSK2). As shown in Figure 5D, 175 genes (69.4%) across both 6 h and 24 h strain contrasts could be classified into functional categories. For ease of representation, the fifteen largest categories are shown. For functional groups with three or less differentially expressed members, these were merged into a "Three or less representatives" category (full list of DEGs shown in Supplementary Table S1).
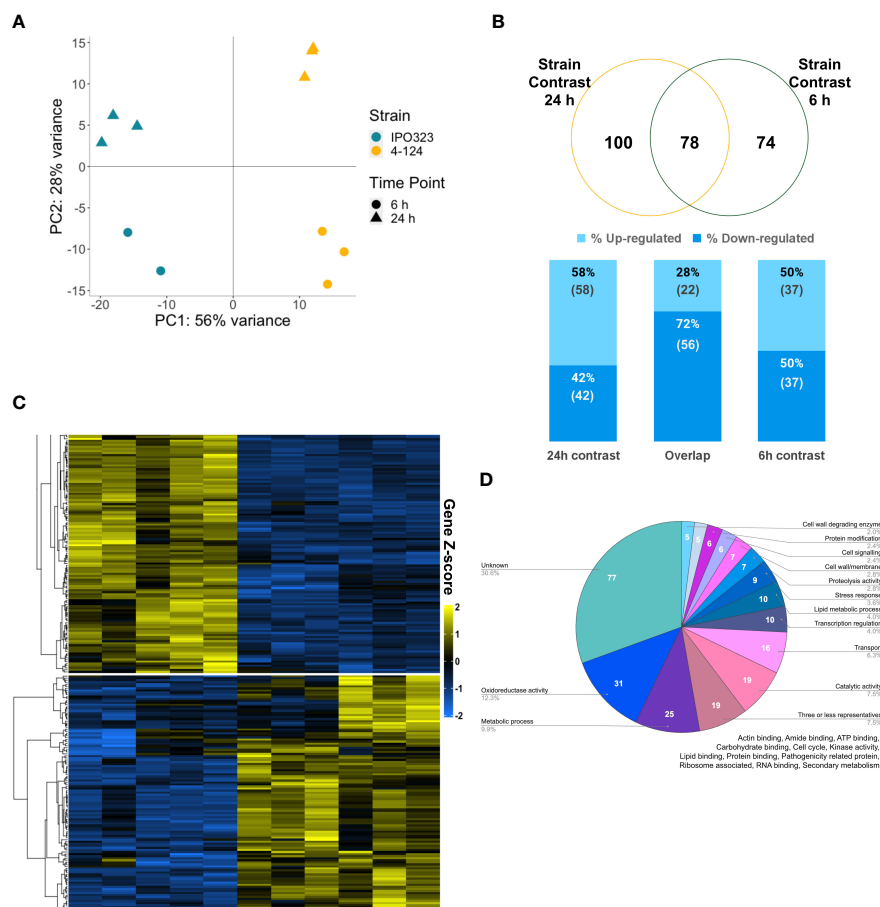
FIGURE 5
The SSK2 MAPKKK affects the fungal transcriptome during the early colonisation of wheat leaves. **(A)** Principal component analysis (PCA) plot of sample distances based on vsd transformed gene count data of the eleven sequenced RNA samples mapped to the *Z. tritici* transcriptome. PC1 explains 56% of the sample variance; this splits IPO323 (blue) and 4-124 (yellow) RNA samples. PC2 explains 28% of the variance, and this splits RNA samples by time, 6 h (triangle) and 24 h (spot). **(B)** Venn diagram showing the number of differentially expressed genes (DEGs) shared and unique to these two contrasts of 4-124 versus IPO323 at 24 h and 6 h timepoints. Stacked percentage bar chart showing the percentage of genes up-regulated (lighter blue) versus down-regulated (darker blue) in the mutant versus WT. These include those which contrast individually at 24 h,6 h and overlapping DEGs in "Both contrasts". Numbers in brackets below the percentage are the actual number of DEGs. **(C)** Expression patterns of the differentially expressed genes using a heatmap generated with "vsd" normalised and log-transformed count data and clustered using PAM (partition around medoids). Gene Z-score scale represents the number of standard deviations away from the mean, averaging across the samples. Cluster 1 broadly represents the genes down-regulated in the 4-124 mutant (yellow bar) vs *Z. tritici* IPO323 (blue bar), and Cluster 2 represents up-regulated genes in the mutant versus the IPO323—generated using DeSeq2 and ComplexHeatmaps in R studio. **(D)** Classification of genes into 44 broad predicted functional groups. Expressed genes annotated through GO and Joint Genome Institute data, combined with results retrieved from BLASTp, InterProScan and Blast2GO analyses.

To determine whether any functional category was overrepresented in the RNAseq data, we performed a GO enrichment analysis using OmicsBox (v.1.3.11). Fisher's Exact test identified one over-represented GO term that met the false discovery rate (FDR) p-value <0.05, which was "oxidoreductase activity" (GO:0016491, FDR p = 4.75E^{-2}). Supplementary Table S1 provides all data for the fungal DEGs and shows the numbers of genes in the functional categories in Figure 5D and for the clusters identified in the heatmap in Figure 5C. Interestingly, the total number of "Stress response" associated genes was lower in cluster two, where expression is up-regulated for the mutant. This may again indicate the reduced activation of HOG1 in 4-124 has

downstream for the expression of genes involved in stress responses.

Finally, we sought to identify any expression changes for any known HOG1 transcriptionally regulated genes, bringing in literature from other fungi and yeasts. For this, we again used the Zymoseptoria KnetMiner tool (https://knetminer.com/Zymoseptoria_tritici/). The KnetMiner keyword search function was used to identify a list of candidate genes putatively associated with HOG1, response to various stresses and developmental stage associated genes from model fungi and the yeast *S. cerevisiae*. These search terms "HOG1", "oxidative stress", "osmotic stress", "cell wall integrity", "hyphal growth", "filamentous growth", and

"dimorphism" generated a list of 1964 genes purportedly linked. A total of 29 of these genes were identified as DE within the 24 h strain comparison (Supplementary Table S1). Matching the same search terms to Yemelin et al. (2021) *in vitro* RNAseq delta HOG1 mutant data identified 47 total genes linked, 6 of which are also within the 24 h strain comparison presented in this study (Supplementary Table S1). These represent strong candidates for SSK2-HOG1 regulation. Table 3 displays the combined results of these analyses from our study and highlights several specific proteins which may confer oxidative and other stress responses through activated ZtSSK2 and HOG1 in *Z. tritici*.

Zt*SSK2* mutants still undergo similar early developmental changes on the leaf surface and do not distinctly affect the wheat transcriptome

Figures 1C, 3D indicated that both the T-DNA *SSK2* mutants were affected for hyphal growth on water agar, when measured at later timepoints after agar inoculation. It was, therefore, possible that this defect may also be responsible for the failure of the mutants to cause full disease on wheat leaves. To test this, we inoculated wheat leaves with spores of mutants and WT strains and analysed cells qualitatively for surface germination at 1, 3 and 9 days post-inoculation using SEM. Qualitative assessments were only made due to simplicity and the fact that if stable genetic ablation of *SSK2* function arrested initial yeast to hyphal growth, this should be apparent in all cells analysed compared to the WT. Figure 6A shows representative images from 9 dpi. Overall, this analysis revealed no major differences in the frequency or level of germination, indicating that the initial germination events are similar in both mutants and WT. The figure also shows that some stomatal penetration events occur and that some hyphae grew across stomates without penetration. This analysis suggests that any hyphal growth (or other) infection-related morphological defects in these Zt*SSK2* mutants likely occurs later in the infection process and not at the initial point of spore germination on leaves.

Similarly, analysis of the wheat transcriptome data suggested that the host does not detect a significant early change in the infection biology between the WT and *SSK2* mutant strains of the pathogen (Figure 6B and Supplementary Table S2). Although some genes were differentially expressed, many lacked functional annotation, and there was no clear change in the expression of pathogenesis-related (or other gene categories) in the gene lists. The overall similarity of the host transcriptome response was emphasised in the PCA analysis (Figure 6B), which demonstrated samples (and replicates) separated on time, not by fungal strain.

Discussion

Whole-genome re-sequencing confirms the genetic instability of the *Z tritici* genome

Our analysis of the small set of random ATMT mutants demonstrated that only single T-DNA inserts in each isolate were

observed. It has previously been shown that, on average, ATMT integrates only one copy of a T-DNA insert into the host genome, reducing the analyses' complexity as there should be fewer functionally impacted genes (Michielse et al., 2005). This consistency also reduces the chances of multiple affected genes contributing to an observed phenotype. However, as shown here, the method (or other handling/storage steps) may also introduce "untagged" genomic variation. These are sequence changes not associated with the T-DNA integration event. In addition, T-DNA integrations have also been associated with other chromosomal aberrations, including rearrangements, deletion, duplication, and inversion (Weld et al., 2006).

Nevertheless, with the random ATMT collection, only a few common untagged variants were observed. The small numbers suggest that the parental strain had changed from the original sequence at a low level. A few putative mechanisms explaining how "untagged" variants arise during the transformation process have been suggested, including that the procedure itself is innately mutagenic; ergo, the stress applied to the genome by the transformation, selection, and regeneration process likely generates untagged effects (Kahmann & Basse, 1999; Maier & Schäfer, 1999; Mullins and Kang, 2001). The absence of chromosome 18 from the IPO323 version used in RNAseq is another extreme example of the high genome instability recognised for this fungus (Möller et al., 2018).

The power of casting a genome-wide net for untagged variants in the mutagenomics approach

Z. tritici was the first genome of a filamentous fungus to have a fully sequenced, all chromosomes from telomere to telomere, reference isolate genome (IPO323) (Goodwin et al., 2011). This sequence has been an excellent scaffold for re-sequencing projects like the mutagenomics analyses described here. Current knowledge of the genome has built on the earlier studies that identified the presence of dispensable/accessory chromosomes, chromosome length, and number polymorphisms (McDonald & Martinez, 1991; Zhan et al., 2002; Wittenberg et al., 2009; Testa et al., 2015). However, next-generation sequencing technologies, and a reduction in the cost of using those technologies, have enabled an approach that has more power to identify changes that would have previously gone unseen. In addition, multiple studies have highlighted the diversity and instability of some areas of *Z. tritici* chromosomes (McDonald et al., 2016; Habig et al., 2017). Whilst the variation in mutant isolates detected here is relatively small compared to natural variation between strains in field populations, the fact it occurs points to significant genome instability in this organism, which may also contribute to its rapid evolution rate.

Identifying tagged integration events has traditionally used selective techniques for laboratory-generated mutants, including chromosome/primer walking, plasmid rescue and PCR-based methods. These have also been used successfully to identify T-DNA insertion and REMI integration sites in other fungi (Michielse et al., 2005; Urban et al., 2015). Whole-genome sequencing also enables the identification of other "untagged" mutations too. To add to the power of this approach in future, the parental strains used in the mutagenesis experiment

TABLE 3 Summary of KnetMiner searches.

| Z. tritici differentially expressed genes 24 h			KnetMiner Search Match (Y/N)						
Gene Name	Description	Log2 FC	HOG1	Oxidative stress	Osmotic stress	Cell wall integrity	Hyphal growth	Filamentous growth	Dimorphism
ZtritIPO323_04g10603	Linoleate diol synthase	−2.59	N	Y	N	N	N	N	N
ZtritIPO323_04g11352	Glucan 1,3-beta-glucosidase	−2.05	N	N	N	Y	N	N	N
ZtritIPO323_04g02810	Siderophore-dependent iron transporter	1.87	N	N	N	N	Y	N	N
ZtritIPO323_04g00700	THI5-LIKE	−2.04	N	Y	N	N	Y	N	N
ZtritIPO323_04g00819	NADP-dependent alcohol dehydrogenase like	−2.72	Y	Y	N	N	N	N	N
ZtritIPO323_04g01183	Monomeric glyoxalase I	−2.26	Y	Y	Y	N	N	N	N
ZtritIPO323_04g01615	Basic-leucine zipper domain	3.29	N	Y	N	N	N	N	N
ZtritIPO323_04g07726	Related to Woronin body major	1.99	N	Y	N	N	N	N	N
ZtritIPO323_04g10309	Glycoside hydrolase family 17	2.08	Y	Y	N	Y	N	N	N
ZtritIPO323_04g02407	Aryl-alcohol dehydrogenase Aad14	−2.69	N	Y	N	N	N	N	N
ZtritIPO323_04g02517	Glutathione-s-transferase like	−2.43	N	Y	N	N	N	N	N
ZtritIPO323_04g01836	Zinc finger transcription factor ace1 like	2.4	N	N	Y	N	N	N	N
ZtritIPO323_04g11895	MDR multidrug transporter	−3.04	N	Y	N	N	N	N	N
ZtritIPO323_04g13735	G-coupled receptor	−1.79	Y	Y	Y	Y	Y	Y	Y
ZtritIPO323_04g05630	Peptidase M3A/M3B catalytic domain	3.07	Y	Y	N	Y	N	N	N
ZtritIPO323_04g10608	Carboxylesterase B family	−2.43	N	Y	N	N	N	N	N
ZtritIPO323_04g08711	RNA binding	−2.26	N	Y	N	N	N	N	N
ZtritIPO323_04g09472	Lysophospholipase 2	3.37	N	Y	N	Y	Y	N	N
ZtritIPO323_04g02648	Phospholipase D/ Transphosphatidylase	−2.59	N	N	N	N	Y	N	Y
ZtritIPO323_04g11589	Alcohol dehydrogenase -like domain-containing	−3.5	Y	Y	N	N	N	N	N
ZtritIPO323_04g00114	NADP-dependent mannitol dehydrogenase	−2.47	N	Y	N	N	N	N	N
ZtritIPO323_04g06038	2,3-butanediol dehydrogenase like	3.9	N	Y	N	N	N	N	N
ZtritIPO323_04g07298	Acid trehalase	−3.2	Y	Y	N	Y	N	N	Y
ZtritIPO323_04g08522	Glutamate decarboxylase	−2.92	Y	Y	N	N	N	N	N
ZtritIPO323_04g10685	Alternative oxidase	3.53	N	Y	N	N	Y	N	N
ZtritIPO323_04g12868	ABC transporter	2.87	Y	Y	N	Y	N	N	N
ZtritIPO323_04g08156	CAT1 catalase	−2.51	Y	Y	Y	Y	Y	N	N
ZtritIPO323_04g10208	Zinc-binding alcohol dehydrogenase like	−3.19	N	Y	N	N	N	N	N
ZtritIPO323_04g13370	3-ketoacyl-ACP reductase like	−2.93	N	Y	N	N	N	N	N
ZtritIPO323_04g03984	Lipase 3	4.15	N	Y	N	N	N	N	N
ZtritIPO323_04g04239	Helicase superfamily 1/2	3.25	N	Y	N	Y	Y	N	N
ZtritIPO323_04g04241	Acetate transporter GPR1/ FUN34/SatP family	4.75	N	Y	N	N	N	N	N
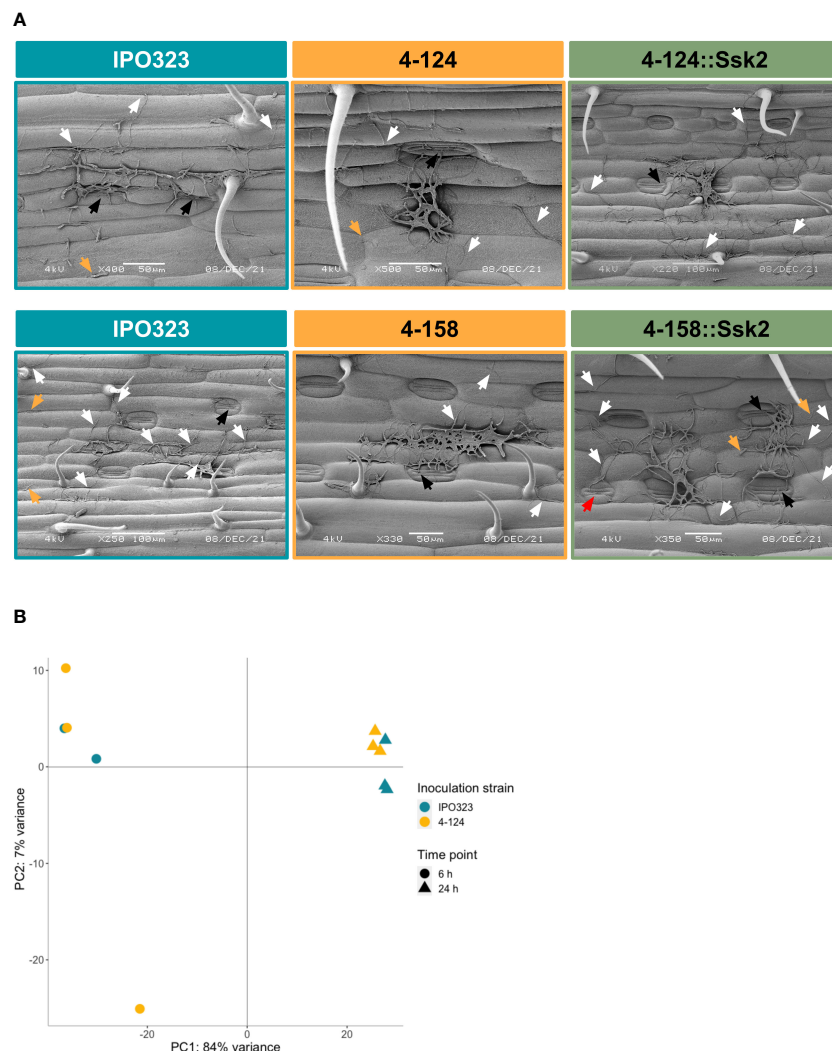
FIGURE 6
Microscopy and gene expression analyses suggest that wheat does not differentially recognise fungal SSK2 mutants from WT during early leaf infection. **(A)** SEM images were taken nine days post-inoculation of WT and SSK2 mutants on the wheat leaf surface. This analysis failed to identify any consistent differences between the tested strains suggesting that early developmental changes are not profoundly affected by the loss of SSK2 function during this initial infection stage. White arrows indicate spore germination, with ungerminated spores labelled by yellow arrows and attempts to penetrate stomata indicated by black arrows. In the representative image for the complemented 4-158 mutant, a red arrow indicates a filament extending over a closed stoma. **(B)** Principal component analysis (PCA) plot of sample distances based on vsd transformed gene count data of the eleven sequenced RNA samples mapped to the Chinese Spring wheat genome assembly. PC1 explains 84% of the sample variance; this splits the RNA samples by time, 6 h (triangle) and 24 h (spot). Only 7% of the variance is explained by PC2 (fungal strain). Overall, these data suggest that wheat is not differing in its response to early infection attempts by the WT and SSK2 mutant fungi.

should also have their genomes re-sequenced at the outset. This inclusion would help identify putative untagged effects as either "background" mutations in isolate stocks from those potentially commonly induced mutations due to the mutagenesis experiment. The fact that the reduced virulence and stress phenotypes in strain 4-158 were shown to be caused by a SNP mutation in *SSK2*, which was independent of the integration of the T-DNA, emphasises the importance of using whole genome re-sequencing approaches. How this mutation occurred remains currently unclear.

There also remain mutant strains from this analysis which require further characterisation, namely 15-120 and 5-51. Previous attempts to link candidates associated with intergenic T-DNA insertion sites in 5-

51 and 15-120 (Table 1) to their respective phenotypes (Figure 1) were unsuccessful. However, after checking their whole genomes for untagged mutations the other likely candidates uncovered in this study (Table 2), highlighting the power of this mutagenomic approach. In the case of 5-51, a frameshift mutation in ZtritIPO323_04g03036 (Mycgr3G76651.1), the White Collar-1 (Zt*WCO1*) gene, we consider the most likely candidate given the recent literature on the importance this gene in dimorphic switching and the role of light-responsive proteins in orchestrating the *Z. tritici* infection (Kilaru et al., 2022). We considered the intergenic T-DNA insertion (Table 1) in 5-51 unlikely to explain the phenotype, and the other untagged variants (Table 2) are common to 4-124 which has a

different phenotype (Figure 1). However, we recognise there could be other undetected chromosomal (or other) rearrangements that could also impart phenotypic changes in these strains.

Efficient stress response pathways are interlinked with fungal virulence and hyphal growth traits

Fungi continuously sense and respond to environmental cues; molecular and genetic circuitry behind those mechanisms make "decisions" that affect the transitions into lifecycle phases (Lengeler et al., 2000). Therefore, the accuracy of detection and efficiency of those circuits is paramount for an organism's survival. For example, the invading *Z. tritici* hyphae are exposed to the leaf apoplast environment of the wheat host. Keon et al. (2007) reported that this is a low-nutrient environment, and upon detection by the host, the fungus is exposed to several stressors. Reactive oxygen species, ions, plant signalling hormones and enzymes attacking major fungal cell wall components, and other microorganisms are just some examples of elements that an apoplastic fungal pathogen must "overcome" to cause infection (Rodriguez-Moreno et al., 2018). Fungal enzymes with oxidoreductase activity are involved in various cellular processes and have been linked to pathogenicity and protection against host-defence responses (Singh et al., 2021). Previous transcriptomic studies in *Z. tritici* identified a subset of oxidoreductases, namely secreted chloroperoxidases, which displayed up-regulation at 1 dpi peaking later at 4 dpi (Rudd et al., 2015). Similarly, in Palma-Guerrero et al. (2016), oxidoreductases were identified as the most up-regulated category at seven dpi of WT infection. Furthermore, oxidoreductases have previously been shown to be up-regulated in response to UV radiation to reduce the levels of free radicals (McCorison & Goodwin, 2020).

The HOG1 pathway has been described as a conserved and prolific regulator of fungal growth, involved in multiple stress responses, cell cycle progression, morphogenesis, cell wall biogenesis and virulence (Hohmann, 2009; Brewster & Gustin, 2014). Despite this, the control, upstream sensors, activation, and functions of the orthologous HOG1 pathways vary between fungi. The RNA sequencing results highlighted that the between the Zt*SSK2* mutant and WT *in planta* the largest differentially expressed category were genes with the GO term relating to oxidoreductase activity. Combined with the Zt*SSK2* mutants displayed enhanced sensitivity to oxidative stresses, it appears likely that the MAPKKK regulates the HOG1 pathway to improve resilience to this stress through regulating oxidoreductase activities. The western blot result indicated that in the Zt*SSK2* mutant, the activation of the HOG1 kinase is impacted under oxidative stress conditions. Whilst the lack of activation of HOG1 observed in the SSK2 mutant could also have been either delayed or extremely short-lived, the data presented suggest that the MAPKKK, Zt*STE11* cannot compensate for the loss of SSK2 function in responses to oxidative stress, fungicides or in virulence. In Kramer et al. (2009), it was noted that Zt*STE11* null mutants were impacted in their virulence but were not sensitive to the fungal growth stressors tested, including oxidative stress using H_2O_2. Together these data suggest that SSK2p functions as the major arm in the HOG1 activation pathway in response to oxidative stress. The fact

that both the MAPKKKs STE11 and SSK2 are independently required for full virulence on wheat suggests they may both be responsible for full (maximal) HOG1 activation to achieve this or that either or both proteins can affect virulence independent of HOG1. Double mutants (should they be viable) may be needed to test these ideas. However, what we report here parallels work from the animal pathogen *Candida albicans* which demonstrated that only SSK2 was able to activate HOG1 (Cheetham et al., 2007). Therefore, it may be that the STE11 MAPKKK may not function through the HOG1 MAPK in *Z. tritici*.

The SSK2-HOG1 pathway is important for infection-related stress gene expression

Much remains to be understood about the pre-symptomatic latent phase of *Z. tritici* infection, particularly in the early pre-stomatal penetration period. However, evidence exists that this provides minimal external nutrition to early hyphal growth (Rudd et al., 2015; Palma-Guerrero et al., 2016). Previous transcriptomic studies *in planta* typically sample at 24h dpi as the earliest timepoint, to capture surface germination and early penetration of the leaf surface (Rudd et al., 2015). However, a consideration brought to attention by Fantozzi et al. (2021) is the asynchronous development of *Z. tritici in planta*. In short, invading hyphae follow their individual asynchronous developmental program, and expression profiles likely reflect this. However, our data showed a clear separation of overall transcriptomic data between the WT and mutant fungus, indicating that *SSK2* gene loss was a key driver for this, and was still exerting effects on the fungal transcriptome irrespective of any asynchronous development.

Before this work, the earliest time point for dual transcriptomic studies *in planta* was reported by Benbow et al. (2020). This study aimed to determine the plant responses to *Z. tritici* in two wheat cultivars, a resistant cultivar (cv. Stigg) and a susceptible (cv. Longbow), at four timepoints, starting at 6 h. They focused on the differing stress responses mounted by wheat against the fungus and identifying disease response genes involved in the early response to *Z. tritici*. As such, they did not detail any differences in the fungal transcriptome between cultivars. Whilst Benbow et al. (2020) saw a difference between host responses to infection in susceptible versus resistant cultivars, we show that there is a limited difference between the expression profiles of a susceptible cultivar responding to a reduced virulence mutant compared to a wild-type virulent strain, particularly at this early time point. This is supported by the observation that only a few germinated spore filaments were seen to have penetrated.

The leaf surface SEM imaging indicated little appreciable visual difference between the WT and defective Zt*SSK2* mutant strains, despite the noticeable phenotypic differences seen macroscopically *in vitro*. So, unless there is a significant difference in the surface PAMPs presented by the WT and mutant strains, it is difficult to envisage how the host would respond differently at such early stages. This could, however, change for later stages. It is conceivable that the reduced virulence of *SSK2* mutants could arise from a combination of reduced hyphal growth at later stages and greater sensitivity to some of the plant-imposed stresses

discussed. Therefore, the exact phase of the infection cycle which imposes the most significant stress on the defective *SSK2* mutant, hindering its virulence, awaits further resolution. Despite this, the strains and tools developed in this initial "mutagenomic" analysis pave the way for an accelerated understanding of the genes and processes required for wheat infection by *Z. tritici*; more broadly, this offers a pipeline which could be exploited to understand the pathogenesis of fungal plant pathogens in general further.

Data availability statement

The datasets presented in this study can be found in onlinerepositories. The names of the repository/repositories and accession number(s) can be found below: https://www.ncbi.nlm.nih. gov/, GSE225623, SAMN33272753, SAMN33272754, SAMN33272755, SAMN33272756.

Author contributions

Funding

Conflict of interest

The authors declare that the research was conducted in the absence of any commercial or financial relationships that could be construed as a potential conflict of interest.

Publisher's note

All claims expressed in this article are solely those of the authors and do not necessarily represent those of their affiliated organizations, or those of the publisher, the editors and the reviewers. Any product that may be evaluated in this article, or claim that may be made by its manufacturer, is not guaranteed or endorsed by the publisher.

Supplementary material

The Supplementary Material for this article can be found online at: https://www.frontiersin.org/articles/10.3389/fpls.2023.1140824/ full#supplementary-material

SUPPLEMENTARY TABLE 1
The differentially expressed fungal genes (WT vs SSK2 mutant) at 6 and 24 hpi on the wheat leaf surface (.xls).

SUPPLEMENTARY TABLE 2
The differentially expressed wheat genes following early infection by WT and SSK2 mutant strains (.xls).

References

Anand, L., and Rodriguez Lopez, C. M. (2022). ChromoMap: an R package for interactive visualization of multi-omics data and annotation of chromosomes. *BMC Bioinf.* 23 (1), 33. doi: 10.1186/s12859-021-04556-z

Benbow, H. R., Brennan, C. J., Zhou, B., Christodoulou, T., Berry, S., Uauy, C., et al. (2020). Insights into the resistance of a synthetically-derived wheat to Septoria tritici blotch disease: Less is more. *BMC Plant Biol.* 20 (1), 1–23. doi: 10.1186/s12870-020-02612-z

Benjamini, Y., and Hochberg, Y. (1995). Controlling the false discovery rate: A practical and powerful approach to multiple testing. *J. R. Stat. Society Ser. B. (Methodological)* 57 (1), 289–300. doi: 10.1111/j.2517-6161.1995.tb02031.x

Bolger, A. M., Lohse, M., and Usadel, B. (2014). Trimmomatic: a flexible trimmer for illumina sequence data. *Bioinformatics* 30 (15), 2114–2120. doi: 10.1093/bioinformatics/btu170

Brewster, J. L., and Gustin, M. C. (2014). Hog1: 20 years of discovery and impact. *Sci. Signaling* 7 (343). doi: 10.1126/scisignal.2005458

Cheetham, J., Smith, D. A., da Silva Dantas, A., Doris, K. S., Patterson, M. J., Bruce, C. R., et al. (2007). A single MAPKKK regulates the Hog1 MAPK pathway in the pathogenic fungus *Candida albicans*. *Mol. Biol. Cell* 18 (11), 4603–4614. doi: 10.1091/mbc.e07-06-0581

Chen, H., King, R., Smith, D., Bayon, C., Ashfield, T., Torriani, S., et al. (2023). Combined pangenomics and transcriptomics reveals core and redundant virulence processes in a rapidly evolving fungal plant pathogen. *BMC Biol.* 21 (1), 24. doi: 10.1186/s12915-023-01520-6

Fantozzi, E., Kilaru, S., Gurr, S. J., and Steinberg, G. (2021). Asynchronous development of *Zymoseptoria tritici* infection in wheat. *Fungal Genet. Biol.* 146, 103504. doi: 10.1016/j.fgb.2020.103504

Fisher, M. C., Henk, D. A., Briggs, C. J., Brownstein, J. S., Madoff, L. C., McCraw, S. L., et al. (2012). Emerging fungal threats to animal, plant and ecosystem health. *Nature* 484 (7393), 186–194. doi: 10.1038/nature10947

Francisco, C. S., Ma, X., Zwyssig, M. M., McDonald, B. A., and Palma-Guerrero, J. (2019). Morphological changes in response to environmental stresses in the fungal plant pathogen *Zymoseptoria tritici*. *Sci. Rep.* 9 (1), 9642. doi: 10.1038/s41598-019-45994-3

Goodwin, S. B., M'Barek, S., Dhillon, B., Wittenberg, A. H. J., Crane, C. F., Hane, J. K., et al. (2011). Finished genome of the fungal wheat pathogen *Mycosphaerella graminicola* reveals dispensome structure, chromosome plasticity, and stealth pathogenesis. *PloS Genet.* 7 (6), e1002070. doi: 10.1371/journal.pgen.1002070

Grandaubert, J., Bhattacharyya, A., and Stukenbrock, E. H. (2015). RNA-seq-Based gene annotation and comparative genomics of four fungal grass pathogens in the genus zymoseptoria identify novel orphan genes and species-specific invasions of transposable elements. *G3 Genes|Genomes|Genetics* 5 (7), 1323–1333. doi: 10.1534/g3.115.017731

Habig, M., Quade, J., and Stukenbrock, E. H. (2017). Forward genetics approach reveals host genotype-dependent importance of accessory chromosomes in the fungal

wheat pathogen *Zymoseptoria tritici*. *MBio* 8 (6), e01919-17. doi: 10.1128/mBio.01919-17

Han, J., Lee, J.-D., Bibbs, L., and Ulevitch, R. J. (1994). A MAP kinase targeted by endotoxin and hyperosmolarity in mammalian cells. *Science* 265 (5173), 808–811. doi: 10.1126/science.7914033

Hassani-Pak, K., Singh, A., Brandizi, M., Hearnshaw, J., Parsons, J. D., Amberkar, S., et al. (2021). KnetMiner: a comprehensive approach for supporting evidence-based gene discovery and complex trait analysis across species. *Plant Biotechnol. J.* 19 (8), 1670–1678. doi: 10.1111/pbi.13583

Hodgens, C., Chang, N., Eric Schaller, G., and Kieber, J. J. (2020). Mutagenomics: A rapid, high-throughput method to identify causative mutations from a genetic screen. *Plant Physiol.* 184 (4), 1658–1673. doi: 10.1104/pp.20.00609

Hohmann, S. (2009). Control of high osmolarity signalling in the yeast saccharomyces cerevisiae. *FEBS Lett.* 583 (24), 4025–4029. doi: 10.1016/j.febslet.2009.10.069

Kahmann, R., and Basse, C. (1999). REMI (Restriction enzyme mediated integration) and its impact on the isolation of pathogenicity genes in fungi attacking plants. *Eur. J. Plant Pathol.* 105 (3), 221–229. doi: 10.1023/A:1008757414036

Kellner, R., Bhattacharyya, A., Poppe, S., Hsu, T. Y., Brem, R. B., and Stukenbrock, E. H. (2014). Expression profiling of the wheat pathogen *Zymoseptoria tritici* reveals genomic patterns of transcription and host-specific regulatory programs. *Genome Biol. Evol.* 6 (6), 1353–1365. doi: 10.1093/gbe/evu101

Keon, J., Antoniw, J., Carzaniga, R., Deller, S., Ward, J. L., Baker, J. M., et al. (2007). Transcriptional adaptation of *Mycosphaerella graminicola* to programmed cell death (PCD) of its susceptible wheat host. *Mol. Plant-Microbe Interact.* 20 (2), 178–193. doi: 10.1094/MPMI-20-2-0178

Kilaru, S., Fantozzi, E., Cannon, S., Schuster, M., Chaloner, T. M., Guiu-Aragones, C., et al. (2022). *Zymoseptoria tritici* white-collar complex integrates light, temperature and plant cues to initiate dimorphism and pathogenesis. *Nat. Commun.* 13 (1), 5625. doi: 10.1038/s41467-022-33183-2

Kim, D., Paggi, J. M., Park, C., Bennett, C., and Salzberg, S. L. (2019). Graph-based genome alignment and genotyping with HISAT2 and HISAT-genotype. *Nat. Biotechnol.* 37 (8), 907–915. doi: 10.1038/s41587-019-0201-4

King, R., Urban, M., Lauder, R. P., Hawkins, N., Evans, M., Plummer, A., et al. (2017). A conserved fungal glycosyltransferase facilitates pathogenesis of plants by enabling hyphal growth on solid surfaces. *PloS Pathog.* 13 (10), e1006672. doi: 10.1371/journal.ppat.1006672

Kramer, B., Thines, E., and Foster, A. J. (2009). MAP kinase signalling pathway components and targets conserved between the distantly related plant pathogenic fungi *Mycosphaerella graminicola* and *Magnaporthe grisea*. *Fungal Genet. Biol.* 46 (9), 667–681. doi: 10.1016/j.fgb.2009.06.001

Lendenmann, M. H., Croll, D., Stewart, E. L., and McDonald, B. A. (2014). Quantitative trait locus mapping of melanization in the plant pathogenic fungus *Zymoseptoria tritici*. *Genes|Genomes|Genetics* 4 (12), 2519–2533. doi: 10.1534/g3.114.015289

Lengeler, K. B., Davidson, R. C., D'souza, C., Harashima, T., Shen, W.-C., Wang, P., et al. (2000). Signal transduction cascades regulating fungal development and virulence. *Microbiol. Mol. Biol. Rev.* 64 (4), 746–785. doi: 10.1128/MMBR.64.4.746-785.2000

Liao, Y., Smyth, G. K., and Shi, W. (2014). FeatureCounts: An efficient general purpose program for assigning sequence reads to genomic features. *Bioinformatics* 30 (7), 923–930. doi: 10.1093/bioinformatics/btt656

Love, M. I., Huber, W., and Anders, S. (2014). Moderated estimation of fold change and dispersion for RNA-seq data with DESeq2. *Genome Biol.* 15 (12), 1–21. doi: 10.1186/s13059-014-0550-8

Maeda, T., Takekawa, M., and Saito, H. (1995). Activation of yeast PBS2 MAPKK by MAPKKKs or by binding of an SH3-containing osmosensor. *Science* 269 (5223), 554–558. doi: 10.1126/science.7624781

Maier, F. J., and Schäfer, W. (1999). Mutagenesis *via* insertional or restriction enzyme-mediated integration (REMI) as a tool to tag pathogenicity related genes in plant pathogenic fungi. *Biol. Chem.* 380 (7–8), 855–864. doi: 10.1515/BC.1999.105

McCorison, C. B., and Goodwin, S. B. (2020). The wheat pathogen *Zymoseptoria tritici* senses and responds to different wavelengths of light. *BMC Genomics* 21 (1), 1–15. doi: 10.1186/s12864-020-06899-y

McDonald, B. A., and Martinez, J. P. (1991). Chromosome length polymorphisms in a septoria tritici population. *Curr. Genet.* 19 (4), 265–271. doi: 10.1007/BF00355053

McDonald, M. C., McGinness, L., Hane, J. K., Williams, A. H., Milgate, A., and Solomon, P. S. (2016). Utilising gene tree variation to identify candidate effector genes in *Zymoseptoria tritici*. *G3: Genes Genomes Genet.* 6 (4), 779–791. doi: 10.1534/g3.115.025197

Mehrabi, R., van der Lee, T., Waalwijk, C., and Gert, H. J. K. (2006a). MgSlt2, a cellular integrity MAP kinase gene of the fungal wheat pathogen mycosphaerella graminicola, is dispensable for penetration but essential for invasive growth. *Mol. Plant-Microbe Interact.* 19 (4), 389–398. doi: 10.1094/MPMI-19-0389

Mehrabi, R., Zwiers, L.-H., de Waard, M. A., and Kema, G. H. J. (2006b). MgHog1 regulates dimorphism and pathogenicity in the fungal wheat pathogen *Mycosphaerella graminicola*. *Mol. Plant-Microbe Interact.* 19 (11), 1262–1269. doi: 10.1094/MPMI-19-1262

Meile, L., Croll, D., Brunner, P. C., Plissonneau, C., Hartmann, F. E., McDonald, B. A., et al. (2018). A fungal avirulence factor encoded in a highly plastic genomic region triggers partial resistance to septoria tritici blotch. *New Phytol.* 219 (3), 1048–1061. doi: 10.1111/nph.15180

Michielse, C. B., Hooykaas, P. J. J., van den Hondel, C. A. M. J. J., and Ram, A. F. J. (2005). *Agrobacterium*-mediated transformation as a tool for functional genomics in fungi. *Curr. Genet.* 48 (1), 1–17. doi: 10.1007/s00294-005-0578-0

Mohammadi, N., Mehrabi, R., Mirzadi Gohari, A., Roostaei, M., Mohammadi Goltapeh, E., Safaie, N., et al. (2020). MADS-box transcription factor ZtRlm1 is responsible for virulence and development of the fungal wheat pathogen *Zymoseptoria tritici*. *Front. Microbiol.* 11. doi: 10.3389/fmicb.2020.01976

Möller, M., Habig, M., Freitag, M., and Stukenbrock, E. H. (2018). Extraordinary genome instability and widespread chromosome rearrangements during vegetative growth. *Genetics* 210 (2), 517–529. doi: 10.1534/genetics.118.301050

Motteram, J., Küfner, I., Deller, S., Brunner, F., Hammond-Kosack, K. E., Nürnberger, T., et al. (2009). Molecular characterisation and functional analysis of MgNLP, the sole NPP1 domain-containing protein, from the fungal wheat leaf pathogen *Mycosphaerella graminicola*. *Mol. Plant-Microbe Interact.* 22 (7), 790–799. doi: 10.1094/MPMI-22-7-0790

Motteram, J., Lovegrove, A., Pirie, E., Marsh, J., Devonshire, J., van de Meene, A., et al. (2011). Aberrant protein n-glycosylation impacts upon infection-related growth transitions of the haploid plant-pathogenic fungus *Mycosphaerella graminicola*. *Mol. Microbiol.* 81 (2), 415–433. doi: 10.1111/j.1365-2958.2011.07701.x

Mullins, E. D., and Kang, S. (2001). Transformation: a tool for studying fungal pathogens of plants. *Cell. Mol. Life Sci.* 58 (14), 2043–2052. doi: 10.1007/PL00000835

Nan, G.-L., and Walbot, V. (2009). Plasmid rescue: Recovery of flanking genomic sequences from transgenic transposon insertion sites. In *Methods Mol. Biol.* 526 (1), 101–109. doi: 10.1007/978-1-59745-494-0_8

Oggenfuss, U., Badet, T., Wicker, T., Hartmann, F. E., Singh, N. K., Abraham, L., et al. (2021). A population-level invasion by transposable elements triggers genome expansion in a fungal pathogen. *ELife* 10, 1–25. doi: 10.7554/eLife.69249

Østergaard, L., and Yanofsky, M. F. (2004). Establishing gene function by mutagenesis in *Arabidopsis thaliana*. *Plant J.* 39 (5), 682–696. doi: 10.1111/j.1365-313X.2004.02149.x

Palma-Guerrero, J., Torriani, S. F. F., Zala, M., Carter, D., Courbot, M., Rudd, J. J., et al. (2016). Comparative transcriptomic analyses of *Zymoseptoria tritici* strains show complex lifestyle transitions and intraspecific variability in transcription profiles. *Mol. Plant Pathol.* 17 (6), 845–859. doi: 10.1111/mpp.12333

Penna, S., and Jain, S. M. (2017). Mutant resources and mutagenomics in crop plants. *Emir. J. Food Agric.* 29 (9), 651–657. doi: 10.9755/ejfa.2017.v29.i9.86

Plissonneau, C., Hartmann, F. E., and Croll, D. (2018). Pangenome analyses of the wheat pathogen *Zymoseptoria tritici* reveal the structural basis of a highly plastic eukaryotic genome. *BMC Biol.* 16 (1), 5. doi: 10.1186/s12915-017-0457-4

Raudvere, U., Kolberg, L., Kuzmin, I., Arak, T., Adler, P., Peterson, H., et al. (2019). g:Profiler: a web server for functional enrichment analysis and conversions of gene lists, (2019 update). *Nucleic Acids Res.* 47 (W1), W191–W198. doi: 10.1093/nar/gkz369

Rodriguez-Moreno, L., Ebert, M. K., Bolton, M. D., and Thomma, B. P. H. J. (2018). Tools of the crook-infection strategies of fungal plant pathogens. *Plant J.* 93 (4), 664–674. doi: 10.1111/tpj.13810

Rossman, A. Y., Crous, P. W., Hyde, K. D., Hawksworth, D. L., Aptroot, A., Bezerra, J. L., et al. (2015). Recommended names for pleomorphic genera in *Dothideomycetes*. *IMA Fungus* 6 (2), 507–523. doi: 10.5598/imafungus.2015.06.02.14

Rudd, J. J., Kanyuka, K., Hassani-Pak, K., Derbyshire, M., Andongabo, A., Devonshire, J., et al. (2015). Transcriptome and metabolite profiling of the infection cycle of *Zymoseptoria tritici* on wheat reveals a biphasic interaction with plant immunity involving differential pathogen chromosomal contributions and a variation on the hemibiotrophic lifestyle definition. *Plant Physiol.* 167 (3), 1158–1185. doi: 10.1104/pp.114.255927

Rudd, J. J., Keon, J., and Hammond-Kosack, K. E. (2008). The wheat mitogen-activated protein kinases TaMPK3 and TaMPK6 are differentially regulated at multiple levels during compatible disease interactions with *Mycosphaerella graminicola*. *Plant Physiol.* 147 (2), 802–815. doi: 10.1104/pp.108.119511

Singer, T., and Burke, E. (2003). "High-throughput TAIL-PCR as a tool to identify DNA flanking insertions." in *Plant Functional Genomics* (Humana Press) 236, 241–272. doi: 10.1385/1-59259-413-1:241

Singh, Y., Nair, A. M., and Verma, P. K. (2021). Surviving the odds: From perception to survival of fungal phytopathogens under host-generated oxidative burst. *Plant Commun.* 2 (3), 100142. doi: 10.1016/j.xplc.2021.100142

Steinberg, G. (2015). Cell biology of *Zymoseptoria tritici*: Pathogen cell organisation and wheat infection. *Fungal Genet. Biol.* 79, 17–23. doi: 10.1016/j.fgb.2015.04.002

Testa, A., Oliver, R., and Hane, J. (2015). Overview of genomic and bioinformatic resources for *Zymoseptoria tritici*. *Fungal Genet. Biol.* 79, 13–16. doi: 10.1016/j.fgb.2015.04.011

Urban, M., King, R., Hassani-Pak, K., and Hammond-Kosack, K. E. (2015). Whole-genome analysis of *Fusarium graminearum* insertional mutants identifies virulence associated genes and unmasks untagged chromosomal deletions. *BMC Genomics* 16 (1), 261. doi: 10.1186/s12864-015-1412-9

Weld, R. J., Plummer, K. M., Carpenter, M. A., and Ridgway, H. J. (2006). Approaches to functional genomics in filamentous fungi. *Cell Res.* 16 (1), 31–44. doi: 10.1038/sj.cr.7310006

Wittenberg, A. H. J., van der Lee, T. A. J., M'Barek, S. B., Ware, S. B., Goodwin, S. B., Kilian, A., et al. (2009). Meiosis drives extraordinary genome plasticity in the haploid fungal plant pathogen *Mycosphaerella graminicola*. *PloS One* 4 (6), e5863. doi: 10.1371/journal.pone.0005863

Yemelin, A., Brauchler, A., Jacob, S., Foster, A. J., Laufer, J., Heck, L., et al. (2021). Two novel dimorphism-related virulence factors of *Zymoseptoria tritici* identified using *Agrobacterium*-mediated insertional mutagenesis. *Int. J. Mol. Sci.* 23 (1), 400. doi: 10.3390/ijms23010400

Yemelin, A., Brauchler, A., Jacob, S., Laufer, J., Heck, L., Foster, A. J., et al. (2017). Identification of factors involved in dimorphism and pathogenicity of *Zymoseptoria tritici*. *PloS One* 12 (8), e0183065. doi: 10.1371/journal.pone.0183065

Zhan, J., Kema, G. H., Waalwijk, C., and McDonald, B. (2002). Distribution of mating type alleles in the wheat pathogen *Mycosphaerella graminicola* over spatial scales from lesions to continents. *Fungal Genet. Biol.* 36 (2), 128–136. doi: 10.1016/S1087-1845(02)00013-0

Zhong, Z., Marcel, T. C., Hartmann, F. E., Ma, X., Plissonneau, C., Zala, M., et al. (2017). A small secreted protein in *Zymoseptoria tritici* is responsible for avirulence on wheat cultivars carrying the Stb6 resistance gene. *New Phytol.* 214 (2), 619–631. doi: 10.1111/nph.14434

Zwiers, L. H., and De Waard, M. A. (2001). Efficient *Agrobacterium tumefaciens*-mediated gene disruption in the phytopathogen *Mycosphaerella graminicola*. *Curr. Genet.* 39 (5–6), 388–393. doi: 10.1007/s002940100216

Quantitative and qualitative plant-pathogen interactions call upon similar pathogenicity genes with a spectrum of effects

Camilla Langlands-Perry[1,2], Anaïs Pitarch[1], Nicolas Lapalu[1], Murielle Cuenin[1], Christophe Bergez[1], Alicia Noly[1], Reda Amezrou[1], Sandrine Gélisse[1], Célia Barrachina[3], Hugues Parrinello[3], Frédéric Suffert[1], Romain Valade[2] and Thierry C. Marcel[1]*

[1]Université Paris-Saclay, INRAE, UR BIOGER, Palaiseau, France, [2]ARVALIS Institut du Végétal, Boigneville, France, [3]MGX-Montpellier GenomiX, Univ. Montpellier, CNRS, INSERM, Montpellier, France

Septoria leaf blotch is a foliar wheat disease controlled by a combination of plant genetic resistances and fungicides use. *R*-gene-based qualitative resistance durability is limited due to gene-for-gene interactions with fungal avirulence (*Avr*) genes. Quantitative resistance is considered more durable but the mechanisms involved are not well documented. We hypothesize that genes involved in quantitative and qualitative plant-pathogen interactions are similar. A bi-parental population of *Zymoseptoria tritici* was inoculated on wheat cultivar 'Renan' and a linkage analysis performed to map QTL. Three pathogenicity QTL, *Qzt-I05-1, Qzt-I05-6* and *Qzt-I07-13*, were mapped on chromosomes 1, 6 and 13 in *Z. tritici*, and a candidate pathogenicity gene on chromosome 6 was selected based on its effector-like characteristics. The candidate gene was cloned by *Agrobacterium tumefaciens*-mediated transformation, and a pathology test assessed the effect of the mutant strains on 'Renan'. This gene was demonstrated to be involved in quantitative pathogenicity. By cloning a newly annotated quantitative-effect gene in *Z. tritici* that is effector-like, we demonstrated that genes underlying pathogenicity QTL can be similar to *Avr* genes. This opens up the previously probed possibility that 'gene-for-gene' underlies not only qualitative but also quantitative plant-pathogen interactions in this pathosystem.

KEYWORDS

quantitative pathogenicity, quantitative trait loci, small secreted proteins, Septoria tritici blotch (STB), *Triticum aestivum* (L.)

1 Introduction

Plant-pathogenic microorganisms employ a variety of strategies to successfully infect crops and effectors are very often involved in infection mechanisms (Koeck et al., 2011; Fouché et al., 2018 ; Shao et al., 2021). Effectors are molecules that manipulate host immunity to enable parasitic infection (Kamoun, 2006; Pradhan et al., 2021). They are generally cysteine-rich small secreted proteins (SSP) (Houterman et al., 2009; Stergiopoulos and Wit, 2009; Oliva et al., 2010) and show low similarities with other species (Plissonneau et al., 2017). They are among the most polymorphic genes found in pathogen genomes (Win et al., 2012), often found in highly plastic transposable element-rich regions of the genome (Ma et al., 2010; Soyer et al., 2014; Fouché et al., 2018; Plissonneau et al., 2018).

As an answer to the onslaught brought on by effectors, host-plants have evolved *R* resistance genes that encode proteins capable of recognizing effectors, thus triggering a defensive response (Petit-Houdenot and Fudal, 2017). In this context, effectors are referred to as avirulence (*Avr*) genes, and the *R/Avr* interaction follows a gene-for-gene interaction as defined by Flor (Flor, 1971). Gene-for-gene interactions have been described in many pathosystems (Wit, 1995; Jia et al., 2000; Gout et al., 2006; Hall et al., 2009; Stukenbrock and McDonald, 2009). Almost exclusively associated with qualitative resistance, these interactions pose an issue for disease resistance durability in crops because of the strong selective pressure they impose on pathogen populations. Indeed, a single mutation in the *Avr* gene is sufficient to overcome the disease resistance provided by the *R* gene as the effector will no longer be recognized by the plant's defence mechanisms (Niks et al., 2015).

Quantitative resistance imposes lower selective pressure on populations as it is polygenic, based on a combination of loci with varying effects all contributing to an overall more or less resistant phenotype (Niks et al., 2015). It is therefore widely thought to be able to slow pathogen adaptation and to be more durable than qualitative resistance. Mechanisms underlying quantitative resistance are not well known but have been hypothesized (Poland et al., 2009). Some hypotheses suggest that gene-for-gene interactions similar to those involved in qualitative resistance are in play, but this has been shown only in very isolated cases (Leonards-Schippers et al., 1994; Qi et al., 1999; Arru et al., 2003; González et al., 2012; Meile et al., 2018; Jiquel et al., 2021).

Septoria tritici blotch (STB), caused by the ascomycete fungus *Zymoseptoria tritici*, is one of the most devastating diseases of wheat in Europe. It is responsible for high yield losses worldwide, 30 to 50% loss when environmental conditions are favourable to the disease's development (Eyal et al., 1987; Fones and Gurr, 2015). Known sources of resistance in wheat to STB comprise 22 major resistance genes (Brown et al., 2015; Yang et al., 2018) and over 100 resistance quantitative trait loci (QTL) detected genome-wide (Brown et al., 2015; Gerard et al., 2017; Vagndorf et al., 2017; Karlstedt et al., 2019; Yates et al., 2019; Langlands-Perry et al., 2022). Very few genes are known to be involved in pathogenicity for *Z. tritici* (Marshall et al., 2011; Poppe et al., 2015; Rudd et al., 2015; Hartmann et al., 2017; Kettles et al., 2017; Yemelin et al., 2022), and qualitative gene-for-gene interactions have been demonstrated for

the *T. aestivum*-*Z. tritici* pathosystem with the *Stb6*/*AvrStb6* and *Stb9*/*AvrStb9* interactions (Brading et al., 2002; Zhong et al., 2017; Amezrou et al., 2022). Though there are qualitative components to *Z. tritici* pathogenicity, it is regarded as being largely quantitative as phenotypes observed are mostly intermediate and do not correspond to a typically qualitative black or white situation (Hartmann et al., 2017; Stewart et al., 2018). Quantitative components of pathogenicity can be evaluated using different quantitative traits such as infection efficiency, latency period, pycnidia density, spore production, duration of the infectious period and lesion size (Pariaud et al., 2009; Lannou, 2012; Gohari et al., 2015; Stewart et al., 2018).

The only other gene-for-gene interaction that has been demonstrated is between *Stb7* or *Stb12* and *Avr3D1* (Meile et al., 2018). This interaction was shown to be linked to quantitative phenotypes despite the involvement of major resistance genes (Meile et al., 2018), a first for this pathosystem. Both *AvrStb6* and *Avr3D1* encode SSP (Zhong et al., 2017; Meile et al., 2018), and *AvrStb9* encodes a large, secreted protein with a protease-like domain (Amezrou et al., 2022). While the *Z. tritici* genome is composed of 13 core chromosomes, present in every known strain, and 8 accessory chromosomes, which are subject to presence/absence polymorphisms (Goodwin et al., 2011), to date, no QTL linked to pathogenicity have been identified on accessory chromosomes, though a small effect of these accessory chromosomes on pathogenicity has been detected (Habig et al., 2017).

Wheat cultivar 'Renan' displays quantitative resistance to *Z. tritici* strains I05 and I07 with three resistance QTL mapped on chromosomes 1D, 5D and 7B, the first two showing strain specificities between I05 and I07 (Langlands-Perry et al., 2022). We studied the progeny of a cross between the strains I05 and I07, aiming at deciphering the genetic architecture of pathogenicity in quantitative interactions and characterizing the underlying genes. We hypothesized that pathogenicity in this cross is also of quantitative and polygenic nature, with pathogenicity QTLs being involved in gene-for-gene interactions with the two strain-specific resistance QTL previously identified in Renan. We therefore aimed at demonstrating that gene-for-gene mechanisms do not exclusively underlie qualitative interactions, but are also involved in quantitative plant-pathogen interactions.

2 Materials and methods

2.1 Fungal material

The two *Z. tritici* strains "I05" (INRA09-FS0813, Mat1-1) and "I07" (INRA09-FS0732, Mat1-2), sampled in 2010 from STB lesions on wheat cv. Soissons in Grignon, France (48510 N, 1580 E), were crossed by co-inoculating adult plants with an equiproportional suspension of parental blastospores. After ascosporogenesis, 167 offspring individuals were collected from yeast-like colonies on Petri dishes placed upside down above wheat debris fragments to collect discharged ascospores as described in Suffert et al. (2016). The population of the 167 individuals resulting from the cross is hereafter referred to as "I05×I07".

2.2 Inoculation procedure

148 chosen randomly among the I05×I07 progeny strains, and the two parental strains were phenotyped over three replications on 16-day-old seedlings of the wheat cultivar 'Renan' grown in a growth chamber as previously described in Langlands-Perry et al. (2022).

The strains were precultured in YPD (Yeast extract Peptone Dextrose), composed of 1% yeast extract, 2% peptone, 2% glucose and 95% distilled water, 10 days prior to inoculation, and each preculture was then grown on a PDA solid culture medium (potato dextrose agar), as described in Langlands-Perry et al. (2022). 150 mL of blastospores were prepared in advance from these cultures, each with a concentration of $10^6 \pm 1.10^5$ spores.mL^{-1}, kept at -80°C between 1 to 3 months to be used for each of the three replicated inoculations. Before inoculation, a drop of Tween 20$^®$ was added per 15 mL of inoculum to ensure adherence of the inoculum to the leaf.

The day before the inoculation, only three plants were kept per pot. On the first true leaf (about 3 cm from the base) of each plant, a surface of 7.5 cm in length was delineated with two black marks from a felt tip. Inoculation was carried out with cotton swabs, one per inoculum, in six passages (3 times back and forth), within the marks. After inoculation, the pot was covered with a plastic bag closed off at the top with a paper clip to not only create a water-saturated atmosphere, which encourages infection (Shaw, 1991; Boixel et al., 2022), but also to isolate the pots from one another to prevent cross contamination. The paper clips were removed after three days, a 72 h incubation period being the time it takes for the fungus to reach the mesophyll, which is necessary to the rest of the colonisation process (Kema et al., 1996). To optimise conditions for the survival of the inoculated leaf and to homogenise the quantity of light received by each leaf, new leaves were cut 2 to 3 cm above the first node 14 days post-inoculation (dpi).

2.3 Evaluation of phenotypic traits

2.3.1 Visual evaluation of symptoms

The areas of the 7.5 cm-long inoculated leaf segment which were green, necrotic and sporulating (i.e. presented pycnidia) were assessed as percentages of the total inoculated area at 14, 20 and 26 dpi. The phenotypic traits S20 and S26 correspond to the percentage of the inoculated area presenting with pycnidia at 20 and 26 dpi, respectively. AUDPCs (Area Under the Disease Progress Curve) for the green, necrotic and sporulating areas (AUDPCG, AUDPCN and AUDPCS, respectively) were calculated as described by Langlands-Perry et al. (2022) using the three assessments realized over the course of the infection.

2.3.2 Evaluation of sporulation by image analyses

Inoculated parts of the leaves were scanned and the images analysed with ImageJ, following the method of Stewart & McDonald (2014) and Stewart et al. (2016), modified by Langlands-Perry et al. (2022). The necrotic leaf surface and the

total number of pycnidia were determined and used to calculate pycnidia density (PYC).

Sporulation for each three-leaf sample was quantified with the use of the particle size & shape analyser Occhio Flowcell FC200S+HR (www.occhio.be) according to the protocol followed by Langlands-Perry et al. (2022) and divided by the number of pycnidia of the three-leaf sample to calculate the number of pycnidiospores per pycnidium (NBS).

2.4 Statistical analysis of phenotypic data

The obtained data sets were analysed with the R software (R Core Team, 2019). For each trait an analysis of variance (ANOVA) was performed with the following model:

$$Yij = \mu + Ii + rj + Irij + \epsilon ij$$

Where Yij is the trait which is being studied, μ is the mean value for this trait, Ii is the individual genotype, rj the replication, $Irij$ the interaction and ϵij the residual. For the following analyses, $Irij$ was included in the residual.

The following hypotheses were tested after the variance analyses.

$\epsilon \sim N(o, \sigma^2)$

$cov(\epsilon, \epsilon') = 0$ Homoscedasticity (homogeneity of $var(\epsilon)$)

Broad-sense heritability is defined by the following formula:

$$H^2 = \frac{\sigma g^2}{\sigma g^2 + \sigma e^2}$$

Where H^2 is the heritability, σg^2 the genotypic variance and σe^2 the residual variance.

Two ANOVAs were carried out as 30 individuals were missing from the experiment for replicate 3. The first ANOVA included the data for all three replicates but with the 30 individuals missing from replicate 3 removed. The second ANOVA included the data for all individuals but only for the replicates 1 and 2.

The correlation between traits was studied using the Bravais-Pearson correlation.

2.5 RAD-sequencing of I05×I07 progeny isolates

The 167 progeny and two parental strains were grown over 7 days in a 250 mL Erlenmeyer flask containing 100 mL of YPD inoculated with 30 μL of inoculum. Growth chambers were fixed at 17°C, a hygrometry of 70%, constant agitation at 160 rpm and under neon lights (two Osram L 58W/840 Lumilux Cool White tubes). Then, spores were washed and transferred into 50 mL Falcon tubes to be lyophilized for 24 to 30 hours. The dry samples were ground in liquid nitrogen with a mortar and pestle. DNA was extracted following a phenol/chloroform-based protocol adapted from Fagundes et al. (2020). After drying, extracted DNA samples were suspended in 250 μL of Tris buffer at 10 mM. Sample purity was verified with a Nanodrop (Desjardins and Conklin, 2010)

measurement while concentrations were measured with a Qubit 2.0 (Anon, 2011). All samples were subjected to an electrophoresis to verify that they were not degraded.

Samples were sequenced following the RADseq (Restriction site Associated DNA sequencing) strategy (Etter et al., 2011), on the Platform MGX (MGX-Montpellier GenomiX) on a HiSeq 2500 (Illumina) in paired-end 2*125nt mode. This type of sequencing enables one to target 1 to 10% of the genome *via* the use of a restriction enzyme and tagging of digested strands. Sequencing depth per sequenced locus is higher than classic sequencing, while the price is considerably lower. The restriction enzyme used was *Pst1*, following a previous study by Lendenmann et al. (2014), corresponding restriction sites were present throughout the IPO323 genome (Figure S1).

2.6 QTL mapping

A genetic map containing 18,316 SNP markers for 1,332 genetic bins covering the whole *Z. tritici* genome bar chromosomes 14 and 18 was built using the Multipoint ultra-dense software (MultiQTL Ltd, Haifa University, Israel) (details in Supporting information 2) and was used for QTL mapping.

A linkage analysis was carried out using the R/qtl software (Broman et al., 2003) version 1.42-8. This analysis included for each trait an initial Simple Interval Mapping (SIM), followed by a Composite Interval Mapping (CIM). Analyses were performed replication by replication. For SIM, 1000 genome-wide permutations were used to calculate the significant logarithm of odds (LOD) threshold. Were considered significant only QTL that showed P-values<0.05. The CIM was carried out with the QTL with the highest LOD used as a covariate. QTL intervals were evaluated with the LOD support interval with a drop in LOD of 1 and the "expandtomarkers" argument as true. QTL effects were calculated with the "effectplot" and "effectscan" functions. Possible epistatic interactions between QTL were looked into using the "addint" function.

2.7 Identification of a candidate pathogenicity gene

2.7.1 QTL gene content

The gene content of the QTL identified on chromosome 6 was looked into using the annotation by Grandaubert et al. (2015). Certain reannotations were carried out using data from Haueisen et al. (2019) and RepeatMasker (Smit et al., 2013) for TE annotation. Functions of candidate genes were predicted using the translated protein sequences as input for the InterPro database (http://www.ebi.ac.uk/interpro/search/sequence/).

2.7.2 Structural differences between I05 and I07 at the detected QTL

A *de novo* genome assembly of parental strains I05 and I07 was realized with previously available PE-100 sequences obtained on an

Illumina HiSeq 2000 sequencing system with a 70x mean genome coverage (BioProject: PRJNA777581, accessions SRR16762604 and SRR16762605). Illumina paired-end reads were assembled using a combination of VELVET (Zerbino and Birney, 2008), SOAPDENOVO and SOAPGAPCLOSER (Luo et al., 2012), as previously described for the assembly of the *Botrytis cinerea* genome (Mercier et al., 2021).

The contigs from the I05 and I07 assemblies covering our regions of interest were identified by BLAST of the assembled genomes on the IPO323 reference genome (Goodwin et al., 2011). These enabled us to identify polymorphism between I05 and I07 for our candidate genes and TE presence/absence polymorphisms in both strains. The TE were annotated using ReapeatMasker (Smit et al., 2013) and a previously generated TE library for this organism (Grandaubert et al., 2015) according to the nomenclature defined by Wicker et al. (2007).

2.7.3 Expression profiles for the top candidate gene

The relative expression of the candidate gene from *Qzt-I05-6* was assessed by analysing qPCR data following the $2^{-\Delta\Delta Ct}$ method (Livak and Schmittgen, 2001), the detail for which is in Supporting information 3 and all primers used are referenced in Table S4.

2.8 Molecular cloning

A detailed version is presented in Supporting information 4.

2.8.1 Bacterial strains and DNA manipulation

For all PCR performed to obtain cloning fragments, the Taq polymerase Phusion® (Thermo Fisher Scientific Inc., Waltham, MA, USA) was used under adapted PCR conditions using primers referenced in Table S6. All DNA assembly manipulations were conducted with the Gibson Assembly Cloning Kit (New England Biolabs, Ipswich, MA, USA). Plasmids carrying a hygromycin resistance gene flanked by two regions of approximately 1000 bp for homologous recombination were generated for knock-out mutants. Plasmids carrying a sulfonylurea resistance gene and a DNA fragment comprising at least 499 bp upstream of the start codon and at least 1 kb downstream of the stop codon of the candidate gene were generated for complementation and ectopic integration mutants. NEB 5-alpha Competent *Escherichia coli* (High Efficiency) (New England Biolabs, Ipswich, MA, USA) were transformed by heat shock with the generated plasmids and used for their amplification. Successfully transformed colonies were identified by PCR and mini-prepped plasmid constructs validated by Sanger sequencing (Eurofins, Luxembourg). *Agrobacterium tumefaciens* strain AGL1 was transformed by heat shock with each generated plasmid. Colonies were screened by PCR.

2.8.2 *A. tumefaciens*-mediated transformation of *Z. tritici*

The *Z. tritici* strains I05 and I07 were transformed by ATMT (Bowler et al., 2010) following the standard protocol to generate

knock-out mutants and ectopic integration mutants. This enabled us to obtain I05_ΔG07189 and I07_ΔG07189 mutants. I05_ΔG07189 was transformed following the same protocol to generate complementation mutants I05_ΔG07189 + G07189$_{I05}$ and I05_ΔG07189 + G07189$_{I07}$ and ectopic integration mutant I05 + G07189$_{I07}$.

Mutant strains were selected by hygromycin or sulfonylurea screening. Obtained strains were verified by PCR on genomic DNA extracted with the DNeasy® Plant Mini Kit (Qiagen, Hilden, Germany) according to the supplier's protocol.

2.8.3 Phenotypic characterization of mutant strains

All generated mutant strains were inoculated on 'Renan' and 'Chinese Spring' (susceptible control) according to the same protocol as the previously described assays. Only visual evaluations were performed. Three clones of each mutant strain type and I05 and I07 were tested, three times each per replication. Four replications were carried out. The results obtained were analysed with a Kruskal-Wallis test and a Wilcoxon pairwise comparison.

2.9 Diversity and selection analysis of the candidate effector from Qzt-I05-6

In addition to the I05 and I07 *de novo* assemblies, the assemblies of 103 *Z. tritici* strains collected in France in 2009-2010 (BioProject: PRJNA777581) and 126 strains collected in France in 2018-2019 (BioProject: PRJNA881220) were also available to us, enabling us to look into the sequence diversity of the pathogenicity gene. We extracted gene sequences from genome assemblies of the 229 *Z. tritici* strains using the ncbi-blast+ software (Camacho et al., 2009). Prior to performing the population genetic analysis, we first verified population structure in our dataset, to ascertain that there is no inflation due to population structure. We constructed a protein sequence phylogenetic tree using the RaxML algorithm with the GAMMA JTT model and 100 bootstrap replicates (Stamatakis, 2014). Phylogenetic trees were visualized using iTOL (Letunic and Bork, 2016); https://itol.embl.de/ . We used the R package Popgenome (Pfeifer et al., 2014) to calculate sliding-window analyses of nucleotide diversity (π) of the effector gene, including ~500 bp upstream and downstream of the coding sequence. We used a window length of 20 bp and a step size of 5 bp. To verify whether the effector gene exhibits signatures of positive diversifying selection, we calculated the rates of ω, the ratio of nonsynonymous to synonymous mutational rates using the codon-based selection analysis codeML (Yang et al., 2004). The ratio indicates negative purifying selection (0< ω< 1), neutral evolution (ω = 1), or positive diversifying selection (ω > 1). We compared different evolutionary models and used the statistical likelihood ratio test (LRT) to determine the model that best fitted our data. The Bayes empirical Bayes method (BEB) was then used to evaluate the posterior probability of sites considered to have been positively selected.
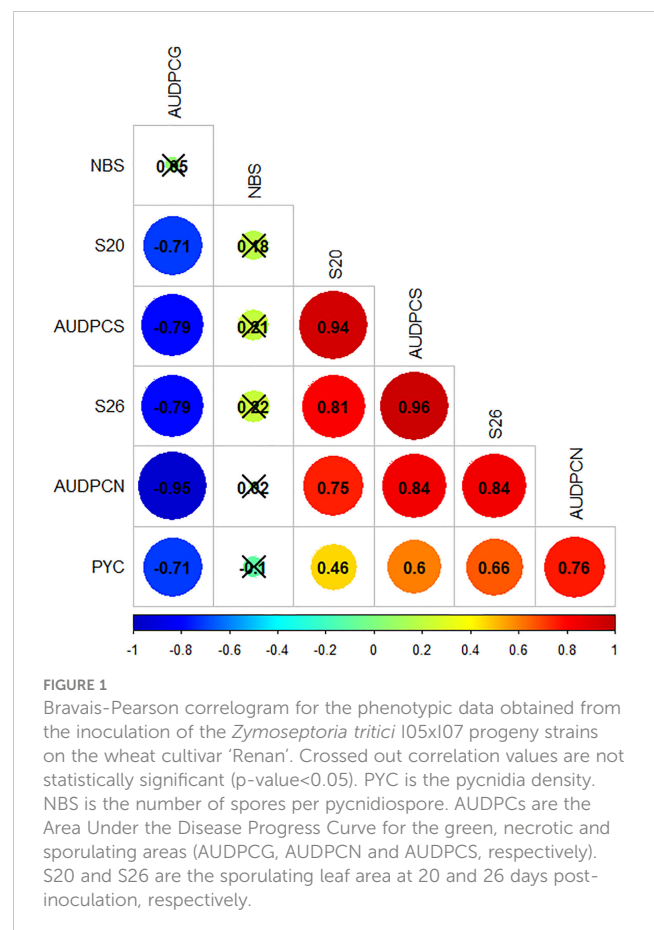
3 Results

3.1 Phenotypic data analysis

A representation of the distribution of the different traits for all three replicates shows that they do not follow a normal distribution (Figure S2), as confirmed by a Shapiro-Wilk normality test. For all traits, transgressive individuals are observed.

Bravais-Pearson correlation results show that all traits but NBS were correlated (Figure 1). The most strongly correlated traits were S26 and AUDPCS with a correlation coefficient of 0.96, both traits linked to the sporulating area. AUDPCN and AUDPCG were also strongly negatively correlated with a correlation coefficient of -0.95. PYC was less strongly correlated overall than the other traits, it was however significantly correlated, with absolute correlation coefficient values ranging from 0.46 to 0.76 for PYC (NBS values excluded).

Both ANOVAs (Table S3) showed that the genotype had a significant effect on phenotypes, though the significance was milder for PYC and NBS. They also showed that, overall, the replication had high statistical significance. This led to all subsequent analyses being carried out replication by replication. The traits that best performed in the statistical analyses were AUDPCG, AUDPCN and PYC with the ANOVA assumptions respected. For the other traits, the assumptions were not so well respected and heritability may not be optimally estimated. Heritability ranged from 0.45 to 0.59 for

FIGURE 1
Bravais-Pearson correlogram for the phenotypic data obtained from the inoculation of the *Zymoseptoria tritici* I05xI07 progeny strains on the wheat cultivar 'Renan'. Crossed out correlation values are not statistically significant (p-value<0.05). PYC is the pycnidia density. NBS is the number of spores per pycnidiospore. AUDPCs are the Area Under the Disease Progress Curve for the green, necrotic and sporulating areas (AUDPCG, AUDPCN and AUDPCS, respectively). S20 and S26 are the sporulating leaf area at 20 and 26 days post-inoculation, respectively.

S26, AUDPCG, AUDPCN and AUDPCS, values that are reasonably high. The values were lower for S20, PYC and NBS, ranging from 0.16 to 0.36.

3.2 Linkage analyses of I05×I07 progeny reveal three pathogenicity QTL

The linkage analyses enabled us to detect three repeatable QTL: *Qzt-I05-1*, *Qzt-I05-6* and *Qzt-I07-13*, on core chromosomes 1, 6 and 13, respectively (Table 1, Figure 2, Table S7). *Qzt-I05-1* and *Qzt-I05-6* were detected for all three replicates, while *Qzt-I07-13* was detected only for replicates 2 and 3 (Table 1). *Qzt-I05-1* is in a sub-telomeric region of chromosome 1. It covers a 4.96 cM-long region on the genetic map spanning 138 kb based on the physical position of the flanking markers. The mean phenotypic variation explained by this QTL is 6.37% and the parental strain carrying the pathogenic allele for this QTL is I05.

Qzt-I05-6 covers a 13.48 cM-long region corresponding to a physical interval of 169 kb on chromosome 6. The mean phenotypic variation explained by this QTL is 24.91%, the highest among the three repeatable QTL detected, and the parental strain carrying the pathogenic allele for this QTL is I05. This QTL presents itself as being the most robust of the three.

Finally, *Qzt-I07-13* is found at a sub-telomeric region of chromosome 13. It covers an 8.64 cM-long region corresponding to a physical interval of 186 kb. The mean phenotypic variation explained by this QTL is 6.93% and, contrary to the other two QTL, the parental strain carrying the pathogenic allele is I07.

Significant epistatic interactions were detected between *Qzt-I05-1* and *Qzt-I05-6* and between *Qzt-I05-6* and *Qzt-I07-13* (Table 2). *Qzt-I05-6* and *Qzt-I07-13* had the highest and most significant epistatic interaction explaining on average 7.12% of phenotypic variation. This epistatic interaction explains why strains carrying the pathogenic allele for these two QTL led to the highest S26 values among the strains combining the pathogenic allele for two QTL (Figure 3).

For further investigation, we chose to focus our efforts on *Qzt-I05-6* which was the most robust QTL, with the strongest effect on phenotypic variation.

3.3 Qzt-I05-6 harbours a previously unannotated effector-like gene in a dynamic region

The interval defined by *Qzt-I05-6* holds 36 genes annotated in Grandaubert et al. (2015). There is a 60 Kb-long TE-rich region in the middle of the QTL, with markers that came out as peak markers during the linkage analysis on either side. None of these 36 genes has any predicted functions; we therefore predicted functions with the InterPro database (http://www.ebi.ac.uk/interpro/search/sequence/) (Table S8). We searched for genes that have characteristics of known effectors, as these are often involved in fungal pathogenicity. Out of the 36 annotated genes, two had a signal peptide. The first, named *Zt09_6_00095* in the Grandaubert et al. (2015) annotation, comes out as being in the PTHR35523 family in the panther classification system (http://www.pantherdb.org/), which regroups cell wall proteins. As a component of the cell structure, this gene does not seem to be a good candidate. The second gene, *Zt09_6_00123*, is predicted to encode a FAD binding domain, linking it to an oxidoreductase process. This gene is a little large for an effector with a length of 1272 bp and a corresponding protein of 423 amino acids (aa), the general cut-off being set at 300 aa (Sperschneider et al., 2018). It has a predicted function and only one cysteine in its protein sequence. It does not seem to be a good candidate either.

RNAseq data from Haueisen et al. (2019) enabled us to notice some reads that mapped to a position that was not annotated, right next to the central TE region. As pathogenicity genes can be found in regions such as this (Plissonneau et al., 2018), we looked further into the corresponding position. The RNAseq data produced by Haueisen et al. (2019) was used to make a read coverage file which was used in the integrative genomics viewer (IGV) software (Robinson et al., 2011) as a means of annotating a previously unidentified gene. On chromosome 6 of IPO323, this gene is positioned at 470,027-470,324 bp. It has two exons with coding sequence (CDS); the first has a predicted signal peptide (https://services.healthtech.dtu.dk/service.php?SignalP) (Teufel et al., 2022), and there is no predicted function or family for the protein (http://www.ebi.ac.uk/interpro/search/sequence/). It has an intron which is 61 bp long and has canonical splice site combination GT-AG (Kupfer et al., 2004; Frey and Pucker, 2020). The CDS is 237 bp

TABLE 1 QTL for pathogenicity detected through linkage analysis using the phenotypic data and the genetic map generated from the *Zymoseptoria tritici* I05xI07 population inoculated on wheat cultivar 'Renan'.

L	Number of detections	Maximal phenotypic variance (%)	Mean phenotypic variance (%)	Parent carrying the pathogenic allele	Traits[1]
Qzt-I05-1	8	7.43	6.37	I05	S26, AUDPCG, AUDPCN, AUDPCS
Qzt-I05-6	17	40.15	24.91	I05	S20, S26, AUDPCG, AUDPCN, AUDPCS, PYC, NBS
Qzt-I07-13	6	9.40	6.93	I07	S20, S26, AUDPCN, AUDPCS, NBS

[1]AUDPCs are the Area Under the Disease Progress Curve for the green, necrotic and sporulating areas (AUDPCG, AUDPCN and AUDPCS respectively). S20 and S26 are the sporulating areas (%) at 20 and 26 days post-inoculation respectively. PYC is the pycnidia density. NBS is the number of pycnidiospores per pycnidium.
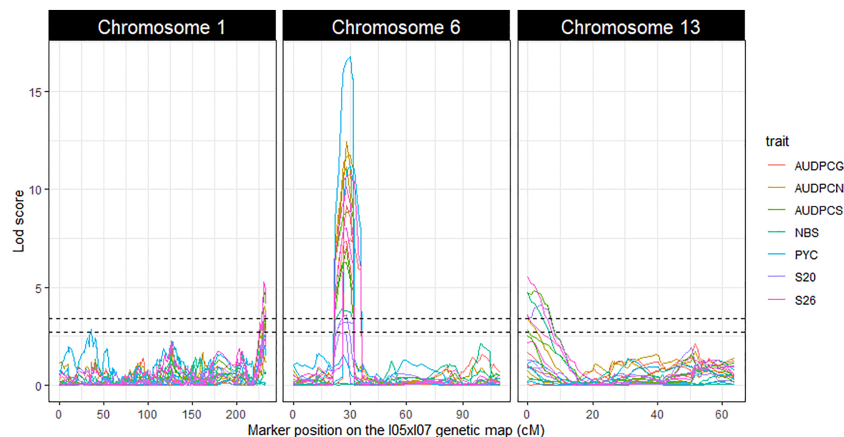
FIGURE 2

LOD score profiles for the linkage analyses performed on the phenotypic and genetic data generated from the *Zymoseptoria tritici* I05xI07 population. The X-axis represents the position of the markers on the I05xI07 genetic map in cM. The Y-axis represents the LOD score associated with the markers. Dotted lines represent the minimal and maximal LOD threshold values obtained in the linkage analyses after 1000 permutation tests. Each column corresponds to a chromosome, chromosomes 1, 6 and 13 respectively. The colours in the graphs correspond to the studied traits. AUDPCs are the Area Under the Disease Progress Curve for the green, necrotic and sporulating areas (AUDPCG, AUDPCN and AUDPCS, respectively). S20 and S26 are the sporulating areas (%) at 20 and 26 days post-inoculation, respectively.

long and encodes a 78-aa protein with 11 cysteines in its sequence (14% of the protein sequence). We identified four mutations between parental strains I05 and I07. In a recent, yet unreleased, annotation of the *Z. tritici* IPO323 genome sequence, specifically improved to detect genes encoding SSP, this gene was identified and named *G_07189* (unpublished data). A BLAST search against the NCBI database (https://blast.ncbi.nlm.nih.gov/Blast.cgi) identified in other *Z. tritici* strains a second, longer protein, with a potential alternative methionine 32 aa before the predicted one. This longer, alternative protein has a cleavage site between the 47th and 48th aa, that is unlikely for a signal peptide. Searches for a GPI anchor did not return positive results. Therefore, the shortest isoform of 78 aa was retained for *G_07189*. The BLAST search did not yield any significant results in other species, indicating that this gene is species specific.

The study of the expression of this gene by RT-qPCR over the course of the infection revealed upregulation at 12 dpi in both I05 and I07 strains (Figure 4), further consolidating its status as a very good effector candidate.

Additionally, comparison of the I05 and I07 assembled contigs revealed that the newly annotated gene lies in a highly dynamic region, with several presence/absence polymorphisms of TE between both parental strains (Figure 5).

3.4 Genetic manipulation and pathology tests validate the involvement of G_07189 in pathogenicity

All knock-out, complementation and ectopic integration mutant strains were successfully generated following an ATMT protocol (Bowler et al., 2010). Three randomly selected mutants per construction were able to successfully infect 'Chinese Spring' and induce sporulation covering on average 99% of the inoculated leaf area (Figure S4).

In the I05 genetic background, deleting gene *G_07189* has no effect on the phenotype, while replacing the I05 allele (G07189$_{I05}$) by the I07 allele (G07189$_{I07}$) induces a suppression of sporulation

TABLE 2   Epistatic interactions detected between the QTL identified with the *Zymoseptoria tritici* I05xI07 population inoculated on wheat cultivar 'Renan'.

Replication	Traits[1]	Chromosomes on which QTL were detected	Range of phenotypic variance due to epistatic effect (%)[2]
1	AUDPCS, S26	1, 6	5.19***-5.8***
2	AUDPCS, S26	1, 6	2.72*-2.74*
3	AUDPCN, AUDPCS	1, 6	2.73*-6.59***
2	S26	6, 13	3.62**
3	AUDPCN, AUDPCS, S20, S26	6, 13	4.07**-10.8***

[1]AUDPCs are the Area Under the Disease Progress Curve for the green, necrotic and sporulating areas (AUDPCG, AUDPCN and AUDPCS respectively). S20 and S26 are the sporulating areas (%) at 20 and 26 days post-inoculation respectively. PYC is the pycnidia density. NBS is the number of pycnidiospores per pycnidium.
[2]Significance codes: 0 '***', 0.001 '**', 0.01 '*'. Detected interactions with very low significance are not shown.

(Figure 6). Indeed, the I05 wild type protein induces a highly susceptible reaction on wheat cultivar 'Renan' (>90% sporulating leaf area) while 'Renan' becomes completely resistant when the I07 allele is introduced (Figure 6). In the I05 genetic background, the I07 allele of *G_07189* behaves as a classic avirulence gene inducing complete resistance in the host.

In the I07 genetic background, deleting the gene *G_07189* also has a strong and significant effect on sporulation as I07 wild type induces 7% sporulating leaf area on average while the knock-out mutants I07_ΔG07189 induce 61% sporulating leaf area on average (Figure 6). In the I07 genetic background, the effect of the I07 allele of *G_07189* remains quantitative.

3.5 G_07189 is highly conserved in French populations of *Z. tritici* but is under diversifying selection

As the cloning experiments validated the effect of *G_07189*, we analysed its genetic diversity in the 229 French *Z. tritici* strains and searched for diversifying selection signatures. This analysis showed that *G_07189* is highly conserved among these strains, regardless of their being collected in 2009-2010 or in 2018-2019, with non-synonymous polymorphism for only 7 amino-acid residues out of 78 (Figure 7). With no collection period-related population structure, the strains carry alleles encoding fifteen isoforms of the *G_07189* protein with four isoforms representing 86% of all strains including the I05 and I07 isoforms (Figure 7). All of the sequence diversity observed for the gene is coded by the second exon, with $\pi_{CDS2} = 0.02254$ while π_{CDS1} and π_{intron} are around 0.0001 (Table S9). The ratio between non-synonymous and synonymous
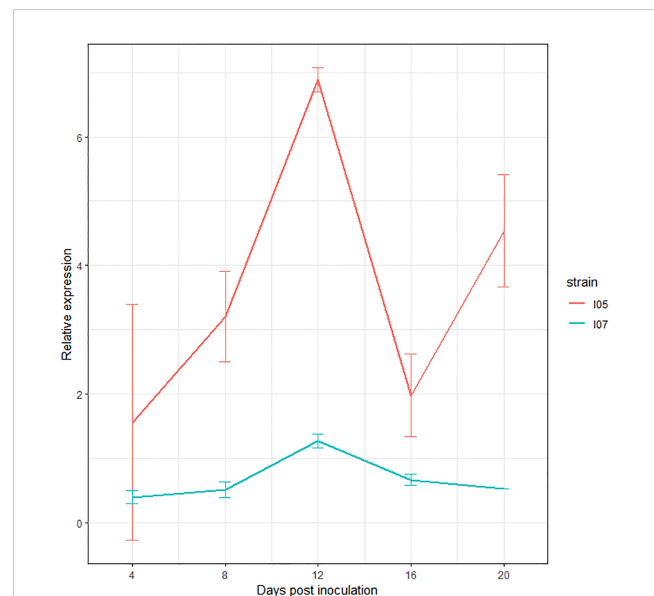

FIGURE 4
Expression profile of *G_07189* in *Zymoseptoria tritici* strains I05 (red) and I07 (blue) during infection on the *T. aestivum* cultivar 'Chinese Spring'. The values shown are the relative expression levels for each gene with respect to the geometric mean obtained for the three housekeeping genes used (*EF1α, UBC* and *β-tubuline*), averaged over at least two biological replicates, except for I07 at 20 dpi, where all samples but one were degraded after RNA extraction and DNase treatment. Error bars represent the 95% confidence intervals of the averages.

mutations (ω=dN/dS) in the panel of strains was calculated at 2.118 for a one-ratio model M0 (Table S10), a high value indicating diversifying selection, further validated by the selection M2 model having the highest lnL value (-487.686, p<0.001) among the three
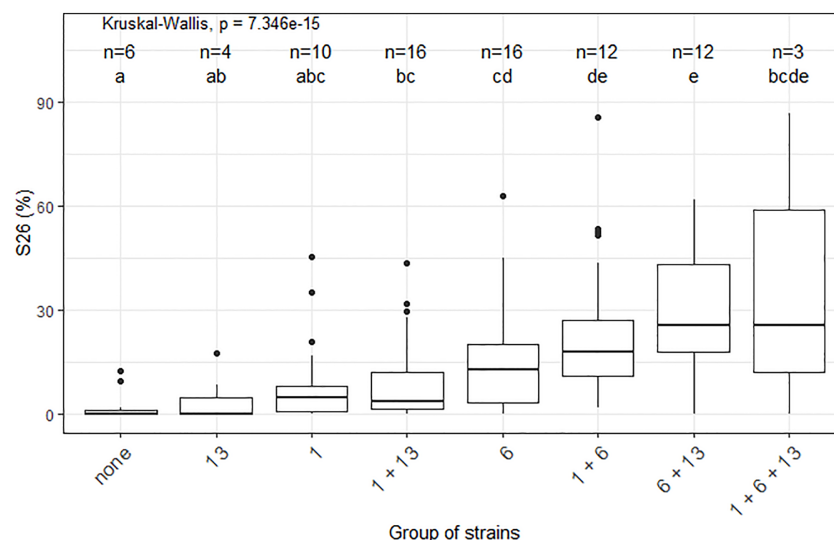

FIGURE 3
Impact of the different combinations of pathogenicity QTL on the performance of strains from the *Zymoseptoria tritici* I05xI07 population on the wheat cultivar 'Renan', strains with recombination within the QTL intervals were excluded. The X-axis represents the different groups of strains concerning their pathogenic allele combination per QTL. For legibility, the QTL are referred to here as 1, 6 and 13. The n values correspond to the numbers of strains per group. The Y-axis represents the phenotypic values obtained. S26 is the sporulating area (%) at 26 days post-inoculation. The Kruskal-Wallis values indicate that the phenotypic value for at least one group of strains is significantly different to the others. Letters a, b, c, d and e indicate a significant difference for a Wilcoxon pairwise comparison at alpha=0.05.
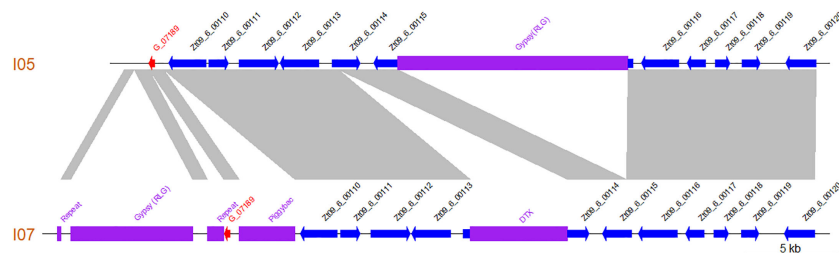
FIGURE 5

The region harbouring gene *G_07189* is highly polymorphic between *Zymoseptoria tritici* strains I05 and I07 as illustrated by this synteny plot comparing the contigs of the I05 and I07 assemblies which carry *G_07189*. Previously annotated genes are represented as blue arrows according to their orientation. The newly annotated gene *G_07189* is represented by a red arrow according to its orientation. Transposable elements are represented by purple blocks. Collinear sequences between contigs are shown in grey.

models tested (Table S10). According to the codon-based maximum likelihood approach, three residues are under significant diversifying selection (p<0.01) at positions 54, 71 and 72 in the protein sequence (Figure 7). We therefore have a highly conserved gene that is under diversifying selection.

4 Discussion

4.1 The interaction between 'Renan' and I05×I07 progeny is polygenic and quantitative

In this study we identified regions in the *Z. tritici* genome, which carry genes that contribute to quantitative pathogenicity

towards *T. aestivum*. The cultivar used was 'Renan', known to carry at least three resistance QTL with different levels of resistance towards I05 and I07 on chromosomes 1D, 5D and 7B (Langlands-Perry et al., 2022). Additionally, the resistance QTL on 'Renan' show strain specificity between I05 and I07 and none of these QTL alone is able to confer total resistance to either I05 or I07, indicating that resistance is polygenic and quantitative in the 'Renan'/I05-I07 interaction (Langlands-Perry et al., 2022). Pathogenicity towards 'Renan' is polygenic, with three QTL identified in this study, each contributing partially to the observed phenotypic variation. For two of these QTL, the parent carrying the pathogenic allele is I05, the parental strain known to be the most pathogenic on 'Renan'. For the third, the parent carrying the pathogenic allele is I07, the least pathogenic parental strain on 'Renan'. We showed that these QTL have varying effects on the
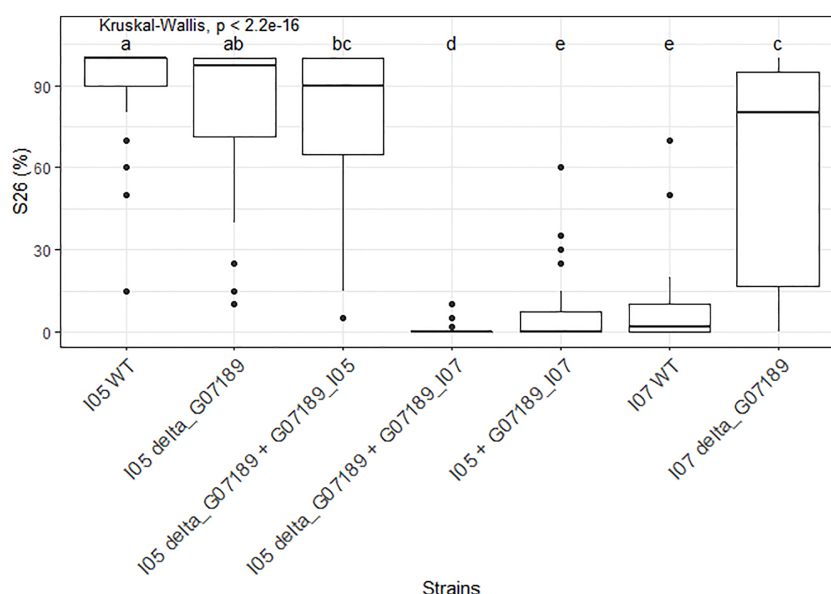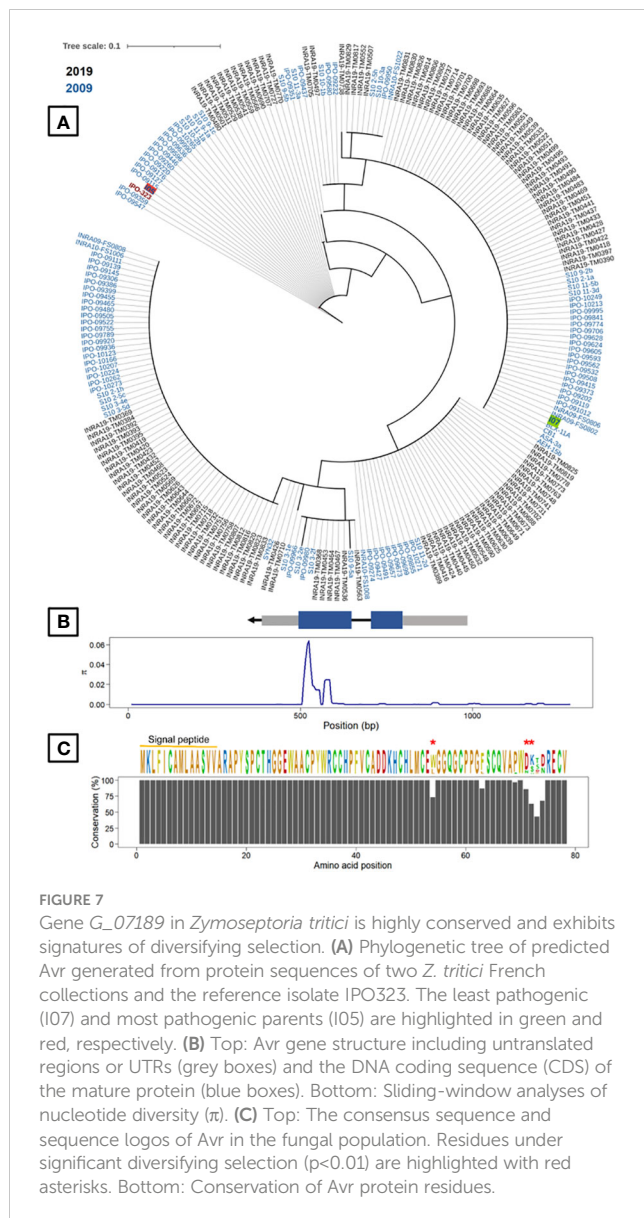

FIGURE 6

S26, the sporulating area (%) at 26 days post-inoculation, values observed for the different mutant *Zymoseptoria tritici* strains obtained for gene *G_07189* inoculated on wheat cultivar 'Renan'. The Kruskal-Wallis value indicates that the phenotypic value for at least one type of strain is significantly different to the others. Letters a, b, c, d and e indicate a significant difference for a Wilcoxon pairwise comparison at alpha=0.05. The X-axis represents the different mutant strains tested. The Y-axis represents the phenotypic values obtained. The phenotypic data presented comprises all replicates for all individuals; the detail per individual is available in Supplementary Figure S4.

FIGURE 7
Gene *G_07189* in *Zymoseptoria tritici* is highly conserved and exhibits signatures of diversifying selection. **(A)** Phylogenetic tree of predicted Avr generated from protein sequences of two *Z. tritici* French collections and the reference isolate IPO323. The least pathogenic (I07) and most pathogenic parents (I05) are highlighted in green and red, respectively. **(B)** Top: Avr gene structure including untranslated regions or UTRs (grey boxes) and the DNA coding sequence (CDS) of the mature protein (blue boxes). Bottom: Sliding-window analyses of nucleotide diversity (π). **(C)** Top: The consensus sequence and sequence logos of Avr in the fungal population. Residues under significant diversifying selection (p<0.01) are highlighted with red asterisks. Bottom: Conservation of Avr protein residues.

phenotype, with *Qzt-I05-6* having the strongest effect, and are subject to epistatic interactions, notably in the case of the *Qzt-I05-6* and *Qzt-I07-13* interaction. None of the detected QTL colocalizes with an already known avirulence gene in *Z. tritici*. Indeed, *AvrStb6* is found on chromosome 5 (Zhong et al., 2017), *AvrStb9* is on chromosome 1 but not in the region defined by *Qzt-I05-1* (Amezrou et al., 2022) and *Avr3D1* is on chromosome 7 (Meile et al., 2018). Looking at progeny strains that did not have any recombination within the QTL intervals, we are able to separate the different strains according to the QTL allele combination that they carry to observe the impact of these allele combinations on the performance of the strains on 'Renan' (Figure 3). We looked into the data for maximal sporulation S26 as this trait led to the detection of all three QTL. S26 was always higher for strains with the pathogenic allele for several QTL compared with strains carrying the pathogenic allele for only one QTL, though the difference was not always statistically significant, indicating incomplete additivity of the QTL effects. None of the non-

pathogenic alleles of the QTL induced a completely resistant phenotype such as that conferred by a major gene like *Stb6* in the presence of *AvrStb6* (Zhong et al., 2017). The only strains that were almost completely non-pathogenic were those that carried the non-pathogenic allele for all three QTL, demonstrating the quantitative and polygenic nature of pathogenicity and mirroring the quantitative and polygenic nature of resistance in 'Renan' (Langlands-Perry et al., 2022).

4.2 Fungal effectors involved in quantitative interactions

An effector-like gene (i.e. coding for SSP) was identified as a candidate to explain *Qzt-I05-6*. This gene had not been previously annotated but was supported by RNA sequences obtained from infected leaves (Grandaubert et al., 2015; Haueisen et al., 2019). Moreover, in a recent reannotation of the *Z. tritici* genome, which aimed at optimizing the detection of SSP (unpublished data), this gene was annotated and named *G_07189*. Additionally, qPCR performed to evaluate relative expression of the gene over the course of infection showed differential expression patterns, with an expression peak at 12 dpi further validating its status as a good effector candidate.

We were able to demonstrate the role of *G_07189* in the pathogenicity of I05 and I07 on the cultivar 'Renan'. The knock-out of this gene from I05 (most pathogenic parental strain on 'Renan') which generated I05_ΔG07189 strains, did not have a significant effect on the phenotype. The inclusion of the I07 (least pathogenic parental strain on 'Renan') allele for this gene, generating strains I05_ΔG07189+G07189$_{I07}$ and I05+G07189$_{I07}$, led to significantly lower S26 regardless of whether or not the I05 allele was present in the genetic background. The same phenomena were observed in the characterization of *Avr3D1* (Meile et al., 2018), where the *Avr3D1* knock-out in the background of the most pathogenic parental strain of the pair in that study (3D7) was unaltered compared to the wild-type. The knock-out however led to increased disease symptoms in the background of the strain with lower pathogenicity used in that study (3D1) compared to the wild-type.

This, corroborated with our results, suggests that *G_07189* encodes an avirulence factor. Additionally we showed that the region in which *G_07189* lies is TE rich and presents with TE presence/absence polymorphisms (Figure 5), similar to what has been previously observed with *AvrStb6* and *Avr3D1* (Zhong et al., 2017; Meile et al., 2018). Moreover, while I07, which carries the avirulent allele for *G_07189*, is able to produce symptoms on 'Renan' (i.e. S26 averaging at 10%), I05_ΔG07189+G07189$_{I07}$ strains, which all carry this same allele, do not produce sporulation on 'Renan' (i.e. S26 averaging at 0.8%). *G_07189* therefore leads to a quantitative phenotype in the I07 background, but to a qualitative, avirulent, phenotype in the I05 background. Rather than acting like a classic avirulence gene in an *R/Avr* interaction, *G_07189* has a spectrum of effects depending on the genetic background of the strain. This is illustrated in Figure 3, where the strains in the "none", "13", "1" and "1+13" categories,

which all carry the avirulent allele for *G_07189*, have different effects, if not always significantly, on the phenotype. These different effects form a gradient depending on the QTL combinations. Such a gradient in phenotypes, or variation of magnitude of the effect of quantitative pathogenicity on the phenotype, was recently demonstrated to also occur depending on the allele of the *Avr* gene in an isogenic background (Meile et al., 2023).

We are able to present conclusive evidence that an *Avr* gene can have a quantitative or qualitative effect on the phenotypes depending on the fungal genetic background. Pathogenicity is therefore not a strictly quantitative or qualitative variable, but rather fits somewhere on the continuum that they form. Recently, another example of an avirulence factor being involved in a quantitative interaction was proposed within the *Leptosphaeria maculans*-rapeseed pathosystem (Jiquel et al., 2021). A gene-for-gene interaction was demonstrated between LmSTEE98, a 'late effector' encoded by *AvrLmSTEE98*, and RlmSTEE98, encoded by the corresponding resistance gene. As a 'late effector', *AvrLmSTEE98* is expressed during stem colonization which is considered to be polygenic and quantitative.

On the plant side, it has been previously suggested that quantitative resistance genes in plants could be weaker forms of major resistance *R* genes (Poland et al., 2009) and that most wheat resistance loci are matched by a specific effector (Plissonneau et al., 2018). We therefore propose that *G_07189* could interact with the wheat resistance QTL identified in 'Renan' on chromosome 5D, designated as *Stb20q*, as this was the only QTL identified in 'Renan' which had specific resistance to I07 (Langlands-Perry et al., 2022). I07 carries the avirulent allele for *G_01789*, meaning that this gene could correspond to *AvrStb20q*.

4.3 Quantitative resistance durability despite gene-for-gene interactions

In a classic *R/Avr* gene-for-gene relationship, disease resistance is not considered durable due to the high probability of adaptation by the fungus with mutations in the *Avr* gene (Niks et al., 2011; Hartmann et al., 2017; Meile et al., 2018; Cowger and Brown, 2019). Here, we observed no loss of *G_07189* in the fungal populations or indeed any mutations in the effector-like features of the corresponding protein, i.e., the signal peptide and cysteine residues, inferring a potential fitness cost of such a loss. We found that the validated effector *G_07189* is highly conserved among French *Z. tritici* strains and shows a signature of positive diversifying selection. This is also what was observed for *Avr3D1*, the only other cloned effector in this pathosystem known to be involved in quantitative interactions (Meile et al., 2018). In the latter case however, a high level of diversity was observed in fungal populations. *G_07189* has the capacity to evolve to adapt to wheat resistance, as demonstrated by the diversifying selection signatures in three residues. The low diversity and fact that the virulent, or most pathogenic, isoform (I05), is not the most abundant in recent strains may therefore seem paradoxical. Two potential explanations for this paradox are, first, that the corresponding resistance gene,

which we hypothesize to be *Stb20q*, has not been largely deployed in the French cultivar landscape, meaning that no selection due to this resistance has been imposed on fungal populations. The cultivar on which *Stb20q* was identified is 'Renan' (Langlands-Perry et al., 2022), mostly used in organic farming, and therefore not one of the majority cultivars in the landscape. The other explanation is that the selective pressure imposed on *G_07189*, despite being present, is low enough that adaptation is slowed down compared to what is observed with major *R/Avr* interactions. Indeed, the least pathogenic allele (I07) does not stop the fungus from completing its life cycle, as illustrated by the presence of pycnidia on the infected leaf surface. This second hypothesis fits in with the narrative that quantitative resistance is more durable than its qualitative counterpart.

An example of a highly conserved effector under diversifying selection is APikL2 in *M. Oryzae* (Bentham et al., 2021). Research has shown that a single amino-acid polymorphism is sufficient to evade host recognition, however, the evolutionary driver of this polymorphism was attributed to the expansion of the host target spectrum rather than immune receptor evasion (Bentham et al., 2021). Moreover, similar to what we observe with *G_07189*, diversifying residues are located at a specific part of the protein (Bentham et al., 2021). This example opens a new avenue of possibilities as to the molecular interactions in which *G_07189* could be involved.

5 Conclusion

This study confirmed that pathogenicity in *Z. tritici* is complex and largely quantitative. We showed that several genes underlying QTL interact and contribute to the *T. aestivum* infection with varied impact on the phenotype. We demonstrated that genes underlying pathogenicity QTL can be effectors or *Avr* genes. These *Avr* genes can produce quantitative or qualitative phenotypes depending on the genetic background of the strains that carry them, advocating for a continuum between qualitative and quantitative notions of pathogenicity. We hypothesize the involvement of these effectors in minor gene-for-minor gene interactions, although this remains to be experimentally validated, in particular in the case of the putative *Stb20q/AvrStb20q* interaction. Furthermore, the low sequence diversity and the few diversifying selection signatures observed for *G_07189* could advocate for the durability of quantitative resistance despite a potential gene-for-gene interaction context. In terms of plant breeding, at this stage one can only hypothesize, however the inclusion of what might be called "weak resistance genes" in breeding programs could be a means of generating durable resistance through disease control in the form of favouring "weak" epidemics over the attempt at complete suppression of a given pathogen, thus reducing the selection of highly virulent strains. These lower effect resistance genes could potentially have advantages of both quantitative and qualitative forms of disease resistance. Indeed, although they are *R* genes from a mechanism-based point of view, they induce relatively low

selection pressure and thus offer more durable resistance than qualitative *R* genes.

Data availability statement

The datasets presented in this study can be found in online repositories. The names of the repository/repositories and accession number(s) can be found below: https://www.ncbi.nlm.nih.gov/, PRJNA777581 https://www.ncbi.nlm.nih.gov/, PRJNA881220.

Conflict of interest

The authors declare that the research was conducted in the absence of any commercial or financial relationships that could be construed as a potential conflict of interest.

Publisher's note

All claims expressed in this article are solely those of the authors and do not necessarily represent those of their affiliated organizations, or those of the publisher, the editors and the reviewers. Any product that may be evaluated in this article, or claim that may be made by its manufacturer, is not guaranteed or endorsed by the publisher.

Supplementary material

The Supplementary Material for this article can be found online at: https://www.frontiersin.org/articles/10.3389/fpls.2023.1128546/full#supplementary-material

References

Amezrou, R., Audeon, C., Compain, J., Gélisse, S., Ducasse, A., Saintenac, C., et al. (2022). A secreted protease-like protein in *Zymoseptoria tritici* is responsible for avirulence on Stb9 resistance in wheat. *bioRxiv* 10, 31. doi: 10.1101/2022.10.31.514577

Anon (2011). The qubit 2.0 fluorometer: the next generation in nucleic acid and protein quantitation. *BioProbes* 64, 12–13.

Arru, L., Francia, E., and Pecchioni, N. (2003). Isolate-specific QTLs of resistance to leaf stripe (*Pyrenophora graminea*) in the "Steptoe" x "Morex" spring barley cross. *Theor. Appl. Genet.* 106, 668–675. doi: 10.1007/s00122-002-1115-x

Bentham, A. R., Petit-Houdenot, Y., Win, J., Chuma, I., Terauchi, R., Banfield, M. J., et al. (2021). A single amino acid polymorphism in a conserved effector of the multihost blast fungus pathogen expands host-target binding spectrum. *PLoS Pathog.* 17, e1009957. doi: 10.1371/journal.ppat.1009957

Boixel, A.-L., Gélisse, S., Marcel, T. C., and Suffert, F. (2022). Differential tolerance of *Zymoseptoria tritici* to altered optimal moisture conditions during the early stages of wheat infection. *J. Plant Pathol.* 104, 495–507. doi: 10.1007/s42161-021-01025-7

Bowler, J., Scott, E., Tailor, R., Scalliet, G., Ray, J., and Csukai, M. (2010). New capabilities for *Mycosphaerella graminicola* research. *Mol. Plant Pathol.* 11, 691–704. doi: 10.1111/j.1364-3703.2010.00629.x

Brading, P. A., Verstappen, E. C. P., Kema, G. H. J., and Brown, J. K. M. (2002). A gene-for-gene relationship between wheat and *Mycosphaerella graminicola*, the septoria tritici blotch pathogen. *Phytopathology* 92, 439–445. doi: 10.1094/PHYTO.2002.92.4.439

Broman, K. W., Wu, H., Sen, Ś., and Churchill, G. A. (2003). R/qtl: QTL mapping in experimental crosses. *Bioinformatics* 19, 889–890. doi: 10.1093/bioinformatics/btg112

Brown, J. K. M., Chartrain, L., Lasserre-Zuber, P., and Saintenac, C. (2015). Genetics of resistance to *Zymoseptoria tritici* and applications to wheat breeding. *Fungal Genet. Biol.* 79, 33–41. doi: 10.1016/j.fgb.2015.04.017

Camacho, C., Coulouris, G., Avagyan, V., Ma, N., Papadopoulos, J., Bealer, K., et al. (2009). BLAST+: architecture and applications. *BMC Bioinf.* 10, 421. doi: 10.1186/1471-2105-10-421

Cowger, C., and Brown, J. K. M. (2019). Durability of quantitative resistance in crops: greater than we know? *Annu. Rev. Phytopathol.* 57, 253–277. doi: 10.1146/annurev-phyto-082718-100016

Desjardins, P., and Conklin, D. (2010). NanoDrop microvolume quantitation of nucleic acids. *J. Visualized Experiments* 45, e2565. doi: 10.3791/2565

Etter, P. D., Bassham, S., Hohenlohe, P. A., Johnson, E. A., and Cresko, W. A. (2011). SNP discovery and genotyping for evolutionary genetics using RAD sequencing. *Methods Mol. Biol. (Clifton N.J.)* 772, 157–178. doi: 10.1007/978-1-61779-228-1_9

Eyal, Z., Scharen, A. L., Prescott, J. M., and Ginkel, M.v. (1987). *The septoria diseases of wheat: concepts and methods of disease management* (Mexico, D.F.: CIMMYT).

Fagundes, W. C., Haueisen, J., and Stukenbrock, E. H. (2020). Dissecting the biology of the fungal wheat pathogen *Zymoseptoria tritici*: a laboratory workflow. *Curr. Protoc. Microbiol.* 59, e128. doi: 10.1002/cpmc.128

Flor, H. H. (1971). Current status of the gene-for-gene concept. *Annu. Rev. Phytopathol.* 9, 275–296. doi: 10.1146/annurev.py.09.090171.001423

Fones, H., and Gurr, S. (2015). The impact of septoria tritici blotch disease on wheat: an EU perspective. *Fungal Genet. Biol.* 79, 3–7. doi: 10.1016/j.fgb.2015.04.004

Fouché, S., Plissonneau, C., and Croll, D. (2018). The birth and death of effectors in rapidly evolving filamentous pathogen genomes. *Curr. Opin. Microbiol.* 46, 34–42. doi: 10.1016/j.mib.2018.01.020

Frey, K., and Pucker, B. (2020). Animal, fungi, and plant genome sequences harbor different non-canonical splice sites. *Cells* 9, 458. doi: 10.3390/cells9020458

Gerard, G., Börner, A., Lohwasser, U., and Simón, M. (2017). Genome-wide association mapping of genetic factors controlling septoria tritici blotch resistance and their associations with plant height and heading date in wheat. *Euphytica* 213, 27. doi: 10.1007/s10681-016-1820-1

Gohari, M. A., Ware, S. B., Wittenberg, A. H. J., Mehrabi, R., Ben M'Barek, S., Verstappen, E. C. P., et al. (2015). Effector discovery in the fungal wheat pathogen *Zymoseptoria tritici*. *Mol. Plant Pathol.* 16, 931–945. doi: 10.1111/mpp.12251

González, A. M., Marcel, T. C., and Niks, R. E. (2012). Evidence for a minor gene-for-minor gene interaction explaining nonhypersensitive polygenic partial disease resistance. *Phytopathology* 102, 1086–1093. doi: 10.1094/PHYTO-03-12-0056-R

Goodwin, S. B., M'Barek, S. B., Dhillon, B., Wittenberg, A. H. J., Crane, C. F., Hane, J. K., et al. (2011). Finished genome of the fungal wheat pathogen *Mycosphaerella graminicola* reveals dispensome structure, chromosome plasticity, and stealth pathogenesis. *PloS Genet.* 7, e1002070. doi: 10.1371/journal.pgen.1002070

Gout, L., Fudal, I., Kuhn, M.-L., Blaise, F., Eckert, M., Cattolico, L., et al. (2006). Lost in the middle of nowhere: the *AvrLm1* avirulence gene of the dothideomycete *Leptosphaeria maculans*. *Mol. Microbiol.* 60, 67–80. doi: 10.1111/j.1365-2958.2006.05076.x

Grandaubert, J., Bhattacharyya, A., and Stukenbrock, E. H. (2015). RNA-Seq-based gene annotation and comparative genomics of four fungal grass pathogens in the genus zymoseptoria identify novel orphan genes and species-specific invasions of transposable elements. *G3 (Bethesda Md.)* 5, 1323–1333. doi: 10.1534/g3.115.017731

Habig, M., Quade, J., and Stukenbrock, E. H. (2017). Forward genetics approach reveals host genotype-dependent importance of accessory chromosomes in the fungal wheat pathogen *Zymoseptoria tritici*. *mBio* 8, e01919–e01917. doi: 10.1128/mBio.01919-17

Hall, S. A., Allen, R. L., Baumber, R. E., Baxter, L. A., Fisher, K., Bittner-Eddy, P. D., et al. (2009). Maintenance of genetic variation in plants and pathogens involves complex networks of gene-for-gene interactions. *Mol. Plant Pathol.* 10, 449–457. doi: 10.1111/j.1364-3703.2009.00544.x

Hartmann, F. E., Sánchez-Vallet, A., McDonald, B. A., and Croll, D. (2017). A fungal wheat pathogen evolved host specialization by extensive chromosomal rearrangements. *ISME J.* 11, 1189–1204. doi: 10.1038/ismej.2016.196

Haueisen, J., Möller, M., Eschenbrenner, C. J., Grandaubert, J., Seybold, H., Adamiak, H., et al. (2019). Highly flexible infection programs in a specialized wheat pathogen. *Ecol. Evol.* 9, 275–294. doi: 10.1002/ece3.4724

Houterman, P. M., Ma, L., Ooijen, G., de, M. J., Cornelissen, B. J. C., Takken, F. L. W., et al. (2009). The effector protein Avr2 of the xylem-colonizing fungus *Fusarium oxysporum* activates the tomato resistance protein I-2 intracellularly. *Plant Journal: For Cell Mol. Biol.* 58, 970–978. doi: 10.1111/j.1365-313X.2009.03838.x

Jia, Y., McAdams, S. A., Bryan, G. T., Hershey, H. P., and Valent, B. (2000). Direct interaction of resistance gene and avirulence gene products confers rice blast resistance. *EMBO J.* 19, 4004–4014. doi: 10.1093/emboj/19.15.4004

Jiquel, A., Gervais, J., Geistodt-Kiener, A., Delourme, R., Gay, E. J., Ollivier, B., et al. (2021). A gene-for-gene interaction involving a 'late' effector contributes to quantitative resistance to the stem canker disease in brassica napus. *New Phytol.* 231, 1510–1524. doi: 10.1111/nph.17292

Kamoun, S. (2006). A catalogue of the effector secretome of plant pathogenic oomycetes. *Annu. Rev. Phytopathol.* 44, 41–60. doi: 10.1146/annurev.phyto.44.070505.143436

Karlstedt, F., Kopahnke, D., Perovic, D., Jacobi, A., Pillen, K., and Ordon, F. (2019). Mapping of quantitative trait loci (QTL) for resistance against *Zymoseptoria tritici* in the winter spelt wheat accession HTRI1410 (Triticum aestivum subsp. *spelta).* *Euphytica* 215, 108. doi: 10.1007/s10681-019-2432-3

Kema, G. H. J., Yu, D., Rijkenberg, F. H. J., Shaw, M. W., and Baayen, R. P. (1996). Histology of the pathogenesis of *Mycosphaerella graminicola* in wheat. *Phytopathology* 86, 777–786. doi: 10.1094/Phyto-86-777

Kettles, G. J., Bayon, C., Canning, G., Rudd, J. J., and Kanyuka, K. (2017). Apoplastic recognition of multiple candidate effectors from the wheat pathogen *Zymoseptoria tritici* in the nonhost plant *Nicotiana benthamiana*. *New Phytol.* 213, 338–350. doi: 10.1111/nph.14215

Koeck, M., Hardham, A. R., and Dodds, P. N. (2011). The role of effectors of biotrophic and hemibiotrophic fungi in infection. *Cell. Microbiol.* 13, 1849–1857. doi: 10.1111/j.1462-5822.2011.01665.x

Kupfer, D. M., Drabenstot, S. D., Buchanan, K. L., Lai, H., Zhu, H., Dyer, D. W., et al. (2004). Introns and splicing elements of five diverse fungi. *Eukaryotic Cell* 3, 1088–1100. doi: 10.1128/EC.3.5.1088-1100.2004

Langlands-Perry, C., Cuenin, M., Bergez, C., Krima, S. B., Gélisse, S., Sourdille, P., et al. (2022). Resistance of the wheat cultivar 'Renan' to septoria leaf blotch explained by a combination of strain specific and strain non-specific QTL mapped on an ultra-dense genetic map. *Genes* 13, 100. doi: 10.3390/genes13010100

Lannou, C. (2012). Variation and selection of quantitative traits in plant pathogens. *Annu. Rev. Phytopathol.* 50, 319–338. doi: 10.1146/annurev-phyto-081211-173031

Lendenmann, M. H., Croll, D., Stewart, E. L., and McDonald, B. A. (2014). "Quantitative trait locus mapping of melanization in the plant pathogenic fungus *Zymoseptoria tritici*. G3: genes Genomes," *Genes Genom. Genet.* 4, 2519–2533. doi: 10.1534/g3.114.015289

Leonards-Schippers, C., Gieffers, W., Schäfer-Pregl, R., Ritter, E., Knapp, S. J., Salamini, F., et al. (1994). Quantitative resistance to *Phytophthora infestans* in potato: a case study for QTL mapping in an allogamous plant species. *Genetics* 137, 67–77. doi: 10.1093/genetics/137.1.67

Letunic, I., and Bork, P. (2016). Interactive tree of life (iTOL) v3: an online tool for the display and annotation of phylogenetic and other trees. *Nucleic Acids Res.* 44, W242–W245. doi: 10.1093/nar/gkw290

Livak, K. J., and Schmittgen, T. D. (2001). Analysis of relative gene expression data using real-time quantitative PCR and the 2−ΔΔCT method. *Methods* 25, 402–408. doi: 10.1006/meth.2001.1262

Luo, R., Liu, B., Xie, Y., Li, Z., Huang, W., Yuan, J., et al. (2012). SOAPdenovo2: an empirically improved memory-efficient short-read *de novo* assembler. *GigaScience* 1, 18. doi: 10.1186/2047-217X-1-18

Ma, L. -J., van der Does, H. C., Borkovich, K. A., Coleman, J. J., Daboussi, , Di Pietro, M.-J. A., et al. (2010). Comparative genomics reveals mobile pathogenicity chromosomes in fusarium. *Nature* 464, 367–373. doi: 10.1038/nature08850

Marshall, R., Kombrink, A., Motteram, J., Loza-Reyes, E., Lucas, J., Hammond-Kosack, K. E., et al. (2011). Analysis of two *in planta* expressed LysM effector homologs from the fungus *Mycosphaerella graminicola* reveals novel functional properties and varying contributions to virulence on wheat. *Plant Physiol.* 156, 756–769. doi: 10.1104/pp.111.176347

Meile, L., Croll, D., Brunner, P. C., Plissonneau, C., Hartmann, F. E., McDonald, B. A., et al. (2018). A fungal avirulence factor encoded in a highly plastic genomic region triggers partial resistance to septoria tritici blotch. *New Phytol.* 219, 1048–1061. doi: 10.1111/nph.15180

Meile, L., Garrido-Arandia, M., Bernasconi, Z., Peter, J., Schneller, A. , Bernasconi, A., et al. (2023). Natural variation in *Avr3D1* from *Zymoseptoria* sp. contributes to quantitative gene-for-gene resistance and to host specificity. *New Phytol.* 238, 1562-1577. doi.org/doi: 10.1111/nph.18690.

Mercier, A., Simon, A., Lapalu, N., Giraud, T., Bardin, M., Walker, A.-S., et al. (2021). Population genomics reveals molecular determinants of specialization to tomato in the polyphagous fungal pathogen *Botrytis cinerea* in France. *Phytopathology* 111, 2355–2366. doi: 10.1094/PHYTO-07-20-0302-FI

Niks, R. E., Parlevliet, J. E., Lindhout, P., and Bai, Y. (2011). Breeding crops with resistance to diseases and pests (The Netherlands: Wageningen Academic Publishers).

Niks, R. E., Qi, X., and Marcel, T. C. (2015). Quantitative resistance to biotrophic filamentous plant pathogens: concepts, misconceptions, and mechanisms. *Annu. Rev. Phytopathol.* 53, 445–470. doi: 10.1146/annurev-phyto-080614-115928

Oliva, R., Win, J., Raffaele, S., Boutemy, L., Bozkurt, T. O., Chaparro-Garcia, A., et al. (2010). Recent developments in effector biology of filamentous plant pathogens. *Cell. Microbiol.* 12, 705–715. doi: 10.1111/j.1462-5822.2010.01471.x

Pariaud, B., Ravigné, V., Halkett, F., Goyeau, H., Carlier, J., and Lannou, C. (2009). Aggressiveness and its role in the adaptation of plant pathogens. *Plant Pathol.* 58, 409–424. doi: 10.1111/j.1365-3059.2009.02039.x

Petit-Houdenot, Y., and Fudal, I. (2017). Complex interactions between fungal avirulence genes and their corresponding plant resistance genes and consequences for disease resistance management. *Front. Plant Sci.* 8. doi: 10.3389/fpls.2017.01072

Pfeifer, B., Wittelsbürger, U., Ramos-Onsins, S. E., and Lercher, M. J. (2014). PopGenome: an efficient Swiss army knife for population genomic analyses in r. *Mol. Biol. Evol.* 31, 1929–1936. doi: 10.1093/molbev/msu136

Plissonneau, C., Blaise, F., Ollivier, B., Leflon, M., Carpezat, J., Rouxel, T., et al. (2017). Unusual evolutionary mechanisms to escape effector-triggered immunity in the fungal phytopathogen *Leptosphaeria maculans*. *Mol. Ecol.* 26, 2183–2198. doi: 10.1111/mec.14046

Plissonneau, C., Hartmann, F. E., and Croll, D. (2018). Pangenome analyses of the wheat pathogen *Zymoseptoria tritici* reveal the structural basis of a highly plastic eukaryotic genome. *BMC Biol.* 16, 5. doi: 10.1186/s12915-017-0457-4

Poland, J. A., Balint-Kurti, P. J., Wisser, R. J., Pratt, R. C., and Nelson, R. J. (2009). Shades of gray: the world of quantitative disease resistance. *Trends Plant Sci.* 14, 21–29. doi: 10.1016/j.tplants.2008.10.006

Poppe, S., Dorsheimer, L., Happel, P., and Stukenbrock, E. H. (2015). Rapidly evolving genes are key players in host specialization and virulence of the fungal wheat

pathogen *Zymoseptoria tritici* (*Mycosphaerella graminicola*). *PloS Pathog.* 11, e1005055. doi: 10.1371/journal.ppat.1005055

Pradhan, A., Ghosh, S., Sahoo, D., and Jha, G. (2021). Fungal effectors, the double edge sword of phytopathogens. *Curr. Genet.* 67, 27–40. doi: 10.1007/s00294-020-01118-3

Qi, X., Jiang, G., Chen, W., Niks, R. E., Stam, P., and Lindhout, P. (1999). Isolate-specific QTLs for partial resistance to *Puccinia hordei* in barley. *Theor. Appl. Genet.* 99, 877–884. doi: 10.1007/s001220051308

R Core Team (2019). *R: a language and environment for statistical computing. r foundation for statistical computing* (Vienna, Austria). Available at: https://www.R-project.org/.

Robinson, J. T., Thorvaldsdóttir, H., Winckler, W., Guttman, M., Lander, E. S., Getz, G., et al. (2011). Integrative genomics viewer. *Nat. Biotechnol.* 29, 24–26. doi: 10.1038/nbt.1754

Rudd, J. J., Kanyuka, K., Hassani-Pak, K., Derbyshire, M., Andongabo, A., Devonshire, J., et al. (2015). Transcriptome and metabolite profiling of the infection cycle of *Zymoseptoria tritici* on wheat reveals a biphasic interaction with plant immunity involving differential pathogen chromosomal contributions and a variation on the hemibiotrophic lifestyle definition. *Plant Physiol.* 167, 1158–1185. doi: 10.1104/pp.114.255927

Shao, D., Smith, D. L., Kabbage, M., and Roth, M. G. (2021). Effectors of plant necrotrophic fungi. *Front. Plant Sci.* 12. doi: 10.3389/fpls.2021.687713

Shaw, M. W. (1991). Interacting effects of interrupted humid periods and light on infection of wheat leaves by *Mycosphaerella graminicola* (*Septoria tritici*). *Plant Pathol.* 40, 595–607. doi: 10.1111/j.1365-3059.1991.tb02424.x

Smit, A., Hubley, R., and Green, P. (2013) *RepeatMasker open-4.0.* Available at: https://www.repeatmasker.org/.

Soyer, J. L., Ghalid, M. E., Glaser, N., Ollivier, B., Linglin, J., Grandaubert, J., et al. (2014). Epigenetic control of effector gene expression in the plant pathogenic fungus *Leptosphaeria maculans*. *PloS Genet.* 10, e1004227. doi: 10.1371/journal.pgen.1004227

Sperschneider, J., Dodds, P. N., Gardiner, D. M., Singh, K. B., and Taylor, J. M. (2018). Improved prediction of fungal effector proteins from secretomes with EffectorP 2.0. *Mol. Plant Pathol.* 19, 2094–2110. doi: 10.1111/mpp.12682

Stamatakis, A. (2014). RAxML version 8: a tool for phylogenetic analysis and post-analysis of large phylogenies. *Bioinformatics* 30, 1312–1313. doi: 10.1093/bioinformatics/btu033

Stergiopoulos, I., and Wit, P. J. G. M. (2009). Fungal effector proteins. *Annu. Rev. Phytopathol.* 47, 233–263. doi: 10.1146/annurev.phyto.112408.132637

Stewart, E. L., Croll, D., Lendenmann, M. H., Sanchez-Vallet, A., Hartmann, F. E., Palma-Guerrero, J., et al. (2018). Quantitative trait locus mapping reveals complex genetic architecture of quantitative virulence in the wheat pathogen *Zymoseptoria tritici*. *Mol. Plant Pathol.* 19, 201–216. doi: 10.1111/mpp.12515

Stewart, E. L., Hagerty, C. H., Mikaberidze, A., Mundt, C. C., Zhong, Z., and McDonald, B. A. (2016). An improved method for measuring quantitative resistance to

the wheat pathogen *Zymoseptoria tritici* using high-throughput automated image analysis. *Phytopathology* 106, 782–788. doi: 10.1094/PHYTO-01-16-0018-R

Stewart, E. L., and McDonald, B. A. (2014). Measuring quantitative virulence in the wheat pathogen *Zymoseptoria tritici* using high-throughput automated image analysis. *Phytopathology* 104, 985–992. doi: 10.1094/PHYTO-11-13-0328-R

Stukenbrock, E. H., and McDonald, B. A. (2009). Population genetics of fungal and oomycete effectors involved in gene-for-gene interactions. *Mol. Plant-Microbe Interact.* 22, 371–380. doi: 10.1094/MPMI-22-4-0371

Suffert, F., Delestre, G., Carpentier, F., Gazeau, G., Walker, A.-S., Gélisse, S., et al. (2016). Fashionably late partners have more fruitful encounters: impact of the timing of co-infection and pathogenicity on sexual reproduction in *Zymoseptoria tritici*. *Fungal Genet. Biol.* 92, 40–49. doi: 10.1016/j.fgb.2016.05.004

Teufel, F., Almagro Armenteros, J. J., Johansen, A. R., Gíś lason, M. H., Pihl, S. I., Tsirigos, K. D., et al. (2022). SignalP 6.0 predicts all five types of signal peptides using protein language models. *Nat. Biotechnol.* 40, 1023–1025. doi: 10.1038/s41587-021-01156-3

Vagndorf, N., Nielsen, N. H., Edriss, V., Andersen, J. R., Orabi, J., Jørgensen, L. N., et al. (2017). Genomewide association study reveals novel quantitative trait loci associated with resistance towards septoria tritici blotch in north European winter wheat. *Plant Breed.* 136, 474–482. doi: 10.1111/pbr.12490

Wicker, T., Sabot, F., Hua-Van, A., Bennetzen, J. L., Capy, P., Chalhoub, B., et al. (2007). A unified classification system for eukaryotic transposable elements. *Nat. Rev. Genet.* 8, 973–982. doi: 10.1038/nrg2165

Win, J., Chaparro-Garcia, A., Belhaj, K., Saunders, D. G. O., Yoshida, K., Dong, S., et al. (2012). Effector biology of plant-associated organisms: concepts and perspectives. *Cold Spring Harbor Symp. Quantitative Biol.* 77, 235–247. doi: 10.1101/sqb.2012.77.015933

Wit, P. J. G. M. (1995). Fungal avirulence genes and plant resistance genes: unraveling the molecular basis of gene-for-gene interactions. *Adv. Bot. Res.* 21, 147–185. doi: 1016/S0065-2296(08)60012-9

Yang, N., McDonald, M. C., Solomon, P. S., and Milgate, A. W. (2018). Genetic mapping of Stb19, a new resistance gene to *Zymoseptoria tritici* in wheat. *Theor. Appl. Genet.* 131, 2765–2773. doi: 10.1007/s00122-018-3189-0

Yates, S., Mikaberidze, A., Krattinger, S. G., Abrouk, M., Hund, A., Yu, K., et al. (2019). Precision phenotyping reveals novel loci for quantitative resistance to septoria tritici blotch. *Plant Phenomics* 2019, 3285904. doi: 10.34133/2019/3285904

Yemelin, A., Brauchler, A., Jacob, S., Foster, A. J., Laufer, J., Heck, L., et al. (2022). Two novel dimorphism-related virulence factors of *Zymoseptoria tritici* identified using agrobacterium-mediated insertional mutagenesis. *Int. J. Mol. Sci.* 23, 400. doi: 10.3390/ijms23010400

Zerbino, D. R., and Birney, E. (2008). Velvet: algorithms for *de novo* short read assembly using de bruijn graphs. *Genome Res.* 18, 821–829. doi: 10.1101/gr.074492.107

Zhong, Z., Marcel, T. C., Hartmann, F. E., Ma, X., Plissonneau, C., Zala, M., et al. (2017). A small secreted protein in *Zymoseptoria tritici* is responsible for avirulence on wheat cultivars carrying the *Stb6* resistance gene. *New Phytol.* 214, 619–631. doi: 10.1111/nph.14434

Frontiers in
Plant Science

Cultivates the science of plant biology and its applications

The most cited plant science journal, which advances our understanding of plant biology for sustainable food security, functional ecosystems and human health.

Discover the latest Research Topics

See more →

frontiers

Frontiers in
Plant Science

frontiers | Research Topics